Book of Proceedings of

MATERIALS SCIENCE AND TECHNOLOGY SOCIETY OF NIGERIA

Kaduna State Chapter
2017 Conference

A Publication of
MATERIALS SCIENCE AND TECHNOLOGY SOCIETY OF NIGERIA
Kaduna State Chapter

13th EDITION

ISBN 978-060-609-31



PROCEEDINGS

OF THE

MATERIALS SCIENCE AND TECHNOLOGY SOCIETY OF NIGERIA (MSN)

KADUNA STATE CHAPTER

PUBLISHED BY

THE MATERIALS SCIENCE AND TECHNOLOGY SOCIETY OF NIGERIA (MSN)

ISBN 978-060-609-31

msnkadunachapter@gmail.com

COPYRIGHT © 2017

FOREWORD

The Kaduna State Chapter of the Materials Science and Technology Society of Nigeria (MSN) was chartered in the year 2003 by the then National President of the Society, Late Prof. O. O. Adewoye – DG NASENI. The National Headquarters of the Society is located at Engineering Materials Development Institute, Akure in Ondo State, Nigeria. Since its inception, the Chapter has been able to bring together academicians and researchers from its catchment areas (i.e., Zaria, Kaduna, Kano, Nasarawa, Bauchi and Yobe). The Chapter successfully hosted the 4th Nigerian Materials Congress (NIMACON2005) and the 15th Nigerian Materials Congress (NIMACON2016) in conjunction with Ahmadu Bello University, Zaria, on 21st – 25th November, 2016 at the famous ABU Hotels (formerly Kongo Conference Hotels), Ahmadu Bello University Zaria, Kaduna State.

The Kaduna State Chapter, since coming into being, has been growing from strength to strength. Presently, the Chapter boasts of about 325 (as at last count in November, 2017) members consisting of academicians, professionals and students from diverse fields of materials science and technology.

The Chapter has continued to encourage members, especially young academics and researchers, to improve themselves through hardwork, exchange of ideas and facilities, as well as paper presentations. This year, the 4th Kaduna State Chapter Conference was organised and held on Saturday 4th of November, 2017 at the Conference Hall of the Department of Polymer and Textile Engineering, Ahmadu Bello University, Zaria. This effort has culminated in the accrual of papers which have made possible the production of the ***13th edition*** of this Book of Proceedings. It is hoped that this publication will further spur our members into full and active participation in MSN activities at local, national and international levels.

We thank Prof. Abu S. Lawal (HOD – Polymer and Textile Engineering) for hosting the Conference, the National President of MSN – Prof. A. S. Ahmed, the immediate past Kaduna State Chapter Chairman – Prof. Peter O. Nkeonye, my indefatigable Secretary – Mr. E.O. Achukwu and also the rest of the EXCO members of MSN Kaduna State Chapter and all other members of the Kaduna State Chapter for their unflinching support throughout my 4-year tenure of 2 terms. I am indeed very grateful, and may Allah reward you all.



Prof. A. Giwa
Chairman, MSN Kaduna Chapter
msnkadunachapter@gmail.com

OFFICERS OF THE KADUNA STATE CHAPTER 2016 – 2017

Prof. A. Giwa	Chairman
Dr. N. S. Maina	Vice Chairman (Materials Engineering)
Dr. E.N. Oparah	Vice Chairman (Materials Science)
Dr. H. Abba	Chairman Publications Committee
Mrs. J. T. Tagwoi	Treasurer
Dr. J. Tagang	Financial Secretary
Mr. Bulus Habila	PRO
Prof. P. O. Nkeonye	Ex-Officio
Prof. A.S. Ahmed	Ex-Officio
Engr. Bello Atiku	Ex-Officio
Mr. E. O. Achukwu	Secretary

PUBLICATIONS COMMITTEE, MSN – KADUNA STATE CHAPTER

DR. H. ABBA (CHAIRMAN)
Department of Chemistry,
Ahmadu Bello University, Zaria

PROF. P. O. NKEONYE (MEMBER)
Department of Textile Science and Technology,
Ahmadu Bello University, Zaria

PROF. K. J. OSINUBI (MEMBER)
Department of Civil Engineering,
Ahmadu Bello University, Zaria

ENGR. (Dr.) O. A. AJAYI (MEMBER)
Department of Chemical Engineering,
Ahmadu Bello University, Zaria

TABLE OF CONTENTS

	Title Page	i
	Foreword	ii
	Officers of the Kaduna State Chapter	iii
	Publications Committee MSN – Kaduna State Chapter	iii
	Table of Contents	iv
1	A DESIGN OF A BIOMIMETIC, HYPER-REDUNDANT ROBOTS JOINTS WITH RUBBER **AFOLAYAN MATTHEW OLATUNDE**	1-6
2	PROSPECTS OF BIOSORBENTS DEVELOPMENT FOR OIL SPILL CLEANUP IN NIGERIA: A REVIEW **AGIDA, I. R., OLAWALE A. S. AND ISA M. T.**	7-13
3	EFFECT OF DRAG REDUCING POLYMER ON THE QUALITY OF DRINKING WATER **LAWRENCE C. EDOMWONYI-OTU, AND DANIEL O. ADELAKUN**	14-21
4	INVESTIGATION OF THE EFFECTIVENESS OF ALUM FROM SOME NIGERIAN KAOLINITES **LAWRENCE C. EDOMWONYI-OTU, IFEANYI E. ALAZU, JONAH U. IRANDE**	22-25
5	PHYSICO-CHEMICAL ANALYSIS OF NANOCRYSTALLINE CELLULOSE FROM RICE HUSK **GBADEGESIN ADENIKE MARIAM AND KOGO A. ABDULLAHI**	26-30
6	COMPARATIVE STUDY OF THE CHARACTERISTICS STRENGTH OF REINFORCEMENT BARS IN THE LOCAL MARKET (A CASE STUDY OF GUSAU METROPOLIS) **SHOLADOYE, I. O AND UCHECHUKWU ANYA**	31-35
7	EFFECTS OF THERMAL RADIATION AND VARIABLE VISCOSITY ON NATURAL CONVECTION FLOW PAST A VERTICAL PLATE IN A SLIP FLOW REGIME **PRINCELY O. OJEAGBASE**	36-45
8	TECHNO-ECONOMIC ANALYSIS OF AGRICULTURAL WASTES AS FEEDSTOCKS FOR BIOETHANOL PRODUCTION IN NIGERIA **A. SANNI, A.S. OLAWALE, Y.M. SANI**	46-52
9	ANTIMICROBIAL DETERGENT FROM CARAWAY OIL **S. MUKTARI, M.M. BAMALLI, AND U.S AMEURU**	53-56
10	EFFECT OF PARTIALLY TREATED SEWAGE WATER ON SANDCRETE BLOCKS **SALAHUDEEN, A. B. AND ABDULLAHI, U.**	57-60
11	POINT AND NON-POINT SOURCE SEWAGE WATER QUALITY ANALYSIS FOR IRRIGATION FARMING **SALAHUDEEN, A. B. AND AMPITAN, A. A.**	61-68
12	MOULDING OF EARTH BLOCKS USING CONTAMINATED WATER **SALAHUDEEN, A. B. AND POPOOLA, F. M.**	69-72
13	ESTERIFICATION OF PROPANOIC ACID WITH N-BUTANOL IN $ZnCl_2$/UREA DEEP EUTECTIC SOLVENT **YAHAYA MUHAMMAD SANI AND LEVI INUWA**	73-76
14	GEOTECHNICAL IMPROVEMENT OF WEAK PAVEMENT BASE SOIL IN BAURE L.G.A OF KATSINA STATE USING LIME **SADEEQ, J. A., HARUNA M. I. AND SALAHUDEEN A. B.**	77-82
15	GROUNDNUT SHELL ASH MODIFICATION OF LATERITIC SOIL **SADEEQ, J. A., ADAMS, M. D. AND SALAHUDEEN A. B.**	83-88
16	MODIFICATION OF LATERITIC SOIL USING CORNCOB ASH **SADEEQ, J. A., DANGNE, K. Z. AND SALAHUDEEN A. B.**	89-94

17 OPTIMIZATION OF ACTIVATING CONDITIONS AND COLOUR REMOVAL EFFICIENCY OF MAIZE HUSK IN THE REMOVAL OF COLOUR FROM TEXTILE WASTE WATER 95-103
R.O. OKPUWHARA, B.M. DAUDA AND K.O. FASHOLA

18 APPLICATION OF ASPEN TECH FOR THE DESIGN OF HEAT EXCHANGERS IN THE PRODUCTION OF BUTADIENE FROM BIOETHANOL 104-108
NUHU M, SAMSON J.N, IMEH E. O

19 DE-CHROMING CHROME TANNED TANNERY SOLID WASTE WITH *SACCHAROMYCES CEREVISIAE* 109-112
IMEH ETIM ONUKAK, NUHU M, ABDULLAHI S. MIKAILU , ISUWA K. ADAMU AND ADEYI A. AMEH

20 OIL-WELL PLACEMENT FOR MAXIMUM PRODUCTION IN ALWYN-NORTH FIELD 113-123
IGBEN ENOHOR, GODWILL PEPRAH, BABA JIBRIL EL-YAKUBU, YAHAYA MUHAMMAD SANI, LAWRENCE EDOMWONYI-OUT

21 DESIGN, FABRICATION AND PERFORMANCE EVALUATION OF KENAF MINI-SPINNING MACHINE 124-130
AKANG I.V., BARMINAS J.F., GADIMOH S., OTSAI O.J., OKECHUKWU T.U., AYUBA N.L. AND AL-KASIM U.

22 NATIONAL INDUSTRIALISATION ROADMAP: THE NARICT FABRICATION ENGINEERING INPUT (A CASE STUDY IN TEXTILE 131-144
AKANG I.V., GADIMOH S., OTSAI O.J., OKECHUKWU T.U., AKANG J., AYUBA N.L. AND AL-KASIM U.

23 PHYSIO-MECHANICAL ANALYSIS OF FABRICATED PLASTIC INTERLOCK USING RECYCLED WASTE LOW DENSITY POLYETHYLENE (WATER SACHET) FILLED PALM KERNEL SHELL PARTICLES 145-151
SANI, M. TAOFEEQ, SALAMI, WASIU OYEYEMI AND ALI, SANI MOHAMMED

24 A NEW APPROACH TO ROBUST IMAGE WATERMARKING ALGORITHM USING DISCRETE ORTHONORMAL STOCKWELL TRANSFORMATION TECHNIQUE 152-157
B. A. JIBRIN, S. M. SANI AND A. M. S. TEKANYI

25 ENHANCEMENT OF SELECTIVE MAPPING TECHNIQUE FOR PEAK-TO-AVERAGE POWER RATIO REDUCTION IN OFDM USING NORMALIZED HILBERT MATRIX 158-165
H. I. YARIMA, A. M. S. TEKANYI, S. M. SANI AND M. B ABDULRAZAQ

26 DESIGN AND SIMULATION OF A PASSIVE BELOW KNEE PROSTHETIC LEG 166-171
U. M. ABDULLAHI, S. UMARU, AND M.A. ADAMU

27 SYNTHESIS AND EVALUATION OF METAL-LOADED ZEOLITE Y FOR CONTROL OF INDOOR CO EMISSIONS 172-175
M. PETER, D.M KULLA, N.O OMINSANYA, D.O. OBADA AND A.Y. ATTA

28 EVALUATION OF THE DYEING PROPERTIES OF SOME AMINOTHIOPHENE BASED DISPERSED AZO DYES 176-181
O.R.A. IYUN, K.A. BELLO, O. J. ABAYEH, A. JAURO AND G.Y. KANTIOK

29 KINETIC MODEL FOR GLUCOSE PRODUCTION FROM ELEPHANT GRASS (STEM) USING ASPERGILLUS NIGER 182-188
JIBRIL, A., ADEREMI, B.O., MOMOH, O.R. AND EBENEZER O.

30 GLUCOSE PRODUCTION FROM ELEPHANT GRASS (*PENNISETUM PURPUREUM*) 189-196
JIBRIL, A., ADEREMI, B.O., MOMOH, O.R. AND EBENEZER O.

31 DEVELOPMENT OF PEROVSKITE BASED CATALYSTS FOR DIESEL SOOT EMISSION CONTROL 197-199
R.T YUSUF, A. ANDREWS, S. UMARU, U.A UMAR, D.O. OBADA AND D. DODOO-ARHIN

32 EFFECTS OF CONCENTRATION AND MOLECULAR WEIGHT ON THE PLASTICIZING EFFICIENCY OF SOME DIALKYL ADIPATES IN PVC SHEETS 200-207
ABBA, H. AND BUKHARI, M. M.

33 INVESTIGATION OF CORROSION INHIBITION EFFECT OF MINT LEAVES AND GUAVA LEAVES EXTRACTS IN ACIDIC MEDIA 208-216
B. O. SAMUEL AND B. DAN-ASABE

34 DEVELOPMENT OF COMPOSITE MATERIAL USING PALM KERNEL SHELL PARTICLES/PHENOLIC RESIN FOR BRAKE PAD APPLICATION 217-221
A.A. IBRAHIM, O.P. MICHAEL, A. ALIU, M.B. BALOGUN, S. ABUBAKAR AND N.D. FACI

35 ENERGY CONSERVATION WITH EFFICIENT LIGHTING: A CASE STUDY OF A PETROLEUM PRODUCTS PRICING REGULATION AGENCY (PPPRA) BUILDING 222-228
J. SALEH, P.U. OKORIE AND E. O. OCHUOKPA

36 CHARACTERISATION OF UNTREATED AND NATURAL LATEX TREATED BORASSUS AETHIOPUM PALM LEAF STALK FIBRE 229-234
ALABI, A.S., SHEHU, U., AUSE, T., MBADA, N. I., AND USMAN, I.

37 EVALUATION OF CERAMIC WASTE AS PARTIAL REPLACEMENT OF COARSE AGGREGATE IN HOT MIX ASPHALT 235-243
IJIMDIYA, T. S., MANASSEH, J., SANI, J. E., CHUKWUJAMA, I. A AND BAKARE, S. M.

38 A REVIEW OF MATERIALS, METHODS AND MODERN TECHNOLOGY OF SIZING AND DESIZING OF COTTON IN TEXTILE INDUSTRIES 244-246
SALISU ABDULRAHMAN

39 COMPARATIVE STUDY OF HYDROXYAPATITE NANOCRYSTALS SYNTHESIZED AT PHYSIOLOGICAL CONDITIONS USING THE CHEMICAL PRECIPITATION AND HYDOTHERMAL TECHNIQUES 247-255
V. OCHIGBO, V.O. AJIBOLA, E.B. AGBAJI, A. GIWA, J.T. BARMINAS, P. MANNIVASAKAN, V. RAJENDRAN

40 PRELIMINARY INVESTIGATION OF THE EFFECT OF PRECURSOR CONCENTRATION AND CALCINATION TEMPERATURES ON HYDROXYAPATITE NANOCRYSTALS SYNTHESIZED AT PHYSIOLOGICAL CONDITION USING WET PRECIPITATION METHOD 256-264
V. OCHIGBO, V.O. AJIBOLA, E.B. AGBAJI, A. GIWA, J.T. BARMINAS, B.S. ZURU, P. MANNIVASAKAN, V. RAJENDRAN

41 INFLUENCE OF PROCESS VARIABLES ON ADSORPTION OF COLOUR FROM TEXTILE WASTE WATER USING ACTIVATED CARBONS FROM SOME AGRICULTURAL WASTES 265-280
R.O. OKPUWHARA, B.M. DAUDA AND K.O. FASHOLA

42 EVALUATION OF VARIATIONS IN INDOOR AIR QUALITY IN SELECTED HOUSEHOLDS WITHIN KADUNA METROPOLIS 281-287
F.B. IBRAHIM AND D. E. ASUKU

43 COMPOSITES FABRICATION AND CHARACTERIZATION 288-294
J. BABA ALI AND A. GIWA

A DESIGN OF A BIOMIMETIC, HYPER-REDUNDANT ROBOTS JOINTS WITH RUBBER

AFOLAYAN MATTHEW OLATUNDE
Mechanical Engineering Department, Ahmadu Bello University, Zaria, Nigeria
tunde_afolayan@yahoo.com

ABSTRACT
Robot designs can be classified based on the number of concurrent joints they posses. The convectional robots can best be described as discrete manipulators where the designs are based on a small number of active joints. Another category are the hyper-redundant robots that have much larger number of joints while the third group are referred to as continuum robots with theoretically no joints or the joints are not distinct. In hyper-redundant robot joint design, the problem many researchers have to solve includes how to control the multiple degree of freedom joints to produce usable motion since an hyper-redundant body can take a very large number of possible shapes without a constraint. This work therefore presents a design of a biologically inspired joint using vulcanized carbon black rubber. An hydrostatic joint model was imitated. Simulation on the designed joint shows that it will not fail in service due to warping. The maximum von Mises stress of 42.61kPa will occur at the rubber-aluminum interface when the joint is loaded as a cantilever with an 0.001N load. The maximum von Mises strain is 0.31m/m.

Keywords*: Biomimetic, Joint, Simulation, Robot, Hyper-Redundant Robot*

INTRODUCTION

There are three forms of robots when classified based on their joints, namely, discrete joints, hyper-redundant joints and continuum joints. Most industrial robots have discrete joints made up of identifiable links. The hyper-redundant joints have much higher number of links while continuum joints have no identifiable or fixed joints. The more the links, the more flexible the robotic manipulator based on them are.

Joint types found in biological models are two categories; bony joints (such as in mammals, reptiles) and hydrostatic joints. Hydrostatic joints are further divided into two categories; fluid-filled hydrostat and muscular hydrostat (Kier and Smith, 1985). Organisms that use fluid-filled balloon like elastic structure used it for support (Skierczynski et al, 1996; Alscher and Beyn, 1998; Kelly, 2007). The organism themselves have very simple body structure, mostly tubular. The fluid includes blood, intracellular fluid, seawater etc depending on the animal *Taxa*. The incompressibility of these water based fluid and a flexible restraints/container act as the support hence hydrostatic skeleton. Hydrostatic skeleton are common among the vertebrates. Examples of Muscular Hydrostat are Trunk (elephant and opossum), Tentacles (Octopus and Squid), Tongue, and Intestine, Mammalian Penis, Cochlea. Fluid filled hydrostatic joints are of two forms in terms of volume; sectional isochoric and whole body isochoric. In the sectional isochoric implementation, the hydrostatic joint is chambered and fluid exchange is not permitted as exemplified by Leeches; *Hirudo medicinalis* (Skierczynski et al, 1996; Sfakiotakis and Tsakiris, 2006; Alscher, 1990). whereas fluid exchange is permitted in the other form. see figures 1 and 2.

In an attempt to reproduce a biological model, many researchers commonly extend the usual rigid links found in industrial systems (Trimmer *et al*., 2006). Examples of such works are listed in Table 1.



Leech (*Hirudo medicinalis*)

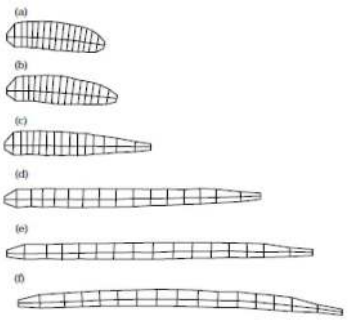


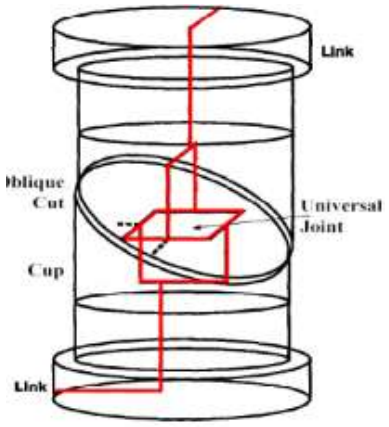
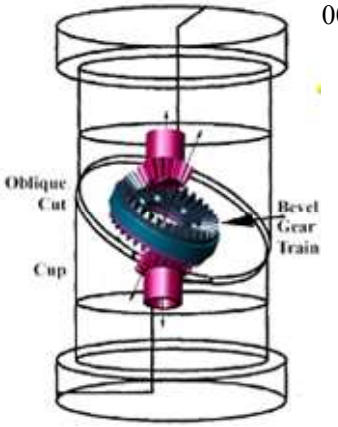
Figure 1 Segementally isochoric Leech body. The body grows thinner when extending to keep volume constant. Also each section maintains constant volume (isochoric) while in action. Source: Skierczynski *et al.* (1996)



Figure 2 Caterpillar (Source: Anonymous).

Caterpillar's body have internally connected chambers that allows exchange of fluid.

Table 1. Examples of joints implementations for biologically inspired robots

 Revolute Joint as used by NASA snakebot (Kevin, 2003)	 Universal Joint was used by Miller (2010), (William, 2006), Yamada and Hirose (2006) and Mori and Hirose (2006). It is the most popular joint adopted for hyper-redundant robot designs.	 Parallel mechanism as used by Masayuki *et al.* (2008).
 Angular swivel joint with universal joint (Elie *et al*., 2003; William, 2006)	Angular swivel joint with bevel 001; 	multi-axis joints (Shammas *et al*., 2003)

Justification for this work

The main reasons behind this work are:

(a) The complexity of biological system when implemented using man-made systems.

(b) How to control the multiple degree of freedom joints to produce usable motion since an hyper-redundant body can take a very large number of possible shapes without a constraint.

(c) How can the complex control strategy be simplified just like that of the biological systems.

Simple Hookes law cannot be used in analyzing biological bodies because the substance they are made up (protein such as collagen and elastin) exhibit nonlinear behaviour. The non linear phenomenon is due to the large strains they normally experienced (>100%). Soft tissues are modeled as Hyperelastic material using models such as Neo-Hookean and Fung-Elastic exponential model - Richard and Thomas (2008). This numerical method is normally done in an iterative process of hypothesis, verification, several steps of modeling, computer simulation and experimental measurements according to

Peterson and Bronzino (2008).

A well know problem (Kier and Smith, 1985; Skierczynski *et al.,* 1996; Choset and Lee, 2001; Ma and Mitsuru, 2002; Wilbur *et al.,* 2002; Crespi *et al.,* 2005 and Masayuki *et al.*, 2008) of hyper-redundant bodies is how to control the body parts so as to produce a useable motion

Aim of this present work

This work aims at presenting a design of elastomer (vulcanized rubber to be precise) as a support and joint for hyper-redundant robot system while imitating nature. This work is based on Dorfmann *et al.* (2007) finding that rubber (unfilled and carbon filled) and biological tissues are qualitatively similar.

METHODOLOGY

A biologically inspired muscular hydrostatic joint is presented in figure 3. It is designed as a segmented backbone made up of a hardened material (such as aluminum and plastics or wood) and a polymeric material (such as Neoprene rubber, Carbon black rubber and Silicone rubber) glued together in alternating series or inserted into each other as depicted in figure 3. For this work, vulcanized rubber acts as the elastomer while aluminum is used for the support.

A preliminary multiphysics analysis (using ANSYS 10 multiphysiscs) on the joint is needed in other to visualize the stress and strain pattern that the joints will experience in service.

Simulation Procedures/Steps

Theoretical backgrounds

1. The aluminum is treated as a linear material and the following mechanical properties were used in its finite element analysis;
   a. Stress $\sigma = \frac{Load}{Area}$ (1)
   b. Strain $\epsilon = \frac{Chan \quad in\ leng}{Original\ length}$ (2)
   c. Modulus of elasticity or Young's modulus; $E = \frac{Stress}{Strain}$ (3)
   d. Poisson's ratio $v = \frac{Lateral\ strain}{Longitudinal\ strain}$ (4)
   e. Density, (5)
   f. Yield strength (von Mises stress)
   $$\sigma_v = \sqrt{\frac{(\sigma_1-\sigma_2)^2+(\sigma_2-\sigma_3)^2+(\sigma_1-\sigma_3)^2}{2}} \quad (6)$$
   where σ_1, σ_2 and σ_3 are the principal stresses
2. Stresses and strain within an elastomer (rubber) are determined using finite strain elasticity theory or constitutive equations because it has unique properties; in particular, it has exceptionally low shear modulus and high elastic strain capability. The Mullin effect is taking into cognizance in stresses and strain analysis. Preconditioning rubber material by uniaxial loading and unloading is known as stress-softening and is referred to as Mullins effect (Beatty, 2002). Since the elastomer will be used in an oscillatory environment, Payne effect – frequency induced softening has to be taken into cognizance also.

The simulation parameters/constraints

The following steps were taken in setting up the finite element tool;

(a) Specification of the material physical data- The following data was used as the physical property of the aluminum material: Young's modulus ($7x10^{10}$ Pa), Poisson's ratio (0.33), density ($2770kg/m^3$), Tensile yield strength ($2.8x10^8$ Pa), Compressive yield strength ($2.8\ x10^8$ Pa), Tensile ultimate strength ($3.1x10^8$Pa) and Compressive ultimate strength (0 Pa). For the rubber material: the inputs are uniaxial and biaxial test data shown graphically in Figure 4. The lines are the ANSYS prediction of the material behaviour, while the smooth lines are the inputs data (uniaxial and biaxial) from experimental measurements.

(b) Selecting constitutive equation - Determining which constitutive equation will best predict the behaviour of the particular sample rubber being tested require curve fiting using the tools provided in the ANSYS Multiphysis version 10. The tool indicates that Mooney–Rivlin parameter (equation 8) constitituve equation is adequate to predict the behaviour of the rubber sample.

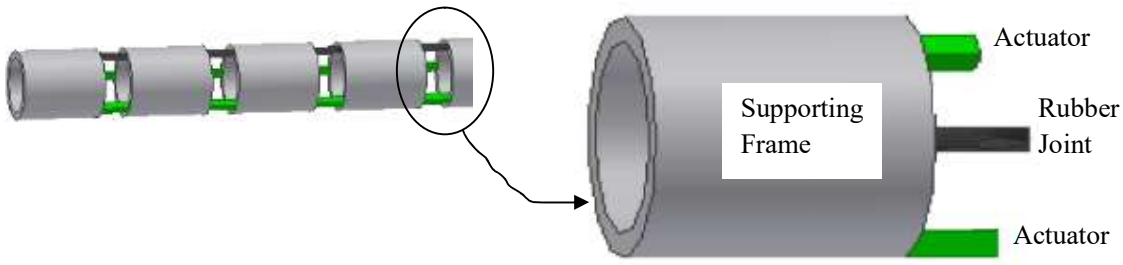


Figure 3 The design uses two actuators and the rubber acts as the connector or joint

$$W = c_{10}(\bar{I}_1 - 3) + c_{01}(\bar{I}_2 - 3) + c_{20}(\bar{I}_1 - 3)^2 + c_{11}(\bar{I}_1 - 3)(\bar{I}_2 - 3) + c_{02}(\bar{I}_2 - 3)^2 + c_{30}(\bar{I}_2 - 3)^3 + c_{21}(\bar{I}_1 - 3)^2(\bar{I}_2 - 3) + c_{12}(\bar{I}_1 - 3)(\bar{I}_2 - 3)^2 + c_{03}(\bar{I}_2 - 3)^3 + \frac{1}{d}(J - 1)^2 \quad (8)$$

where W = strain energy
J = determinant of the elastic deformation gradient *F*
$\bar{I}_1$= first deviatoric strain invariant
$\bar{I}_2$= second deviatoric strain invariant
c_{10}, c_{01} = material constants characterizing the deviatoric deformation of the material
d = material incompressibility parameter

The initial shear modulus is defined as:

$\mu = 2(c_{10} + c_{01})$

and the initial bulk modulus is defined as:

K = 2/d where $d=(1-2*\nu)/(c_{10} + c_{01})$

(c) Mesh element design - The mesh element design Figure 5 was done using the mesh tools built into the ANSYS multiphysis 10. The number of elements is 639, the number of nodes is 3435 and the depth of refinement is 2. These values were able to give convergence (i.e. solution). Higher values will also work but experience shows for each increase in refinement for example, the processing time increases greatly.

(d) Frequency induced softening of the rubber (PAYNE effect) - This was determined experimentally using a frequency loss machine design presented by Afolayan *et al.* (2011).

Items simulated

The simulation was performed specifically to find the range and load distribution experienced by the rubber based joint. Also the possibility of warping of the design was checked using directional deformation tool built into ANSYS especially in twist and twist plus cantilever load input modes. The behavior of the glue interfaces was also checked using contact analysis tool.

RESULTS AND DISCUSSIONS

The results of the simulation is summarized in figures 7 and 8; von Mises Stress (A), von Mises Strain (B), total deformation (C) and directional deformation (D) in that order for each figure. The simulation without the moment load is shown in figure 7 while figure 8 shows simulation with the force (cantilever load) suppressed. Under pure cantilever loading, the von Mises stress ranges from 0.22 kPa to 42.61 kPa (figure 7A) while it experience strain of 0m/m to 0.31m/m (figure 7B). The maximum total deformation (8.436mm) or deviation from original shape occurred at the tip (figure 7C) as expected but the highest direction deformation occurred within the rubber at 0.4765mm (tensile) and -1.353mm (compressive). Furthermore, the mesh pattern does not show warping of the shape (figure 7D).

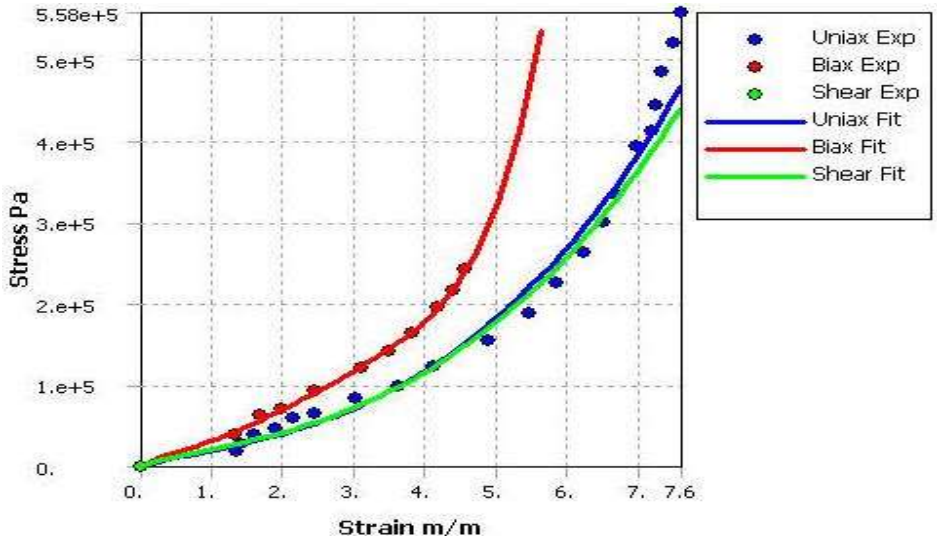


Figure 4. Mooney-Rivling parameter constitutive equation used within the ANSYS 10 shows very close prediction of the rubber sample behavior. It means that Mooney-Rivling parameter can be safely used for the finite element analysis of the rubber sample.

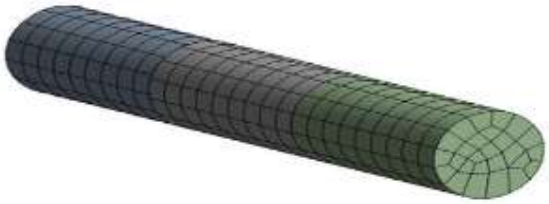


Figure 5. Optimized ANSYS 10 generated mesh pattern used for the finite element analysis

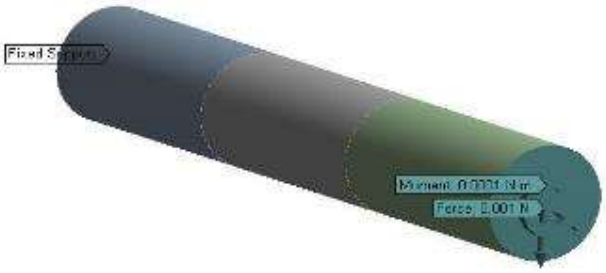


Figure 6. The simulation inputs and constraints showing combined loading

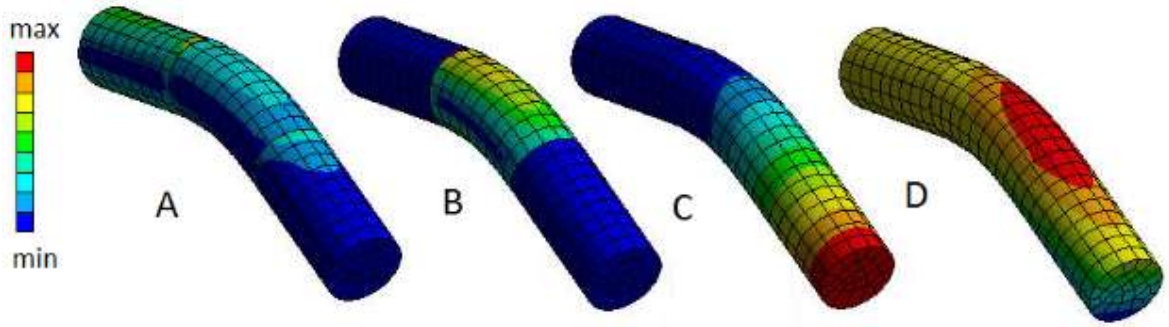


Figure 7 Simulation results under pure cantilever loading; von Mises Stress (A), von Mises Strain (B), total deformation (C) and directional deformation (D)

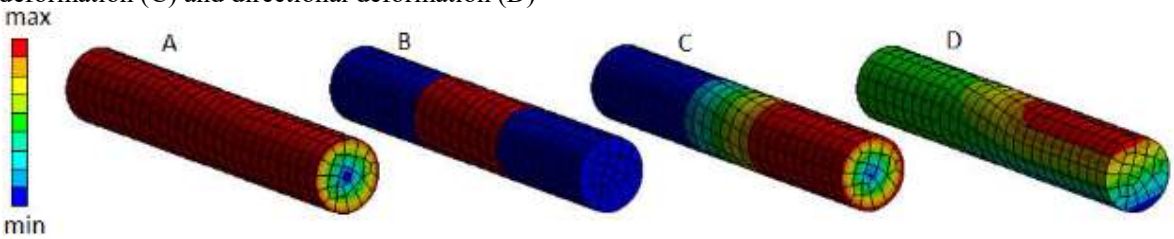


Figure 8 Simulation results under pure moment; von Mises Stress (A), von Mises Strain (B), total deformation (C) and directional deformation (D)

The maximum von Misses stress of 7.48kPa is uniformly distributed over the assembly for the pure moment simulation. The minimum value is 0.346kPa and occurred at the core of the assembly (figure 8A). The rubber experienced very high strain of 0.13m/m and whereas the supports had close to 0.0mm strain value (figure 8B). The maximum total deformation (1.42mm, figure 8C) from the original shape occurred outside the aluminum support while it is distributed in the rubber. The directional deformation is polarized (figure 8D) and ranges from -1.22mm to 1.24mm. The mesh pattern shows twisting as expected and the lines are gradual- which also implies no warping of the assembly using the simulated load of 0.0001Nm.

The same rubber material used by Afolayan *et al.* (2011) was used and the critical frequency was determined to be 25Hz, that is, the oscillation should not exceed this value if the system (joint) is not to fail due to frequency induced softening.

CONCLUSIONS AND RECOMMENDATION

The maximum stress experienced (42.61kPa) occurred during the cantilever loading and it is at the rubber-support interface. It means serious attention must be given to this interface in real life scenario. Screwing or interlocking connection is suggested for the rubber-support interfaces.

Building efficient and cheap robots is a universally desired goal in the field of robotics especially for civil / home use. Materials such as magneto/electro sensitive rubbers (that is, a rubber material that will adjust its volumetric dimension under the influence of magnetic field or electrical field) can be used as an actuator. The design used in this work can be adapted to use such materials as actuator and support at the same time. A typical scenario of possible application of magneto/electro

sensitive rubbers based hyper-redundant joint is in robot assisted surgery (minimally invasive surgery). Endoscope and laparoscope are common manipulators used in minimally invasive surgery. The design presented in this work will be very useful in implementing such devices.

REFERENCES

Afolayan M.O., Yawas D.S., Folayan C.O. and Aku S.Y. (2011). Mechanical Performance of Polyisoprene used in Building a Flapping Foil Underwater Robot. Research Journal of Applied Sciences, Engineering and Technology 3(6): 474-485.

Alscher, C. and Beyn, W.J. (1998). Simulating the motion of the Leech, A biomechanical application of DAEs, *Numerical Algorithms* 19 (1998): 1-12.

Choset, H and Lee, J. Y. (2001). Sensor-Based Construction of a Retract-Like Structure for a Planar Rod Robot. *IEEE Transactions on Robotics*. pp 435- 449.

Crespi, A, Badertscher, A, Guignard, A and Ijspeert, A. J. (2005). Amphibot I: an amphibious snake-like robot. *Robots and Autonomous System*, 50: 163-175.

Dorfmann, A., Trimmer, B.A. and Woods, W.A. Jr. (2007). A constitutive Model for Muscle properties in Soft-bodied Arthropod. *Journal of Royal Society International*. 4: 257-269.

Elie, S., Wolf, A., Brown, H.B., Jr. and Choset, H. (2003). New Joint Design for Three-dimensional Hyper Redundant Robots. *Proceedings of the 2005 IEEE International Conference on Robotics and Automation, Las Vegas, Nevada,* October 2003. pp 3594- 3599.

Kelly, D.A. (2007). Penises as Variable-Volume Hydrostatic Skeletons. *Ann N.Y. Academic. Science* 1101: 453-463.

Kevin, B. (2003). How snakebots work. *Available online at: http://electronics.howstuffworks.com /snakebot.htm.* Accessed 8.00pm 11, August 2007

Kier, W.M and Smith, K. K. (1985). Tongues, tentacle and trunks: the biomechanics of movement in muscular-hydrostat. *Zoological Journal of the Linnean Society*. 83: 307-324.

Masayuki, A., Yoshinori, T. and Hirose, S. (2008). Development of "Souryu-VI" and "Souryu-V:" Serially Connected Crawler Vehicles for in-Rubble Searching Operations. *Journal of Field Robotics*, 25: 31–65. (DOI: 10.1002/rob.20229)

Mori, M. and Hirose, S. (2006). Locomotion of 3D Snake-Like Robots; Shifting and Rolling Control of Active Cord Mechanism ACM-R3. *Journal of Robotics and Mechatronics*. 18(5): 521-528.

Peterson, D. R. and Bronzino, J. D. (2008). Biomechanic: Priciples and Applications. *CRC Press, New York* pp 1-10.Richard and Thomas (2008).

Robinson, G. and Davies, J.B.C. (1999) "Continuum Robots - A State of the Art," *IEEE Conference on Robotics and Automation*, pp. 2849-2854.

Shammas, E., Wolf, A., Brown, H. B., and Choset, H. (2003). New Joint Design for Three-dimensional Hyper Redundant Robots. *Proceedings of the 2005 IEEE International Conference on Robotics and Automation, Las Vegas, Nevada*, October 2003. pp 1-10.

Ma, S. and Mitsuru, W. (2002). Time-optimal control of kinematically redundant manipulators with limit heat characteristics of actuators. *Advanced Robotics.* 16(8) : 735-749.

Skierczynski, B.A., Wilson, R.J.A., Kristian, W.B. Jr and Skalak, R. (1996). A model of the Hydrostatic Skeleton of the Leech. *Journal of Theoretical Biology* 181: 329-342

Trimmer, B.A., Takesian, A.E., Sweet, B.M., Rogers, C.B., Hake, D.C. and Rogers, D.J. (2006). Caterpillar Locomotion and Burrowing Robots. *7th International Symposium on Technology and Mine Problem, Monterey*, CA. pp 1-10

Wilbur, C., Vorus, W., Cao, Y., and Currie, S. (2002) A Lamprey-Based Undulatory Vehicle. *Neurotechnology for Biomimetic Robots, Edts: J. Ayers, J. Davis and A. Rudolph. MIT Press*, pp 285-296.

William, C. (2006). Snake-Like Robot Can Crawl on Land or Swim. *Available online at http://www.gorobotics.net/The-News/Latest-News/Snake%11Like-Snake-Like-Robot-Can-Crawl-on-Land-or-Swim/*

Wolf, A., Brown, H.B., Casciola, R., Costa, A., Schwerin, M., Shamas, E. and Choset, H. (2003). *Proceedings of the 2003 IEEE/RSJ International Conference on Intelligent Robots and Systems, Las Vegas, Nevada*, October 2003. pp 1-10

Yamada, H. and Hirose, S. (2006). Development of Practical 3-Dimensional Active Cord Mechanism ACM-R4. *Journal of Robotics and Mechatronics*, 18(3): 305-311.

PROSPECTS OF BIOSORBENTS DEVELOPMENT FOR OIL SPILL CLEANUP IN NIGERIA: A REVIEW

***AGIDA, I. R., OLAWALE A. S. AND ISA M. T.**
Department of Chemical Engineering, Ahmadu Bello University, Zaria
*Corresponding author: **Tel: +2347035585968; E-mail:Raymoski4uall@yahoo.com**

ABSTRACT
In this work effort has been made to assess the potentials and prospects for the development of biosorbents for oil spill cleanup in Nigeria. Numerous lignocellulosic biomass have been identified to possess promising adsorption ability of oil in preference to water. The biomass include kapok, cotton fibre, rice straws, kenaf fibre, groundnut husk, coconut coir fibre, wheat straw, milkweed and rice husk among others. They are usually generated in large amount yearly and can effectively serve as low cost raw materials for the development of biosorbents with the expectancy of reduced production cost and as an alternative to synthetic sorbents. The development of biosorbents from these abundantly available lignocellulosic biomass and the necessity for their modification to improve oleophilicity and hydrophobicity becomes imperative. Approaches to achieve this include physical and/or chemical modification of the biomass and, embedding of additives in the biomass as part of the formulations of the biosorbents. Various chemical modification methods including acetylation, esterification and salinization of the identified lignocellulosic biomass were assessed. Prospects and potentials for biosorbents development were established.

Introduction

Oil spill is a major source of marine pollution which has continue to wreak havoc on marine life and environment. The spill usually affects the ecosystem of the contaminated areas, causing death of birds, other marine animals and plants as well as the environment (Lee *et. al.,* 1999; Huang and Lim, 2005; Hussein *et. al.,* 2009; Nelson, 1972). For these reasons, greater attentions have continued to be paid to these undesirable phenomena from 1970s.

Major spills include those in Persian Gulf in 1991, Gulf of Mexico in 1979/80 and Trinidad and Tobago in 1979 among others (Wikipedia.org, 2009). In Nigeria, majority of environmental pollution in the Niger Delta region is due to oil spill in one form or another. This has devastated the once fertile oil producing areas of the Niger Delta region of the country. There is, therefore, no doubt that oil spill need to be contained as much as it needs to be prevented.

The economic losses and environmental nuisance arising from oil spill are usually taken care of by recovery, dispersal and/or bioremediation. Oil sorption is one of the recovery methods usually employed in oil spill cleanup. Sorbents used in oil spill clean-up could be inorganic minerals, synthetic sorbents or natural organic matters like cotton, kapok, wool and feathers. Though synthetic sorbents have been found to be superior in sorption capacity (70 g/g), the natural sorbents (with 3-15g/g sorption capacity) have the advantage of cheapness, availability and biodegradability (Aboul-Gheit *et. al.,* 2006), though some natural sorbents such as cotton, kapok, poplar hair fibre, milkweed floss, *Pistia stratiotes*, *Salvinia molesta* and kenaf have been found to sorb 1.5 to 3 times as much as synthetic sorbents (Huang and Lim, 2005; Hussein *et. al.,* 2009; Johnson *et. al.,* 1973; Choi and Moreau, 1992; Choi, 1996, Zeigler *et. al.*, 2016).

The low hydrophobicity and/or poor fibre strength of many natural organic sorbents is a drawback to their use in sorption of oil spill cleanup and recovery. This might be the reason for the lack of interest in developing natural sorbents (biosorbents) as substitutes for the very pervasive synthetic sorbents in commercial oil spill cleanup operations. Therefore, the prospects and potentials for biosorbents development and use in remediation of oil spill and oil recovery will be assessed in this work.

Materials (Lignocellulosic Wastes) Assessment

Biosorbents can be developed from natural organic materials which are of plant or animal origin. Most of the natural organic materials from plant sources are largely lignocellulosics agricultural wastes. These agricultural wastes are usually abundantly available in Nigeria,

Africa and many tropical countries and because they are otherwise not of much competitive

use, they are cheap. The properties of these lignocellulosics that determine their application in oil spill remediation and oil recovery are their morphological structures (indicative of pore size, surface area, fibre strength), biodegradability and oleophilicity/hydrophobicity (Sharzberg, 1971; Choi and Moreau, 1996; Melvold *et. al.*, 1988). Availability and costs, chemical and physical characteristics as well as sorption performance

(characteristics) of the common lignocellulosics obtainable in Nigeria, Africa and tropical countries are evaluated in the subsequent sections.

Availability, cost and uses

A very large quantity of lignocellulosic agricultural wastes are produced as by-products of food and industrial crops in Nigeria yearly. These large volume of waste constitute environmental nuisance in many cases; finding means of utilizing them will remove the nuisance while converting the wastes to wealth. Among the many lignocellulosic wastes are straws (rice, wheat, millet), stalks (maize, banana, plantain, sorghum, okra, sorrel, bagasse), husks (groundnut, soyabean, rice, various edible and oil containing seeds) pawpaw stem, waste of cotton processing, kapok, milkweed floss, kenaf bast fibre and coconut coir fibre. Others are waste woods, saw dust, palm fibre, luffa, poplar seed hair fibre, hemp and super hydrophobic plant leaves such as species of *Salvinia* (aquatic fern), water lettuce, water hyacinth, lotus leaves (Olawale and Saidu, 2010; Likon *et. al.*, 2013; Ogunye, 1988; Zeigler *et. al.*, 2016). The availability of some of the common lignocellulosic wastes are presented in Table 1 (Sanni *et. al.*, 2017).

Table 1: Availability, and cost of lignocellulosic biomass in Nigeria

Lignocellulosic feedstocks	Quantity (tonnes/annum)	Price ($/kg)	Price (₦/kg) at 1$ = ₦315
Corn cob	2,454,000	0.180	56.7
Corn stover	4,907,800	0.189	59.535
Rice husk	870,000	0.11	34.65
Sugarcane bagasse	18,900	0.05	15.75
Rice straw	660,000	0.12	37.8
Saw dust	1,800,000	0.05	15.75
Waste wood	5,200,000	0.05	15.75
Sorghum stalk	277,000	0.045	14.175
Millet straw	284,000	0.045	14.175

Source: Sanni *et. al.*, 2017

Wheat straw is usually disposed of as waste from a typical domestic wheat production recorded of 70,000 tonnes in 2013-14 season. Nigeria's northern states of Borno, Yobe, Jigawa, Kano, Zamfara, Katsina, Adamawa, Sokoto are Kebbi are the major wheat producers (Uche, 2014). Cotton wastes could be obtained from ginneries located in Northern Nigeria; the crop is produced majorly in the North West, North East and North Central part of Nigeria (Odedokun, 2014). Water hyacinth (*Eichorina crassipes*) is nuisance aquatic weed along the waterways in Southern Nigeria. Other important macrophytes found in Nigeria are *Pistia stratiotes*, *Salvinia* species and *Mimosa pigra* (Ogunye, 1988). Water lettuce, water lily, water fern and water hyacinth are found along River Niger, as well as in Anambra, Niger, Delta and Cross river basins while *Pistia stratiotese* are vastly distributed in Nigeria (Bolenz *et. al.*, 1990; Poddlar *et. al.*, 1991; Gressel, 2008). Kenaf is available in commercial quantities in North East, North Central and South West parts of Nigeria, covering about eighteen states to the tune of 1,300 tonnes per year (Webber *et. al.*, 2002).

The straws, stalks, husks and shells are left to waste in the farmyards and usually constitute environmental nuisances. These categories of lignocellulosic by-products are therefore of little economic value and are available as relatively cheap materials. Attempts have been made to find uses for kenaf and water hyacinth in paper production (Bidin *et. a.l,* 2015). Kenaf bast has also found use as blend in plastic composites and drilling mud (Kenaf, 2010). Kapok is used in bedding and upholstery industries as well as in the production of life-saving equipment and thermally insulated and sound proof covers and walls (Zheng *et al*, 2015).

Characteristics

- *Physical and chemical properties*

The chemical and physical properties of biomass have effects on their sorption performances. Important properties in this respects are cellulose, hemicellulose, lignin and wax which are the main components of hemicellulosics. Other important characteristics of this biomass type are pore size, density and fibre length.

Cellulose (β-1,4-glucan), shown in Figure 1, is the major constituents of plant materials. It is a polysaccharide, of glucose monosaccharides, made up of cellubiose units as the elementary microfibrils which are wound into macrofibril bundles. This structure makes cellulose resistant to

biological and chemical agents (Delmar and Amor, 1995; Morohosi, 1991; Ha *et. al.*, 1998). The cellulose fibrils are joined together or covered by hemicellulose and lignin, which are the two other major constituents. The presence O-H bonds in these components' molecules make them hydrophilic with degree hydrophilicity increasing in the order in which they are mentioned above.

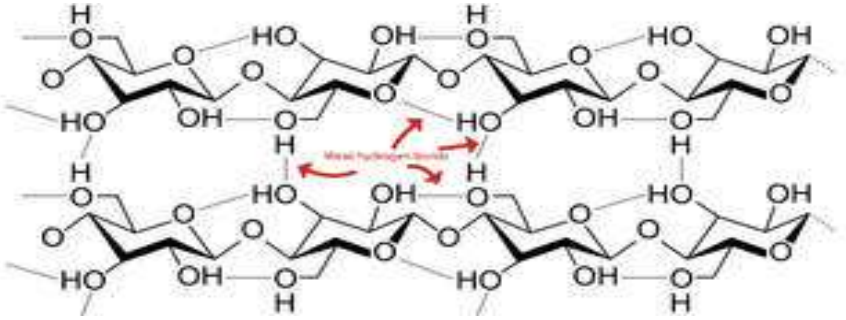


Figure 1: Structure of cellulose

Table 2: Properties of lignocellulosic materials used in oil sorption

Biomass	Fibre length (mm)	Wax deposit	Cellulose (%)	Hemicell-ulose (%)	Lignin (%)	Others (%)	Density (g/cm^3)
Kapok fibre	25	Yes	64	-	13	23	
Cotton	15-56	0.5-1 %	80-90	4-6	-		
Barley straw	-	Yes	40-45	20-31	15-20		
Peanut husk	-	Yes	34-45	-	27-38		0.08-0.1
Kenaf bast fibre	1.5-2.7	Yes	65	13	21.6	3-5	0.34
Milkweed floss	20	Yes	39.6	-	15.1		0.9
Banana stalk	2-9		63-64	10	5		0.15
Corn husk (stover)			40-45	20-31	15-20		0.06
Soyabean husk		Yes	14-25	14-20	3-4		0.12
Rice husk			40	-	30	20 (SiO_2)	
Water hyacinth			20	33	10		
Wheat straw	1.4	Yes	41	32.5	15.4		
Rice straw	1.4	Yes	40-45	20-31	15-20		
Pith bagasse	2-4	Yes	32-48	19-24	23-32		
Hemp	5-55	Yes	68-85	10-17	3-5		
Palm fibre	20-30	Yes	33.5	55.6	21.6		
Luffa		Yes	60	30	10		
Jute	2-5	Yes	70-75	12-15	10-15		
Sorghum stalk		Yes	32-35	24-27	15-21		

Source: Mullin *et. al.*, (2001); Batra (1985); Hurter (1988); Eman (2005); Reddy *et. al.*, (2004); Bilba *et. al.*, (2007), Bismark *et. al*., (2005); Sessa and Wolf (2001); Mullin and Xu (2001); Saidu and Olawale (2010).

The presence of wax deposits on lignocellulosic materials confer affinity for oil on the materials. From the data provided in Table 1, the top candidates among the listed materials expected to have good oleophilicity and hydrophobicity would include cotton, kapok, kenaf, milkweed floss, hemp and jute. The fibre (cellulose) content of lignocellusic materials influences the mechanical strength of the materials. The longer the fibre length the greater should be mechanical strength of the material, if we give allowance for the deficits attributable to the non-fibril constituents like hemicellulose, lignin and the non-crystalline constituents. Kapok and milkweed floss are known to have relatively large and non-collapsible lumen (Choi and Choi, 1992). The greater pore volume resulting enables absorption of large volume of oil while the strong lumen allows for longer reusability of the materials in oil sorption.

- *Sorption characteristics*

Sorption process, as we have with oil and water, involve adsorption and absorption. While adsorption is favoured by chemical affinity (which reduces interfacial tension), surface area and pore size, absorption is linked to ease of transport of fluid (oil, water) by capillary action and so depend on pore size (Huang and Lim, 2005; Johnson *et. al.*, 1973; Choi, 1996; McCabe *et. al.*, 1985). Absence of oxygen, nitrogen and sulphur of the material enhances its oleophilicity and hydrophobicity as well as when hydrocarbons constitute the bulk of the material or are present as wax. Sorption capacity, release rate for oil and strength of the capillary and lumen (pores) on reuse are measures of sorbent's reusability. This is thus related to the fibre strength as well as fibre's affinity for oil. Buoyancy is dependent on the bulk density of the material and hydrophobicity. It is in light of these factors that kapok, cotton, milkweed floss, kenaf bast fibre and marine plant leaves such as species of *Salvinia*, water lettuce and lotus leaves have been found to be excellent oil sorbents (Choi and Moreau, 1992, Spielman *et. al.*, 1972; Huang and Lim, 2005; Zeigler *et. al.*, 2016). Kapok, cotton, milkweed floss and kenaf bast fibre and *Pistia stratiotes*, *Salvinia molesta* have been found to perform 1.5 – 3 times better than synthetic sorbents (Huang and Lim, 2005; Johnson *et. al.,* 1973; Choi and Moreau, 1992; Choi, 1996; Zeigler *et. al.*, 2016). At pH 5.0 the sorption capacity of chitosan and walnut shell were determined as 96 and 99.9 mg/g respectively (Srinivasan et. al., 2010). Sorption capacities have been reported for raw cotton (35.5 g/g), poplar seed fibre (55-60 g/g), carbonised cotton fibre (32-77 g/g), raw luffa fibre (15-27 g/g), coated kapok fibre (59.5 – 63.2 g/g) and silkworm cocoon waste (37-60 g/g) on different oils (Moriwaki *et. al.*, 2009; Wang *et. al.*, 2013; Abdel Wahab, 2014; Likon *et. al.*, 2013; Singh *et. al.*, 2013). Particles of plants like groundnut husk, kenaf bast fibre, soyabean husk, corn husk or stover, banana stem, sawdust as well as perlite, vermiculite and glass wool sorbed 4-12 times their weights of oil (Saidu, 2011; Olawale and Saidu, 2010; Saidu and Olawale, 2010; Olawale and Saidu, 2015; Teas *et. al.*, 2001; Adebajo *et. al.*, 2003; Bayat *et. al.*, 2005).

From the foregoing reviews it is obvious that there are some good and abundantly available biosobent materials in Nigeria. Among them are cotton fibre, kapok fibre, kenaf bast fibre and super oleophilic marine plants like *Pistia stratiotes* and *Salvinia molesta*.

Biosorbents Development

Biomass-based materials that are used for oil recovery in an oil spill cleanup operation are called biosorbents. These materials are biodegradable and should be able to compete with the commercial synthetic sorbents with characteristically high oleophilicity, hydrophobicity and mechanical strength as well as reusability. Since no biomass, and in particular lignocellulosics, has all these desirable attributes, it is necessary to manipulate the base biomass to improve sorption and recovery capacity. This could be done by modification (physically or chemically) and or addition of materials to obtain sorbent formulations with the desired characteristics.

Techniques

- *Chemical modification*

Available chemical treatment processes attempt to modify the lignocellulosic fibres by

a) altering the fibre chemistry by new covalent bond formation on the reactive sites of the fibre

b) changing the fibre chemistry by radiation treatment and polymer coating with degradation resistant chemicals on fibre surface.

The hydroxyl groups present on or within lignocellulosic fibre matrix are mainly targeted in the chemical processes involving substitution of hydroxyl group by hydrophobic functional group. The hydroxyl groups in lignocellulosic fibre are blocked by a number of chemical treatment processes such as esterification, transesterification, etherification, silane treatment and grafting.

Acetylation involves replacement of hydroxyl groups with acetyl functional group (CH_3CO-)

Esterification with benzoyl chloride involves surface modification with alkaline benzoyl chloride solution. It has been used for enhancing tensile strength and hydrophobicity. Esterification of plant based cellulose substrate with penta fluorobenzoyl chloride has led to enhanced hydrophobicity.

Esterification with fatty acid and fatty acid salts involves stearic acid dissolved in ethyl alcohol being used to esterify the hydroxyl groups of lignocellulosic fibres. Bagasse fibres and cellulose pulp esterified by long –chain aliphatic fatty acid treatments developed greater hydrophobicity and possibly greater resistance against biodegradation.

Transesterification of cellulose and lignocellulosic fibres is also known to make the fibres by hydrophobic jute and coir fibres trans-esterified using n-butyl acrylate and methyl acrylate in pyridine as organic solvent reportedly led to increased hydrophobicity and resistance against chemical degradation. Transesterification of cotton with organic solvent based vegetable oil emulsion led to greater hydrophobicity.

Etherification: Etherified lignocellulosic fibres also exhibit greater hydrophobicity, tensile strength and degradation resistance. Alkali treated saw dust has been etherified with benzoyl chloride or alkyl

chloride in presence of alkali catalyst for use in the manufacture of mechanically strong and more hydrophobic composites. Steam treated flax fibre were also found to become less hydrophobic after etherification with alkaline ethyl iodide at reduced pressure

Silane treatment: Hydrophobic chemical derivative of SiH_4 called silane can be hydrolyzed and bonded to the hydroxyl groups of cellulose chains or hemicelluloses in lignocellulosic fibres through covalent bonding.

Grafting: Chemical or photo catalyzed graft copolymerization is also used to modify lignocellulosic fibres. Polymeric acrylate functionality (CH_2=CHCOO-) has been grafted on alkali treated fibres of plant *Hibiscus sadariffa, Saccaharum cilliare*. (Thakur *et. al.,* 2011) These modifications lead to increased tensile strength, thermal and chemical resistance and hydrophobicity of treated fibres due to blocking of fibre hydroxyl groups by polymer grafting. Lignocellulosic fibres obtained from *Grewia optive* plant are reported to be rapidly grafted with poly (methyl acrylate) chains using ferrous ammonium sulphate potassium per sulphate to reduce the swelling of lignocellulosic fibre toward polar solvents. These methods impart greater tensile strength as well as thermal and chemical resistance, to treated fibres (Thakur *et al*, 2013 & Thakur *et al*, 2014).

Grafting of polymeric chains of methyl acrylate onto surface of lignocellulosic fibres collected from *Eulaliopsis binata* plant was found to reduce the swelling tendency of fibres in different types of solvents with enhanced acid-alkali resistance of treated fibres. (Thakur *et. al.,* 2013)

Grafting can be induced with electromagnetic radiations instead of using chemical agents. Jute yarn has been grafted with acrylamide monomer (AA) under ultra violet radiation to increase its hydrophobicity, tensile strength and degradation resistance (Hassan *et al,* 2002).

- *Physical modification*

Coating or blocking: Lignocellulosic fibres have been coated with phenol formaldehyde resin, boric acid-oil emulsion, neem seed extract and other water repellent reagents to reduce their hydrophobicity.

Vegetable oil treatment: The use of vegetable oil and fatty acid for enhancing durability and hydrophobicity is a recent treatment method for lignocellulosic fibres which is eco-friendly, non-toxic plant based ingredients. Jute and sisal fibres were treated with an aqueous emulsion of neem oil and plant based resin (cardanol) at elevated temperature for enhancing their tensile strength, hydrophobicity and resistance against biological and chemical degradation (Saha *et al* 2012).

A range of chemical treatments and coating has been developed for enhancing tensile strength, hydrophobicity and degradation resistance of lignocellulosic fibres. The treatments based on coating are expected to be prone to leaching and less stable compare to the processes involving hydroxyl group substitution. Blocking or substitution of hydroxyl group of lignocellulosic fibres therefore appear to be the most appropriate strategy for imparting greater strength and degradation resistance to lignocellulosic fibres. The processes are based on the use of hazardous or expensive chemical that generate by products that are difficult to dispose. Complex process design and high energy requirement pose additional problems in using some of these chemical processes in manufacturing expensive products.

Many works have been reported on chemical modification of lignocellusic biomass. These include the works of Ibrahim *et. al.* (2013), Teli and Valia (2013) and Sidik *et. al.*, (2012) which carried out chemical modifications of different lignocellulosics by acetylation and esterification with good results. A recent work also acetylated groundnut husk particles and obtained improved oleophilicity and hydrophobicity (Umar, 2017).

Applications

Sorbents are normally applied in oil spill cleanup in various forms. These forms include particles, granules, sheets, pillow, pads, etc. most lignocellulosic-based sorbents can be made into different forms since cellulose are fibres. Biosorbents with adequate sorption capacity to handle oil spill cleanup and recovery could be developed from the agricultural wastes, chemicals and technology that are available in Nigeria. The developed sorbents could be applied in granules, sheets, pads or pillow forms depending on the size and location of the oil spill.

Looking Ahead

All these findings indicate the possibility of developing biosorbents that can perform well in oil spill cleanup and recovery and at a competitive cost to commercial sorbents. Since the biosorbents to be developed are expected to rival or even surpass the characteristic high oil sorption and recovery capacity of synthetic sorbents in addition to the bonus of biodegradability, their utilization in oil spill cleanup should be sustainable. The future is thus bright for biosorbents development in Nigeria.

Conclusion

The abundant availability of some agricultural (lignocellulosic) wastes with excellent oil sorption characteristics in Nigeria have been established. These include cotton, kapok, kenaf bast fibre and some marine plants. In addition, the required treatments of these native lignocellulosics to improve their sorption characteristics (oleophilicity, hydrophobicity, oil recovery, reusability. mechanical strength and buoyancy) were identified and assessed from works available in the literature. The sustainability of the biosorbents utilization in oil spill cleanup and recovery in Nigeria is alluded to.

References

Abdelwahab O. (2014) Assessment of raw luffa as a natural hollow oleophilic fibrous sorbent for oil spill cleanup.

Aboul-Gheit A.K.., Khalil F.H. and Abdel-Maghny T. (2006). Adsorption of spilled oil from seawater by waste plastic. Oil and Gas Science and Technology-Rev. IFP, 61 (2), 259-268.

Adebajo M. O., R.L. Frost, J.T. Kloprogge, O. Carmody and S. Kokot (2003). Porous materials for oil spill clean-up: A review of synthesis and absorbing properties. Journal of Porous Materials, Vol.10 (No.3) 159-170.

Batra S. K. (1985). Other long vegetable fibres. In: Fibre Chemisry-Handbook of Fibre Science and Technology. $;727-808.

Bayat A., Agbamiri S. F., Moheb A. and Vakili-Nezhaad G. R. (2004). Chemical Engineering and Technology. 28 (12): 1525-1528.

Bidin, N., Zakaria, M. H., Bujang, J. S., and Abdul Aziz, N. A. (2015). Suitability of aquatic plant fibres for handmade papermaking. International Journal of Polymer Science Vol. 2015, Article ID 165868, 9

Bilba K., Arsene M. A., Ouesanga A. (2007). Study of banana and coconut fibers: Botanicalcomposition, thermaldegradationand textural observations. Bioresources Technology. Vol 98:58-60.

Bolenz S., Omran H.,Gierschner K. (1990). Treatment of water hyacinth tissue to obtain useful products. Bio-Waste Vol 33: 263-274

Choi H.-M, and Moreau J. P.(1992). Oil sorption behaviour of various sorbents studied by sorption capacity measurement and environmental scanning electron. Microscopy Research and Techniques. 25(5-6), 447-456

Choi H.-M. (1996). Needle punched cotton non-woven and other natural fibers as oil spill cleanup sorbents. Journal of Environmental Science and Health, A31 (6), 1441-1457

Choi H.-M. and Moreau J. P. (1996). Understanding the sorbents for cleaning up spills, Plant Engineering. Vol 3, 219-221

Eman A. A. (2005).an investigationon the feasibilityof peanut hull as an adsorbent. Alexandria Engineering Journal, Vol 44; 129-139.

Gressel J. (2008). Transgenics are imperative for biofuel crops. Plant Science, Vol 174:246 – 263

Han J. S. (1998). Properties of non-wood fibers. In: Proceedings of the Korea Society of Wood Science and Technology 3-12

Huang X. and Lim T. (2005). Experimental evaluation of natural hollow hydrophobic-oleophilic fibre for its potential application in non-aqueous phase liquid spill cleanup. International Oil Spill Conference. Singapore.

Hurter A. M. (1988). Utilization of annualplantsand agricultural residuesfor production of pulp and paper. Proceedings of TAPPI Pulping Conference (TPC'88), New Orleans, LA USA. Pp139-160.

Hussein M. Amer A. A. El-Maghraby A. and Taha, N. A. (2009). International Journal of Environmental Science and Technology, 6 (1), 123-130

Ibrahim W. A.W., Tahiruddin N. S. M., Jaluddin N. S. M. (2013). Natural fruit peel- potential bisorbents for combating oil pollution. Journa Intelek, Vol 8b (1), 2013.

Johnson R., Manjrekar T. and Halligan J. (1973). Removal of oil from water surfaces by sorption on unstructured fibers., Environ. Science and Technology. 7 (5), 439- 443

Kenaf (2010).Living Green Enterprises Inc. http://www.living-green.ca/kenaf.html. (accessed June, 17 2010).

Lee B. G., Han J. S. and Rowell R. M. (1999). Oil sorption by lignocellulosic fibres. In: Kenaf properties, processing and products. Mississippi State University: Agric and Bio Engineering. (35), 423-433

Likon, M.; Remškar, M.; Ducman, V.; Švegl, F. (2013). Populus seed fibers as a natural source for production of oil superabsorbents, Journal of Environmental Management 114:158–167.

McCabe W. L., Smith J.C and Herriot P. (1985). Unit Operations in Chemical Engineering 4th ed., McGraw Hill Book Co., New York.

Melvold, R.W., Gibson S.C., Scarberry R. (1988). Sorbents for liquid hazardous substances cleanup and control. Noyes Data Corp., NJ.

Moriwaki H., Kitajima S., Kurashima M., Haigiwara A., Haraguchi K., Shirai K., Kanekatsu R., Kiguchi K. (2009). Utilization of silkworm cocoon waste as a sorbent for the removal of oil from water. Journal of Hazardous Materials. Vol. 165: 266–270

Mullin W. J. and Weili X. (2001). Study of soyabean seedcoat componentsand their relationships to water absorption. Journal of Agricultural and Food Chemistry. Vol49: 5331-55335.

Nelson S. (1972). Oil Polluted and Marine Ecology, Leek Scientific, London.

Odedokun, O. V. (2014). Economic analysis of cotton production and supply trend estimation in Zamfara State, Nigeria. A Ph.D. Dissertation. Department of agricultural economic and rural sociology, Ahmadu Bello University, Zaria. Nigeria.

Ogunye, O. (1988). Water hyacinth - Nigerian experience. In: O. L. Oke, A. M. A. Imevbore and T. A. Farri (Eds.) Water Hyacinth Menace and Resource. Proceedings of International Workshop, COSTED, Lagos

Olawale A.S. and B.B. Saidu (2010). Oil sorption characteristics of lignocellulics' particulates. Proceedings of International Conference on Engineering Research and Development, Benin City. Nigeria. September.7-9

Olawale A.S. and B.B. Saidu (2015). Study of oil sorption capacity of some agricultural wastes. Journal of Fuels, Energy and Environment. Vol.1 (Issues1), 1-12.

Poddar K., Mandal L., Banerjee G. C. (1991). Studies on water hyacinth (*Eichnornia crassipes*) - Chemical composition of the plant and waterfrom different habitats. Ind Vet J., Vol 68; 833-837

Reddy N. and Yang Y. (2004). Structure of novel cellulosic fibres from corn husks. Polymer Preprints (American Chemical Society, Division of Polymer Chemistry) 45: 411

Saidu B.B. (2011). 'Study of oil spill clean-up by selected natural organic sorbents'. MSc. Thesis. Department of Chemical Engineering, Ahmadu Bello University, Zaria. Nigeria.

Saidu B.B. and A.S Olawale (2010). Utilization of agricultural wastes in oil spill clean-up. Paper presented at 8th ChemClass Conference, Zaria, Nigeria. June 10

Sanni, A., Olawale A. S. and Sani Y. M. (2017). Techno-economic analysis of agricultural wastes as feedstocks for bioethanol production in Nigeria. Paper presented at 13th Chapter Conference/AGM of Material Science and Technology Society of Nigeria (MSN), Kaduna State Chapter. 4th November. Zaria. Nigeria

Scharzberg P. (1971). U. S Coast Guard report no. 724110. 1/2/2001, U.S Coast Guard Headquarters Washington DC

Sessa D. J. and Wolf W. J. (2001). Bowman- bark inhibitors in soybean seed coats. Industrial Crops and Products. Vol. 14;73-83

Sidik S. M., Jalil A. A., Triwahyono S., Adam S. H., Satar M. A. H.and hameed B. H. (2012). Modified oil palm leaves adsorbent with enhanced hydrophobicity for crude. Chemical Engineering Journal, Vol 203: 9-18.

Singh, V., Ronald J. K., Kater H. and Seshadri R. (2013)Crude Oil Sorption by Raw Cotton, Industrial & Engineering Chemistry Research 52, 18: 6277-81

Srinivasan, A. and T. Viraraghavan. (2010). Oil removal from water using biomaterials. Bio Resource Technology, Vol.101 (17): 6594-6600.

Sun, C., (Editor). 'Biomaterials and Biofuels: Chemistry of extractives, lignins, hemicelluloses, and cellulose'. Chapter 7. 1st edition, Elsevier. Oxford, U K. 209-217.

Suni, S., A. L. Kosunen, M. Hautala, A. Pasila and M. Romantschuk. (2004). Use of a by-product of peat excavation, cotton grass fibre, as a sorbent for oil- spills. Marine pollution bulletin, Vol 49 (11): 916-921.

Teas Ch, Kalligeros S., Zanikos F., Stournas S. Lois E. and Anastopoulos G. (2001). Investigation of the effectiveness of absorbent materials in oil spills clean. Desalination. 140 (3), 259-264

Teli, M. D., and Valia, P. S. (2012). Acetylation of banana fibre to improve oil absorbency. Carbohydrate Polymers. Vol 92: 328 -333

Teli, M. D., and Valia, P. S. (2015). Modification of biomaterialsfor functional application. Cellulose Chemistry and Technology. Vol 49 (1).: 3-6

Uche M. N. (2014). USDA Foreign Agricultural Service. Nigeria Grain and Feed Annual Report.

Umar D. A. (2017). 'Modification of groundnut husk particulates for oil spill cleanup'. B. Eng. Research Project Report, Department of Chemical Engineering, Ahmadu Bello University, Zaria. Nigeria.

Wang, J., Zheng, Y. and Wang, A. (2012). Effect of kapok fibre treated with various solvents on oil absorbency. Industrial Crops and Products. Vol. 40: 178-184

www.wikipedia.org (accessed October 3, 2009)

Zeigler, C., da Silva, I. C. R., Mail, M., Kavalenka, M. N., Barthlott, W. and Holscher H. (2016). Microstructure of superhydrophobic plant leaves-inspiration for efficient oil spill cleanup materials. Bioinspiration and Biomimetic. Vol 11, 10pp.

Zheng, Y., Wang, J., Zhu, Y. and Wang, A. (2015). Research and application of kapok fibre as an absorbing material: A mini review. Journal of Environmental Sciences, Vol 27, 21 – 32.

EFFECT OF DRAG REDUCING POLYMER ON THE QUALITY OF DRINKING WATER

LAWRENCE C. EDOMWONYI-OTU, AND DANIEL O. ADELAKUN
Chemical Engineering Department, Ahmadu Bello University, Zaria, Nigeria
Corresponding Email: lcotu@abu.edu.ng

Abstract
The transport of fluids in pipes results in huge energy losses due to pressure drop. In addition, it has been established that the use of minute quantities of heavy molecular weight polymers leads to substantial reduction in the occurring frictional pressure drop in pipelines. Up to 80% reduction in pressure drop for water flows have been reported. These materials have been known to insignificantly affect the physico-chemical and rheological properties of their host solvents. However, the use of drag reducing polymer and its effect on the quality of drinking water has not been well reported. In this work, the detailed study of the effect of addition varying concentrations of a drag reducing polymer (DRP) (Magnafloc 1011; hydrolysed copolymer of polyacrylamide and sodium acrylate) in treated water samples was carried out. The physicochemical parameters such as pH, biochemical oxygen demand, chemical oxygen demand, dissolved oxygen, total dissolved solid, total hardness, alkalinity, electrical conductivity, temperature and turbidity was determined after injecting concentrations of 5ppm, 10ppm, 20ppm and 50ppm of the DRP. The samples with the polymer was left over ten days while the parameters were measured at intervals. The results were compared with the World Health Organisation water quality standards in order to note the deviations and carefully consider the health effects on the consumers at large. The results showed that the DRP could also serve as a coagulating agent for water treatment. It was observed that the tested parameters were within the limit of the water quality standards for all the days investigated. The result also showed an optimum concentration of 10 ppm of the DRP and that the water is safe for drinking even after 10 days. The result is promising and thus encouraging the use of this technology in transporting our drinking water with the attendant reduction in operational cost.

Keywords*: Drag reducing polymer, health, turbidity, parameters, fluids,*

Introduction

Pipelines are a predominant part in any chemical industry and finds application in most engineering operations. It is an essential component to transport fluids, liquid and gas over long distances. It finds application in water treatment plants, petroleum industries etc. (Ann, 2010). In fluid flow, resistance encountered by flowing fluid touching the pipe wall is due to the frictional pressure drop. Adding certain polymeric substances to fluids during flow in pipes shows large reductions in frictional drag and pumping requirements (Edomwonyi-Otu and Angeli, 2014). This phenomenon is known as drag reduction (Edomwonyi-Otu, 2015).

Drag Reducing Agents (DRA) also known as flow improvers are additives which are injected into pipeline fluids to reduce turbulence and allow fluids to flow more efficiently. The associated reduction in frictional pressure drop provides significant benefits to pipeline throughput. It allows operation at reduced pressure drop conditions, savings in pumping power, and reduction in pipeline insulation costs (Edomwonyi-Otu and Angeli, 2014). DRA (s) can be broadly classified under Polymers, Solid-Particle suspensions, Biological additives and Surfactants. These agents are produced from high molecular weight polymers or micellar systems (Shenoy, 1984).

Water may be clear, still does not guarantee its safety for consumption. Drinking water passed fit for human consumption must meet the World Health Organisation (WHO) standard. Drinking water should be void of chemical and physical substances and micro-organisms that can be dangerous to health. The standards for drinking water describes the parameters set for quality of drinking water (Yusuf et al, 2015). According to Venus (2016), water treatment is any process that makes water more acceptable for a specific end use. A water treatment plant involves usage of pipelines to transport water over long distances. The use of drag reducing polymers (DRPs) could prove useful in enhancing the throughput and reducing the pumping requirements of the water line. Edomwonyi-Otu and Angeli, (2014), Edomwonyi-Otu et al, (2015), and Singh, (2004) reported that use of 20 ppm of hydrolysed polyacrylamide in water resulted in over 80% drag reduction. It is also known that addition of these polymeric materials in small quantities has no significant effect on the physico-chemical and rheological properties of the solvents (Edomwonyi-Otu and Angeli, 2014; Yusuf et al, 2015). The use of DRPs in the petroleum

industry for fluid transportation is common with high savings in pumping cost. The effect of this addition on the quality of drinking water has however not been investigated.

The addition of DRP in water pipelines will increase water throughput and reduce pumping requirements. There is therefore need to study these effects on drinking water quality in terms of changes in its physico-chemical properties when DRP is added if it still conforms to quality drinking water standards. This forms the thrust of the current study, and if passed fit, it will be a major technological advancement for the water industry in Nigeria.

This research project aims to study the effect of drag reducing polymer on the quality of drinking water. The objectives are to prepare the polymer stock solution at several concentrations, to obtain physicochemical analysis of quality drinking water before and after injecting the DRP of different concentrations in the water samples and to analyse and compare these results with other drinking water standards (WHO standard).

Materials and Methods

The polymer used in this study is a very high molecular weight anionic polyacrylamide (magnafloc 1011) produced by BASF Chemicals and it was used as received without further purification. 1000 ppm stock solution of the polymer was prepared following procedures given by Abdullah et al... Smaller polymer solution concentrations of 5, 10, 20 and 50 ppm was further prepared from the stock solution.

Ahmadu Bello University Water Board (AWB) and Kaduna State Water Board (KSWB) quality drinking water samples was collected and kept in clean sterile containers to avoid contamination. The physico-chemical properties of the quality drinking water samples collected was taken for analysis. Analysis for the following parameters was carried out: pH, Total Hardness, Biological Oxygen Demand (BOD), Chemical Oxygen Demand (COD), Dissolved oxygen (DO), Total Dissolved Solids (TDS), Electrical Conductivity (EC), Turbidity and Alkalinity using standard laboratory techniques and procedures set by Department of Water Resources and Environmental Engineering, ABU Zaria. Furthermore, the already prepared polymer solution of different concentrations (5 ppm, 10 ppm, 20 ppm, 50 ppm) was added to both AWB and KSWB water samples and the physico-chemical analysis was carried out observing its effects over a period of 0 – 10 days. The results and observations was carefully noted and recorded. The analysis was carried out at the Departments of Water Resources, Chemical Engineering and ABU water works of Ahmadu Bello University, Zaria, Nigeria.

Results and Discussion

After carefully carrying out the experimental procedures to determine the effect of the drag reducing agent (magnafloc) on the quality of drinking water when added to AWB and KSWB drinking water sample. The following results of their physico-chemical properties were obtained.

Effect on Turbidity

The turbidity of the water samples is shown in Figures 1 & 2. It is observed that addition of the polymer solution in the water samples over a period of ten days resulted in less turbid water. Increasing concentration of HPAM in the water samples doesn't cause any change as turbidity remained at equilibrium. This change in turbidity on addition of partially hydrolysed polyacrylamide (HPAM) is attributed to the clarification ability of the polymer which has been demonstrated in other researches but there is little information on the interactions between HPAM properties and that of the water samples (Nathanael, 2017). However, HPAM has been used as a flocculant (CIBA Chemicals, UK) and the resulting water is suitable for drinking and conforms to the quality drinking water standard of <5 NTU (SON).

Effect on pH

It is observed that there is no change in the pH after the addition of the polymer in both water samples as concentration of HPAM increased even with increasing number of days as shown in Figures 3 & 4 for both water samples. This is an important observation since this is one of the key properties in determining water quality. The result also shows that the pH of water used within Kaduna and the Ahmadu Bello University communities fall within quality drinking water standard of 6.5 – 8.5 (WHO). It also implies that the use of DRP in transporting drinking water will not result in enhanced corrosion of the pipeline since the alkalinity/acidity is not affected (WHO, 2007).

Effect on electrical conductivity (EC)

The results obtained for electrical conductivity of the water samples as shown in Figures 5 & 6. It can be observed that for both water samples that no change in electrical conductivity with increasing polymer concentration except after 10 days. This gradual increase in the conductivity of the water samples is as a result of the substitution of the sodium formate functional unit in the

polyacrylamide molecule to allow aqueous dissociation of Na^+ to release positively charged sodium ions present in the polymer as it hydrolysis which increases the conductivity of the water considerably (Entry, 2000). Generally, at all concentrations and for all days, the electrical conductivity of the water samples falls within the standard limit for quality drinking water. The results obtained is within acceptable standard for quality drinking water which is 1000 µs at 25°C (SON).

Effect on total dissolved solids (TDS)

Figures 7 & 8 shows the results obtained for the amount of total dissolved solids in the water samples before and after the addition of different polymer concentrations. It can be observed that there is minimal increase in the amount of total dissolved solids present in the water samples upon addition of the polymer at different concentrations with increasing number of days. Upon addition of the polymer in the water samples, the TDS remained at equilibrium until after day 03. The steady increase observed from day 05 in the amount of TDS can be related to the sum of cations and anions in the water from the ionization of the polymer added. The polymer contains sodium acrylate and polyacrylamide with the resultant carboxylic anions completely neutralized by the sodium cation. This may also explain why there is no change in the measured pH already explained. Therefore, addition of HPAM in drinking water has insignificant effect on the TDS of the water sample. Generally, at all concentrations at several days, the amount of TDS in the water samples falls within the standard limit for quality drinking water which is 500 mg/l (SON).

Effect on dissolved oxygen (DO)

Figures 9 & 10, shows the effect of addition of different concentrations of the DRP on the dissolved oxygen (DO) of the two water samples. It can be observed that the addition of the polymer has no effect on the DO level of the water samples at all concentrations and for all days investigated. It implies that the addition of the DRP does not affect the oxygen equilibrium in the water, making it safe for drinking. The result also implies that the integrity of the pipe is retained as an increase in DO will enhance the corrosion of the pipes (USGS, 2017). The acceptable DO standard for quality drinking water is <5.0 mg/l (NSWDET, 2009).

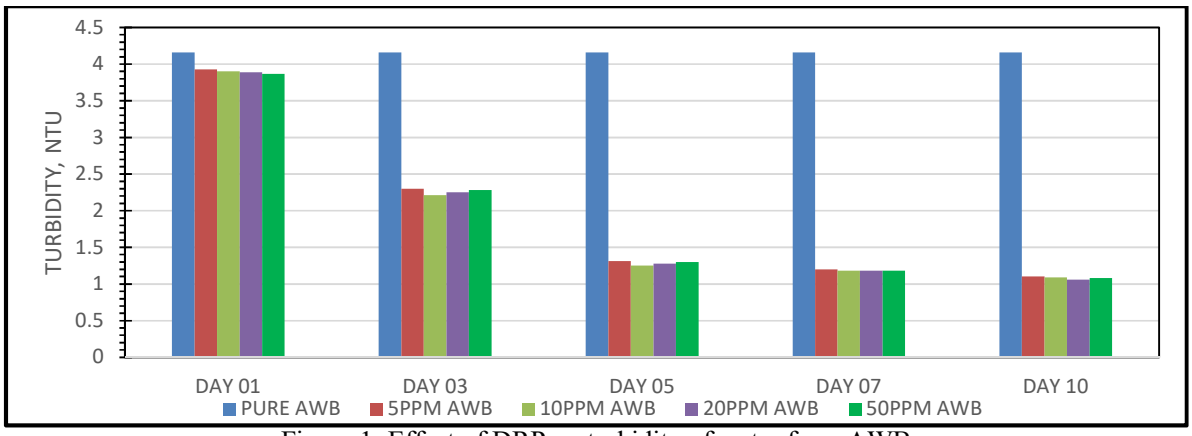


Figure 1: Effect of DRP on turbidity of water from AWB

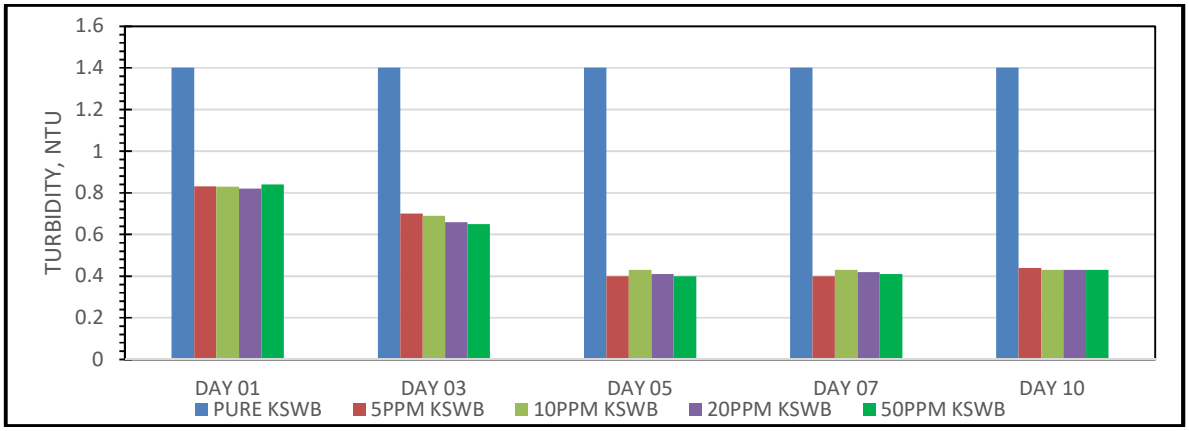


Figure 2: Effect of DRP on turbidity of water from KSWB

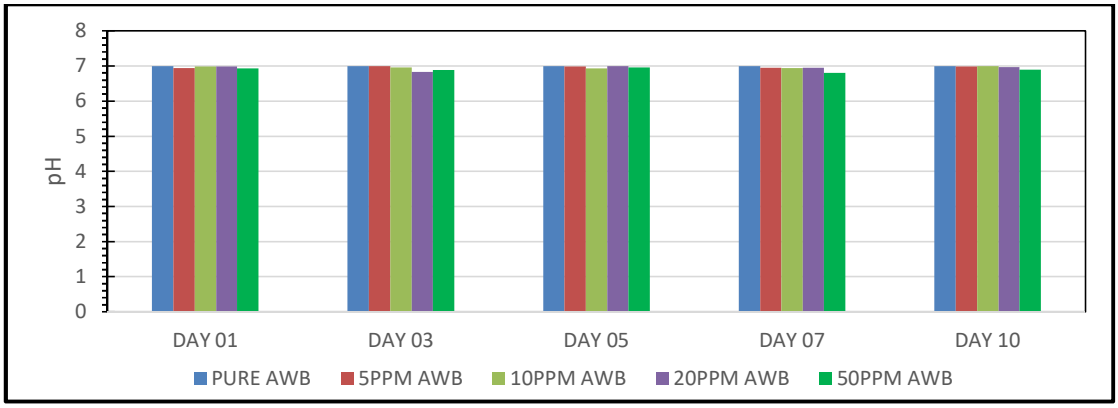


Figure 3: Effect of DRP on pH of water from AWB

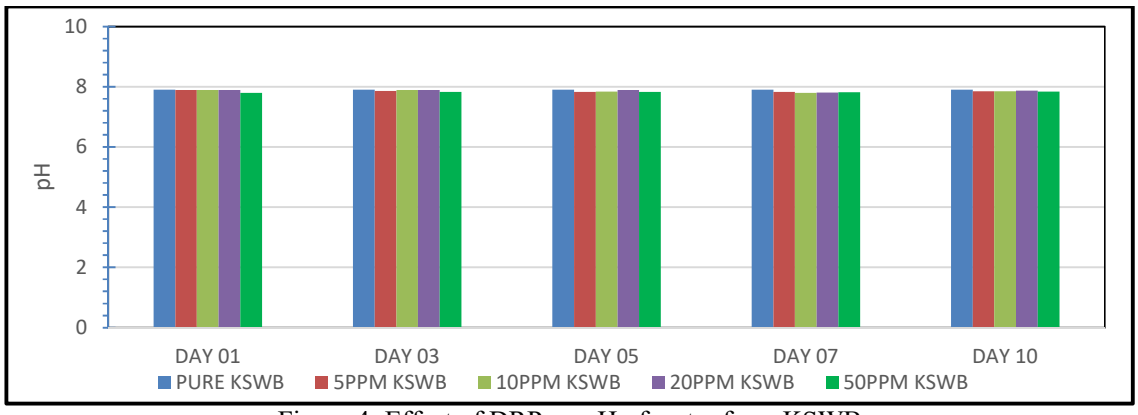


Figure 4: Effect of DRP on pH of water from KSWB

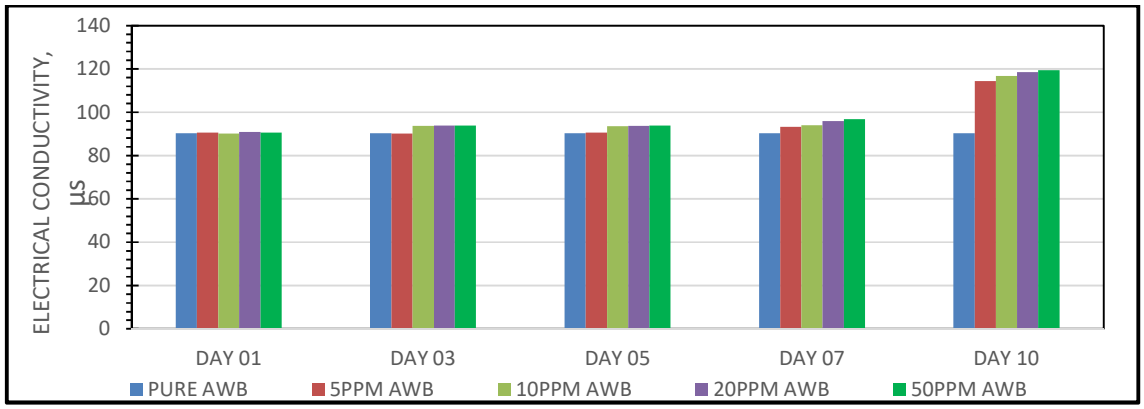


Figure 5: Effect of DRP on electrical conductivity of water from AWB

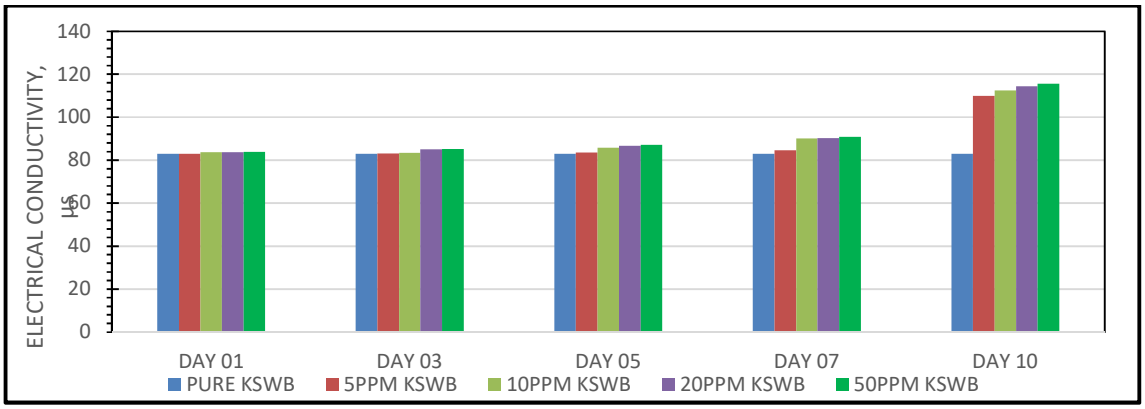


Figure 6: Effect of DRP on electrical conductivity of water from KSWB

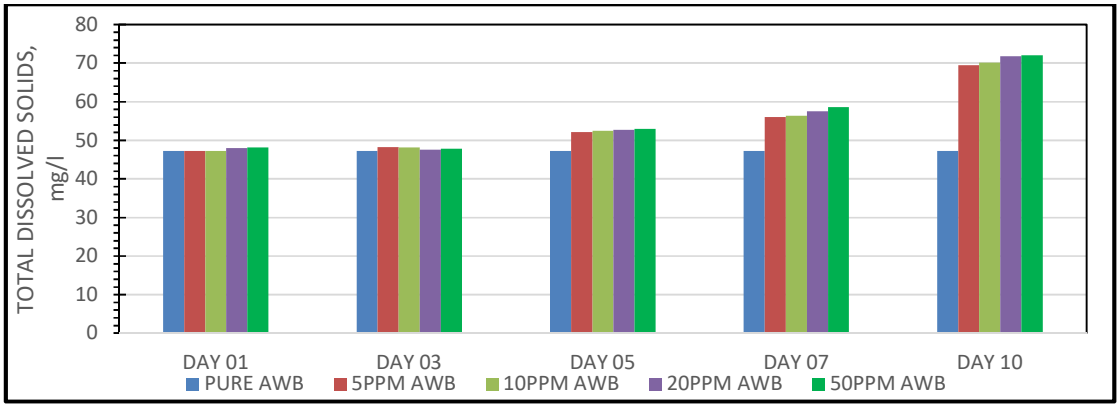


Figure 7: Effect of DRP on total dissolved solids of water from AWB

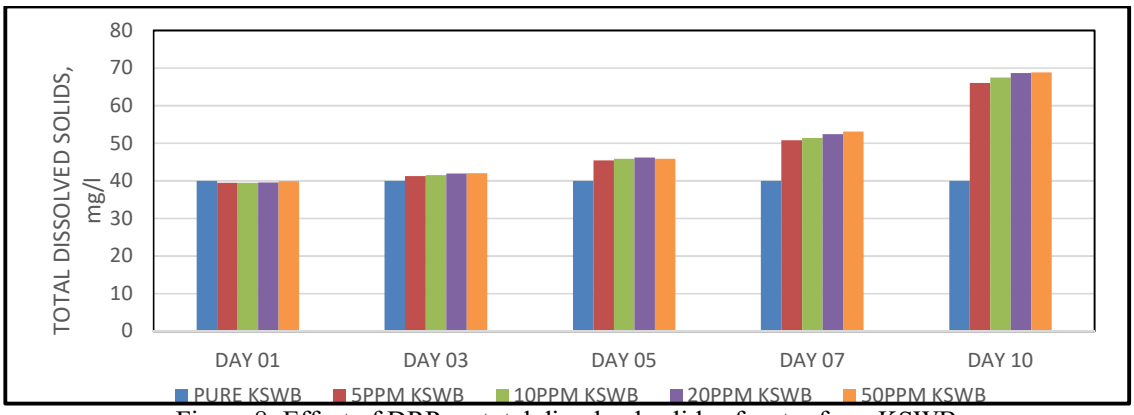


Figure 8: Effect of DRP on total dissolved solids of water from KSWB

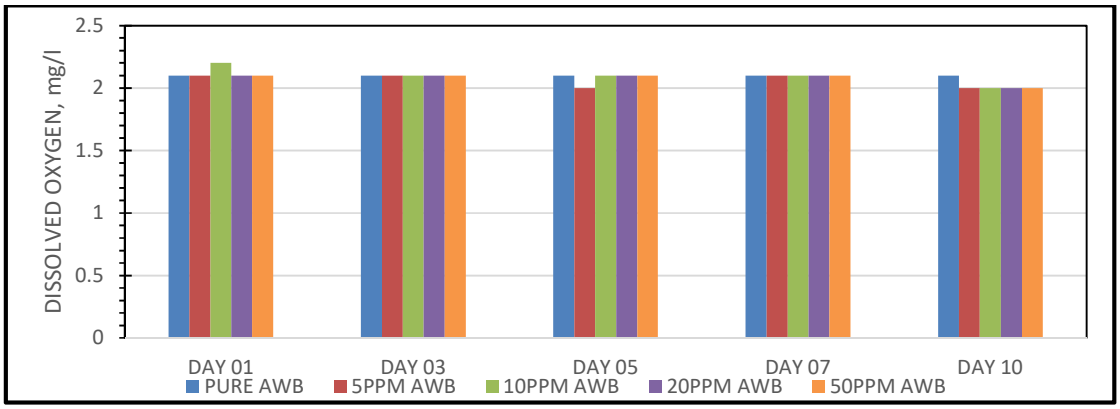


Figure 9: Effect of DRP on dissolved oxygen of water from AWB

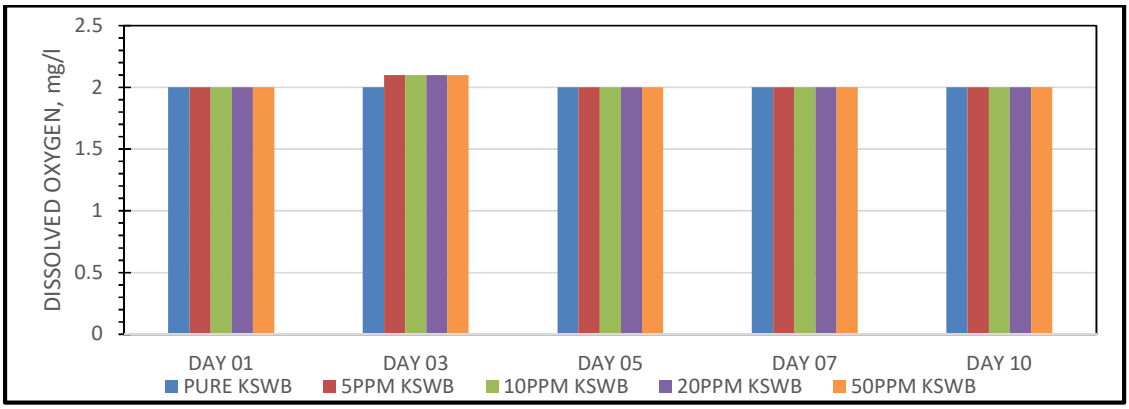


Figure 10: Effect of DRP on dissolved oxygen of water from KSWB

Effect on total hardness
For AWB water sample upon addition of the polymer, the total hardness did not change even with increasing concentration throughout the entire 10-day period which is the same trend for the KSWB water sample as observed in Figures 11 & 12.

Therefore, presence of the polymer in the water samples has no effect on the hardness of the drinking water samples as they are all within acceptable limits for quality drinking water; < 60 mg/l for soft water; 60 – 120 mg/l for moderately hard water; 120 – 180 mg/l for hard water (NSWDET, 2009).

Effect on biological oxygen demand (BOD)
The BOD of the water samples can be gotten only after every five days by taking the difference between the initial DO of day 01 and DO of day 05, difference between DO of day 05 and day 10. The values obtained for several concentrations of the water samples as shown in Figures 15 & 16.

Figure 15 & 16 shows that the BOD values of both water samples are at equilibrium i.e. the amount of BOD remained constant even with increasing concentrations of HPAM and number of days. This equilibrium observed for BOD is due to the fact that the DO level of both water samples remained constant since BOD is a direct measure of DO needed in water (Entry et al, 2000) as earlier discussed. In addition, the BOD values obtained for both water samples are within the acceptable limit for drinking water which usually should be between 1 mg/l and 5 mg/l (NSWDET, 2009).

Effect on chemical oxygen demand (COD)
It can be observed from Figures 17 & 18 that there are no significant changes in COD of the water samples with increased DRP concentration and for all days tested. Therefore, the addition of HPAM in the drinking water samples has no effect on its chemical oxygen demand. It is observed that the COD values of both water samples are within the range of 0 mg/l and 6.4 mg/l, although, there is no maximum acceptable limit set for drinking water but it is specified not to exceed 3.0 times the BOD value. i.e. average ratios of 2 – 3 mg/l COD to 1 mg/l BOD is to be expected (WHO, 2017).

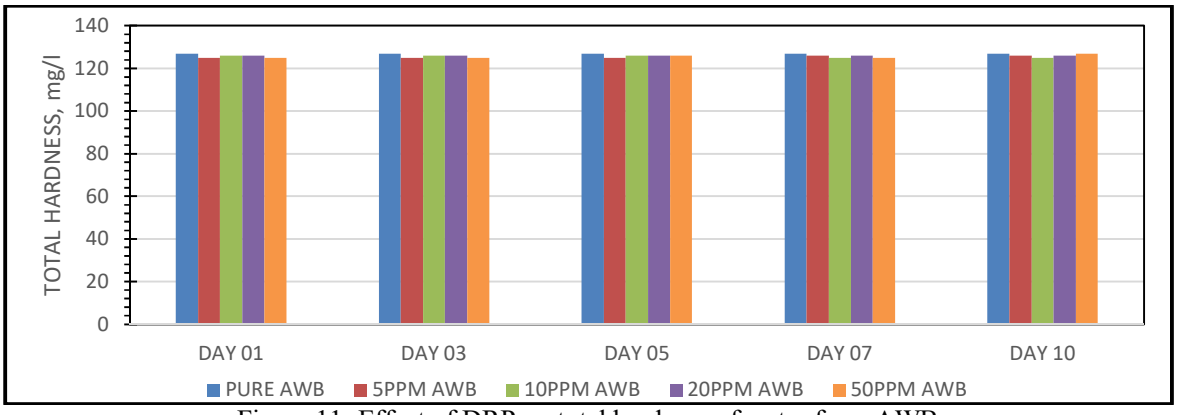


Figure 11: Effect of DRP on total hardness of water from AWB

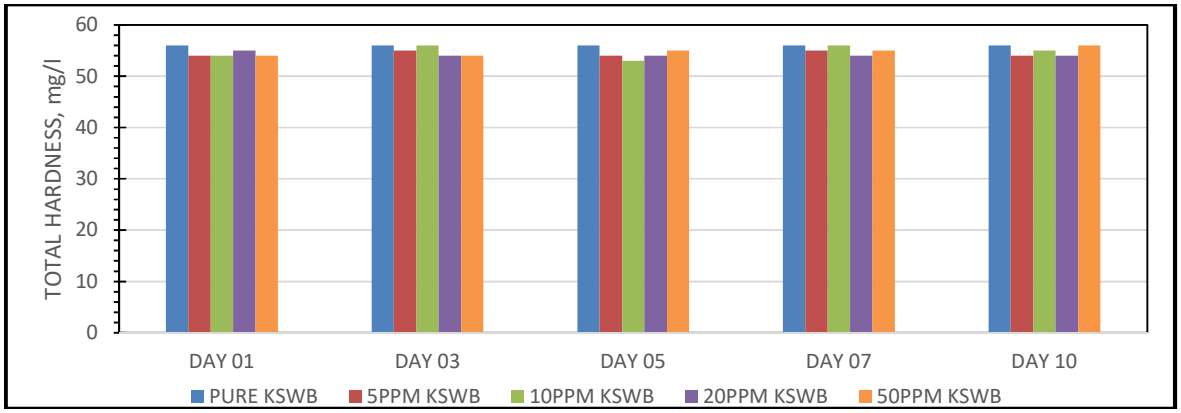


Figure 12: Effect of DRP on total hardness of water from KSWB

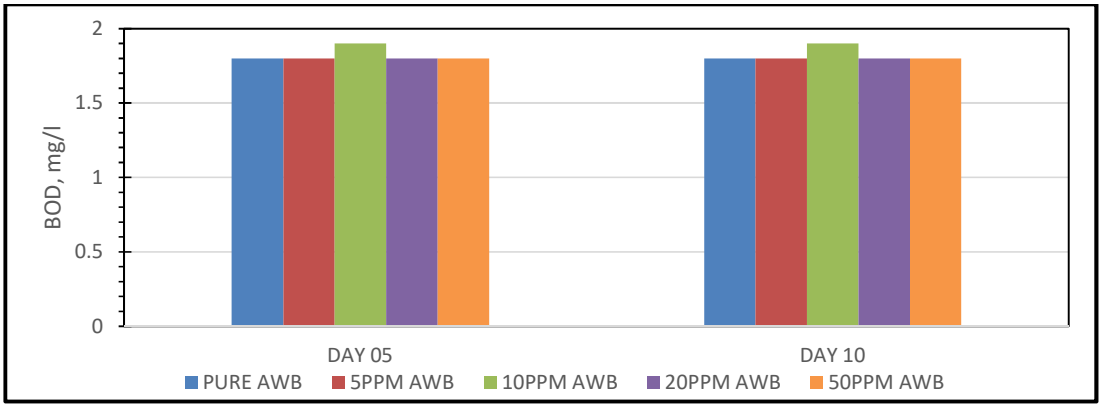


Figure 15: BOD deviation plot of pure AWB and polymer added AWB

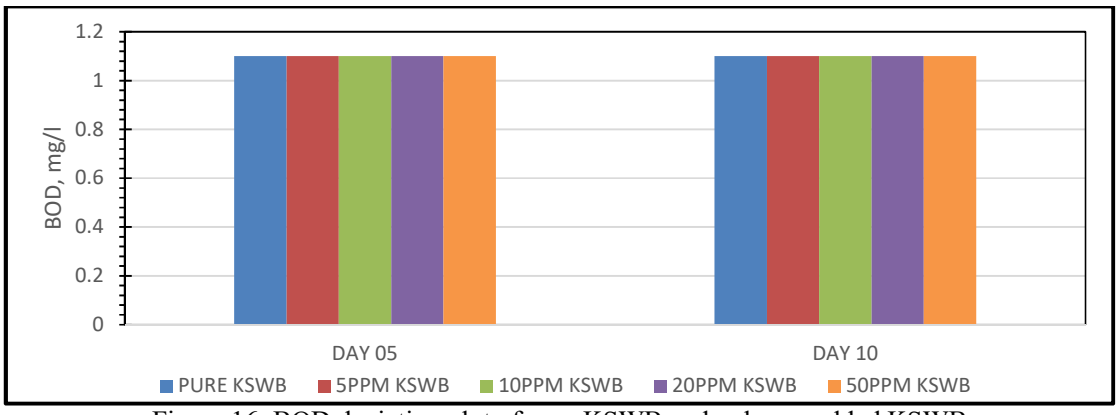


Figure 16: BOD deviation plot of pure KSWB and polymer added KSWB

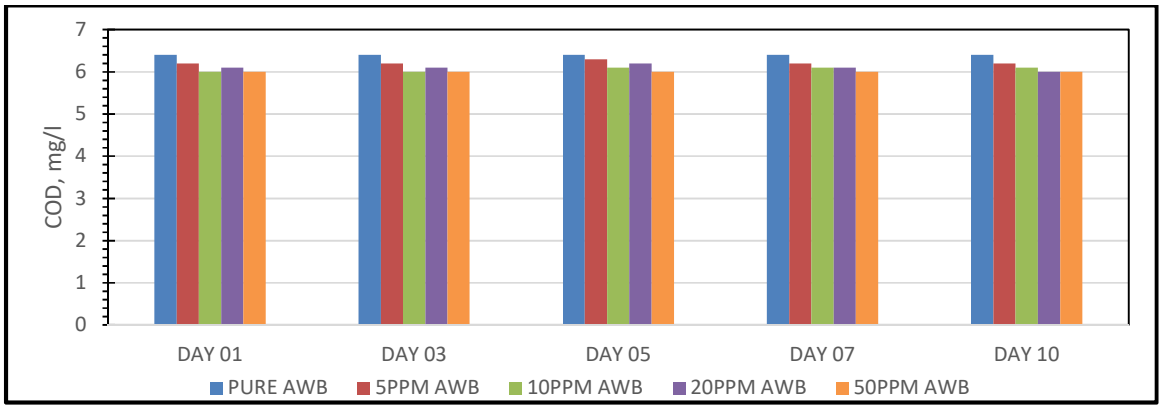


Figure 17: COD deviation plot of pure AWB and polymer added AWB

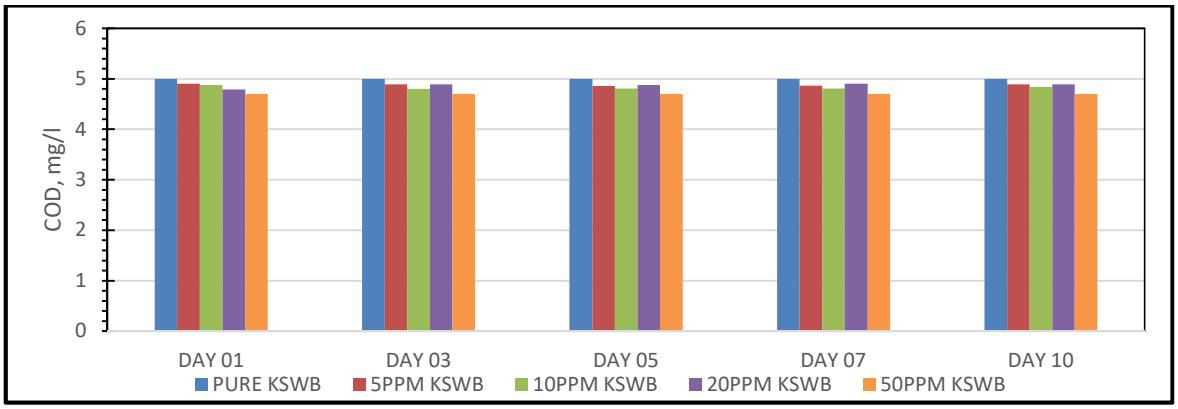


Figure 18: COD deviation plot of pure KSWB and polymer added KSWB

Conclusion

The effect of drag reducing polymer addition to drinking water from ABU and KSWB has been investigated. From the results, it can be concluded that the addition of partially hydrolysed polyacrylamide in concentration up to 50 ppm has no effect on the quality of drinking water. The resultant solution possesses properties which fall within the limit for acceptable and quality drinking water. The result also shows the reduction in turbidity which is a reflection of the coagulation capability of the tested polymer. These implies that DRP can be used in transporting drinking water to consumption points with enhanced throughputs resulting in more efficient and flexible operations.

Recommendations

- The effect of DRP on the quality of drinking water should be investigated with natural DRP's
- The optimal concentration of DRP in addition to drinking water can be set at 10 ppm, as differences are observed to be very minimal for all physico-chemical parameters at this concentration with significant drag reduction reported.

Acknowledgements

The Authors thank the staff of the ABU water works, Estate Department, Kaduna State Water Board, and Department of Chemical Engineering, Ahmadu Bello University, Zaria for their support and advice in conducting this study.

References

1. Ann, J. L. (2010). Formulation of natural drag-reducing agent from malabar spinach for aqueous liquid flowing in turbulent mode through pipelines. B.Eng thesis. Faculty of Chemical & Natural Resources Engineering, University Malaysia Pahang.
2. CAWST, Centre for Affordable Water and Sanitation Technology (2009). Introduction to drinking water quality testing (2009th ed.). 12, 2916. Calgary, Alberta, Canada.
3. Edomwonyi-Otu, L. C. (2015). Drag reduction in oil-water flows. PhD thesis. Department of Chemical Engineering, University College London.
4. Edomwonyi-Otu, L. C., & Angeli, P. (2014). Effects of polymer addition on pressure drop and interfacial waves in horizontal oil-water flows. *International Journal of Petroleum Technology Development*, 2(July), 41–48.
5. **Edomwonyi-Otu, L.C**., Chinaud, M., Angeli, P. (2015). Effect of Drag Reducing Polymer on Horizontal Liquid-Liquid Flows. Exp. Therm. Fluid Sci. 64, 164 – 174.
6. Entry, J.A., Sojka, R.E., Verwey, S.A., Ross, C.W. (2000). Polyacrylamide removes microorganisms and nutrients from surface water. United States Department of Agriculture (USDA). Retrieved October 19, 2017, from 222.lib.ncsu.edu/1840.16/158.
7. SON, Standard Organization of Nigeria. (2007). Nigerian Standard for Drinking Water Quality. Nigerian Industrial Standard (3rd ed., Vol. NIS 554), 5-30. Lekki, Lagos.
8. Nathanael, B.R. (2017). Polyacrylamide for turbidity control in runoff. *Journal of polymer and colloid science*, 1(4), 36-77.
9. NSWDET, New South Wales Department of Education and Communities. (2009). Water quality testing. Retrieved March 6, 2017, from www.irrpublic.cli.det.nsw.edu.au
10. Yusuf, Y. O., Jimoh, A. I., Onaolapo, E. O., & Dabo, Y. (2015). An assessment of sachet water quality in Zaria area of Kaduna state, Nigeria. *Journal of Geography and Regional Planning*, 8(7), 174–180.
11. USGS, United States Geological Survey (2017). Water properties: Dissolved oxygen, in USGS science school. www.water.usgs.gov/edu/dissolvedoxygen.html. Accessed 02/11/17
12. WHO, World Health Organization (2007). pH in drinking-water; In WHO Guidelines for drinking-water quality, WHO/SDE/WSH/07.01/

INVESTIGATION OF THE EFFECTIVENESS OF ALUM FROM SOME NIGERIAN KAOLINITES

LAWRENCE C. EDOMWONYI-OTU, IFEANYI E. ALAZU, JONAH U. IRANDE
Chemical Engineering Department, Ahmadu Bello University, Zaria
Corresponding Email: lcotu@abu.edu.ng

Abstract
Alum is an indispensable material both for water treatment (coagulant and disinfectant) and leather tanning purposes. High quality alum has recently been produced from some Nigerian kaolinite (Bauchi and Kankara) via the energy-saving process. However, its effectiveness in actual water treatment process, compared to commercial alum, has not been investigated. This forms the thrust of the current study. Tests were carried out on several parameters of the raw water before and after the addition of varying volume of the alum for a fixed volume of the raw water. The results showed that while the total dissolved solids (TDS) and conductivity increased with alum volume, the biological oxygen demand (BOD), chemical oxygen demand (COD), alkalinity of the water showed reduction. The coagulating effectiveness of the alum was demonstrated by over 95% reduction in the turbidity of the water sample. The results showed that the alum from Nigerian kaolinite showed remarkable and desirable water treatment qualities and compares well with the commercial alum for all the tested parameters. Since the water treatment process was not complete, comparison of the results with water quality standard such as Nigerian Standard Drinking Water Quality (NSDWQ) and the World Health Organization (WHO) was not carried out. The development of alum production plant using Nigerian kaolinite is therefore recommended as it can serve as alternative to the present commercial alum that is majorly imported.

Keywords: *Alum, Drinking water, coagulation, kaolinite, turbidity,*

INTRODUCTION

Nigeria as a nation is faced with the challenge of harnessing her abundant natural resources to meet the needs of her teeming population. The current effort by the Federal Government to develop its economy can only be achieved under a diversified economic system, which underscores the need to explore other resources in the country (Edomwonyi-Otu et al., 2012). Chemical precipitation and flocculation with various salts of aluminium (alum), iron, lime and other organic and inorganic chemicals are widely used for treatment of water to remove colloidal particles and microbes. Treatment of water by addition of chemical coagulants and precipitants has been practised from ancient times (Ahirrao, 2008). Potash alum is also a common household product for water treatment (Aung et al., 1993) and it also has a disinfecting property (Chaudhary et al., 1997; Chigondo et al., 2015)

Bauxite is the main raw material for alum production but this is not readily available in Nigeria (Edomwonyi-Otu 2008; Aderemi et al., 2009; Edomwonyi-Otu and Aderemi, 2010). These researchers have established the feasibility of producing alum from kaolinites (Babatunde, 1999) which is next to bauxite in alumina content. Kaolinites have several industrial applications and have been used since ancient times (Obaje et al., 2013; Jide 2014). Over 85% yield was reported for alum production from Nigerian kaolinites (Edomwonyi-Otu et al., 2012) and this has prompted the need to develop this resources to commercial scale.

Despite these strides in producing alum from kaolinites, there is no systemic work on testing the effectiveness of these alum from Nigerian kaolinites in water treatment processes.

In this present investigation, alum from Bauchi and Kankara kaolinites are used for treating raw water from the Ahmadu Bello University (ABU) dam. The data obtained will give an indication of the effectiveness of these alums. This is a needed step in the development of the alum production process from bench scale to commercial scale.

MATERIALS AND METHODS

Alum (aluminum sulphate) was synthesized from Kankara and Bauchi kaolinites following steps described by Edomwonyi-Otu (2008). Raw water sample were obtained from the Ahmadu Bello University dam and tested for its turbidity, pH, conductivity, Total Dissolved Solid (TDS), Hardness, Alkalinity, Biological Oxygen Demand (BOD), and Chemical Oxygen Demand (COD) (Patil et al., 2012; Soni et al., 2013). Then, 5, 10, 15, 20, 25 and 30 ml of alum solution was added to 100 ml raw water samples and the previous tests were repeated following procedure established by

the Department of Water and Environmental Engineering, Ahmadu Bello University, Zaria. Commercial alum was obtained from the open market and added to raw water samples in same volume as the synthesized alum for the purpose of comparison. The tests were repeated thrice and the average values obtained were recorded.

RESULTS AND DISCUSSION

Figures 1 to 6 show the variation in the parameter of the raw water, treated water using commercial alum and alum from Nigerian kaolinite. The estimated values for commercial and alum from Kankara kaolinite indicates high variation from that of raw water, and close comparable estimates for the use of the alums.

The results of the coagulation study in varying alums concentration with equal volume of water sample is shown as the turbidity test in Figure 1. It can be observed that the both alums perform similarly in reducing the turbidity by over 90% with as low 5 ml of alum solution. The turbidity is seen to thereafter reduce with increasing alum volume. This attest to the coagulating capability of the alum synthesized from Nigerian kaolinite.

The key attraction here is the close performance of the synthesized alum when compared with the commercial alum. Expectedly, the total dissolved solids (TDS) of the water sample is observed to reduce (See Figure 2) for both alums. This corroborates the result on turbidity and may be due to the precipitation and subsequent coagulation of some of the dissolved ions that constitute impurity in the water sample.

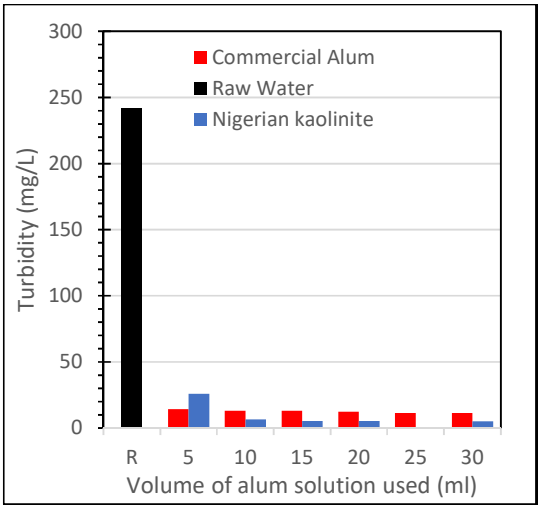


Figure 1. Turbidity Trend

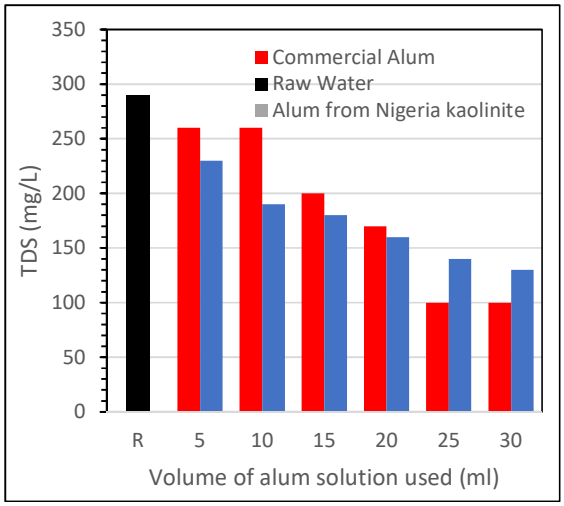


Figure 2. TDS Trend

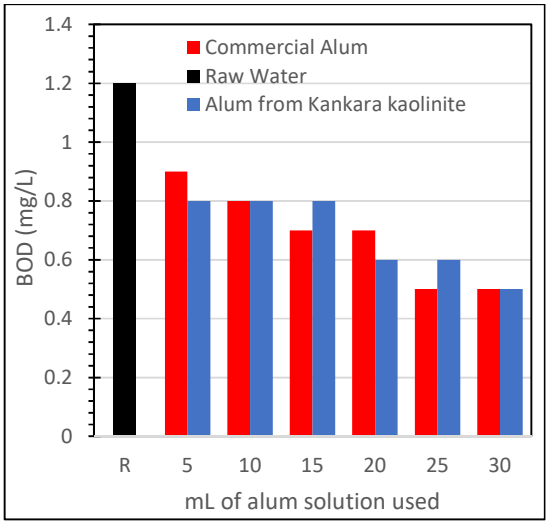


Figure 3. BOD Trend

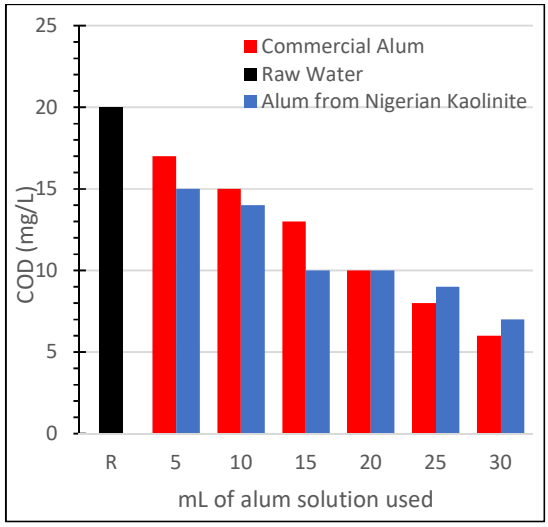


Figure 4. COD Trend

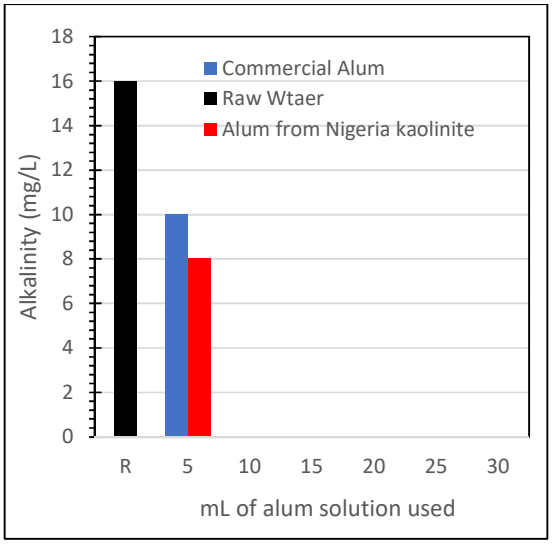


Figure 5. Alkalinity Trend

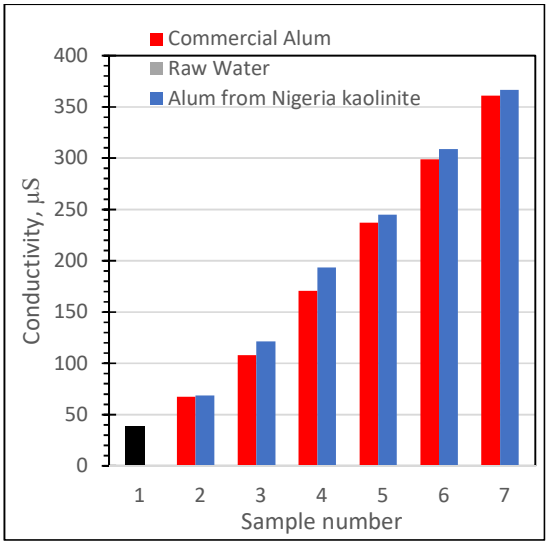


Figure 6. Conductivity Trend

Similarly, Biological Oxygen Demand (BOD) and Chemical Oxygen Demand (COD), which are measures of the amount of organic compounds in water, are observed to reduce with increasing volume of alum (Figures 3 & 4). Although the BOD and COD of the raw water are both within acceptable limit for drinking water, their reduction is an indication of the effectiveness of the alums since both are considered conventional pollutants (Clair et al., 2003). The result also shows their disinfectant property (Aung et al., 1993; Chaudhary et al., 1997). The acidic nature of the alum resulted in the observed reduction of the alkalinity of the water sample after the alum solution was added as can be seen in Figure 5. The reduction towards neutrality shows the effectiveness of the alum in controlling the pH of the water. The combined use of hydrated lime and the alum helps to attain the desired pH for drinking water for the complete water treatment process. The increase in electrical conductivity (EC) observed in Figure 6 is the result of the addition of aluminium and sulphate ions from the aluminium sulphate (alum) to the water sample. The observation agrees with the report by Ahirrao (2008) who treated municipal water with potash alum and observed an increase in the EC.

Comparison of the results with WHO and NSDWQ was not undertaken because the alum treated water is not the final product in water treatment processes. The key objective was to compare the performance of the synthesised alums, from Nigerian Kaolinites, with the commercially available alum in the market.

CONCLUSION

The effectiveness of alum from some Nigerian kaolinites in water treatment has been studied. From the results obtained, it can be concluded that the alums from Nigerian kaolinites have good coagulating and disinfectant properties and can be used for water treatment purposes. Their effectiveness was found to compares well the commercial alum currently used for water treatment processes in Nigeria. Hence, it can serve as alternative to the commercial alums when the production process is fully commercialized. This will lead to savings in foreign exchange, job creation, economic improvement and value addition to the kaolinite deposits in Nigeria.

REFERENCES

Ahirrao, S. D. (2008). Effect of a common water purifier potash alum on drinking water quality and human health. *Nature Environment and Pollution Technology*, *7*(1), 79–81.

Aung, K. S. O., Knine, W. W. T., Sow, M. M. and Aye, T. (1993). EFFECT OF potash alum in decontaminating household water. *Journal of Diarrheal Disease Research* 1(3) 172-174

Aderemi, B. O., Edomwonyi-Otu, L., & Adefila, S. S. (2009). A New Approach to Metakaolin Dealumination. *Australian Jounal of Basic and Applied Sciences*, *3*(3), 2243–2248.

Babatunde, A. O. (1999). Alum From Kaolin: Production, Analysis And Quality Studies, MSc Thesis. Ahmadu Bello University.

Badmus, B. S., & Olatinsu, O. B. (2009). Geophysical evaluation and chemical analysis of kaolin clay deposit of Lakiri village , southwestern Nigeria. *Intenational Journal of Physical Science*, *4*(10), 592–606.

Chaudhary, M. A., Haq, B., Xu F. J. B., Maderia and Colwell. R. R. (1997). Effect of alum on free living and copepods associated *V. Cholerae. Applied and Environmental Microbiology,* 3323-3326

Chigondo, et al. (2015). Extraction of Water Treatment Coagulant from Locally Abundant Kaolin Clays. *Comparative Journal of Chemistry*, *2015*, 1–8.

Edomwonyi-Otu, L. C., Adenowo, A. S., & Aderemi, B. O. (2013). Ferric Alum Production from Brown Kankara Kaolin Clay. *Petroleum Technology Development Journal*, *3*(2), 81–87.

Edomwonyi-Otu, L.C and Aderemi, B.O. (2009). Alums from Kankara Kaolin. Jour. of Res.in Eng. Vol 6 (1)105-111.

Edomwonyi-Otu, L. C., Aderemi, B. O., Edomwonyi-Otu, O., Simo, A., & Maaza, M. (2012). Alum Production from some Nigerian Kaolinite Deposits. *International Journal of Engineering Research in Africa*, *7*, 13–19

Jide, A. (2014). Characterisation of the Nigerian Kankara Kaolinite Clay Particulates for Automobile Friction Lining Material Development. *Chemcal and Process Engineering Research*, *29*, 24–35.

Obaje, S. O., Omada, J. I., & Dambatta, U. A. (2013). Clays and their Industrial Applications : Synoptic Review. *Internal Journal of Science and Technology*, *3*(5), 264–270.

Patil, P., Sawant, D., & Deshmukh, R. (2012). Physico-chemical parameters for testing of water A review. *International Journal of Environmental Sciences*, *3*(3),1194–1207.

Sawyer, N. C., McCarty, P. L., Parkin, F. G. (2003). Chemistry for environmental engineering and sciences (5th edition). McGraw-Hill, New York.

Soni, V., Visavadia, M., Gosai, C., Hussain, D. Mewada, M., Gor, S., & Salahuddin, K. (2013) Evaluation of physico-chemical and microbial parameters on water quality of Narmada River, India. *African Juurnal of Environmental Science*, *7*(6), 496–503.

PHYSICO-CHEMICAL ANALYSIS OF NANOCRYSTALLINE CELLULOSE FROM RICE HUSK

GBADEGESIN ADENIKE MARIAM AND KOGO A. ABDULLAHI
Department of Polymer and Textile Engineering, Ahmadu Bello University, Zaria, Nigeria

ABSTRACT
Rice husk is a residue from agro-industry that can be used to produce nanocellulose. Cellulose has been extracted from rice husk by chemical treatment with aqueous solution of sodium hydroxide. After bleaching, the compact structure around the cellulosic fibers was removed, and the lignin content of the residue decreased from 7.00 to 4.00%. Acid hydrolysis was performed at a mild temperature of 50˚C followed by ultrasonication. The obtained nanocellulose presented a higher crystallinity of about 70%, higher thermal stability than the raw material. The physical properties of derived nanocrystalline cellulose has been investigated by performing a swelling and density test. The morphology and chemical structure were investigated by Fourier transform infrared spectroscopy (FTIR) and Scanning electron microscopy (SEM) techniques, respectively.

1.0 Introduction

Cellulose-based nanomaterials have been of increasing interest as potential nano-reinforcing filler into biocomposites for industrial and biomedical applications. Two general classes of cellulose nanomaterials (CNs) that can be extracted from different resources such as plant, animal, or mineral plants are cellulose nanocrystals (CNCs) and cellulose nanofibrils (CNFs). Cellulose nanocrystals can be referred as cellulose nanowhiskers (CNW) or nanocrystalline cellulose (NCC) while cellulose nanofibrils can be referred as nanofibrillated cellulose (NFC), (Dong *et al*., 2013).

Nanocrystalline cellulose (NCC) is typically a rod-shaped monocrystalline cellulose with tens to hundreds of nanometers in length and 1-100nm indiameter (Ruiz *et al*., 2000). It is an emerging renewable nanomaterial that holds promise in many different applications such as foods, pharmaceuticals, personal care etc. It is a uniform, re-dispersible natural nanoparticle obtained from the crystalline regions of cellulose fibers.

Agricultural wastes are additional materials from harvested crops that have different usages. Rice is the largest cereal crop in the world. Rice husks are the hard protecting coverings of grains of rice. In addition to protecting rice during the growing season, rice husk can be put to use as building material, fertilizer, insulation material, or fuel. Rice husk is an important agricultural waste that can be easily found in some states in Nigeria. Previous reports on the commercial use of rice husk have focused more on surface modification to improve filler-matrix interaction in composite application (Ahmad *et al*., 2007). The rice husk can also undergo combustion to produce rice husk ash that is rich in silica. Another way to use rice husk is exploitation of its cellulose content. Rice husk consist of 35% cellulose, 25% hemicellulose, 20% lignin and 17% ash. Therefore, the use of rice husk as the primary source for producing nanocrystalline cellulose is promising.

The aim of this study is to extract and characterize nanocrystalline cellulose (NCC) from rice husk.

2.0 Materials and methods

2.1 Materials

The rice husk used as raw material was obtained from zaria city, Zaria, Nigeria. Sodium hydroxide (Supplied by Trust chemical laboratories, United Kingdom, 98% purity) was used for the alkaline treatment. Acetic acid (Supplied by Guangdong Guandgua chemical factory co. Ltd. Shantou, China, 99.5% purity) and hydrogen peroxide (Supplied by BDH chemicals Ltd. Poole, England) were used as bleaching agents while sulphuric acid (Supplied by Guangdong Guandgua chemical factory co. Ltd. Shantou, China, 99% purity) was used for hydrolysis. All chemicals were used without further purification.

2.2 Preparation of Nanocrystalline cellulose from rice husk

The obtained rice husk was washed with distilled water thoroughly and dried in an oven at 35˚C for 24hrs.The rice husk were then reduced to regularly formed particles and carefully sieved into 75µm sizes.

2.2.1 Alkali treatment

30g of the ground rice husk were immersed in 300ml of NaOH 5% (w/v) at 90˚C for 60mins under constant stirring. The solid was then filter and washed several times using distilled water. This treatment was repeated thrice and the solid was dried at 40˚C for 24hrs.

2.2.2 Bleaching process

Following alkaline treatment, the bleaching process was completed by adding a buffer solution of acetic acid, hydrogen peroxide and distilled water at reflux (using an oil bath at 100-130˚C) for 4hr. The mixture was allowed to cool and was filtered using excess distilled water. The bleaching process was repeated thrice.

2.2.3 Acid hydrolysis

The acid hydrolysis treatment was conducted on the fibres after alkaline and bleaching treatment at a temperature of 50˚C using 10.0mol/L of sulphuric acid (preheated) for 40mins under continuous stirring. The hydrolysed material was washed by centrifugation at 5,000rpm for 15mins. The centrifugation step was repeated three times before the suspension was dialysed against distilled water for 3 days until constant PH in the range of 5-6 was reached. The resulting suspension was sonicated for 30mins.

2.3 Characterization of rice husk fibres and Nanocrystalline cellulose.

2.3.1 Swelling test

The swelling capacity of the NCC powder was estimated as described by Maigari, (2015). 3g of the NCC powder was placed in a measuring cylinder, 20ml of water was added into the cylinder and the volume of the NCC was then recorded as V_i. This was allowed for one hour and the volume of the NCC was again observed and recorded. The volume was observed and recorded at an hour interval until there was a constant volume V_f. The swelling index was then calculated as follows:

$$Swelling\ index = \frac{Vf - Vi}{Vf} \times 100 \quad \ldots\ldots\ldots\ldots\ldots\ldots (1)$$

2.3.2 Density Test

2g of the NCC powder was weighed on a weighing balance. The weighed sample was then transferred into a suitable graduated cylinder, with the base of the cylinder gently tapped on a book until the height of the sample in the cylinder was at minimum i.e. the sample height does not reduce by further tapping, care was taken so that some of the sample did not bounce out of the top of the cylinder during tapping. The volume of the sample was then read in ml. The density was then calculated as follows:

$$Density = \frac{Mass\ (g)}{volume\ (ml)} \quad \ldots\ldots\ldots\ldots\ldots\ldots (2)$$

2.3.3 Scanning electron microscopy (SEM)

Scanning electron microscopy (SEM) (model Quorum Q15ORES) was used to observe the surface morphology of the rice husk fibres. The effect of the different chemical treatments was assessed using a comparison of the untreated and the acid hydrolysed fibres. Rice husk fibres were placed on the aluminium stub and incubated in the oven at 60˚C. The samples were then coated with 5nm of gold using a vacuum sputter coater thereby making it conductive. The sample is transferred to the sample holder of the machine and with the aid of a navigation camera using secondary detector the structure of each samples was viewed at different magnification.

2.3.4 Fourier transform infrared spectroscopy (FTIR)

Fourier transform infrared spectra were recorded using ATR spectrophotometer (model CARY 630). Untreated and acid hydrolysed rice husk fibres samples were analysed. The samples were finely grounded and then compressed into pellet form. FTIR spectral analysis was performed within the wave number range of 400-4000cm^{-1}.

3.0 Results and discussion

3.1 Swelling Test

The result obtained from the swelling index below indicates that NCC have a very low swelling capacity. This is true because the NCC is much more compacted and since the amorphous regions were hydrolysed, this leaves little or no spaces for water retention which will subsequently lead to swelling.

The swelling index was determined using the formula in Equation 1 above. Thus:

$$Swelling\ index = \frac{6.3 - 4.8}{6.3} \times 100\% = 23.8\%$$

3.2 Density test

There was a slight increase in density from rice husk to NCC as we can see below, this can be explained on the basis of the concept of density itself. Density of any material is inversely proportional to the volume it occupies at a constant mass. The rice husk will occupy higher molecular volume because of the high level of amorphousity and thus less dense. On the other hand, NCC is made up of more compact structure and occupies less volume and therefore appears denser than rice husk. We can say here that: Density can be directly proportional to crystallinity.

By using Equation 2 above, the density of the NCC powder and the untreated rice husk was calculated.

a) Density of NCC powder:

$$Density = \frac{2}{3.2} = 0.625 g/ml$$

b) Density of untreated rice husk:

$$Density = \frac{2}{3.8} = 0.526 g/ml$$

3.3 Scanning Electron Micrograph

The scanning electron microscope images shown in Plate 1 (a) and (b) shows a clear difference between the two samples. The smooth surface of untreated rice husk fibre in Plate 1 (a) can be attributed to the fact that the rice husk powder contains all its components such as cellulose, hemicellulose etc. After alkaline treatment, bleaching and subsequent hydrolysis, the fibre surface tends to become rougher as observed in (image b). This indicates the removal of the outer non-cellulosic layer composed of materials such as hemicelluloses, lignin, pectin, wax, and other impurities contained in the rice husk. Both wax and pectins are known to surround the surface of natural fibres as a protective layer. There was a decrease in the diameter of the fibrous material which indicates that under strong chemical treatment conditions, almost all the components that bind the fibril structure of the rice husk was removed thus enabling the fibres to separate into individual forms.

The SEM images of both the rice husk and NCC sample at magnification of × 1000 are shown Plate 1a and 1b.

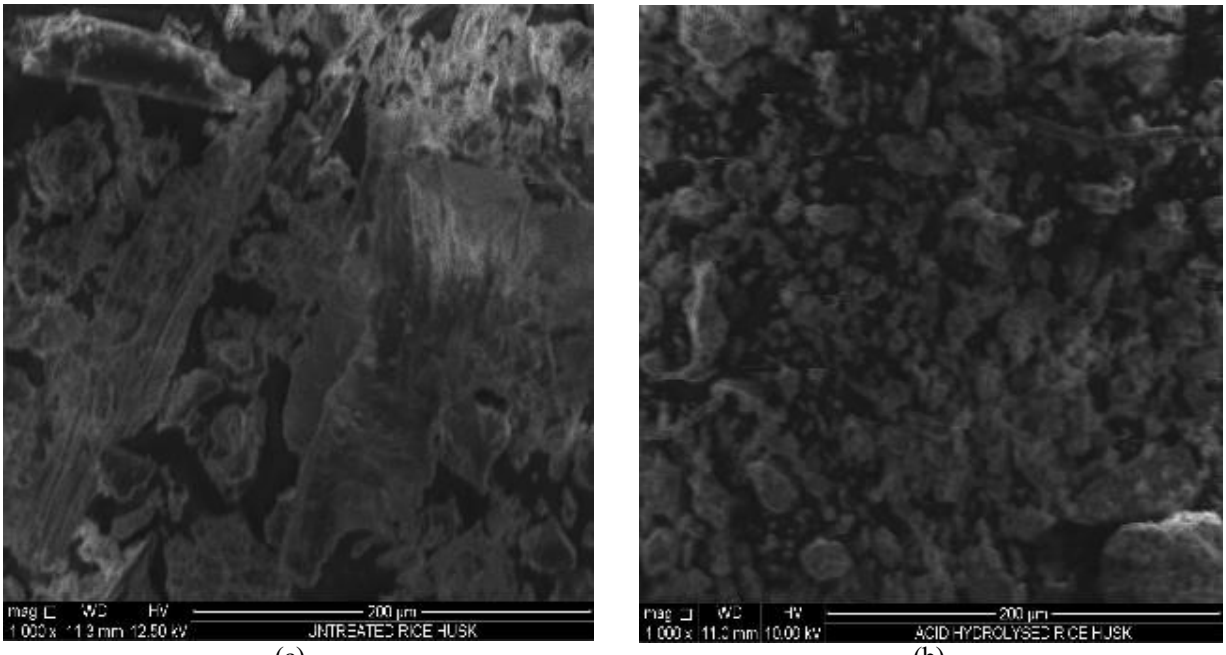
3.4 Fourier-Transformed Infrared Spectroscopy

The FTIR spectra gives us useful information on the functional groups present in the sample.
The two spectra shown in Plate 2 (a) and (b) above are similar with little shift in position of certain peaks and also change in intensity. This suggest the unaltered chemistry of the starting material.

The peak around 3400-3300cm^{-1}, 3000-2900cm^{-1} which was observed in both spectra, is representative of the C-H and O-H group. The peak located around 1423cm^{-1} in both spectrum corresponds to O-H bending vibrations. According to Sun et al., the C–O–C pyranose ring skeletal vibration occurs in the region of 1076–1023 cm^{-1}.

The peak around 1636cm^{-1} in both spectra correspond to the absorption of water. These peaks are ascribed to the stretching of hydrogen bonds and bending of hydroxyl (OH) groups bound to the cellulose structure. These results indicate that the cellulose component was not removed during the chemical treatment carried out on the rice husk fibres and is the common material found in both samples.

The graphs of the IR absorption of both the rice husk and NCC are shown in plate 2a and 2b.



(a) (b)

Plate 1. SEM images of: (a) Rice Husk (b) NCC

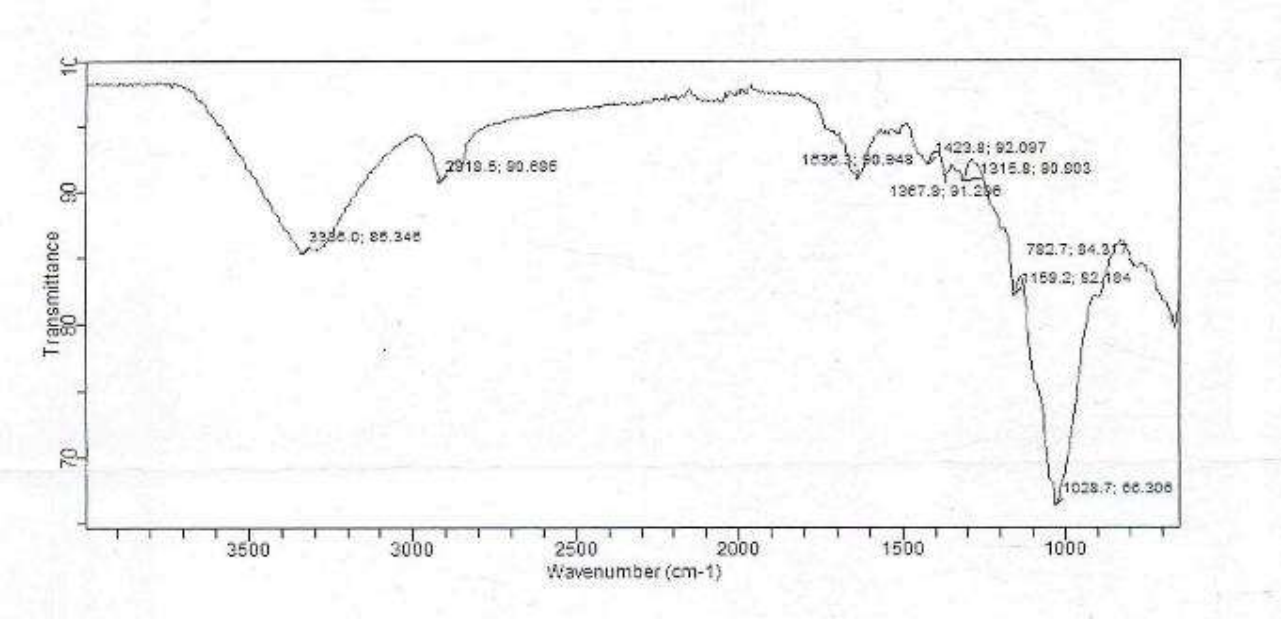


Plate 2a: FTIR graph of rice husk

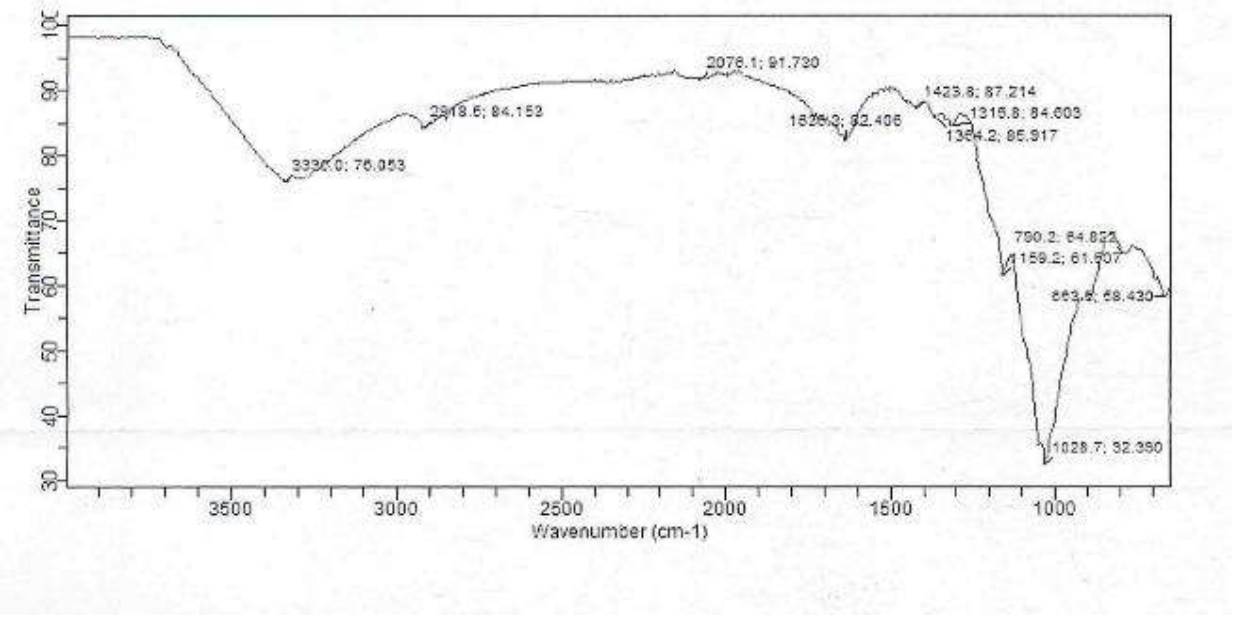


Plate 2b: FTIR graph of NCC powder

4.0 Conclusion

Purification of cellulose was performed using classical chemical treatments involving alkaline and bleaching treatments. It was observed that the former treatment was efficient in removing hemicellulose while the latter fully removed lignin. Cellulose nanocrystals were successfully extracted from the purified rice husk using an acid hydrolysis treatment at a temperature of 50˚C. Morphological investigation, Fourier transformed infrared spectroscopy confirmed the removal of non-cellulosic materials. The extraction time did not affect the properties of the cellulose nanofibers, which demonstrated an increased crystallinity index (up to 70%) and thermal stability than the raw material. The crystallinity hardly exceeds this range due to the complex nature of cellulose and the thermal stability is proportional to the chain length of the polymer.

References

Ahmad, I., Abubakar, D. R., Ramli, A., (2007). "Direct usage of products of PET glycolysis for manufacturing rice husk/ unsaturated polyester composite". Iran polym. J. 14, 233-239.

Bhammathidas, N., Mehtra, P. K., (2004). "Concrete mixtures made with tenary blended cements containing fly ash and rice husk ash", In: Malhotra, V. M. (Ed),

international conference proceeding seventh, 199-22. CANMET-Chennai, India, pp. 379-391.

Chen, W., Yu, H., Liu, Y., Hai, Y., Zhang, M., Chen. P. (2011). "Isolation and characterization of cellulose nanofibers from four plant cellulose fibers using a chemical-ultrasonic process", *Cellulose* 18(2), 433-442.

Dong, H., Snyder, J. F., Tran, D.T., Leadore, J. L. (2013). "Hydrogel, aerogel and film of cellulose nanofibrils functionalized with silver nanoparticles", Carbohydr. Polym, 95, 760-767, 2013.

Ioelovich M. (2012). Optimal Conditions for Isolation of Nanocrystalline Cellulose Particles. *Nanoscience and Nanotechnology,* 2(2): 2-13.

Habibi Y., Lucian A. L. Orlando J. R. (2010). Cellulose Nanocrystals: Chemistry, Self – Assembly and Applications. *Chemical Review*, 110: 3479-3500.

Ruiz M. M., Cavaille J. Y., Dufresne A., Gerard J. F., Graillat C. (2000). Processing and Characterization of New Thermoset Nanocomposites Based on Cellulose Whiskers, *composite interfaces* 7(2): 117-131.

Maigari, S., Bukhari, M. M. (2015). "Assessment of dyeing and some fastness properties of Nanocrystalline cellulose extracted from corn cub".

Matori K.A., Haslinawati M.M. (2009). "Producing Amorphous White Silica from Rice Husk," *MASAUM Journal of Basic and Applied Sciences*, Vol. 1, No. 3, 512.

Moon, R. J., Martini, A., Nairn, J., Simonsen J., Youngblood, J., (2011). "Cellulose nanomaterials review: structure, properties and nanocomposites", Chem. Soc. Rev., 40, pp (3941-3994).

Moran, J. I., Alvarez, A. V., Cyras, P. V., Vazquez, A. (2008). "Extraction of cellulose and preparation of nanocellulose from sisal fiber", *Cellulose* 15, 149-159.

Nakagaito, A. N., Yano, H. (2004). "The effect of morphological changes from pulp fiber towards nano-scale fibrillated cellulose on the mechanical properties of high- strength plant fiber based composites", *Applied Physics A: Materials Science & Processing* 78(4), 547-552.

Pandey A., Mathew, G. M., Sukumaran, R.K., Singhania, R. R. (2008). "Progress in Research on Fungal Celluloses for Lignocellulose Degradation", *Journal of Scientific and industrial Research,* 67:898-907.

Peng, B. L., Dhar, N., Liu, H. L., Tam, K. C. (2011). "Chemistry and applications of nanocrystalline cellulose and its derivatives: a nanotechnology perspective", Can. J. Chem. Eng., 89, 1191-1206.

Piva, A., Steudner, S., and Wiebeck, H. (2004). Physico- mechanical properties of rice husk powder filled polypropylene composites with coupling agent study. In: Proceedings of the Fifth International Symposium on Natural Polymer and Composites; São Pedro/SP, Brazil.

COMPARATIVE STUDY OF THE CHARACTERISTICS STRENGTH OF REINFORCEMENT BARS IN THE LOCAL MARKET (A CASE STUDY OF GUSAU METROPOLIS)

***SHOLADOYE, I. O AND UCHECHUKWU ANYA**
Department of Civil Engineering Technology, Federal Polytechnic Kaura Namoda, Zamfara State, Nigeria
*Corresponding author: e-maill: kemtalsi@yahoo.com

ABSTRACT
This study is a reawaking of the consciousness of all key players in the construction industries on the need to properly examine the properties of building materials in this case of reinforcing steel in the market. Tensile strength, bending, bar size identification and elongation behaviour was investigated for reinforcing steel bars sold in Gusau metropolis; this was done to ascertain the level of conformity of the tested parameters with the standards. A total of 30 samples were collected from Gusau and taken to KADPOLY for the various tests to be carried out. This research evaluates the behavior of reinforcing steel used in Nigerian concrete structures. The research considers the test results of 16mm reinforcing bars adopted for structural purposes within Gusau. 80% of 16mm bars failed to meet the BS code prescription of 460N/mm^2 yield strength and 600 N/mm^2 of the ultimate yield strength, 25% of 16mm bar failed to meet the Nigerian's professional's prescription 580 N/mm^2. The elongation test was satisfactory, but showed high level of ductility, the bending test was ok there was no sign of crack or residue.

INTRODUCTION

An understanding of the properties of materials is essential in both design and applications of any engineering project if it is to prove satisfactory for its intended purpose (Anthony, 2010). Engineering failure frequently caused by misuse of materials or the engineer did not understand the properties of the materials (Ashby *et al.*, 1990).

Most local construction companies in Nigeria make all their reinforcing steel procurements from the open local markets without any technical information that guide users on the appropriate use (Arum, 2008). The aim of the research was to determine the characteristics strength of 16mm reinforcement steel bars sold in Gusau metropolis.

REINFORCING OF STEEL

Concrete is strong in compression but weak in tension. The tensile strength is generally rated about 10 percent of the compression strength. For this reason, concrete works well for columns and posts that are compression members in a structure. But, when it is used for tension members, such as beams, girders, foundation walls, or floors, concrete must be reinforced to attain the necessary tension strength.

METHODOLOGY

MATERIALS

Reinforcement steel bars of different sizes (12mm, 16mm)
Weighing balance (weighing machine).
Vanier calliper.
Measuring tape.
Electric universal testing machine.
Compression machine was used in the absence of brenner bending machine.

COLLECTION OF MATERIALS

Reinforcement steel bars for test were gotten from Igbo line in Gusau Zamfara State. The reinforcement steel bars were collected from different shops. Reinforcement steel bars of 16mm of averagely 500mm in height was collected and was taken to Kaduna polytechnic college of engineering in civil engineering department to determine the mechanical properties of steel bars.

SAMPLES PREPARATION

The various samples specimens were arrange according to their product which where label as company A, B and C in other to achieve an accurate results. The specimens were first measured to know the actual length of each specimen which is 500mm diameter of average length the material was also weighed.

TENSILE STRENGTH TEST

The tension test specimen are measured to know the original length by using tape and the size of the steel is measure to know the original size of the steel bars by using the venire caliper before it was gage to the tension machine (DOH 15). When it is place in the machine the piece is grip or hold in the machine before the transmission of the load from

the heads of the machine to the specimen under test then release it to allow the specimen until it break as shown with plate 1(Charles and Mark 2002). Then all the readings or data are recorded for all the specimens. All this is done for all the samples specimens.

The load at which there is a halt or hesitation of the load indicating pointer is noted and termed the "yield point". The stress at this point is computed and termed the yield stress. The yield stress is calculated by dividing the load at the "yield point" by the nominal cross-sectional area of the test specimen.

Tensile Strength – Calculate the tensile strength of the Deformed Bar by dividing the maximum load the specimen sustains during a tension test by the original cross sectional area of the specimen as in Equations (1) and (2).

$$Yield\ Stress = \frac{Load\ at\ yield\ point}{Nominal\ Cross\ sectional\ Area} \quad (1)$$

$$Tensile\ Strength = \frac{Maximum\ load}{Nominal\ Cross\ sectional\ Area} \quad (2)$$

ELONGATION

The percentage of elongation is determined by fitting the ends of the fractured Specimens together carefully and measure the distance between the gage marks to the nearest 1/8" (0.32 cm). The elongation is the increase in length of the gage length, expressed as a percentage of the original gage length. In reporting elongation values, give both the percentage increase and the original gage length using Equation (3).

$$EL = \frac{(elongation\ at\ rapture) \times 100}{(initial\ gage\ lengt\ )} \quad (3)$$

where EL = percentage elongation

BENDING TEST

The bend test is one method for evaluating ductility, but it cannot be considered as a quantitative means of predicting service performance in bending operations (Restrepo, *et al.,* 1999). The severity of the bend test is primarily a function of the angle of bend and inside diameter to which the specimen is bent, and of the cross-section of the specimen (Parker, 2008). These conditions are varied according to location and orientation of the test specimen and the chemical composition, tensile properties, hardness, type, and quality of the steel specified. Bend the test specimen at room temperature to an inside diameter, as designated by the applicable product specifications, to the extent specified without major cracking on the outside of the bent portion as shown on plate 2.

RESULTS AND DISCUSSION

The results obtained from laboratory tests were used, to determine the percentage pass and failure rate of the materials being tested using a standard of 460N/mm^2 from BS 4449: 1997. But in Nigeria, structural designers are forced to adopt yield strength of 410N/mm^2 due to the substandard quality of reinforcement produced within the country and imported from other countries.

TENSILE STRENGTH TEST AND ANALYSIS OF 16 MILLIMETRE DIAMETER BARS

The yield strength values obtained with the samples which are gotten from the Tables 1 and 2 for COMPANY A and B have values which are lower than the standard limit of 460N/mm^2 set by BS; 1997, but also below limits of 415N/mm^2 and 420 N/mm^{2}set by ASTM A706, but COMPANY C as shown on Table 3 have values which are above the standard required. The ultimate or maximum tensile strength of all the steel product samples from COMPANY A, B and C tested were lower than the recommended limit of 600N/mm^2 by BS449, 1997 and Nst65-Mn1994 limit of 580 N/ mm^2 by ASTM A706 only 6 out of 10 met the ultimate tensile test.

The permissible elongation (%) stated by BS 4449: 1997 Table 7 is 14% for grade 460Bd steel reinforcement. The high percentage elongation values gotten from the samples from the bar sizes of 16mm from companies A, B, and C indicates high ductility as shown in Tables 4, 5 and 6. High percentage of ductility is not a desirable property in reinforcement bar as it makes it susceptible to bending. These materials will behave more as mild still rather than high strength still desired for reinforcement.

BENDING TEST

The bend test was carried out in accordance with the BS4449 (1997) provisions using compression machine. The result of the test showed no evidence of cracks or residue that dropped from the reinforcement steel bars during the bending.

TABLE 1: Company A, summary of samples in tension.

S/No	Identification no	Actual Diameter	Area	Yield Load (kN)	Maximum Load (kN)	Yield Stress (N/mm^2)	Maximum Stress (N/mm^2)
1	$A_{16}T1$	16	201.216	89	89	442	442
2	$A_{16}T2$	16	201.216	81	92	403	457
3	$A_{16}T3$	16	201.216	79	91	391	452
4	$A_{16}T4$	16	201.216	80	92	399	457
5	$A_{16}T5$	16	201.216	81	92	401	456
6	$A_{16}T6$	16	201.216	82	92	409	456
7	$A_{16}T7$	16	201.216	84	91	415	451
8	$A_{16}T8$	16	201.216	80	92	396	456
9	$A_{16}T9$	16	201.216	82	92	405	455
10	$A_{16}T10$	16	201.216	79	91	392	451

TABLE 2: Company B, summary of samples in tension.

S/No	Identification no	Actual Diameter	Area	Yield Load (kN)	Maximum Load (kN)	Yield Stress (N/mm^2)	Maximum Stress (N/mm^2)
1	$B_{16}T1$	16	201.216	79	89	393	442
21	$B_{16}T2$	16	201.216	80	92	398	457
3	$B_{16}T3$	16	201.216	82	91	408	452
4	$B_{16}T4$	16	201.216	81	89	403	441
5	$B_{16}T5$	16	201.216	80	91	398	453
6	$B_{16}T6$	16	201.216	82	92	406	459
7	$B_{16}T7$	16	201.216	80	92	399	456
8	$B_{16}T8$	16	201.216	81	91	403	455
9	$B_{16}T9$	16	201.216	82	91	405	451
10	$B_{16}T10$	16	201.216	81	90	401	449

TABLE 3: Company C, summary of samples in tension.

S/No	Identification no	Actual Diameter	Area	Yield Load (kN)	Maximum Load (kN)	Yield Stress (N/mm^2)	Maximum Stress (N/mm^2)
1	C16T1	16	201.216	110	119	547	591
2	C16T2	16	201.216	98	101	487	502
3	C16T3	16	201.216	105	125	522	621
4	C16T4	16	201.216	103	121	512	600
5	C16T5	16	201.216	113	101	560	503
6	C16T6	16	201.216	108	115	537	570
7	C16T7	16	201.216	103	122	509	608
8	C16T8	16	201.216	96	121	476	604
9	C16T9	16	201.216	98	119	487	593
10	C16T10	16	201.216	117	109	581	541

TABLE 4: Company A, summary of samples in elongation test.

S/No	Identification no	Length (mm)	Guage Length (mm)	Actual Dia. (mm)	Reduced dia. (mm)	% Reduced in dia. at fracture (mm)	Elongation % at Max. Stress
1	$A_{16}E1$	500	150	16	14	13	30
2	$A_{16}E2$	400	150	16	13	19	38
3	$A_{16}E3$	400	150	16	14	13	38
4	$A_{16}E4$	500	150	16	14	13	30
5	$A_{16}E5$	500	150	16	13	19	30
6	$A_{16}E6$	40	150	16	14	13	30
7	$A_{16}E7$	450	150	16	13	19	33
8	$A_{16}E8$	400	150	16	14	13	38
9	$A_{16}E9$	550	150	16	12	25	27
10	$A_{16}E10$	400	150	16	14	13	38

TABLE 5: Company B, summary of samples in elongation test.

S/No	Identification no	Length (mm)	Guage Length (mm)	Actual Dia. (mm)	Reduced dia. (mm)	% Reduced in dia. at fracture (mm)	Elongation % at Max. Stress
1	$B_{12}E1$	530	135	12	9	25	25
2	$B_{12}E2$	530	135	12	10	17	25
3	$B_{12}E3$	530	135	12	10	17	25
4	$B_{12}E4$	530	135	12	9	25	25
5	$B_{12}E5$	530	135	12	10	17	25
6	$B_{12}E6$	530	135	12	10	17	25
7	$B_{12}E7$	530	135	12	9	25	25
8	$B_{12}E8$	530	135	12	10	17	25
9	$B_{12}E9$	530	135	12	10	17	25
10	$B_{12}E10$	530	135	12	11	8	25

TABLE 6: Company C, summary of samples in elongation test.

S/No	Identification no	Length (mm)	Guage Length (mm)	Actual Dia. (mm)	Reduced dia. (mm)	% Reduced in dia. at fracture (mm)	Elongation % at Max. Stress
1	$C_{16}E1$	500	150	16	13	19	30
2	$C_{16}E2$	500	150	16	14	13	30
3	$C_{16}E3$	500	150	16	15	6	30
4	$C_{16}E4$	500	150	16	13	19	30
5	$C_{16}E5$	500	150	16	14	13	30
6	$C_{16}E6$	500	150	16	15	6	30
7	$C_{16}E7$	500	150	16	13	19	30
8	$C_{16}E8$	500	150	16	14	13	30
9	$C_{16}E9$	500	150	16	15	6	30
10	$C_{16}E10$	500	150	16	13	19	30


Plate 1: Tensile Test


Plate 2: Bending Test

CONCLUSION AND RECOMMENDATIONS

CONCLUSION

The study will help practice engineers to appreciate the place of steel in civil engineering works and their specific use. It also draws the attention of the government as well as the regulatory bodies to critically examine the properties of steel used in the construction industries with a view of to making efficient laws to properly control the steel industries in Nigeria so as to put a lasting solution to incidence of collapse of building.

RECOMMENDATIONS.

A constant check and re-evaluation by Government agency within the industry is recommended and cannot be over emphasized.

There should be technical information on all steel reinforcement sold in the open markets so as to guide the designers on their strength and deformation characteristics.

Regulatory authorities such as the Standards Organisation of Nigeria, Council for the Regulation of Engineering in Nigeria and tertiary institutions should strengthen their collaborations on ensuring quality standards through materials testing.

REFERENCES

Anthony N. E. (2010), Building Collapse in Nigeria, International Journal for Civil and Environmental Vol. 10 No. 0632.

Arum, C. (2008): "Verification of Properties of Concrete Reinforcement Bars:- Nigerian Case Study" - Published by : A Journal of Indoor and Built Environment by SAGE Publications. http:ibe.sagepub.com PP.370-376

BS 4449 (1997): Specification for Carbon Steel Bars for the Reinforcement of Concrete

ASTM E 290-97A, 2006, *"Standard Test Methods for Bend Testing of Material for Ductility"*, ASTM International, PA, USA. (www.astm.org).

Babaei, K. and Hawkins, N. M., (1991): *"Development of Standard Specifications for Bending/Straightening Concrete Reinforcing Steel",* Washington State Transportation Center (TRAC), Seattle, Washington

Babaei, K. and Hawkins, N. M., 1992, *"Field Bending and Straightening of Reinforcing Steel",* Concrete International, Journal of ACI, Januari 1992, page 67-72

British Standards Institution BS 4482 (1985)" Cold Reduced Steel Wire for the Reinforcement of Concrete" pp. 1-26

Charles K.K. and Mark A (2002) "Strength & Ductility Characteristics of Reinforcing Steel Bar milled from Scrap Metals"- Materials and Design 23 pp.537-545

DOH 15: Testing of Reinforcing Steel: pp. D-39-D41

Parker, F., (2008): *"To Bend or Not to Bend",* Monolithic Dome Articles, 177 Dome Park Palace. Italy

Restrepo, J.I., Crissafulli, F.J. and Park, R., (1999): *"How Harmful is Bending/Straightening of Reinforcing Bars?",* Concrete International, Journal of ACI, April 1999, page 45-48

EFFECTS OF THERMAL RADIATION AND VARIABLE VISCOSITY ON NATURAL CONVECTION FLOW PAST A VERTICAL PLATE IN A SLIP FLOW REGIME

PRINCELY O. OJEAGBASE
Department of Mathematics, Ahmadu Bello University, Zaria, Nigeria

ABSTRACT
In this present study, thermal radiation and variable viscosity on natural convection flow past a vertical porous plate in a slip flow regime is investigated. The temperature jump, concentration jump as well as the velocity slip is taken into account. The governing equations are transformed into a set of non linear ordinary differential equations and solved using the perturbation method. The influence of the flow parameter on fluid temperature, concentration and velocity are presented graphically. From the course of investigation, it was revealed that increasing thermal radiation parameter increases both fluid temperature and velocity. In addition, increasing rarefraction parameter increases fluid velocity and boundary layer thickness while it decreases fluid temperature and concentration and the boundary layer thickness.

Keywords *– free convection; incompressible fluid; variable viscosity; heat transfer; thermal radiation; boundary jumps.*

1. Introduction

The phenomenon of free convective flow with thermal radiation has been a subject of interest of many researches because of its importance in processes involving high temperatures such as in space technology, nuclear power plants, gas turbines and underground energy transport. The effect of radiation on natural convection flow of s gas past a semi- infinite flat plate using the Cogley- Vincentine Giles equilibrium model was investigated by Saundalgekar and Takhar [1].

The effect of radiation using the Rosseland diffusion approximation which leads to non similar solutions for the forced and free convection flow of an optically dense viscous incompressible fluid past a heated vertical plate was analyzed by Hassain and Takhar [2]. They considered gray gases that emit and absorb which do not scatter thermal radiation. Hossain et al [3] have studied the effect of radiation on natural convection flow of an optically uniformly heated vertical plate with uniform suction using the Rosseland diffusion approximation. Ganesan and Loganadhen [4] have investigated the radiation and mass transfer effects flow of incompressible viscous fluid past a moving vertical cylinder using Rosseland approximation by the Crank-Nicolson finite difference method.

Ramanchandra et al [5] studied the interaction of free convection with thermal radiation of a viscous incompressible unsteady flow past an impulsively started vertical plate with heat and mass transfer using Rosseland approximation. They considered an implicit finite difference method of Crank-Nicolson type for solution of the governing equations. The effect of thermal radiation on a steady two- dimensional mixed convection laminar flow of viscous incompressible optically thick fluid along a vertical wavy surface has been investigated using the Keller box method and the straight forward finite difference method by Moller and Hossain [6].

In all the above mentioned work, the fluid viscosity was assumed constant. However, flow of fluids significantly requires variation of viscosity with temperature. Carey and Mollendorf [7] have investigated the effect of variable viscosity in several natural convection flows using a regular perturbation method. Pozzi and Lupo [8] used Pade- approximation techniques to investigate the effect of variable property in free convection. Recently, Kafoussias and William [9] and Rees and Kafoussias [10] studied the effect of temperature dependent viscosity on the mixed convection flow from a vertical flat plate in the region that is near the leading edge using the local non- similarity method.

The effect of thermal radiation on natural convection flow along a uniformly heated vertical porous plate with variable viscosity and uniform suction velocity has been investigated numerically by Hossain et al [11]. Elbashbeshy and Dimian [12] have solved the effect of radiation on the flow and heat transfer over a wedge with variable viscosity using the Runge- kutta method. The effects of radiation and variable fluid viscosity on flow and heat transfer along a symmetric wedge were investigated by Mukhopadhyay [13]. In his work, the fluid viscosity is assumed to vary as a linear function of temperature.

The rarefraction effect in gases is the ratio of the mean free path to the characteristic length. Its effect on the slip flow regime cannot be neglected and remain applicable in engineering and industries provided the velocity slip, temperature jump and concentration jump are taken into account at the boundary wall. Balamurugan et al [14] investigated the effect of chemical reaction on natural convection flow past a moving vertical plate with time dependent suction in a slip flow regime using the perturbation technique. Swati and Iswar [15] studied the effects of velocity slip and thermal slip on MHD boundary layer mixed convection flow and heat transfer of an incompressible fluid past a vertical plate in the presence of suction/ blowing using numerical method. Sharma [16] studied the effect of combined heat and mass transfer on unsteady free convective flow past a vertical flat plate in a slip flow regime using the perturbation technique. This present study extends the work of Sharma [16] with thermal radiation, temperature dependent viscosity and boundary jumps as they have significant applications in industries.

2. Formulation of Problem

We consider the free convective heat and mass transfer flow of a viscous incompressible fluid past an infinite vertical porous plate in a slip flow regime. Also, the suction velocity $\left[V = -\frac{\nu}{h}\left(1 + \varepsilon A e^{i\omega^* t^*}\right)\right]$ is assumed to vary with time while the viscosity of the fluid is temperature dependent. The flow is assumed to be in the x^*- direction which is taken vertically upward along the vertical porous plate and the y^*-axis is taken normal to the plate. Since the plate is considered infinite in length, the velocity, temperature and concentration fields are function of y^* and t^* only. The flow is considered optically thick gray gas with natural convection and radiation. The physical configuration of the problem is given in figure 1. Neglecting viscous dissipation and assuming variation of density in the body force term (Boussinesq's approximation), the problem is governed by the following set of equations:

$$\frac{\partial u^*}{\partial t^*} + V^* \frac{\partial u^*}{\partial y^*} = g\beta(T^* - T_\infty^*) + g\beta^0(C^* - C_\infty^*) + \frac{1}{\rho}\frac{\partial}{\partial y^*}\left(\mu \frac{\partial u^*}{\partial y^*}\right) \quad (1)$$

$$\frac{\partial T^*}{\partial t^*} + V^* \frac{\partial T^*}{\partial y^*} = \frac{\kappa}{\rho c_p}\frac{\partial^2 T^*}{\partial y^{*2}} - \frac{1}{\rho cp}\frac{\partial q_r}{\partial y} \quad (2)$$

$$\frac{\partial C^*}{\partial y^*} + V^* \frac{\partial C^*}{\partial y^*} = D\frac{\partial^2 C^*}{\partial y^{*2}} \quad (3)$$

The boundary conditions of the problem are:

$$T^* = T_w^* + \varepsilon(T_w^* - T_\infty^*)e^{i\omega^* t^*} + L\frac{\partial T^*}{\partial y^*}, u^* = L\frac{\partial u^*}{\partial y^*} \quad (4)$$

$$C^* = C_w^* + \varepsilon(C_w^* - C_\infty^*)e^{i\omega^* t^*} + L\frac{\partial C^*}{\partial y^*} \text{ at } y^* = 0$$

$u^* \to 0$, $T^* \to T_\infty^*$, $C^* \to C_\infty^*$ as $y^* \to \infty$ (5) the fluid viscosity μ is assumed to vary with temperature as:

$$\mu = \mu_0[1 - a(T^* - T_\infty^*)] \quad (6)$$

where 'a' is a constant with the dimension of β (thermal expansion of the fluid) and its value depend on the reference state of the fluid. Also, $\mu = \mu_0$ is the viscosity constant at $T^* = T_\infty^*$.

In general, a>0 is for liquids such as water, benzene, crude oil in which fluid viscosity decreases with growing temperature whereas a<0 is for gases like air, helium or methane in which fluid viscosity increases as temperature increases.

Simplifying the radiative heat flux term using the Rosseland approximation for radiation of an optically thick boundary layer given by Siegel and Howell [17] and Raptis et al [18], we have:

$$q_r = -\frac{4\sigma^*}{3k^*}\frac{\partial T^{*4}}{\partial y^*} \quad (7)$$

where σ^* and k^* are the Stefan- Boltzmann constant and Rosseland mean absorption coefficient respectively.

We assume that the temperature difference within the flow is sufficiently small such that T^{*4} may be expressed as a linear function of temperature. Hence, expanding T^{*4} in a Taylor series about T^* and neglecting higher order terms, we get:

$$T^{*4} \cong 4T_\infty^{*3}T^* - 3T_\infty^{*4} \quad (8)$$

Substituting equations (7) and (8) into equation (2), we obtain:

$$\frac{\partial T^*}{\partial t^*} + V^* \frac{\partial T^*}{\partial y^*} = \frac{k}{\rho cp}\left(1 + \frac{16\sigma^* T_\infty^{*3}}{3kk^*}\right)\frac{\partial^2 T^*}{\partial y^{*2}} \quad (9)$$

where $R = \dfrac{kk^\bullet}{4\sigma^* T_\infty^{\bullet 3}}$ is the thermal radiation parameter

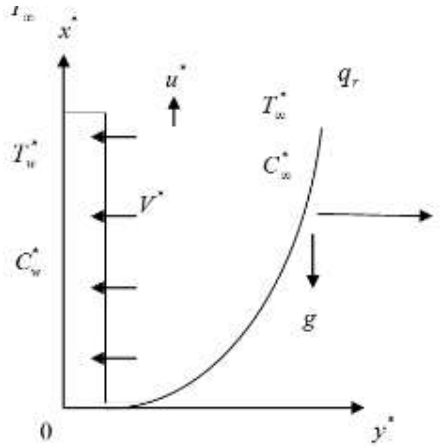


Figure 1: The physical configuration of the problem

We introduce the following non- dimensional quantities

$$y = \frac{y^*}{h},\ t = t^*\frac{\nu}{4h^2},\ u = \frac{u^*}{V_0^*},\ \omega = \frac{4h^2\omega^*}{\nu},\ \theta = \frac{T^* - T_\infty^*}{T_w^* - T_\infty^*},\ C = \frac{C^* - C_\infty^*}{C_w^* - C_\infty^*}$$

$$Gr = \frac{g\beta h^2(T_w^* - T_\infty^*)}{\nu V_0},\ Gc = \frac{g\beta^0 h^2(C_w^* - C_\infty^*)}{\nu V_0^*},\ \Pr = \mu\frac{c_p}{\kappa} = \frac{\nu\rho c_p}{\kappa},\ Sc = \frac{\nu}{D} \quad (10)$$

$$Kn = \frac{L}{h},\ \lambda = a(T_w^* - T_\infty^*)$$

where $(*)$ stands for dimensional quantities, g is the acceleration due to gravity, T^* is the fluid temperature, c_p is the specific heat of the fluid at constant pressure κ is the thermal conductivity of the fluid. Pr is the prandtl number, Sc is the Schmidt number, Kn is the rarefaction parameter, A is the suction parameter, ω^* is the frequency parameter, the subscript ∞ denotes the free stream condition, w denotes condition at the wall and λ is the dimensionless viscosity parameter.

Equations (1) to (3) reduces to the following non- dimensional form using the transformation equation (10).

$$\frac{1}{4}\frac{\partial u}{\partial t} - (1 + \varepsilon A e^{i\omega t})\frac{\partial u}{\partial y} = Gr\theta + GcC + (1 - \lambda\theta)\frac{\partial^2 u}{\partial y^2} - \lambda\left(\frac{\partial u}{\partial y}\frac{\partial \theta}{\partial y}\right) \quad (11)$$

$$\frac{1}{4}\frac{\partial\theta}{\partial t}-(1+\varepsilon Ae^{i\omega t})\frac{\partial\theta}{\partial y}=\frac{(1-\lambda\theta)(1+\frac{4}{3R})}{\Pr}\frac{\partial^2\theta}{\partial y^2} \quad (12)$$

$$\frac{1}{4}\frac{\partial C}{\partial t}-(1+\varepsilon Ae^{i\omega t})\frac{\partial C}{\partial y}=\frac{1}{Sc}\frac{\partial^2 C}{\partial y^2} \quad (13)$$

The boundary conditions to the problem in the dimensionless form are:

$$u=Kn\frac{\partial u}{\partial y},\ \theta=1+\varepsilon e^{i\omega t}+Kn\frac{\partial\theta}{\partial y},\ C=1+\varepsilon e^{i\omega t}+Kn\frac{\partial C}{\partial y}\ \text{ at }\ y=0$$

$$u\to 0,\ \theta\to 0,\ C\to 0\ \text{ as }\ y\to\infty \quad (14)$$

3. Solution of the Problem

In order to solve the differential equations (11) to (13), we assume the amplitude Oscillation ($\varepsilon << 1$) to be very small. The solutions of the velocity u, temperature θ and concentration C near the plate are as follow:

$$u(y,t)=u_0+\varepsilon u_1(y)e^{i\omega t}$$

$$\theta(y,t)=\theta_0+\varepsilon\theta_1(y)e^{i\omega t} \quad (15)$$

$$C(y,t)=C_0+\varepsilon C_1(y)e^{i\omega t}$$

Substituting equation (15) into equations (13) to (15), equating the coefficients of harmonic and non harmonic terms, neglecting the coefficients of ε^2, we get:

$$(1-\lambda\theta_0)u_0''+(1-\lambda\theta_0')u_0'=-Gr\theta_0-GcC_0 \quad (16)$$

$$(1-\lambda\theta_0)\theta_0''+\Pr d\theta_0'=0 \quad (17)$$

$$C_0''+ScC_0'=0 \quad (18)$$

$$(1-\lambda\theta_0)u_1''+(1-\lambda\theta_0')u_1'+\frac{i\omega u_1}{4}=-Gr\theta_1-GcC_1-Au_0'+\lambda\theta_1u_0''+\lambda u_0'\theta_1' \quad (19)$$

$$(1-\lambda\theta)\theta_1''+\Pr d\theta_1'-\frac{\Pr di\omega\theta_1}{4}=-A\Pr d\theta_0'+\lambda\theta_1\theta_0'' \quad (20)$$

$$C_1''+ScC_1'-\frac{Sc\omega C_1}{4}=-AScC_0' \quad (21)$$ The modified boundary conditions are:

$$u_0=Knu_0',\ u_1=Knu_1',\theta_0=1+Kn\theta_0',\theta_1=1+Kn\theta_1',$$

$$C_0=1+KnC_0',\ C_1=1+KnC_1'\ \text{ at }\ y=0$$

$$u_0\to 0,u_1\to 0,\ \theta_0\to 0,\ \theta_1\to 0,\ C_0\to 0,C_1\to 0,\ \text{as}\ y\to\infty \quad (22)$$

Where $d=\dfrac{1}{1+\frac{4}{3}R}$ and primes denote differentiation with respect to y

Equations (16), (17), (19) and (20) are still coupled for the variables u_0, u_1, θ_0 and θ_1. To solve them, we again use a regular perturbation technique with λ as a perturbation parameter and u_0, u_1, θ_0 and θ_1 take the form:

$$u_0=u_{00}+\lambda u_{01},\ u_1=u_{10}+\lambda u_{11},\ \theta_0=\theta_{00}+\lambda\theta_{01},\ \theta_1=\theta_{10}+\lambda\theta_{11} \quad (23)$$

with λ as a very small parameter. Substituting (3.31) into equations (3.24) to (3.27) and equating the like powers of λ, we get:

$$u_{00}''+u_{00}'=-Gr\theta_0-GcC_0 \quad (24)$$

$$u_{01}^{''} + u_{01}^{'} = \theta_0 u_{00}^{''} + \theta_0^{'} u_{00}^{'} \quad (25)$$

$$u_{10}^{''} + u_{10}^{'} - \frac{i\omega u_{10}}{4} = -Gr\theta_1 - GcC_1 - Au_{00}^{'} \quad (26)$$

$$u_{11}^{''} + u_{11}^{'} - \frac{i\omega u_{11}}{4} = \theta_0 u_{10}^{''} + \theta_0^{'} u_{10}^{'} - Au_{01}^{'} + \theta_1 u_{00}^{''} + \theta_1^{'} u_{00}^{'} \quad (27)$$

$$\theta_{00}^{''} + \Pr d\theta_{00}^{'} = 0 \quad (28)$$

$$\theta_{01}^{''} + \Pr d\theta_{01}^{'} = \theta_{00}\theta_{00}^{''} \quad (29)$$

$$\theta_{10}^{''} + \Pr d\theta_{10}^{'} - \frac{\Pr di\omega\theta_{10}}{4} = -\Pr dA\theta_{00}^{'} \quad (30)$$

$$\theta_{11}^{''} + \Pr d\theta_{11}^{'} - \frac{\Pr di\omega\theta_{11}}{4} = -\Pr dA\theta_{01}^{'} + \theta_{00}\theta_{10}^{''} + \theta_{10}\theta_{00}^{''} \quad (31)$$

subject to the boundary conditions:

$$\begin{gathered} u_{00} = Knu_{00}^{'},\ u_{01} = Knu_{01}^{'}, u_{10} = Knu_{10}^{'}, u_{11} = Knu_{11}^{'}, \theta_{00} = 1 + Kn_{00}^{'} \\ \theta_{01} = 1 + Kn_{01}^{'},\ \theta_{10} = 1 + Kn_{10}^{'},\ \theta_{11} = 1 + Kn_{11}^{'} \ at \ \ y \to 0 \\ u_{00} = u_{01} = u_{10} = u_{11} \to 0,\ \theta_{00} = \theta_{01} = \theta_{10} = \theta_{11} \to 0 \text{ as } y \to \infty \end{gathered} \quad (32)$$

Solving equations (18), (21), (24) to (31) - (3.40) under the boundary conditions (32) , we get:

$$C_0 = A_1 e^{-Scy}$$

$$C_1 = A_2 e^{-Scy} + A_3 e^{-m_2 y}$$

$$\theta_{00} = A_4 e^{-\Pr y}$$

$$\theta_{01} = A_6 e^{-\Pr y} + A_5 e^{-2\Pr dy}$$

$$\theta_{10} = A_8 e^{-m_1 y} + A_7 e^{-\Pr dy}$$

$$\theta_{11} = A_{12} e^{-m_1 y} + A_{10} e^{-\Pr dy} + A_{10} e^{-2\Pr dy} + A_9 e^{-(m_1 + \Pr d)y} \quad (33)$$

$$u_{00} = A_{19} e^{-y} - A_{16} e^{-\Pr dy} - A_{17} e^{-2\Pr dy} - A_{18} e^{-Scy}$$

$$u_{01} = A_{27} e^{-y} + A_{20} e^{-(1+\Pr d)y} - A_{21} e^{-2\Pr dy} - A_{22} e^{-3\Pr dy} - A_{23} e^{-(\Pr d + Sc)y} + A_{24} e^{-(1+2\Pr d)y} - A_{25} e^{-4\Pr dy} - A_{26} e^{-(2\Pr d + Sc)y}$$

$$u_{10} = A_{28} e^{-m_3 y} - B_8 e^{-m_1 y} - B_9 e^{-\Pr dy} - B_{12} e^{-2\Pr dy} - B_{14} e^{-Scy} - B_{11} e^{-m_2 y} + B_{13} e^{-y} - B_{10} e^{-(m_1 + \Pr d)y}$$

$$u_{11} = A_{48} e^{-m_3 y} + A_{29} e^{-(m_3 + \Pr d)y} - A_{30} e^{-(m_1 + \Pr d)y} - A_{31} e^{-2\Pr dy} - A_{34} e^{-3\Pr dy} - A_{38} e^{-(\Pr d + Sc)y} - A_{33} e^{-(m_2 + \Pr d)y} + A_{36} e^{-(1+\Pr d)y} - A_{32} e^{-(m_1 + 2\Pr d)y} + A_{35} e^{-(m_3 + 2\Pr d)y} - A_{39} e^{-4\Pr dy} - A_{42} e^{-(Sc + 2\Pr d)y} - A_{41} e^{-(m_2 + 2\Pr d)y} + A_{40} e^{-(1+2\Pr d)y} - A_{37} e^{-(m_1 + 3\Pr d)y} + A_{43} e^{-y} - A_{45} e^{-(m_1 + Sc)y} + A_{46} e^{-(1 + m_1 + \Pr d)y} - A_{47} e^{-(m_1 + \Pr d + Sc)y} + A_{44} e^{-(1+m_1)y}$$

Applying (15) and (23) with (33), the temperature, concentration and velocity become:

$$C = A_1 e^{-Scy} + \varepsilon e^{i\omega t}(A_2 e^{-Scy} + A_3 e^{-m_2 y}) \quad (34)$$

$$\theta = A_{13} e^{-\Pr dy} + A_5 \lambda e^{-2\Pr dy} + \varepsilon e^{i\omega t}(A_{14} e^{-m_1 y} + A_{15} e^{-\Pr dy} + A_{10} \lambda e^{-2\Pr dy} + A_9 \lambda e^{-(m_1 + \Pr d)y}) \quad (35$$

$$u = (A_{19} + \lambda A_{27}) e^{-y} - A_{16} e^{-\Pr dy} - (A_{17} + A_{21}\lambda) e^{-2\Pr dy} - A_{18} e^{-Scy} + \lambda A_{20} e^{-(1+\Pr d)y} - \lambda A_{22} e^{-3\Pr dy} - A_{23} \lambda e^{-(\Pr d + Sc)y} + A_{24} \lambda e^{-(1+2\Pr d)y} - A_{25} \lambda e^{-4\Pr dy} - A_{26} \lambda e^{-(2\Pr d + Sc)y} + \varepsilon e^{-i\omega t}[(A_{28} + A_{48}\lambda) e^{-m_3 y} - B_8 e^{-m_1 y} - B_{14} e^{-Scy} - B_9 e^{-\Pr dy} - B_{11} e^{-m_2 y} - (B_{12} + A_{31}\lambda) e^{-2\Pr dy} + (B_{13} + A_{43}\lambda) e^{-y} - (B_{10} + A_{30}\lambda) e^{-(m_1 + \Pr d)y} + A_{29} \lambda e^{-(m_3 + \Pr d)y} - A_{34} \lambda e^{-3\Pr dy} - A_{38} \lambda e^{-(\Pr d + Sc)y} - A_{33} \lambda e^{-(m_2 + \Pr d)y} + A_{36} \lambda e^{-(1+\Pr d)y} - A_{32} \lambda e^{-(m_1 + 2\Pr d)y} + A_{35} \lambda e^{-(m_3 + 2\Pr)y} - A_{39} \lambda e^{-4\Pr dy} \quad (36)$$

$$- A_{42}\lambda e^{-(Sc+2\Pr d)y} - A_{41}\lambda e^{-(m_2+2\Pr d)y} + A_{40}\lambda e^{-(1+2\Pr d)y} - A_{37}\lambda e^{-(m_1+3\Pr d)y} - A_{45}\lambda e^{-(m_1+Sc)y}$$
$$+ A_{46}\lambda e^{-(1+m_1+\Pr d)y} - A_{47}\lambda e^{-(m_1+\Pr d+Sc)y} + A_{44}\lambda e^{-(1+m_1)y}]$$

where the coefficients $A_i (i = 0,1,2,....48)$ and $B_j (j = 1,2,....32)$ are defined in appendix I

4. Skin friction

The skin friction in the non- dimensional form on the plate $y = 0$ is given by:

$$\tau = (1-\lambda\theta)\left.\frac{\partial u}{\partial y}\right|_{y=0} \quad (37)$$

where: $\theta\big|_{y=0} = A_{13} + A_5\lambda + \varepsilon e^{i\omega t}[A_{14} + A_{15} + A_9\lambda + A_{10}\lambda]$

$$\left.\frac{\partial u}{dy}\right|_{y=0} = -(A_{19} + A_{27}\lambda) + \Pr dA_{16} + 2\Pr d(A_{17} + A_{21}\lambda) + ScA_{18} - A_{20}\lambda(1+\Pr d) + 3\Pr d\lambda A_{22} +$$
$$A_{23}\lambda(\Pr d + Sc) - A_{24}\lambda(1+2\Pr d) + 4\Pr dA_{25}\lambda + A_{26}\lambda(2\Pr d + Sc) + \varepsilon e^{i\omega t}[-m_3(A_{28} + A_{48}\lambda)$$
$$+ m_1 B_8 + ScB_{14} + \Pr dB_9 + m_2 B_{11} + 2\Pr d(B_{12} + A_{31}\lambda) - (B_{13} + A_{43}\lambda) +$$
$$(m_1 + \Pr d)(B_{10} + A_{38}\lambda) - A_{29}\lambda(m_3 + \Pr d) + 3\Pr dA_{34}\lambda + A_{38}\lambda(\Pr d + Sc) + A_{33}\lambda(m_2 + \Pr d)$$
$$- A_{36}\lambda(1+\Pr d) + A_{32}\lambda(m_1 + 2\Pr d) - A_{35}\lambda(m_3 + 2\Pr d) + 4\Pr dA_{39}\lambda + A_{42}\lambda(Sc + 2\Pr d)$$
$$+ A_{41}\lambda(m_2 + 2\Pr d) - A_{40}\lambda(1+2\Pr d) + A_{37}\lambda(m_1 + 3\Pr d) + A_{45}\lambda(m_1 + Sc) -$$
$$A_{46}\lambda(1 + m_1 + \Pr d) + A_{47}\lambda(m_1 + \Pr d + Sc) - A_{44}\lambda(1 + m_1)$$

5. Heat Transfer

The Nusselt number in non- dimensional form on the plate $y = 0$ is given by:

$$Nu = -\left(\frac{\partial\theta}{\partial y}\right)_{y=0} \quad (38)$$

$$Nu = \Pr dA_{13} + 2\Pr dA_5\lambda + \varepsilon e^{i\omega t}[m_1 A_{14} + \Pr dA_{15} + 2\Pr dA_{10}\lambda + A_9\lambda(m_1 + \Pr d)] \quad (39)$$

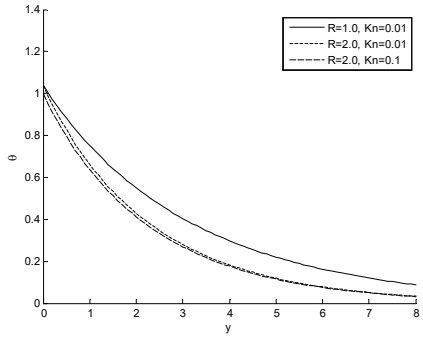


Figure 2: Temperature profile for different values of Kn and R when $\boldsymbol{\omega = 10}, \boldsymbol{\omega t = 0}$, $A = 5$, $\boldsymbol{\varepsilon = 0.02}$, $\lambda = 0.02$ and $\Pr = 0.71$

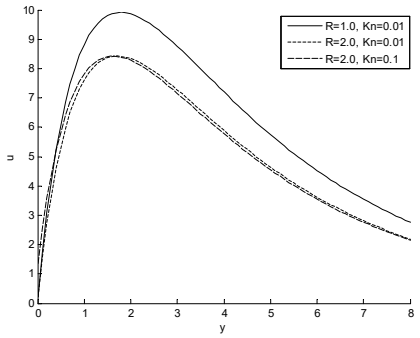


Figure 3: Velocity profile for different values of Kn and R when $Gr = 2$, $Gc = 2$, $A = 5$ $\lambda = 0.02$ $\boldsymbol{\omega = 10}, \Pr = 0.71, Sc = 0.22$ $\boldsymbol{\omega t = 0}$ and $\boldsymbol{\varepsilon = 0.02}$

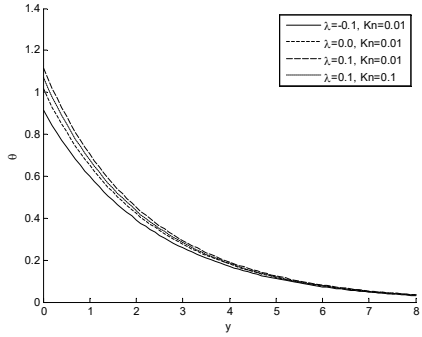


Figure 4: Temperature profile for different values of Kn and λ when $\boldsymbol{\omega = 10}, \boldsymbol{\omega t = 0}$, $A = 5$, $\boldsymbol{\varepsilon = 0.02}$, $R = 2$, $\lambda = 0.02$ and $\Pr = 0.71$

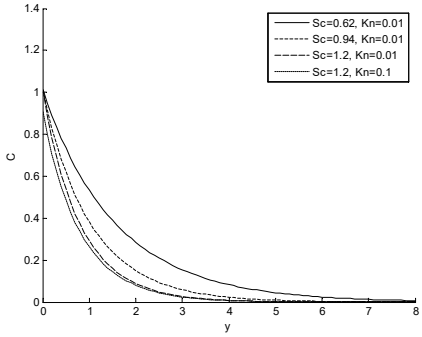


Figure 7: Concentration profile for different values of Kn and $Sc = 0.94$ when $\boldsymbol{\omega = 10}, \boldsymbol{\omega t = 0}$, $A = 5, R = 2$, $\boldsymbol{\varepsilon = 0.02}$, $\lambda = 0.002$ and $\Pr = 0.71$

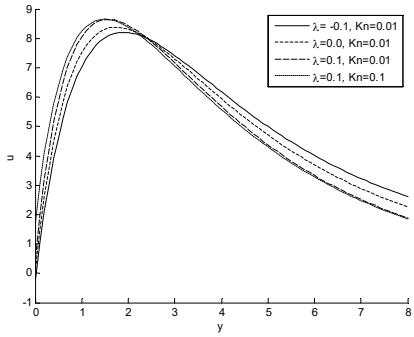


Figure 5: Velocity profile for different values of Kn and λ when $Gr = 2$, $Gc = 2$, $A = 5$ $\lambda = 0.02$ $\boldsymbol{\omega = 10}$, $R = 2$, $\Pr = 0.71$, $Sc = 0.22$ $\boldsymbol{\omega t = 0}$ and $\boldsymbol{\varepsilon = 0.02}$

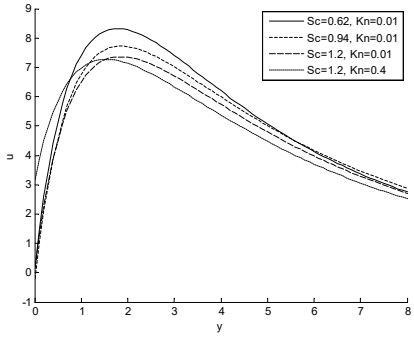


Figure 8: Velocity profile for different values of Kn and Sc when $Gr = 2$, $Gc = 2$, $A = 5$ $\lambda = 0.002$ $\boldsymbol{\omega = 10}$, $R = 2$, $\Pr = 0.71$, $\boldsymbol{\omega t = 0}$ and $\boldsymbol{\varepsilon = 0.02}$

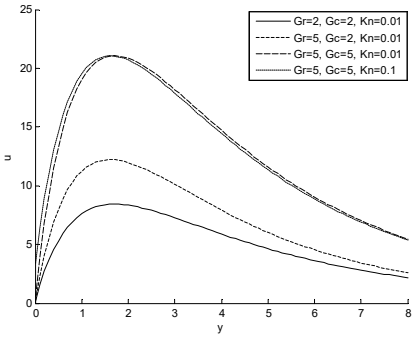


Figure 6: Velocity profile for different values of Kn, Gr and Gc when $A = 5$ $\lambda = 0.002$ $\boldsymbol{\omega = 10}$, $R = 2$, $\Pr = 0.71$, $Sc = 0.94$ $\boldsymbol{\omega t = 0}$ and $\boldsymbol{\varepsilon = 0.02}$

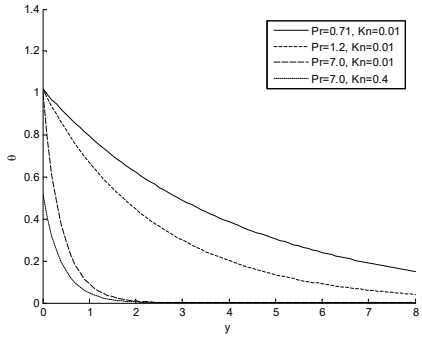


Figure 9: Temperature profile for different values of Kn and $\Pr$ when when $\boldsymbol{\omega = 10}, \boldsymbol{\omega t = 0}$, $A = 5$, $\boldsymbol{\varepsilon = 0.02}$, $R = 2$ and $\lambda = 0.002$

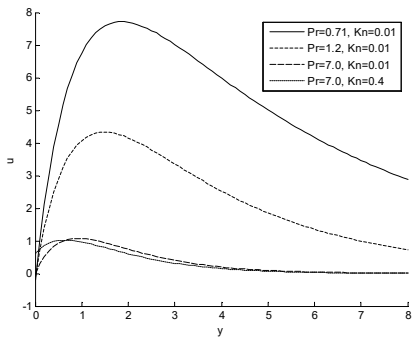


Figure 10: Velocity profile for different values of Kn and $\Pr$ when $Gr = 2$, $Gc = 2$, $A = 5$ $\lambda = 0.002\,\omega = 10,\ R = 2,\ Sc = 0.94,\ \omega t = 0$ and $\varepsilon = 0.02$

6. RESULTS AND DISCUSSIONS

This present article presents an unsteady natural convection heat and mass transfer flow of a vertical porous plate in a slip flow regime. The governing equations have been solved by perturbation technique to obtain the expressions for concentration, temperature and velocity fields. For the purpose of discussion, the concentration, temperature and velocity profiles are presented graphically by the use of MATLAB for different values of the governing parameters. The values of the Schmidt and Prandtl numbers are chosen to be $Sc = 0.94$(carbon dioxide) and $\Pr = 0.71$(air) while the boundary jumps and slip parameters are taken to be $Kn = 0.01$.

Table 1: The Skin friction (τ) and Nusselt number (Nu) for different values of viscosity parameter λ when $Gr = 2$, $Gc = 2$, $A = 5$, $Kn = 0.01$ $\boldsymbol{\omega = 10}$, $R = 2$, $Sc = 0.94$, $\boldsymbol{\omega t = 0}$ and $\boldsymbol{\varepsilon = 0.02}$

λ	τ	Nu
0.0	10.86723607	0.25447082
-0.2	8.00918223	0.17769244
-0.4	6.24531333	0.10091406
-0.6	5.25799747	0.02413568
-0.8	4.72960273	-0.05264270
-1.0	4.34249720	-0.12942108

Table 2: The Skin friction (τ) and Nusselt number (Nu) for different values of Radiation parameter R when $Gr = 2$, $Gc = 2$, $A = 5$ $\boldsymbol{\omega = 10}$, $\lambda = 0.002$ $Sc = 0.94$, $\boldsymbol{\omega t = 0}$, $Kn = 0.01$ and $\boldsymbol{\varepsilon = 0.02}$

R	τ	Nu
0.0	5.06273888	0.75885569
0.2	5.64755825	0.63288276
0.4	6.23203862	0.54292697
0.6	6.81627216	0.47547788
0.8	7.40032009	0.42302883
1.0	7.98422469	0.38107641

Table 3 Comparison of values of velocity and skin friction

A	Sharma [16] $Kn = 0,\ \varepsilon = 0.2$		Present work $\lambda = 0,\ \varepsilon = 0.2,\ Kn = 0, R = 0$	
	Velocity	Skin friction	Velocity	Skin friction
0.0	0.1513336	5.1409241	0.1513336	5.1409241
0.2	0.1513301	5.2128375	0.1513301	5.2128375
0.4	0.1513266	5.2847508	0.1513266	5.2847508
0.6	0.1513231	5.3566642	0.1513231	5.3566642
0.8	0.1513195	5.4285775	0.1513195	5.4285775
1.0	0.1513160	5.5004909	0.1513160	5.5004909

The influence of thermal radiation has been investigated in figures 2 and 3. It is observed that increasing the thermal radiation parameter decreases both fluid temperature and velocity. This is physically true because radiation add up energy to the fluid which significantly increases the movement of the fluid particles for temperature and velocity distributions within the boundary layers. In addition, the hydrodynamic boundary layer thickness decreases as a result of increasing the radiation parameter (R).

Also, from the figures, it is noticed that growing rarefraction parameter (Kn) decreases fluid temperature and the boundary layer thickness while the fluid velocity increases with the boundary layer thickness.

The temperature and velocity profiles for different values of viscosity parameter λ ($\lambda < 0$ for gas) are presented in figures 4 and 5. It is observed that fluid temperature decreases while fluid velocity increases near the plate. The figures further reveal a decrease in boundary layer thickness for

temperature and an increase in boundary layer thickness for growing Kn

Figure 6 illustrates the variation of velocity profile for different values buoyancy parameters Gr and Gc for the binary mixture of carbon dioxide in air. The fluid velocity increases near the plate and the decreases exponentially towards the free stream. Furthermore, increasing rarefraction parameter Kn increases the fluid velocity and the boundary layer thickness.

Figures 7 and 8 represent the variation of concentration and velocity for different values of Schmidt number Sc. It is noticed from these figures that as the fluid concentration and velocity decreases for increasing values of Sc. This causes the concentration buoyancy effects to decrease leading to a decrease in the fluid velocity. The figures further reveal that increasing rarefraction parameter lead to an increase in boundary layer thickness for fluid velocity and a decrease in boundary layer thickness for concentration.

The influence of Prandtl number $\Pr$ on temperature and velocity are presented if figures 9 and 10. It is seen from these figures that the fluid temperature and velocity decreases with increasing values of Prandtl number in the boundary layer.

The reason is that smaller values of $\Pr$ have more uniform temperature distribution across the thermal boundary layer as compared to larger values of the Prandtl number. The thickness of the boundary layer decreases with an increase in the values of $\Pr$. Also, increasing jump temperature decreases the boundary layer thickness while increase in velocity slip increases the boundary layer thickness.

Table 1 shows that both skin friction and rate of heat transfer decreases for increasing viscosity parameter ($\lambda < 0$ for gas). It is observed in table 2 that on increasing the thermal radiation parameter R, the skin friction increases while the rate of heat transfer decreases. The comparison of velocity and skin friction is shown in table 3. The numerical values presented in this work are in good agreement with those obtained by Sharma [16].

7. CONCLUSION

In this present paper, thermal radiation and variable viscosity on natural convection flow past a vertical plate in a ship flow regime has been considered. It can be concluded from this work that:

1. Increase in radiation parameter tend to increase both fluid temperature and velocity
2. Increase in radiation parameter increases skin friction while rate of heat transfer decreases
3. Increasing viscosity parameter decreases fluid temperature.

8. Nomenclature

a viscosity constant with dimension of β $[K^{-1}]$
A suction parameter
C^* species concentration
c_p specific heat at constant pressure $[ms^{-1}]$
C_∞^* concentration in free stream
C_w^* concentration at the wall
D molecular diffusivity of the species $[m^2 s^{-1}]$
g acceleration due to gravity $[ms^{-2}]$
Gc modified Grashof number (solutal)
Gr Grashof number
h characteristic length $[m]$
Kn Knudsen number
L molecular mean free path length $[m]$
Nu Nusselt number
q_r component of radiative flux
R radiation parameter
Pr Prandtl number
Sc Schmidt number
t^* time $[s]$
t dimensionless time
T^* temperature $[K]$
T_∞^* temperature of fluid in free stream $[K]$
T_w^* temperature of wall $[K]$
u dimensionless velocity
u^* velocity component $[ms^{-1}]$
V suction velocity $[ms^{-1}]$
V_0^* constant mean suction velocity $[ms^{-1}]$

GREEK LETTERS

ε amplitude

β coefficient of thermal expansion $[K^{-1}]$

β^0 coefficient of solutal expansion

κ thermal conductivity $[kgs^{-2}]$

θ dimensionless temperature

λ dimensionless viscosity parameter

μ_0 viscosity constant $[Nsm^{-2}]$

μ variable viscosity $[Nsm^{-2}]$

ν kinematic viscosity $[m^2 s^{-1}]$

ρ density $[kgm^{-3}]$

τ dimensionless shearing stress

τ^* shearing stress $[Nm^{-2}]$

ω dimensionless frequency

ω^* frequency $[s^{-1}]$

References

1. Soundalgekar V M and Takhar H S. Natural convection flow past a semi- infinite vertical plate. Modelling, Measur. and Cont. 1992; 51: 31- 40.
2. Hossain M A and Takhar H S. Radiation effect on mixed convection along a vertical plate with uniform surface temperature. International Journal Heat Mass Transfer. 1996; 31: 243- 248.
3. Hossain M A, Alim M A and Rees D A S. Effect of radiation on free convection from a porous vertical plate. International Journal Heat Mass Transfer. 1999; 42: 181- 191.
4. Ganesan P and Loganadan P. Radiation and mass transfer effects on flow on flow of an incompressible viscous fluid past a moving cylinder. International Journal Heat and Mass Transfer. 2002; 45: 4281- 4288.
5. Ramachandra P V, Bhaskar N R and Muthucumaraswamy R. Radiation and mass transfer effects on two- dimensional flow past an impulsively started infinite vertical plate. International Journal of Thermal Science. 2007; 46(12): 1251- 1258.
6. Molla M M and Hossain M A. Radiation effect on mixed convection laminar flow along a vertical wavy surface. International Journal of Thermal Science. 2007; 46(9): 926- 935.
7. Carey and Mollendorf. Variable viscosity effects in several natural convection flows. International journal of Heat and Mass Transfer. 1980; 23(1): 95- 109.
8. Pozzi A and Lupo M. Variable property effects in free convection. International Journal of Heat and Fluid Flow. 1990; 11(2): 135- 141.
9. Kafoussias NG and Williams EW. The effect of temperature- dependent viscosity on free-forced convective laminar boundary layer flow past a vertical isothermal flat plate. Acta Mechanica 1995; Vol.110: issue 1-4, pp.123-137.
10. Kafoussias NG and Rees DAS, and Daskalakis JE. Numerical study of the combined free-forced convective laminar boundary layer flow past a vertical isothermal flat plate with temperature dependent viscosity. Acta Mech 1998; vol.127:no. 1-4, pp. 39-50.
11. Hossain M A, Khalil K H and Kambiz V. The effect of radiation on free convection flow of fluid with variable viscosity from a porous plate. International Journal of Thermal Science. 2001; 40(2): 115- 124.
12. Elbashbeshy E M A and Dimian M F. Effect of radiation on the flow and heat transfer over a wedge with variable viscosity. Applied Mathematics and Computation. 2002. Vol. 132: 445- 454.
13. Mukhopadhyay S. Effects of radiation and variable fluid viscosity on flow and heat transfer along a symmetric wedge. Journal of Applied Fluid Mechanics. 2009; 2(2): 29-34.
14. Balamurugan K S , Raraprasad J L, Viyaya S and Varma K. Unsteady MHD free convective flow past a moving vertical plate with time dependent suction and chemical reaction in a slip flow regime. International Conference of Computational Heat and Mass Transfer. 2015; 127: 516-523.
15. Swati M and Iswar C M. MHD mixed convection slip flow and heat transfer over a vertical porous plate. Engineering Science and Technology, an International Journal. 2015; 18(1): 98- 105.
16. Sharma PK. Influence of periodic temperature and concentration on unsteady free convective viscous incompressible flow and heat transfer past a vertical plate in slip flow regime. Matematicas: Ensenanza Universitaria 2005; XIII (1): 51-62.
17. Siegel R and Howel J R. Thermal radiation heat transfer. 2002; 4th Edition, Taylor and Francis , New York.
18. Raptis A, Rerdikis C and Takhar H S. Effect of thermal radiation on MHD flow. Appl. Math. Comp. 2004; 153: 645-649.

TECHNO-ECONOMIC ANALYSIS OF AGRICULTURAL WASTES AS FEEDSTOCKS FOR BIOETHANOL PRODUCTION IN NIGERIA

A. SANNI*, A.S. OLAWALE, Y.M. SANI
Department of Chemical Engineering, Ahmadu Bello University, Nigeria.
*Corresponding author: sanniabdulkadeem@yahoo.com

ABSTRACT
Economic analyses of bioethanol production from some agricultural wastes, which are abundantly available in Nigeria, were conducted using superPro Designer® simulation software. The agricultural wastes considered were; corn cob, corn stover, rice husk, rice straw, saw dust, and waste wood. The flowsheet included four bioethanol production pathways, namely: pretreatment (dilute acid and liquid hot water), hydrolysis and fermentation and purification technologies. The paper attempted to ensure a safe, reliable, and efficient production of fuel-grade bioethanol from six lignocellulosic feedstocks, which are agricultural wastes. The established economic minimum bioethanol plant capacity utilised was 75,000 m^3/annum. The plant using corncob as the feedstock has the highest return on investment (ROI) of 75.98% followed by that using rice straw (49.86%) with matching payback periods of 1.3 and 2.0 years respectively. The least profitable plant was based on waste wood.

1.0 INTRODUCTION

Nigeria is blessed with abundance of lignocellulosic biomass most of which are agricultural wastes (Cardona and Sanchez, 2008). These lignocellulosic biomass are known to be useful as second-generation feedstocks in bioethanol production. The agricultural wastes among the biomass are under-utilised as energy sources rather they are left in the field to decay and thereby, constituting environmental nuisance (Ogundare *et al.*, 2010). This is in spite of the fact that these feedstocks are relatively cheap and do not engender the risk of food scarcity unlike the first-generation feedstocks such as sucrose-containing and starchy biomass. Nigeria is endowed with energy resources which include natural gas, crude oil, coal, biomass, and tar sand (Ogundare *et al.*, 2010). However, the almost absolute dependence on fossil fuels as revenue and energy sources is not sustainable economically or environmentally.

The consumption of petrol in Nigeria as at November, 2016 was 12.7 billion litres (National Bureau of Statistics, 2016). It is in realization of this that Nigerian government biofuel policy stipulated the substitution of petrol (PMS) consumption with 10% bioethanol blend to be used in Nigeria (NNPC, 2017). As of now the very limited number of bioethanol processing plant in Nigeria uses cassava and in many cases capacity utilization has never been above 65%. For commercial-scale bioethanol production it is desirable to use cheap and relatively more abundant feedstocks such as agricultural wastes. The commonly available ones are; corn cob, corn stover, sugarcane bagasse, rice husk, rice straw, saw dust, stalk (sorghum, wheat and millet), waste wood and wheat straw.

Taking these afore-mentioned scenarios the prospect of utilization of lignocellulosic agricultural wastes as bioethanol feedstocks in Nigeria is bright. Economic viability of bioethanol production using different feedstocks is dependent on factors such as local cost and composition of the feedstocks, energy cost, technologies adopted, plant capacity, etc. The influence of these economic factors have been demonstrated from economic perspective ascribed to some lignocellulosic feedstocks when utilized in different countries and/or under different conditions (Njoku *et al*., 2012; Binod *et al*., 2010; Pandey *et al*., 2000; Sukumaran *et al*., 2010; and Sánchez and Cardona, 2008) .

Consideration of these economic factors requires the case by case analysis of bioethanol produced from different lignocellulosic feedstocks in different climes. Despite this bright prospect, no work has been carried out on technical and economic assessment of these abundant lignocellulosic feedstocks for bioethanol production in Nigeria. Thus, assessment of bioethanol production using Nigeria agricultural wastes is needed to assist policy makers and bioethanol producers in feedstocks selection.

In this work economic analysis of bioethanol production from second (lignocellulosic) generation feedstocks that are available in Nigeria was carried out as well as comparative assessment of the pathways utilizing the feedstocks.

2.0 METHODOLOGY

The method comprises four stages: Selection of feedstocks and technology, data gathering and generation, and economic analysis.

2.1 Feedstocks Selection

Nigeria agricultural wastes were identified and six were selected. The basis for selection was feedstock availability to meet the economic minimum scale of 75,000 m^3/annum and costs as presented in Table 1.

TABLE 1: AVAILABILITY AND COSTS OF NIGERIA-BASED LIGNOCELLULOSIC FEEDSTOCKS

Lignocellulosic feedstocks	Quantity (tonnes/annum)	Price ($/kg)	Price (₦/kg) at $ = ₦315	EtOH yiels (w/w)
Corn cob	2,454,000[y]	0.038[*]	12.250	0.358*
Corn stover	4,907,800[y]	0.189[a]	59.530	0.221*
Rice husk	3,300,000 [x]	0.110[a]	34.650	0.265*
Sugarcane bagasse	18,900[a]	0.050[*]	15.750	0.297*
Rice straw	4,350,000[x]	0.042[a]	13.500	0.248*
Saw dust	1,800,000[b]	0.050[*]	15.750	0.265*
Waste wood	5,200,000[b]	0.050[a]	15.750	0.210*
Sorghum stalk	277,000[c]	0.045[*]	14.175	0.340*
Millet straw	284,000[c]	0.045[*]	14.175	0.300*

Source: a= Anyanwu *et al*., (2013); b= Sambo *et al*., (2013); c= Jekins *et al*., (2015); x=Muhammad, (2017); *=Alibaba.com; y=USDA, (2013)

2.2 Selection of Technologies and Operating Conditions

Figure 1 shows typical flow-diagram scheme for processing the feedstock category studied in this project. The flow sheet containing different units (pretreatment, hydrolysis, fermentation and purification) as applicable to the lignocellulosic feedstocks were identified from literature (Scott *et al.,* 2012). Those capable of achieving the best yields of bioethanol with slight environmental impacts and cost were selected.

Hot water pretreatment was preferred for its advantages such as cost minimization, elimination of the need for chemical recovery, prevention of corrosion, inhibitory substance formation and environmentally friendliness. Enzymatic hydrolysis using hydrolase, *Trichoderma reesei* followed afterwards (NREL, 2012). *Zymomonas mobilis* was selected as fermentation microbe because of its ability to ferment both pentoses and hexoses simultaneously for low lignin content (<18%) lignocellulosic feedstocks and resistance to glucose restraint (Balat *et al*., 2011). Separate hydrolysis and fermentation (SHF) was selected for feedstocks with lignin content greater than 18% (such as saw dust 21-23%, waste wood 29-31%, and rice husk 19-21%) and *Saccharomyces cerevisiae* as the ideal fermentation microbes as lignin content within this range limits the activity of *Zymomonas mobilis* (Balat *et al.,* 2011). The purifications of the fermentation broths obtained were carried out as described in this section. Double-effect totally heat integrated distillation columns favoured the distillation section. They promote energy savings at a low cost (Dias *et al*., 2011; Suleiman *et al*., 2014). The first column performed at best condenser temperature (107.6°C) and reboiler condition (temperature = 111.3°C, pressure = 1.013bar). The second distillation column performed at condenser temperature (84.1°C) and reboiler condition (temperature = 99.9°C and pressure = 1.013bar) for ethanol recovery (see Figure 1). While the first column produced 43% ethanol solution in the distillate, the second column produced 95% ethanol (azeotropic composition). This approach concentrated the bottom of the first column and solids of the pretreatment section in a multi-effect evaporator. The dried solids sent to boiler for steam generation. Bottom of second column with recycled stream of evaporator join distillation stream. Because of the cost of hydrophilic membrane, complexity of installing pervaporation and solvents recovery costs for azeotropic and extractive distillations (Aden *et. al*., 2002) molecular sieve adsorption was selected for all the feedstocks categories. The purification flowsheet was also recommended by Suleiman *et al*., 2014).

2.3 Process Simulation and Economic Analysis

Having selected the feedstocks and the technologies continuous process of 90% (329 days = 7896h) annual running time (Sinnott, 2005) were input in superPro Designer® simulation startup window. The process flow models for the selected technologies in Figure 1 were represented on superPro Designer® simulation environment. Updated engineering plant and raw material costs were estimated using cost indices for November, 2016 (which are 100.3 and 99.7 respectively) and November, 2013 (106.8) as the base cost using Equation 1.

$$\text{Cost in year Y} = \text{Cost in year X}\ \frac{\text{Index in year Y}}{\text{Index in year X}} \quad (1)$$

where, X = year 2013, Y = November, 2016.

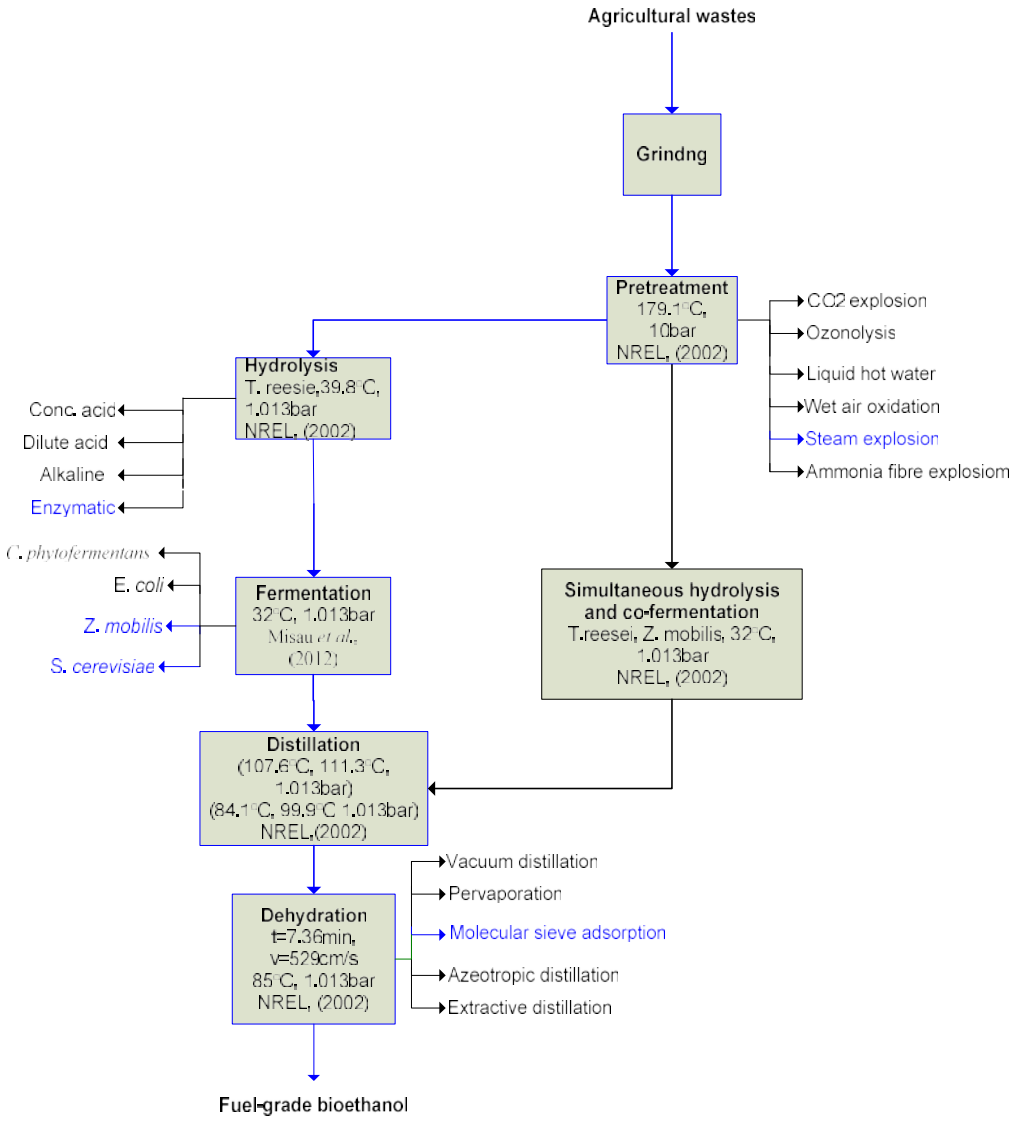


Figure 1: Feedstocks processing pathway

Economic parameters extracted from Sinnott, (2005) as given in Table 3 were input in 'Economic Evaluation Parameter' window, and startup period of 4 months was input on the 'Time Valuation' window. The discounted cash flow parameters presented in Table 2 and net present value interest of 14% (CBN report, 2017) were input on the 'Finances' window. The indirect and fixed costs presented in Table 3 were input on 'Main Section' window comprising capital cost and operating cost adjustments panes. The cost and size of equipment on flow models were registered on 'Equipment Data' panes. Similarly, the costs of feedstocks were registered on 'Pure Component' pane. The prices were registered on per kilogram basis and the price of the products (ethanol) set at ₦350/litre (News agency of Nigeria, 2016). Average cost of co-product (electricity) set at ₦23.6/kWh. Utility steam and cooling water requirement costs within the programme were set at US$ 17.08 per 1000 kg and US$ 0.1 per 1000 kg respectively (NNPC report, 2017). The exchange rate used was $ = ₦315 (CBN, 2017). The costs of major equipment were obtained from www.matche.com (2013), quotations from equipment suppliers and erectors. Equipment of varying capacities from received quotations had their costs adjusted using scaling expression given by Equation 2.

$$C = Co \times \left(\frac{Q}{Q_b}\right)^n \left(\frac{I}{I_o}\right) \qquad (2)$$

where C = current cost, dollars, C_0 = base cost, dollars, Q = current capacity, Q_b = base capacity, I = current index, dimensionless, I_o = base index, dimensionless n = exponent number or cost factor.

Prices of the various feedstocks were obtained from recently published market prices in Nigeria (see Tables 1) and information collected from Alibaba.com (website of a supplier of most lignocellulosic feedstocks). Three products got from converting the selected starchy feedstocks to ethanol were ethanol, pomace/bagasse, and carbon dioxide. The equivalent electricity generated from pomace or bagasse resulting from the used lignocellulosics and sucrose-containing biomass were considered. The carbon dioxide produced was released because of high cost of purifying and transport to end user (Jason *et al*., 2006).

The plant capacity selected for bioethanol production from agricultural wastes investigated in this work was 75,000 m^3/annum (Hexagon renewable, 2013).

3.0 RESULTS AND DISCUSSION

The result presented in Figures 2 showed that the total capital investment (TCI) and annual operating cost (AOC) were lowest for bioethanol production process utilizing corn cob.

TABLE 2: PARAMETERS USED FOR DISCOUNTED CASH FLOW CALCULATIONS

Parameter	Assumption
Discount rate	14 %[a]
Plant life time	10 years
Working capital	15% of fixed capital investment
Construction period	3 years
Project life	10 years
Tax rate	30%[b]
Depreciation	Straight line method

Source: Peters *et al*., (2003), a-CBN report, (2017), b-Deloitte corporate tax rate, (2017)

TABLE 3: ASSUMED PARAMETERS' VALUES

Parameter	Assumptions
Indirect cost	
Engineering and supervision	8% of TIE
Legal expenses	2% of TIE
Construction and contractor fee	15% of TIE
Project contingency	10% of TIE
Working capital	15% of TIE
Total capital investment (TCI)	TIE + indirect cost
Fixed cost	
Maintenance	7% of TCI
Operating labour	15% of product cost
Laboratory cost	15% of operating labour
Operating supplies	15% of maintenance cost
Supervision	10% of operating labour
Local taxes	2% of TCI
Insurance	1% of TCI
Plant overhead	60% of (operating labour + supervision + maintenance)

Source: Peters *et al*., (2003); TIE: Total installed equipment

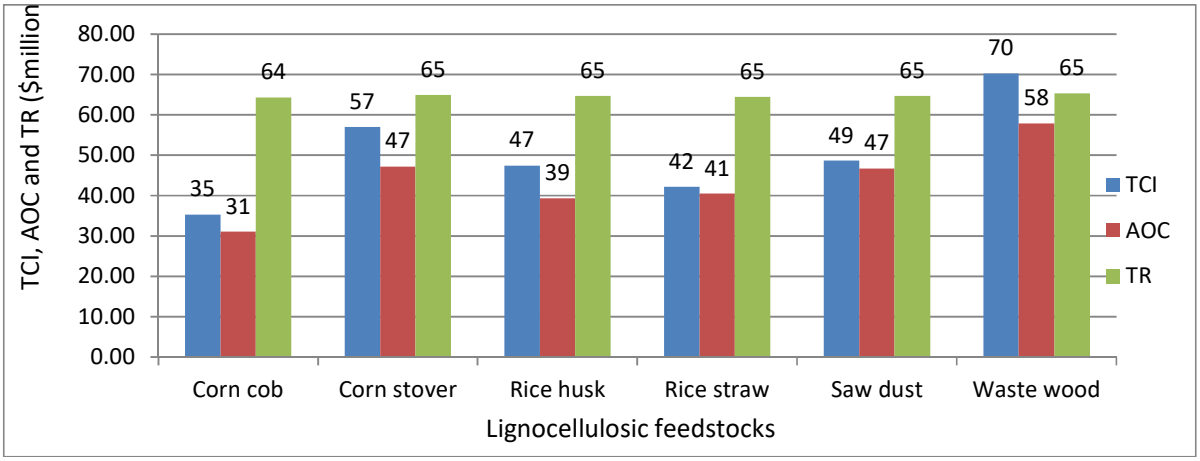


Figure 2: TCI, AOC and TR of bioethanol produced from the selected Lignocellulosic Feedstocks

TCI= total capital investment; AOC= annual operating cost; TR=total revenue

Bioethanol production from these wastes required TCI of between 35-70 million dollars with corn cob based plant recording the highest gross profit. However, the waste wood based bioethanol production required the highest capital cost ($70m) while the same product based on the five other feedstocks (corn cob, corn stovert, rice husk, rice straw and saw dust) fell between 35 and 57 million dollars.

From Figures 2 the two highest gross profits were recorded with plants using corncob and rice husk to be $33.2 million and $25.3 respectively. They represent the two most economically viable plants among the selected lignocellulosic agricultural wastes. Large gross profit observed in corn cob compared to other feedstocks was due to cheap price and high bioethanol yield of corn cob.

Return on investment (ROI), a measure of profitability of a process is shown in Figures 3. Ethanol from corn cob and rice straw gave the two highest ROI of 75.98% and 49.86%. The lowest ROI from these lignocellulosic feedstocks was observed with waste wood based bioethanol plant (17.36%). This trend in ROI is expected as cost of feedstocks accounted for over 75% of the annual operating cost (NREL, 2002). The market prices of corn cob, rice straw, and their pretreatment technology are extremely low in relative term.

Figure 4 shows the payback period (PBP) for the bioethanol plants based on six selected feedstocks. This is a fraction of profit after tax (PAT) with depreciation and TCI. It is indirectly proportional to ROI. Therefore, the least PBP signifies the highest profitability of the process. Corn cob and rice straw in decreasing order of economic viability proved to be the best alternatives feedstocks for bioethanol production. The relatively low bioethanol yield of corn stover, waste wood, saw dust and rice husk (see Table 1) have made them less competitive.

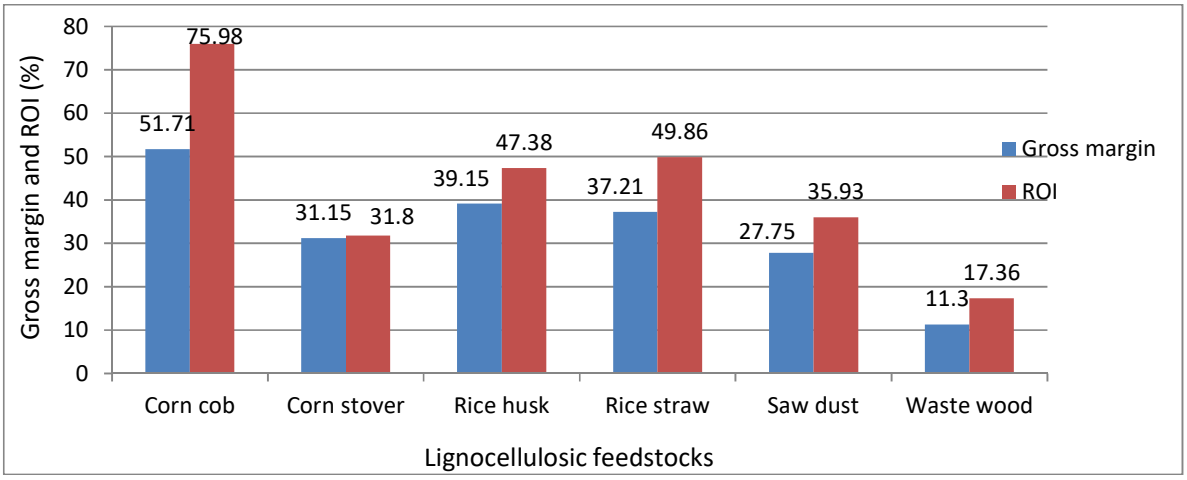


Figure 3: Gross margin and return on investment (ROI) of bioethanol produced from lignocellulosic feedstocks

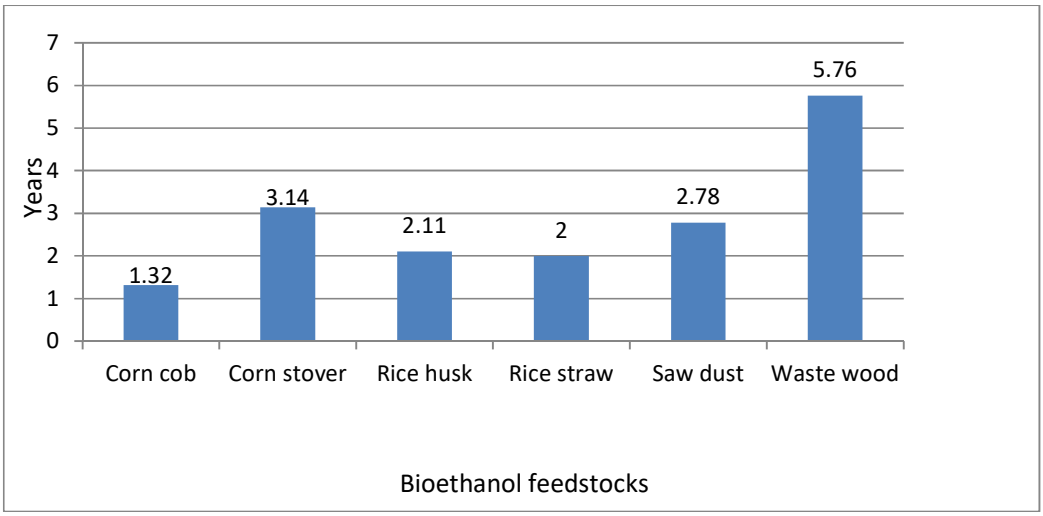


Figure 4: Payback periods for the selected feedstocks

TABLE 4: COMPARATIVE BIOETHANOL PRODUCTION COST IN THIS AND PREVIOUS STUDIES

	Cost ($/gal) of bioethanol production from selected feedstocks	
Feedstocks	Corn cob	Rice straw
This work	1.88	2.48
Past work	0.45[m]	

m- Ricardo and Robert, (2005)

Table 4 compares the cost variation in bioethanol production from some bioethanol feedstocks assessed in this work and previous studies. Bioethanol production cost varies from region to region depending upon a number of factors as agreed by previous workers. Among these factors are prices of feedstocks, raw materials species, geographical location, climatic conditions and process technology alternatives (Xavier, 2007; Shampouri *et al*., 2006; Pimentel *et al*., 2005).

4.0 CONCLUSION

The following lignocellulosic (agricultural wastes) biomass were identified to be abundantly available in Nigeria in the following decreasing order: waste wood, corn stover, rice straw, rice husk, corn cob, saw dust, millet straw, sorghum stalk, sugarcane bagasse. The technical and economic analysis carried out on the bioethanol production from the six most abundant agricultural by-products in Nigeria showed that the process utilizing corn cob was the best, followed by those using rice straw, rice husk, saw dust, corn stover, and waste wood in that order. The bioconversion technology adopted in this study involved steam explosion pretreatment, hydrolysis, fermentation, thermally heat integrated distillation and molecular sieve adsorption processes.

REFERENCES

Aden, A., Ruth, M., and Iechura, J. (2002). Lignocellulosic Biomass to Ethanol Process Design and Economics Utilizing Co-Current Dilute Acid Prehydrolysis and Enzymatic Hydrolysis for Corn Stover (National Renewable Energy Laboratory-NREL, Report TP510-32438).

Anyanwu, I.S., Eze, O.U., Oparaku, V.K., Sharma, G., Braccio, and Contuzzi. (2013). "Biofuels: An alternative resource for mitigating primary energy shortfalls in Nigeria," Int. Energy J. 9(Special Issue 61), 31–36

Balat, M., Balat, H., Oz, C., (2011). Progress in bioethanol processing. Progress in Energy and Combustion Science 34, pp 551- 573

Binod, P., Sindhu, R., Singhania, R.R., Vikram, S., Devi, L., Nagalakshmi, S., Kurien, N., Sukumaran, R.K., Pandey, A., (2010). Bioethanol production from rice straw: an overview. Bioresour. Technol. 101 (13), 4767–4774.

Cardona, C.A., Sanchez O.J. (2008). Fuel ethanol production: process design trends and integration opportunities. *Bioresource Technol*; 98:2415–57.

Central Bank of Nigeria (CBN). (2017) "Contributions of the Agricultural Credit Guarantee Scheme (ACGS) to Improved Agricultural Financing in Nigeria: Past, Present and Future", in Ade S. Olomola and S. O. Akande (eds.) *Agricultural Finance Issues in Nigeria*, NISER, Ibadan

Chemical Engineering Plant Cost Index (CEPCI). (2016). *Chemical Engineering*. November 2016.

Jason R.K., Andrew J. M., Frank T., David B.J. (2006). Modeling the process and costs of fuel ethanol production by the corn dry-grind process. U.S. Department of Agriculture. Industrial Crops and Products. 23, 288–296

Jenkins, B. (2015). Properties of Biomass, Appendix to Biomass Energy Fundamentals, EPRI Report TR-102107

Muhammed, A., (2017). Rice Production in Nigeria. Premium Times. October 30th, 2017

Njoku, S.I., Ahring, B.K., Uellendahl, H., (2012). Pretreatment as the crucial step for a cellulosic ethanol biorefinery: testing the efficiency of wet explosion on different types of biomass. Bioresour. Technol. 124, 105–110.

National Bureau of Statistics. (2016). Petroleum Products Consumption Statistics in Nigeria. National Bureau of Statistics.

News Agency of Nigeria report. (2016). (Accessed 26 December 2016).

NNPC, (2017). Biofuels Development in Nigeria. International Renewable Energy Conference, Abuja, March 16-19

Ogundare, I.O. (2010): Techno-Economic Assessment of Biofuel as an Alternative Energy Source for Transportation in Nigeria. Technology Planning and Development Unit, Obafemi Awolowo University, Ile-Ife (MSc Thesis)

Pandey, A., Soccol, C.R., Nigam P., Soccol V.T. (2000). Biotechnological potential of agroindustrial residues I: sugarcane bagasse. Bioresource Technology.74:69–80.

Peters M.S., and K.D., Timmerhaus. (2003). Plant Design and Economics for Chemical Engineers, 4th Edition, McGraw-Hill, Inc., New York.

Pimentel D., Patzek T.W. (2005). Ethanol production using corn, switchgrass, and wood; biodiesel production using soybean and sunflower. Nat Resources Res 2005;14:65–76.

Sánchez, Ó.J, Cardona, C.A. (2008). Trends in biotechnological production of fuel ethanol from different feedstocks. Bioresour. Technol. 99(13):5270-5295.

Sambo, A. (2013). The Place of Renewable Energy in the Nigerian Energy Sector. *World Future Council Workshop on Renewable Energy Policies*. 10th October, Addis Ababa, Ethiopia.

Scott, F., Quintero, J., Morales, M., Conejeros, R., Cardona, C., & Aroca, G. (2013). Process design and sustainability in the production of bioethanol from lignocellulosic materials. *Electronic Journal of Biotechnology*, *16*(3). https://doi.org/10.2225/vol16-issue3-fulltext-7

Shapouri H., Salassi M., Nelson J. (2006). The economic feasibility of ethanol production from sugar in the United States. Washington, DC, USA: US Department of Agriculture (USDA); July.

Sinnott R.K., Coulson, J.M., and Richardson, J.F. (2005). Coulson and Richardson's Chemical Engineering. Vol. 6. Oxford: Elsevier Butterworth-Heinemann.

Sukumaran, R.K, Singhania. R.R, Mathew, G.M, Pandey. A. (2009) Cellulase production using biomass feed stock and its application in lignocellulose saccharification for bio-ethanol production. Renew Energy 34: 421-424.

Suleiman B., Olawale A.S., and Waziri S.M. (2014). Exergetic and Economic Assessment of Distillation Hybrid Configurations for Bioethanol Refining. Nigerian Journal of Engineering. Vol 21. no 2. pp 81-91.

United States Department of Agriculture. (2013). The economic feasibility of ethanol production from sugar in the United States. Available at: http://www.usda.gov/oce/reports/energy/EthanolSugarFeasibilityReport3.pdf

Xavier M. (2007). *The Brazilian sugarcane ethanol experience*. Washington, DC: Competitive Enterprise Institute (CEI), Issue Analysis. [cited; available from: /www.cei.org/pdf/5774S].

ANTIMICROBIAL DETERGENT FROM CARAWAY OIL

***S. MUKTARI, M.M. BAMALLI, AND U.S AMEURU**
Department of Polymer and Textile Engineering, Ahmadu Bello University, Zaria, Nigeria
*Corresponding author: muktarisuleiman@gmail.com, +2347064545407

ABSTRACT
The basic function of a detergent is to remove dirt. In Nigeria most people wash clothes with their hands, the detergent which removes the dirt and grime from the clothes also degreases the skin while washing. Linear Alkyl Benzene Sulphonate (LABS) - a primary ingredient of modern day detergents and other alkaline builders and fillers added to make detergents antimicrobial can penetrate the epidermis causing irritation of the skin. This work is aimed at capturing the antimicrobial property of caraway into the detergent synthesized from it. Liquid detergent (100ml) was synthesized. Antimicrobial Test with three organisms (Staphylococcus aureus, Pseudomonas aeruginosa, and Candida albican) showed sensitivity to two of the organisms: Staphylococcus aureus and Candida albican. The detergent reduced the surface tension of water from 0.0735Nm^{-1} to 0.0294Nm^{-}1.The detergent is confirmed with antimicrobial effect and can be used as excellent wetting and cleansing agent.

Keywords: *Detergent, Antimicrobial, Organism, Clean, Caraway.*

INTRODUCTION

Generally, detergent is a substance used to enhance the cleansing action of water. It serves as an emulsifier, which penetrates and breaks up the oily film that binds dirt particles and a wetting agent which helps them to float off [1].

These emulsifier molecules have an oil like non polar portion which is drawn into the oil, and a polar group that is water soluble; by bridging the oil-water interface, they break the oil into dispersible droplets (emulsion). Hence on this account soap can be seen as a detergent [2].

The basic function of a detergent is to remove dirt [3, 4]. In Nigeria most people wash clothes with their hands[5]. The detergent which removes the dirt and grime from the clothes also degreases the skin while washing the clothes. Thus natural oils from the skin are removed which may lead to certain skin diseases [6].

Linear Alkyl Benzene Sulphonate (LABS) - a primary ingredient of modern day detergents, can penetrate the epidermis causing irritation of the skin [7]. More over the alkaline builders and fillers added to the detergents are also harmful to the sensitive skin. If the clothes are not washed very well with water, the residual detergent sticking to the cloth also may irritate the skin [8, 9].

Phosphates used as detergent builders cause eutrophication [10]. Another active ingredient in laundry detergent is household bleach, or sodium hypochlorite. Responsible for the majority of the household poisonings, this chemical is a forerunner to chlorine. When it reacts with other organic materials, the results are even more harmful. Carcinogenic and toxic compounds are created. These can cause damage or disorder to the reproductive system, endocrine and immune system [11, 12].

From fragrance to whiteners, detergents have become increasingly dangerous to use, especially on a regular basis [13]. Hence the Mother to this Research Work; to Synthesize Detergent from Caraway Oil - an essential oil with health benefits attributed to its properties as a galactogogue, anti-histaminic, antiseptic, cardiac, anti-spasmodic, carminative, digestive, stomachic, disinfectant, diuretic, emanagogue, expectorant, aperitif, astringent, insecticide, stimulant, tonic and vermifuge substance .

Chemical Properties of Caraway Oil

Common name: Caraway Oil (Black Cumin seed oil).
Scientific name: Carum carvi
Principal constituent: Carvone
Molecular formula: $C_{10}H_{14}O$
Molar mass: 150.22g/mol
Appearance: Clear Blackish Yellow liquid.

MATERIALS AND METHODS

Materials

Caraway oil, Sodium hydroxide pellets (NaOH), Potassium hydroxide pellets (KOH), Conc. Sulphuric acid (H_2SO_4), Distilled water.

Equipment.

Beakers, Soap pot, Wooden stirrer, Electric balance, Glass rod, Heating mantle, Thermometer, pH meter, Mould, Burette, Pipette, Conical flask, Volumetric flask.

Synthesis
50g caraway oil was placed in a stainless beaker and the temperature raised and kept constant at 50^0C . 10.4g KOH dissolved in 29.952ml distilled water was gradually added with stirring and immediately followed with gradual addition of 5ml conc. H_2SO_4 with stirring. The cooking and stirring continued for 30mins. The mixture separated into two layers. It was decanted and the detergent (lower layer) collected. It was diluted with 50ml of boiled distilled water.

Characterization
Chemical analysis of The detergents were made according to ASTM D455-69

pH Determination
10ml of the detergent was collected in a beaker. The pH was determined with a pH meter and recorded in Table 1.

Determination of Surface Tension (Capillary Rise Method).
20ml of the detergent was measured into a 250ml beaker (washed with dilute NaOH and rinsed thoroughly with distilled water) and filled up with distilled water.

A clean capillary tube of diameter 1mm (washed with dilute NaOH and rinsed thoroughly with water) was pushed into the beaker containing the soap solution. The capillary tube was removed and clamped gently so that the tip just touch the surface of the liquid. When the liquid inside the capillary tube has fallen to a constant position the height of this liquid from the surface of the soap solution was measured with a transparent rule and recorded as liquid height in metres(h). The surface tension was calculated with the formula;$\gamma = \frac{rh\rho g}{2}$ where; γ = surface tension, r = radius of capillary tube in metres, h = liquid height in metres, ρ = density of water = 1000kgm^{-3}, g = acceleration due to gravity = 9.8ms^{-2} Results obtained are shown in Table 2.

Anti Microbial Test
A Fungus and two bacteria were used. All been clinical isolates from the Department of Microbiology, Ahmadu Bello University Zaria. These isolates were: Candida albican (fungus), Pseudomonas aeruginosa (bacteria), Staphylococcus aureus (bacteria)

Culture Media
The culture media used for the analysis include Mueller Hinton Agar (MHA), Nutrient Agar (NA) and Mueller Hinton Broth (MHB). They were all used for the sensitivity test, determination of minimum inhibitory concentration (MIC) and minimum bactericidal concentration (MBC) respectively. All the media were prepared according to manufacturer's instructions.

Sensitivity Test of the Detergent Using Agar Well Diffusion Method.
The bacterial isolates were standardized and streaked uniformly onto freshly prepared Mueller Hinton Agar plates using a sterile swab stick. Four wells were punched on the agar plates with the aid of a sterile cork borer (8mm) in diameter. The well were properly labeled according to different concentrations of the soap prepared (50, 25, 12.5 & 6.25mg/ml). The wells were then filled up with 0.2ml of different concentration of the soap respectively. The plates were left on the bench for 1hr for the soap to diffuse in the agar, after which they were incubated at 37^0c for 24hrs. After the incubation period, the plates were observed for any evidence of inhibition, which will appear as a clear zone that was completely devoid of growth around the wells (zone of inhibition). The diameter of the zones were measured using a transparent rule calibrated in millimeter (mm) as shown in Table 3.

Determination of Minimum Inhibitory Concentration (MIC)
The minimum inhibitory concentration (MIC) of the detergents were determined using the tube dilution method. Serial dilution of the soap was carried out in well labeled test tubes using Mueller Hinton Broth as a diluent. The lowest concentration of the soap showing inhibition for each organism when the soaps were tested using agar well diffusion method was serially diluted in the test tubes containing Mueller Hinton Broth. Each organism was inoculated into each tube containing the diluted detergent. The tubes were then incubated at 37^0C for 24hrs.

After the incubation period, the tubes were examined for the presence or absence of growth using turbidity as criterion. The lowest dilution (concentration) in the serial without visible signs of growth (turbidity) was considered to be the minimum inhibitory concentration (MIC). Results are shown in Table 4.

Determination of Minimum Bactericidal Concentration (MBC)
The results from the minimum inhibitory concentration were used to determine the minimum bactericidal concentration of the detergent. A sterile wire loop was dipped into the test tubes that did not show turbidity in the MIC

test, it was then streaked on a freshly prepared nutrient agar plates. The plates were incubated at 37^0C for 24hrs. After the incubation period, the plate were examined for the presence or absence of growth. This was done to determine if the antibacterial effect of the detergent is bactericidal or bacteriostatic.

Washing Test

14 pieces (1g each) of bleached cotton was cut into 5x5cm dimension and 7 stained with black engine oil and the remaining stained with palm oil and dried. Each of the stained fabric was washed with 5g of solid samples and for the liquid samples 20ml was used using a liquor to specimen ratio of 50:1 at 400C for 30min. with continuous stirring. The stained fabric were also washed with water only with the same condition as above. After washing, the samples were rinsed thoroughly with distilled water and dried. The change in colour of the washed fabrics and the originally stained ones were observed with a grey scale. The soaps were graded according to the extent of colour change. This grading is based on; the further the change in colour the lower the number on the grey scale and the more efficient the soap. On the other hand, the smaller the change in colour the bigger the number on the grey scale and the less efficient the soap. The results obtained are shown in Table 5.0

RESULTS AND DISCUSSION

Table 1: pH of the Detergent Samples.

SAMPLES	pH
A	9.50
B	10.00

KEY A= Detergent, B = control (Dettol)

From the result, the detergent have pH within the normal pH range for detergent 8-10.5 [14] and compete well with the control 10.00. This indicate that the prepared detergents are not corrosive to the skin. This alkalinity favours detergency [14].

The detergent (A) had a value 0.0294 Nm^{-1} exactly the same with the control irrespective of the builder due to the presence of sulphate ($-O-SO_3^-$) group. The lower the surface tension the more efficient the detergent and vice versa [15, 16].

Table 2: Surface Tension of Distilled Water, and Detergent Solutions.

Sample	r (m)	h (m)	ρ (kgm^{-3})	g (ms^{-1})	γ (Nm^{-1})
Distilled H_2O	0.0005	0.0300	1000	9.8	0.0735
A	0.0005	0.0120	1000	9.8	0.0294
B	0.0005	0.0120	1000	9.8	0.0294

where;γ= surface tension, r = radius of capillary tube in metres, h = liquid height in metres, ρ = density of water = 1000kgm^{-3}, and g = acceleration due to gravity = 9.8ms^{-2}.

Table 3: Sensitivity Test

Test Organisms	A				B			
	50	25	12.5	6.25	50	25	12.5	6.25
Candida albican	20	18	16	12	21	19	17	14
Pseudomonas aeruginosa	R	R	R	R	R	R	R	R
S. aureus	20	19	17	15	23	20	18	16

Zones on Inhibition (mm) at Varying Concentrations of the Soap (mg/mL)
where R = Resistant.

Table 4: MBC and MIC Test

Test Organism	MIC (mg/ml)		MBC (mg/ml)	
	A	B	A	B
Staph. aureus	1.625	1.562	3.250	3.125
Candida albican	1.700	1.630	3.500	3.320

The detergent and the control had sensitivity to two of the organisms- Candida albican and Staphylococcus aureus but were resistant to Pseudomonas aeruginosa. This sensitivity indicates inhibition to the organism whereas resistant indicates no inhibition. The wider the zone of inhibition the more antibacterial effect of the detergent. The minimum Inhibitory Concentration (MIC) values tells the lowest concentration of the detergent that will stop the further growth of organisms. The lower the value, the more effective is the detergent.

The Minimum Bactericidal Concentration (MBC) values indicate the minimum concentration of the detergent that will completely kill the organism. The lower this value the more effective the detergent.
The detergent is found Bactericidal and Bacteriostatic to some but not all organisms.

Table 5: Washing Test.

Sample	Grade
Water only	4/5
A	½
B	1

Note: x/y is read; in between x and y.

The cleansing power of water only was 4/5 which shows only a small removal of stain. The detergent and the control have almost the same cleansing power of ½ and 1 respectively. These indicate complete removal of stain. The detergent can be used for the removal of both domestic and industrial stain.

CONCLUSION

Liquid detergent was successfully prepared from caraway oil. Chemical analysis showed that the detergent conform to standard- ASTM D455-69. Antimicrobial Test revealed the detergent can be used as a bactericidal and bacteriostatic agent against some harmful organisms particularly Staphylococcus aureus and Candida albican without any external builder. The detergent can be used excellently for stain removal because of their ability to lower the surface tension of wash water.

REFERENCES

1. Essential Oils (2012). Encyclopedia Britannica, vol. 4.Chicago: Encyclopedia Britannica. pp 563
2. Jubb,,A.H,and,Nechvatal,,A.(2014).,Organic,Chemistry”.,London:,John,Wiley,& Sons. pp 453, 457, 462-466.
3. Pandey, G. (2013). A Textbook of Chemical Technology, vol. 2. New Delhi: Vikas Publishing House Ltd. pp 7.1-7.47
4. David, T. (2015). Experimental Organic Chemistry. New Jersey: Prentice-Hall, Inc. pp 400.
5. Detergent,(2015).,Encyclopedia,of,Science,and,Technology,,vol.,5.,London:,MC,Graw, Hill,,Inc.,pp 411-412.
6. James, K.A (2015). Riegel’s Handbook of Industrial Chemistry, 9th Ed. India: CBS publishers., pp1040
7. Janardhanan, K. (2014). /http:/ issstindian.or/../art.6.pdf/soaps and detergent.
8. Kirschenbauer, H.G. (2016). Fats and Oil; an outline of their chemistry and technology, 6th Ed. New York: Chapman & Hall, Ltd. pp 5, 24, 27-34.
9. Lewkowitsch, M.A. (2014). Chemical Technology and Analysis of Oils, Fats and Waxes, 9th Ed, vol. 3. London: Macmillan & Col ltd. pp 237, 313.
10. Mak-Mensah, E.E and. Firempong C.K (2016) Chemical characteristics of toilet soap prepared from neem (Azadirachtaindica A. Juss) seed oil”. Asian Journal of Plant Science and, Research, 1(4):1-7.
11. Martin, G. (2016). The Modern Soap and Detergent Industry, vol. 2. London: Elsevier Applied,Science. pp 4-7, 10.
12. Mercola, E.D (2014). Laundry Soap Detergent; Harmful Side Effects for Humans. Green Health Technologies. Annual publication, pp 40.
13. Nicholson, N.L (2005). Detergents are Bad for Health and Environment. Green HealthTechnologies. Annual publication, pp 25.
14. Nkeonye, P.O (2009). Textile Preparatory Processes and Waste liquor Treatment. Zaria: Asekome & Co. pp 22-34.
15. Perry, Anthony, et al (2005): Surface Active Agents and Detergents. New York: MC Graw-Hill,,Inc. pp 32, 40, 55.
16. Soap and detergent (2015). The New Encyclopedia Britannica, vol. 21. Chicago: Encyclopedia Britannica. pp 352-357.

EFFECT OF PARTIALLY TREATED SEWAGE WATER ON SANDCRETE BLOCKS

[*]SALAHUDEEN, A. B. AND ABDULLAHI, U.
Samaru College of Agriculture, Division of Agricultural Colleges, Ahmadu Bello University, Zaria
[*]**Corresponding Author:** basalahudeen@gmail.com

ABSTRACT
The study to access the effects of partially treated sewage water on sandcrete blocks was carried out by casting of blocks with different proportion of partially treated sewage water and tap water as control. The block samples were designated as S1, S2, S3, S4, S5 and S6 according to the percentage of sewage/tap water used.. Total number of thirty (30) blocks were casted with five (5) samples belonging to each designation. All samples were casted with sand/cement ratio of 1:6 and water/ cement ratio of 0.5. The compressive strength test of the prepared block samples was determined after 7, 14 and 28 days curing age using compressive testing machine and absorption rate of the block samples was also determined at Civil Engineering Department concrete laboratory, Ahmadu Bello University, Zaria. The results obtained show that there is no significant different in compressive strength values of samples when prepared using partially treated sewage water or tap water in moulding the block samples. Most of the sandcrete block samples met the recommendations of British Standard (BS) and Nigeria Industrial Standard (NIS) of 2.5-3.45 N/mm^2.

Keywords: Treated Sewage Water, Sandcrete Blocks, Compressive strength, Absorption rate

1.0 INTRODUCTION

Sandcrete blocks are the most prominent of the concrete masonry units in the building industry today especially in the construction of residential, industrial and commercial buildings (Ejeh, 1982). Sandcrete blocks are the most widely used walling unit in Nigeria, accounting for 90% of houses (Ewa and Ukpata 2013). They could be used as external walls (i.e. 460 mm thick blocks) or as partition walls (the 150 mm thick blocks.). The later (150 mm) is usually non-load bearing. They are made from a cement/sand mix usually 1 part of cement to 6 or 8 parts of sand (1:6 or 1:8) with a water/cement ratio of between 50 and 75% (B.S. 3921: 1969).

Historically, most concrete masonry units are manufactured on the local level and industry standards are not always adhered to (Ewa and Ukpata 2013, Aiyewalehinmi and Tanimola 2013, Mahmoud *et al* 2010, Abdullahi 2005). Currently there are no special tests developed to determine the suitability of mixing water except comparative tests. Generally, comparative tests require that, if the quality of water is not known, the strength of the sandceret block made the with water in question should be compared with the strength of concrete made with water of known suitability. Both blocks should be made with cement proposed to be used in the construction works.

Baiden and Tuuli (2004) confirmed that mix ratio, materials quality, and mixing of the constituent materials affect the quality of sandcrete blocks. Afolayan et al. (2008) tested the compressive strength values of sandcrete blocks produced by different block industries in Ondo State, Nigeria and found that they were very much lower than those stipulated by the relevant Codes and Standards. The blocks also had high coefficient of variation that indicate very poor quality control in the production processes. Wenapereand (2009) found that the compressive strength of sandcrete blocks increased with age of curing for all mixes tested at the water-cement ratio of 0.5. The strength at ages 7, 14, and 21 days were 43%, 75%, and 92% of the 28-day strength respectively.

According to NIS 87 (2000), sandcrete blocks pose intrinsic low compressive strength, indicating that they are susceptive to any natural disaster such as earth quakes or seismic activities. Previous studies have also indicated that sandcrete blocks are produced in various standards and some are below the requirement standards for the construction of the buildings. The deficiency found is that sandcrete has no standard engineering definition. The engineering definition of sandcrete is to suit the purpose of use. Sandcrete blocks are rough in physical appearance; due to the nature and origin of pure morphological definition. However, there is a general engineering materials standard definition such as sand, cement and water. In addition, the application of Geotechnical methods such as sieve analysis, silt/clay content and bulk density appeared to have consolidated engineering definition. The time mixing sandcrete with cement and also the time lapse between mixing compaction appear to have direct impact on the strength. Increase in strength with age and curing temperature, also seems to contribute to stabilization of sandcrete.

According to Smith (1976), water used for curing block can impair the strength of the block. Impurities and deleterious substances which are largely introduced from water used in mixing block are likely to interfere with the process of hydration, preventing effective bond between the mixtures and matrix. The impurities sometimes reduce the durability of the mixture (Neville, 1995). Therefore, there is need to investigate the effect of partially treated sewage water on sandcrete blocks made with different proportions of the sewage water using compressive strength test. This is what this study aimed at.

2.0 MATERIALS AND METHODS

2.1 Materials

The clean (uncontaminated) water used in this study was a normal tap water from borehole. It was a colourless, odourless and tasteless, portable water that was fit for drinking. The partially treated sewage water was obtained from ABU dam sewage unit section. The sand used was sharp sand and the cement was ordinary Portland cement obtained from an open market in Samaru, Zaria.

2.2 Methods

A rectangular metal cuboid (mould) of 150x75x75 mm was constructed which was used as standard size for all the block samples. The cement and sand were mixed uniformly with hand trowel at ratio 1:6 respectively and water cement ratio of 0.5 using compaction of 25 blow 3layers according to British Standard (BS) recommendation. The water was added in the following proportions:

Sample 1: 100% Tap water.
Sample 2: 100% Partially treated sewage water.
Sample 3: 80% Partially treated sewage water + 20% Tap water.
Sample 4: 60% Partially treated sewage water + 40% Tap water.
Sample 5: 40% Partially treated sewage water + 60% Tap water.
Sample 6: 20% Partially treated sewage water + 80% Tap water.

Samples 1 – 6 were designated as S1 – S6 throughout this study. A total number of 5 sandcrete blocks per sample was casted. All the casted block samples were cured for 7, 14 and 28 days before carrying out the compressive strength test. The compressive strength and absorption rate tests were carried out in the Civil Engineering Department, Ahmadu Bello University Zaria Concrete Laboratory.

3.0 RESULTS AND DISCUSSIONS

3.1 Properties of Water Used

Qualities of partially treated sewage water (PTSW) and tap water (TW) used for this study were analysed and the results are presented in Table 1.

Table 1: CHEMICAL PROPERTY OF WATER.

S/N	Parameters	Unit	PTSW	TW
1.	pH	-	6.9	8.5
2.	Total solid (TS)	Mg/l	17,410	280
3.	Total dissolve solid (TDS)	Mg/l	630	-
4.	Biological oxygen demand (BOD)	Mg/l	60	35
5.	Chemical oxygen demand (COD)	Mg/l	1800	133
6.	Dissolve oxygen (DO)	Mg/l	110	-

The partially treated sewage water (PTSW) and tap water (TW) samples have pH values of 6 and 8.5 which according to the findings of Neville (1995), that pH range between 6.0 and 8.0 have no significant effect on the compressive strength of concrete and sandcrete, show that the compressive strength values of sandcrete samples are not expected to be affected by the used water. And according to BS 3148: Methods of test for water for making sandcrete block and concrete, the permissible limit of total dissolved solids (TDS) is 2000 ppm (part per million) 1 Mg/l = 1ppm. It was observed that both water samples tested have their TDS within the acceptable limit.

3.2 Compressive Strength of Sandcrete Blocks

The compressive strength of the block samples was determined after 7, 14, and 28 days of curing. The prepared blocks were tested using the Compressive Testing Machine. The results are presented in Figure 1. In general, the compressive strength values increased with increase in curing age. The peak compressive strength value of 9.78 N/mm^2 was observed in sample S5 (100% tap water) at 28 days curing period while the least compressive strength value of 4.27 N/mm^2 was observed in sample S1 (40% partially treated sewage water + 60% tap water) at 7 days curing period.

This is in confirmation of some studies in the literatures that observed that water with the properties observed for the sewage water used in this study do not affect the compressive strength values of sandcrete blocks. It was further observed that the sewage water used in this study caused an increase in the compressive strength value of the sandcrete blocks. This observation may be due to the chemical properties of the partially treated water, which is presented in Table 1.

Sandcrete block samples made of partially treated sewage water show improvement in strength throughout the curing days. This observation may be as a result of the organic contents present in the partially treated sewage water which may be acting as dispersing agents improving the dispersion of particles of cement and reducing clumping. However, the long term performance and durability of sandcrete made from these water samples have not been ascertained. Also the effects of biological constituents, turbidity and presence of E-coli may not be insignificant on compressive strength of sandcrete block especially in long-term period. The observed trends are in agreement with similar research findings reported by Saricimen (2008).

3.3 Absorption Test

The variation of absorption rate with sandcrete block samples is shown in Figure 2. It was observed that the peak value of 11.11 % occurred in sample S3 (80% partially treated sewage water + 20% tap water) while the least absorption rate value of 7.69 % was observed in sample S4 (60% partially treated sewage water + 40% tap water). It was observed that there is significant difference in the absorption rate values of samples prepared with different proportions of partially treated sewage water and tap water.

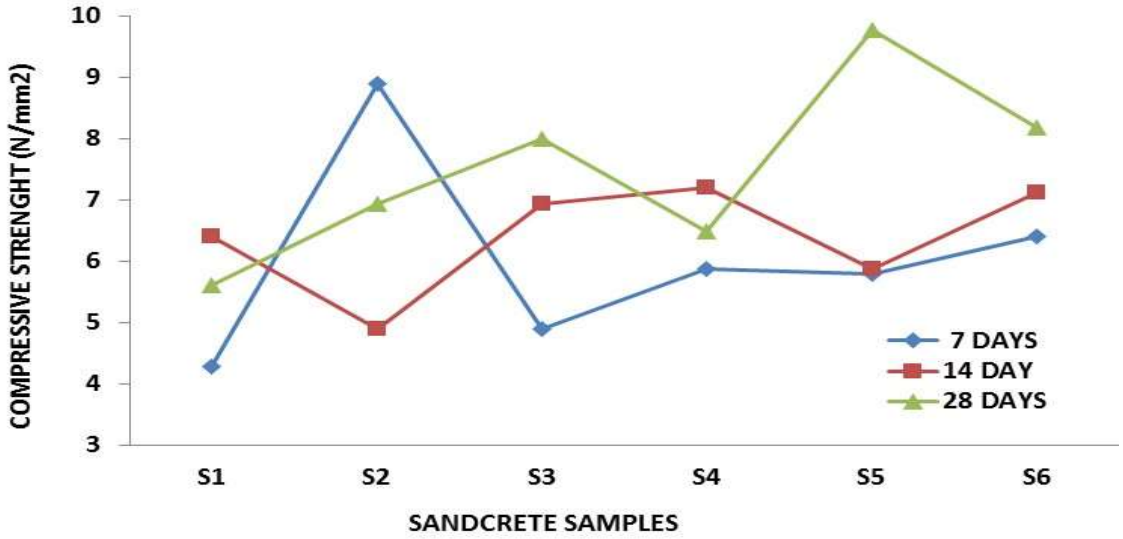


Figure 1: Variation of compressive strength values of block samples with curing period

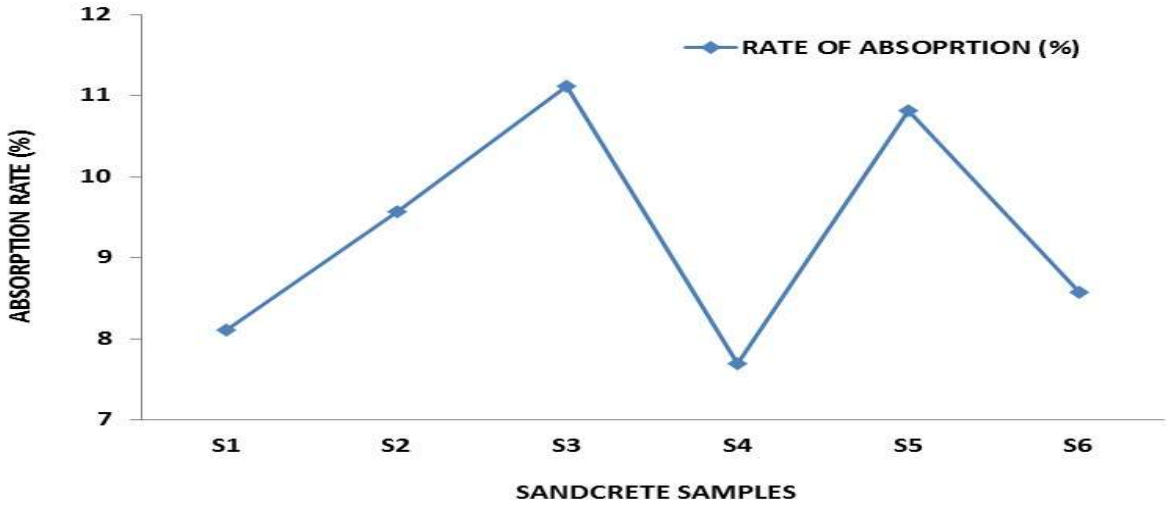


Figure 2: Variation of absorption rate with sandcrete block samples

4.0 CONCLUSION

Based on the results of the study carried out on the effect of partially treated sewage water on sandcrete blocks, the following conclusions were derived:

1. The partially treated sewage water (PTSW) and tap water (TW) samples have pH values of 6 and 8.5 which indicate lack of significant effect on the compressive strength of sandcrete blocks.
2. The compressive strength of the block samples was determined after 7, 14, and 28 days of curing. In general, the compressive strength values increased with increase in curing age.
3. The peak compressive strength value of 9.78 N/mm^2 was observed in sample S5 (100% tap water) at 28 days curing period while the least compressive strength value of 4.27 N/mm^2 was observed in sample S1 (40% partially treated sewage water + 60% tap water) at 7 days curing period.
4. It was observed that the peak value of 11.11 % occurred in sample S3 (80% partially treated sewage water + 20% tap water) while the least absorption rate value of 7.69 % was observed in sample S4 (60% partially treated sewage water + 40% tap water).
5. It was observed that there is significant difference in the absorption rate values of samples prepared with different proportions of partially treated sewage water and tap water.

5.0 REFERENCES

Abdullahi, M. (2005).Compressive Strength of Sandcrete Blocks in Bosso and Shiroro Areas of Minna, Nigeria, A.U. J.T. 9(2): 126-132.

Afolayan, J. O., Arum, C., and Daramola, C. M. (2008).Characterization of the Compressive Strength of Sandcrete Blocks in Ondo State, Nigeria. Journal of Civil Engineering Research and Practice, 5 (1): 15-28.

Aiyewalehinmi, E. O., Tanimola, M. O. (2013). Strength Properties of Commercially Produced Sandcrete block In Akure: Ondo State, International Journal of Engineering Science Invention, 2(5): 22-33.

Baiden, B. K. and Tuuli, M. M. (2004). Impact of quality control practices in sandcrete blocks production. Journal of Architectural Engineering, 10 (2): 53-60.

BS (British Standard) 3921 (1969).Specification for bricks and blocks of fired brick earth, clay or shale.

Ejeh, S. P. (1982). Comparative strength of Soilcrete blocks in Zaria, (Unpublished) Msc Thesis, Department of Civil Engineering, Ahmadu Bello University, Zaria.

Ewa, D. E., Ukpata, J. O. (2013). Investigation of the Compressive Strengths of Commercial Sandcrete Blocks in Calabar Nigeria. International Journal of Engineering and Technology, 3(4): 477 - 482.

Mahmoud, H., Hamma, H. A. and Abba, H. A. (2010).Compressive Strength of Marketed Sandcrete Blocks Produced in Yola, Nigeria, Journal of Engineering and Applied Sciences, 2: 74 – 81.

Neville, A.M. (1995). Properties of Concrete and Sandcrete, Addison Wesley Longman Limited, England

NIS (Nigerian Industrial Standard) (2000).Standard for Sandcrete Blocks. The Standard organization of Nigeria.

Saricimen, H., Shameem, M., Barry, M., and Ibrahim, M. (2008).“Testing of treated effluent for use in mixing and curing of concrete.”<e-printshttps://eprints.kfupm.edu.sa/1745/> (Sep. 21, 2009).

Smith, B., (1976) “Curing of Concrete”. In the Proceedings of the Lewis H. Tuthill International Symposium onConcrete and Concrete Construction, ACI SP-104, American Concrete Institute, Michigan, USA, pp: 145-159.

Wenapere, D. A. and Ephraim, M. E. (2009).Physico-mechanical behaviour of sandcrete block masonry units. Journal of Building Appraisal 4: 301–309. doi:10.1057/jba.2009.8

POINT AND NON-POINT SOURCE SEWAGE WATER QUALITY ANALYSIS FOR IRRIGATION FARMING

***SALAHUDEEN, A. B. AND AMPITAN, A. A.**

Samaru College of Agriculture, Division of Agricultural Colleges, Ahmadu Bello University, Zaria, Nigeria

***Corresponding Author:** basalahudeen@gmail.com

ABSTRACT

This research was carried out to investigate the quality of treated, partially treated and untreated sewage water when used for irrigation farming. The sewage water used in this study was obtained from Ahmadu Bello University Dam sewage unit. The water was collected at three different locations labeled Sections A – C. The study was aimed at investigating and recommending the best level of treatment sewage water should undergo before been discharged for irrigation purpose. The study results were compared with three standards; Federal Ministry of Environment (FME), Food and Agricultural Organization (FAO) and World Health Organization (WHO) and recommendations were based on compliance with these standards. Results obtained show that sewage water obtained from Section C gave close range values to those recommended in the used standards and it is therefore recommended for irrigation farming for better and improved yield of crops.

Keywords: *Point source, Non-point source, Sewage Water, Irrigation Farming*

1.0 INTRODUCTION

Water is an important constituent of the ecosystem; it is the most abundant substance on earth. It exists in a variety of forms such as sea water, snow, surface water, soil moisture, groundwater and water vapour. In addition, water is particularly important to life; the earliest string of life on earth started in water and even though some forms have strayed away from their natural habitat to be sustained on land water is still considered for their survival. Man can live several weeks without food, but not without water, the longest he can live is ten days (Chaturvedi, 1987). However, water is not only for sustenance of life, but is also essential for socioeconomic development. Agriculture, the first step in enabling the development of societies, requires vast amount of water. In a single growing season, a plant may absorb as much as 2000 times its grain yield (Ahaneku *et al.,* 2004). Crops can be grown without fertilizers and even without soil, but they cannot survive without water.

Nigerian agriculture is basically rain fed, characterised by low productivity and subjected to the vagaries of weather. Water is therefore a limiting factor to agricultural production in most parts of the country. According to Musa (2001), there are a number of reasons why water and not land may become the most important constraint for Nigeria's food security. First, is Nigeria's extreme inter and intra annual climate variability. Second, is the strong indication that discharges from West African rivers including Nigeria have dropped significantly over the past 25 years. Third, the population growth and growing urbanisation is increasing water demand for domestic, industrial and environmental uses. Lastly, when upstream riparian countries develop water resources fully, transborder flows drop considerably leaving less internal flow for downstream users (Ahmed *et al.,* 2008).

The accumulation of some chemicals in the water used for irrigation farming could affect the farm produce and/or cause serious health hazards to human beings and animals. Certainly, the quality of crop yield is dependent on the quality of water used. Water of inadequate quality has the potential to be a direct source of contamination and a vehicle for spreading localised contamination in the field, facility or transportation environments in the production of fresh produce crops. Therefore there is need to analyse the quality of water used for irrigation so as to ascertain the effect of the water on the crops and to recommend crops that are best grown with the sewage water. These make it necessary to evaluate the quality of the water before use. The study was aimed at evaluation of the sewage water quality for irrigation farming purpose.

2.0 MATERIAL AND METHODS

2.1 Material

2.1.1 Sewage water

The sewage water used was collected from the Sewage unit of Ahmadu Bello University Dam.

The water was collected at three different locations labelled section A, B and C. The sewage water was collected into a plastic container and transported directly to the laboratory where some parameters were tested.

2.2 Methods

All tests conducted on the water samples were conducted based on the standard laboratory procedures. Three laboratories in Ahmadu Bello University were used to carried out the analysis base the kind of test they can perform in their laboratories. These laboratories are: Ahmadu Bello University Multipurpose Laboratory in Chemistry Department, Department of Water Resources Engineering Laboratory and Institutes of Agricultural research Multipurpose Laboratory. Some of the parameters tested include temperature, pH and Dissolved oxygen. The rest of the samples were kept inside refrigerator for preservation. Acid digestion was carried out on the samples for heavy metals analysis. These analysis results were compared with three different standards; Federal Ministry of Environment (FME), Food and Agricultural Organization (FAO) and World Health Organization (WHO) in order to determine the suitability of the sewage water for irrigation purpose.

3.0 RESULTS AND DISCUSSIONS

3.1 Results of Sewage Water Analyses

The types of analyses carried out on the sewage water samples used in this study are presented in Table 1. The concentration of most of the chemical constituents are higher in sections A and B compared with section C which is the water released to the farmers for irrigate farming. These analysis results were compared with three different standards; Federal Ministry of Environment (FME), Food and Agricultural Organization (FAO) and World Health Organization (WHO) in order to determine the suitability of the sewage water for irrigation purpose. All results are in mg/l.

Table 1: Results of Sewage Water Analyses

Parameters	Section A	Section B	Section C
Temperature	28	28	28
pH	6.7	6.9	6.5
Dissolved oxygen	120	110	100
B.O.D	70	60	60
C.O.D	260	180	120
Total solids	1200	1741	1070
TDS	780	630	790
Ammonia	1.4	1.7	1.8
Nitrite	0.0708	0.0236	0.047
Nitrate	0.0525	0.0175	0.035
Sulphate	34.795	46.79	29.15
Phosphate	13.71	17.29	12.52
Nitrogen	0.7	1.4	2.45
Cadmium	0.019	0.019	0.024
Lead	0	0	0
Cobalt	0.119	0.164	0.098
Copper	0.02	0.027	0.031

3.2 Comparison of Results of Sewage Water Analyses with Standards

3.2.1 Temperature; The temperature results of all the three sections were the same. The temperature was found to be 28°C which is close to the requirement of 25°C by WHO.

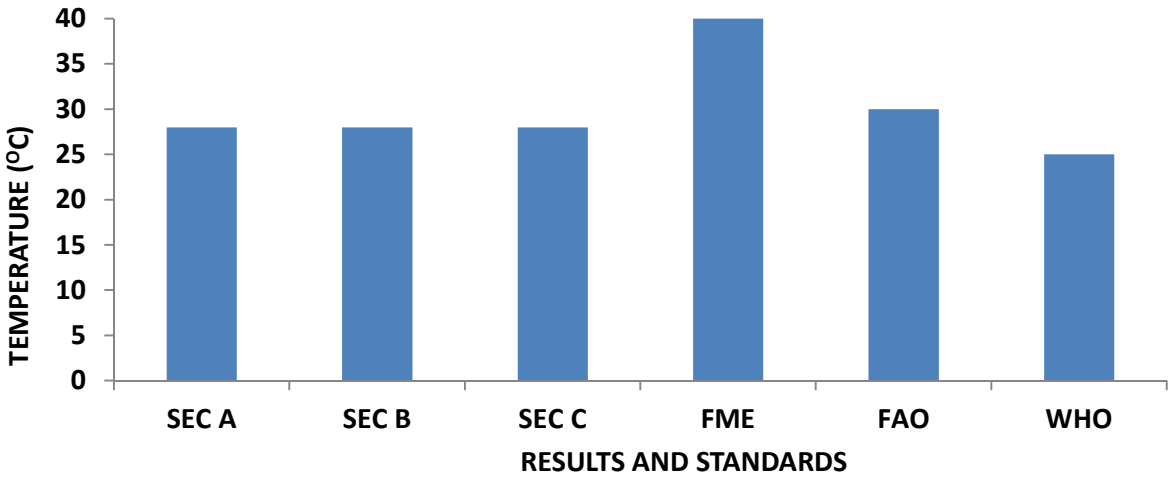


Figure 1: Temperature results and comparison with standards

3.2.2 Cadmium: The concentration of cadmium is higher in all the three sections compared with the standards.

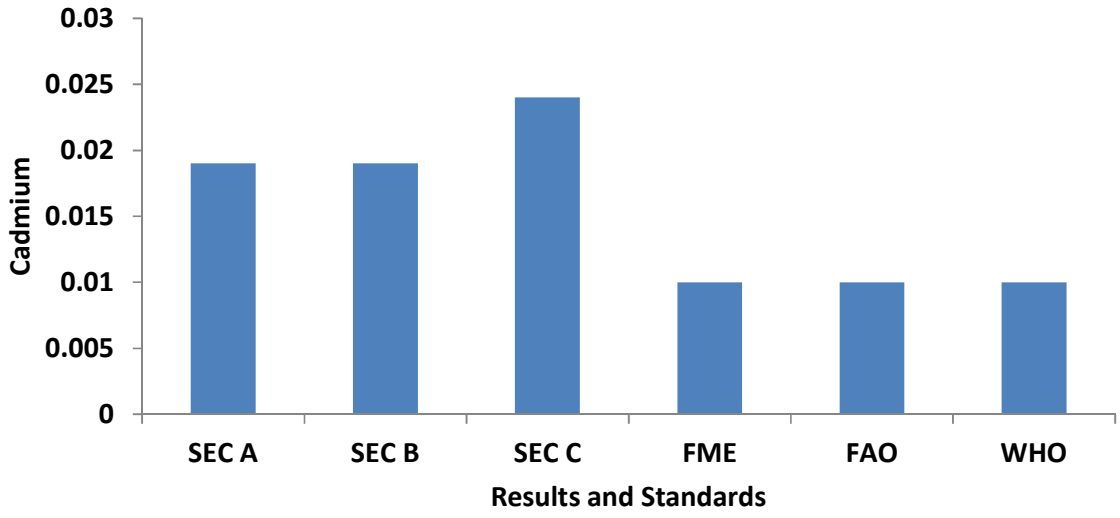


Figure 2: Cadmium results and comparison with standards

3.2.3 pH: The pH values of all sections are close to the standard requirements. The pH results are presented in Figure 3.

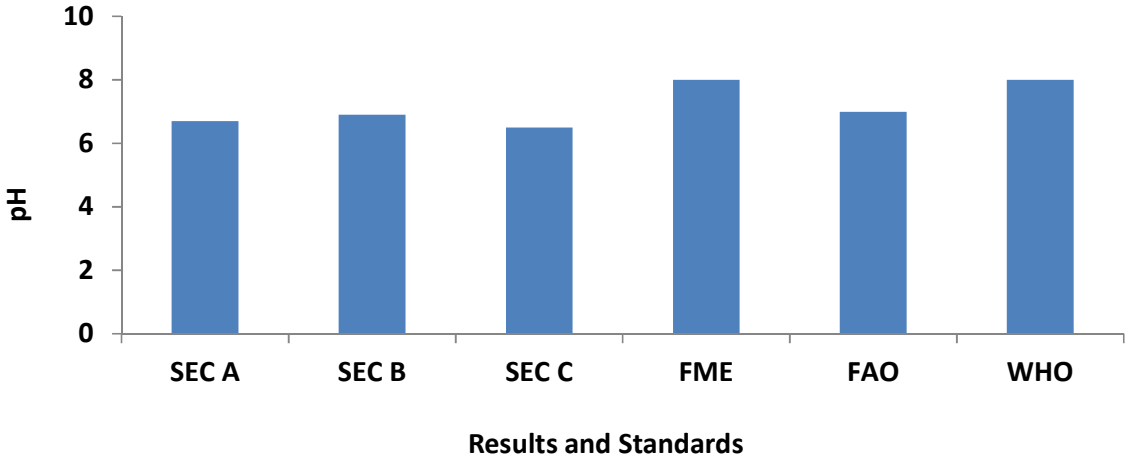


Figure 3: pH results and comparison with standards

3.2.4 Dissolved Oxygen: The dissolved oxygen results are presented in Figure 4.

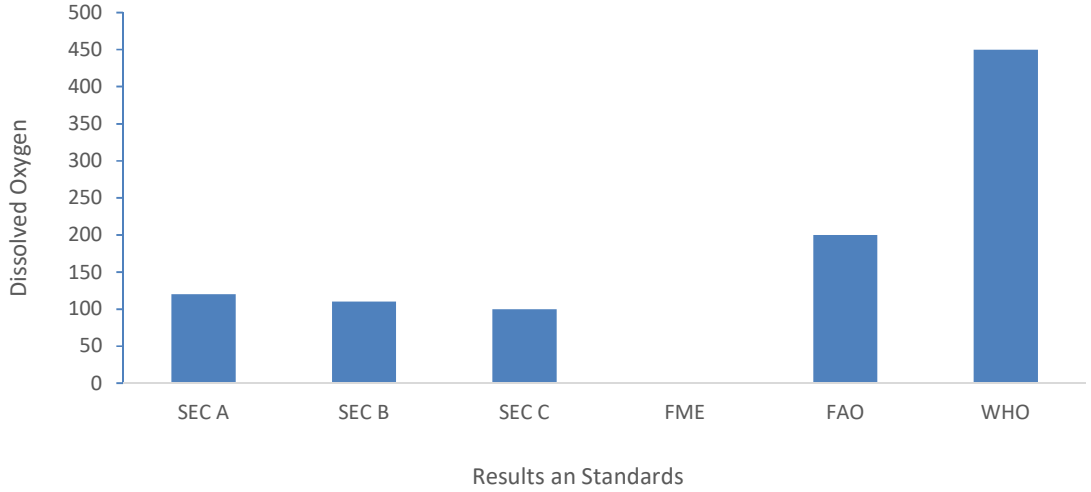


Figure 4: Dissolved oxygen results and comparison with standards

3.2.5 BOD_5: The $B.O.D_5$ results all the three sections are higher than the standards requirements. The BOD results are presented in Figure 5.

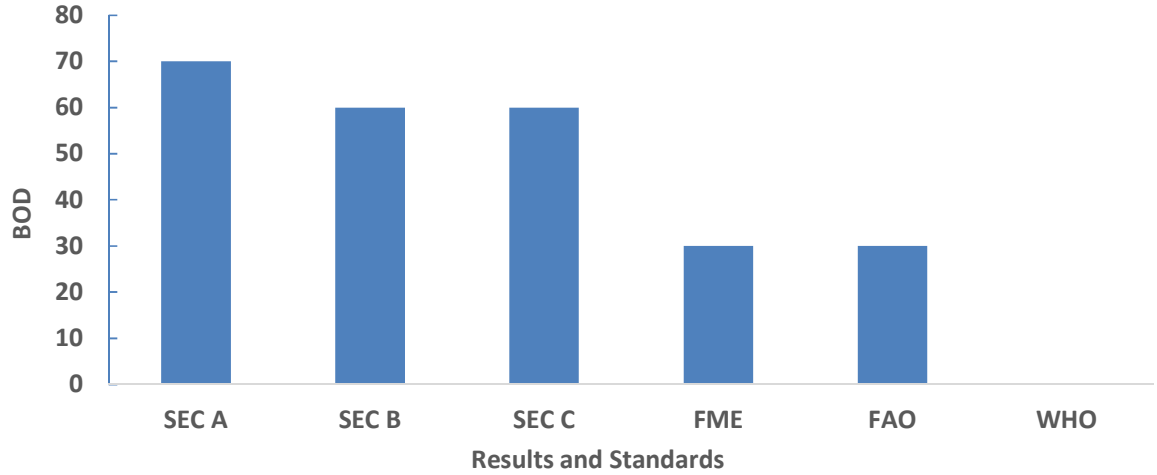


Figure 5: The BOD results and comparison with standards

3.2.6 Chemical Oxygen Demands: The COD results of all the three sections are higher than the standards requirements. The COD results are presented in Figure 6.

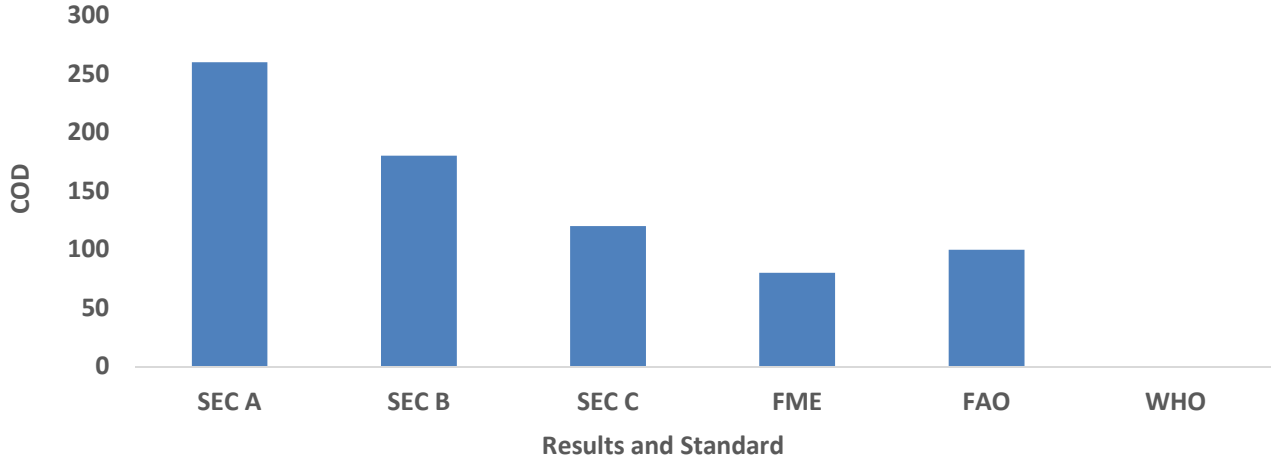


Figure 6: COD results and comparison with standards

3.2.7 Total Solids: The total solids results of sections A and C are in close range with the provision of FAO. The total solid results are presented in Figure 7.

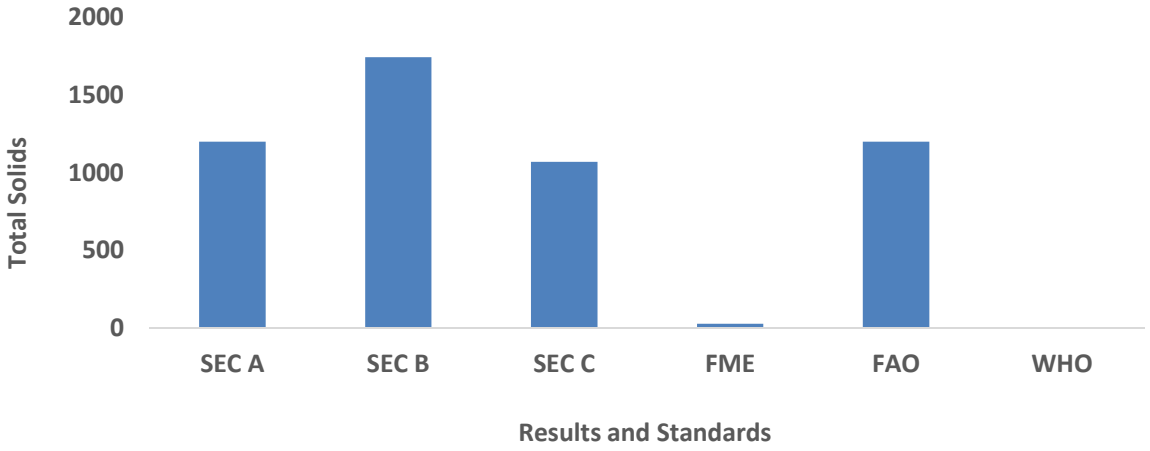


Figure 7: Total solids results and comparison with standards

3.2.8 Total Dissolved Solids: The TDS results of all the three sections fell below standards requirements. The TDS results are presented in Figure 8.



Figure 8: Total dissolved solids results and comparison with standards

3.2.9 Ammonia: The Ammonia results of all the three sections are very high compared with the standards requirements.

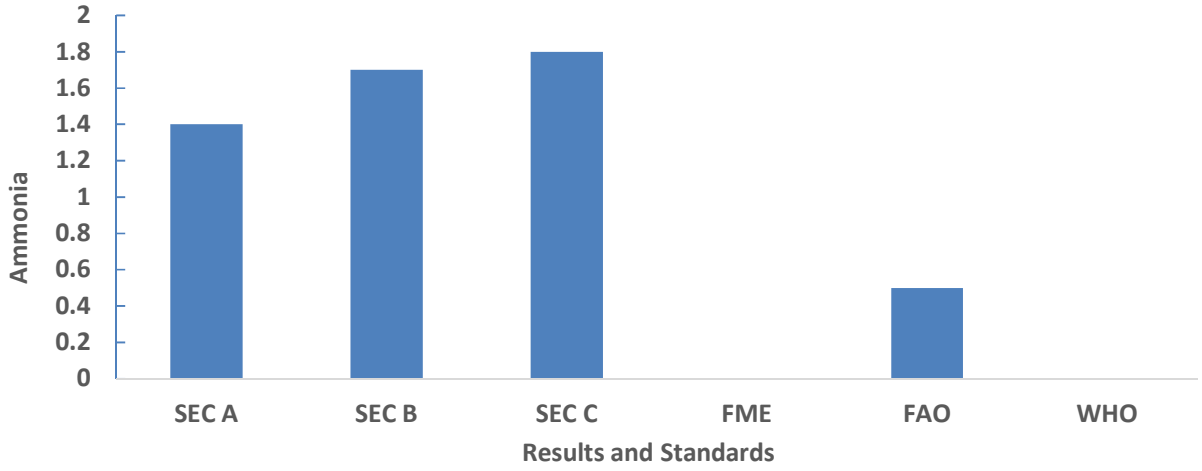


Figure 9: Ammonia results and comparison with standards

3.2.10 Copper: The Copper results of all the three sections are very low compared with the standards requirements.

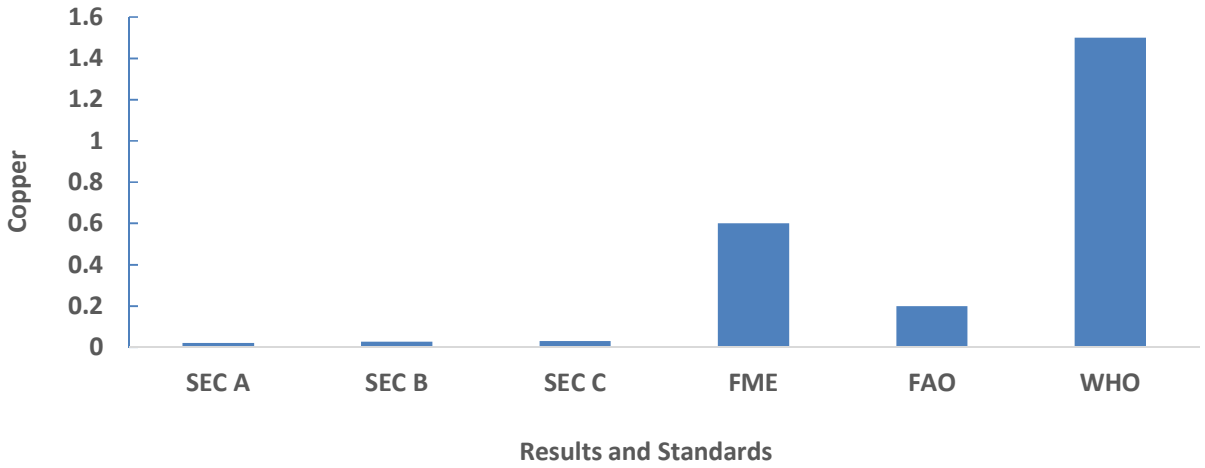


Figure 10: Copper results and comparison with standards

3.2.11 Nitrate (NO_3): The Nitrate results of all the three sections are very low compared with the standards requirements.

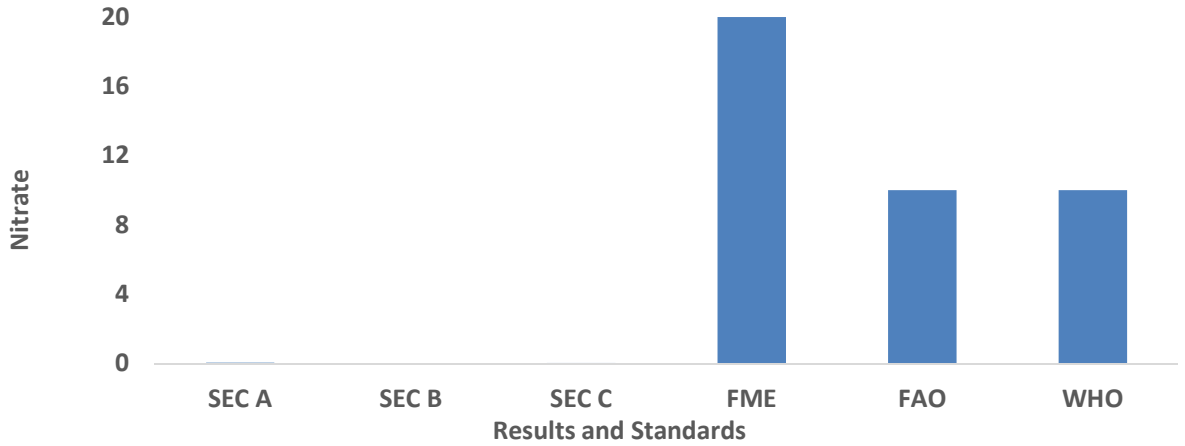


Figure 11: Nitrate results and comparison with standards

3.2.12 Nitrite (NO_2): The Nitrite results of all the three sections are very low compared with the standards requirements.

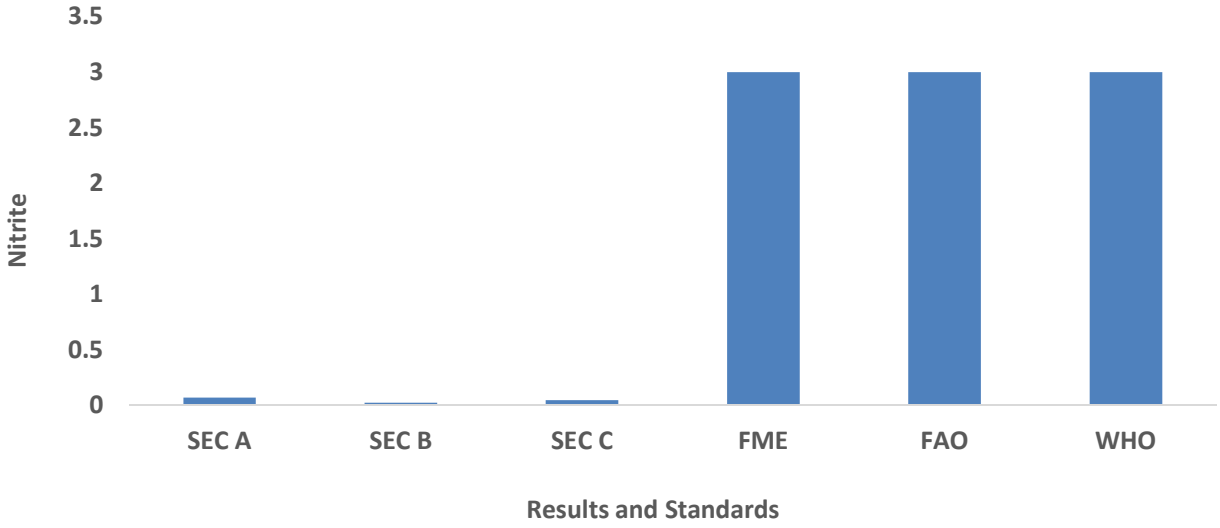


Figure12: Nitrite results and comparison with standards

3.2.13 Sulphate (SO_4): The Sulphate results of all the three sections are very low compared with the standards requirements.

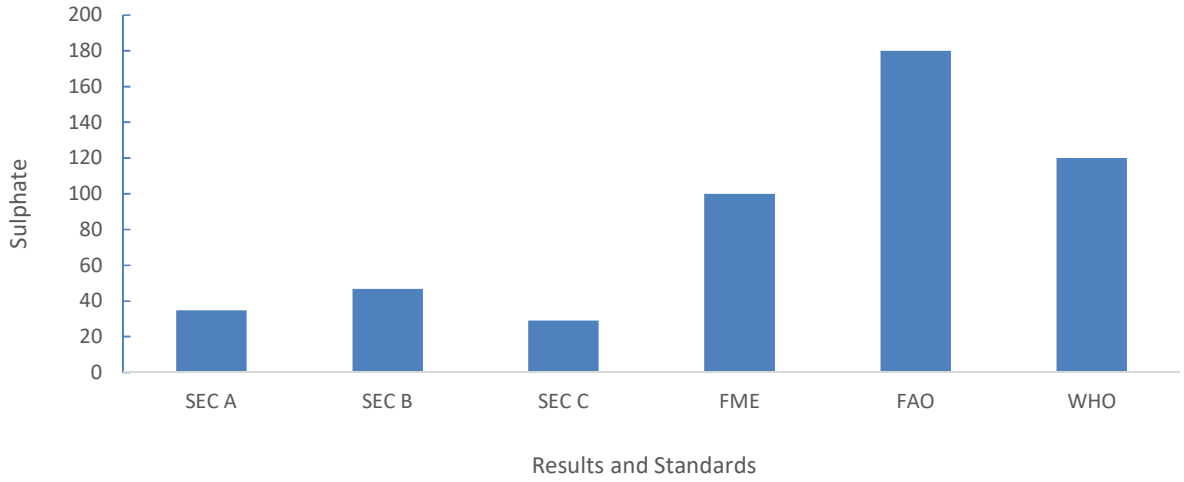


Figure13: Sulphate results and comparison with standards

3.2.14 Phosphate (PO_4): Variation of Phosphate results is shown in Figure 14.

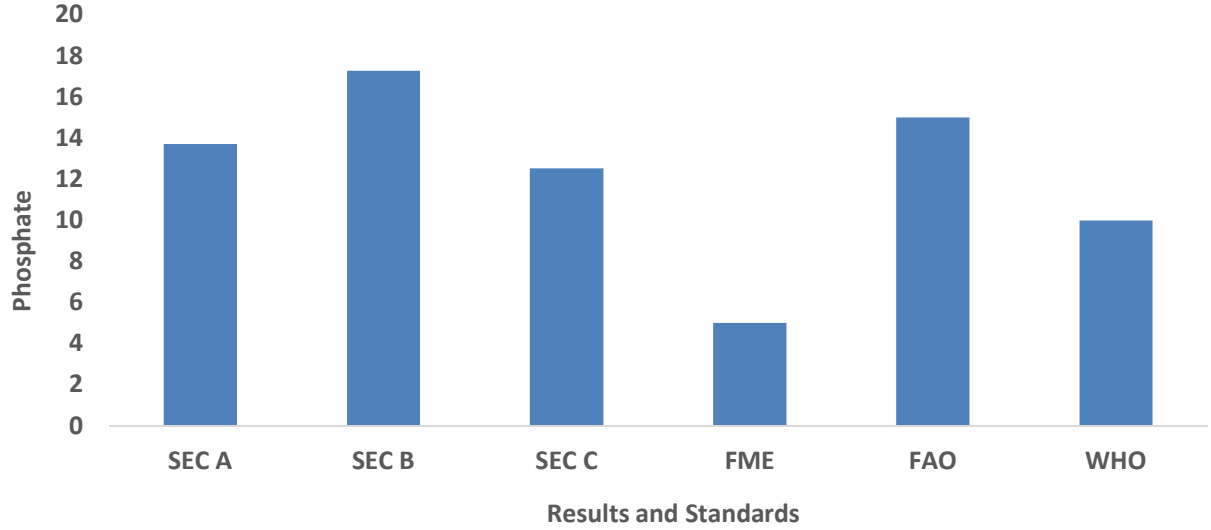


Figure 14: Phosphate results and comparison with standards

3.2.15 Lead: The results of Lead of all section samples is zero.

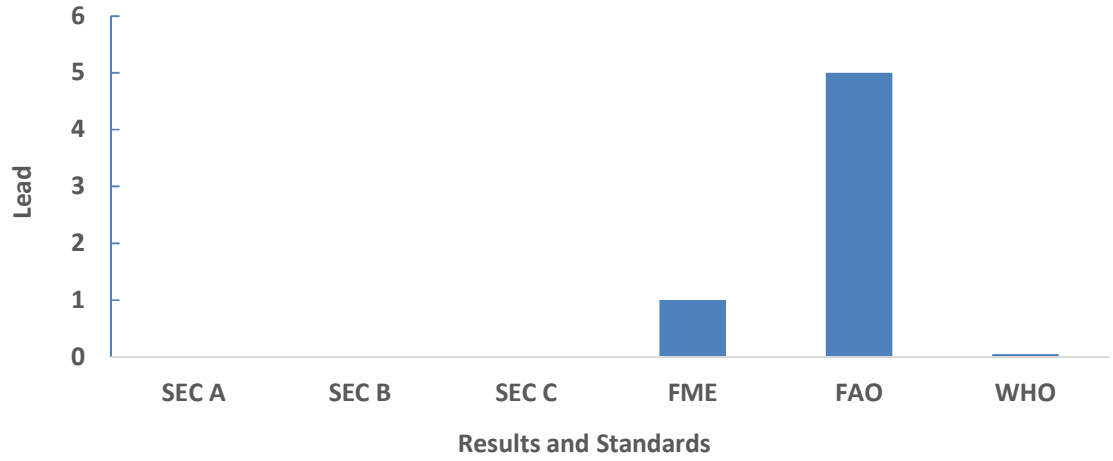


Figure 15: The lead results and comparison with standards

3.2.16 Nitrogen: The Nitrogen test results of section C is close to the specification of the three standards considered.



Figure 16: The Nitrogen results and comparison with standards

3.2.17 Cobalt: The Cobalt results of section A and C are in close range with those specified by FME and FAO.

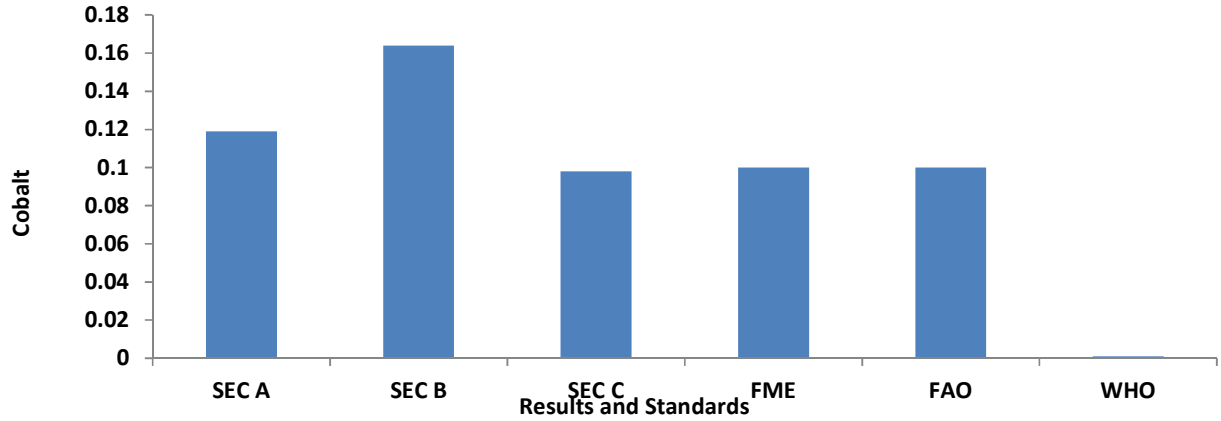


Figure 17: The Cobalt results and comparison with standard

4.0 CONCLUSION

The quality of irrigation water available to farmers and other irrigators has a considerable impact on what plants can be successfully grown, the productivity of these plants, and water infiltration and other soil physical conditions. The first step in understanding how an irrigation water source can affect a soil-plant system is to have it analyzed by a reputable lab and compared with the recognized standards. The trace elements and heavy metals are minutes and within the range of the standard and the production of crops. section C gave close range values to the recommendations in the standards and it is therefore recommended for irrigation farming for better yield of crops. Results obtained shows that sewage water obtained from section C gave close range values to the recommendations in the standards and it is therefore recommended for irrigation farming for better yield of crops.

REFERENCES

Ahaneku IE, James D, Edogi KS (2004). Changes in Soil Quality Indicators Induced by Field Incorporation of Selected Animal Wastes. J. Agric. Environ. Eng. Technol. 1(1): 78-85

Ahmed, M., R.A. Khattak and D. Mohammad. 2008. Soil evaluation of Kafoor Dheri farm for crop production. Soil & Environ., 27(1): 43-51.

Chaturvedi MC (1987). Water Resources Systems Planning and Management. Tata McGraw-Hill Publishing Company Limited, New Delhi 110 007, India

Musa IK (2000). Land and Water Use in Sustainable Agriculture: An Integrated Land and Water Resource Management for Food and Rural Development. Lead Paper presented at International Conference of NIAE 22: 8-15.

Musa IK (2001). Challenges and Opportunities for Sustainable Irrigation Development in Nigeria. Proceeding of NIAE 23: 13-22

MOULDING OF EARTH BLOCKS USING CONTAMINATED WATER

[*]SALAHUDEEN, A. B. AND POPOOLA, F. M.
[1]Samaru College of Agriculture, Division of Agricultural Colleges, Ahmadu Bello University, Zaria
[*]**Corresponding email:** basalahudeen@gmail.com

ABSTRACT
This study was carried out to determine the effect of partially treated sewage water on earth blocks. The soil used in this project work was obtained from Samara College of Agriculture, Division of Agricultural Colleges, Ahmadu Bello University, Zaria. The soil was mixed with a predetermined percentage of partially treated sewage water, which was gotten from the sewage unit of Ahmadu Bello University water board. To prepare the control samples, the soil was mixed with a predetermined percentage of tap water, gotten from the College Department of Agricultural And Bio- Environmental Engineering Programme. Results obtained from the study show that there is considerable difference in the compressive strength values of earth block samples prepared with partially treated sewage water and those treated with tap water. Peak compressive strength value of 2.22 N/mm2 was observed for S1 (100% tap water), S2 (100% partially treated sewage water) and S3 (80% partially treated sewage water + 20% tap water) all at 7 days curing period while the least compressive strength value of 1.51 N/mm^2 was observed in sample S5 (40% partially treated sewage water + 60% tap water) at 14 days curing period.

Keywords: *Contaminated water, Earth blocks, Compressive strength, Absorption rate, Sewage water*

1.0 INTRODUCTION

Many benefits that are offered by earth construction are often underutilized in the developed world where the use of earth as a low-embodied material is often the case (Midden, 2001). Historically, earth has been the most widely known and used building material in construction and probably has been the most important of all building materials (Legget, 1960). According to Midden (2001) recorded cases of the use of earth bricks dates back to Mesopotamia "around 8000 BC". Recent reports indicated that, about half of the world's populations are still living in earth buildings (McHenry, 1984). Of all urban housing units worldwide there are about 25 % that does not conform to building regulations while18 % are considered non-permanent structures (Habitat, 2001).

Earth as a building material is available everywhere and exists in many different compositions. It is most efficiently used in developing countries to house the greatest number of people with the least demand. The world map below shows the distribution of buildings units using earth material and construction around the world. However, it must be noted that earth buildings are not a phenomenon only of the Third World countries, but also in developed countries(EBA New Zealand, 1998). There are many benefits of earth buildings. For example, earth structures are completely recyclable, so sun-dried bricks return to the earth without polluting the soil (Rigassi, 1995).

It is important to ensure that the materials used in construction meet all the specification in every respect. This means that all relevant properties must be checked properly before construction (Tuffin, 2007). There are many benefits of earth buildings. For example, earth structures are completely recyclable, so sun-dried bricks return to the earth without polluting the soil (Rigassi, 1995). Using earth for such environmental-friendly buildings will be a strong component in the future of humankind (Bossel, 1998; Hochella, 2002). In addition, energy requirement to produce adobe block is only 5 (kWh)/cubic meter, while it is about 1000 (kWh)/ cubic meter for fired brick and 400-500 (kWh)/ cubic meter for concrete.

Generally, people are re-discovering the benefits of having earth walls in developing countries (Midden, 2001). This is because better properties can be obtained by using additives to the earth material. In addition, earth construction is possible with a wide variety of building methods. Egyptian architect, Hassan Fathy (1973) argues that housing design should not be based solely on imported forms, but rather on traditional forms of architecture as well. In 1998, 88% of Yemeni families were living in villages and in their own made houses. There are many economical, demographic and social problems associated with housing issues as the need for housing in Yemen which is increasing rapidly (Al-Jahdari et al., 1998). For example, there is a clear shortage of houses compared to the number of families. A study about the housing situation in the Republic of Yemen has indicated that the average yearly demand has been about 149,500 units, from 1992 to 2005 (Al-Jahdari et al., 1998).

Sewage (or domestic wastewater or municipal wastewater) is a type of wastewater that is produced from a community of people. It is characterized by volume or rate of flow, physical condition, chemical and toxic constituents, and its bacteriologic status (which organisms it contain and in what quantities). It consist mostly of grey water (from the sinks, tubs, showers, dishwashers, and cloth washers), black water (the water used to flush toilets combined with the human waste that its flushes away); soap and detergent; and toilet paper. It also contain surface runoff depends on the design of sewage system. Since local residents use contaminated water including effluents for their block making works, this study aimed at evaluating the effects of partially treated sewage water on earth blocks in terms of compressive strength test, absorption rate test and water quality tests.

2.0 MATERIALS AND METHODS

2.1 Materials

2.1.1 Soil

The soil sample used for this study was obtained from the College Farm. Samaru College of Agriculture, Division of Agricultural Colleges. Ahmadu Bello University, Zaria, Nigeria located at latitude 11^0 10' N and longitude 7^0 38' E. The soil sample was obtained using disturbed sampling method from trial pit dug to a depth between 0.6 – 1.0 m below the top soil to avoid organic matter influence. The soil sample was dried in the sun to obtain the actual weight of the natural soil and it was sieved to remove stones and unwanted materials before mixing with the right proportion of sewage/tap water used.

2.1.2 Water

The clean (uncontaminated) water used in this study was a normal tap water from borehole. It was a colourless, odourless and tasteless, portable water that was fit for drinking. The partially treated sewage water was obtained from ABU dam sewage unit section. The sand used was sharp sand and the cement was ordinary Portland cement obtained from an open market in Samaru, Zaria.

2.2 Methods

A rectangular metal cuboid (mould) of 150x75x75 mm was constructed which was used as standard size for all the earth block samples. The soil was mixed uniformly with hand trowel. The water was added in the following proportions:
Sample 1: 100% Tap water.
Sample 2: 100% Partially treated sewage water.
Sample 3: 80% Partially treated sewage water + 20% Tap water.
Sample 4: 60% Partially treated sewage water + 40% Tap water.
Sample 5: 40% Partially treated sewage water + 60% Tap water.
Sample 6: 20% Partially treated sewage water + 80% Tap water.
Samples 1 – 6 were designated as S1 – S6 throughout this study. A total number of 7 earth blocks per sample was casted resulting to a total of 42 blocks. All the casted block samples were cured for 7, 14 and 28 days before carrying out the compressive strength test. The compressive strength and absorption rate tests were carried out in the Civil Engineering Department, Ahmadu Bello University Zaria Concrete Laboratory.

3.0 RESULTS AND DISCUSSIONS

3.1 Properties of Water Used

Qualities of partially treated sewage water (PTSW) and tap water (TW) used for this study were analysed and the results are presented in Table 1.

Table 1: CHEMICAL PROPERTY OF WATER.

S/N	Parameters	Unit	PTSW	TW
1.	pH	-	6.9	8.5
2.	Total solid (TS)	Mg/l	17,410	280
3.	Total dissolve solid (TDS)	Mg/l	630	-
4.	Biological oxygen demand (BOD)	Mg/l	60	35
5.	Chemical oxygen demand (COD)	Mg/l	1800	133
6.	Dissolve oxygen (DO)	Mg/l	110	-

The partially treated sewage water (PTSW) and tap water (TW) samples have pH values of 6 and 8.5 which according to the findings of Neville (1995), that pH range between 6.0 and 8.0 have no significant effect on the compressive strength of blocks. And according to BS 3148: Methods of test for water for making blocks, the permissible limit of total dissolved solids (TDS) is 2000 ppm (part per million) 1 Mg/l = 1ppm. It was observed that both water samples tested have their TDS within the acceptable limit.

3.2 Compressive Strength of Sandcrete Blocks

The compressive strength of the block samples was determined after 7, 14, and 28 days of curing. The prepared blocks were tested using the Compressive Testing Machine. The results are presented in Figure 1. In general, the compressive strength values decreased with increase in curing age. The peak compressive strength value of 2.22 N/mm^2 was observed in sample S1 (100% tap water), S2

(100% partially treated sewage water) and S3 (80% partially treated sewage water + 20% tap water) all at 7 days curing period while the least compressive strength value of 1.51 N/mm^2 was observed in sample S5 (40% partially treated sewage water + 60% tap water) at 14 days curing period.

3.3 Absorption Rate Test

The variation of absorption rate with earth block samples is shown in Figure 2. It was observed that the peak value of 15.08 % occurred in sample S4 (60% partially treated sewage water + 40% tap water) while the least absorption rate value of 6.58 % was observed in sample S1 (100% tap water). It was observed that there is significant difference in the absorption rate values of samples prepared with different proportions of partially treated sewage water and tap water.

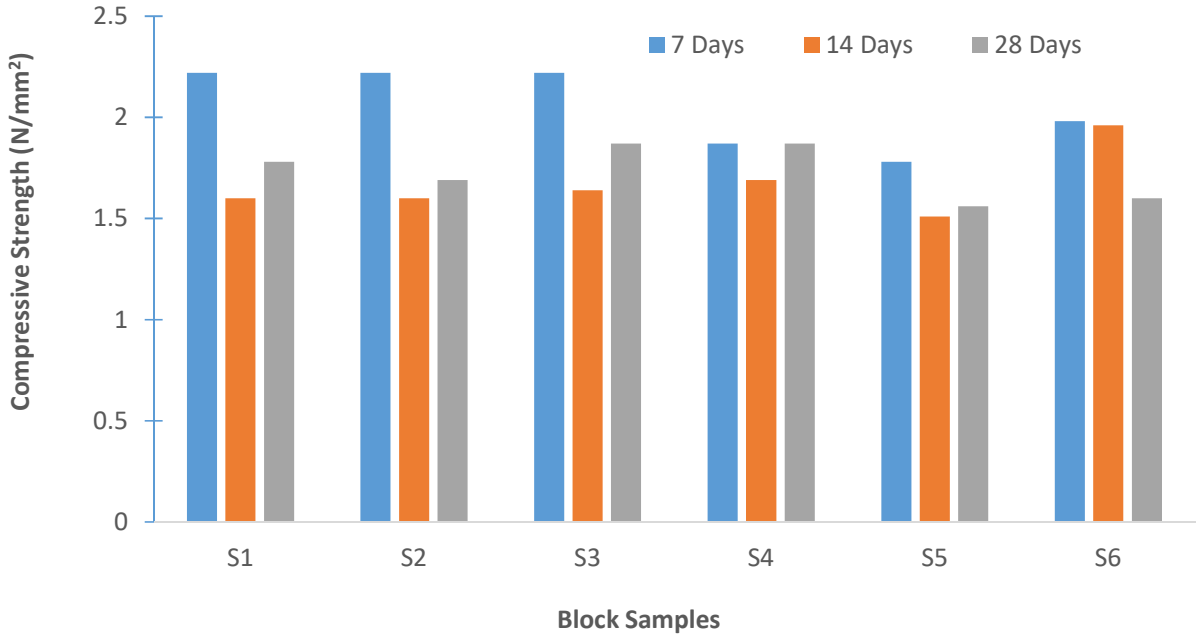


Figure 1: Variation of compressive strength values of block samples with curing period

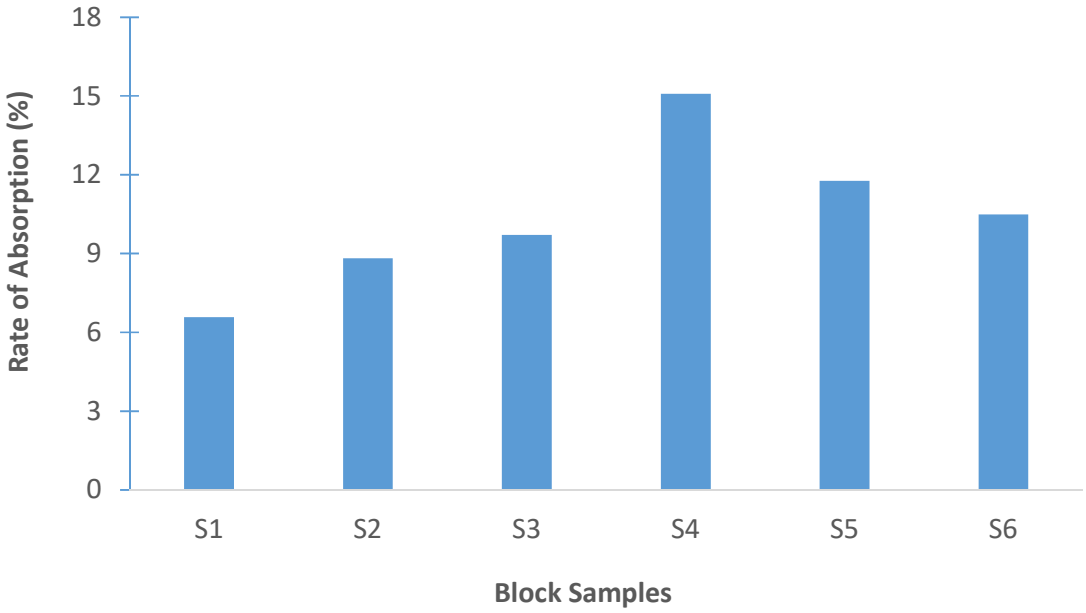


Figure 2: Variation of absorption rate with earth block samples

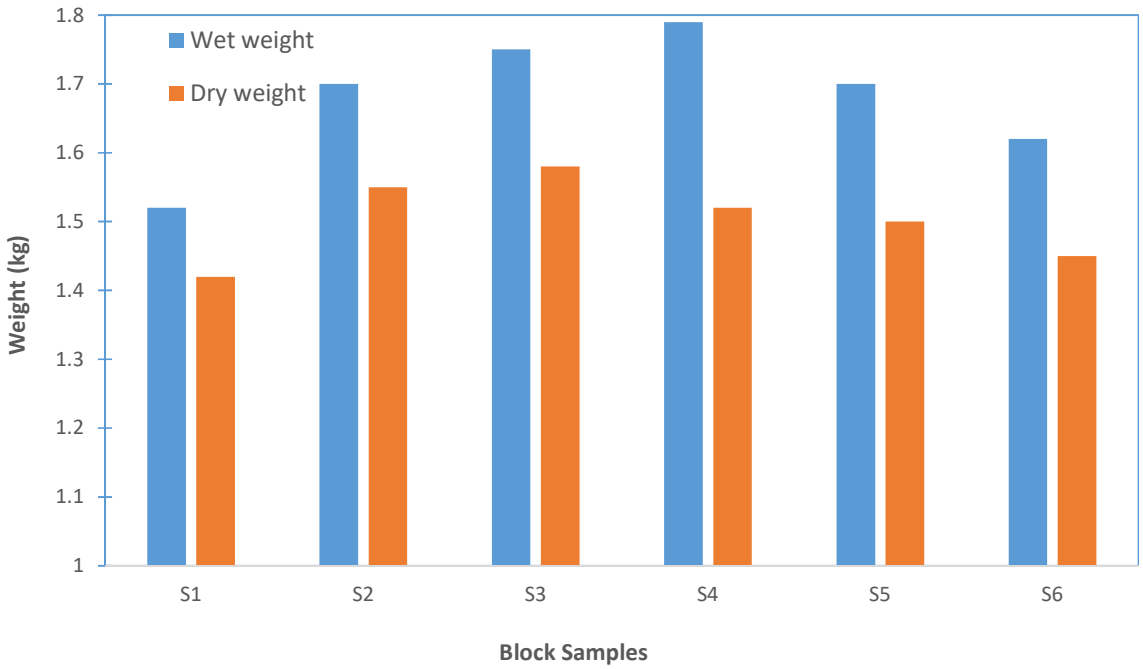


Figure 3: Variation of wet and dry weights of the prepared block samples

4.0 CONCLUSION

Based on the results of the study carried out on the effect of partially treated sewage water on earth blocks, the following conclusions were derived:

1. The compressive strength of the block samples was determined after 7, 14, and 28 days of curing. In general, the compressive strength values decreased with increase in curing age.
2. The partially treated sewage water (PTSW) and tap water (TW) samples have pH values of 6 and 8.5.
3. The peak compressive strength value of 2.22 N/mm^2 was observed in sample S1 (100% tap water), S2 (100% partially treated sewage water) and S3 (80% partially treated sewage water + 20% tap water) all at 7 days curing period while the least compressive strength value of 1.51 N/mm^2 was observed in sample S5 (40% partially treated sewage water + 60% tap water) at 14 days curing period.
4. The peak value of 15.08 % occurred in sample S4 (60% partially treated sewage water + 40% tap water) while the least absorption rate value of 6.58 % was observed in sample S1 (100% tap water).
5. It is recommended that earth blocks should not be cured above seven days before placement.

5.0 REFERENCES

Al-Jahdari (1998) "A study about the housing situation in the Republic of Yemen"

Bahar and Naik, T.R. (2004), Earth construction from shrinkage, cracking, durability and low strength.

Bossel (1998). Research on importance of using earth block for building.

Hochella (2002). Importance of using earth block for building.

Hassan F. (1973) "Housing design".

McHenry, 1984; EBAA. Australia (Recent reports about half of the world's populations living in earth buildings).

Midden D. (2001), States the benefit of using earth block for construction of buildings.

Rigassi, (1995) "Benefits of earth buildings).

Tuffing (2007), Properties of soil that needs to be check before using for construction.

ESTERIFICATION OF PROPANOIC ACID WITH N-BUTANOL IN $ZNCL_2$/UREA DEEP EUTECTIC SOLVENT

YAHAYA MUHAMMAD SANI*AND LEVI INUWA
Department of Chemical Engineering, Ahmadu Bello University, 870001 Nigeria.
*Corresponding author Tel.: 0903 965 4787; e-mail: ymsani@abu.edu.ng; ayeashah@yahoo.com

ABSTRACT
Esterification reaction between Propanoic acid and n-Butanol produces esters and water. Usually, the process is a slow equilibrium reaction, which requires the activity of a catalyst for it to reach completion. The present study utilized varying molar ratio (1:1 mmol, 1:2 mmol, 1:3 mmol 1:4 mmol, and 1:5 mmol) of $ZnCl_2$/Urea; a green Deep Eutectic Solvent at constant temperature of 100 °C. This saves the cost as well as environmental impact of utilizing H_2SO_4 catalyst. The percentage yields obtained were 87.6%, 90.4%, 93.3%, 94.5%, and 97.2% respectively at a shorter reaction time of 40 min, compared to conventional methods. Molar ratio 1:5 favoured high yield of the butylpropanoate; an ester with high demand in the soap and perfume industries. Further, the DES satisfied the conditions of green chemistry in terms of its recyclability and non-corrosiveness. This implies that the $ZnCl_2$/Urea DES is a potential substitute as a catalyst in the esterification reaction.

1 INTRODUCTION

The reaction between carboxylic acids and alcohols gives esters through the process of esterification. Esterification is an essential reaction in organic material production. This method of ester production is commonly a single step, atom-efficient process of synthesis. The process of direct esterification of alkanoic acids with alcohols signifies a familiar classification of liquid-phase reactions (Dupont & Lefebvre, 1996). Esterification is of substantial engineering concern as a result of vast useful significance of the chemical products obtained. Low-molecular-weight carboxylic groups are broadly reprocessed to address vital problems owing to their simplicity, convenience, and less toxicity. In general, esters are considerable organic compounds with proper kinetic evidence.

The esterification reaction between direct alcohol groups and alkanoic acid can occur conservatively without the use of catalyst. The rate of alkanoate formation is faster when an acid or base catalyst is used. In most chemical and industrial cases, the use of catalyst is more preferable to cut expenditure and to manage time. The use of acid catalyst to improve the rate of esterification was developed by Emil Fischer (1852-1919). This form of reaction was an equilibrium reaction. There are other industrial and laboratory methods of production of esters, though Emil Fischer method is easy and motivating. In many industrial fields and research institutes, esterification reaction was termed as an equilibrium reaction. During esterification, inorganic catalyst such as H_2SO_4, HF and H_3PO_4 were the considerable inorganic solvents used. Nevertheless, the catalyst used as inorganic acids needs to be treated and neutralized after esterification has been successfully carried out. This was necessary because the catalyst were highly toxic, on-renewable and not eco-friendly (Williamson et al., 1994). Also, the elimination of absorbed substances present in catalyst is time-consuming, uses large amount of organic liquids and very expensive. Because of the problems associated with organic solvent, Discovery of better method of esterification was necessary. Synthetic method was preferable as an environmental friendly process with high yield of esters (Metody & Oczyszczania, 2011).

Deep eutectic solvents (DESs) are organic substances whose constituents form a low melting point below that of each separate component. The use of this organic catalyst delivers a better material use for synthesis of progressive products. Organic catalyst is economical with less time-wasting during the improvement of organic substance production. Deep Eutectic Solvents (DESs) are substances composed of a quaternary ammonium mixed with a metal salt or a hydrogen bond donor (HBD) that has the capability to form a complex with the halide anion of the quaternary ammonium salt. DESs display comparable physical and chemical characteristics to ionic substances. DE_s are better, less expensive, and not highly dissolvable in water (Liu & Tan, 2001).

The focus of this work is to study the esterification of n-Butanol with Propanoic acid using $ZnCl_2$/Urea as an organic catalyst and varying the molar ratio of the catalyst to obtain a better yield of ester.

2 METHOD

2.1 Preparation of Des ($ZnCl_2$/Urea)

A mixture of $ZnCl_2$ and Urea at a mole ratio of 1:1mmol, 1:2mmol, 1:3mmol 1:4mmol and 1:5mmol was carried out correspondingly. Each

mixture was heated to a constant temperature of about 100 °C and stirred vigorously to obtain a uniform mixture with no odour. Each mixture was cooled to room temperature separately of 25 °C.

2.2 Esterification of Propanoic Acid and N-Butanol with $ZnCl_2$/Urea Catalyst

An amount of 0.03 mole of n-Butanol was mixed with 0.09 mole of Propanoic acid in a 100ml round bottom flask. Five drops of $ZnCl_2$/Urea at a ratio 1:1 mmol was added to whole solution as a catalyst to increase the rate of reaction. Small boiling stones were also put in the mixture to ensure uniform rate of heating. The round bottom flask was then attached firmly to a condenser while the bottom rests on the inside part of the heating mantle. The heating mantle was set to a temperature of 100 °C. The reflux from condensation was tolerable to run and run down the bottom flask.

The whole mixture was heated at this constant temperature until it reaches boiling point. The whole set up was allowed to run for 40 minutes as the reaction continues. After 40 minutes, the heating mantle was turned off. The whole mixture was cooled to room temperature of about 25 °C. The flask was then detached from the condenser and put and emptied into a tube using funnel. 1ml of Methylene Chloride was added to the mixture in the test tube. The mixture was shaken gradually to obtain a homogeneous solution. Excess carboxylic acid present in the solution was removed by addition of 3 ml of 5% anhydrous Sodium bicarbonate. The mixture stirred vigorously to ensure complete removal of Carbon IV Oxide. The vial was capped with small aperture and shaken until gas removal was comprehensive. The mixture was then allow4d to settle into layers before it was transmitted into a separating funnel. Two scoops of anhydrous Sodium Sulphate were introduced into the organic layer in the test tube with the using spatula. The solution was allowed to rest for 10minutes and was stirred at intervals. The liquid solution was decanted into a preweighed beaker. The Methylene Chloride was removed through air evaporation. The weight of the Ester (Butyl propanoate) in the beaker was then determined using a weighing balance and then recorded.

2.4 Varying Molar Ratio of $ZnCl_2$/Urea Catalyst

The same procedure were also repeated using $ZnCl_2$/Urea Catalyst at a ratio; 1:2 mmol, 1:3 mmol 1:4 mmol and 1:5 mmol. This was carried out constant temperature of 100 °C to monitor the effect of varying molar ratio in esterification of n-Butanol and Propanoic acid using $ZnCl_2$/Urea Catalyst.

3 RESULT AND DISCUSSION

From the experimental data obtain during the esterification reaction of n-Butanol with Propanoic acid represented in table 3.1, at a constant temperature of 100 °C, the increase in molar ratio of the $ZnCl_2$/urea to the n-Butanol from 1:1, 1:2, 1;3, 1:4 to 1:5 result to a corresponding increase in reaction time. This occurrence is due to the fact that as the number of moles of the limiting reactant (n-Butanol) increases, more butylpropanoate is produce. A gradual increase in the total mass of butyl propanoate was also observed.

Table 3.2 represents the percentage yield of the esterification of Propanoic acid with n-butylpropanoate which was calculated using the equation 1:

$$\text{yield} = \frac{\text{actual yield of butylpropanoate}}{\text{theoretical yield of butylpropanoate}} \times 100\%$$

Eqn. 1

Table 3.1: Esterification Reaction of Propanoic acid with Butanol at a constant temperature of 100 °C and varying catalyst ratio

Ratio $ZnCl_2$/urea	Product mass, 1st run (g)	Product mass, 2nd (g)	Product mass, 3rd (g)	Product mass, 4th (g)	Product mass, 5th (g)	Reaction time (minutes)
1:1	3.42	3.41	3.43	3.42	3.42	15.18
1:2	3.53	3.52	3.51	3.53	3.52	15.39
1:3	3.63	3.64	3.64	3.63	3.64	15.63
1:4	3.69	3.68	3.69	3.68	3.67	15.81
1:5	3.78	3.77	3.79	3.77	3.78	16.02

Table 3.2: Esterification Reaction of Propanoic acid with Butanol showing percentage yield at a constant temperature of 100 °C and varying catalyst ratio

Ratio $ZnCl_2$/urea	1st Yield (%)	2nd Yield (%)	3rd Yield (%)	4th Yield (%)	5th Yield (%)	Average Yield (%)
1:1	87.7	87.5	87.6	87.7	87.7	87.6
1:2	90.5	90.3	90.4	90.5	90.3	90.4
1:3	93.2	93.3	93.3	93.2	93.3	93.3
1:4	94.6	94.5	94.6	94.5	94.4	94.5
1:5	97.2	97.3	97.2	97.1	97.2	97.2



Propanoic Acid n-Butanol butyl-propanoate water

From the stoichiometric reaction shown above, increasing the amount of the limiting reactant (n-Butanol) supports the forward reaction as more of the butyl acetate is formed.

It was observed the increasing the molar ratio of the deep eutectic solvent used result to an increase in the percentage yield from 87.6% to 97.2% which is a reasonable. This high percentage yield is observed at the ratio 1:5 which shows that an increase in the molar ratio is favoured most at 1:5 if the temperature is kept at 100 °C.

The relationship between the percentage yield and the reaction time is represented in figure 3.1 above. The increase in reaction time result to a corresponding increase in the percentage yield. This means that as the molar ratio increases, more time is needed for conversion to occur though a very high percentage of the reactant will be converted to butylpropanoate. The increase in molar ratio implies that more of the limiting reactant are been added and more time will be needed for complete product formation.

3.2 FTIR Analysis of Butyl Propanoate

The FTIR analysis (Figure 3.3) was carried out at the National Research Institute of Chemical Technology (NARICT), Zaria, Kaduna state to determine the presence of functional groups and types of carbon and hydrogen bonds present. The molecule of butyl propionate was allowed to absorbed infra-red radiations in order to cause molecular vibrations, stretching and compression of molecular bonds as shown below.

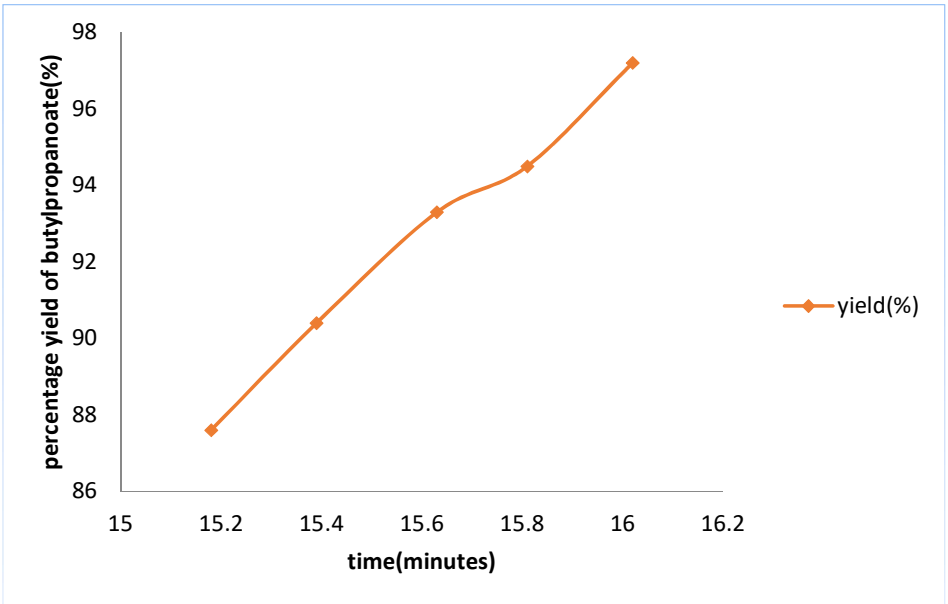
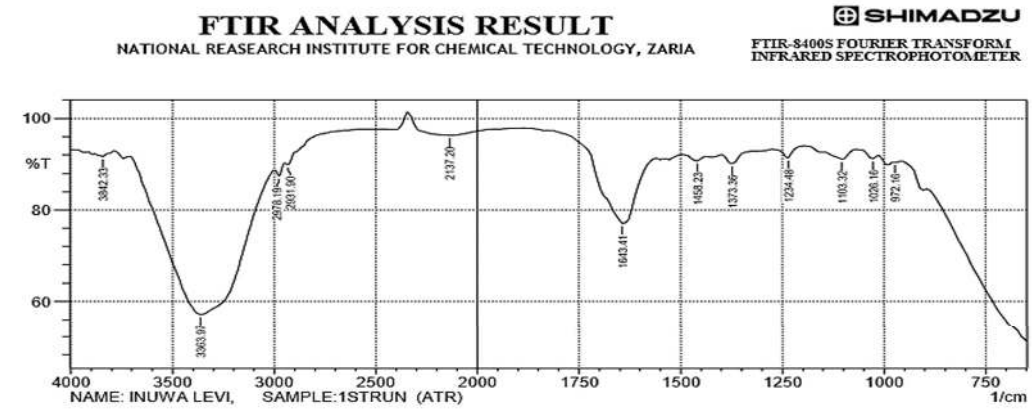


Figure 3.2 percentage yield of esterification of Propanoic acid with n-Butanol



	Peak	Intensity	Corr. Intensity	Base (H)	Base (L)	Area	Corr. Area
1	972.16	90.445	0.095	979.87	956.72	1.003	0.008
2	1026.16	91.26	0.963	1064.74	1010.73	1.905	0.081
3	1103.32	91.028	2.414	1195.91	1064.74	4.416	0.646
4	1234.48	91.422	2.211	1273.06	1195.91	2.469	0.264
5	1373.36	90.116	2.228	1404.22	1327.07	2.95	0.309
6	1458.23	90.786	0.993	1496.81	1442.8	2.11	0.123
7	1643.41	77.096	16.109	1828.58	1558.54	14.402	7.507
8	2137.2	96.322	0.01	2152.63	2129.48	0.376	0.001
9	2931.9	89.898	0.692	2947.33	2584.7	7.241	-2.676
10	2978.19	87.43	1.955	3001.34	2947.33	2.834	0.23
11	3363.97	57.164	33.095	3703.45	3001.34	107.218	75.761
12	3842.33	91.727	0.854	3888.62	3788.32	3.554	0.208

Figure 3.3 FTIR Analysis of butyl propanoate

From Figure 3.3, there is a broad signal shape with a peak of 3363.97 and intensity of 57.163 in the diagnostic region between the wavelengths of 3000 and 3500 cm^{-1}. This broad shape represents the presence OH (alcohol) and C=O group. This phenomenon occurs due to the presence of hydrogen bond and polar bonds of carbon atoms. This region shows that about 60% of the infra-red radiation was absorbed while 40% of the radiation was only transmitted through the butyl propanoate.

The next peak to consider is peak 1643.41 which lies between the wavelengths of 1500-1750cm^{-1}, with an intensity of about 77.096. This region represents a sharp and strong signals with only 30% absorption of the infra-red radiations. The peaks fall within the limit of a carboxylic group such as a propionic acid. The decrease in wave length shows a resulting decrease in the frequency of molecular vibration and energy during the reaction.

The peaks 1458.23,1373.36, 1234.48, 1103.32, 1026.16 all falls within the range of molecular wavelength of about 1000-1500cm^{-1} corresponds to that of an ester which should be within a range of 100-1700cm^{-1}. This area represents the region of butyl propanoate formation with low e energy absorption of almost 10% with weak shape signals.

4 CONCLUSION

In summary, the esterification of Propanoic acid with n-Butanol was carried out at constant temperature of 100 °C by varying the molar ratio of the deep eutectic; solvent used at values 1:1, 1:2, 1:3, 1:4 to1:5. A high conversion is obtained at the ratio 1:5 which favours more production butylpropanoate. Further, the DES satisfied the conditions of green chemistry in terms of its recyclability and non-corrosiveness. This implies that the $ZnCl_2$/Urea DES is a potential substitute as a catalyst in the esterification

REFERENCE

Abbott, A. P., Capper, G., Davies, D. L., & Rasheed, R. K. (2004). Ionic Liquid Analogues Formed from Hydrated Metal Salts, 3769–3774. https://doi.org/10.1002/chem.200400127

Anonymous (2009). Acid and Base Catalyzed Esterification, 132–147. Accessed from: http://www.hwscience.com/chemistry/ap/aplab/ester.pdf.

Deruiter, J. (2005). Carboxylic Acid Structure and Chemistry : Part 1. H The dipolar nature of acids, 1–11.

Dupont, P., & Lefebvre, F. (1996). Esterification of propanoic acid by butanol and 2-ethylhexanol catalyzed by heteropolyacids pure or supported on carbon

Izci, A. A., & Hosgun, B. H. L. (2007). Synthesis of isobutyl propionate using Amberlyst 15 as a catalyst, (September), 16–20.

Liu, Y., Lotero, E., & Jr, J. G. G. (2006). Effect of carbon chain length on esterification of carboxylic acids with methanol using acid catalysis, *243*, 221–228.

GEOTECHNICAL IMPROVEMENT OF WEAK PAVEMENT BASE SOIL IN BAURE L.G.A OF KATSINA STATE USING LIME

[1]SADEEQ, J. A., [1] HARUNA M. I. AND [2*]SALAHUDEEN A. B.
[1]Department of Civil Engineering, Ahmadu Bello University, Zaria, Nigeria
[2]Samaru College of Agriculture, Division of Agricultural Colleges, Ahmadu Bello University, Zaria
[*]**Corresponding email:** basalahudeen@gmail.com

ABSTRACT
This study was carried out to evaluate the effect of lime on the bearing strength of weak base soil in Baure Local Government Area of Katsina State, north-west Nigeria. The geotechnical properties of the weak base soil and their suitability for road construction was evaluated for selected locations in Baure L.G.A of Katsina State, Nigeria. Several analysis were performed on natural and lime treated soil samples in accordance with BS 1377 (1990) and BS 1924 (1990) respectively. Treated specimens were prepared by mixing the soil with lime in steps of 0, 3, 6, and 9% by weight of dry soil. The preliminary investigation carried out on the natural soil shows that the soil falls under class A-4 using AASHTO classification and inorganic clay material, CL, according to Unified Soil Classification System (USCS). The specific gravity of the soil samples decreased from 2.62 for the natural soil to 2.52 at 9% lime content.. The liquid limit ranged from 24% for the natural soil to 36% at 6% lime content while the plastic limits varied from 18% for natural soil to 27.7% when treated with 9% lime content. The maximum dry density (MDD) of the untreated soil increased from 1.4Mg/m^3 to a peak value of 1.66Mg/m^3 at 9% lime content, while the optimum moisture content (OMC) decreased from a value of 25% for the natural soil to a minimum value of 18.5% at 9% lime content. This geotechnical information obtained and presented herein can serve as base-line information for future road design and construction in the study area and other locations with similar soil properties.

Keywords: *Geotechnical improvement, Weak pavement base soil, Lime Atterberg limits, MDD, OMC*

1.0 INTRODUCTION

Subgrade layer is the lowest layer in the pavement structure underlying the base course or surface course, depending upon the type of pavement. Generally, subgrade consists of various locally available soil materials that sometimes might be soft and/or wet that cannot have enough strength/stiffness to support pavement loading (Sadeeq et al., 2014a; b) A sound knowledge of performance of the subgrade soil under prevailing in-situ condition is necessary prior to the construction of the pavement. The better the strength/stiffness quality of the materials the better would be the long-term performance of the pavement (Salahudeen et al., 2014). Hence, the design of pavement should be focused on the efficient, most economical and effective use of existing subgrade materials to optimize their performance. In case of soft and or wet (weak) subgrades, proper treatment might be needed in order to make the subgrade workable for overlying layers (e.g., creating working platform) for pavement and other engineering constructions. Understanding the engineering properties of subgrade is crucial to obtain strength and economic performance (Amadi, 2015).

In the road construction, there is much need for soil material in the construction of pavements. When a section of the road is to be filled with soil, the material is either obtained from other cut section along the road or from borrow pit where the suitable material is present, (if the material from the road does not meet the required standards). A major cost that would be incurred in "borrowing" the soil material is that involved in hauling the material from the borrow pit to the construction site. The cost effective, in terms of finance, resources and time, could however be achieved by simply improving the engineering properties of subgrade material that was earlier rejected (Anderson, 2012).

The replacement of the subgrade soil might not always be the best option due to associated hauling cost of the excavated materials as well as the imported quality materials. In some developing regions or even urban areas, the unviability of the aggregate or the shortage of the suitable fill materials makes replacement of weak subgrade soil uneconomical (Salahudeen et al., 2013). In such conditions, the strength/stiffness properties of the existing weak subgrade soil can be improved by the use of proper compaction technique as well as by using some chemical stabilizers. Portland cement, lime and fly ash are the most common types of chemical stabilizers used by most of states to stabilize the weak subgrades; thus creating a proper working platform and/or sub-base layer for pavement construction.

Geotechnically, soil improvement could either be by modification or stabilization, or both. Soil modification is the addition of a modifier (cement, lime, cement kiln dust, etc) to a problem soil to improve its index properties for better usefulness, while soil stabilization is the treatment of problem soils to improve their index properties and strength characteristics such that they permanently become suitable for construction and meet engineering design standards (Salahudeen and Akiije 2014). Stabilization is the process of blending and mixing materials with a soil to improve the soil's strength and durability Butalia et al. (2003). Shriram (2015) describes soil stabilization as the treatment of natural soil to improve its engineering properties. In general, soil stabilization is the process of creating or improving certain desired properties in a soil material so as to render it stable and useful for specific purpose at minimum cost. Amadi (2015), states that the improvements in engineering properties caused by stabilization can include the following: increase in soil strength (shearing resistance), stiffness (resistance to formation) and durability (wearing resistance), reduction in swelling potential or dispersivity (tendency to deflocculates) of wet clay soils and other desirable characteristics, such as dust proofing and water proofing unsealed roads.

According to national association of lime (Texas), "lime", either alone or in combination with other materials, can be used to treat a range of soil types. The mineralogical properties of the soils will determine their degree of reactivity with lime and the ultimate strength that the stabilized layers will develop. In general, fine-grained clay soils (with a minimum of 25 percent passing the No. 200 sieve (74mm) and a Plasticity Index greater than 10) are considered to be good candidates for stabilization. Soils containing significant amounts of organic material (greater than about 1 percent) or sulfates (greater than 0.3 percent) may require additional lime and/or special construction procedures.

The scarcity of good construction material plus inherent economy in utilizing locally available materials in the construction of modern highway systems and other engineering projects in Baure local government area of Katsina State in particular, has placed emphasis on the stabilization of weak soil materials to meet the present as well as the anticipated engineering specifications of subgrade materials. The study is aimed at improving the engineering properties of weak soil of Baure L.G.A Katsina State, using lime as an admixture.

2.0 MATERIALS AND METHODS

2.1 Materials

2.1.1 Soil

The disturbed soil sample used for this study was collected in February 2017 at Tsamiyar-kwance (Latitude $12^0$47'15"N and longitude $8^0$27'43"E), Baure Local Government Area of Katsina State along Gangarawa, which is 1km from Baure town. The soil samples were sealed in plastic bags and put in sacks to avoid loss of moisture during transportation. The soil sample was then air–dried, pulverized and then sieved through several standard sieves for different types of tests with the largest sieve been BS No. 4 sieve (4.76 mm aperture).

2.1.2 Lime

The lime used for this study was obtained from Sokoto Cement Factory, Sokoto the capital of Sokoto State of Nigeria. The lime was passed through British Standard No. 200 sieve and kept to be mixed with the soil in the appropriate percentages.

2.2 Methods

2.2.1 Laboratory tests

Laboratory tests were performed to determine the index properties of the natural soil and lime treated weak subgrade soil in accordance with BS 1377 (1990) and BS 1924 (1990), respectively.

2.2.2 Compaction

The compaction tests were performed on the natural soil and the lime treated soils using the British Standard light (BSL) energy. All tests carried out in this study were done at 0, 3, 6 and 9 % lime treatment by dry weight of the natural soil.

3.0 RESULTS AND DISCUSSION

3.1 Properties of the Natural Soil

Preliminary tests performed show that the natural soil is an A-4 (2) soil according to the AASHTO classification system (AASHTO, 1986) and low plasticity clay (CL), using the Unified Soil Classification System, USCS (ASTM, 1992). The natural soil has low moisture content of 14.70 %, specific gravity of 2.62, liquid limit of 25.00%, plastic limit of 18.30%, plasticity index of 6.70 % with 67.30% of the soil particles passing through the BS. No 200 sieve. Table 1 and Figure 1 respectively show the summarized properties of the natural soil and its particle size distribution curve.

Table 1: Properties of the Natural Lateritic Soil

Properties	Description
Natural moisture content (%)	14.70
Percentage passing BS No. 200 (%)	67.30
Liquid limit (%)	25
Plastic limit (%)	18.3
Plasticity index (%)	6.7
Linear shrinkage (%)	10.4
Free Swelling (%)	40
Group Index	2
AASHTO classification	A – 4
USCS	CL
Specific gravity	2.62
Maximum dry density (Mg/m3)	1.4
Optimum moisture content (%)	25
Colour	Black

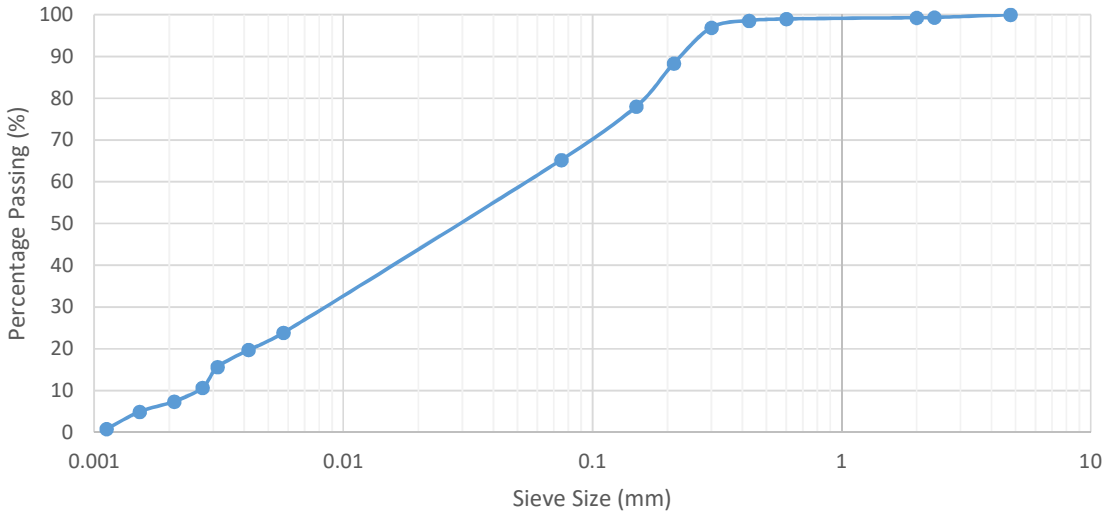


Figure 1: Particle size distribution curve for the natural soil

3.2 Effect of Lime on Particle Size Distribution of Weak Subgrade Soil

The particle size distribution curves for soil treated with lime content are shown in Figure 2. It can be observed that with increase in admixture (lime content), the particle size distribution curves shifted to the right thereby showing decrease in the percentage of fines at the steps 0, 3, 6 and 9% of lime content. A little change is noticed in the coarser sizes; this is an indication that with increase in lime content, modification reaction between lime and clay minerals increased which facilitated the formation of relatively coarser particles (Salahudeen, 2014).

3.3 Effect of Lime on Specific Gravity of Weak Subgrade Soil

The variation of specific gravity of weak subgrade with lime content is shown in Figure 3. The Specific gravity of untreated soil was found to be 2.62. The addition of admixture (lime) in steps of 0, 3, 6 and 9% by weight of dry soil led to the decrease in Specific Gravity of untreated weak soil having the lowest value at 9 % treatment. The decrease in specific gravity is due to the lower specific gravity of lime (2.34) compared to that of the untreated soil (2.62) (Salahudeen, 2014).

3.4 Effect of Lime on Atterberg Limits of Weak Subgrade Soil

Figure 4 shows the variation of Atterberg limits (liquid limit, plastic limit and plasticity index) of subgrade soil with lime content. The introduction of lime into the soil caused a continuous increase in the Atterberg limit. The increase can be attributed to addition of lime which introduced more pozzolanic substance into the specimen that required more water for hydration to be completed (Salahudeen et al. 2014). This observed trend is in agreement with Ramzi et al. (2001), Venkaramuthyalu et al. (2012), Salahudeen and Ochepo (2015), Sadeeq et al. (2014 a, b, c) Sadeeq et al. (2015), Salahudeen and Sadeeq (2016a; b) and

Sadeeq and Salahudeen (2017). The plastic limit increased continuously while the plasticity index decreased with increased RHA content.

3.5 Effect of Lime on Compaction Characteristics of Weak Subgrade Soil

The variations of maximum dry density (MDD) and optimum moisture content (OMC) of the weak subgrade soil used in this study with lime content are shown in Figure 5. According to Alhassan (2008) and Salahudeen (2014), the increase in the MDD can be attributed to the replacement of soil by lime in the mixture. It may also be attributed to coating of the soil by the lime which resulted to formation of larger particles and hence the increase in MDD. The increase in the MDD may also be explained by considering the lime as a filler in the soil voids which increased the weight of the soil/lime matrix. According to Salahudeen et al. (2014) and Salahudeen (2014), the increase in MDD could be due to lime occupying the voids within the soil matrix as well as the flocculation and agglomeration of the clay particles due to exchange of ions. There was a continuous decrease in OMC with increased lime contents. The trend is in line with Osinubi (1999) and Salahudeen (2014). The decrease may be due to the addition of lime, which decreased the quantity of free silt and clay fraction and coarser materials with larger surface areas were formed. The decrease in OMC with increase in lime content might also be due to cation exchange reaction that caused the flocculation of clay particles (Salahudeen and Akiije, 2014; Salahudeen et al. 2014; Salahudeen, 2014, Sadeeq and Salahudeen, 2017).

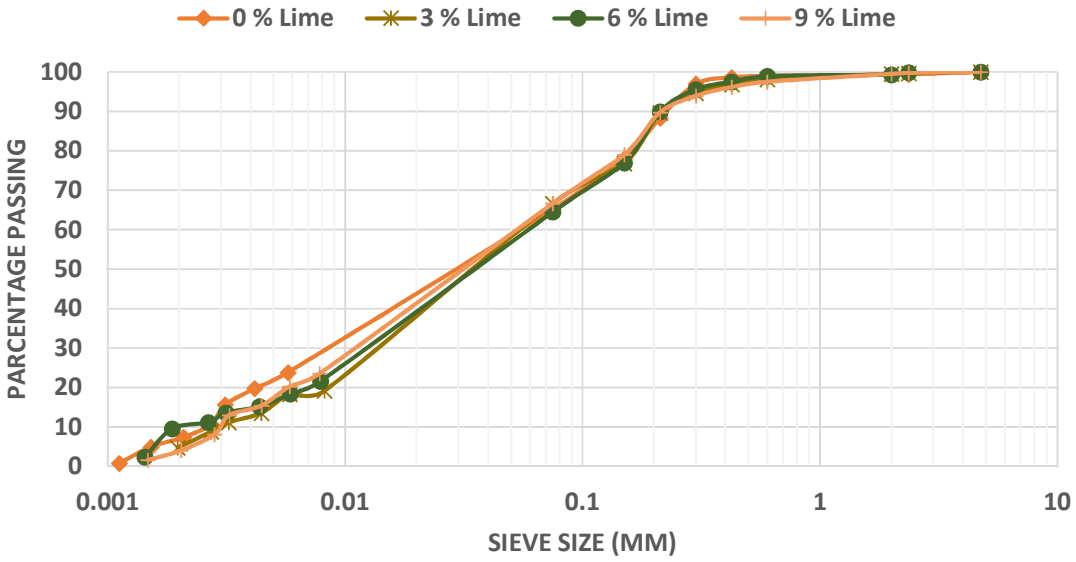


Figure 2: Particle size distribution curve for the natural and lime modified weak subgrade soil

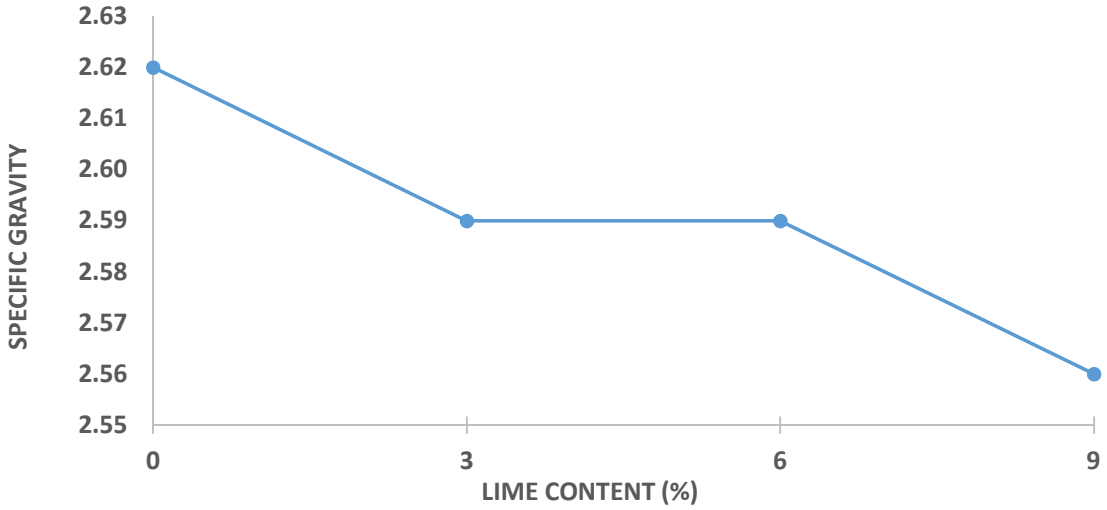


Figure 3: Variation of specific gravity of weak subgrade soil with lime content

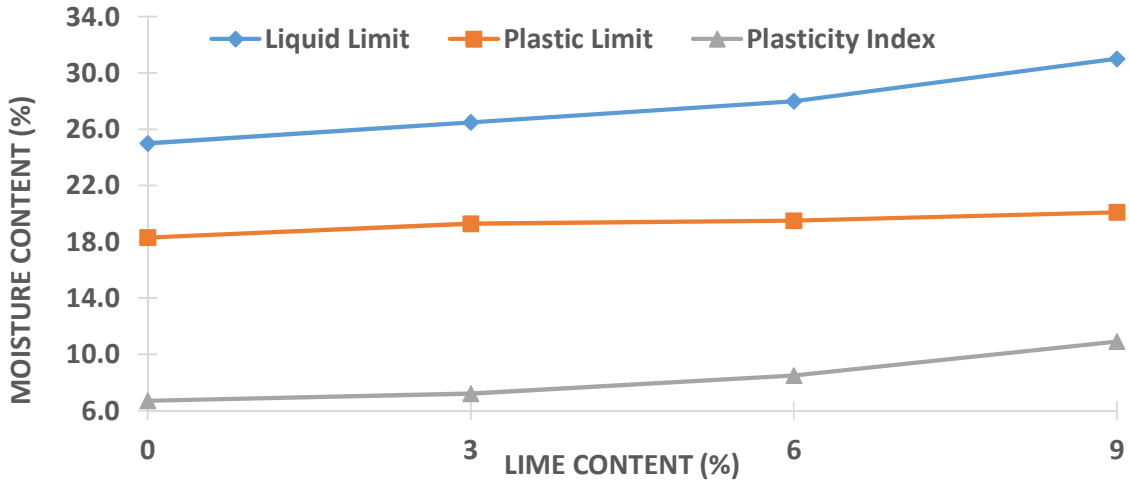


Figure 4: Variation of Atterberg limits of of weak subgrade soil with lime content

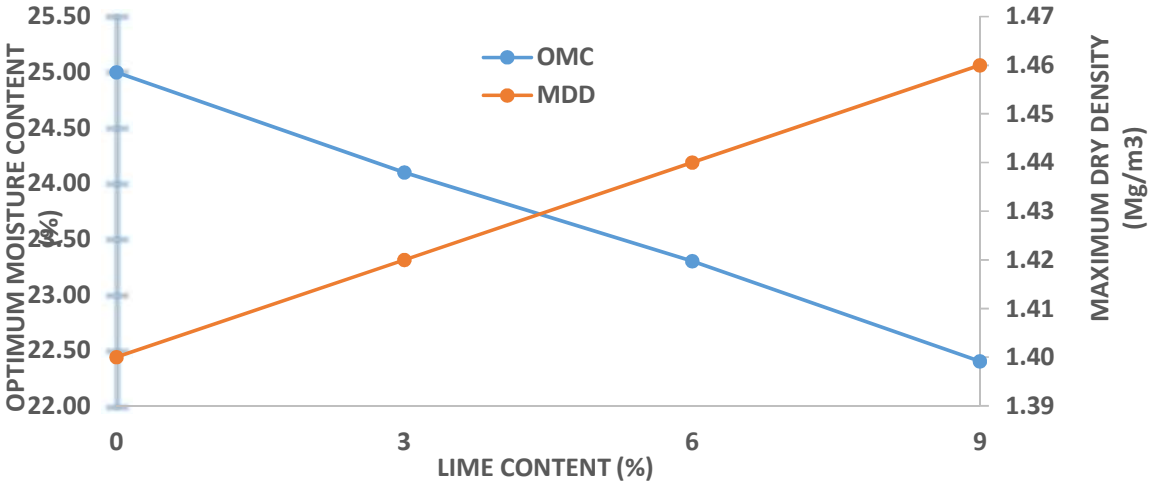


Figure 5: Variation of maximum dry density and optimum moisture content of weak subgrade soil with lime content

4.0 CONCLUSION

From the results of this study, the following conclusions were drowned:

- The specific gravity decreased with increased lime content.
- The plasticity index increased with increase in lime content. However, none of the values of plasticity indices went below the 12 % plasticity index specified by clause 6201 of the Nigerian General Specifications (1997) for sub base materials.
- Treatment with lime showed a general increase in the MDD and decrease in OMC with increased lime content.

5.0 ACKNOWLEDGEMENT

The authors are grateful to all the technical staff in the Geotechnical research laboratory, Department of civil engineering of Ahmadu Bello University, Zaria for the role they played in the laboratory work of this research particularly Malam Lawal.

6.0 REFERENCES

Alhassan, M. (2008). *"Potential Of Rice Husk Ash For Soil Stabilization"*. *Assumption University Journal of Technology*. Vol. 11, No. 4. pp.246-250.

Amadi A.N.1, A. W. (2015). Assessment of the Geotechnical Properties of Lateritic Soils in Minna, North Central Nigeria for Road design and Construction . *Journal of Science and Education*, 2 - 7.

American Association of State Highway and Transportation Officials (AASHTO), (1986) Washington, D. C.. "Standard Specifications for Transportation Materials and Methods of Sampling and Testing, Twentieth Edition".

Anderson, J. N. (2012). Soil Cement Stabilization - Mix Design, Control and Results during

Construction. *International Symposium on Ground Improvement IS-GI Brussels*, 1 - 5.

ASTM C618-93 specification (1992) "Fly Ash and Raw or Calcined Natural Pozzolan for use as Mineral Admixture in Portland Cement Concrete".

Bhattacharja, S. A. (2003). *Comparative performance of the Portland cement and lime stabilization of moderate to high plasticity soils.* Washington D.C: CD-ROM publication, National research council, Washington D.C.

British Standard (BS) 1377 (1990) "Methods of Test for Soils for Civil Engineering Purposes".

British Standard (BS) 1924 (1990). *Methods of Tests for Stabilized Soils.* British Standards Institute, London.

Nigerian General Specification (1997): Road Works and Bridges, Federal Ministry of Works and Housing, Abuja, Nigeria.

Osinubi, K. J. (1999). "Evaluation of admixture stabilization of Nigerian black cotton soil." *Nigerian Society of Engineers Technical Transactions*, Vol. 34, No 3, pp 88-96.

Ramzi, T., Amer, A., Ali, A. and Hilia A. (2001). "*Use Of Cement Kiln Dust In Soil Stabilization*". EJUQ. Vol.14 pp.61-76.

Sadeeq, J. A., Ochepo, J. and Salahudeen, A. B. (2014 a). "Effect of used oil contamination on the volumetric shrinkage of lateritic soils." Proceedings of the Third International Conference on Engineering and Technology Research, Ladoke Akintola University of Technology , Ogbomoso, Nigeria Volume 3, pp 167-175.

Sadeeq, J. A., Ochepo, J. and Salahudeen, A. B. (2014 b). "Assessment of bagasse ash effect on the volumetric shrinkage of lateritic soils for flexible pavements." Proceedings of the Nigerian Engineering Conference, Ahmadu Bello University, Zaria, Nigeria, pp 241-248.

Sadeeq, J. A., Ochepo, J. and Salahudeen, A. B. (2014 c). Effect of bagasse ash on consolidation settlement characteristics of lateritic soils. Proceedings of the national conference on "Bridging the gap between academia and industry in Nigeria-Refocosing the engineering discipline." Faculty of Engineering, Bayero University, Kano, Nigeria, pp 573 – 587.

Sadeeq, J. A., Ochepo, J., Salahudeen, A. B. and Tijjani, S. T. (2015). Effect of bagasse ash on lime stabilized lateritic soil. Jordan Journal of Civil Engineering (JJCE), Vol. 9, No.2.

Sadeeq, J. A. and Salahudeen, A. B. (2017). Strength characterization of foundation soils at Federal University Lokoja based on standard penetration tests data. *Nigerian Journal of Technology (NIJOTECH),* Vol. 36 No. 3, Pp. 671 – 676.

Salahudeen, A.B., Akiije, I. and Usman, G.M. (2013). Effect of sectional modulus on universal and hollow steel columns subjected to flexure. IJERT. Vol. 2 issue 9, pp 1848-1864.

Salahudeen, A. B. (2014). Stabilization of black cotton soil with cement kiln dust. Unpublished M.Sc. thesis*, Department of Civil Engineering,* Ahmadu Bello University, Zaria.

Salahudeen, A. B. and Akiije, I. (2014). Stabilization of highway expansive soils with high loss on ignition content kiln dust. *Nigerian journal of technology (NIJOTECH),* Vol. 33. No. 2, pp. 141 – 148.

Salahudeen, A. B., Eberemu O. A. and Osinubi, K. J. (2014). Assessment of cement kiln dust-treated expansive soil for the construction of flexible pavements. Geotechnical and Geological Engineering, Springer, Vol. 32, No. 4, PP. 923-931.

Salahudeen, A. B. and Ochepo, J. (2015). Effect of bagasse ash on some engineering properties of lateritic soil. Jordan Journal of Civil Engineering (JJCE), Vol. 9, No.4.

Salahudeen, A. B. and Sadeeq, J. A. (2016a). Effect of rice husk ash on the index properties and hydraulic conductivity of lateritic soils for flexible pavement construction. *Proceedings of the International Conference and Nigerian Material Congress 2016 (NIMACON 2016), Material Science and Technology Society of Nigeria (MSN),* Ahmadu Bello University, Zaria, pp. 1 – 6.

Salahudeen, A. B. and Sadeeq, J. A. (2016b). Strength characteristics of lateritic soils treated with rice husk ash for earth road construction. *Proceedings of the International Conference and Nigerian Material Congress 2016 (NIMACON 2016), Material Science and Technology Society of Nigeria (MSN),* Ahmadu Bello University, Zaria, pp. 7 – 11.

Shriram M., A. K. (2015). Stabilization of Lateritic Soil Subgrade Using Cement, Coconut Coir and Aggregates. *International Journal of Innovative Research in Science, Engineering and Technology*, 2 - 6.

Venkaramuthyalu, P., Ramu, K., and Prasada, R.G.V.R. (2012). "*Study on performance of chemically stabilized expansive soil*". IJAET, Vol. 2, Issue 1, pp 139-148.

GROUNDNUT SHELL ASH MODIFICATION OF LATERITIC SOIL

[1]SADEEQ, J. A., [1]ADAMS, M. D. AND [2*]SALAHUDEEN A. B.,
[1]Department of Civil Engineering, Ahmadu Bello University, Zaria, Nigeria
[2]Samaru College of Agriculture, Division of Agricultural Colleges, Ahmadu Bello University, Zaria
[*]**Corresponding email:** basalahudeen@gmail.com

ABSTRACT
This study investigated the effect of groundnut shell ash (GSA) on lateritic soil. The preliminary investigations of the natural soil collected from Shika, Zaria show that the soil belongs to A-7-6 in AASHTO classification system and CL in USCS classification system which is an indication of a poor soil for engineering purposes. Groundnut shell ash (GSA) blend in stepped concentration of 0, 3, 6, and 9% by dry weight of soil was used to treat the soil. Compaction was carried out using British Standard Light (BSL) energy. The liquid limit and plasticity index values of the natural soil are 44.0% and 20.5% respectively. The specific gravity of the soil sample decreased from 2.60 for the natural soil to 2.46 at 6% GSA content. The liquid limit ranged from 44% for the natural soil to 39.5 at 9% GSA. The maximum dry density (MDD) increased from 1.62Mg/m^3 for the natural soil to a peak value of 1.72Mg/m^3 when treated with 9% GSA, while the optimum moisture content (OMC) increased from a value of 18.05% for the natural soil to 14.53% at 3% GSA treatment. The study shows that the lateritic soil can be modified with GSA for road construction works.

Keywords: *Groundnut shell ash, Modification, Lateritic soil, Atterberg limits, MDD, OMC*

1.0 INTRODUCTION

In engineering works, the need for adequate provision of infrastructure to be considered with good and sound material is necessary so as to comply with the proposed design requirements. Highway and structural engineers are faced with the problems of providing suitable material for civil engineering constructions (Sadeeq et al., 2014a). To this end, continuous researches have been carried out by individuals, firms and institutions on the ways to improve the engineering properties of soil. The most available soils do not have, in most cases, adequate engineering properties to really bear the expected loads. So improvising has to be made to make these soils better. These lead to the concept called soil stabilization or modification; which is any treatment applied to a soil to improve its index properties, workability, strength and to reduce its vulnerability to water. If the treated soil is able to withstand excessive deformation then it is generally regarded as stable (Osinubi, 1999).

Lateritic soils are widely available throughout the warm sub-humid parts of the tropical regions of the world. While some lateritic soils are suitable for use in roads (sub-base and base course) construction, others require one form of stabilization or the other to make them suitable for construction work. Cement and lime are commonly used for stabilization of lateritic soils. Cement stabilization becomes more difficult as the fine contents increases above 25% and lime is then generally considered as more appropriate for the stabilization of soils with high clay contents (Osinubi, 1995).

The geotechnical characteristics of laterite are influenced considerably by their formation (genesis) degree of weathering and mineralogical composition and environmental factors. (Gidigasu, 1976) Laboratory test carried out in some of the soils using different pre-test preparation and listing procedure lead to essentially the same result. Normal laterite soil may thus be identified and classified on the basis of standard soil classification system (USCS) (ASTM, 1992) the American Association of state Highway and transportation Officials, (AASHTO, 1986) specification could be used. Groundnut shell can be used to improve soil stabilization in the ground because it is good water proofer and its binding properties are adequate for stabilization (Osinubi, 1999). And also, because of its being usually rich in calcium carbonate, which is good binding agent and its other pozzolana with good stabilization properties, it can be used in a cement based construction material to improve soil in the ground (Salahudeen, 2014).

Lateritic soil vary in their plasticity and strength among other engineering properties even within a borrow pit, area or soil deposits (Sadeeq et al., 2014a). Behavior of soils and there responds to engineering applications (either as foundation or bearing materials for all kind of structures or as construction material) is strictly dedicated by the mode of formation. Groundnut shell ash is a waste material which is commonly disposed off in land fill, but with rising disposal cost ecological friendly alternative are becoming more attractive conventionally, lime, Portland cement and bitumen have been used to appropriately improve properties

of most soils to make them meet requirement of construction works. Groundnut shell ash which is a wastes product is difficult to dispose off, therefore ways of making it useful are derived by using it to solving engineering problems (Osinubi 2000). This research was aimed at improving the performance, workability and some geotechnical properties of lateritic soil using groundnut shell ash as admixture.

2.0 MATERIALS AND METHODS

2.1 Materials

2.1.1 Lateritic Soil

The lateritic soil used in this study was collected from a borrow pit in Shika village, Zaria, Kaduna State in the northern part of Nigeria (latitude $11^0$15' N and longitude 7^0 45' E), by using the method of disturbed sampling at 1m depth from the natural earth surface to avoid organic matter influence. This depth corresponds to the B – horizon usually characterized by the accumulation of material leached from the overlying A – horizon. A study of Nigerian soils by Salahudeen (2017) reveals that the soil belongs to the group of ferruginous tropical soils derived from acid igneous and metamorphic rocks.

2.1.2 Groundnut Shell Ash

The groundnut shell used for this research was collected from Giwa in Kaduna State of Nigeria. The groundnut shell was burnt in an enclosed area at atmospheric temperature. After it was collected to the laboratory, the groundnut shell ash (GSA) was passed through British Standard No 200 (0.0075m aperture) sieve, stored in a tight polythene bag to avoid any form of hydration, and kept to be mixed with the soil.

2.2 Methods

2.2.1 Laboratory tests

Laboratory tests were performed to determine the index properties of the natural soil and groundnut shell ash (GSA) treated lateritic soil in accordance with BS 1377 (1990) and BS 1924 (1990), respectively.

2.2.2 Compaction

The compaction tests were performed on the natural soil and the groundnut shell ash (GSA) treated soils using the British Standard light (BSL) energy. All tests carried out in this study were done at 0, 3, 6 and 9 % groundnut shell ash (GSA) treatment by dry weight of the natural soil.

3.0 RESULTS AND DISCUSSION

3.1 Properties of the Natural Soil

Preliminary tests performed show that the natural soil is an A-6 (18) soil according to the AASHTO classification system (AASHTO, 1986) and low plasticity clay (CL), using the Unified Soil Classification System, USCS (ASTM, 1992). The natural soil has low moisture content of 15.50 %, specific gravity of 2.60, liquid limit of 44.00%, plastic limit of 22.50%, plasticity index of 22.50 % with 81.80 % of the soil particles passing through the BS. No 200 sieve. Table 1 and Figure 1 respectively show the summarized properties of the natural soil and its particle size distribution curve.

3.2 Effect of GSA on Particle Size Distribution of Lateritic Soil

The results in Figure 2 show the particle size distribution of lateritic soil with GSA content. A slight increase in the coarser particles was observed at 3% GSA content. This change is an indication that with increase in GSA content of 3%, modification reaction between GSA and clay minerals increased which facilitated the formation of relatively coarser particles (Salahudeen, 2014). However, a sharp increase in fine content was observed at 9% GSA content

Table 1: Properties of the Natural Lateritic Soil

Properties	Quantities
Percentage passing BS sieve no. 200	81.80
Liquid Limit (LL) (%)	44.0
Plastic Limit (PL) (%)	21.5
Plasticity index (PI) (%)	22.5
AASHTO classification	A-6
USCS	CL
Group index	17.74
Specific gravity	2.60
Natural moisture content (%)	15.50
Colour	Reddish brown
Optimum moisture content (OMC) (%)	21.52
Maximum dry density (MDD) (%)	1.64
Dominant clay mineral	Kaolinite

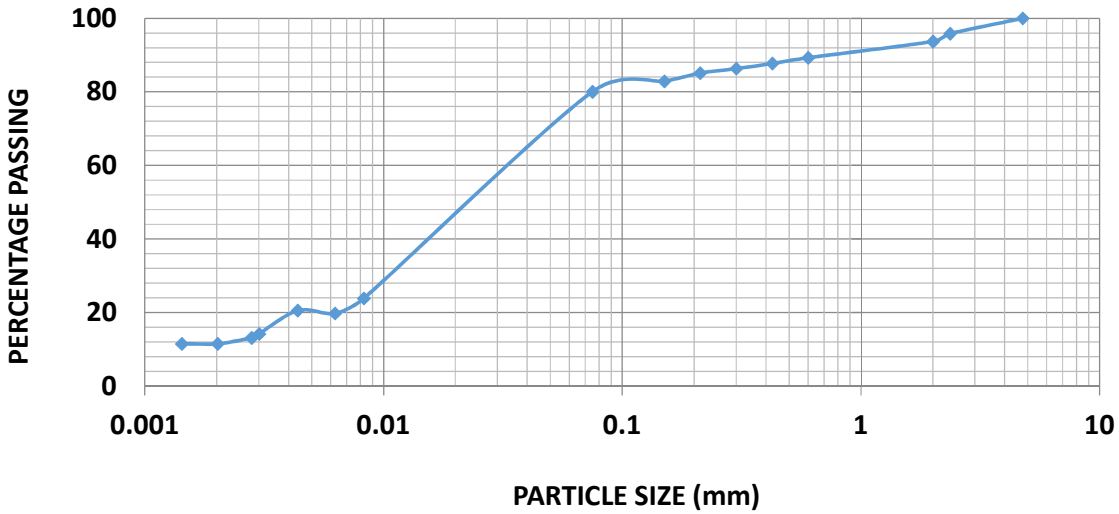


Figure1: Particle size distribution for the natural soil

3.3 Effect of GSA on Specific Gravity of Lateritic Soil

The specific gravity of solid particles is the ratio of the mass of a given volume of solids to the mass of an equal volume of water. Specific gravity an important parameter used for the determination of the void ratio and particle size of any soil particle (Salahudeen and Sadeeq, 2016a; b). The variation of specific gravity with GSA is shown in Figure 3.The specific gravity of natural soil (2.60) decreased consistently with the addition of GSA content. The decrease in specific gravity is due to the lower specific gravity of GSA compared to that of the untreated soil (Salahudeen, 2014).

3.4 Effect of GSA on Atterberg Limits of Lateritic Soil

The variation of Atterberg limits (liquid limit, plastic limit and plasticity index) of subgrade soil with GSA content is shown in Figure 4. The liquid limits decreased while the plastic limits of the lateritic soil increased with increased GSA content. This decrease in liquid limit can be associated with the agglomeration and flocculation of the clay particles which is as a result of exchange ions at the surface of the clay particles (Salahudeen et al. 2014). An increase in plastic limit (PL) was also observed as GSA content increased. The increase can be attributed to addition of GSA which introduced more pozzolanic substance into the specimen that required more water for hydration to be completed. Ramzi et al. (2001), Suhail et al., (2008), Venkaramuthyalu et al. (2012) and Salahudeen and Sadeeq (2016a; b) reported that the reduction in plasticity index with chemical treatment could be attributed to the depressed double layer thickness due to cation exchange by potassium, calcium and ferric ions. This observed trend is in agreement with Salahudeen and Ochepo (2015), Sadeeq et al. (2014a; b; c) Sadeeq et al. (2015), Salahudeen and Sadeeq (2016a; b) and Sadeeq and Salahudeen (2017).

3.5 Effect of GSA on Compaction Characteristics of Lateritic Soil

The variations of maximum dry density (MDD) and optimum moisture content (OMC) of the lateritic soil used in this study with GSA content are shown in Figure 5. According to Alhassan (2008) and Salahudeen (2014), the increase in the MDD can be attributed to the replacement of soil by GSA in the mixture. It may also be attributed to coating of the soil by the GSA which resulted to formation of larger particles and hence the increase in MDD. The increase in the MDD may also be explained by considering the GSA as a filler in the soil voids which increased the weight of the soil/GSA matrix. According to Salahudeen et al. (2014) and Salahudeen (2014), the increase in MDD could be due to GSA occupying the voids within the soil matrix as well as the flocculation and agglomeration of the clay particles due to exchange of ions. There was a continuous increase in OMC with increased CCA contents. The trend is in line with Osinubi (1999) and Salahudeen (2014). An explanation for this trend was the increased demand for water commensurate with the higher amount of GSA required for its hydration reaction and dissociation needed for cation exchange reaction (Salahudeen and Akiije, 2014; Salahudeen et al. 2014; Salahudeen, 2014, Sadeeq and Salahudeen, 2017).

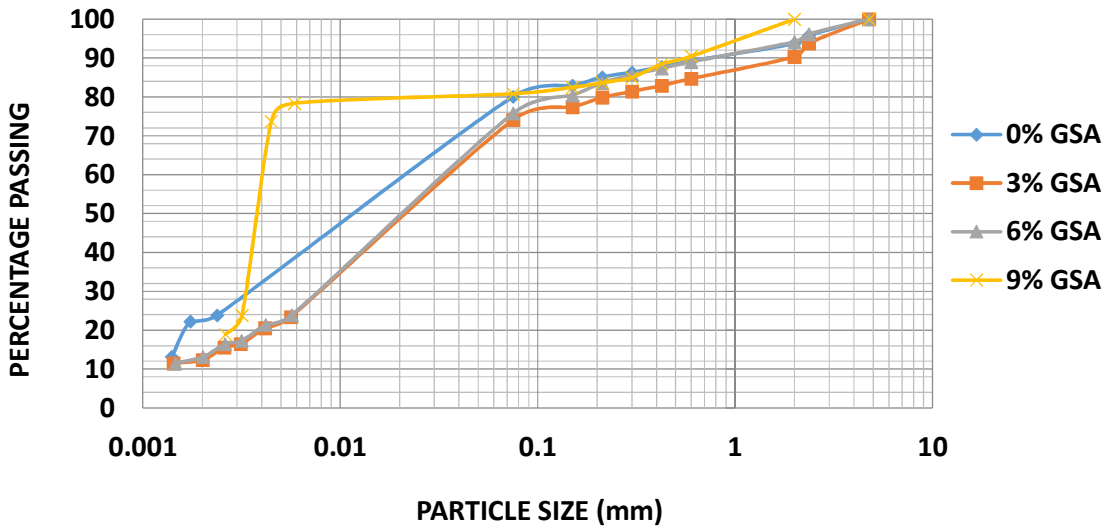


Figure 2: Particle size distribution curve for the natural and GSA modified lateritic soil

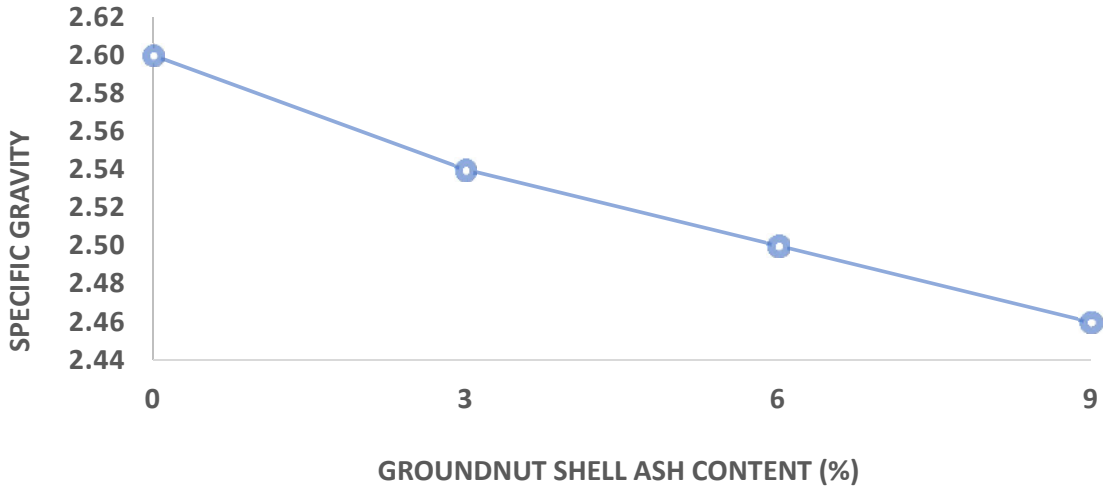


Figure 3: Variation of specific gravity of lateritic soil with GSA content

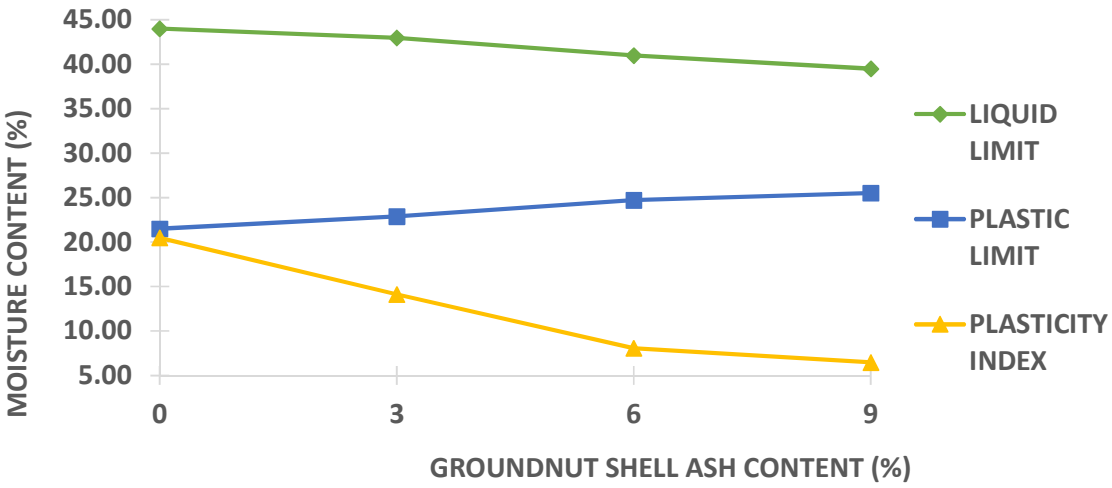


Figure 4: Variation of Atterberg limits of of lateritic soil with GSA content

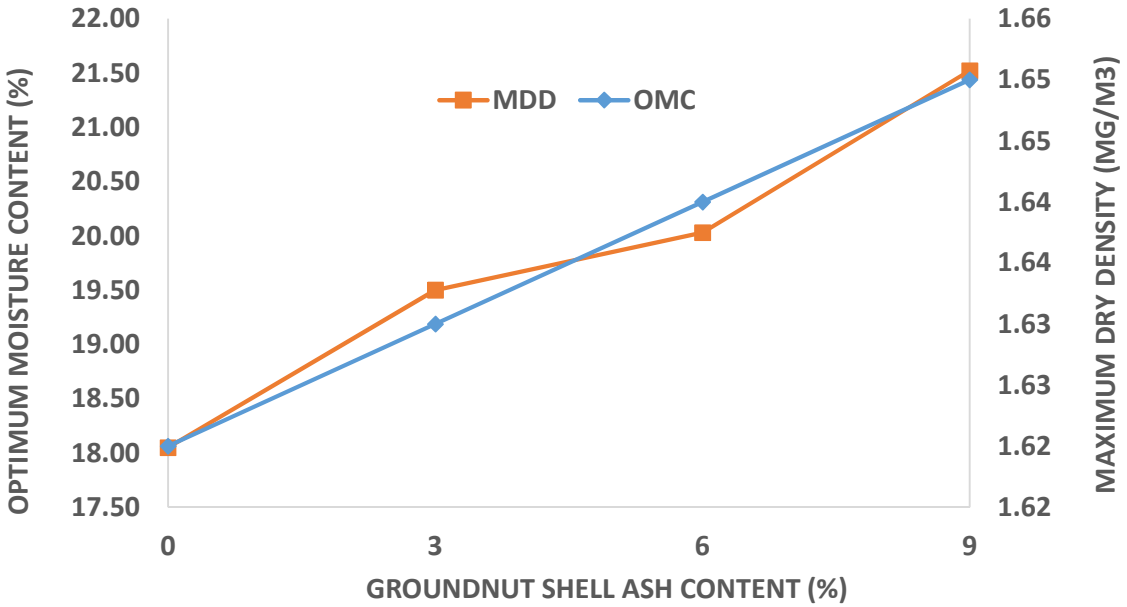


Figure 5: Variation of maximum dry density and optimum moisture content of lateritic soil with GSA content

4.0 CONCLUSION

Based on the results of this study, the following conclusions were drowned:

- The specific gravity decreased with increased GSA content.
- The plasticity index decreased with increase in CCA content meeting the value of plasticity index of 12 % specified by clause 6201 of the Nigerian General Specifications (1997) for sub base materials at GSA content of 6% and above.
- Treatment of lateritic soil with GAA showed a general increase in the MDD with increased GSA content.

5.0 ACKNOWLEDGEMENT

The authors are grateful to all the technical staff in the Geotechnical research laboratory, Department of civil engineering of Ahmadu Bello University, Zaria for the role they played in the laboratory work of this research particularly Malam Lawal.

6.0 REFERENCES

Alhassan, M. (2008). *"Potential Of Rice Husk Ash For Soil Stabilization"*. *Assumption University Journal of Technology*. Vol. 11, No. 4. pp.246-250.

American Association of State Highway and Transportation Officials (AASHTO), (1986) Washington, D. C.. "Standard Specifications for Transportation Materials and Methods of Sampling and Testing, Twentieth Edition".

ASTM C618-93 specification (1992) "Fly Ash and Raw or Calcined Natural Pozzolan for use as Mineral Admixture in Portland Cement Concrete".

British Standard (BS) 1377 (1990) "Methods of Test for Soils for Civil Engineering Purposes".

British Standard (BS) 1924 (1990). *Methods of Tests for Stabilized Soils.* British Standards Institute, London.

Nigerian General Specification (1997): Road Works and Bridges, Federal Ministry of Works and Housing, Abuja, Nigeria.

Osinubi, K. J. (1995). "Lime modification of black cotton soils." *Spectrum Journal*, Vol. 2, Nos 1 and 2, pp. 112 – 122.

Osinubi, K. J. (1999). "Evaluation of admixture stabilization of Nigerian black cotton soil." *Nigerian Society of Engineers Technical Transactions*, Vol. 34, No 3, pp 88-96.

Osinubi, K. J. (2000). "Laboratory trial of soil stabilization using pulverised coal bottom ash." *Nigerian Society of Engineers Technical Transactions*, Vol. 35, No 4 pp 13 – 21.

Ramzi, T., Amer, A., Ali, A. and Hilia A. (2001). "*Use Of Cement Kiln Dust In Soil Stabilization*". EJUQ. Vol.14 pp.61-76.

Sadeeq, J. A., Ochepo, J. and Salahudeen, A. B. (2014 a). "Effect of used oil contamination on the volumetric shrinkage of lateritic soils." Proceedings of the Third International Conference on Engineering and Technology Research, Ladoke Akintola University of Technology , Ogbomoso, Nigeria Volume 3, pp 167-175.

Sadeeq, J. A., Ochepo, J. and Salahudeen, A. B. (2014 b). "Assessment of bagasse ash effect on the volumetric shrinkage of lateritic soils for flexible pavements." Proceedings of the Nigerian Engineering

Conference, Ahmadu Bello University, Zaria, Nigeria, pp 241-248.

Sadeeq, J. A., Ochepo, J. and Salahudeen, A. B. (2014 c). Effect of bagasse ash on consolidation settlement characteristics of lateritic soils. Proceedings of the national conference on "Bridging the gap between academia and industry in Nigeria-Refocosing the engineering discipline." Faculty of Engineering, Bayero University, Kano, Nigeria, pp 573 – 587.

Sadeeq, J. A., Ochepo, J., Salahudeen, A. B. and Tijjani, S. T. (2015). Effect of bagasse ash on lime stabilized lateritic soil. Jordan Journal of Civil Engineering (JJCE), Vol. 9, No.2.

Sadeeq, J. A. and Salahudeen, A. B. (2017). Strength characterization of foundation soils at Federal University Lokoja based on standard penetration tests data. *Nigerian Journal of Technology (NIJOTECH),* Vol. 36 No. 3, Pp. 671 – 676.

Salahudeen, A. B. (2014). Stabilization of black cotton soil with cement kiln dust. Unpublished M.Sc. thesis*, Department of Civil Engineering,* Ahmadu Bello University, Zaria.

Salahudeen, A. B. and Akiije, I. (2014). Stabilization of highway expansive soils with high loss on ignition content kiln dust. *Nigerian journal of technology (NIJOTECH),* Vol. 33. No. 2, pp. 141 – 148.

Salahudeen, A. B., Eberemu O. A. and Osinubi, K. J. (2014). Assessment of cement kiln dust-treated expansive soil for the construction of flexible pavements. Geotechnical and Geological Engineering, Springer, Vol. 32, No. 4, PP. 923-931.

Salahudeen, A. B. and Ochepo, J. (2015). Effect of bagasse ash on some engineering properties of lateritic soil. Jordan Journal of Civil Engineering (JJCE), Vol. 9, No.4.

Salahudeen, A. B. and Sadeeq, J. A. (2016a). Effect of rice husk ash on the index properties and hydraulic conductivity of lateritic soils for flexible pavement construction. *Proceedings of the International Conference and Nigerian Material Congress 2016 (NIMACON 2016), Material Science and Technology Society of Nigeria (MSN),* Ahmadu Bello University, Zaria, pp. 1 – 6.

Salahudeen, A. B. and Sadeeq, J. A. (2016b). Strength characteristics of lateritic soils treated with rice husk ash for earth road construction. *Proceedings of the International Conference and Nigerian Material Congress 2016 (NIMACON 2016), Material Science and Technology Society of Nigeria (MSN),* Ahmadu Bello University, Zaria, pp. 7 – 11.

Salahudeen, A. B. (2017). "Prediction of foundation settlement based on standard penetration test results using empirical and numerical techniques." Unpublished PhD thesis, Department of Civil Engineering, Ahmadu Bello University, Zaria, Nigeria. Pp 70 – 77.

Suhail, A.A.A., Khawla, A.K.A. and Ibrahaim, M.A.A. (2008). "*Strength Durability And Hydraulic Properties Of Clayey Soil Stabilized With Lime And Industrial Waste Lime*". Al-Rafidain Engineering. Vol. 16. No. 1. Pp.102-116.

Venkaramuthyalu, P., Ramu, K., and Prasada, R.G.V.R. (2012). "*Study on performance of chemically stabilized expansive soil*". IJAET, Vol. 2, Issue 1, pp 139-148.

Gidigasu, M.D. (1976). *Laterite Soil Engineering: Principles*. Elsevier, Amsterdam, the Netherlands.

Osinubi, K. J. (1995). "Lime modification of black cotton soils." *Spectrum Journal*, Vol. 2, Nos 1 and 2, pp. 112 – 122.

Osinubi, K. J. (1999). "Evaluation of admixture stabilization of Nigerian black cotton soil." *Nigerian Society of Engineers Technical Transactions*, Vol. 34, No 3, pp 88-96.

MODIFICATION OF LATERITIC SOIL USING CORNCOB ASH

[1]SADEEQ, J. A., [1] DANGNE, K. Z. AND [2*]SALAHUDEEN A. B.
[1]Department of Civil Engineering, Ahmadu Bello University, Zaria, Nigeria
[2]Samaru College of Agriculture, Division of Agricultural Colleges, Ahmadu Bello University, Zaria
[*]**Corresponding email:** basalahudeen@gmail.com

ABSTRACT
The growing cost of traditional modifying agents and the need for the economical utilization of industrial and agricultural waste for beneficial engineering purposes has lead to extensive research on the use of industrial and agricultural wastes as alternative soil modifying agents. The soil used in this study was collected from a borrow pit in Shika area of Zaria and The soil was classified as inorganic clay of law plasticity (CL) based on the unified soil classification system (USCS) and as A-6 using the American Association of State Highway and Transportation officers (AASHTO) classification system. The effect of Corncob ash (CCA) on the soil was investigated with respect to Atterberg limits and compaction characteristics. The maximum dry density (MDD) results show an increase in the values having a peak value of 1.85 Mg/m^3 at 9% CCA content. The OMC decreased to a minimum value at 9% CCA contents and thereafter increased with higher CCA content.

Keywords: *Corncob Ash, Lateritic soil, Atterberg limits, Modification, OMC, MDD*

1.0 INTRODUCTION

Laterite is a soil and rock type rich in iron and aluminium, and is commonly considered to have formed in hot and wet tropical areas. Nearly all laterites are of rusty red coloration, because of high iron oxide content. Typical lateritic is porous and claylike. It contains the Iron oxide minerals, goethite (HFeO2); lepidocrocite (FeO[OH]) and hematite(Fe2O2). It also contains titanium oxides and hydrated oxide of aluminium, the most common and abundant of which is gibbsite (Al2O3.3H2O). The aluminium rich representative of lateritic are bauxites (Osinubi, 1995; 2000).

A lot of laterite gravels, which are good for gravely roads , occur in tropical counties of the world ,including Nigeria (Osinubi,1994).there are instances where a laterite may contain substantial amount of clay minerals that its strength and stability cannot be guaranteed under load ,especially in presence of moisture. These types of laterite are also common in many tropical regions including Nigeria where in most cases sourcing for alternative soil may prove economically unwise but rather to improve the available soil to meet the desired objective (Osinubi 1994).the need for good road network are extremely increase with increase in population so also the maintenance of the existing ones. The physical properties of laterite can be improve (Salahudeen et. al., 2014). Soil improvement could either be by modification or stabilization or both. However due to the increasing cost of cement and lime which are the two conventional materials used for stabilizing soils, the use of industrial wastes, such as corncob ash (CA) will considerable reduce the cost of constructions as well as reducing environment hazards they cause if found to be useful.

Cement is the oldest binding agent since the invention of soil stabilization technology in 1960's. It may be considered as primary stabilizing agent or hydraulic binder because it can be used alone to bring about the stabilizing action required (Sherwood, 1993; EuroSoilStab, 2002).

Corn cob is the waste product obtained from maize or corn, which is the most important cereal crop in sub-Saharan Africa. According to food and agriculture organization (FAO) data, 589 million tons of maize were produced worldwide in the year 2000. The United States was the largest maize producer having 43% of world production. Africa produced 7% of the world's maize. Nigeria was the second largest producer of maize in Africa in the year 2001 with 4.62 million ton. South Africa has the highest production of 8.04 million ton .

Geotechnically, soil improvement could either be by modification or stabilization, or both. Soil modification is the addition of a modifier (cement, lime, cement kiln dust, etc) to a problem soil to improve its index properties for better usefulness, while soil stabilization is the treatment of problem soils to improve their index properties and strength characteristics such that they permanently become suitable for construction and meet engineering design standards (Salahudeen and Akiije 2014).

The over dependence on the utilization of industrially manufactured soil improving additives (cement, lime, etc.) have kept the cost of

construction of stabilized road financially high (Salahudeen, 2014). Thus, the possible use of industrial and/or agricultural wastes such as corncob will considerably reduce the cost of construction and as well as reduce or eliminate the environmental hazards caused by such wastes. In a bid to achieve alternative low cost roads where the production of aggregates for road work is very expensive, corncob ash, a waste product is substituted as a soil stabilizer. Corncob Ash (CCA) is cheaply available locally and is obtained through the burning of maize waste which is agricultural by-product .Therefore the use of corncob ash as an additive for soil stabilization will go a long way in reducing the cost of soil stabilization. The aim of this study is to evaluate the possibility of using Corncob Ash (CCA) as a modifier of lateritic soil to improve the index properties and workability of lateritic soil.

2.0 MATERIALS AND METHODS

2.1 Materials

2.1.1 Lateritic Soil

The lateritic soil used in this study was collected from a borrow pit in Shika village, Zaria, Kaduna State in the northern part of Nigeria (latitude $11^0$15' N and longitude 7^0 45' E), by using the method of disturbed sampling at 1m depth from the natural earth surface to avoid organic matter influence. This depth corresponds to the B – horizon usually characterized by the accumulation of material leached from the overlying A – horizon. A study of Nigerian soils by Salahudeen (2017) reveals that the soil belongs to the group of ferruginous tropical soils derived from acid igneous and metamorphic rocks.

2.1.2 Corncob Ash

Corncob was locally obtained from maize in Samaru, Zaria area of Kaduna State. The corn waste (Corncob) was collected, air-dried and burnt under atmospheric conditions. The residue obtained after burning was the ash that was collected in sacks and transported to the Geotechnical Research Laboratory, Department of Civil Engineering, Ahmadu Bello University, Zaria. The ash was then passed through B.S. sieve no. 200 (0.075 mm) to meet the requirements of BS 1924 (1990).

2.2 Methods

2.2.1 Laboratory tests

Laboratory tests were performed to determine the index properties of the natural soil and corncob ash (CCA) treated lateritic soil in accordance with BS 1377 (1990) and BS 1924 (1990), respectively.

2.2.2 Compaction

The compaction tests were performed on the natural soil and the corncob ash (CCA) treated soils using the British Standard light (BSL) energy. All tests carried out in this study were done at 0, 3, 6 and 9 % corncob ash (CCA) treatment by dry weight of the natural soil.

3.0 RESULTS AND DISCUSSION

3.1 Properties of the Natural Soil

Preliminary tests performed show that the natural soil is an A-6 (15) soil according to the AASHTO classification system (AASHTO, 1986) and low plasticity clay (CL), using the Unified Soil Classification System, USCS (ASTM, 1992). The natural soil has low moisture content of 15.82 %, specific gravity of 2.73, liquid limit of 45.00%, plastic limit of 22.00%, plasticity index of 23.00 % with 70.85 % of the soil particles passing through the BS. No 200 sieve. Table 1 and Figure 1 respectively show the summarized properties of the natural soil and its particle size distribution curve.

Table 1: Properties of the Natural Lateritic Soil

Properties	Description
Percent passing BS sieve No.200	70.85
Liquid limit (%)	45
Plastic limit (%)	22
Plasticity index	23
Linear shrinkage (%)	3.6
Group index	15
AASHTO classification	A-6
UCS classification	CL
Specific gravity	2.73
Maximum Dry Density (Mg/m^3)	1.7
Optimum Moisture content (%)	18.9
Natural moisture content (%)	15.82
Colour	Reddish brown

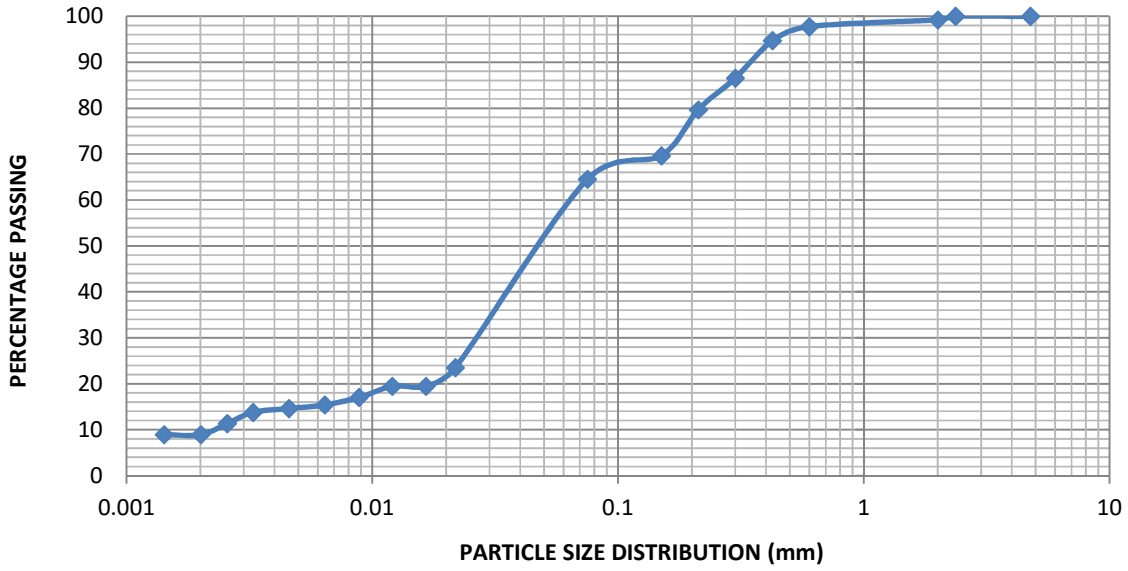


Figure1: Particle size distribution for the natural soil

3.2 Effect of CCA on Particle Size Distribution of Lateritic Soil

The results in Figure 2 show that there is no significant influence of CCA on the particle size distribution of lateritic soil. However, a slight increase in the coarser particles was observed. This change is an indication that with increase in CCA content, modification reaction between CCA and clay minerals increased which facilitated the formation of relatively coarser particles (Salahudeen, 2014).

3.3 Effect of CCA on Specific Gravity of Lateritic Soil

The specific gravity of solid particles is the ratio of the mass of a given volume of solids to the mass of an equal volume of water. Specific gravity an important parameter used for the determination of the void ratio and particle size of any soil particle (Salahudeen and Sadeeq, 2016a; b). The variation of specific gravity with CCA is shown in Figure 3.The specific gravity of natural soil (2.73) decreased consistently with the addition of CCA content. The decrease in specific gravity is due to the lower specific gravity of CCA compared to that of the untreated soil (Salahudeen, 2014).

3.4 Effect of CCA on Atterberg Limits of Lateritic Soil

The variation of Atterberg limits (liquid limit, plastic limit and plasticity index) of subgrade soil with CCA content is shown in Figure 4. The liquid and plastic limits of the lateritic soil increased with increased CCA content. This increase in liquid limit is an indication of increasing value of compression index and higher proneness of the soil towards settlement (Salahudeen et al. 2014). An increase in plastic limit (PL) was also observed as CCA content increased. The introduction of CCA into the soil first caused an increase in the liquid limit and plasticity index and thereafter decreased. The increase can be attributed to addition of CCA which introduced more pozzolanic substance into the specimen that required more water for hydration to be completed. The subsequence decrease can be associated with the agglomeration and flocculation of the clay particles which is as a result of exchange ions at the surface of the clay particles.

This observed trend is in agreement with Ramzi et al. (2001), Venkaramuthyalu et al. (2012), Salahudeen and Ochepo (2015), Sadeeq et al. (2014a; b; c) Sadeeq et al. (2015), Salahudeen and Sadeeq (2016a; b) and Sadeeq and Salahudeen (2017). Ramzi et al. (2001), Suhail et al., (2008), Venkaramuthyalu et al. (2012) and Salahudeen and Sadeeq (2016a; b) reported that the reduction in plasticity index with chemical treatment could be attributed to the depressed double layer thickness due to cation exchange by potassium, calcium and ferric ions.

3.5 Effect of CCA on Compaction Characteristics of Lateritic Soil

The variations of maximum dry density (MDD) and optimum moisture content (OMC) of the lateritic soil used in this study with CCA content are shown in Figure 5. According to Alhassan (2008) and Salahudeen (2014), the increase in the MDD can be attributed to the replacement of soil by CCA in the mixture. It may also be attributed to coating of the soil by the CCA which resulted to formation of larger particles and hence the increase in MDD. The increase in the MDD may also be explained by considering the CCA as a filler in the soil voids which increased the weight of the soil/CCA matrix.

According to Salahudeen et al. (2014) and Salahudeen (2014), the increase in MDD could be due to CCA occupying the voids within the soil matrix as well as the flocculation and agglomeration of the clay particles due to exchange of ions. There was a continuous decrease in OMC with increased CCA contents. The trend is in line with Osinubi (1999) and Salahudeen (2014). The decrease may be due to the addition of CCA, which decreased the quantity of free silt and clay fraction and coarser materials with larger surface areas were formed. The decrease in OMC with increase in CCA content might also be due to cation exchange reaction that caused the flocculation of clay particles (Salahudeen and Akiije, 2014; Salahudeen et al. 2014; Salahudeen, 2014, Sadeeq and Salahudeen, 2017).

4.0 CONCLUSION

From the results of this study, the following conclusions were drowned:

- The specific gravity decreased with increased CCA content.
- The plasticity index increased then decreased with increase in CCA content. However, none of the values of plasticity indices met the 12 % plasticity index specified by clause 6201 of the Nigerian General Specifications (1997) for sub base materials.
- Treatment of lateritic soil with CCA showed a general increase in the MDD and decrease in OMC with increased CCA content.

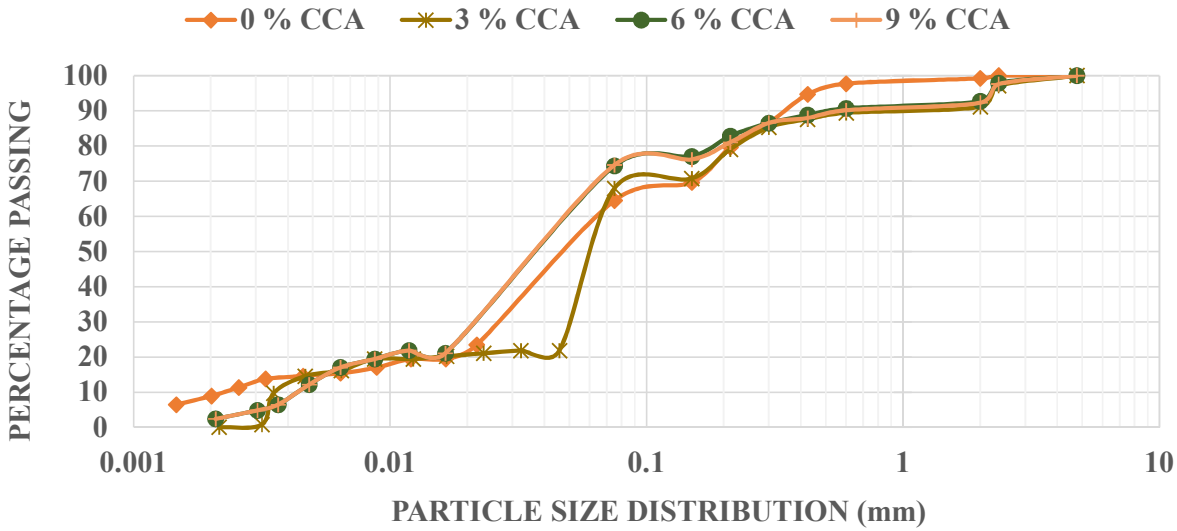


Figure 2: Particle size distribution curve for the natural and CCA modified lateritic soil

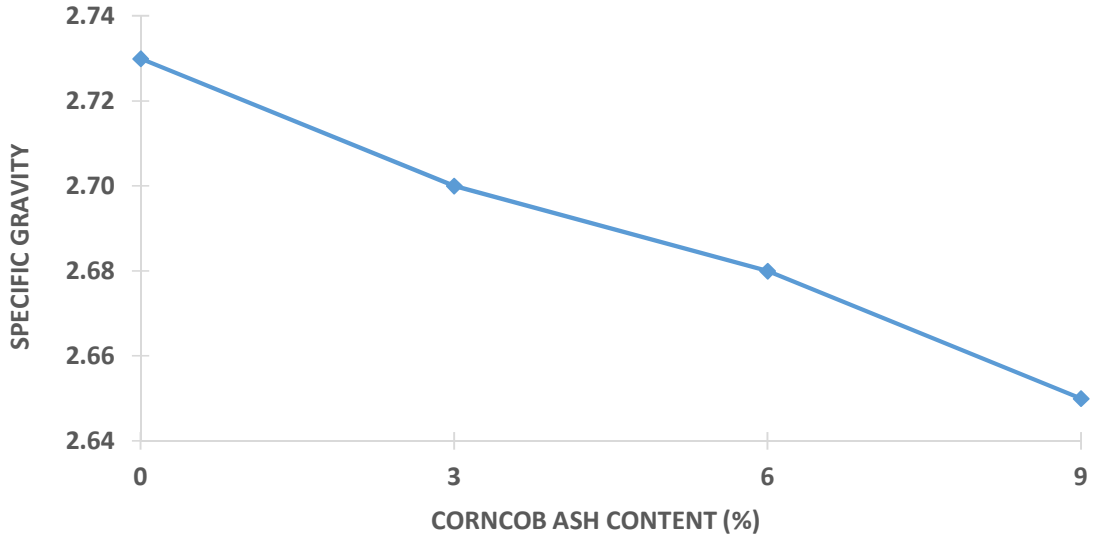


Figure 3: Variation of specific gravity of lateritic soil with CCA content

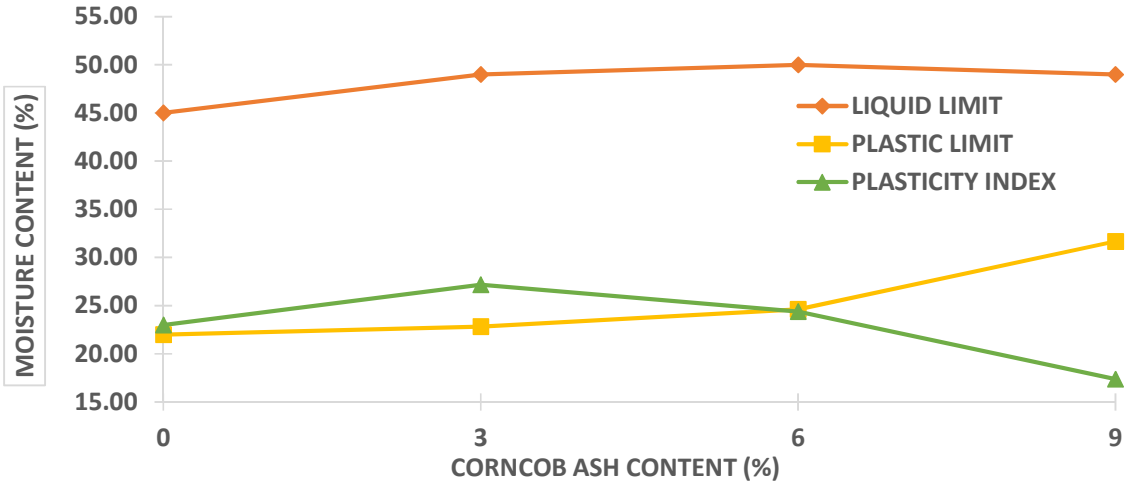


Figure 4: Variation of Atterberg limits of of lateritic soil with CCA content

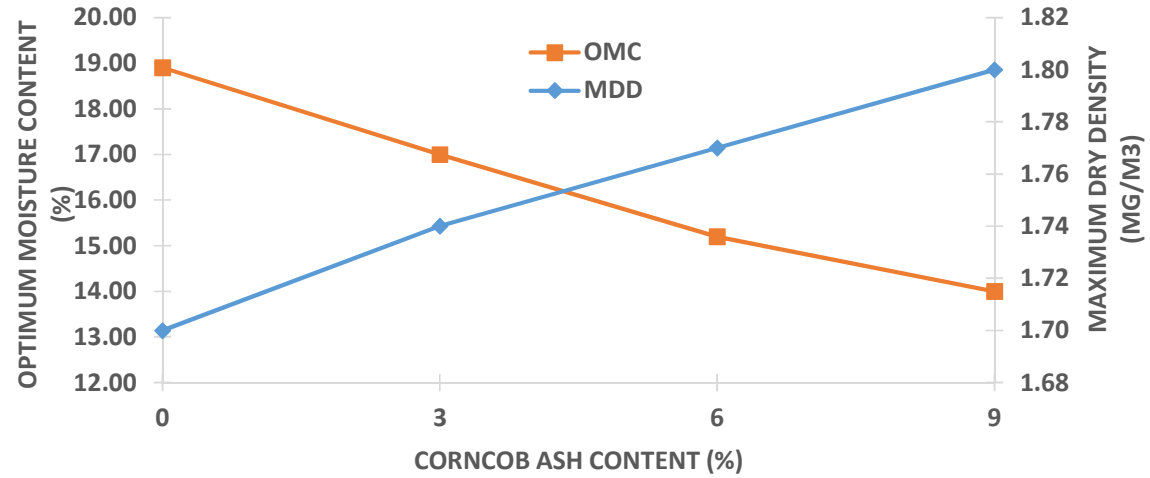


Figure 5: Variation of maximum dry density and optimum moisture content of lateritic soil with CCA content

5.0 ACKNOWLEDGEMENT

The authors are grateful to all the technical staff in the Geotechnical research laboratory, Department of civil engineering of Ahmadu Bello University, Zaria for the role they played in the laboratory work of this research particularly Malam Lawal.

6.0 REFERENCES

Alhassan, M. (2008). *"Potential Of Rice Husk Ash For Soil Stabilization"*. *Assumption University Journal of Technology*. Vol. 11, No. 4. pp.246-250.

American Association of State Highway and Transportation Officials (AASHTO), (1986) Washington, D. C.. "Standard Specifications for Transportation Materials and Methods of Sampling and Testing, Twentieth Edition".

ASTM C618-93 specification (1992) "Fly Ash and Raw or Calcined Natural Pozzolan for use as Mineral Admixture in Portland Cement Concrete".

British Standard (BS) 1377 (1990) "Methods of Test for Soils for Civil Engineering Purposes".

British Standard (BS) 1924 (1990). *Methods of Tests for Stabilized Soils.* British Standards Institute, London.

EuroSoilStab. (2002). Development of Design and Construction Methods to Stabilize Soft Organic Soils: Design Guide for soft soil stabilization. CT97-0351, European Commission, Industrial and Materials Technologies Programme (Rite-EuRam III) Bryssel.

FAO. Records, Retrieved December 15, 2002, from http://apps.- fao.org/default.htm.

cement. The Professional Builder 2001;June:3–10.

Nigerian General Specification (1997): Road Works and Bridges, Federal Ministry of Works and Housing, Abuja, Nigeria.

Osinubi, K. J. (1995). "Lime modification of black cotton soils." *Spectrum Journal*, Vol. 2, Nos 1 and 2, pp. 112 – 122.

Osinubi, K. J. (1999). "Evaluation of admixture stabilization of Nigerian black cotton soil." *Nigerian Society of Engineers Technical Transactions*, Vol. 34, No 3, pp 88-96.

Osinubi, K. J. (2000). "Laboratory trial of soil stabilization using pulverised coal bottom ash." *Nigerian Society of Engineers Technical Transactions*, Vol. 35, No 4 pp 13 – 21.

Ramzi, T., Amer, A., Ali, A. and Hilia A. (2001). "*Use Of Cement Kiln Dust In Soil Stabilization*". EJUQ. Vol.14 pp.61-76.

Sadeeq, J. A., Ochepo, J. and Salahudeen, A. B. (2014 a). "Effect of used oil contamination on the volumetric shrinkage of lateritic soils." Proceedings of the Third International Conference on Engineering and Technology Research, Ladoke Akintola University of Technology , Ogbomoso, Nigeria Volume 3, pp 167-175.

Sadeeq, J. A., Ochepo, J. and Salahudeen, A. B. (2014 b). "Assessment of bagasse ash effect on the volumetric shrinkage of lateritic soils for flexible pavements." Proceedings of the Nigerian Engineering Conference, Ahmadu Bello University, Zaria, Nigeria, pp 241-248.

Sadeeq, J. A., Ochepo, J. and Salahudeen, A. B. (2014 c). Effect of bagasse ash on consolidation settlement characteristics of lateritic soils. Proceedings of the national conference on "Bridging the gap between academia and industry in Nigeria-Refocosing the engineering discipline." Faculty of Engineering, Bayero University, Kano, Nigeria, pp 573 – 587.

Sadeeq, J. A., Ochepo, J., Salahudeen, A. B. and Tijjani, S. T. (2015). Effect of bagasse ash on lime stabilized lateritic soil. Jordan Journal of Civil Engineering (JJCE), Vol. 9, No.2.

Sadeeq, J. A. and Salahudeen, A. B. (2017). Strength characterization of foundation soils at Federal University Lokoja based on standard penetration tests data. *Nigerian Journal of Technology (NIJOTECH),* Vol. 36 No. 3, Pp. 671 – 676.

Salahudeen, A. B. (2014). Stabilization of black cotton soil with cement kiln dust. Unpublished M.Sc. thesis*, Department of Civil Engineering,* Ahmadu Bello University, Zaria.

Salahudeen, A. B. and Akiije, I. (2014). Stabilization of highway expansive soils with high loss on ignition content kiln dust. *Nigerian journal of technology (NIJOTECH),* Vol. 33. No. 2, pp. 141 – 148.

Salahudeen, A. B., Eberemu O. A. and Osinubi, K. J. (2014). Assessment of cement kiln dust-treated expansive soil for the construction of flexible pavements. Geotechnical and Geological Engineering, Springer, Vol. 32, No. 4, PP. 923-931.

Salahudeen, A. B. and Ochepo, J. (2015). Effect of bagasse ash on some engineering properties of lateritic soil. Jordan Journal of Civil Engineering (JJCE), Vol. 9, No.4.

Salahudeen, A. B. and Sadeeq, J. A. (2016a). Effect of rice husk ash on the index properties and hydraulic conductivity of lateritic soils for flexible pavement construction. *Proceedings of the International Conference and Nigerian Material Congress 2016 (NIMACON 2016), Material Science and Technology Society of Nigeria (MSN),* Ahmadu Bello University, Zaria, pp. 1 – 6.

Salahudeen, A. B. and Sadeeq, J. A. (2016b). Strength characteristics of lateritic soils treated with rice husk ash for earth road construction. *Proceedings of the International Conference and Nigerian Material Congress 2016 (NIMACON 2016), Material Science and Technology Society of Nigeria (MSN),* Ahmadu Bello University, Zaria, pp. 7 – 11.

Salahudeen, A. B. (2017). "Prediction of foundation settlement based on standard penetration test results using empirical and numerical techniques." Unpublished PhD thesis, Department of Civil Engineering, Ahmadu Bello University, Zaria, Nigeria. Pp 70 – 77.

Sherwood, P.T. (1993): "Soil Stabilization with Cement and Lime: A State-of-The-ArtReview" Department of Transport, Transport Research Laboratory, United Kingdom.

Suhail, A.A.A., Khawla, A.K.A. and Ibrahaim, M.A.A. (2008). "*Strength Durability And Hydraulic Properties Of Clayey Soil Stabilized With Lime And Industrial Waste Lime*". Al-Rafidain Engineering. Vol. 16. No. 1. Pp.102-116.

Venkaramuthyalu, P., Ramu, K., and Prasada, R.G.V.R. (2012). "*Study on performance of chemically stabilized expansive soil*". IJAET, Vol. 2, Issue 1, pp 139-148.

OPTIMIZATION OF ACTIVATING CONDITIONS AND COLOUR REMOVAL EFFICIENCY OF MAIZE HUSK IN THE REMOVAL OF COLOUR FROM TEXTILE WASTE WATER

R.O. OKPUWHARA, B.M. DAUDA AND K.O. FASHOLA
Department Of Textile Science and Technology, Ahmadu Bello University, Zaria, Nigeria.
oghenetega7@gmail.com

ABSTRACT
Activated carbons (ACs) have been produced from maize husk and used for colour removal from textile effluent. The colour removal efficiency of the activated carbons was evaluated using textile wastewater as adsorbate. The optimization of activating conditions of temperature, time and acid ratio for the activation of maize husk was investigated. Results showed that the optimized condition for conversion the maize husk into AC is at a temperature of 550°C for 45min using 60% acid ratio using phosphoric acid. Charaterization studies of the activated carbon were carried out for the BET surface area, pore volume, ash content, carbon yield, moisture content, and volatile content. The results obtained showed that the colour removal efficiency was influenced by various operational variables such as, pH, time, adsorbent dose, particle size and adsorbate concentration.

Keywords: *colour, carbon, activation, maize, husk.*

INTRODUCTION

Maize is the world's most widely distributed crop from the tropics to the temperate zone. It is an important food in Sub – Saharan Africa and one of the five major crops accounting for 60% to 70% of total cereal production (UNDP, 2009).

In Nigeria, maize has become a major food item. It is consumed in many forms and thus, the maize husks cause littered environment because the husks and cobs are often discarded indiscriminately after being eaten cooked or roasted as green maize. The husks and cobs are often burnt as a means of waste disposal.
Although some economical benefits of maize husk are its use as livestock feeds, in weaving of baskets, mats and maize husk dolls (Bond, 2008), its use for production of AC would increase its economic value and help reduce its environmental nuisance factor. Maize husk has rarely been used in biosorption researches in the past.

Some related works on maize plant include: Khodaie *et al*. (2007) investigated the removal of methylene blue by Corn Husk Activated Carbon using $ZnCl_2$ (CHACZ). Dada *et al.* (2012) studied the comparative adsorption of dyes unto activated carbon prepared from maize stems and sugar cane stems.

In this study activated carbons have been produced from maize husk and used for colour removal from dye containing-textile effluent obtained from a textile mill. The optimum conditions for chemical activation were established.

MATERIALS AND METHODS

MATERIALS

Chemicals and Reagents

All chemicals and reagents used are of analytical grade and include the following:
Phosphoric acid, Zinc chloride, Sulphuric acid, Sodium hydroxide, Sodium hydrogen carbonate,

Glass Wares/Apparatus

Beakers, measuring cylinders, funnels, burettes, wash bottles, shaking vessels stoppers, volumetric flasks, Pyrex dishes, desiccator, crucibles, and filter paper (whatman 110mmø).

Equipment

Water still, Grinding mill, Digital weighing balance, Muffle furnace, Oven, Laboratory blender, Electronic test sieve shaker, Digital pH meter, Test tube shaker, Scanning spectrophotometer, Spectro UV – VIS dual beam split beam, Surface area and porosity analyser.

Adsorbents /Adsorbates

Maize husk was used as adsorbent while Dye effluent (mixture of basic green dye and basic lemon yellow dye) was used as adsorbate.

Collection and Preparation of Biomass Waste Samples

The maize husk samples were collected locally from Zaria environs, washed with water to remove dirt, other particulate matter and air dried. The dried samples were crushed using grinding mill fitted with sieve of 1mm mesh. The samples were then labelled and stored in tight plastic containers.

Collection and Preparation of Adsorbate

The Adsorbate (industrial dye wastewater) was collected from the untreated effluent reservoir at Chellco Textiles Nigeria Limited, Kaduna, Nigeria. The dye-containing wastewater was used without further purification and diluted to the required concentration. A 1000ppm (1000mg/l) concentration was first prepared and from which series of working concentrations of 2ppm, 4ppm, 5ppm, 6ppm, 8ppm and 10ppm were prepared as described by Kardirvelu *et al*. (2003).

PRODUCTION OF ACTIVATED CARBON (AC)

Chemical Activation of Maize Husk

Phosphoric acid was used as the activating chemical and the activation process was carried out in stages as stated in the procedures below.

Preparation of carbonised maize husk

Carbonization of Maize Husk (MH) was carried out by placing 200g of 2mm size MH sample in a crucible kept in a furnace at 400ºC for 30min. The char produced was used for chemical activation.

Preparation of activating chemical (acid concentration)

The activating chemical was produced using different phosphoric acid impregnating ratios of 40%, 60% and 80%. The acid ratio is defined as the ratio of percentage volume of phosphoric acid utilized for impregnation to the percentage volume of distilled water.

Preliminary test for the optimization of activating conditions for MHAC

Activating conditions of temperature, time and acid concentration were determined by using 6cm^3 of each acid: water ratio from the prepared acid concentrations of 40%, 60% and 80% phosphoric acid. 2g of the carbonised MH precursor was used for each test run. Tests were carried out at 3 different temperatures and 3 varied periods.

The different acid impregnating ratios of 40%, 60% and 80% phosphoric acid were kept constant for each batch test. Time was varied at 15min, 30min and 45min respectively. Temperatures were varied at 500ºC, 550ºC and 600ºC respectively and kept constant for a particular batch test. After activation, the Maize Husk Activated Carbon (MHAC) was immediately quenched in distilled water.

The samples were then washed repeatedly in distilled water. To optimize percentage removal of colour, the MHAC samples were shaken with 10cm^3 of the effluent sample for 60min, it was filtered out with filter paper and the absorbance reading taken with a UV - spectrophotometer. The carbon yield and percentage dye removal from the preliminary tests were then calculated as shown in Equations 1.0 and 2.0 respectively to know the optimized temperature, time, and acid concentration to carry out the activation of the MH adsorbent to be used for the adsorption experiments. The carbon yield and percentage dye removal results are shown in Table 1.0

The method of Fapetu (2000) was used forcarbon yield determination as shown in Equation 1.0 The carbon Yield is defined as the ratio of weight of AC produced to the dry weight of precursor.

$$Y = 100\left[\frac{W_{ch}}{W_o}\right] \ldots\ldots\ldots (1.0)$$

where:

Y = Carbon Yield

W_{ch}= Weight of carbon retrieved from the furnace

W_o= Dried weight of the carbon sample

$$\text{Dye removal} = 100\left[\frac{Abs_0 - Abs_1}{Abs_0}\right] \ldots\ldots\ldots (2.0)$$

where:

Abs_0 = Spectrophotometric reading of initial absorbance of adsorbate before shaking.

Abs_1 =Spectrophotometric reading of final absorbance of adsorbate mixed with adsorbent after shaking.

Preparation of activated maize husk adsorbent for adsorption experiments using optimised condition.

The experimental sample was prepared by mixing 100g of carbonized MH precursor with 300cm^3 phosphoric acid based on optimised impregnating ratio. This was utilized for soaking the precursor so as to promote the formation of slurry. The phosphoric acid soaked sample was left overnight in a desiccator and the excess water was evaporated in an oven at 100ºC to ensure complete absorption of phosphoric acid onto the carbonized maize husk.

The acid soaked carbonized samples were then activated in a muffle furnace at optimal activation condition. After activation, the MHAC was immediately quenched in distilled water. The sample was then washed repeatedly in distilled water to remove residual acid. The effectiveness of the washing process was confirmed with a neutral or near neutral pH using a pH meter. It was finally dried in an oven for 180min at 120±5ºC, ground into fine powder with laboratory blender and sieved to get different particle sizes. The sample was then characterized and the results are shown in Table 2.0.

3.4 CHARACTERIZATION OF ACTIVATED CARBON

Characterization of Activated Carbon

The MHAC from the agricultural wastes were characterized for their properties as follow:

Surface Area (m^2/kg): The Brunauer – Emmett – Teller (BET) method was used to calculate the surface area, based on selected N_2 adsorption data. (Brunauer *et al*., 1938).

Pore Volume (cm^3/g) , Micro - Pore Volume (cm^3/g) And Pore Size (Å): These were derived from the Barrett, Joyner and Halenda (BJH) method. The micro–pore volume and pore size were also calculated from the BJH method (Barrett *et al*., 1951).

Carbon Yield (Percent): The carbon yield Y_{cb} was determined using the method of Fapetu, (2000).

pH: The pH of the ACs was determined using the standard test of ASTM D3838 – (2011).

Ash Content (Percent): The ash content of the ACs was determined using the ASTM procedures D2866 – (1994).

Moisture Content (Percent): Moisture content was determined according to the AOAC (1980) Method.

Volatile Content: Volatile content was determined according to the AOAC (1980) Method.

All characterization results are displayed in Table 2.0.

ADSORPTION EXPERIMENT

The UV spectrophotometer was used to determine the absorbance of the dyes before and after decolourization; to know optimal conditions for dye removal and calculations was carried out by the equation 3.0 as given below and their lander max displayed in figure 1.0.

$$\text{Dye removal} = 100\left[\frac{C_i - C_e}{C_i}\right] \ldots\ldots\ldots (3.0)$$

where:

C_i= Initial concentration before shaking

Ce = Equilibrium concentration after shaking.

The optimal conditions for dye removal were carried out by varying the influence of the following parameters:

Effect of pH

0.02g of Adsorbents of particle size 500µm were thoroughly mixed with $10cm^3$ adsorbate at a concentration of 10ppm in $60cm^3$ shaking vessels. The initial pH of the adsorbate was included in test runs and was also adjusted to the required pH value, by varying at 2.00, 4.00, 6.00 and 8.00, 10.00 depending on the case by either 0.1M sulphuric acid or 0.1M Sodium hydroxide solution. The mixtures were agitated at a speed of 400rpm with test tube shaker at 25±0.5°C for 60min. After shaking, the adsorbents were separated from solution by filtration and absorbance measured with a spectrophotometer. The percentage removal of dyes was calculated as stated in Equation 3.0 above and the graph of percentage removal of dyes was plotted against pH. Figure 2.0 shows the comparative pH analysis for the mixture of dye-containing effluent. From the plotted graph, the optimal pH, X_{pH} for the experiment were determined.

Determination of Equilibrium Time

$10cm^3$ of adsorbates at a concentration of 10ppm and 0.02g adsorbent dose of particle sizes 500µm were used and kept constant during the experiment. Batch experiments were carried out in $60cm^3$ shaking vessels. The optimal solution pH, X_{pH} previously determined was kept constant. The mixtures were agitated at a speed of 400rpm with test tube shaker at 25±0.5°C periods of times varied at 15min, 30min, 45min, 60min and 75min. After shaking, the adsorbent were separated from solution by filtrations and absorbance measured with a spectrophotometer. The percentage removals of dyes were calculated as stated in Equation 3.0 and the graphs of percentage removal of dyes were plotted against time. Figure 3.0 shows the comparative time analysis for the mixture of dye-containing effluent. From the plotted graphs, the highest contact time X_T for the experiment were determined.

Effect of Adsorbent Dosage

0.01g, 0.02g, 0.03g, 0.04g, 0.05g and 0.06g of particle sizes 500µm and placed in $60cm^3$ shaking vessels and $10cm^3$ of adsorbates at a concentration of 10ppm were added. The optimal solution pH of the mixture $X_{pH}$and the optimal time (X_T) determined were used and kept constant throughout the experiment. The mixtures were agitated at a speed of 400rpm in shaking vessels at 25±0.5°C. After shaking, the adsorbents were separated from solution by filtration and absorbance measured with a spectrophotometer. The percentage removal of dyes was calculated as stated in Equation 3.0 and the graph of percentage removal of dye was plotted against adsorbent dose.

Figure 4.0 shows the comparative dosage analysis for the mixture of dye-containing effluent. From the plotted graphs, the optimal adsorbent dose, X_{AD} were determined.

Effect of Particle Sizes

Particle sizes of adsorbent samples determined from different sieve sizes of 0 – 75µm, 75µm, 90µm, 150µm, 250µm and 500µm were placed in 60cm^3 shaking vessels. In all sets of experiment, 10cm^3 of adsorbate at a concentration of 10ppm were used and kept constant during the experiment. The determined optimal solution pH (X_{pH}), determined equilibrium time (X_T) and optimal adsorbent dose (X_{AD}) were used. The mixture was agitated in 60cm^3 vessels at a speed of 400rpm with test tube shaker at 25±0.5°C for X_T min. After shaking, the adsorbent were separated from solution by filtration and the absorbance was measured with a spectrophotometer. The percentage removal of dyes was calculated as stated in Equation 3.0 and the graph of percentage removal of dye was plotted against particle size. Figure 5.0 shows the comparative particle size analysis for the mixture of dye-containing effluent. From the plotted graphs, the optimal particle sizes (X_P) for the experiments were determined.

Effect of Adsorbate Concentration

10cm^3 of adsorbate with varied concentrations of 2ppm, 4ppm, 5ppm, 6ppm, 8ppm and 10ppm were placed in a 60cm^3 shaking vessels. The determined optimal solution pH of the mixture (X_{pH}), the optimal time (X_T), optimal absorbent dose (X_{AD}) and the predetermined particle size (X_P) from the previous tests were used and kept constant throughout the experiments. The mixtures were agitated at a speed of 400rpm in shaking vessels at 25±0.5ºC. After shaking, the adsorbents were separated from solution by filtrations and absorbance measured with a spectrophotometer.

The percentage removals of dyes were calculated as stated in Equation 3.0 and the graphs of percentage removal of dyes were plotted against concentration of adsorbates. Figure 6.0 shows the comparative concentration analysis for the mixture of dye-containing effluent. From the plotted graphs, the optimal concentration of adsorbate, X_{Aconc} for the experiments was determined.

RESULTS AND DISCUSSION

SPECTROPHOTOMETRIC ANALYSES OF EFFLUENT SAMPLES

Figure 1.0 shows the spectrophotometric reading of effluent sample which contains a mixture of the BYD and BGD at 430nm and 620nm respectively.

PRELIMINARY TEST ON MAIZE HUSK ACTIVATED CARBON

Generally, the yield of MHAC decreased with increase in activation temperature, activation time and impregnation ratio, while the pore characteristic improved with increase in the above stated parameters, mostly to an optimum value of 99.93% of dye removal at 550ºC, 30min at 40%, 550ºC, 30min at 80%, 550ºC at 45min and 60% acid ratio as shown in Table 1.0 This trend is expected since the optimum temperatures have been reported to be between 400°C to 500°Cby most of the earlier researchers irrespective of the time of activation and impregnation ratio for different raw material. Moreover, it is well known that carbons from plant species origin show the highest specific surface area while they are obtained in the 450 – 500°C temperature range (Molina- Sabio and Rodriguez-Reinoso, 2004).

This trend is almost maintained up to 600ºC which shows that percent yield remained almost constant on increase of temperature and time because there is no volatile matter left for release. Amongst the three optimised values of percent dye removal, 550ºC at 45min and 60% acid ratio had the highest yield hence was chosen as the best optimized condition for the production of MHAC.

The result of percentage yield for variation in activation temperature and time are in good agreement with the statements from Adiante *et al*., (2007), Guo *et al*., (2003) and Malik *et al*., (2008) that percentage yield decreases with increase in temperature.

Results on Colour Removal

After 60min of contact time, the adsorptions of BYD and BGD on the MHAC were found to be highly pH dependent. pH results showed that lower pH gave higher percentage dye removal and showed colour change at pH 2 than that of 4, 6,8 and at pH 10. For both BYD and BGD, the best pH for dye removal with MHAC is at pH 2. BGD with 96.78% and BYD with 87. 59%. Although, overall BGD was better adsorbed than BYD. This maybe so because pH influences the dissociation of functional groups on the active sites of the adsorbent, but also the solution dye chemistry (Crini *et al*., 2007).

The highest yellow and green dyes percentage removal by MHAC from the effluent was obtained at 75min and the lowest was obtained at 15min. Thereby, the longer the time, the better the dye percentage removal. This also agrees with literature that the longer the time, the more

complete the adsorption will be (Kannan and Meenakshisundaram, 2002Gratuito *et al*., 2010).

MHAC had the highest dye removal with 0.02g and the lowest at 0.06g for both BYD and BGD. The relative increase in the percentage removal of dye is found to be insignificant after an optimum dose because of the fluctuating trend. This may be due to overlapping and aggregation of adsorption sites when dose increased (Lata*et al*., 2008; Nuhoglu and Malkoc, 2009)

For BYD, MHAC had the highest dye removal with 500µm and the lowest with 0 – 75µm While for BGD; MHAC had the highest dye removal with 90µm and 250µm, and the lowest at 500µm. The rate of removal efficiency did not follow any significant trend, especially regarding smaller particle sizes having higher efficiency. It is cited in literature that smaller particle sizes reduce internal diffusional and mass transferlimitation to the penetration of the adsorbate inside the adsorbent that is, equilibrium is more easily achieved and nearly full adsorption capability can be attained (Pagnanelli*et al*., 2003; Tarley and Arruda, 2004 and Singh *et al*., 2008).

For BYD, MHAC had the highest dye removal at 2ppm and 2.5ppm; the lowest was at 1ppm. and for BGD, MHAC had the highest dye removal at 2ppm and 5ppm; the lowest was at 1ppm.
It was observed that the removal efficiency decreased with increase in concentration of adsorbate concentration to an optimum but again, the change in trend may have been caused by aggregation of particles thereby minimising the availability of active sites for adsorption.

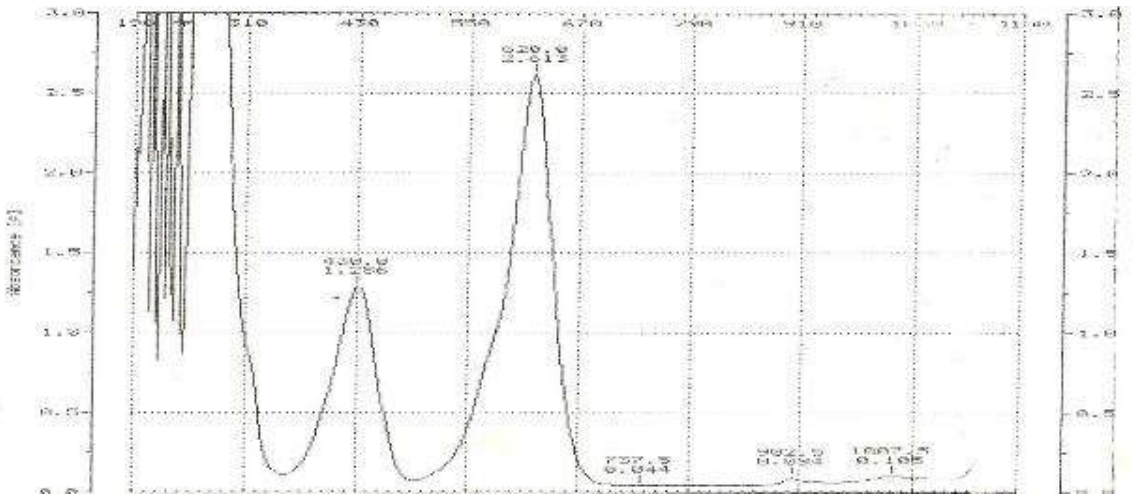
Table 1.0. : Yield Percent and Percentage Dye Removal from Preliminary Test on Maize Husk.

Temperature (˚ C)	Time (min)	Concentration (%)	Yield (%)	Dye Removal (%)
500	15	40	99.95	98.81
500	15	60	99.95	99.75
500	15	80	99.9	99.81
500	30	40	99.85	99.56
500	30	60	99.75	98.75
500	30	80	99.45	99.12
500	45	40	99.5	98.31
500	45	60	95.95	99.12
500	45	80	95.55	99.62
550	15	40	89.95	99.62
550	15	60	79.70	99.37
550	15	80	54.15	99.68
550	30	40	80.95	99.93
550	30	60	72.20	99.87
550	30	80	60.55	99.93
550	45	40	55.95	99.87
550	45	60	91.60	99.93
550	45	80	94.10	99.31
600	15	40	58.80	99.87
600	15	60	55.05	99.00
600	15	80	56.65	99.75
600	30	40	46.00	99.06
600	30	60	56.95	96.93
600	30	80	56.65	99.62
600	45	40	27.80	94.44
600	45	60	22.35	97.06
600	45	80	12.50	98.93

RESULTS OF THE PHYSICO-CHEMICAL CHARACTERIZATION/ANALYSES OF THE ACTIVATED CARBON PRODUCED

Table 2.0. : Characteristics of the Activated Carbon(s) Produced

PARAMETER	RESULT
pH	5.36
BET surface area (m^2/g)	206.57
Pore volume (cm^3/g)	0.12
Micropore volume (cm^3/g)	0.06
Mean pore width (Å)	22.89
Carbon yield (%)	41.97
Ash content (%)	6.80
Moisture content (%)	8.00
Volatile content (%)	93.20



Wavelenght (nm)

Figure 1.0. Absorbance vs Wavelenght of Effluent Sample.

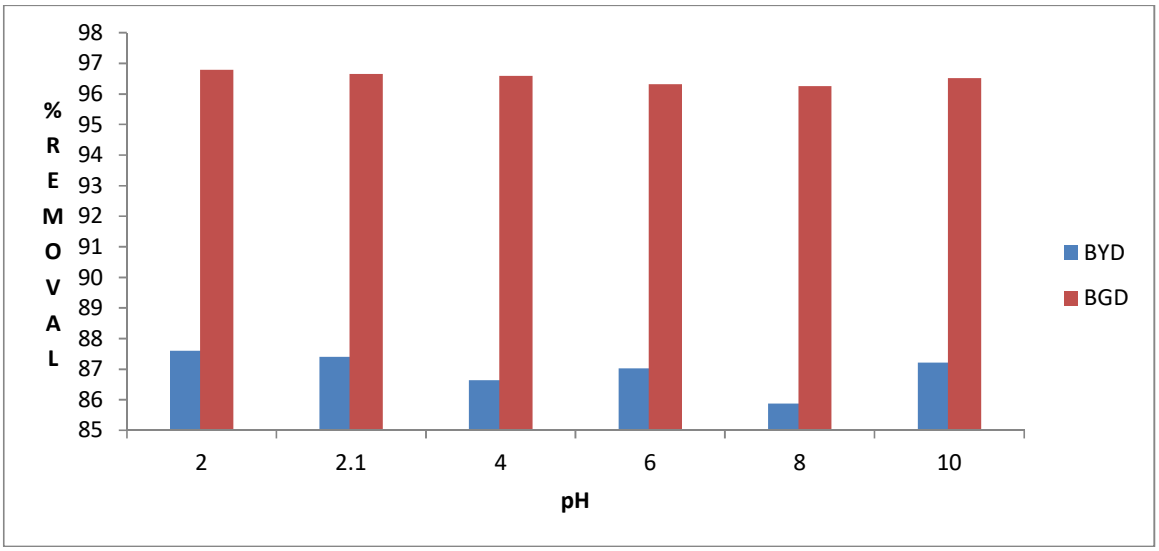


Figure 2.0: Effect of pH on dye removal in Effluent.

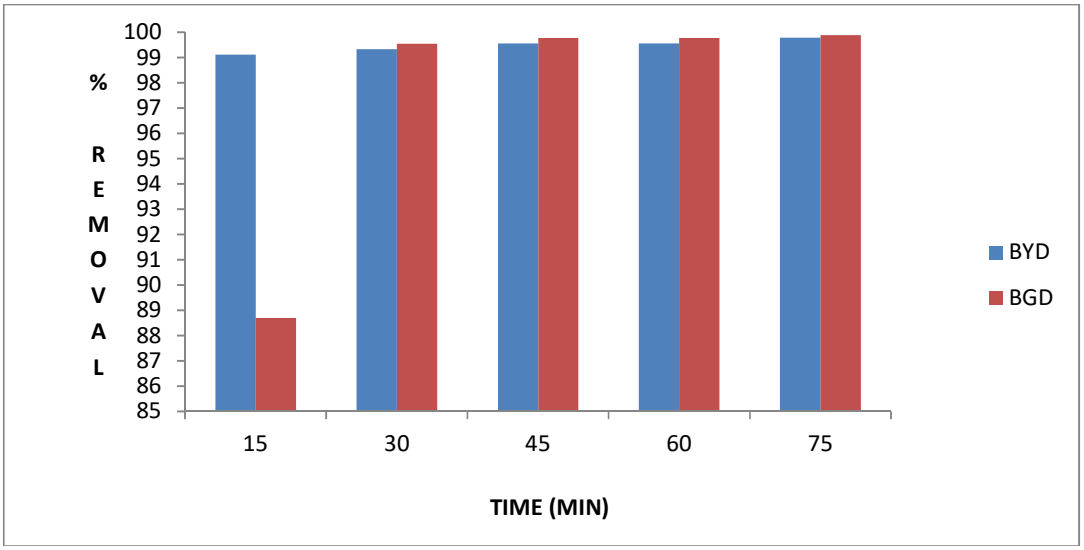


Figure 3.0: Effect of Time on dye removal in Effluent.

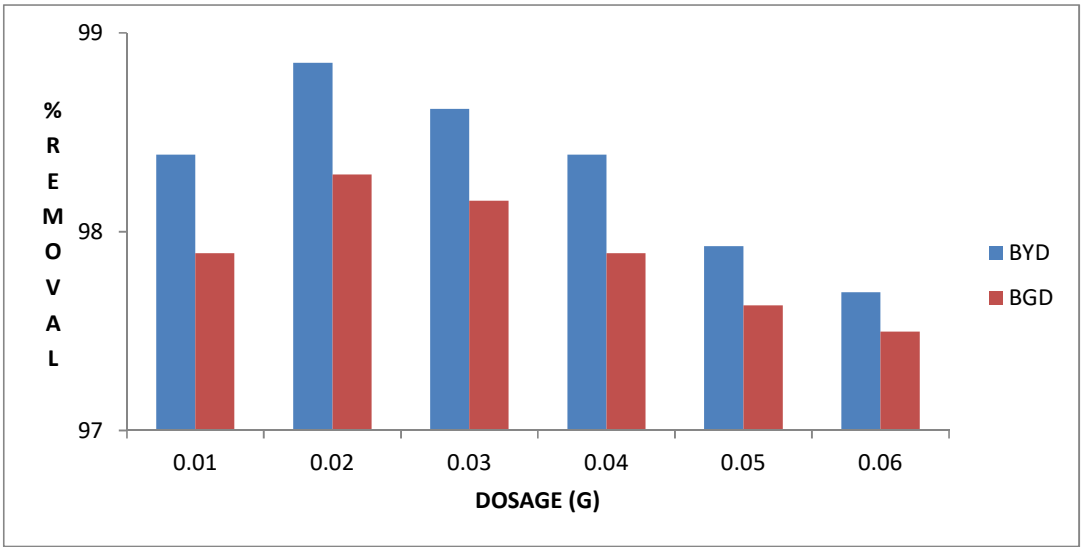


Figure 4.0: Effect of Dosage on dye removal in Effluent.

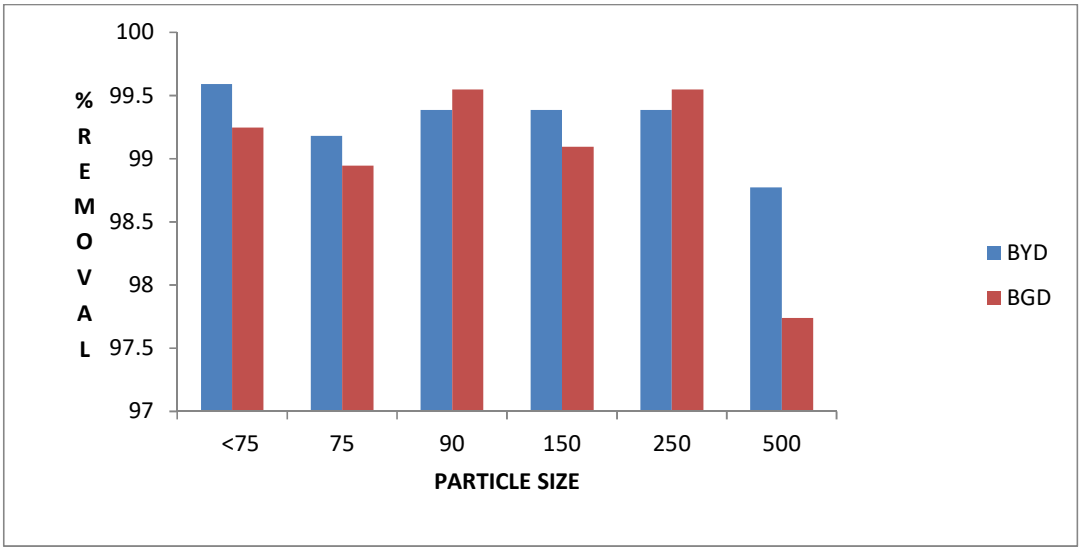


Figure 5.0: Effect of Particle size on dye removal in Effluent.

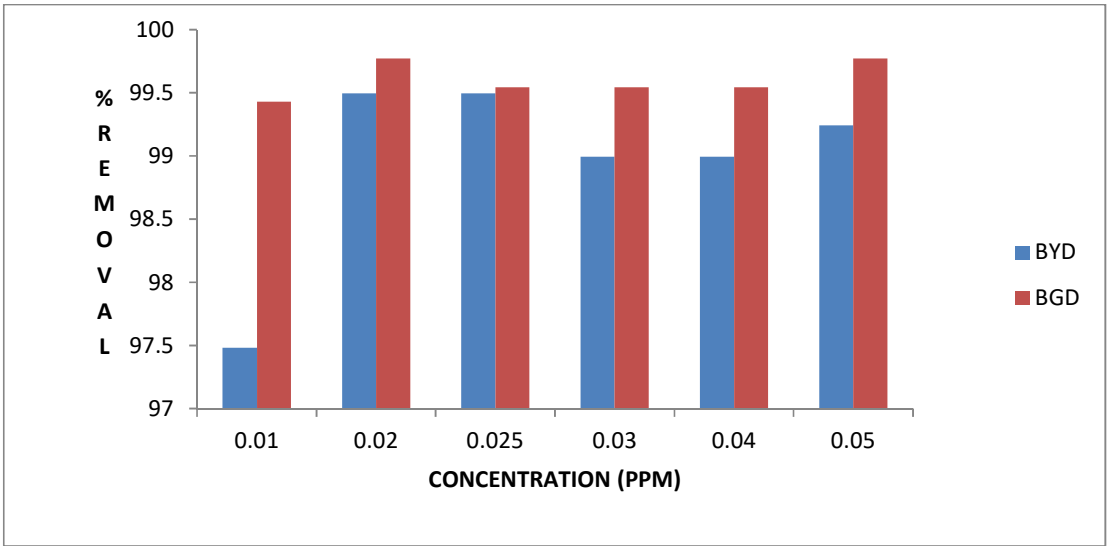


Figure 6.0: Effect of Concentration on dye removal in Effluent.

CONCLUSION

The adsorbent, MHAC at its optimized condition, as shown from the table was at 550ºC, 45min of activating time and impregnation ratio of 60% using phosphoric acid.

Generally percentage colour removals were high within the range of 70 to 90% resulting in colourless residual sample in each case after adsorption. The results mostly did not give any particular trend but the green dye was better removed than the yellow dye from the effluent dye mixture thus resulting in higher percentage dye removal for the green dye with the optimizing parameters. pH value of a dye solution plays an important role in the whole adsorption process and particularly on the adsorption capacity (Aksu, 2005).

The optimum activation time is reported to vary between 30min and 120 min depending upon the activation method. However a lower activation time is desirable as it improves the process economics and increases the product yield (Gratuito*et al*., 2010).

The use of 0.02g adsorbent dose is justified for economical purposes because when dosage is increased, the adsorbed dye may either block the access to the internal pores of the ACs or may have caused particles to aggregate and thereby minimising the availability of active sites for adsorption.

The results for the dyes and effluent were not consistent with past literature for particle size experiments, adsorption takes place, then desorption takes place, then adsorption again, leading to optimal results at different particle sizes. This may be due to the effect of chemical activation, whereby pores that are well defined, and might have surface complex formation, gives higher efficiency irrespective of the particle size.

In the concentration studies, the samples have been optimised to their respective conditions of pH, time, dosage, particle size and can be said to be at their maximum state of colour removal efficiency.

For BYD, MHAC had the highest dye removal at 2ppm and 2.5ppm; the lowest was at 1ppm. and for BGD, MHAC had the highest dye removal at 2ppm and 5ppm; the lowest was at 1ppm.

It was observed that the removal efficiency decreased with increase in concentration of adsorbate concentration to an optimum but again, the change in trend may have been caused by aggregation of particles thereby minimising the availability of active sites for adsorption.

REFERENCES

1. Adinata, D., Daud,W.M.A.W. and Aroua, M.K.(2007)Bioresource Technology.98: pp 145-149.
2. American Standard of Testing Material. (2011). *Standard Test Method for Determination For pH of Activated Carbon*, ASTM Annual Book. Annual Book of ASTMstandards, D 3838.
3. American Standard of Testing Material.(1994). *Standard Test Method for Total Ash Content of Activated Carbon*. Annual Book of ASTMstandards, D 2866.
4. Association of Analytical Chemist.(18th Ed), (1980). *Official Methods of Analysis*.

AOAC, George Banta Company Incorporation, Mensasha.
5. Barrett, E.P., Joyner, L.G., Halenda, P.H. (1951). *Journal of America Chemical Society*, 73: 373.
6. Bond, A.B. (2008). *How to Dry Corn Husks? Ask Annie*. Retrieved July, 25, 2012, from
7. Brunauer,S., Emmett P. H. and Teller, E. *J. Am. Chem. Soc.*, 1938, **60**, 309.
8. Crini, G., Peindy, H.N., Gimbert, F., Robert, C., 2007. Removal of C.I.Basic Green 4 (Malachite Green) from aqueous solutions by adsorptionusing cyclodextrin-based adsorbent: kinetic and equilibriumstudies. Sep. Purif. Technol. 53, 97–110.
9. Fapetu, O.P. (2000). Production of Carbon from Biomass for Industrial and Metallurgical Processes.*Nigerian Journal of Engineering Management*, 1: 34-37.
10. Gratuito, M.K.B., Panyathanmaporn, T., Chumnankiang, R.A. , Sirinuntawittaya, N. and Dutta, A.(2008). Bioresource Technology.99:pp4887-4895.
11. Guo, J.,Lua, A.C.(2003).Material chemistry and physics 80:pp 114-119.

http://www.care2.com/greenliving/how-to-dry-corn-husks-ask-annie.html

12. Kadirvelu, K., Kavipriya, M., Karthika, C., Radhika, M., Vennilamani, N. and Pattabhi, S.(2003). Utilisation of Various Agricultural Wastes for Activated Carbon Preparation and Application for the Removal of Dyes and Metal Ions from Aqueous Solutions. *Bioresource Technology,* 87: 129-132.
13. Kannan, N. and Meenakshsundaram, M. (2002). Adsorption of Congo Red on Various Activated Carbons. A Comparative Study.*Water, Air, and Soil Pollution*, 138: 289 – 305.
14. Khodaie, M., Ghasemi,N., Moradi, B., and Rahimi, M. (2007). Removal of Methylene Blue from Wastewater by Adsorption onto Zncl2 Activated Corn Husk Carbon Equilibrium Studies.
15. Lata, H., Garg, V.K. and Gupta, R.K. (2008). Sequestration of Nickel from Aqeous Solution onto Activated Carbon Prepared from *Parthenium hysterophorus* L. *Journal of Harzadaous Material*, 157: 503 – 509.
16. Malik, R.; Ramteke, D.S. and Wate, S.R. (2006).Physico - Chemical and Surface Characterization of Adsorbent Prepared from Groundnut Shell by Zncl2 Activation and Its Ability To Adsorb Colour. *India Journal of Chemical Technology*, 13: 319-328.
17. Nuhoglu, Y. and Malkoc, E. (2009).Thermodinamic and Kinetic Studies for Environmental Friendly Ni (II) Biosorption Using Waste Pomace of Olive Oil Factory. *Bioresource Technology*, 100: 2375 – 2380.
18. Pagnanelli, F., Mainelli, S., Veglio, F. and Toro, L. (2003). Heavy Metal Removal by Olive Pomace: Biosorbent Charaterization and Equilibrium Modelling.Chemical Engineering Science, 58(20): 4709 – 4717.
19. Singh, C.K., Sahu, J.N., Mahalik, K.K., Mohanty, C.R., Mohan, B.R. and Meikap, B.C. (2008). Studies on the Removal of Pb (II) from Wastewater by Activated Carbon Developed from Tamarind Wood Activated With Sulphuric Acid. Journal of Hazardous Materials, 153:221 – 228.
20. Tarley, C.R.T. and Arruda, M.A.Z. (2004). Biosorption of Heavy Metals Using Rice Milling By-Products, Characterization and Application for Removal of Metals from Aqueous Effluents. *Chemosphere*, 54: 987 – 995.
21. United Nations Development Programme (UNDP) Green Commodities Facility. (2009).*A Scoping Paper: Global Maize Production, Environmental Impacts and Sustainable Production*. Retrieved July 25, 2012 fromhttp://greencommodities.org/attachments /037UNDP%20GCF%20Maize%20Scoping%20Paper.pdf

APPLICATION OF ASPEN TECH FOR THE DESIGN OF HEAT EXCHANGERS IN THE PRODUCTION OF BUTADIENE FROM BIOETHANOL

NUHU M*, SAMSON J.N[1], IMEH E. O[2]
[*]Department of Chemical Engineering, Ahmadu Bello University Zaria, Nigeria
[1]Department of Chemical Engineering, University of Abuja, Nigeria
[2]Directorate of Research and Development, Nigerian Institute of Leather and Science Abuja, Nigeria
*Corresponding author email: nmohammed@abu.edu.ng
Co-authors emails: samsonjohnndaa@yahoo.com; imykk224@gmail.com

ABSTRACT
The heat exchangers were successfully design with the application of Aspen software simulation results, which provide most of the design parameters during the manual design. Ivan Murray et al process was chosen out of the three technologies originally selected. Aspen plus software was used to simulate the whole butadiene process plant from which the heat exchanger unit was considered for this report. The heat exchangers were successfully design with the application of Aspen software simulation results, which provide most of the design parameters during the manual design. These parameters are; hot and cold stream mass flow rate of 3.08 and 2.0 kg/s, heat capacity, viscosity and thermal conductivity of 1.78 kJ/kg-K, 0.00034 Ns/m^2 and 0.26 W/m. K respectively. Their respective heat duties are 437, 1629, 1471 and 2712 kW while the required areas are 33, 62, 36 and 230 m^2 for HE-101, HE-102, HE-103 and HE-104 respectively. Other values such as provisional area, total pressure drop, percentage over (under) design, thermal effectiveness, number of transfer unit, maximum Reynolds number, shell and tube side maximum cross-flow velocity, actual tube and shell side baffle clearance which can't be easily calculate manually are obtained easily with the help of the Aspen process simulator.

Keywords: *Design, simulation, technology, shell and tube, flow stream*

INTRODUCTION

Butadiene is an important raw material in chemical process industries. It is produced from different sources which include butane acetylene and ethanol among others. After the second war a substantial part of the butadiene for manufacturing synthetic rubber was produce from ethanol (Toussaint *et al*, 1947). The development of this process was facilitated by the recognition that crotonaldehyde is the intermediate product in the ostromislensky reaction, in which ethanol and acetaldehydes are converted to butadiene. Initially a process was developed for converting crotonaldehyde and ethanol to butadiene (Toussaint *et al*, 1947) with a catalyst of silica gel, but suitable modification of the catalyst afforded equally efficient production of butadiene from acetaldehyde and ethanol.

The need for the conversion of the bio-ethanol to other useful products that will be economical is in a high pressing which provide an option for the conversion of ethanol to butadiene. Amongst the other raw material used for butadiene production, in Nigeria the cheapest of these materials is ethanol due to its renewing ability via crops production. Since Nigeria is rich in oil deposition and gas deposits (natural and associated gas) there is no much to convert the ethanol to fuel for power consumption, therefore the option for butadiene production from bio-ethanol rise to diverse of products that are so useful.

However, by incorporating dehydrogenating components in the catalyst, the lebedev type of process was affected for converting ethanol more directly to butadiene. The preferred catalyst for the acetaldehyde ethanol reaction consisted silica gel impregnated with tantalum oxide (2% Ta_20_5-98% Sio_2) while that of ethanol directly to butadiene was ($A1_20_3$: Zno) in a ratio of 60:40 with catalyst efficiencies of 67% from ethanol as the ultimate raw material were obtained in the laboratory and the results were substantially reproduced in plant operations. Ivan Murray et al process was chosen out of the three technologies originally selected.

Aspen plus T^M was developed by Aspen Tech, a company founded in 1981, with the sole objective of commercializing technology developed as part of the advanced system for process Engineering (ASPEN) project at the Massachusetts Institute of technology (MIT). Aspen plus T^M is the major component of Aspen Engineering suite ^{TM}. The process simulation software is widely used in many industries for process design, simulation, optimization and costing. It uses mathematical models to predict the performances of a chemical process. This accurate modeling of thermodynamic properties is particularly important in the separation of ideal and non ideal mixtures. The software can handle very complex processes, such as multiple- column separation systems, chemical reactions, distillation of chemically reactive

compounds and even electrolyte solutions like mineral acids and sodium hydroxide solutions. This work aim at the application of Aspen Tech Software for heat exchanger design, in the production of Butadiene from Bioethanol.

Background

The principal types of heat exchanger used in the chemical process and allied industries are listed below.

- Double-pipe exchanger: the simplest type used for cooling and heating
- Shell and tube exchangers: used for all applications.
- Plate and frame exchanger (plate heat exchanger): used for heating and cooling.
- Plate-fin exchangers.
- Spiral heat exchangers
- Direct contact: coolers and quenching.
- fired heater among others

For this design shell and tube will be consider because it is usually application to all process (Sinnott, 2004). The steps in designing the heat exchanger are given below:

Process Selection

The general concern of a chemical engineer is to developed and maintain process that serve to convert raw material into desires products which is environmental friendly, high quality and less cost. The Technologies used for production of butadiene from ethanol are; S.k. Bhattacharyya et al, Sergei Lebedev, Ivan osromislensky and Ivran L. Murray et al process. However, in selecting the best process route about three criteria have to be considered. These are availability of raw material, efficiency and ease of operation and economic viability of the process.

Design Equations

Several design equations were used for the detail heat exchanger design. These equations are used in determining the input parameters needed in complete process design of the heat exchangers using the aforementioned Aspen software.

$Q = U A_T \Delta T$ Eq1

$LMTD = \frac{\Delta T_1 - \Delta T_2}{\ln \frac{\Delta T_1}{\Delta T_2}}$ Eq2

$\Delta T_1 = T_1 - t_1$ Eq3

$\Delta T_1 = T_2 - t_2$ Eq4

$R = \Delta T / \Delta t$ Eq5

$\Delta T = T_1 - T_2$ Eq6

$\Delta t = t_2 - t_1$ Eq7

$S = \Delta t / (t_1 - T_1)$ Eq8

$Q = m C_p \Delta T$ Eq9

$At = 3.412 d_0 L$ Eq10

$N_t = A_T / At$ Eq11

$Db = d_0 (N_t/K)^{1/n}$ Eq12

$Ds = Db + B_c$ Eq13

$Pt = 1.25 d_0$ Eq14

$h_i d_i = j_h Re Pr^{0.33} (\mu / \mu_w)^{0.14}$ Eq15

$1/U_0 = 1/h_t + 1/h_s + 1/f_i + 1/f_s + d_o \ln (d_o/d_i)$ Eq16

where,

N_t = total number of tubes
A_T = total cross sectional area
At = area for one tube
D_b = bundle diameter
d_0= outer tube diameter
B_C = bundle diametrical clearance
L = length of the tube
P_t = triangular pitch
Ds = inner shell diameter

METHODOLOGY

For this design, shell and tube will be considered due to its applicability to almost all processes (Sinnott, 2004). The steps in designing the heat exchanger are;

- Define the duty: heat-transfer rate, fluid flow-rates, and temperatures
- Collected together the fluid physical properties: density, viscosity, thermal conductivity
- Decide on the type of heat exchanger to be used
- Select a trail value for the overall coefficient, U
- Calculate the log mean temperature difference, ΔTm
- Calculate the area required
- Decide the exchanger layout
- Calculate the individual coefficients
- Calculate the overall coefficient and compare with the trail value
- Calculate the pressure drop
- Optimize the design: by repeating steps 4 to 10, as necessary, to determine the cheapest exchanger that will satisfy the duty. Usually this will be the one with the smallest area.

RESULT AND DISCUSSION

Acetaldehyde Reactor Heat Exchanger (HE-101)

The main function of this heat exchanger was to heat the ethanol fed to acetaldehyde reactor (RC-101) to the reaction temperature of 280 ^{0}C for the dehydrogenation reaction. The flow direction is countercurrent, with the cold fluid in the tube and hot fluid (steam) in the shell.

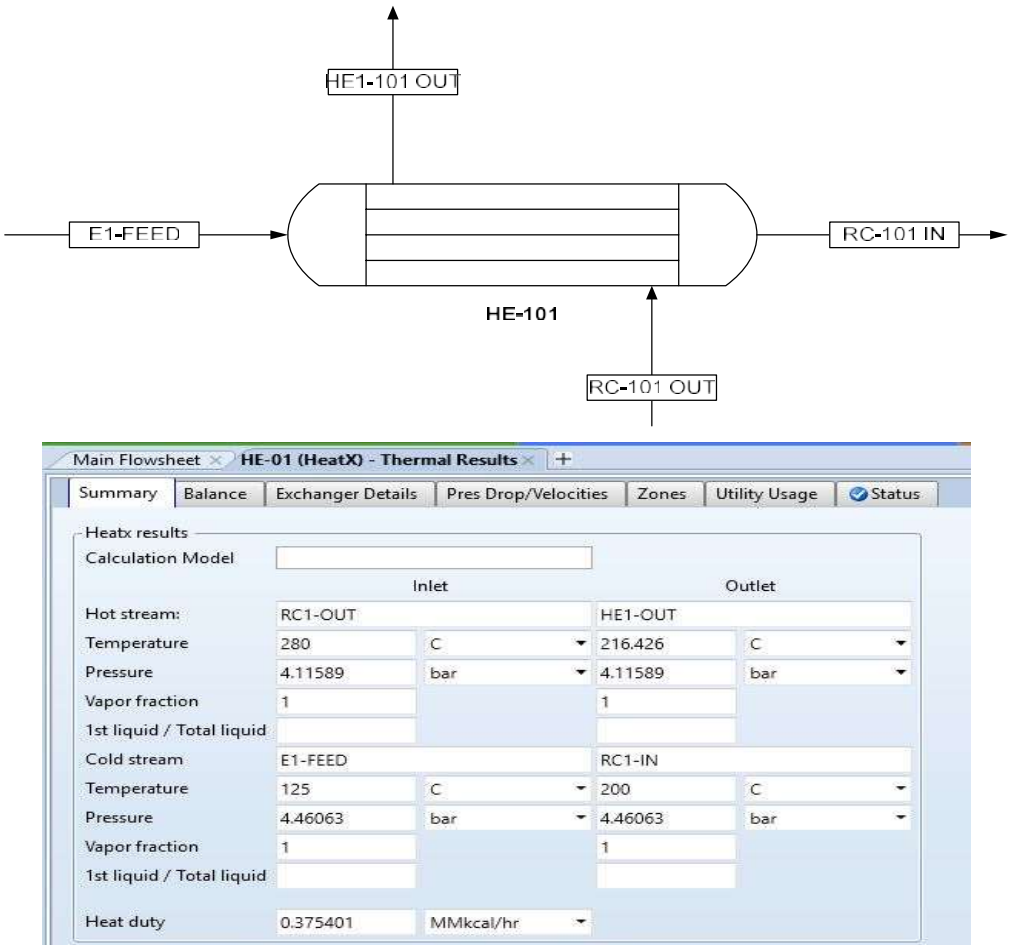


Figure 1: Heat exchanger configuration

LMTD = 85.705 ^{0}C, R = ΔT / Δt, ΔT = 75 ^{0}C, Δt = 64 ^{0}C, R = 1.17 and S = 0.7

Base on the value of R and S, the correction factor Ft is 0.88 (Sinnott, 2004). Therefore, LMTD corrected = 85.705 * 0.88 = 75.42 ^{0}C

Heat gain cold stream = heat loss by hot stream

$Q = m C_p \Delta T$ Eq17

m = 3.08 kg/s (from simulation)

Cp = 1.78 kJ/kg-K (from simulation)

ΔT = 200 – 125 = 75 ^{0}C

Q = 3.08 * 75 * 1.78 = 435.585 kW

Also,

Q = U A ΔT

A = Q / U*ΔT

U = 200 W/m^2 K (Sinnott, 2004)

ΔT = 75 ^{0}C

Therefore, A_T = 435.585 * 1000 / (200 * 75) = 33.43 m^2

Area of one tube (At) = 3.412 d_0 L

The outer diameter, inner diameter and tube length are 20 mm, 16 mm and 4.88 m respectively (Sinnott, 2004)

At = 3.142 * 0.02 * 4.88 = 0.307 m^2

$N_t = A_T/At$ = 33 / 0.3833 = 108

$Db = d_0 (N_t/K)^{1/n}$

The constants K and n are obtain base on the number of tubes passes. For the basis of the design K and n are 0.249 and 2.207 respectively.

$Db = 0.025 (108/0.249)^{1/2.207}$ = 327 mm

The bundle diametrical clearance (B_C) = 55 mm (from appendix)

Ds = Db + B_c = 327 + 55 = 383 mm

Pt = 1.25 d_0 = 1.25 * 20 = 25 mm

Shell-Side Coefficient

Mean cold steam temperature = 280 + 216 / 2 = 248 ^{0}C

Tube cross-sectional area = 3.142 * 16^2 / 4 = 201 mm^2

Tube per pass = 108 / 2 = 54

Total flow area = 54 * 210 * E-06 = 0.011 m^2

Steam flow rate = 2.002 kg/s (from simulation)

Steam mass velocity = 2.002 / 0.011 = 200 kg/s m^2

Density of water = 995 kg/m^3 (Sinnnott, 2004)

Water linear velocity = 200 / 995 = 0.2 m/s

The coefficient can also be calculated using the equation below;

$h_s d_i = j_h$ Re Pr $^{0.33}$ $(\mu / \mu_w)^{0.14}$

Viscosity of steam = 0.0001322 Ns/m^2 (Sinnott, 2004)

Thermal conductivity = 0.17 W/m^2-C

Reynolds number (Re) = density * inner diameter * linear velocity / viscosity Eq18
= 995 * 0.2 * 0.016 / 0.000132 = 24003.333
The baffle cut and frictional factor (j_h) are 0.1 and 0.0025 respectively (from appendix)
The prandle number (Pr) = heat capacity * viscosity / thermal conductivity Eq19
= 4200 * 0.0008 / 0.19 = 5.7
Neglecting $(\mu / \mu_w)^{0.14}$, assuming the viscosity of the main stream and water are almost equal
$L/d_i = 4.83 / 0.016 = 302$
From appendix $j_h = 0.00039$, $h_s = 0.17 * 0.00039 * 24003.33 * 5.7^{0.33} / 0.016 = 175$ W/m^2- K

Tube-Side Coefficient
Choose baffle spacing = Ds/5 =383 /2 = 191.5 mm, Tube pitch (Pt) = 1.25 * 20 = 25 mm
Cross-flow area A_s = (Pt – di) * Ds * baffle spacing / Pt Eq20
= (25 – 20) * 383 * 191.5 *E-06 / 25 = 0.015 m^2
Mass velocity, Gs = 3.08 / 0.015 = 205.333 kg/s m^2
Equipment diameter, de = 1.1 * (Pt^2- 0.917 * d_o^2) / d_o Eq21
=1.1 * (25^2- 0.917 * 20^2) / 20 = 14.4mm
Mean tube side temperature = (125 + 200) /2 = 162.5 ^{0}C
Viscosity = 0.00034 Ns/m^2 (from simulation),
Heat capacity = 1.78 kJ/kg-K (from simulation)
Thermal conductivity = 0.26 (from simulation)
Re = Gs * de / μ Eq22
= 205.333 * 0.00144 / 0.00034 = 265,721.18
Pr = Cp * μ / k_f Eq23
= 1780 * 0.00034 / 0.26 = 2.33
Using 10 % baffle cut, j_h = 0.0025 (Sinnott, 2004), solving without the viscosity term
$H_t = 0.26 * 0.0025 * 265721.18 * 2.33^{0.33} / 0.0144$
= 184.32 W/m^2- K

Overall Coefficient
Thermal conductivity of cupronickel alloys = 45 W/m^2- K (Sinnott, 2004), taking the fouling factor for the tube and shell side to be 5000 and 3000 W/m^2- K respectively (Sinnott, 2004)
$1/U_0 = 1/h_i + 1/h_s + 1/f_i + 1/f_s + d_o$ In (d_o/d_i) = 1/175 + 1/184.32 + 1/5000 + 1/3000 = 0.0056
U_0 = 1/ 0.0056 = 180 W/m^2- K
The overall heat transfer coefficient obtained was 10% lower than the initial guess of 200 W/m^2- K, which falls within the acceptable limit of 5-10% (Sinnott, 2004). The same procedures was also applied in the designing the other three heat exchangers.

Table 1: Heat exchanger design results summary

Parameters	**HE-01**	**HE-02**	**HE-03**	**HE-04**
Heat Duty, (kW)	436.59	1629	1471.1	2711.8
ΔT_m corrected, (^{0}C)	75.418	80.698	62.668	50.187
Assumed Uo, W/m^2- K	200	300	500	300
Provisional Area, (m^2)	29.945	67.288	78.25	180.11
Actual length, (m)	4.83	4.83	4.83	4.83
Inner tube diameter, mm	16	16	16	16
Outer tube diameter, mm	20	20	20	20
Area of one tube, (m^2)	0.307	0.307	0.307	0.307
Number of tubes	119	215	163	779
Bundle diametrical clearance (Bc) mm	55	56	53	70
Shell Diameter Ds, (mm)	382	483	430	850
Tube Crossectional Area, (mm^2)	314.16	314.16	314.16	314.16
Tubes per pass	96	107	81.5	425
Total flow area, (m^2)	0.0302	0.038	0.0256	0.134
Choose Baffle Spacing, (mm)	76.4	96.6	86	170
Tube pitch, (mm)	25	25	25	25
Final Uo , W/m^2- K	183	352	570	338
Required exchanger area, m^2	33.096	62.3242	45.8366	229.892
Actual exchanger area, m^2	36.1139	65.248	49.979	236.41
Percent over design, %	9.1174	4.6908	9.0372	2.8349
Total pressure drop, bar	0.152	1.604	0.067	0.06
Outer nozzle tube diameter, m	0.15	0.15	0.15	0.1
Outer shell tube diameter, m	0.3	0.3	0.3	0.2

LEGEND
HE-101------ Acetaldehyde Reactor Heat Exchanger
HE-102------ Butadiene Reactor Heat Exchanger
HE-103------ Butadiene Rectification Column Heat Exchanger
HE-104------ Preheater

Taking a look at the Table 1, HE-104 was doing more work (Q = 2,712 kW) compared with the other heat exchangers. This was due to the high temperature increase of 30 – 125 ^{0}C of the feed, as such more energy duty was needed to achieve the large temperature increase. The heat exchanger with the least duty was HE-101 (Q = 437 kW) as a result of the small temperature raise from 216-280 ^{0}C required for the Acetaldehyde reactor. The actual cost of heat exchanger depends on it required area size. The lowest area size was found to be HE-101 (33 m^2) which is because of it lower heat duty of 437 kW, since it was establish that the lower the area the less the energy consumption during the heat exchange. This followed the same trend regarding the number of tubes which is a function of exchanger area. The extends of heat exchanged from one stream to another was measure as the overall heat transfer coefficient. HE-101 has the lowest percentage deviation of the overall transfer coefficient from the assumed U_o values. These values are 8.5, 17.3, 14 and 12.7% for HE-101, HE-102, HE-103 and HE-104 respectively. The percentage over or under design indicate the differences between the actual and required area values. As can be seen, HE-104 has the lowest area difference; this was followed by HE-102 while the others have the same deviation from the required area value.

Conclusion

The heat exchangers were successfully design with the application of Aspen software simulation results, which provide most of the design parameters during the manual design. These parameters are; hot and cold stream mass flow rate of 3.08 and 2.0 kg/s, heat capacity, viscosity and thermal conductivity of 1.78 kJ/kg-K, 0.00034 Ns/m_2 and 0.26 W/m.K respectively. Other values such as provisional area, total pressure drop, percentage over (under) design, thermal effectiveness, number of transfer unit, maximum Reynolds number, shell and tube side maximum cross-flow velocity, actual tube and shell side baffle clearance which can't be easily calculate manually are obtained easily with the help of the Aspen process simulator.

References

Bhattacharyya S.K and Avasthi B.N (1963), "One-step Catalytic Conversion of Ethanol to Butadiene in a Fluidized Bed", *Industrial and Engineering Chemistry Process Design and Development*, Vol (1) 45-55.

Murray I. L, Marsh J. L and Smith S. P (1946), "Process for Marking Butadiene", U.S Patent 2,403,742, *Carbide and Carbon Chemicals Cooperation.*

Sinnott R. K (20054), Chemical Engieering Design, Vol. 6 fourth edition, *Butterworth-Heinemann.*

Toussaint W. J, Dunn J. T and Jackson D. R (1947), "Production of Butadiene from Alcohol", *Industrial and Engineering Chemistry*, Vol 39(2), 120-125.

DE-CHROMING CHROME TANNED TANNERY SOLID WASTE WITH *SACCHAROMYCES CEREVISIAE*

IMEH ETIM ONUKAK*[1, 2], NUHU M[1], ABDULLAHI S. MIKAILU [2], ISUWA K. ADAMU[3] AND ADEYI A. AMEH[2]

[1]Department of Chemical Engineering, Ahmadu Bello University, Zaria

[2] Directorates of Research and Development, Nigerian Institute of Leather and Science Technology, Abuja

[3] Directorate of Academics, Nigerian Institute of Leather and Science Technology, Zaria

***Correspondence:** Email: imykk224@gmail.com; Tel: +234-803-338-1081

ABSTRACT

Chrome tannage is the most widely adopted tanning process in the leather industry besides vegetable and alum tannage. The most commonly used chromium compound in tanneries is Basic Chromium Sulfate (BCS). Chromium (III) is initially trivalent but gets oxidized when left open to atmosphere to hexavalent chromium [Cr(VI)]. Cr (VI) is highly carcinogenic and causes damage to health and the environment. In this research, yeast recovered from raffia palm wine was used to treat tannery solid waste (chrome shavings and buffing dust). A buffer solution of Sodium dihydrogen orthophosphate ($NaH_2PO_4.12H_2O$) and disodium hydrogen orthophosphate ($Na_2HPO_4.12H_2O$) was prepared and used to wash the mixture of the waste and yeast followed by 0.2 % nitric acid at a pH value of 6.5. Both the substrate and filtrate were analyzed using Atomic Adsorption Spectra (AAS). The result from the analysis of chrome shaving filtrate and substrate showed 4589±5 mg/l of and 1861±16 mg/l Cr(III) compound respectively, while that of the buffing dust revealed 3641±4 mg/l and 1783±60 mg/l of Cr(III) both in the filtrate and substrate as well. The yeast, S. cerevisiae, in a non-viable state, is able to adsorb chrome and other metals from the chrome shavings and buffing dust of chrome tanned pilot tannery plant.

Keywords: *S. cerevisiae, heavy metals, chrome (Cr), bioremediation, buffing dust, chrome shavings, carcinogenic*

INTRODUCTION

Leather is the product obtained by tanning skins and hides by any one of several methods. By convention, the term 'hide' generally refers to the skin-covering of larger animals (cows, steers, horses, buffaloes, etc.), and the term 'skins', to those of smaller animals (calves, sheep, goats, pigs, etc.). The tanned skins and hides are used to produce a variety of finished goods such as shoes, bags, clothing, belts, furniture, stuffed animals, puffs, mats, wallets, footballs and a lot of accessories.

More than 70 % operating tanneries adopt chrome tanning process while the remaining tanneries adopt vegetable tanning process (UNIDO, 2004). Apart from these two, a few of these industries uses alum tanning. Associated solid waste liberated from the leather tanning process contains less chromium but much more aluminum. According to Hazardous Waste (management and handling) Amendment Rule 2000, the sludge and other waste (chrome shavings, buffing dust and trimmings) from tanning industry containing more than 50 mg/kg chromium(VI) and 5000 mg/kg chromium(III) compounds are considered as hazardous waste.

The most commonly used chromium compound in tanneries is Basic Chromium Sulfate (BCS). Chromium sulfate is initially trivalent but gets oxidized if left open to atmosphere to hexavalent chromium [Cr(VI)]. All forms of chromium are influenced greatly by pH, which affects the solubility and subsequent reactivity of chromium ions. Trivalent chromium is chemically basic and insoluble while hexavalent chromium is acidic and soluble. Chromium as heavy metal has no adverse effect. The trivalent form of chromium [Cr(III)] is considered as essential for normal carbohydrates, lipids and protein metabolism (NRC, 1980). Little toxic effect is attributed to trivalent chromium when present in large concentrations compared to the hexavalent chromium (Venkatathri and Alabdraba, 2014). Cr(VI) is highly toxic with a large aqueous solubility (Langard, 1982). Indeed, aqueous Cr(VI) is highly carcinogenic and causes damage to skin, mucous membrane and respiratory tract. It could also lead to infant mutation causing genetoxic effects such as chromosomal aberrations and sister chromatid exchanges (WHO, 2003).

Chrome can be recovered from these wastes and be reused in tanning using standard qualitative and quantitative methods as described by various authors. In this report, the method proposed by Brady and Duncan (1994) was adopted but modified. They used yeast from the brewery but the yeast employed in this report was recovered from local palm wine.

METHODOLOGY

The methodology was categorized into four stages; sample collection, sample pre-treatment, yeast recovery and de-chroming of tannery solid waste.

Sample Collection

Chrome Shavings and buffing dust from chrome leather tanning process were collected from NILEST mini tannery used for student practical. In all, 60 g of the waste were collected for the research. 25 litres of raffia palm wine was gotten from a retailer in Hayan Dogo, Samaru, Zaria.

Sample Pre-treatment

Sample pre-treatment involved, sorting of the sample to remove impurities such as pieces of wood, bone, metal and any other unwanted material, drying at 105 °C in Gallenkamp Oven (model no. OV-010 (9A-122-B9) Leicestershire, UK) to reduce the moisture content (up to 90 % dryness).

Recovery of yeast from palm wine

The yeast was recovered by centrifuging 5 ml of fresh palm wine in sterile centrifuge bottles (Hettich Universal Centrifuge, Model no. 32R, Germany) Centrifuge at 50 rpm for 5 minutes. 1ml of the sediment was inoculated by streaking on plates of glucose yeast agar (GYA) and incubated at 28 ^{0}C for 24 hours [Gallenkamp (illuminated Cooled Incubator) Model no. OC-4225J, UK]. Chloramphenicol was added to 0.005 mg/ml to discourage bacteria growth. The yeast colonies developed were isolated and purified by subsequently washing in ultra-pure water three times. Standard methods for yeast identification were employed (Barneth et al., 1990).

Preparation of Buffer Solution

3.12 g of Sodium dihydrogen orthophosphate ($NaH_2PO_4.12H_2O$) was dissolved in 100 cm^3 of distilled water to get 0.1 mole of $NaH_2PO_4.12H_2O$. 7.17 g of disodium hydrogen orthophosphate ($Na_2HPO_4.12H_2O$) was also dissolved in 100 cm^3 of distilled water to get 0.1 mole of $Na_2HPO_4.12H_2O$. 36.7 cm^3 of $NaH_2PO_4.2H_2O$ was added to 13.2 cm^3 of $Na_2HPO_4.12H_2O$ to get a pH of 6.5.

De-chroming of the Waste Sample

250 ml of distilled water was added to 2 g of the recovered yeast and 5 g of the pre-treated sample in an Erlenmyer flask and suspended in a shaker (Stuart Flask Shaker Model no. 420, UK,) at 110 rpm for 1hr. 50 ml of the mixture was withdrawn using a 10 ml syringe and transferred to a filtration apparatus (Edwards High Vacuum pump Model no. E2M2, West Sussex, UK) using a 25 mm diameter membrane filter paper. The substrate was then washed twice in a 5ml buffer solution (pH 6.5) of sodium dihydrogen orthophosphate and disodium hydrogen orthophosphate. 0.2 ml of 20 % nitric acid was used to wash the substrate. The substrate in a glass centrifuge test tube was placed in a water bath for an hour after adding 4 ml of distilled water, In order to release any metal ions associated to cells. The biomass substrate obtained was finally washed in 20 ml distilled water and dried overnight at 70 ^{0}C in an oven (Brady and Duncan, 1994). Analyses of both the raw samples, filtrates and the substrates were performed by flame atomic absorption spectra (AAS) for metal content (Brady and Duncan, 1994).

RESULT AND DISCUSSION

The result from the analysis of chrome shavings filtrate and substrate showed 4589$\pm$5 mg/l of Cr(III) compound in the filtrate and 1861$\pm$16 mg/l in the substrate. The result for buffing dust analysis revealed that the 3641$\pm$4 mg/l of Cr(III) compound has been reduced to 1783$\pm$60 mg/l as evident in the concentration of the Cr^{3+} in the filtrate and substrate respectively. A total chromium value, greater than 3 g/kg and below 5 g/kg, render these waste as non inert and non-hazardous according to Portuguese law (Decreto-Lei, 2002). Table 1 shows the AAS analysis result for the raw and treated chrome shaving and buffing dust.

According to Gadd and Griffiths (1978), a wide range of organisms has the ability to grow in the presence of high metal concentrations and may be the result of intrinsic or induced features, including specific mechanism(s) of resistance and/or environmental factors that may reduce or eliminate toxicity, for example pH, inorganic anions, cations, particulate and soluble organic matter, clay minerals and salinity.

Further investigations demonstrated that yeasts are capable of accumulating other cations such as copper, iron, Zinc and manganese are superior metal accumulators compared to certain bacteria (Norris *et al*., 1979). The fact that waste brewery's yeast can accumulate heavy metals has been proven with great success by a number of researchers (Gadd and White, 1993; Brady et al., 1994; Brady and Duncan, 1994; Tobin et al., 1990; Volesky and Holan, 1995; Wilhelmi and Duncan, 1995; Unz and Shuttleworth, 1996; Riordan et al., 1997; Bakkaloglu et al., 1998). This is also feasible for raffia palm wine base on the result shown in Table 1.

Table 1: AAS Result for the raw and treated tannery waste samples

Elements	Concentration, mg/l					
	CS	BD	CSF	CSS	BDF	BDS
Na_2^+	6562±7	3054±9	786±8	BD	23±10	BD
Mg^{2+}	BDL	BDL	103±2	BD	5±20	BD
Al_2^{3+}	2129±1	9612±9	121±8	BD	13±70	BD
K_2^+	BDL	BDL	28±80	6±36	3±20	511±10
Ca^{2+}	31440+21	650±26	286±6	29±8	4±30	373±10
Cr^{3+}	6647±8	5605±10	4589±5	1861±16	3641±4	1783±60
Mn_2^{3+}	BDL	58±10	226±8	5±10	20±90	553±10
Fe_2^{3+}	903+57	836±50	722±4	454±6	26±80	2378±60
Zn^{2+}	33+4	29±3	39±5	BD	0.2±10	23±10

NB: CSF and BDF are filtrate of Chrome Shavings and Buffing Dust respectively while CSS and BDS are their substrate.

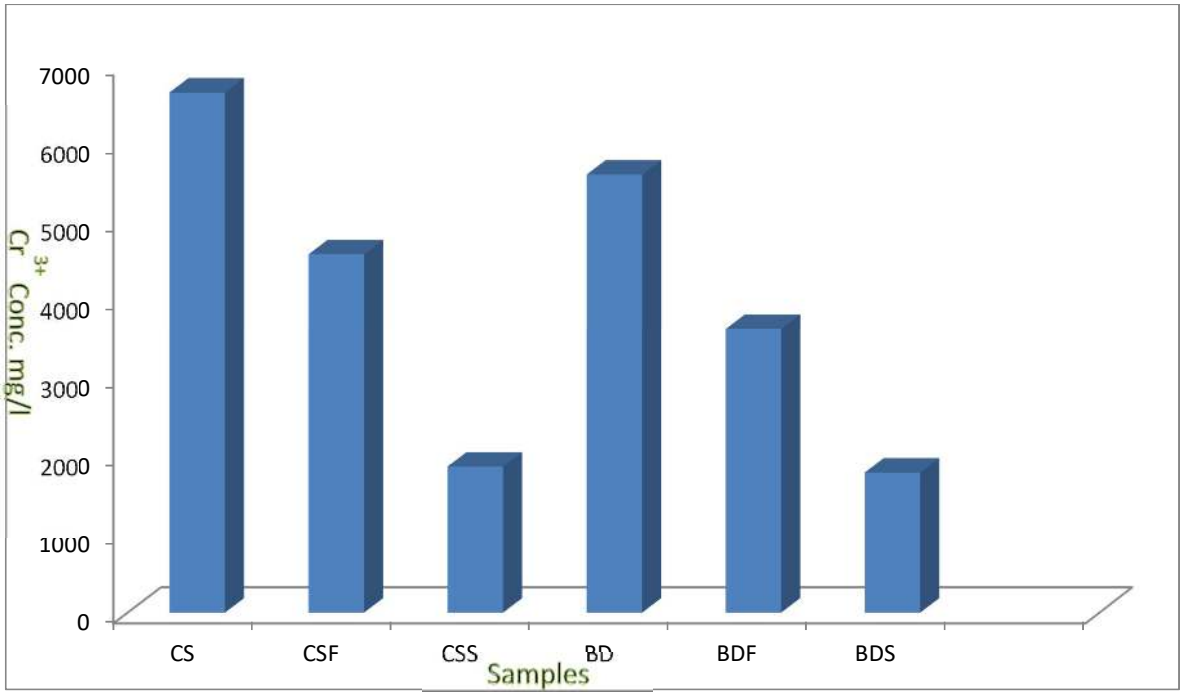


Figure 1: Bar chart for the adsorption of chrome from CS and BD samples

Looking at Figure 1, a total percentage removal of 28% Cr^3 from the chrome shavings (CS) and 32% removal was observed from the chrome shavings (CS) and buffing dust (BD) samples respectively. The yeast biomass was able to adsorb Cr^{3+} from the tannery waste generated.

CONCLUSION

The yeast Saccharomyces Cerevisiae (S. cerevisiae) was a good source for bioremediation of chromium in chrome shavings and buffing dust. The concentration of yeast and acid needs to be increased proportionally in the treatment of chrome shavings having more content of Cr^{3+}. Adsorption of chrome in buffing dust is 4% higher than that of chrome shavings. This study indicates the application of raffia palm wine yeast for biosorption of chrome from buffing dust and chrome shavings tannery waste generated.

REFERENCES

Bakkaloglu I, Butter TJ, Evison LM, Holland FS, Hancock IC (1998). "Screening of various types of biomass for removal and recovery of heavy metals (Zn, Cu, Ni) by biosorption, sedimentation and desorption". In IAWQ 19th Biennial International Conference: Vancouver, Canada.

Brady D, Duncan JR (1994). "Bioaccumulation of metal cations by *Saccharomyces cerevisiae",* Appl. Microbiol. Biotechnol. 41: 149-154.

Brady D, Stoll AD, Starke L, Duncan JR (1994). "Chemical and Enzymatical Extraction of Heavy Metal Binding Polymers from Isolated Cell Walls of *Saccharomyces cervisiae",* John Wiley & Sons, Inc., *Biotechnol. Bioengin.* 44: 297-302.

Brady D, Stoll A, Duncan JR (1994). "Biosorption of heavy metal cations by non-viable yeast biomass". *Environ. Biotechnol*. 15: 429-438.

Basu, D., Blackburn K., Harris B., Neal M., Stoss F. (1983). "HEALTH ASSESSMENT DOCUMENT FOR CHROMIUM. FINAL REPORT". *U.S. Environmental Protection Agency*, Washington, D.C., EPA/600/8-83/014F.

Decreto-Lei n.° 152/2002, Diário da República, (2002). (núm. 119), Série I- Ministério do Ambiente e do Ordenamento do Território.

Gadd GM, White C (1993). "Microbial treatment of metal pollution – a working biotechnology" *TIBTECH* .11: p. 353.

Langard S. 1982. "Biological and Environmental Aspect of Chromium". 1st Ed, *Elsevier Biomedical Press*, Amsterdam, New York, pp: 285.

Norris PR, Kelly DP (1977). "Accumulation of cadmium and cobalt by *Saccharomyces cerevisiae". J. Gen. Microbiol.* 99: 317-324.

Norris PR, Kelly DP (1979). "Accumulation of metals by bacteria and yeasts". *Dev. Ind. Microbiol.* 20: 229-308.

NRC (1980). "Mineral Tolerance of Domestic Animals". *National Academic Press, National Research Council-Washington* DC.\ UNIDO (2004)." Improving Tannery Pollution Control in Kano, Nigeria". *United Nations Industrial Development Organization* (Technical Report), YA/NIR/03/440/11-54.

Riordan C, Bustard M, Putt R, McHale AP (1997). "Removal of uranium from solution using residual brewery yeast: combined biosorption and precipitation". *Biotechnol. Lett.* 19(4): 385-387, Chapman and Hall.

Tobin JM, Cooper DG, Neufeld RJ (1990). "Investigation of the mechanism of metal uptake by denatured *Rhizopus arrhizus* biomass". *Enzyme Microbial Technol*. 12: 591-595.

Unz RF, Shuttleworth KL (1996). "Microbial mobilization and immobilization of heavy metals". *Curr. Opin. Biotechnol*. 7: 307-310.

Volesky B, Holan ZR (1995). "Biosorption of heavy metals". *Biotechnol. Prog.* 11: 235-250.

Wilhelmi BS, Duncan JR (1995). "Metal recovery from *Saccharomyces cerevisiae* biosorption columns". Chapman and Hall. *Biotechnol. Lett*. 17(9): 1007-1012.

WHO (2003). "Chromium in Drinking-water". *Background document for development of World Health Organisation Guidelines for Drinking-water Quality* (1996). Geneva, WHO/SDE/WSH/03.04/04

OIL-WELL PLACEMENT FOR MAXIMUM PRODUCTION IN ALWYN-NORTH FIELD

IGBEN ENOHOR[1], GODWILL PEPRAH[1], BABA JIBRIL EL-YAKUBU[2], YAHAYA MUHAMMAD SANI[2], LAWRENCE EDOMWONYI-OTU[2]

[1]Department of Oil and Gas Engineering, All Nations University College, Koforidua, Ghana
[2]Department of Chemical Engineering, Ahmadu Bello University, Zaria, Kaduna.
Corresponding Author: enohorigben@gmail.com +2348125485634

ABSTRACT

There is increasing emphasis on the accuracy of reservoir modeling and well placement. This leads to optimized exploration and production cost, and enhances safety of lives and working equipment. Hence, reservoir engineers take great caution in modeling and proposing well locations before the commencement of drilling. Seismic surveys and analysis from nearby wells provide data for the development of a 3D reservoir geologic model using MATLAB®. The model shows pressure zones, structural traps and possible production well placement locations. In this work, nine (9) probabilistic well placement locations were determined using Stanford Geomodeling Software®. Eclipse100® reservoir simulator aided the simulation of the field oil efficiency, gas production rate, oil production rate, cumulative production rate, water cut and active drive mechanisms. The presence and the absence of an infinite aquifer were taken into consideration for each simulation. After a period of 3,300 days considering only a primary recovery mechanism, producer wells 3 and 4 proved more promising. They showed a cummulative oil production of 0.77 x 10^6 m^3 and 1.84 x 10^6 m^3, recovery factor of 19.3% and 8%, and solution gas and water as driving force, respectively. It is recommended, that in the absence of an aquifer the drilling should be in the region favourable for well 3, while in the presence of an aquifer, the well should be drilled in the region favourable for well 4.

Keywords*: Reservoir, Drilling, Geomodeling, Safety, Well placement, Simulation.*

INTRODUCTION

The demand for oil products over the years has placed huge effort on the search for oil. This resulted in development of technology to assess the certainty of hydrocarbons and lessen risk associated with recovery. In oil recovery, to avoid expense on drilling dry holes, the use of reservoir simulators has been very useful and promising. Reservoir simulation involves construction and operation of a mathematical model which mimics the behaviour of an actual reservoir with the objective of predicting future reservoir performance (Al-Yousef, 2013). The main purpose of simulation is to provide an information database that can help the oil companies to position and manage wells and well trajectories to maximize the oil and gas recovery (Lie, 2014). Moreover, many Governments of oil producing countries rely on money made from oil and their products. Hence, the reservoir model should be precise for subsequently calculating the oil-in-place, and determining an effective way of economic recovery. During the early stages of field development, well placement is very demanding because the available data is not sufficient to pin-point the exact locations suitable for economic recovery. It depends on reservoir and fluid properties, well, and surface equipment specifications, as well as economic parameters. Likewise, optimum reservoir performance is dependent on well locations. Therefore, determining the well locations requires the use of most reliable techniques to avoid excess drilling costs, and drilling impenetrable areas. This will alleviate the problems associated with placement of oil and gas wells in the initial stages of field development. Furthermore, the use of intuitive judgement alone in determining well locations is not appropriate. This is because aside the non-linear correlation, reservoir engineering and geological variables affecting reservoir performance are also time and process dependent. Hence, there is the need to run simulations for an objective well-placement location considering key production variables.

Development strategies and well placement may significantly depend on field geology, maturity of the depletion stage, technological factor, drive resources and other parameters. (Badru, 2003).Before strategies for the development and management of petroleum fields, it is better to know the life cycle of hydrocarbon field. Reservoir Management begins with exploration leading to discovery followed by appraisal of the reservoir, development of the field under primary and secondary means, IOR and EOR, and finally to abandonment (Akpan, 2012).Accordingly, this study aimed at determining the well placement location for optimum oil and gas production in

Alwyn-North Brent East reservoir from nine well. This was achieved by simulating the field oil, water, and gas production with and without an aquifer using Eclipse. Active drive mechanism in the reservoir facilitated the choice of well location with maximum oil and gas recovery efficiency. The study utilized Matlab Reservoir Simulation Toolbox (MRST) and Schlumberger Eclipse 100 simulator in modelling the reservoir, and simulating production scenarios respectively.

METHODOLOGY

STUDY AREA.

The Alwyn-North Field was discovered in 1974 in the South Eastern part of the East Shetland Basin in the UK North Sea. Its location relative to other fields is shown in Figure 1.0. The Alwyn field lays respectively 4 and 10 km south of Strathspey and Brent field, 7 km east of Ninian field, and 10 km north of Dunbar field. The water depth is around 130 m. The field is in the UKCS Block 3/9 and extends northward into the Block 3/4.

A dynamic flow simulation carried out on an oil field with MRST to determine the best location to drill a well on the field. Running sensitivities on two possible scenarios and predicting production for primary recovery. During primary recovery the natural energy of the reservoir is used to transport hydrocarbons towards and out of the production wells. The earliest possible determination of the drive mechanism is a primary goal in the early life of the reservoir, as its knowledge can greatly improve the management and recovery of reserves from the reservoir in its middle and later life (Glover, 2012). Figure 2 is a flow chart that shows the step by step process carried out in this study.

The reservoir in the field has an anticlinal structure, which is not symmetrical at both ends. In each assumption, 9 cases are simulated. The nine cases are the possible well locations on the field gotten from the SGeMS tool. This tool works based on kriging technique. In Figure 4, the SGeMS tool which works on Kriging principle shows the possible producer and injector wells. It gives a total of nine producer wells which in turn narrows down the large reservoir portion to nine possible locations. It shows the wells with no dynamic (pressure, temperature and saturation) or static (porosity and permeability) parameters description. The anticline nature of the reservoir also affects the position of the wells and it can be seen that most of the wells are positioned at top or flanks of the structure.

Table 1 shows data is used to simulate the model with the two cases with and without an aquifer. This data was acquired from a resource personnel in the department of oil and gas engineering, All nations university college, Ghana.

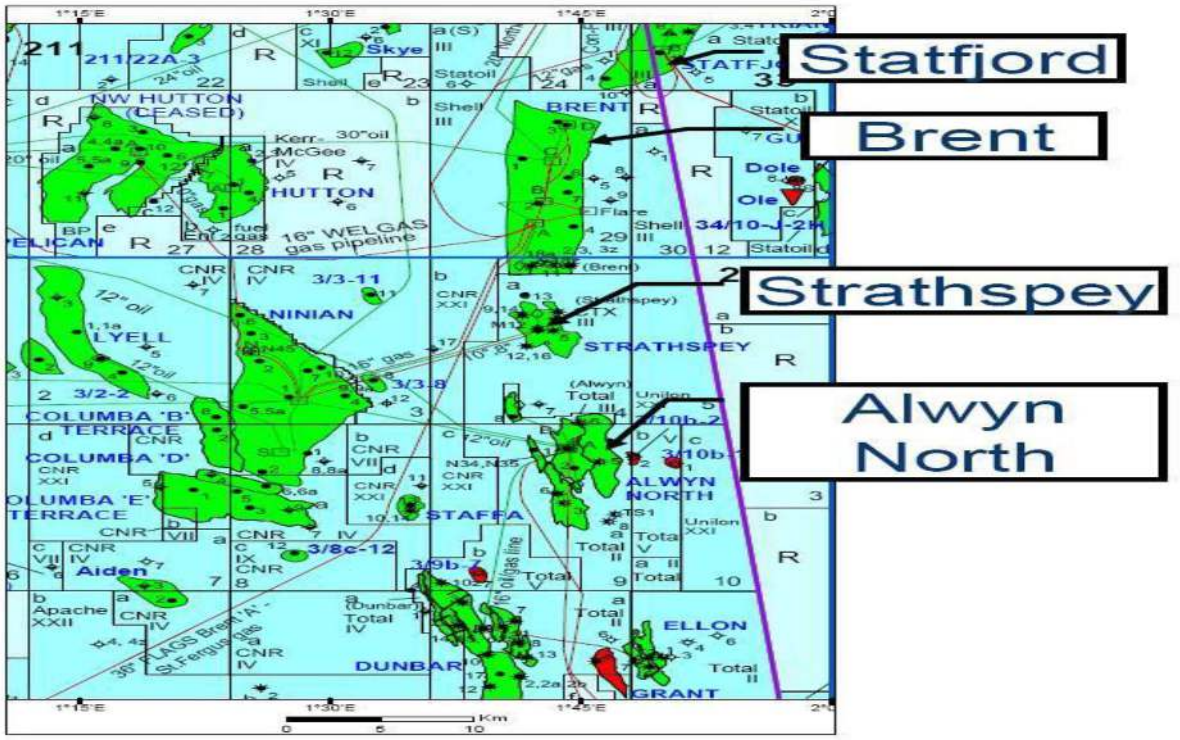


Figure 1: Alwyn North Oil Field (Nwosu, 2015)

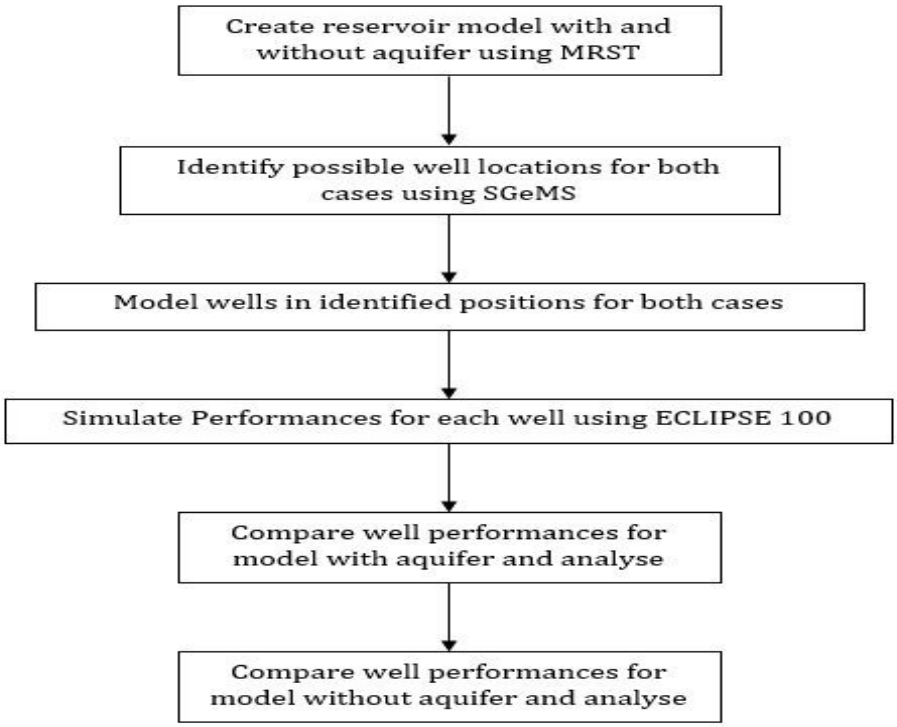


Figure 2: Flow chart indicating the step by step process carried out

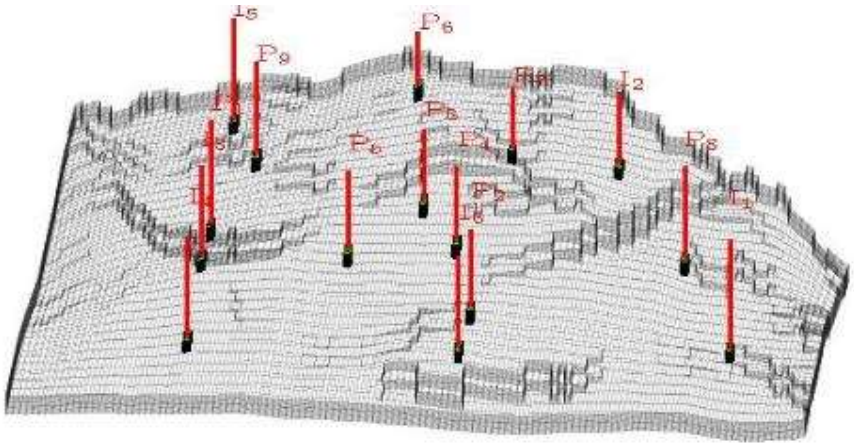


Figure 3: Possible Producer and Injector wells.

Table 1: **Alwyn-North reservoir data**

Parameters	Value	Units
Reference pressure	260	Bar
Water FVF at Pref	1.01	rm^3/sm^3
Water compressibility	4.4E-5	1/bar
Water viscosity at Pref	0.4	cP
Oil density	825.8	kg/sm^3
Water density	1025	kg/sm^3
Gas density	0.982	kg/sm^3
Oil relative permeability, k_{ro}	0.0265	Dimensionless
Oil formation volume factor, β_o	1.63	rb/stb
Oil viscosity, μ_o	0.27	cP
Average reservoir thickness	70	Ft
Total oil in place	2,493,078,669	MMStb
Solution oil-gas ratio, R_s	195.8	Sm^3/rm^3

Original Oil in Place Calculation: $N_p = \frac{7758*A*h*\emptyset*s_o}{\beta_o}$ …1

Oil Recovery Efficiency Calculation: $RE = \frac{\text{Initial oil in place} - \text{Residual oil}}{\text{Initial oil in place}} X\ 100\%$.....2

Where: RE = Recovery Efficiency

Table 2**: Live oil PVT table**

Solution gas ratio, Rs (scf/stb)	PSAT (psia)	Oil formation volume factor, Bo (stb/day)	Viscosity of oil (cP)
0	1.0	1.010	2.87
14.8	25.0	1.048	2.50
28.9	50.0	1.078	2.24
42.9	80.0	1.121	1.96
61.0	110.0	1.170	1.72
78.0	140.0	1.226	1.53
102.3	170.0	1.291	1.36
124.7	200.0	1.362	1.22
140.0	220.0	1.411	1.15
162.0	240.0	1.405	1.16
184.6	260.0	1.403	1.17
206.4	300.0	1.398	1.18
227.0	350.0	1.388	1.22

Table 3**: Dissolved gas PVT table**

PRES (psia)	BG (ft^3/scf)	Viscosity Of Gas (cP)
1.0	1.243	0.0121
25.0	0.0497	0.0131
50.0	0.0249	0.0136
80.0	0.0155	0.0145
110.0	0.0113	0.0158
140.0	0.0089	0.0172
170.0	0.0073	0.0189
200.0	0.0062	0.0207
220.0	0.0057	0.0220

Table 4**: Formation water PVT table**

PRES (psia)	BW (stb/rb)	Water Compressibilty (psi^{-1})	Viscosity of Water (cP)
260.0	1.0100	4.4E-5	0.4

Table 5**: Water-Oil relative permeability table**

Water saturation	Water relative permeabilty	Water-oil relative permeability	Water-oil capilary pressure, (psig)
0.22	0.0000	0.8000	0.600
0.25	0.0002	0.6835	0.390
0.30	0.0022	0.5143	0.210
0.35	0.0074	0.3742	0.124
0.40	0.0168	0.2609	0.079
0.45	0.0310	0.1721	0.053
0.50	0.0507	0.1052	0.037
0.55	0.0765	0.0576	0.027
0.60	0.1088	0.0265	0.020
0.65	0.1482	0.0089	0.015
0.70	0.1951	0.0014	0.0122
0.75	0.2500	0.0000	0.009
1.00	1.0000	0.0000	0.000

Table 6: **Gas-Oil relative permeability table**

Gas saturation	Gas relative permeability	Gas-oil relative permeability	Gas-oil capillary pressure, (psig)
0.00	0.0000	0.8000	0.000
0.05	0.0144	0.6722	0.000
0.1	0.0408	0.5556	0.001
0.15	0.0750	0.4500	0.002
0.20	0.155	0.3556	0.004
0.25	0.1614	0.2722	0.007
0.30	0.2121	0.2000	0.012
0.35	0.2673	1389	0.020
0.40	0.3266	0.0889	0.029
0.45	0.3897	0.0500	0.042
0.50	0.4564	0.0222	0.058
0.55	0.5266	0.0056	0.077
0.60	0.6000	0.000	0.100

RESULTS AND DISCUSSION

The reservoir initial pressure distribution measured in bars is shown in Figure 4. The numeric pressure values with the colour coding are represented with the vertical column above. The bluish to reddish regions indicates low to high pressure zones respectively.

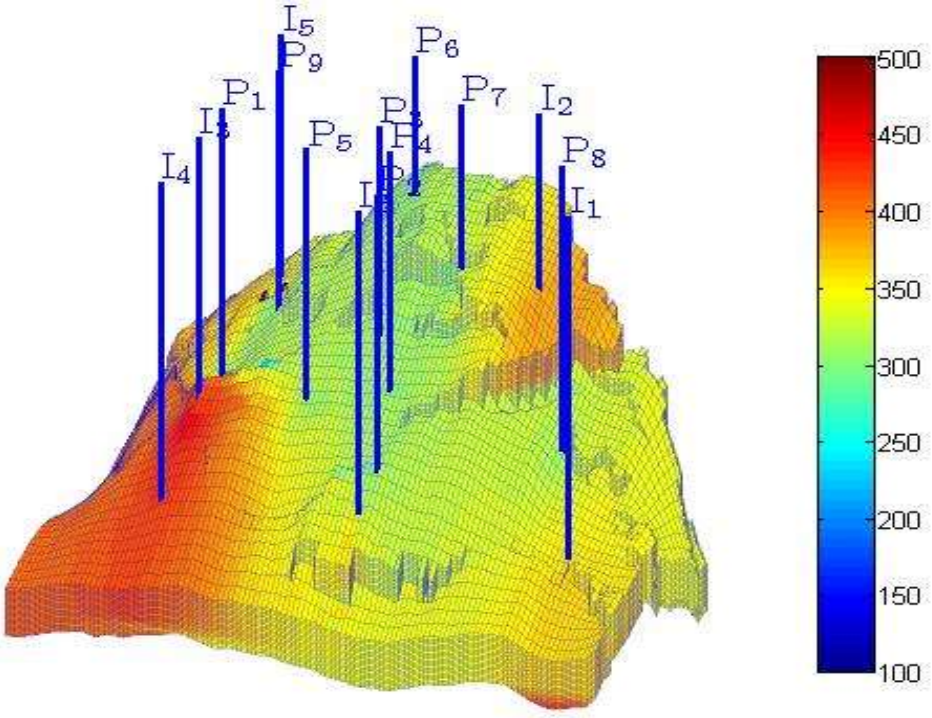


Figure 4: Geologic model showing initial pressure distribution measured in bar

Flow Simulation Results without Aquifer

An aquifer is an underground layer of permeable rock, sediment (usually sand or gravel), or soil that yields water. The pore spaces in aquifers are filled with water and are interconnected, so that water flows through them. In this case scenario, simulation is performed without including the presence of any aquifer. From Figure 5, the total oil reserve is 9,260,000 sm^3. Well 3 had the lowest residual oil volume of 8,500,000sm^3, followed by wells 2, 4, 8, 1, 7, 9, 5 and 6 respectively at the end of 3,300 days. Wells 3, 2, 4 and 8 were more promising than the others.

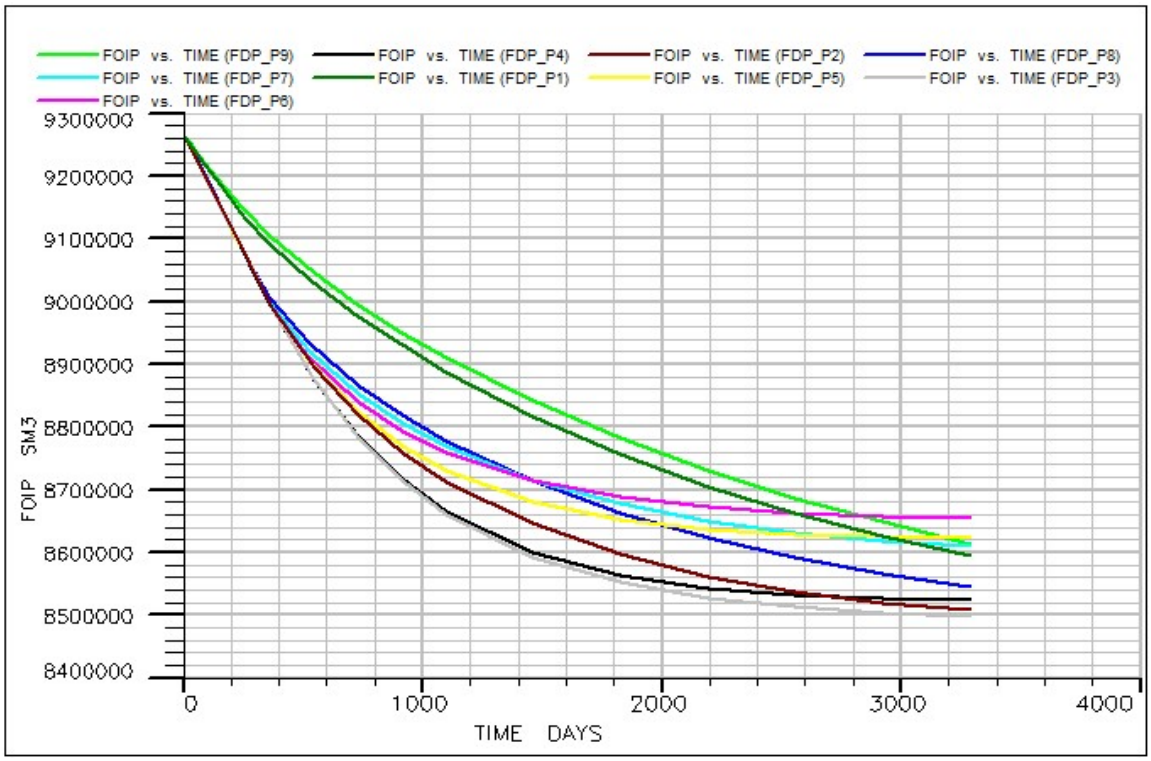


Figure 5: A plot showing field oil in place, before, during and after production

The results achieved in Figure 6 shows well 3 had the highest oil production total of about 770,000 sm^3. Followed by wells 2, 4 and 8, while well 6 had the lowest yield of about 610,000 sm^3. From the simulation, it is evident that the main drive mechanism is solution gas drive, since there is no aquifer and gas cap. The solution gas drive is due to the released of gas from the oil.

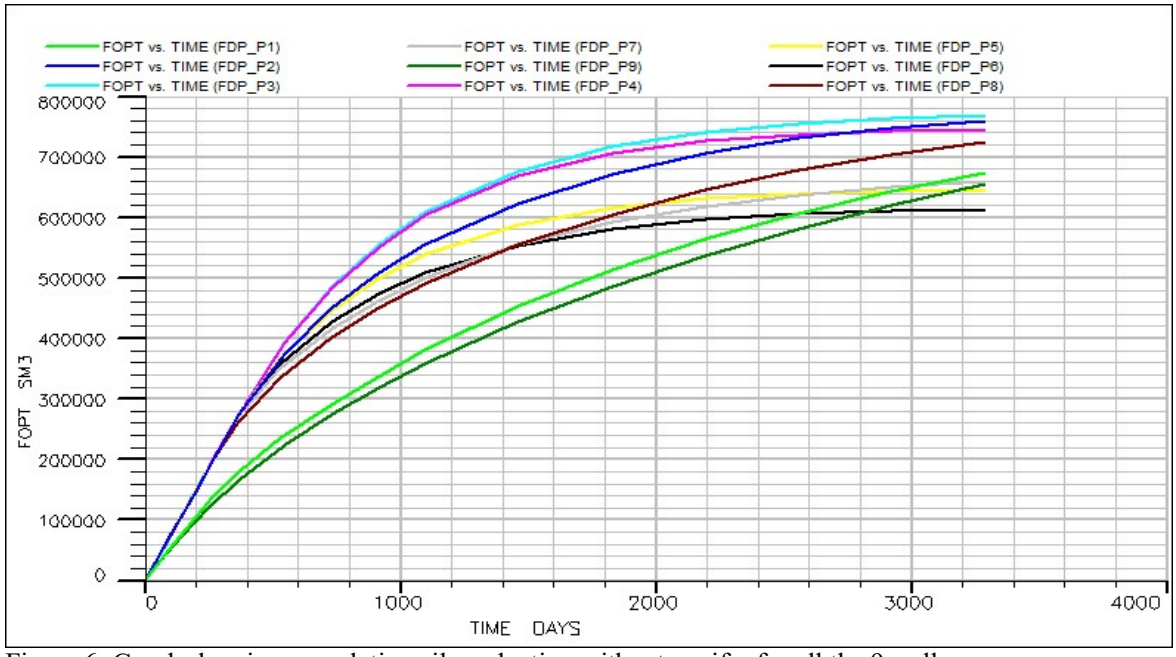


Figure 6: Graph showing cumulative oil production without aquifer for all the 9 wells.

From the Figure 7, the production of gas favours well 4, 3 and 5. This is as a result of the position of the wells in relation to the field geometry (anticlinal) and gravity contrast between the different fluids.

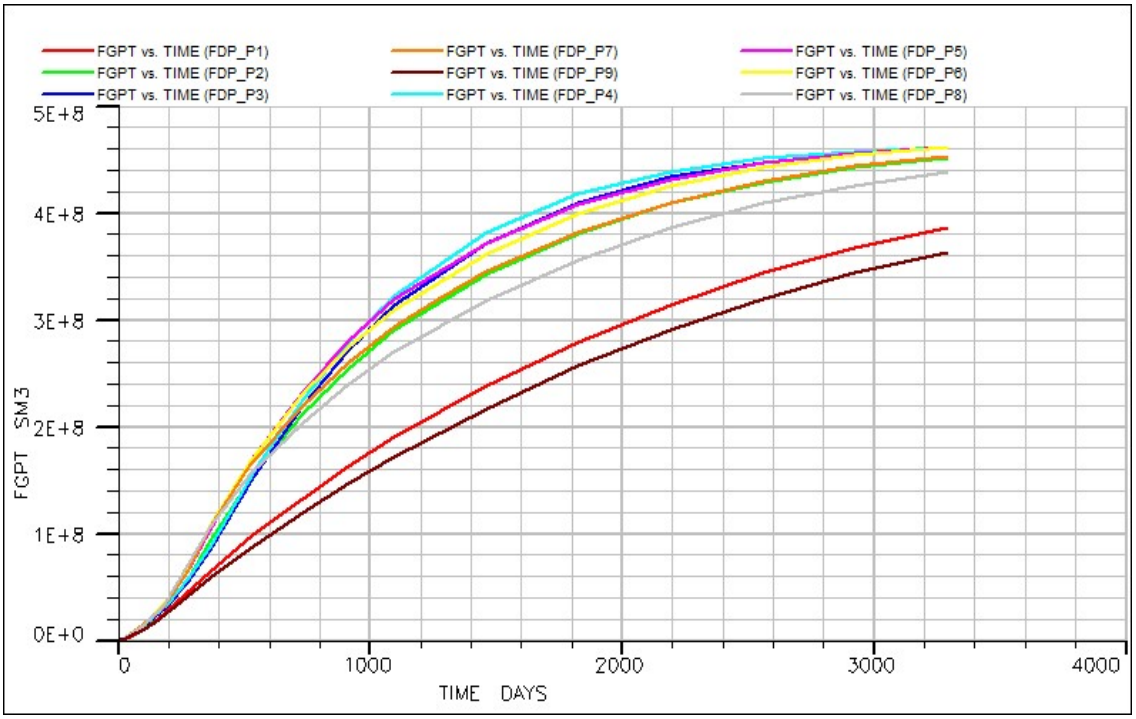


Figure 7: Graph showing cumulative gas production without aquifer for all the 9 wells

From figure 8, well 1 and 9 produce some amount of water even when the simulation is done without aquifer. This is due to the fact that these wells are located at the flank of the anticline, close to the oil water contact (OWC).

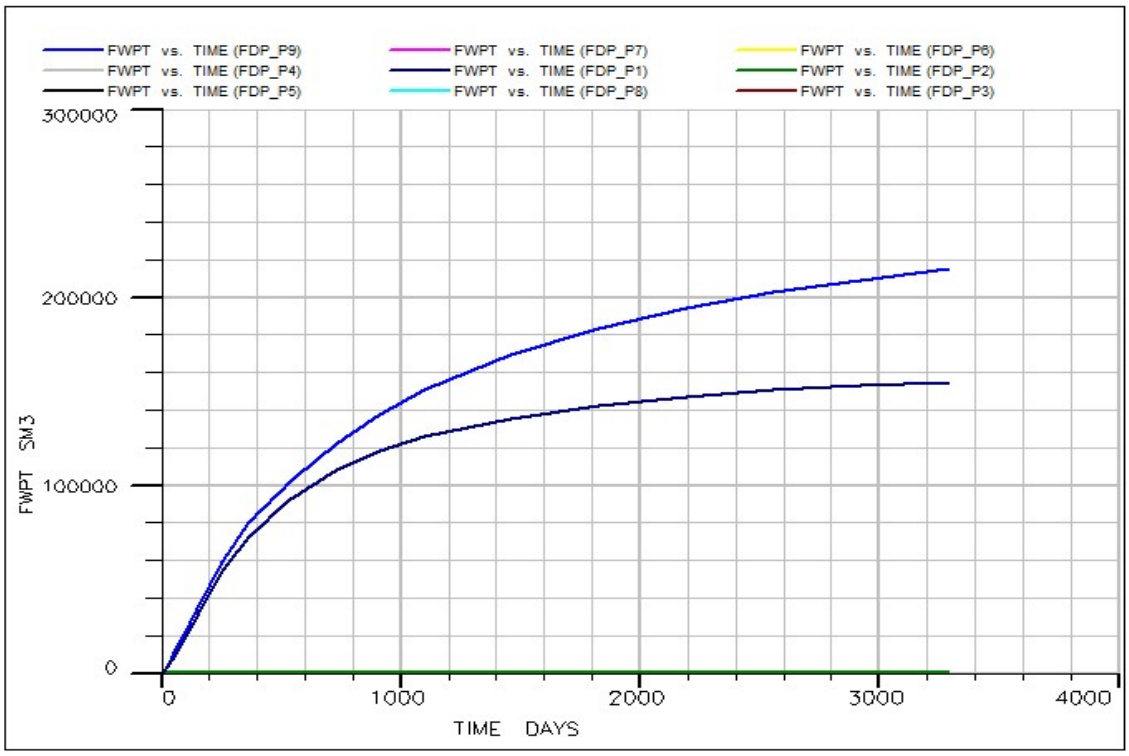


Figure 8: Graph showing cumulative water production without aquifer for all the 9 wells

Major Drive Mechanisms Analysis For Well 3 Without Aquifer

From the figure 9, the major drive mechanism without aquifer is fluid expansion (solution gas drive) as confirmed from the previous plot of FOTP versus time. It shows the four major primary drive mechanisms contributing to the production of oil in well 3.

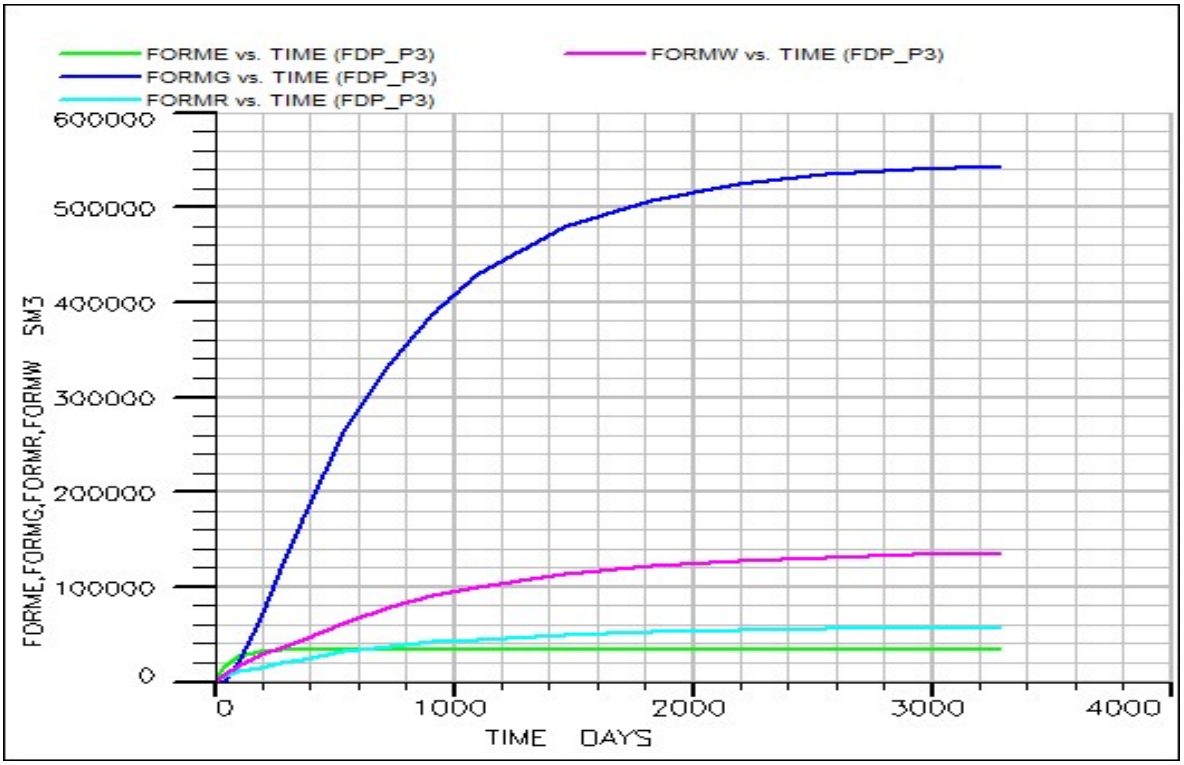


Figure 9: Graph showing the four major drive mechanisms contributing to the production of oil in well 3

Flow Simulation Results with Aquifer

Cumulative Oil Production per Wells with Aquifer

From the Figure 10, it is observed that with an aquifer, well 4 gives the highest oil production, followed by well 3, unlike the case without aquifer. From the simulation, it is evident that the main drive mechanism is water drive with a slight support from solution gas drive.

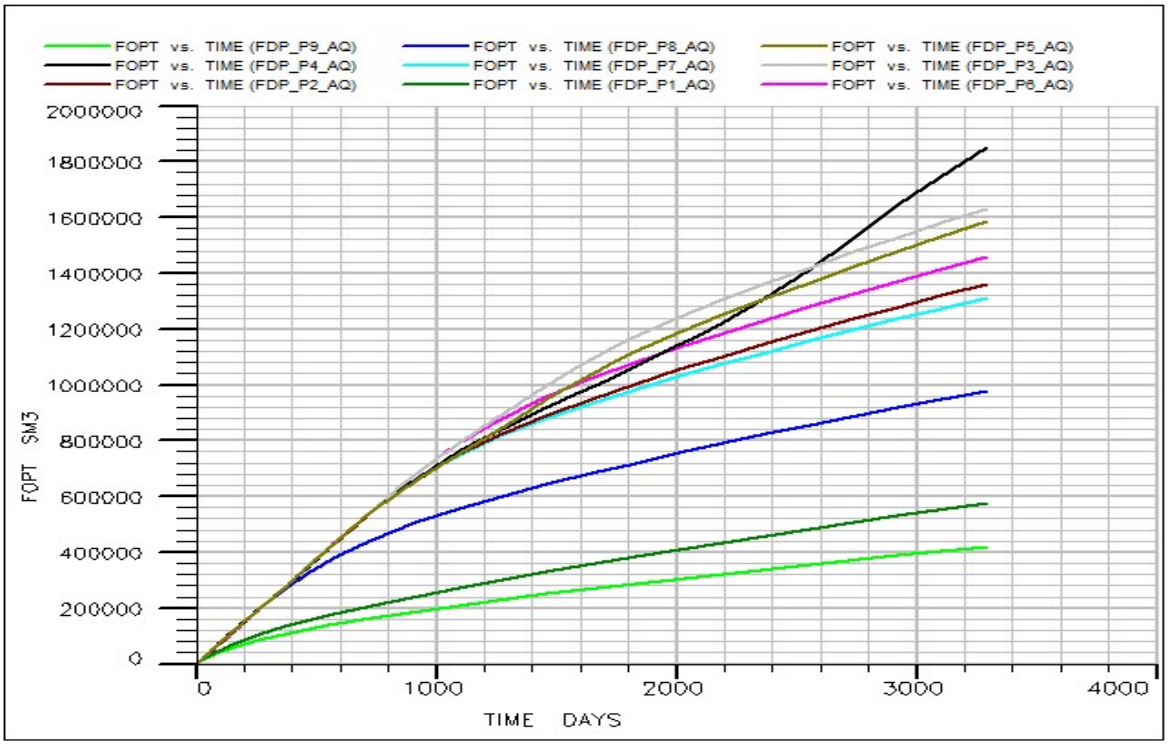


Figure 10: Plot cumulative oil production per wells with aquifer

From Figure 11, there is a decrease in the field oil in place after production commenced. This plot shows the field oil before, during and after production.

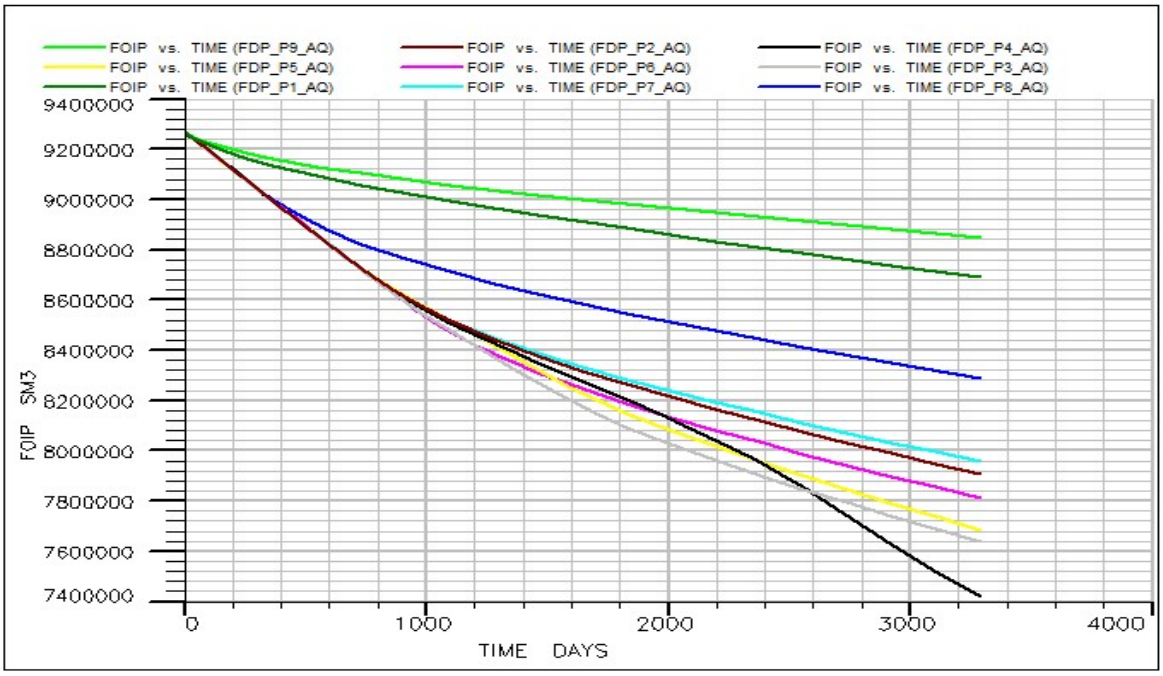


Figure 11: A plot showing field oil in place, before, during and after production

From Figure 12, the highest production of gas favours well 4, followed by 3 and 5. This is as a result of the position of the wells in relation to the field geometry (anticline) and gravity contrast between the different fluids.

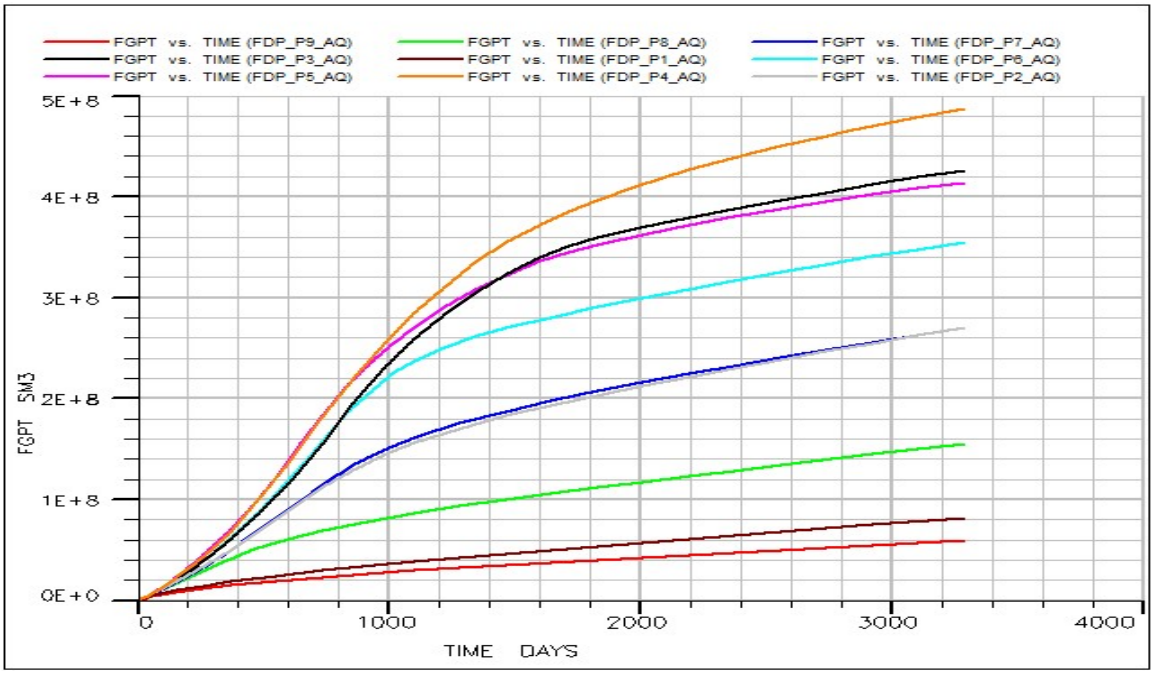


Figure 12: Plot showing gas production from the nine (9) wells

Water Production

From Figure 13, it is observed that all the wells are producing significant amount of water with the exception of well 4 due to its location in the field. Well 1 and 9 produce the highest since they are located at the flank of the anticline, close to the oil water contact (OWC).

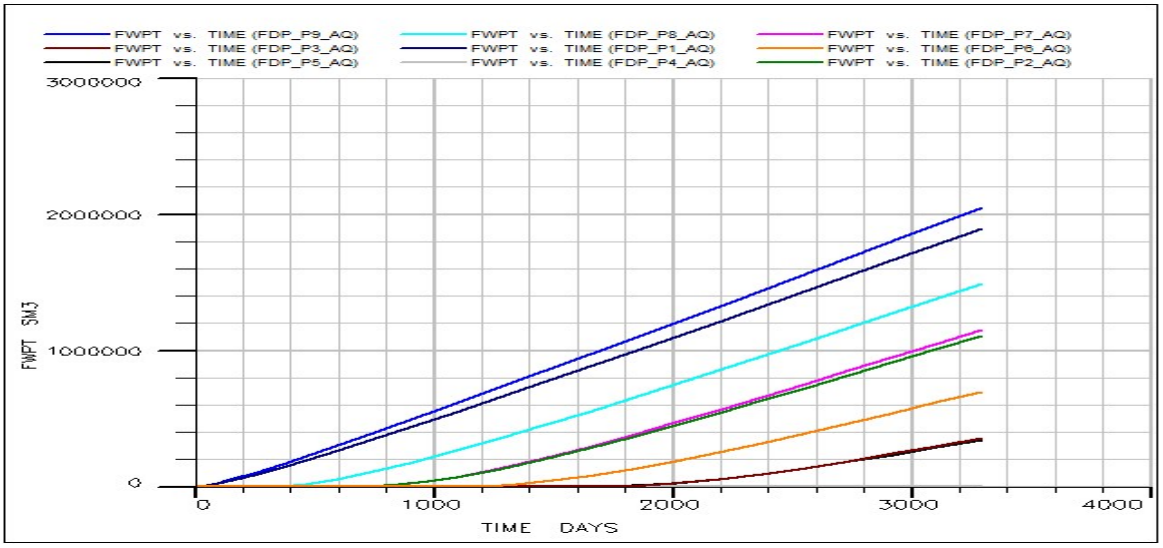
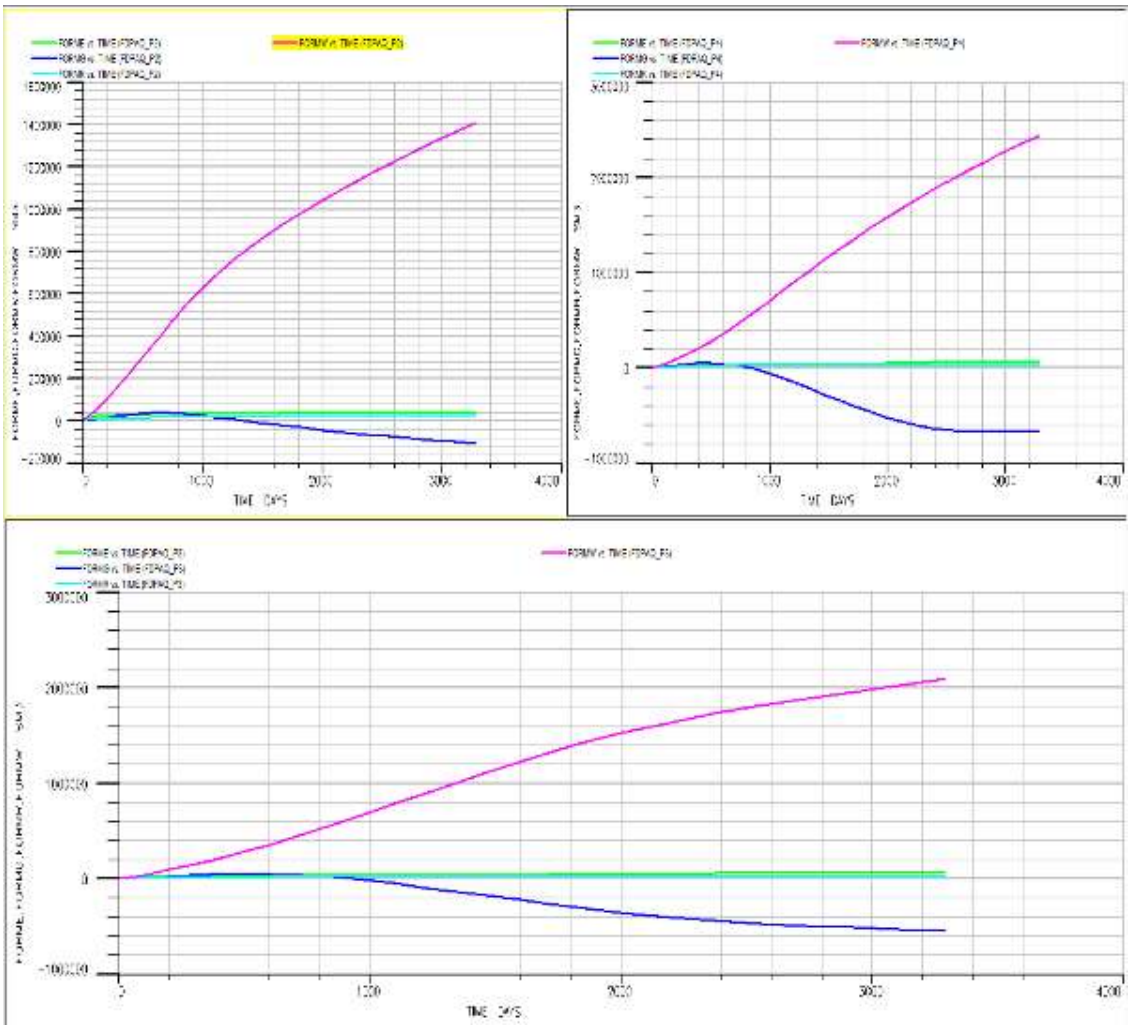


Figure 13: Plot showing water production from the nine (9) wells

Major Drive Mechanisms Analysis per Well With Aquifer for Well 2, 3 and 4

From Figure 14, the major drive mechanism is water drive, unlike in the case without aquifer where solution gas is the main drive mechanism.


Figure 14: Plot showing the major drive mechanisms per well with aquifer

Oil Recovery Analysis

Oil recovery analysis for well 3 (aquifer present) and well 4 (aquifer absent), shows the difference in oil recovery for both case scenarios. For the presence of an aquifer, well 4 had oil recovery efficiency of 19.3% and in the absence of an aquifer, well 3 had a low oil recovery efficiency of 8%.

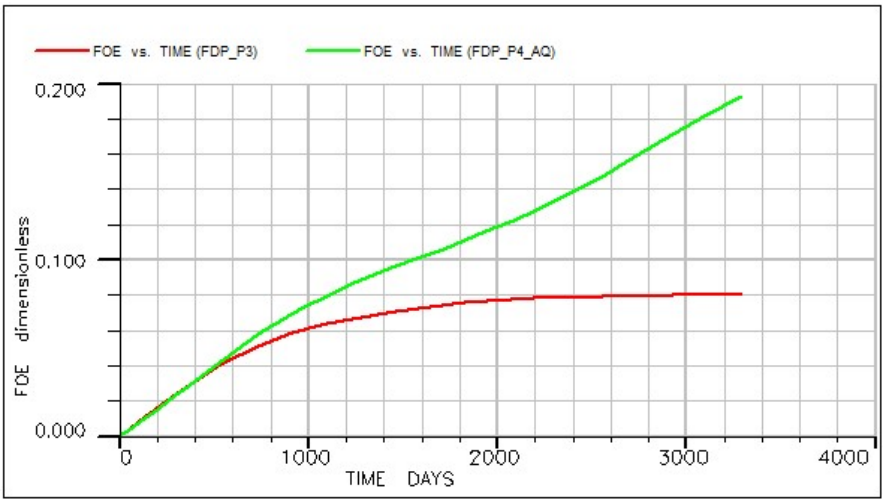


Figure 18: Oil recovery analysis per region for well 2, 3 and 4 without aquifer

The oil recovery analysis from the flow simulation indicates that well 4 and 3 had the highest oil recovery factor with and without an aquifer respectively. The best location for the major producers (3 and 4) is at the top of the anticline.

Conclusion

Analysis on the well placement location considering the presence and absence of aquifer showed that producer wells 3 and 4 were more promising with cummulative oil production of 0.77E6 sm^3 where solution gas was the active drive mechanism and 1.84E6 sm^3 in the case where water drive was the active drive force in the reservoir respectively at the end of the simulation peiod 3300 days. Water production was a significant factor taken into consideration in this work to ascertain the decision on the best well location. In the absence of an aquifer well 3 produced no water due to its location at the top of the anticline, above the oil-water contact (OWC). This was not the case for well 4 in the presence of an aquifer, which had a water production of about about 370,000 sm^3 water. This shows that in the absence of an aquifer, well 3 will produce at an optimum oil rate. Plausibly, the well should be drilled in the location, which is quite favourable for 3 with no aquifer and 4 in the case of an infinite aquifer with a recovery factor of 19.3% and 8% respectively.

NOMENCLATURE

FGOR - Field Gas Oil Ratio
FGPR - Field Gas Production Rate
FGPT Field Gas Production Total
FOE Field Oil Efficiency
FOPR Field Oil Production Rate
FWCT Field Water Cut
FWPR Field Water Production Rate
FORME Field Gas Cap Expansion Drive
FORMW Field Water Drive
FORMG Field Solution Gas Drive

References

Akpan, S. E. (2012). *'Well Placement for maximum production in the Norwegian Sea '*. Norwegian University of Science and Technology, Page 11, 17, 20.

Al-Yousef, D. H. Y. (2013). *'Purpose of Reservoir Simulation '*. Kwame Nkrumah University of Science and Technology, Kumasi, Page 4.

Lie, K. (2014). *'An Introduction to Reservoir Simulation Using MATLA '. User Guide for Matlab Reservoir Simulation Toolbox (MRST)*. SINTE.F ICT, Page 110-111.

Nwosu, U. D. (2015). *'Dynamic Reservoir Simulation of Alwyn field using Eclipse '*. Page 28, 33

DESIGN, FABRICATION AND PERFORMANCE EVALUATION OF KENAF MINI-SPINNING MACHINE

AKANG I.V., BARMINAS J.F., GADIMOH S., OTSAI O.J., OKECHUKWU T.U., AYUBA N.L. AND AL-KASIM U

[1] National Research Institute for Chemical Technology, Zaria

[2] Ahmadu Bello University, Zaria

ABSTRACT

Kenaf fibres generally has some advantages such as eco-friendly, biodegradability, renewable nature and lighter than synthetic fibres. The aim of the study is to design a mini-spinning machine evaluate the potentials of using weaved and un-weaved indigenous Kenaf fibres to produce yarn.In this paper, the strength parameters of Kenaf yarns formed on the mini-spinning machine using the open ended spinning method were analysed. For the open ended spinning, the prime mover is a 1.5hp electrical induction motor, with influence of linear density of the feeding sliver and of yarns on their specific strength, elongation and elasticity was evaluated. For the mini-spinning machine, the following parameters were used:

- *The speed of the rotary drum was determined with a tachometer to be 51.8rev/s. as designed*
- *The speed of the bobbin was also determined to be 11.9rev/s.*
- *The number of twist per cm was also determined to be 25 twist/cm.*
- *Production rate is 2.41cm/s.*
- *linear density of yarns: 18, 20, 25, 30 tex.*

The spinning machine was fed with slivers after the second passage of drawing with the linear densities: 3.5, 4.0, 4.5, 5.0 ktex. On the open end spinning machine, Kenaf yarns of linear densities of 25 and 40 tex were formed from the roving 400 tex. Analysis of the results for the mini-spinning open end spun yarns showed that open ended spun yarns are characterised by higher elasticity, which makes them a very good material for knitting purposes.

KEYWORD: Spinning machine, Kenaf, twisting, fibres, yarn, spinning drum.

INTRODUCTION

Kenaf (*Hibiscus cannabinus* L.) is a fibre plant native to east-central Africa where it has been grown for several thousand years for food and fibre. It is a common wild plant of tropical and subtropical Africa and Asia. It has been a source of textile fibre for such products as rope, twine, bagging and rugs. It is a promising source of raw material fibre for pulp, paper and other fibre products, and has been introduced since World War II in China, USSR, Thailand, South Africa, Egypt, Mexico and Cuba. It is a short-day annual herbaceous plant cultivated from the soft bast fibre in its stem. It grows quickly, rising to a height of 12-14 feet within a period as short as 4 to 5 months. It is considered a hardy plant that has a short life cycle, broad growth area, strong adaptability to environment, low cost of cultivated conditions and requires a minimum quantity of fertilizers and pesticides. It is extracted through retting process, which usually involves moisture with bacteria or chemicals, to remove the unwanted bark material from the fibre strands within the bark. However, power-driven decorticating machines are used. Although the natural water- retting process is still used throughout many parts of the world, newer chemical retting processes have been studied, developed, and implemented to produce fibre of greater chemical and physical uniformity (Charles et al, 1998). Kenaf and sisal fibres generally has some advantages such as eco-friendly, biodegradability, renewable nature and lighter than synthetic fibres, which is what has informed the choice of Kenaf.

Fibres are what fabrics are made of. Just look at the fabric of the dress you are wearing. It is made of the thread prepared from small fibres. A thread from a piece of fabric can be pulled out and opened up by untwisting. Small fibres can be seen. There are a large number of fibres available to us and from which a variety of fabrics are made. This is why in any cloth shop one can find such a variety of fabrics on the shelves of cloth shops in the market.

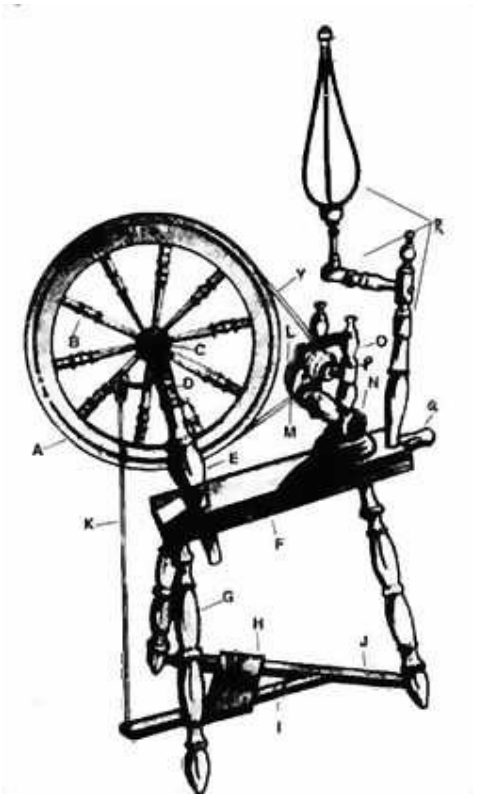
This paper presents the design of an effective mechanism which will convert kenaf yarns into a spun product. Staple fibre yarns can be produced from natural fibres as well as from chemical fibres cut to staple length. In contrast to the chemical fibres, which can be manufactured industrially in almost every desirable length and shape, the various natural fibres are available only in specific lengths, titers, and cross-sections, and with certain

crimp and stress–strain behaviour depending on their type and origin. The development of spinning processes was based on these characteristics. This is another reason that the properties of chemical fibers are often adjusted to those of natural fibres so that they can be mixed or blended and also processed on conventional spinning machines. The functions of the spinning machines are the preparation of the fibres for the actual spinning process, the organization of the fibers in a coherent, continuous structure, and the production of packages or units suitable for further processing. The basic principle of producing a yarn by organizing, parallelizing, drawing, and twisting of the fibers has not changed since the very beginning of spinning thousands of years ago.

Spinning of plant fibres locally in Nigeria has remained in its primitive stage using hand and stick methods and as such research in the area of conversion of fibre to yarn has remained a very difficult task. Similarly, the spinning industries are not ready to stop operation to allow for any research activity on their spinning machines due to down time effect on their business.

As for the earliest conventional spinning machine which was called the Jenny in Britain, it was invented by James Hargreaves in Lancashire in the mid 1760s. To understand what was involved in inventing the jenny, first consider the spinning wheel, which it replaced. The spinning wheel consisted of a vertical wheel, a spindle that was parallel to the axle of the wheel, and a string that acted as a belt so the turning wheel rotated the spindle. Sometimes a treadle was used to turn the wheel; otherwise, the spinner did it with her right hand. In either case, the spindle spun as the wheel turned, and the inertia of the wheel stabilized the speed. The saxony spinning wheel can be shown in the figure below. It is almost the same with the spinning wheel of earliest times.

The objective of this paper is to present the actualization of the spinning of kenaf yarn with a view to transforming the fibre to fabric. In the light of global technological transformation, the department of Textile Technology of the National Research Institute for Chemical Technology Zaria deems it fit to fabricate a spinning machine which is first of its kind in Africa.



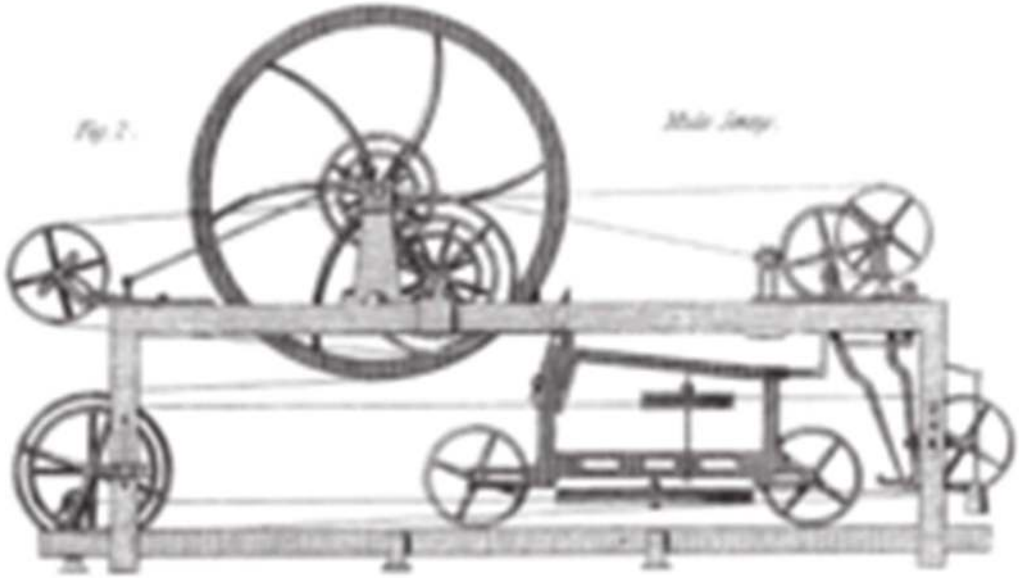
Saxony Spinning Wheel Diagram

A - Drive Wheel
B - Spoke
C - Wheel Hub
D - Crank and Wheel Axle
E - Wheel Support Arm
F - Table or Bench

G - Leg
H - Treadle
I & J - Treadle Bars or Rods
K - Footman
L - Flyer
M - Bobbin
N - Mother-Of-All (An assembly which consists of items L, M, O, P)
O - Maiden
P - Pulley
Q - Tension Knob
R - Distaff Parts

This diagram shows a saxony style treadle-operated spinning wheel, approximately 3' x 3'. These treadle wheels were also made in upright or castle style wheels, with the mother-of-all mounted above or below the drive wheel. Parts are essentially the same. Very large spinning wheels, of approximately 5' in height, with a similar configuration to a saxony wheel, are called walking wheels or great wheels, and sometimes wool wheels. They have no treadle, and instead of a flyer mechanism between two maidens, one would find a pointed metal spindle, approximately 10" in length, with a wooden pulley and disk affixed to it. The large walking wheel or great wheel is the wheel of **Sleeping Beauty** fame.
The spinning machine spins textile fibres into yarn by an intermittent process. The position of spinning is the open-end yarn. In the draw stroke, the lead fibre or roving is pulled through a rolling drum and twisted; on the return it is wrapped onto the spindle. Its rival, the throstle frame or ring frame uses a continuous process, where the roving is drawn, twisted and wrapped in one action. The mule was the most common spinning machine from 1790 until about 1900 and was still used for fine yarns until the early 1980s.

The first mule



An early spinning mule: showing the gearing in the headstock
Samuel Crompton invented the **spinning mule** or **mule jenny** in 1779, so called because it is a hybrid of Arkwright's water frame and James Hargreaves' spinning jenny in the same way that mule is the product of crossbreeding a female horse with a male donkey. The spinning mule has a fixed frame with a creel of bobbins to hold the roving, connected through the headstock to a parallel carriage with the spindles. On the outward motion, the rovings are paid out through attenuating rollers and twisted. On the return, the roving is clamped and the spindles reversed to take up the newly spun thread.
Presently, the short staple, also called cotton or three-roller spinning process, is the most common spinning method worldwide. The name three-roller spinning comes from the arrangement of the rollers in the drafting zone at the most commonly used spinning machine, the ring spinning frame. This spinning principle is suitable for all fibre types with lengths up to 40mm. It is very flexible with regard to the properties and applications of the produced yarns. Yarns manufactured by ring spinning are processed into wovens, hosiery, knits, and braidings in the areas of apparel, home textiles, and technical textiles.

Yarn properties are parameters to describe the yarn, such as
• Fineness or titer,
• Elongation,
• Hairiness,
• Tenacity,
• Twist, and
• Volume.

The current paper addresses the short comings and flaws of these older methods with a view to making a compact, efficient and simple spinning device. Twists given to fibre strands for formation of a yarn can be either **'S-twist'** (clockwise) or **'Z-twist'** (anticlockwise). The quality and strength of yarn is affected by the number of twists in inch. Lesser the number of twists per inch, bulkier and less strong is the yarn and more the number of twists, finer and stronger is the yarn. The spinning machine is a pre-textile production machine and as a processing machine, it consist of a group of elements arranged to perform some useful functions (spinning in our case). This machine consist of mechanisms. A mechanism is a group of elements arranged to produce a definite motion. A machine receives energy from some source from which to perform the function. This energy source is regarded as a prime mover.

MATERIALS AND METHODS
Materials used in the construction of the design include;

- 1/2' mild steel angle iron.
- 1' mild steel angle iron.
- Mild steel shaft.
- 3mm mild steel plate.
- 2mm galvanized steel plate.
- Three phase electric motor.
- Chain and sprocket drive.
- Transmission mechanism.
- Belt and pulley system.

Before establishing our methodology for fabricating the Kenaf mini-spinning machine, it is only proper to define certain terms as relates to our discuss. Parallelizing leads to an orientation of the fibres in one direction. Drawing is the drafting of an oriented fibre web in a drafting field. The purpose of drawing is to provide an optimally straightened, parallel, and uniform fibre orientation.

Processes prior to spinning
Both, the fibres as well as filaments are spun into yarns that are then used for different end uses. Fibres available in the filament form are first cut into short lengths and then made into yarns called spun yarns. Various steps followed for making yarns are :

i) Cleaning: When the natural fibres are harvested or collected, these contain dry leaves, stems, seeds, dirt and unwanted materials that are removed during cleaning.

ii) Carding: The fibres sometimes get matted and stick to each other. Carding opens and arranges the fibres in a parallel manner. The carded web of fibres is turned into a soft rope called **sliver**.

iii) Combing: It is an optional step used for making fine quality yarn. Carded slivers are combed to separate long and short fibres with the help of series of combs. Cleaning, carding and combing steps are omitted while making spun yarns from cut filaments of synthetic fibres. For these synthetic fibres only spinning and winding is done.

iv) Spinning: Carded and combed slivers are further drawn and spun into yarns. The yarn is a single strand but may be plied into several strands:

v) Winding: The yarn is wound into various packages according to the weight or length of the yarn and its end use. Some of the common yarn packages for fabric construction are- ball (yarns for hand knitting), reels or bobbins for sewing; embroidery and hanks, cones, etc.
The Kenaf spinning machine is an electric device. The prime mover is an electric motor which is linked via many drives. The motion of the motor is transmitted and converted to the cone on which the yarn is wound. The yarn after being treated through the processes prior to spinning, it is then passed in loop of the thread holder. To this end a set of rules are followed such as outlining the design requirement from which the design specification is adopted. The link is an element of the mechanism which is capable of transmitting a force.

DESIGN REQUIREMENTS

- Power to be delivered: 15kW
- Input speed: 35rpm
- Output speed: 1.4rpm
- Targeted for uniformly loaded applications, such as belts, chain etc
- Output shaft and input shaft in-line
- Base mounted on four bolts

- Continuous operation
- 4-year life, with8 hour per day, 5 days a week operation
- Low maintenance
- Competitive cost

DESIGN SPECIFICATIONS

- Power to be delivered: 15kW
- Power efficiency: 97%
- Steady state input speed: 35rpm
- Maximum input speed: 2.1rpm
- Steady state output speed: 1.6rpm
- Low shock levels

With these parameters taken into consideration, the fabrication of the spinning machine was done with utmost precision and the dimension is 250 × 700 × 750



Fig 1: The finally assembled NARICT spinning machine.



Fig 2: The top view of the NARICT spinning machine.



Fig 3: An operator spinning fibre using the NARICT spinning machine.

PERFORMANCE TEST AND EVALUATION

Having constructed the spinning machine, the following test procedure was carried out and the evaluation recorded. A tachometer was used to determine the speed of the drum and bobbin. The machine was made to run for twenty-five to thirty minutes to ascertain the readiness of the machine. Then the machine was operated for a period of 6 hrs and continuous feeding was done with the Kenaf yarn for a 5 day duration and the efficiency obtained. Spinning spindle rest on a carriage that travels on a track a distance of 10cm, while drawing out and spinning the yarn. On the return trip, known as putting up, as the carriage moves

back to its original position, the lead spun yarn is wound onto the spindle in the form of a cone-shaped cop. As the spinning spindle travels on its carriage, the roving which it spins is fed to it through rolling orifice geared to revolve at different speeds to draw out the yarn. At the end the production rate was determined. This was found to be 2.41cm/s.

RESULTS AND DISCUSSION

The National Research Institrute for Chemical Technology, Zaria operates a Mini-Spinning Laboratory that contains unique miniature textile machinery that can process much smaller (50 g) quantities of fibre than conventional textile mills. The facility provides a quick method for evaluation of kenaf or kenaf blended with other fibers. The 50-gram spinning test (Landstreet, et.al., 1962) was modified to handle the kenaf/cotton blend. The spinning machine which spins the bast fibre while minimizing fibre breakage, and then blended with cotton for a 80% cotton / 20% kenaf blend. The kenaf was processed and passed through the orifice of the drum while rotating. The cotton was hand blended with the opened kenaf and run through the opener on low speed. The blended fibres were then processed on the mini-spinning system in 50 g quantities. (Landstreet et al., 1962).

The evaluation was carried out as follows;

- The general performance of the machine was satisfactory as all the various components functioned as expected.
- The speed of the rotary drum was determined with a tachometer to be 1.8rev/s. as designed
- The speed of the bobbin was also determined to be 0.9rev/s.
- The number of twist per cm was also determined to be 25 twist/cm.
- Production rate is 2.41cm/s.

CONCLUSION

Having achieved the fit of producing a spinning machine which is a first of its kind, the output was as anticipated from the design. The machine spinning speed was determined to be 1.8rev/s and the production rate was 25 twist/cm.

FURTHER WORK

As a result of the success achieved in the fabrication of the NARICT spinning machine further work is still recommended thus:

- Use the feedback from the Textile and Fibre research group to make any necessary adjustment.
- To optimize the machine developed for higher production.
- To upgrade the machine to a pilot scale.

REFERENCE

Aimin Liu (1999) Proceedings from the First International Workshop on Pulp and Paper making from Kenaf. Yuanjiang, China

American Society for Testing and Materials. (1998). Annual book of ASTM Standards. Section 7. Vol. 07.01. Textiles—Yarns, fabrics, and general test methods. ASTM, Philadelphia.

Boylston, E.K., and J.J. Hebert. (1975). An electron microscopy study of cotton fibers mercerized at elevated temperatures. Text. Res. J. 45:790–796.

Cheek, L., and L. Roussel (1989). Mercerization of ramie:Comparison with flax and cotton. Part 1. Effects on physical, mechanical, and accessibility characteristics. Text. Res. J. 59:478–483.

Chen, L.H., E.P. Columbus, J.W. Pote, M.J. Fuller, and J.G. Black. (1995). Kenaf bast fiber separation. p. 15–19.

In Proc. International KenafAssociation, Ladonia, TX.Mar. (1995). International Kenaf Association, Ladonia, TX.

Kawabata, S.(1980). Standardization and analysis of hand evaluation, 2nd ed. The Textile Machinery Society of Japan.

NATIONAL INDUSTRIALISATION ROADMAP: THE NARICT FABRICATION ENGINEERING INPUT (A CASE STUDY IN TEXTILE

Akang V.I[1]., Gadimoh S[1]., Otsai O.J[1]., Okechukwu T.U[2].,Akang J[3] Ayuba N.L.[1] and Al-Kasim U[1]

(*1) National Research Institute for Chemical Technology, Zaria (2) Ahmadu Bello University, Zaria (3) Nuhu Bamalli Polytechnic, Zaria E-mail:akangiv@yahoo.com. vinakang@yahoo.com*

ABSTRACT

This paper formulates a workable model for industrializing the nation using the textile sector as a reference point. The textile industry is one of the most complicated manufacturing industries because it is a fragmented and heterogeneous sector dominated by small and medium enterprises (SMEs). Electrical power is one of the main cost factors in the textile industry. Especially in times of high energy price volatility, improving marketing efficiency should be a primary concern for the textile sector. There are various energy-efficiency opportunities that exist in every textile plant, many of which are cost-effective. However, policies that should create a level plane field for an even cost-effective option often are not implemented in textile sectors mostly because of limited information on how to implement energy-efficiency measures, especially given the fact that a majority of textile plants are categorized as SMEs or government owned and hence they have limited resources to acquire this information. Know-how on energy-efficiency technologies, marketing opportunity and practices should, therefore, be prepared and disseminated to textile industries. Provision of information on a model to enhance a variety of efficiency technologies and measures applicable to the textile industry is proposed. First, the paper gives a brief overview of the textile industry around the world, with an explanation of major textile processes. The conclusion includes a short section dedicated to highlighting a few emerging technologies in the textile industry as well as the potential for the use of renewable energy and marketing with incentive pattern in the textile industry. The main channels through which emerging economies can access international knowledge and technology are through FDI and domestic investment. The entrepreneur organizes and operates an enterprise for personal gain. He pays current prices for the materials consumed in the business, for the use of the land, personal services he employs and for the capital he requires etc. The net residue of the annual receipts of the enterprises, after all costs have been paid, he retails for himself. These principles and theories apply also to the indigenous entrepreneurs in the textiles and clothing industries. Today most Nigerian indigenous textile and clothing industries have closed down, sending thousands of Nigerian workers to premature retirements. This trend can be improved by adopting the approach outlined in the model.

Keywords: foreign direct investment, multinational enterprises, industrialization, technology, innovation, entrepreneurship,

INTRODUCTION

Nigeria is a middle income, mixed economy and emerging market, with expanding financial, service, communications, technology and entertainment sectors. It is ranked 26th in the world in terms of GDP (nominal: 30th in 2013 before rebasing, 40th in 2005, and 52nd in 2000). It is also on track to become one of the 20 largest economies in the world by 2020. Its re-emergent, though currently underperforming, manufacturing sector is the third-largest on the continent, and produces a large proportion of goods and services for the West African region.

The main focus of this paper on industrialization in general, and manufacturing specifically, is based on the recognition within the traditions of endogenous growth theory, evolutionary economics and institutional economics that manufacturing (industrialization), is important for economic development (Szirmai, 2012). Technological progress is in turn, necessary for successful industrialization (Von Tunzelmann, 1997; Fu, Pietrobelli and Soete, 2010). Hence in this paper we elucidate the workable path through which the nation should traverse for a sustained economic/industrial growth, the path of which is embedded in the model.

Industrialization – the rise of the manufacturing sector – has been a *sine qua non* of structural economic change and development ever since the first Industrial Revolution (Szirmai, 2012a; O'Brien, 2001). It is associated with higher productivity growth and per capita incomes, described as a "structural bonus" (Timmer and

Szirmai, 2000). Among the central issues in the literature on industrialization are technological change, innovation, and the relative contributions of multinational enterprises (MNEs) and domestic investment in facilitating technological upgrading. Technological progress and its diffusion were important for the First Industrial Revolution in Britain in the 18th century. It was also vital for the (second revolution) industrialization of Continental Europe and the USA in the 19th century, and for the (third revolution) industrialization of Japan and the East Asian countries in the 20th century (O'Brien, 2001; Veloso and Soto, 2001). In each case, catch up resulted from lagging countries accessing technology developed in leading nations, adapting it effectively to local circumstances, and subsequently relying more on indigenous innovation. Technology has become more important as ever, in the current modular and flexible production systems that has come to characterize the world economy. Indeed Marsh (2012) claims that the world is experiencing a new industrial revolution, led by networked production, mass customization and new technologies, such as 3-D printing. Multinational Enterprises (MNEs) can diffuse technologies to developing countries in three ways:

(i) By directly transferring technology to affiliate or joint ventures (JV);
(ii) Through spillover effects , and/or
(iii) Through doing R&D within a developing establishment (Lloyd, 1996).

The importance of such diffusion is well recognised. For instance Fu, Pietrobelli and Soete (2010: 1206) states that "foreign direct investment (FDI) has been 'a major vehicle for the transfer of advanced foreign technology to developing countries for a long time" (see also Veloso and Soto, 2001:88). More particularly FDI is "a vehicle through which developing country firms learn about new technology" (Harrison and Rodriguez-Clare, 2010: 4100). With MNEs as the "main engines of innovation in the world economy' (Franco et al., 2011:1249) such industrialization has been labelled "transnational-assisted restructuring" (Lloyd, 1996). Once sufficient absorptive capacities have developed, MNEs can bring technology and know-how to a local economy. This can take place either through FDI and/or through non-equity modes (NEMs) of international production and/or through their global R&D activities. It should be stressed that the context within which technology became available was important. For instance in 18th century Britain, the country's access to cheap energy (coal), its location in terms of seaborne trade, and the substantial investments made by the state in the Royal Navy (lowering transport costs) as well as other measures to protect intellectual capital created a favourable context for industrialization (see O'Brien, 2001; Robinson, 2009; Von Tunzelmann, 1997). Similar considerations apply to China's recent industrial success, as will be made clear: relatively low-cost resources (labour in China vs. coal in Britain), trade (export-driven growth), a large domestic market and government policies and infrastructural investments. Importantly they played this role in conjunction with the adoption or acquisition of existing foreign technology - with the latter first and foremost applied to make existing goods and later improve these through incremental innovations (Puga and Trefler, 2010). Indeed, China's industrialization has been described as foreign technology-led industrialization (Ozawa, 2011). The point thus is that foreign technology-driven industrialization commences through innovations based on the adoption of foreign technologies that require lower-skilled human and entrepreneurial resources. As time passes, a country can begin to add its own innovations, expanding the global technological frontier (Eberhardt et al., 2011). As such innovation, in a broad sense, is inherently part of the structural economic transformation process countries need to undergo (Fagerberg et al., 2010). The much faster industrialization of China, as compared to that of Europe or the USA, reflects in part the "stage skipping" phenomenon, made possible by the country benefitting from the much more rapid diffusion of technologies by foreign firms and domestic efforts for acquisition of technology. The catch up country does not have to go through every stage of technological development. It can immediately jump from relatively backward levels of technology to relatively advanced levels. In recent years it has not only been the technology transfer role of MNEs and FDI that has received attention as a mechanism for industrialization. The global fragmentation of production has also contributed to industrialization through the greater ease through which parts of a product's manufacturing may be outsourced and located in various countries (Nixson, 2012). The emergence of global value chains has been driven by two broad 'unbundling' forces (Baldwin 2003). The "first unbundling" was due to better transport and freight handling and the liberalization of trade.

Since the mid-1980s multinational enterprises (MNEs) used these better technologies and transport to break up their production processes across the globe; described as the spatial 'disintegration of production' (Feenstra, 1998). It

allowed these MNEs to combine 'the high technology they developed at home with low-wage workers abroad' (Baldwin, 2011:7). Through this global value chains (GVCs) ('global production sharing') in production emerged (see for instance Houseman et al. 2010; Grossman and Helpman 2005; Kaplinksi 2011; Nordas 2008; Yi 2003; Hummels et al. 2001). International trade started to shift from 'trade in goods' to 'trade in tasks' (Bournakis et al. 2011). World trade in parts and components increased from US $ 502 billion in 1992/1993 to US $ 1,1762 billion by 2005/2006 (Athukorala and Menon 2010).

For industrially lagging countries the rise of global production sharing has radically changed the range of industrial policy instruments available– and has increased the importance of complementarities between foreign sources of technology and domestic absorption capabilities. This is because successful industrial development now requires countries to be competitive not in the complete production of some goods, but in the production only of a component ('trade in tasks') wherein they need exceptional capabilities. Integrating a country's producers into global value chains may imply that the traditional focus of industrial policy on 'lumpy, complex industry' may not be appropriate anymore (Baldwin 2003; Kaplinksi 2011).

This development has opened up a range of opportunities for poorer countries, which may be more likely to be able to find a niche in which to specialize rather than be competitive along the entire production chain (Gimet et al. 2010). In other words finding a comparative advantage in a 'slice' of the production chain may perhaps be easier than finding a comparative advantage in the entire production chain and can be shaped by industrial policies (Coxhead and Jayasuriya, 2010). According to Baldwin (2011:2) global value chains have made industrialization for lagging countries much easier and quicker, stating that global value chains have *"...opened a new industrialization path. Today, nations can industrialize by joining a supply chain...there is no need to build a supply chain...the concept of a one-nation supply chain has disappeared'*. Global production sharing has also been shown, at least in theory, to result in static and dynamic efficiency gains (Bournakis et al. 2011; Rodriguez-Clare 2010 and Grossman and Rossi-Hansberg 2008). The objective of this paper is to design a pathway for the nation to follow so as to revamp the textile sector, improving the economy, and entrenching R&D in such ventures.

ESSENTIAL ELEMENTS, CONCEPT AND INDICATORS

THE ELEMENTS

The objective here focuses on a result oriented approach proposed by the National Research Institute for Chemical Technology; the fabrication engineering input. There is a model outline presupposing the institutionalization of the *technology* for the revamping of the textile sector by a tripod. This is proposed for a twenty year period. This tripod can be classed as: *the link, the innovator* and *the entrepreneur*. They are the essential elements for the success of the model. The concept behind the formulation of this model, stems from the notion that; Population growth stimulated a surge in production of textiles and other goods of daily usage. The term "Industrial Revolution" signifies accelerated developments of the technology and their applications to the Industry of certain countries in the world (as in the case of England). Supporting an unprecedented increase in industrial production, this revolution reached its peak, at the end of the 18th century and mid 19th century. Although by some authors the term "revolution" is considered to be exaggerated, it is true that between 1750's and 1850's the quality of goods produced increased enormously and machine power began to replace the human power for the first time in history. Workshops turned into factories, artisans to entrepreneurs and labourers to an alienated working class: the industrial proletariat. Output and distribution, passed the limit of local markets and the yield of a mass production began to be directed towards export markets. Briefly, industrial "revolution" was not a sudden incident but a transformation through time resulting in technical, economic, social, political and ideological alterations. If looked at from another aspect, Industrial Revolution also would mean misery of the working people, including women and small children, labouring from early morning until night.

Production technology

The technological innovations accompanied simultaneously the social and economic changes, and this may be considered as a reciprocal process. The driving force of the Industrial revolution was the textile industry and particularly the cotton products. Cotton industry was not considerable through much of the 17th century but exploded one century later. Most cotton was produced in British colonies namely America and India. Because it was a labour intensive agriculture, it fueled the traffic in African slaves to the American plantations. The cotton produced in America imported to the homeland for the use of textile

industry, and the finished products were marketed in Europe and in other countries. At the beginning, having the technological superiority of production, England had almost the monopoly of cotton textiles. This position altered when America became independent and entered into the market as a competitor. The first innovation in cotton manufacture was the then flying shuttle, developed by John Kay in 1733, and was one of the key developments in weaving that helped fuel the Industrial Revolution. James Hargreaves, a carpenter, developed the spinning jenny, which greatly speeded up the process of weaving cotton threads into cloth. In 1793, the American, Eli Whitney, invented the cotton gin, which mechanized the separating of seeds from cotton fibres. By the end of the eighteenth century, the manufacture of thread and cloth had slowly moved out of the family economy and into large factory mills. The invention that really drove the revolution in the eighteenth century was the steam engine.

INDICATOR

The basic source material from which textiles are made is the fibre. Fibres are what fabrics are made of. With a look at the fabric of the dress we are wearing, it can be seen that it is made of the thread prepared from small fibres. Just pull out a thread from a piece of fabric and open it up by untwisting, small fibres can be seen. There are a large number of fibres available to us and from which a variety of fabrics are made. In Nigeria, the production of textiles had flourished at both cottage and industrial levels. Studies show that the industry had been a major employer of labour (about 60% of the labour force) in the manufacturing sector and contributed immensely to the socio-economic and cultural development of the country {Asaju, (2004), Oloyede.(2014), Makinde,(2006)}. It is unfortunate; however, that the current economic low-ebb in Nigeria has developed adversarial forces clamping the proper functioning of the textile industry as a resourceful economic contributor. It becomes germane at this point to briefly trace the history of this development overtime.

The initial development of industrial estate that led to the evolution of the manufacturing sector of the economy started in 1953, by the establishment of Apapa medium large industrial estate. This is followed by the Yaba industrial estate established in 1958 by the federal ministry of Commerce and Industry for small and medium enterprises. Other industrial estates for the medium-large enterprises; the Ikeja Industrial Estate established by Western Nigeria Regional Government 1954 and the Trans-Amadi Industrial layout in Port-Harcourt, established in 1961 by the Eastern Nigeria Regional Government, were the pioneers. Essentially, these were industrial layout, areas provided with roads, railway sidings, transport and utilities, drainage facilities and so on, in which plots were made available to tenants. A unique feature of this pioneer industrial layout was the establishment of residential areas for the accommodation of workers and their managers. Immediately, after the acquisition of these industrial estates, manufacturing industrial tenants started building their factories, warehouses, offices, etc. Textile industries at the time are either fully owed by the indigenous-Nigerian government or in partnership with foreign concern, examples include;

(i) Nigerian Textile Mills, Ikeja established in 1961
(ii) Kaduna Textile Limited, Kaduna established in 1961/63
(iii) Aba Textile Limited, Aba established in1961/63, etc.

METHODOLOGY

PROCESS DESCRIPTIONS AND CURRENT INDUSTRY PRACTICES

The characterization of textile manufacturing is complex because of the wide variety of substrates, processes, components used, and finishing steps undertaken. Different types of fibres or yarns, method of fabric construction, and finishing operations (including preparation, printing, dyeing, chemical/mechanical finishing, and coating), all interrelate in producing a finished fabric. When one of these components is changed, the properties of the end products are affected. There are several properties that can be used to define a fabric and one or more of a fabric's inherent properties may be modified during processing to give it the desired end characteristics. Some examples of fabric properties include weight, appearance, texture, strength, luster, flexibility, and affinity to dyestuff.

Natural Fibre Preparation.

Natural fibres require several steps to open and clean the fibres to prepare them for yarn manufacturing. The first step, termed as opening and blending, is typically to take the natural fibres from compressed bales and sort and clean them to remove dirt and impurities. The next several steps are aimed at teasing out the fibres, lengthening them, and aligning them into thin parallel sheets, with each successive step resulting in a finer product. These steps are carding, combing, drawing, and drafting; all of which prepare the fibre for spinning. Different types of fibres may be

blended (combined) during drawing or following drafting. After drafting, the yarn is wound onto rotating spindles, which are mounted on to spinning frames, where they are set for spinning. These steps will vary according to the fibre being processed and the desired end product.

Man-made Fibre and Yarn Manufacture.
Man-made fibres do not need to go through the same cleaning and fibre preparation steps that natural fibres undergo. The man-made fibres can be manufactured by three different methods, each of which involves forcing a liquid through a small opening, where the liquid solidifies to form a continuous filament. These methods are melt spinning, dry spinning, and wet spinning, and each is used to produce different types of man-made fibres.

Texturing and Heat-Setting.
After spinning, the man-made fibres are drawn to align and orient the polymer molecules and strengthen the filament. This may be followed by texturing. Texturing is a process of crimping, importing random loops, or otherwise modifying continuous filament yarn to increase cover, resilience, abrasion resistance, warmth, insulation, or moisture absorption, or to provide a different surface texture. Texturing basically involves deforming the filaments (such as by imparting a twist) with a mechanical process to give man-made fibres spun-like properties, after which the deformation is set, usually by a heat-setting process (the deformation is not always heat-set). Heat-setting is typically done only for synthetics, does not involve application of any chemicals, and can be done on a semi-contact oven or tenter frame. In false-twist texturing, the deformation is further removed. Heat-setting involves applying high temperatures (350 - 400^0F) to confer dimensional stability to the synthetic fabrics, or blends (e.g., poly-cotton) containing thermoplastic fibres. One function of heat-setting is to prevent creasing during processing. No chemicals are applied; however, the high temperature required for heat-setting will volatilize spin finishes that may have been applied to the fibres, some of which may contain hazardous air pollutants (HAPs). Fibre is heated in a semi-contact oven or tenter frame under tension above its glass transition temperature and held for a period of time. It is typically used on polyester, nylon, and triacetate, and not on rayon, cotton, and acrylics.

Yarn and Thread Spinning.
Yarns are classified either as spun yarns or filament yarns. Spun yarns use staple (finite) length natural or man-made fibres combined to produce a yarn with high strength and structural integrity properties. Spinning may involve additional twisting or texturing, or multiple yarns may be twisted together to form plied yarns (may be further plied to make ropes, thicker cords, and cables). Filament yarns are produced from filament fibres in a process known as throwing. Man-made filaments may require additional drawing. Filament yarns are continuous forms in which the length of the fibre is essentially infinite, resulting in the yarn's structural strength and integrity. The input material is a sliver and the output is yarn on a large cone or tube. Thread bonding is a coating process that some threads may go through to increase the integrity of the construction. During the spinning process, synthetic fibres are often lubricated to aid in future handling or processing. These lubricants can be added to the fibre after converging or to polymer chips prior to melting and extruding. Some of these lubricants include finishes and antistatic agents, the composition of which varies with type of fibre and intended end use.

Fibre, Yarn, and Thread Dyeing
Although dyeing is a wet process, textiles can also be dyed in any of several different steps in the dry processing stage. Dyeing can be done using batch or continuous processes. Fibre dyeing is typically done in a stock dyeing machine where tightly-packed fibres are placed in a cage with perforated sides (or top and base), which is placed in a large vase. Dye solution is pumped through the fibre mass. The process is costly and has low productivity and is used mostly on woolen materials for certain effects. Various batch or continuous processes can be used for yarn dyeing. Advantages of the package dyeing method include savings in energy, water, and space, and lesser labour handling. Chain (tow) machines are used to dye yarn continuously (man-made fibres). For man-made fibres, the polymer itself can be imparted with colour even before yarn or fabric manufacture. Dope dye machines are used to melt dye polymer before extrusion into fibre.

Yarn preparation and Slashing.
Yarn preparation involves processes that improve the quality of woven or knitted fabrics produced from the yarn. In preparation steps, yarns will be inspected, cleared for defects, lubricated (if needed), and tensioned. Other steps to prepare yarn for weaving include warping, a process where single packages of yarn are transferred to an even sheet of yarn representing hundreds of ends, and then wound onto a large cylinder called a warp beam. Warp yarns (in addition to other preparation requirements) need to sustain their elongation and

flexibility during the weaving process. Knitting yarns or filling yarns used in weaving, do not have this requirement. This requirement necessitates a process called slashing or sizing, which is the application of a chemical sizing solution to warp yarns prior to weaving to protect them against snagging or abrasion that could occur during weaving. Slashing is necessary as long as the warp is in tension; to eliminate the need for slashing, there have been some efforts to develop weaving processes with less tension, although these processes are likely to be much slower.

The objectives of slashing are to strengthen, smooth the outer surface, and lubricate the yarn. The chemical nature of the size applied is dependent on the yarn substrate and the type of weaving being used. The three main types of size currently used are natural products (starch), fully synthetic products (e.g., PVA), and semi-synthetic blends (e.g., modified starches and carboxymethyl cellulose or CMC). In addition to these, auxiliary chemicals (lubricants, adhesives, additives, etc.) and water or a solvent are often added. PVA can be applied in pure form (with additives) or blended with natural substances, such as starch. The sizing operation is done on a large range called a slasher using pad/dry techniques. The slasher contains different sections that take up yarn from the warp beam and pass it through a size box that contains the aqueous sizing solution. New sizing technologies include high pressure squeezing, hot melt sizing, and foam sizing.

Weaving.

Weaving is a dry operation, but is normally done in buildings maintained at high humidity to increase flexibility of the yarn and minimize breakage. Weaving is performed on different types of looms, which vary in speed and methods used to transport fill yarns. The warp yarns are arranged so that they run lengthwise and the fill yarns run crosswise (at right angles to warp threads), so that these two yarns can be interlaced to impart a weave to the fabric. The warp yarns are wound on to large metal cylinders called beams and these are the yarns that normally pass through a sizing solution. The fill yarn is transported either by a shuttle or by shuttleless methods, such as using high-speed jets of water, air, or projectiles.

Knitting.

In knitting, fabric is formed by interlocking or intermeshing loops of one or more sets of yarns. Knitting is performed using one of two processes - weft and warp knitting, each is done on several different types of machines. In weft (or filling) knitting, loops are formed by needles knitting the yarn across the width of the fabric. In warp knitting, loops are formed by needles knitting a series of warp yarns fed parallel to the direction of fabric formation.

Tufting.

Tufting involves inserting additional yarns into the fabric to create pile fabric. In modern tufting machines, hollow needles carry and insert the yarn through a substrate cloth, which can range from a thin backing to heavier material. Tufting is used for apparel fabrics, upholstery, and blankets, although most tufting machines are used for carpets. Pattern attachments can be added to basic tufting machines.

Non-woven manufacturing.

In addition to the fabric formation methods described above, man-made fibres can be processed into fabric using non-woven techniques. Non-wovens are typically used in industrial applications and are a growth segment in the textile industry. Non-wovens are essentially sheet or web structures made by bonding and/or interlocking fibres, yarns, or filaments using mechanical, thermal, chemical, or solvent means. Non-wovens have several performance advantages such as moldability, and are typically engineered for specific uses, such as geotextiles, blankets, diapers, electrical insulation, and filters. Non-wovens can be homogenous fibre-web or netlike structures or can be laminates/composites. Typical fibres used in making non-wovens include polyester, polypropylene, rayon, and wood pulp. Raw materials in making non-woven fabrics are supplied either as synthetic polymer chips or as fibres. If a polymer chip is used, it needs to be melted and extruded, whereas fibres need to be opened, separated, and cleaned (using the same methods as in spun yarns). Non-wovens can be manufactured using different processes: dry lay; wet lay; spun bond; and melt spun. Each one of these processes involves web formation and sheet/web entanglement (bonding). The web formation typically involves a series of mechanical processes to feed in the fibre, open/blend, and to comb and straighten it to form a composite web, that varies in size and thickness. In the wet lay process however, the fibres are first suspended in a solvent, which can be water or a chemical solvent. This is followed by web formation, dewatering, and drying. In melt-blown processes, the feed consists of polymer that has been molten using a stream of hot air. After web formation, the sheet is bonded using chemical bonding, thermal bonding, or mechanical entanglement. Examples of mechanical techniques include using needle punching to entangle fibres, using water jets to entangle fibres (spun laced), or stitching sections of the web (stitch bonded).

Mechanical bonding is the oldest technique for consolidating a web, and is used to enmesh or entangle fibres to give strength to what are usually dry-laid webs. The most common methods are needle punching and hydroentangling (spun lacing). In needle punching, barbed needles are punched vertically through the web, hooking tufts of fibres through it and bonding it in the needle punched areas. The hydroentangled process uses fine, high velocity jets of water to impact a fibrous web and cause the fibres to curl and entangle about each other. Binder is not required, though a small amount of binder may be added to increase fabric strength and dimensional stability or to make them liquid repellant on one side. A third mechanical bonding process called stitch bonded uses a continuous filament to sew a web of unbonded fibres into a fabric with a stitch pattern. Mechanical bonding techniques typically are slower than chemical or thermal bonding. However, they yield advantages in strength and aesthetics. The two largest markets for needle punched non-wovens are automotive trim and geotextiles. Other major end uses, in order of importance, are coated/laminated fabric backings, bedding and home furnishing materials, filters, interlinings, roofing, and landscape fabrics. Medical packs and gown are by far the largest spun laced application. Other large uses are wipers and medical sponges. Stitch bonded fabric is used in shoe components, mattress ticking, and coating substrates. Needle punching is also used to manufacture some nonwoven carpets. The needles used differ in design and function as compared to those used for tufting.

Wet Processing

Wet processing includes several steps that involve imparting colours or patterns to the fabric, along with a variety of finishing steps that provide certain desired characteristics to the end product. These finishing steps are important mainly in cotton and synthetic production. For most wool products and some man-made and cotton products (like gingham), the yarn is dyed prior to weaving and the pattern is woven on the fabric.

Preparation

Preparation includes any of several steps that may be taken to clean or prepare the fabric prior to dyeing. Preparation includes, but is not limited to, heat-setting, desizing (woven only), singeing, scouring, bleaching, and mercerization (cotton only). Heat-setting has been described above. Different types of equipment and chemicals are used in different preparation steps, and all these steps are not necessarily undertaken for all fabrics. Desizing, scouring, and bleaching operations all involve removal of impurities and can be done on various types of washers and steamers. The specific chemicals used vary from a simple warm water wash to use of surfactants, chelates, alkali, and oxidizing agents. Drying operations are generally done using ovens or tenter frames. Singeing involves passing the full width of a fabric under tension over open gas flame burners (singer), which remove projecting hairs to clean the fabric and reduce pilling. Singeing is an optional step and does not involve the addition of any chemicals. No HAPs are emitted from this process.

THE MODEL

As outlined, the elements are classed a tripod, viz; link, innovator and entrepreneur.

THE LINK

This is the agent saddled with the responsibility of enactment and execution of laws to enable a level plane field to be created so as to bring together the innovator and the entrepreneur for a productive venture. Usually this is the government. The objective of the model can be achieved by entrenching of a positively focused *linkage. Linkages* then are crucial to "systemic competitiveness" – i.e., with competitiveness that goes beyond the individual firm to become a feature of certain sectors in specific regions or of whole regions and countries. The development of linkages has both supply and demand side effects. The latter determine the magnitude of macroeconomic multipliers; the former are associated with the positive externalities that different economic agents generate among themselves through cost reductions induced by economies of scale and scope in production, lower transport and transaction costs (economies of agglomeration), the induced provision of more specialized inputs or services (economies of specialization), and the sharing of knowledge between firms and the development of human capital that can move between firms (knowledge spillovers). This implies that developing domestic linkages is more important than integration into world markets per se, and that not all patterns of integration into international markets have the same effect on economic growth. Thus, the countries that profit most from FDI are those whose domestic firms and institutions build domestic technological capability, both through investment in own R&D and workforce education and training, and through linkages created between domestic firms and foreign affiliates. At the same time, a successful export strategy is highly dependent on how the export sectors are integrated with other domestic economic activities, not least

in terms of employment generation. Enabling laws are enacted to enhance productivity by the innovator, making of policies that will encourage the entrepreneur to part with his means, venturing into textile business. The creation of clusters of would be distributors, collectors and farmers for effective channelization of the required raw material from source to the innovator, and from the innovator to the final consumer.

THE INNOVATOR

Innovation should be considered in a broad sense, as the development of new economic activities or new ways of doing existing activities. It is important in this regard to recognize the role, not only of technological but also of non-technological innovations. For instance, developing new marketing networks and innovations in marketing, as well as the development of new organisational practices or structures are often more important than the adoption of new production technologies. Indeed, the ability to reap the benefits from new technologies often depends on innovations in distribution and organisation occurring simultaneously. The microeconomics literature has tended to focus too much on production, and too little on sales, marketing and distribution. Schumpeter's concept of "new combinations" captures much better this broad concept of innovation than the usual association of this concept with technological change in production. The innovator in this regard is the *National Research Institute for Chemical Technology, Zaria.* Most of the required machineries for the smooth running of the textile sector are outdated and hardly available, or non existent. Such machines of complex nature are to be procured and the innovator fabricates these and modifies same to suit the local environment. This agent has to also treat the effluent from the numerous activities emanating from the textile production sites to make the environment clean and safe (including research into a variety of methods best for such treatment).

THE ENTREPRENEUR

Entrepreneurs are the ones who organize and lead such forays into unexplored territory. Their appetite for risk may, however, be dulled if the prospect of profiting from a successful discovery is small. Non-technological innovation, such as conquering a new market or developing a new marketing strategy, may be more important in the early stages of development but it can be easily imitated and is also difficult to protect through conventional forms of intellectual property rights. It is also necessary to go beyond the neo-classical view, in which technological progress is exogenous and technology is often embodied in industrial equipment. On the contrary, the process of absorption of technology by firms is an active and costly process. Furthermore, the development of new activities may be fraught with coordination failures and entry costs vary across sectors. Most developing countries enter international markets with commodities or basic manufactures and assembly operations, because the production of high-tech products requires a pre-existing industrial and technological base. One of the main challenges of industrial policy is thus to understand better how to support the development, in a coordinated fashion, of production and technological capabilities in new economic activities. It is in this context that "clusters" of interlinked firms, trading goods and services as well as ideas and personnel, are seen as valuable features of the industrial landscape. This agent engages the working population, assigning them roles to meet up with the targeted objectives. He should also be willing to give out non cash loans of product worth. The entrepreneur in this model is the *NARICT Micro-finance bank*.

A FUNCTIONAL RELATIONSHIP OF THE ELEMENTS OF THE MODEL

Reflection on industrial policies in developing countries are concerned with these three important dimensions: *innovations* (in a Schumpeterian sense), *linkages* (Hirschman), and *surplus labour* (Lewis). In developing countries, a sizeable part of the workforce is underemployed in low-productivity activities. As Lewis argued, this surplus labour is available in virtually unlimited supply to the modern sector, where it could be employed more productively. The absorption of this *surplus labour* or, in the opposite case, the incapacity to do so, is generally a more important determinant of overall factor productivity growth in developing countries than technological change per se. Thus far, globalization has had only a limited impact on surplus labour absorption. In fact, in some parts of the world, informal employment in low productivity sectors has grown with the liberalization of trade and the implementation of efficiency-increasing domestic economic reforms. In these cases, aggregate productivity may show a poor performance even if the modern sectors are immersed in a dynamic process of technological change. Industrial policies should thus aim at reducing surplus labour in the economy. Taking into account surplus labour in the design of industrial policies can lead to very different prescriptions from those emerging from a neo-classical paradigm, which assumes full employment. Thus, industrial policies and the process of production sector restructuring

generated by structural reforms should be measured against their potential effects on surplus labour in the economy. In this regard, linkages are once again crucial, since what matters from an employment perspective is the overall impact of industrial restructuring and development on job creation, even if many of the new jobs are in a growing service sector stimulated by and supporting industrial activity or, for that matter, in producing food crops and other agricultural products to satisfy changing consumer preferences. Let us mention here, two elements that had been taken into account in understanding the links between industrial policies and growth. The first is that domestic factors are not the sole determinant of domestic policies. The regional and global economic environments are also essential determinants of growth, an issue usually overlooked in the massive literature on economic growth in recent decades. During the so-called golden age of 1950-1973, most developing regions experienced rapid economic growth. In contrast, the final two decades of the twentieth century brought a large number of "growth collapses", with only a small number of developing economies able to sustain fast rates of growth. Furthermore, widening international inequality diminishes the growth prospects of the less advantaged countries. This is so because markets did exacerbate inequality, as successful countries accumulate richer endowments and as capital followed success, while those left behind remained more vulnerable to shocks in international financial and commodity markets. Second, development is path-dependent, i.e., long-run growth prospects depend on an economy's trajectory. The importance of dynamic learning economies to economic development implies that the opportunities open to economic agents are largely determined by their production experience. Loss of experience may thus have cumulative effects on growth, as illustrated in the 1980s by the diverging experience of Latin America (which suffered major adverse macroeconomic shocks) and Asia (which did not). Several countries have been able to emerge from extended periods of relative stagnation or high economic volatility to embark on new development paths characterised by consistently high growth. Those experiences do, however, suggest the importance of government policy in helping create an environment which provides sufficient rewards to entrepreneurship and innovation, and also in addressing the coordination failures and informational externalities which can inhibit a sustainable process of industrial development.

The model develops a number of the themes touched upon here – the importance of *patterns* of industrial diversification and the opportunities they provide for linkage and knowledge spillover (Rodrik); the need for a broader view of innovation, encompassing not only technology but also marketing, logistics, management and organization (Dahlman); the realization that FDI, do not per se have a positive impact on the economic development of recipient countries (Aykut and Goldstein); the scope beyond industry – in certain areas of agriculture and services – for innovation, linkage and high-value-added production; the employment-creating and poverty reducing effects of different patterns of industrial development; and the importance of the external environment to shaping industrial development prospects had been considered.

The sector is increasingly dominated by Asian countries

In the past fifteen to twenty years, employment in the sector has increasingly been concentrated in China, Pakistan, Bangladesh, India, Mexico, Romania, Cambodia and Turkey. All of these countries, apart from India, have shown increases in clothing and textile employment from 1997 to 2002 – the global decline in employment in the sector is equally marked in countries such as the USA, Europe and the Philippines. Employment in the clothing and textile sector in EU25 countries fell from one million to 2.7 million between 1995 and 2005. A further one million job losses in the sector are anticipated in the next five years

Innovations have included new production technologies to reduce the labour requirement of garment completion and development of novel 'smart' functions. Pressure from consumers and legislation is likely to drive increasing demands for environmentally sensitive production. In the short term this is likely to focus on the use of chemicals but may extend to include re-use of materials and substitution of alternative materials.

Developing a more sustainable future: the largest part of the work was a wide-ranging scenario analysis of various possible futures. The analysis included prediction of the environmental, economic and social consequences of changes in production structure, material and process innovations and government influence. The main findings of the scenario analysis are: Improvement in the environmental performance of the sector is material specific and depends on the energy and toxicity life-cycle profile of the material. For conventional cotton products, the requirement for energy is driven by laundry, but the use of toxic chemicals is driven by agriculture. In contrast, for viscose, energy use is dominated by production. For products in which production dominates

impacts, process efficiencies should be pursued and the impact will be reduced by extending the life of the product or by re-using materials by some form of recycling. For products in which raw material production dominates, in addition to measures to extend product life, alternative processes or materials should be pursued. A switch from conventional to organic cotton growing would eliminate most toxic releases. Recycling is significant for materials with high impacts in the production phase. Technology innovations may provide a means to extract longer fibres from used textiles, although a recent innovative business for carpet recycling failed to achieve profitability. In order to maximise the programme's full potential, data has been generated and classified in ways that are both consistent with each other, and with methodologies of the other generators of resource flow / waste management data. In addition to the projects having their own means of dissemination to their own constituencies, their data and information has been gathered in a common format to facilitate policy making at corporate, regional and national levels.

Reasons for different models

Why is there such a difference in business models? Actually in both China and India the cost conscious and the profit-conscious models exist. Although focusing on reducing cost, the Chinese companies do not forget to pursue more value-added products and profit. Indian companies also introduce new machinery and enhance management to improve cost-efficiency. However, historic, cultural, and social contexts in each country inform the various emphases and strategies that enterprises use in their decisions. Such decisions cannot be simply explained through static comparative advantages. As we see, labour costs in India are as cheap as in China, and China has as many engineers as India. Only by examining the development path comprehensively can we understand the reasons behind the divergence in business patterns. As mentioned before, today's major Chinese textile companies are pretty young. While the old state-owned textile enterprises lost their competence and went bankrupt, competitive private textile mills and garment factories were set up only after the economic reform in 1978. Since the focus of early economic reform in China was in rural areas, some of the peasants and small hand-workers became the first beneficiaries of reform and established their enterprises. Today 87.5% of the textile and apparel enterprises are based in rural areas. Some of the most famous apparel brands such as "Younger," "Luomen," "Shanshan," and "Sanhong" were all founded and managed by former peasants. Chinese peasants at that time had very limited education: none of the founders of the companies just mentioned have education beyond secondary school, and none of them speaks English. Consequently these companies lag in human capital and technology acquisition. After the devastating Cultural Revolution (1966-1976), there were few engineers and skilled workers left in the urban textile industries and even fewer in rural areas. The typical story is that several young men bought a machine together and commenced the most primitive "production" of cloth, socks, shirts, and trousers. The quality of such "production" was of course pathetic and there was no design, for they simply copied others' products. However, in the early 1980s China was still largely locked into a planned economy. The shortage of consumer products was so serious that the consideration of quality and brand was merely secondary. The basic products were still salable on the world market, and China's textile giants today obtained their first capital in this manner. Because of the lack of skilled workers, experienced engineers, and qualified designers, these enterprises can do little to improve technology or fashion design. Their development is rather based on the efficient organization of mass production, promoting productivity and reducing cost. This also fits the Chinese work ethic. China's cultural background makes Chinese workers relatively disciplined and willing to work hard. From the middle 1980s to the early 1990s, when the foreign orders arrived, Chinese manufacturers had neither modern machinery, nor technology strength, nor communication capability. Their only option was to use their advantage in a highly disciplined workforce and compete with others through astonishing productivity and cut-throat prices. Besides, the emphasis of the Chinese government on infrastructure construction, including road construction, power, and water supply development, provided the fledgling textile enterprises with substantial support that came from lower production and transportation costs. Although the strategies of Chinese textile and apparel companies have changed a lot since then, established business models and existing customer groups still largely influence the direction of the companies' technological development. Reducing costs, increasing productivity and managing mass production continue to be the major themes of Chinese textile industry. In comparison, many Indian textile enterprises have a long and stable development history, which can be traced back to the colonial era. Arvind Mills was founded in 1931; Premier Mills was set up in 1949; The Raymond Group was incorporated in 1925; Lakshmi Mills was established in 1910. Even the

"younger brother" Vardhman, established in 1962, is almost two decades older than its Chinese counterparts. Through a long period of market operation, Indian companies have relatively established market networks and regular customer groups. Not concerned with survival, they are aiming at higher profit. Besides, the founders and managers of Indian enterprises are either experienced experts in the textile industry or industrialists who are able to understand sophisticated technology. The Indian entrepreneurs belong almost exclusively to the upper classes in the social (caste) system. They have the knowledge, the capital, and the social relationships to build up their enterprises. Their good educational background, systematic management, and technological and financial capability enable them to consider more value added and profit, whereas the Chinese village entrepreneurs struggled for survival under circumstances of little technology and little capital for a long period. Apart from management, the external conditions in India are not friendly to mass production. The road traffic, train transportation, and harbour facilities in India are of poor quality. Restrictive labour laws prevent companies from recruiting large numbers of workers. When the enterprises hire more than one hundred workers, they have to deal with worker unions. Under the unions' pressure, only 2% of Indian textile factories have three shifts, whereas about 20% of Chinese counterparts are operating 24 hours a day. In short, the choices between two paths of technological development – promoting productivity or customization – have been decided by the historical, cultural, economic, and social conditions in India and China. Under its particular socio-political conditions, it was reasonable for Chinese enterprises to prioritize a mass production model, which led to the Chinese textile industry's amazing boom. By contrast, Indian companies based their strategies on market experience and mature management, which do not trigger explosive growth, but are stable and effective.

CONCLUSION

The West African countries which produce low-cost high quality cotton have been unable to benefit fully from this boom, as world prices are artificially low due to oversupply of subsidized US cotton. While China, India and Pakistan are also major producers, only the United States is in addition a major exporter. Africa's cotton exports to the US accounted for less than 0.5 per cent of the total supplied to that market in 2004. At the Hong Kong WTO Ministerial it was decided that developed countries would eliminate all forms of export subsidies to cotton in 2006. Since most cotton producers in Africa are small holders, this could have a significant impact on rural incomes and rural poverty. At the same time, although there is in principle scope for developing a textile industry and producing goods with more value added, high energy and transportation costs remain a challenge. Diversification towards products with more value added is particularly important as new competitors enter the market. Although Brazil has traditionally been a net importer of cotton, the introduction of the new high yielding variety has turned the country into a net exporter as of 2003/04 and this change is likely to be sustained (ICAC, 2004; Oxfam, 2002). As of 2005/2006, yields were higher only in Australia. From the model proposed, if adequately implemented, the Nigerian state stands not only to industrialise the textile sector but create employment and generate income. This paper has examined the role of textile and clothing (T&C) industries in growth and development strategies in developing countries. It suggested that textiles and clothing industries are important in economic and social terms, in the short-run by providing incomes, jobs, and foreign currency receipts and in the long-run by providing countries the opportunity for sustained economic development in those countries with appropriate policies and institutions to enhance the dynamic effects of textiles and clothing. The potential of the textile and clothing industries to contribute to long-run growth and development will depend not only on the attributes (desirable or otherwise) of the investors, but also on the quality and effectiveness of government policies and institutions in developing countries to build on this investment.

DISCUSSION

The textiles and clothing sector plays a major role in the development and industrialisation process of countries and their integration into the world economy. The WTO (2006) notes that in 2004, developing countries as a group (low and middle income countries) accounted for more than half of all world exports of textiles and clothing and that in no other category of manufactured goods do developing countries enjoy such a large net-exporting position. Today, clothing and textiles represent about seven per cent of world exports. Globally, the workforce in clothing and textiles production was around 26.5 million in 2000. More than a quarter of the world's production of clothing and textiles is in China, which has a fast growing internal market and the largest share of world trade. Western countries are still important exporters of clothing and textiles, particularly Germany and Italy in clothing and the USA in textiles. Output from the sector is growing in

volume, but prices are dropping, as is employment, as new technology and vertically integrated structures support improved productivity.

REFERENCE

ABRAMOVITZ, M. (1989b). 'Thinking about Growth', in: M. Abramovitz, *Thinking about Growth and other Essays on Economic Growth and Welfare*, Cambridge: Cambridge University Press, pp.3-79.

ALFARO, L. AND RODRIGUEZ-CLARE, A. (2004). 'Multinationals and Linkages: An Empirical Investigation', *Economia*, Spring 4(2). ASAJU, K, etal (2014). "*The Rising Rate of Unemployment In Nigeria: The Socio-Economic and Political Implications"*, Global Business And Economics Research Journal vol. 3(2), 2014

ATHUKORALA, P. AND JAYASURIYA, S., (2000), *"Trade policy reforms and industrial adjustment in Sri Lanka",* The World Economy, 23, 3: 387-404.

ATHUKORALA,P.C. AND MENON, J. (2010), 'Global Production Sharing Patterns and Determinants of Trade Flows in East Asia', ADB *Working Paper Series on Regional Integration no. 41*, Asian Development Bank.

BALDWIN, R. E. (2003). 'Openness and Growth: What's the Empirical Relationship?' Working Paper 9578. Cambridge, MA: National Bureau for Economic Research.

BALDWIN, R.E. (2011). 'Trade and Industrialization after Globalization's 2nd Unbundling: How Building and Joining a Supply Chain are Different and Why it Matters', *NBER Working Paper no.17716*.

BALDWIN, R. (2006)," *Globalization: The Great Unbundling(s)",* paper contributed to event on Globalization Challenges to Europe and Finland organized by the Secretariat of the Economic Council, Prime Minister's Office (June).

BARBER E. J.W. (1991):" *Prehistoric Textiles: The Development of Cloth in the Neolithic and Bronze Ages with Special Reference to the Aegean".* Oxford, Princeton: Princeton University Press.

BOURNAKIS, I., M. VECCHI, AND F. VENTURI (2011). 'Offshoring and Specialization: Are Industries Moving Abroad?', Quaderno no. 98, December. BROUDY E.(1979) *"The book of looms: a history of the handloom from ancient times to the present.* London: Studio Vista.

COXHEAD, I. AND JAYASURIYA, S. (2010). 'China, India and the Commodity Boom: Economic and Environmental Implications for Low-Income Countries', *The World Economy*, 525-551.

FAGERBERG, J. (1994), *"Technology and international differences in growth rates*". Journal of Economic Literature, Vol. 32, No.3, pp. 1147-1175.

FAGERBERG J. AND M.M. GODINHO (2005). 'Introduction', in. J. Fagerberg, D.C. Mowery and R.R. Nelson (eds) (2005) The Oxford Handbook of Innovation, Oxford: Oxford University Press, pp. 514-542.

FAGERBERG, J., SHROLEC, M. AND VERSPAGEN, B. (2010). 'Innovation and Economic Development' (In *Handbooks in Economics*, vol 2, chapter 20, pp. 834-871).

FAGERBERG, J., M. SRHOLEC, AND M. KNELL (2007). 'The Competitiveness of Nations: Why Some Countries Prosper while Others Fall Behind', *World Development*, 35 (10): 1595-620.

FEENSTRA, R. (1998). 'Integration of Trade and Disintegration of Production in the Global Economy', *Journal of Economic Perspectives*, 14 (4). 31-50.

FIGUEIRDO, P. (2007). 'Industrial Policy Changes and Firm-Level Technological Capability Development: Evidence from Northern Brazil', *World Development*, 36 (1): 55-88.

FISCHER, W.A. AND VON ZEDTWITZ, M. (2004). 'Chinese R&D: Naissance, Renaissance or Mirage?",*R&D Management*, 34 (4): 349-365.

FONG, H.D. (1942). 'The Prospects for China's Industrialization', *Pacific Affairs*, 15 (1): 44-60.

FRANCO, E., RAY, S. AND RAY, P.K. (2011). 'Patterns of Innovation Practices of Multinational-Affiliates in Emerging Economies: Evidence from Brazil and India', *World Development*, 39(7): 1249-1260.

FU, X., PIETROBELLI, C. AND SOETE, L. (2010). 'The Role of Foreign Technology and Indigenous Innovation in the Emerging Economies: Technological Change and Catching-up', *World Development*, 39 (7): 1204-1212.

GIMET, C., B. GUILHON AND N. ROUX (2010). 'Fragmentation and Immiserising Specialization: The Case of the Textile and Clothing Sector', *Working Paper 1003*, Groupe D'Analyse et de Theorie Economique Lyon – St Etienne. March.

GROSSMAN, GENE M. AND ELHANAN HELPMAN (1991), *"Innovation and Growth in the Global Economy",* Cambridge, MA: MIT Press.

GROSSMAN, G.M. AND E. ROSSI-HANSBERG (2008). 'Trading Tasks: A Simple Theory of Offshoring', *American Economic Review*, 98 (5): 1978-1997.

GROSSMAN, G.M. AND HELPMAN, E. (2005). 'Outsourcing in a Global Economy', *Review of Economic Studies*, 72 (1). 135-159.

GROSSMAN, G. AND E. ROSSI-HANSBERG (2006), *"The Rise of Offshoring: It's not Wine for Cloth Anymore",* conference paper, Reserve Bank of Kansas, August 23.

HARRISON, A. AND RODRÍGUEZ-CLARE, A. (2010). 'Trade, Foreign Investment, and Industrial Policy for Developing Countries', Chapter 63 of the *Handbook of Development Economics*, volume 5, pp.4039-4214.

HAUSMANN, R. AND B. KLINGER (2006), *"Structural transformation and patterns of comparative advantage in the product space",* mimeo, Harvard University.

HAUSMANN, R., PRITCHETT L,. RODRIK D.(2005), *"Growth Accelerations",* Journal of Economic Growth, 10, 2005, 303–29.

HAUSMANN, R., HWANG J., RODRIK, D (2006)*, "What You Export Matters*", Harvard University, April.

HAUSMANN, R., RODRIK, D. (2006), *"Doomed to Choose: Industrial Policy as Predicament",* Harvard University, September.

HAUSMANN,. KLINGER B. (2006), *"Structural transformation and patterns of comparative advantage in the product space*", mimeo, Harvard University.

HOBDAY, M. (1994). 'Export-Led Technology Development in the Four Tigers: The Case of Electronics', *Development and Change*, 25 (2): 333-361.

HOUSEMAN, S., KURZ, C., LENGERMANN, P. AND MANDEL, B. (2010). 'Offshoring and the State of American Manufacturing', *UPJohn Institute Working Paper no. 10-166*.

HUMMELS, D., J. ISHII AND K.M. YI, (2001), *"The nature and growth of vertical specialization in world trade",* Journal of International Economics vol. 54, no 1. pp. 75-96.

IMBS, J., WACZIARG R., (2003), *"Stages of Diversification*", American Economic Review, 93(1), 63-86.

LLOYD, P.J. (1996). 'The Role of Foreign Investment in the Success of Asian Industrialization', *Journal of Asian Economics*, 7 (3): 407-433.

JOHNSON, S., OSTRY J., SUBRAMANIAN A (2006), "Africa's Growth Prospects"

JONES, B. F. AND B. A. OLKEN (2005), "*The Anatomy of Start-Stop Growth"*, NBER Working Paper No. 11528, Cambridge, MA, National Bureau of Economic Research.

KAPLINSKY, R. (2001) '*Spreading the Gains from Globalisation: What Can be Learnt from Value Chain Analysis'*, IDS Working Paper 110

KAPLINSKY, R. (2006) *"China and the Global Terms of Trade*", IDS Bulletin Volume 37, Number 1, pp43-53 (11)

KAPLINSKY, R. (2011). 'Commodities for Industrial Development: Making Linkages Work', *Development Policy, Statistics and Research Branch Working Paper 01/2011*,

UNIDO. KLINGER, B. AND D. LEDERMAN (2004), "*Discovery and Development: An Empirical Exploration of 'New' Products"*, World Bank, August.

LALL, S. (2003), *"Reinventing industrial strategy: The role of government policy in building industrial competitiveness",* for The Intergovernmental Group on Monetary Affairs and Development (G-24), September, second draft.

LALL, S. (2003), *"Foreign Direct Investment, Technology Development and Competitiveness: Issues and Evidence, in Competitiveness, FDI and Technological Activity in East Asia*", S. Lall and S. Urata, eds., Edgward Elgar, Northampton.

LEWIS, W. A. (1954), *"Economic Development with Unlimited Supplies of Labor"*, Manchester School of Economic and Social Studies, 22, 139-91.

LLOYD, P.J. (1996). 'The Role of Foreign Investment in the Success of Asian Industrialization', *Journal of Asian Economics*, 7 (3): 407-433.

MAKINDE, D.O (2005). *"Old Wine, New Bottle: The Changing Face of Adire in Contemporary Nigerian Arts"*. Paper Presented at the 30th Anniversary of the Department of Fine Arts, Obafemi Awolowo University, Ile-Ife.

MARSH, P. (2013). *The New Industrial Revolution*. Yale: Yale University Press.

NGUYEN TH, SUTHERLAND K AND THOBURN J (2003). *"Globalisation and the Impact of Restructuring in the Textiles Sector on Households in Vietnam"*. Paper (revised) presented at the workshop on Globalisation and Poverty in Vietnam, organized by the Department for International Development (DFID) of the United Kingdom in Hanoi, September 2002.

NIXSON, F. (2012). *The Dynamics of Global Value Chain Development: A BRICS Perspective*, Paper prepared for the UNIDO project: The Untold Story: Structural Change for Poverty Reduction: The Case of the BRICS, September 2012.

NORDÅS, H.K., (2003A), *"A note on the impact of Trade liberalization on women's job opportunities and earnings in developing countries*", Trade Policy Review, 2: 2, 221-231.

NORDÅS, H.K., (2003B), *"Vertical specialization and the quality of infrastructure",* WTO Working Paper ESRD 2003-04. NORDAS, H. (2004) *"The Global Textile and Clothing Industry post the Agreement on Textiles and Clothing",* WTO Discussion Paper No. 5,

O'BRIEN, P.K. (2001). 'Industrialization; Typologies and History of', *International Encyclopedia of the Social and Behavioural Sciences*, pp. 7360 – 7367. OLOYEDE, Z.O (2014). *"An Assessment of Factors Militating Against Fabric Production In Contemporary Nigerian Textile Industry"*. Paper Presented At a Workshop Organized By The Entrepreneurial Unit of Obafemi Awolowo University. Ile-Ife.

PRASAD, E., R. RAJAN AND A. SUBRAMANIAN (2006), *"Foreign Capital and Economic Growth"*, Research Department, IMF, August.

PUGA, D. AND TREFLER, D. (2010). 'Wake Up and Smell the Ginseng: International Trade and the Rise of Incremental Innovation in Low-Wage Countries', *Journal of Development Economics*, 29 (4): 304-313.

ROBINSON, J. A. (2009). 'Industrial Policy and Development: A Political Economy Perspective'. Paper prepared for the 2009 World Bank ABCDE Conference, Seoul, Korea, 22–24 June.

RODRIK, D. (2004), "*Industrial Policy for the Twenty-First Century"*, Harvard University.

RODRIK, D. (2006), "*What's So Special About China's Exports, China & World Economy"*, 14(5), 1-19

RODRIK, D. (2006) *"Industrial Development: Stylised Facts and Policies",* John F Kennedy School of Government,

SZIRMAI, A. (2012a). 'Industrialization as an Engine of Growth in Developing Countries, 1950-2005', *Structural Change and Economic Dynamics*, 23 (4), December 2012, pp. 406-20, http://www.sciencedirect.com/science/article/pii/S0954349X1100018X

SZIRMAI, A (2012b). *Proximate, Intermediate and Ultimate Causality: Theories and Experiences of Growth and Development,* Working Papers on Institutions and Economic Growth: IPD WP01),

UNU-MERIT Working Paper Series, 2012-32, May 2012 (76 pp).

SZIRMAI, A. (2012c). 'Explaining Success and Failure in Economic Development' in D.S. Prasada Rao and B. van Ark, (eds.), *World Economic Performance. Past, Present and Future*, Edward Elgar, chapter 9.

SZIRMAI, A., NAUDÉ, W.A. AND ALCORTA, L. EDS. (2013). *Pathways to Industrialization in the 21st Century*. Oxford: Oxford University Press.

TIMMER, M. AND SZIRMAI, A. (2000). 'Productivity Growth in Asian Manufacturing: the Structural Bonus Hypothesis Examined', *Structural Change and Economic Dynamics*, 11: 371-392.

TIMMER, C.P. (2004), *"The road to pro-poor growth: The Indonesian experience in regional perspective"*. Working Paper 38, Center for Global Development, April 2004.

VELOSO, F. AND SOTO, J.M. (2001), *"Incentives, infrastructure and institutions: Perspectives on industrialization and technical change in late-developing nations"*. Technological Forecasting and Social

VON TUNZELMANN, G.N. (1995). *Technology and Industrial Progress: The Foundations of Economic Growth.* Aldershot: E. Elgar Publishers.

VON TUNZELMANN, G.N. (1997). 'Innovation and Industrialization: A Long-Term Comparison', *Technological Forecasting and Social Change*, 56: 1-23.

STURZENEGGER, F. AND E.L. YEYATI (2006), Fear of Floating or Fear of Sinking? Exchange Rate regimes in the 2000s, unpublished paper.

PHYSIO-MECHANICAL ANALYSIS OF FABRICATED PLASTIC INTERLOCK USING RECYCLED WASTE LOW DENSITY POLYETHYLENE (WATER SACHET) FILLED PALM KERNEL SHELL PARTICLES

[1]SANI, M. TAOFEEQ, [2]SALAMI, WASIU OYEYEMI AND [2]ALI, SANI MOHAMMED

[1]Institute of Education, Ahmadu Bello University, Zaria – NIGERIA.

[2]Department of Polymer Technology, Directorate of Polymer and Environmental Technology, Nigeria Institute Leather and Science Technology (NILEST) Zaria – Kaduna State.

Correspondence: sanimtaofeeq@gmail.com; 08030570307

ABSTRACT

Recycled low density polyethylene (used water sachet) was reinforced with palm kernel shell particles as filler at percentage proportion 0, 10, 20, 30, 40, and 50 for production of plastic inter-locks. Six (6) different were produced. Phyco-mechanical analysis such as compression strength, hardness, impact strength, abrasion resistance and water absorption were carried out. The result shows a consistence increase in compressive strength, hardness, abrasion resistance with increasing % palm kernel shell particle from 0% to 50%. This could be due to inherent property of palm kernel shell been a non-compressive material. There is also decrease in the impact strength with increases % palm kernel shell particles loading from 0% to 50%. It was concluded that the sample with 30% filler have good quality for the interlock based on the findings.

Keywords: *Low density polyethylene (water-sachet), Palm kernel shell, Reinforcement, Production and Phyco-mechanical analysis.*

1.0 INTRODUCTION

A lot of waste materials are found littered in most places around the country; some of them are polyethylene bags and agricultural wastes. These wastes are usually in very large amounts; among these are the palm kernel shells, while polyethylene bags form a major eyesore on virtually all streets of the suburbs and even the urban areas.

Annual plastics waste generation in Nigeria increased from 546,537 tonnes in 2001 to 684,400 tonnes in 2008, which is about 11.5% of the total waste generated. However, the recycling rate remained very low at about 13% as compared to other forms of waste (e.g. 12% for food waste; 48% for paper/cardboard; 98% for construction debris; 71% for wood/timber; 42% for horticultural waste; 99% for used slag; 18% for glass; 88% for scrap tyres) Used plastics are usually sent to incineration plants and landfills for disposal, which is a waste of valuable, non-renewable petrochemical resources. (NEA, 2009).

Agricultural wastes residues during harvest seasons in most African countries are enormous and often constitute environmental menace. Most of these materials are lingo cellulosic and could be used as reinforcements in developing composite materials. (Son J.I. *et al*, 2001).

The wide use of plastic products in various applications has greatly increased due to their unique properties, which include good mechanical properties, resistance to chemical attack and corrosion, ease of processing and recycling, cost effectiveness, light weight, and others. However, these properties are affected by many factors such as stress, temperature and environment when they are exposed to service. In fact, this led to vehement objection of plastics in some specific applications. The attempts to overcome these obstacles led to incorporation of fillers (inorganic and organic) into plastics with a view to obtaining a plastic composite whose constituents act synergistically to withstand the challenges, thereby making plastics more reliable during use or processing. Generally, the composite properties are influenced by many factors such as filler characteristics, filler content, and interfacial adhesion and dispersion due to combination of more than one material (Abdullahi *et al.,* 2011).

This research aim is to produce plastic inter-lock using recycled Low density polyethylene 'RLDPE' (waste water sachet) and palm kernel shell particles, with a view to reducing some of the menace of huge volume of agricultural and polymeric waste generation in the country as well as creating of wealth from the wastes.

- Palm kernel is a waste material usually obtained in kernel oil processing. It constitutes environmental pollution due to its low economic value.
- Low Density Polyethylene is one of the most consumable plastic in form of shopping bags and packaging sachets especially the common pure water. Pure water sachets become a big environmental

problem as the water is consumed due to its non-bio-degradable nature.

Therefore, its use in this research will help solving environmental menace cause by this material.

The conventional inter-lock is produced from aggregate of sand, gravel and cement which are costly materials. Hence, the use of waste materials for production of inter-lock could yield a cost effective product that complete favorably with the conventional inter-lock.

Chemical Composition for Palm Kernel Shell

Palm kernel shell can be considered as pellet form because of it nature form, due to its high grade solid, high calorific value, low ash and low sulfur content.

2.0 MATERIALS AND METHODOLOGY

Materials

Table 1: The materials used in this research work and source

S/No	MATERIALS	SOURCES
1	Recycled low density polyethylene (RLDPE)	NILEST, Zaria.
2	Palm kernel shell (particulate filler)	SabonGari Market
3	Processing oil	NILEST, Polymer Recycling Workshop.

Table 2: Chemical Composition of Palm Kernel Shell

PROPERTY	VALUE
Moisture (%)	13
Calorific kg	20100KJ
Sulphur (%)	0.09
Ash (%)	3

Methodology

Sample Collection

Waste water sachets (RLDPE) were sourced from various dump sites in Nigerian Institute of Leather and Science Technology [NILEST], Samaru Zaria while the palm kernel shell was sourced from Ota-Efon village, Oyo east Local Government, Oyo State, Nigeria.

Sample Preparation

The Palm kernel shell was milled on a milling machine to obtain particulate filler. The low density polyethylene was shredded using a shredding machine.

Mixing of Palm Kernel Shell and Recycled (LDPE) Composites

Each sample as shown in the table 3 was mixed on two-roll mill. The shredded waste water sachets were introduced into the nip of the rolls rotating in anti-clockwise direction and allow to run until plastic paste was achieved. The conditions for mixing were temperature 120°C and pressure of 3bar for 10mins. The samples were labeled accordingly.

Formation of Plastic Inter-Locks

The palm kernel shell/recycled LDPE composite was filled into the provided metal mold having a dumbbell shape with dimension. The sample was then pressed on a hydraulic press at temperature of 130°C and pressure of 3bar. Moreover, specimens samples were also prepared by the same method using a mould with a dimension 100mm×100mm×3mm.

Formulation

Table 3: Formulation for palm kernel shell/Recycled Low Density Polyethylene Inter-Locks.

	SAMPLES (g)					
MATERIALS	**A**	**B**	**C**	**D**	**E**	**F**
Recycled LDPE	90	80	70	60	50	100
Palm kernel shell Filler	10	20	30	40	50	0





Sample A **Sample B** **Sample C**





Sample D **Sample E** **Sample F**

Hardness Test

The hardness tests were carried out using the Durometer Hardness tester with model no. 5019 on shore A scale. The sample was placed on the mounting stage and the dial gauge adjusted to zero (0), the hand lever was used to raise the stage such that the sample come in contact with the dial point and exact pressure/force on the sample and the reading was taking. This was repeated three (3) times at different positions on the sample. Average hardness value was determined using the equation

$$\text{Average Hardness} = \frac{1\text{st} + 2\text{nd} + 3\text{rd readings}}{3} \quad \ldots 1$$

Impact Strength

The impact test was carried out to the standard specified by ISO 179 ASTM D-156. Impact strength is the capacity of material to withstand a suddenly applied load and it is expressed in term of the thickness of specimen. The specimen was cut to (50x10) mm at 6mm thickness from all the produced samples.

$$\text{Impact Strength} = \frac{Impact\ energy}{Thickness\ of\ Sample}\ (J/mm) \quad 2$$

Abrasion Test

A known mass of a circular sample was subjected to an abrading surface at a constant revolution/speed for 5minutes each. The percentage weight lost for each tested specimen was determined and recorded after brushing to remove any dust or abrading material adhering to the surface of the specimen. The Percentage weight lost shows in the equation 3.4 was used to express the abrasion resistance of the material tested.This is the resistant of a material or sample wear.

$$\%\ \text{Weight Remaining} = \frac{wf - wi}{Wi} x\ 100\% \quad 3$$

where; W_i= Initial weight (g)
Wf = Final weight (g)

Percentage Water Absorption

The specimens were prepared with dimension 50mm x50mm x 3mm. Water absorption test (ASTM D570) was done by total immersion of specimens in distilled water at room temperature for 7 days. The water absorbed was determined by weighing the samples at regular intervals of 12hrs, with the aid of digital weighing balance. The water adhering on the surface of the specimen was carefully wiped off using filter paper. The water uptake in the composite was measured by the weight gain method of the material using the equation below;

% Water absorbed = $Wf - W \,/_{Wi}\; x\; 100\%$ 4

where; Wi= Initial weight (g)

W_f= Final weight (g)

3.0 RESULTS AND DISCUSSIONS

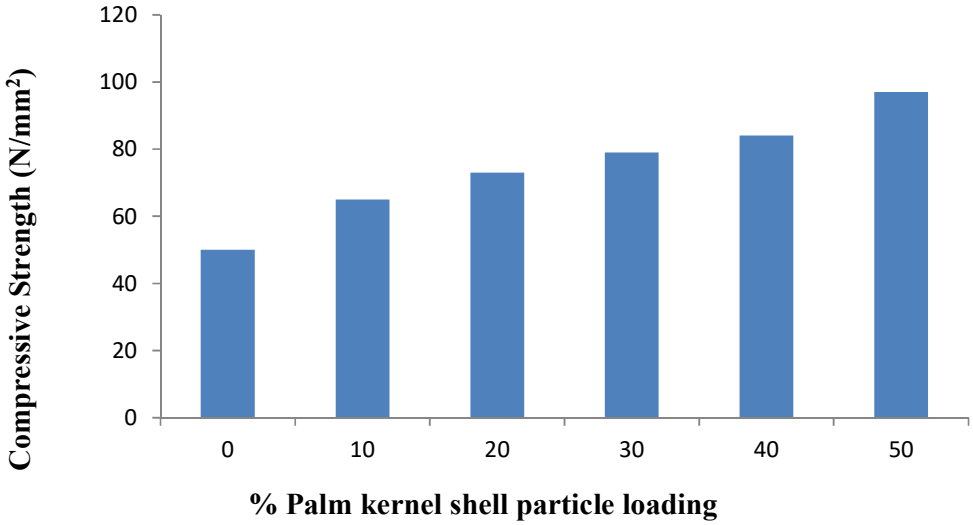


Fig. 1: Compressive strength test result for the produced plastic inter-lock

Compressive strength describes the strength of a material to withstand inward stress (Cooke, 19901). The result shows a consistence increase in compressive strength with increasing % palm kernel shell particle from 0% to 50%. This could be due to inherent property of palm kernel shell been a non-compressive material(Adewuyi, 2008).The inter-lock samplesproduced show compressive strength above 55N/mm2 the require standard for heavy duty vehicle (ESS4382-1/2004).

Hardness property of material describes it ability to resist indentation (Cooke, 1991). A consistent increase in hardness was observed with increasing filler loading from 0% to 50% respectively.The consistent in hardness properties of the composite with increased % filler loading could be related to the fact that palm kernel shell which a hard material in the polymer matrix may stiff the polymer core making it more resistance to indentation (Isiaka, *et al.* 2013).

Impact Strength is a property of material that describes amount of energy it can absorb before it fracture and the higher the impact strength the better the material(Aisien, 2014).The result as shows a steady decrease in the impact strength with increases % palm kernel shell particles loading from 0% to 50%. This could be due to decreasing in ductility of the samples as the filler loading increase (Isiaka, *et al.* 2013).

Abrasion resistance is ability of material to resist wear under constant shear force (Cooke, 1991). Percentage weight lost was used to express abrasion resistance of the produced inter-lock samples. The lower the percentage weight lost the better the material abrasion resistance. It was observed that the percentage weight lost of the samples decreased with increasing palm kernel (PKS) particle loading from 0% to 50%. However, the sample filled 30% PKS shows the least percentage weight lost among others. Hence, the sample filled with 30% PKS shows better abrasion resistance among other samples. The better abrasion resistance observed at the samples filled with 30% PKS could due to proper filler-matrix distribution and strong interfacial adhesion that could have formed in the composite since filler–matrix composition has effect on the distribution and interfacial adhesion of the filler and the matrix as evident by (Josmin, 2012).

Percentage water absorption is the extent to which a material can absorb water in liquid or gaseous form (vapour) during service life (Cooke, 1991). Lower percentage water absorption of a material is an indication of better water absorption property of the material. The results obtained shows that the percentage water absorption of the samples increase progressively with increasing % PKS loading from 0% to 50%. The progressive increased in water absorption could be related to the fact that palm kernel shell is an agro-filler which is expected to have possibility of moisture absorption property (hydrophilic) (Abdullah et. al, 2011).

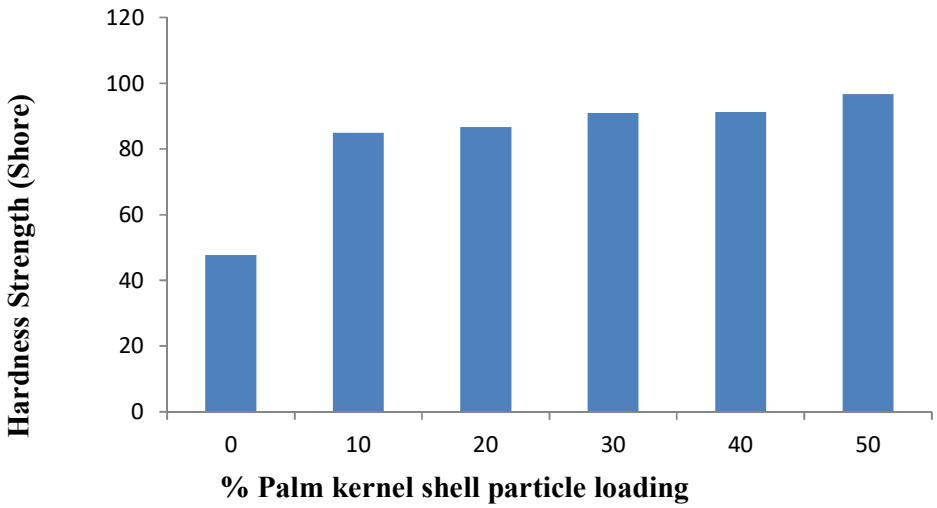


Fig. 2: Hardness strength test result for the produced plastic inter-locks

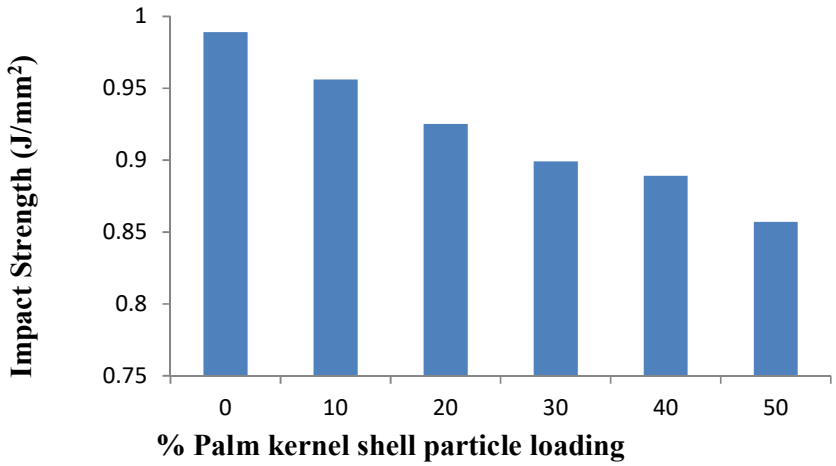


Fig. 3: Impact strength test result for the produced plastic inter-locks

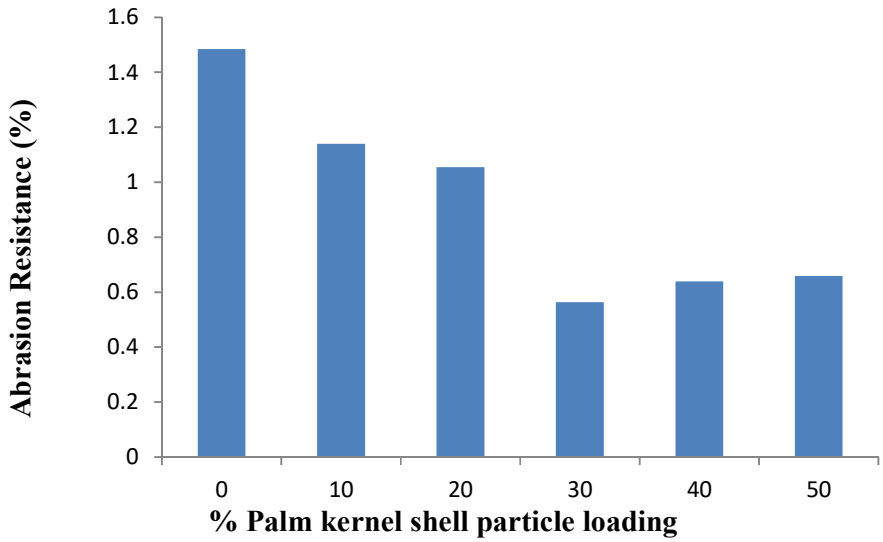


Fig. 4: Abrasion resistance test result for the produced plastic inter-locks

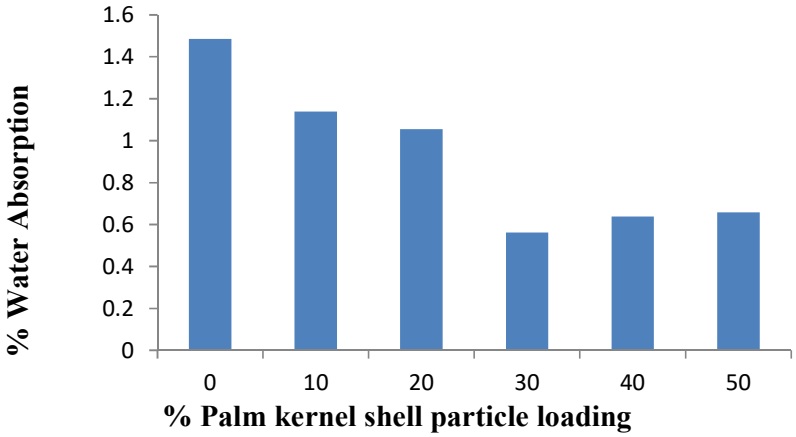


Fig. 5: Percentage water absorption test result for the produced plastic inter-locks

Table 3: Summary of the average results obtained and required standard for concrete inter-lock

Property	Result Obtained for the Plastic Inter-lock Produced						Required Standard Property for Inter-lock (ASTM C-140)
	Contr.	A	B	C	D	E	
Compressive Strength (N/mm^2)	50.00	65.00	73.00	79.00	84.00	97.00	55
Hardness Strength	47.7	85.0	88.67	91.00	91.33	96.67	Not less than 80
Izod Impact Strength (J/mm)	0.989	0.956	0.925	0.899	0.889	0.854	-
Abrasion Resistance (%)	1.485	1.140	1.055	0.563	0.639	0.659	Not exceed 3mm/1.05 lost in thickness or % mass
Water Absorption (%)	0.319	0.447	0.570	0.887	1.125	1.170	Not greater than 7%

4.0 CONCLUSION

This research reveals that reinforced low density polyethylene (water satchet) and palm kernel shells can also be used for interlock when compared with the conventional concrete interlock standard. The result shows a consistence increase in compressive strength with increasing % palm kernel shell particle from 0% to 50%. A consistent increase in hardness was observed with increasing filler loading from 0% to 50% respectively. The result as shows a steady decrease in the impact strength with increases % palm kernel shell particles loading from 0% to 50%. It was observed that the percentage weight lost of the samples decreased with increasing palm kernel (PKS) particle loading from 0% to 50%. The results obtained shows that the percentage water absorption of the samples increase progressively with increasing % PKS loading from 0% to 50%.

RECOMMENDATION

From this research work, it is recommended that palm kernel filled low density polyethylene(LDPE) should be used for the production of interlock from its comparison with the concrete composite. And more work on the properties of the produced interlock samples are still in progress like the FTIR, SEM, Weathering etc.

5.0 ACKNOLWEDGEMENT

The authors wish to express their gratitude to the staff of the Directorate ofPolymer and Environmental Technology, Nigerian Institute of Science and Leather Technology (NILEST), Zaria

– Nigeriafor their patience, hospitality and contribution to ensure the research success.

6.0 REFERENCE

Abdullah, A.H, Russell, D.S, and Abdulwahab, A.S. (2011) Particle reinforced polymers, *J. Bas. Res (Sci),* 37(3A), 36-42).

Adewuyi, A. P. and Adegoke, T. (2008) Exploratory Study of Periwinkle Shells as Coarse Aggregate in Concrete Works.Journal *Science Resources.* 4(12):1678-1681.

Aisien, F. A, Amenaghawon, N. A, Oshomogho, F. O (2014)Application of periwinkle shell ash as photocatalyst in the heterogenousphotocatalytic degradation of aniline in aqeoussolution.J. *Mat. Environ. Sci.* 6(2) (2014) 572-579.

American Society for Testing and Materials (1993) - Standard Test Methodfor Determining Aerobic Biodegradation of Plastic Materials under Controlled Composting Conditions - *ASTM D 5338-92 Annual Book of ASTM Standards*

Cooke, T.F. (1991) Biodegradability of Polymers and Fibers- A Review of the Literature.*Journal of Polymer Engineering*. 9: 171-211.

Isiaka, .O.O, and Temitope, .A.A. (2013): Influence of Cow Bone Particle Size Distributionon the Mechanical Properties of Cow Bone-Reinforced Polyester Composites.*Biotechnology Research International* Volume 2013, Article ID 725396, 5 pages.

National Environment Agency (NEA). (2009). *Environment information: waste minimization -data and statistics.* Retrieved Mar. 6, 2009, from: http://app.nea.gov.sg/cms/htdocs/article.asp?pid=2706

A NEW APPROACH TO ROBUST IMAGE WATERMARKING ALGORITHM USING DISCRETE ORTHONORMAL STOCKWELL TRANSFORMATION TECHNIQUE

B. A. JIBRIN [1], S. M. SANI [2] AND A. M. S. TEKANYI [3],
Department of Electrical and Computer Engineering, Ahmadu Bello University, Zaria
bjabba4real@gmail.com, smsani@abu.edu.ng, amtekanyi@abu.edu.ng

ABSTRACT
Digital multimedia data are rapidly spreading everywhere due to advances in computer networking and high speed computer processors. This spread has brought about problems of unauthorized duplication, distribution, and manipulation of multimedia data. To address these problems requires copyright protection using techniques like digital image watermarking. This is a process of embedding code or some watermark information into image without affecting its visual quality. Therefore, this paper developed an image watermarking algorithm to mitigate both signal processing manipulations and geometric attacks on watermarked images. The novelty in this work from the traditional transformation algorithms used in image watermarking standards was the introduction of Discrete Orthonormal Stockwell Transform (DOST) for more efficient image decomposition and energy de-correlation and Arithmetic Progression (AP) technique to eliminate the need for scaling factor. The developed watermarking algorithm was implemented using MATLAB R2015b and its performance on three standard images of Lena, Baboon, and Barbara was evaluated against the traditional watermarking scheme using Peak Signal to Noise Ratio (PSNR) as performance indices and it was found better in both robustness and imperceptibility.

Keywords: *Digital Image Watermarking; Discrete Orthonormal Stockwell Transform; PSNR; DWT; DCT; SVD; MSE*

1.0 INTRODUCTION

Advances in computer networking and high speed computer processors have made unauthorized duplication and distribution of multimedia data easy and virtually costless and have also made copyright protection of digital media an ever urgent challenge. An effective way for copyright protection is digital watermarking, a process which embeds (hides) a watermarked signal in the host signals to be protected (Sinha et al., 2014). Such information is embedded for many different purposes such as copyright protection, source tracking, telemedicine, piracy deterrence, etc., and therefore it is embedded in a way that makes it difficult to be removed (Nin & Ricciardi, 2013). At the same time, the watermark should not transform the content of the work and it should be practically impossible for illicit users to remove or alter it (Bansal et al., 2016). Watermarking techniques can be divided into four categories based on the type of information to be watermarked, namely: text watermarking, image watermarking, audio watermarking, and video watermarking (Sinha et al., 2014).

There are two types of digital image watermarking schemes, that is, visible watermarking and invisible watermarking. The invisible watermarking requirements are imperceptibility and robustness. Similarly, the requirements of visible watermarking should be perceptibility, ease of identifying the hidden data (Santhi & Arulmozhivarman, 2013). A variety of techniques have been proposed for copyright protection of digital images which include spatial domain and transform domain watermarking (Sinha *et al.*, 2014). Figure 1 shows categories of digital image watermarking techniques.

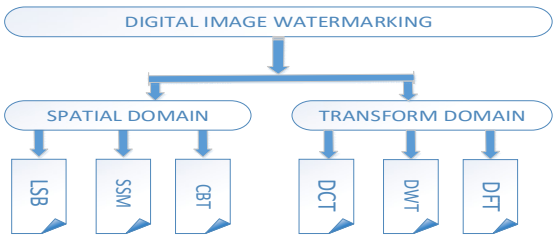


Figure 1: Digital Image Watermarking (Chahal & Khurana, 2013)

Simplicity and ease of implementation are the two advantages provided by spatial domain algorithms over transform domain watermarking algorithms (Zheng *et al.*, 2007). Spatial domain algorithms are less robust than other types of watermarking algorithms because they are more vulnerable to noise attacks, compression, or filtering due to watermark insertion in selected locations of the image. The spatial domain techniques include Least Significant Bit (LSB), Spread Spectrum Technique (SSM) and Correlation Based Technique (CBT) (Lai & Tsai, 2010). On the other hand, the transform domain technique is more robust and compatible to popular image

compression standards than that of spatial domain. The transform domain techniques include Discrete Cosine Transform (DCT), Discrete Wavelet Transform (DWT), and Single Value Decomposition (SVD) (Chahal & Khurana, 2013). The information hiding and extraction operation of these transform algorithms is relatively complex, but due to its strong anti-attack ability, it is suitable for the copyright protection of digital works (Li *et al.*, 2010). Although some of these methods present a robust technique against attacks, they do not preserve quality of host image after embedding in a transform domain. Some methods have a high performance for imperceptibility, but they are not robust enough against different attacks. Therefore, this work is developing a new algorithm for image watermarking against attacks using Discrete Orthonormal Stockwell Transformation (DOST) technique which will improve performance on both imperceptibility and robustness, simultaneously.

1.1 Review of Similar Works

A number of studies have been conducted on image watermarking algorithm in frequency domain such as: **Kashyap and Sinha, (2012)** implemented 2-level 2-D DWT based image watermarking algorithm, in which the watermark was embedded using alpha blending technique. In this algorithm, a host image was decomposed using 2-level 2-D DWT. Watermark image was also decomposed using 2-level 2-D DWT. The decomposed 2-level Low-Low (LL) frequency components of the host image and that of watermark image were multiplied by a scaling factor and then added using alpha blending formula, then finally inverse 2-level 2-D DWT was applied to obtain watermarked image. The performance of the algorithm was tested using gray scale standard images of Lena image as original image and cameraman image as the watermark image, both the images were of equal size of 256×256. The values of MSE and PSNR were calculated for different values of the scaling factors. Experimental results showed that the quality of the watermarked image was dependent only on the scaling factor. The work did not consider the robustness and imperceptibility of the algorithm against intentional and unintentional attacks, which was its problem.

Singh et al., (2014) proposed a new robust image watermarking approach in transform domain for image authentication using DWT, DCT, and SVD. In this algorithm, DCT was applied over DWT to improve imperceptibility and robustness. 1-level 2-D DWT was applied to decompose the host image and it was followed by applying DCT and SVD on the High-High (HH) sub-band of the decomposed 1-level 2-D DWT host image. The SVD watermark image was embedded into SVD host image using orthogonal matrix to get the final watermarked image. The algorithm was complex and when the watermark data was embedded in high frequency components of the image, high frequency content of an image behaved like added noise and therefore noise removal algorithms such as filtering and sharpening destroyed it.

Ahmad et al., (2014) implemented image watermarking algorithm in transform domain using DWT. The host image and the watermark image were decomposed using 3-level 2-D DWT and then embedded LL sub band of decomposed watermark image into the LL sub band of decomposed host image using alpha blending technique. The performance of the algorithm was evaluated using PSNR. The algorithm recorded high performance for no attack cases. When attacks were applied, especially JPEG compression, by adding noise and filtering attacks, the watermarked image quality was below the minimum required level of 30 dB.

Rahman and Rabbi, (2015) designed the image watermarking algorithm in transform domain using combination of DWT and SVD with decomposition error. In this approach a host color image was separated into three respective color bands namely R G, and B and 4-level 2-D DWT was applied to decompose R band of the host image. SVD technique was applied to watermark matrixes and then embedded into the HL sub band of the decomposed R band of the host image and finally the inverse 4-level 2-D DWT was applied to obtain the watermarked image. The performance of the algorithm was evaluated using RGB image of size 512×512 as a host image and secret matrixes of size 64×64 as a watermark image. The designed scheme registered less robustness against attacks such as rotation and Gaussian high pass filtering with PSNR values not above the 30dB required by robust algorithm.

Malonia and Agarwal, (2016) proposed a digital image watermarking scheme in frequency domain using DWT and AP algorithms. This technique inserted the binary watermark bits into the host image using AP. In the embedding process, 1-level 2-D DWT was applied to decompose RGB host image and then watermark bits were embedded into the HH, HL, and LH sub bands of the decomposed host image. The performance was tested using different host standard images of Lena, Baboon, and Barbara of size 512 × 512 and a QR code image of size 48 × 48 as watermark image. The result showed that by applying different signal processing manipulations and geometric attacks on watermarked images, the technique revealed that the PSNR and SSIM

values were above 50 dB and 0.2, respectively.
It is evident from the reviewed literatures that the effects of both geometric attacks and signal processing manipulations on watermarked images are major challenges in digital image copyright protection. Consequently research has focused on developing robust algorithms to mitigate these effects using 2-D transformation algorithms such as: DCT, SVD, DWT or combinations of two or all of these transform methods for image transformation and these have been identified to possess limited properties that make them less efficient. Therefore, the algorithm in this research employs Discrete Orthonormal Stockwell Transform (DOST) to achieve improved robustness and imperceptibility of watermarked image.

1.2 Discrete Orthonormal Stockwell Transform

The Discrete Orthonormal Stockwell Transform (DOST) is an orthonormal version of the Discrete Stockwell Transform (DST) capable of producing N-point time-frequency representation for a signal of length N. The DOST reduces the information redundancy of the DST to zero and leads to the maximum efficiency of each representation. The DOST is defined as an inner product between a time series $h(.)$ and a set of orthonormal functions $D[k]_{[v,\beta,\tau]}$ defined as Wang & Orchard, (2009);

$$D[k]_{[v,\beta,\tau]} = \frac{1}{\sqrt{\beta}}\sum_{f=v-\frac{\beta}{2}}^{v+\frac{\beta}{2}-1} exp^{-2\pi\frac{k}{N}f}\, exp^{i2\pi\frac{\tau}{\beta}f}\, exp^{-i\pi\tau} \quad (1)$$

where the parameters v, β, and τ represent the center frequency, bandwidth, and time of the function, respectively. If the parameters are chosen so that the different values of v and β do not overlap in frequency, and $\tau = 1,2,\dots,\beta$ -1, then the function is orthonormal. Here to ensure the orthogonality of thet functions, v, β and τ must satisfy the following conditions (Wang & Orchard, 2009):

i. τ=0, 1, 2,…, β -1.
ii. v and β must be selected such that each of frequency sample is used once and only once.

1.3 Arithmetic Progression Technique

The Arithmetic Progression (AP) is a sequence of numbers with finite terms, where every next term is generated by adding a constant known as common difference to the previous term. Common difference of an AP is the difference between two consecutive terms (Malonia & Agarwal, 2016) and it influences the nature of arithmetic progression. Generally, a represents the first term of the sequence, d represents common difference between successive terms. Therefore, first sequence can be written as; $\mathrm{a}, \mathrm{a}+\mathrm{d}, \mathrm{a}+2\mathrm{d}, \dots . a+[(n-1)\times d]$. The nth term of the sequence (Malonia & Agarwal, 2016) is expressed as:

$$n^{th} = a + [(n-1)\times d] \quad (2)$$

In this work, the positions of the binary watermark bits to be inserted into the host image are replaced by the binary watermark bits using the following equations (Malonia & Agarwal, 2016):

$$d(j) = [z(j) - au(j) \div (n-1)] \quad (3)$$
$$au(j) = a + [1.5\times(j+1)] \quad (4)$$
$$z(j) = zm - [5.5\times(j-1)] \quad (5)$$
$$an(j) = au(j) + [(j-1)\times d(j)] \quad (6)$$

where; $d(j)$ is the common difference, a is first position of the sub band which is 1, zm is the last position of the sub band which is 256, n is the number of terms, which is 3, $au(j)$ is the first term of the sub band of the host image, $z(j)$ is the last term of the sub band of the host image, $an(j)$ is the positions to be replaced by binary watermark bits, $j = 1\ to\ 8$, after every 8th row positions are repeated.

Equations (3), (4), (5), and (6) are used to locate the pixel positions of the sub band to be replaced with the watermark bits during the embedding process.

2.0 DEVELOPED ALGORITHM

The following are the steps and procedures followed to develop the algorithm used in this work:

i. Conversion of any RGB digital image of size 512×512 into grey scale.
ii. Conversion of the watermark image into binary image of size 48×48.
iii. Reshaping the binary watermark to 1×2304 and again to 3×768 elements, take 1×768 element and reshape it into 256×3 elements that are to be inserted into each high frequency sub band.
iv. Decomposition of the grey scale image using 2-D DOST algorithm to obtain an array of transformed coefficients.
v. Embedding the watermark bits (256×3) into each of the transformed DOST high frequency sub bands using AP by locating the positions in the sub band to be replaced with the watermark bits.
vi. Performing inverse 2-D DOST to

obtain the watermarked image.

vii. Application of the attacks such as addition of noise, rotation, and cropping to the watermarked image:.

The flowchart of the developed algorithm is shown in Figure 2.

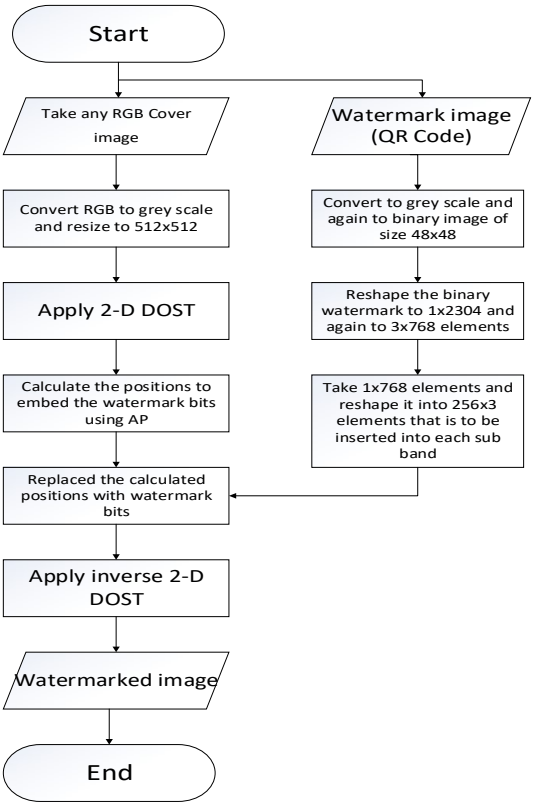


Figure 2: Flowchart of developed algorithm

3.0 RESULTS AND DISCUSSION

4.0

This section, simulation was done in MATLAB R2015b software environment using Laptop (Toshiba with Intel(R) core(TM) i5 processor). Three RGB images of Lena, Baboon, and Barbara of size 512 x 512 are selected as host image and a Quick Response (QR) code image was used as watermark information. Figure 3 shows the host images and Figure 4 shows the watermark image.

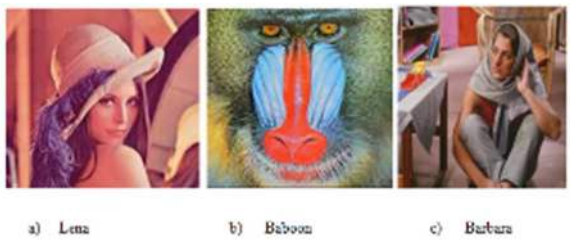


Figure 3: Host Standard Images



Figure 4: QR Code (Watermark Image)

Figure 5 shows the watermarked images without attack. It can be observed that the developed method preserves the perceptual quality of the watermarked mage.

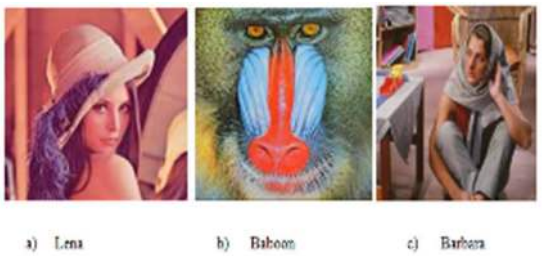


Figure 5: watermarked images without attack

The developed watermarking algorithm was tested to investigate the robustness of the algorithm by subjecting the watermarked images against attacks such as noise addition, rotation, and cropping. Figure 6 shows the attacked watermarked images, where Figure 6(a) was Gaussian noise (mean = 0 and variance = 0.01) attack, (b) rotation (45°) attack, and (c) cropping attack

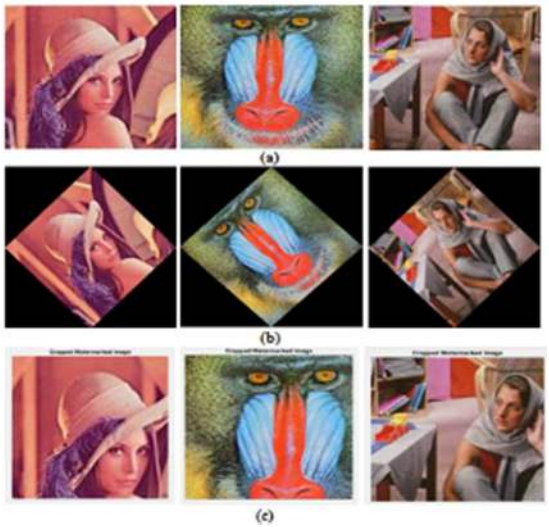


Figure 6: Attacked Watermarked Images

The developed algorithm was evaluated using two metrics, that is, imperceptibility and robustness. The imperceptibility and the robustness of the watermarked images were tested using PSNR

PSNR is a mathematical measure of image quality and is calculated between the original host image and watermarked image. The higher the value of the PSNR, the more similar is the watermarked image to the original host image. This metric is defined in decibels (ITU-T Rec. J.147, 2002):

$$PSNR = 10log_{10}\frac{255\times255}{MSE} \quad (7)$$

$$\text{MSE} = \frac{1}{M \times N}\sum_{i=1}^{M}\sum_{j=1}^{N}(X(i,j) - X'(i,j))^2 \quad (8)$$

where: $X(i,j)$ is original image, $X'(i,j)$ is watermarked image, M is numbers of row in the image, and N is numbers of column in the images.

If the PSNR value is equal to or greater than 35dB then the perceptual quality of the algorithm is acceptable (ITU-T Rec. J.147, 2002).

Table 1 shows the PSNR values in dB of Lena, Barbara, and Baboon standard images with different attacks

TABLE 1: PSNR VALUES OF LENA, BARBARA, AND BABOON IMAGES

Attacks	**Lena**	**Baboon**	**Barbara**
Without Attack	82.4785	80.8988	79.9666
Gaussian noise	71.8381	72.5356	74.1824
Rotation	64.2520	64.2862	65.1868
Cropping	77.5877	78.7436	76.1862

5.0 CONCLUSION

In this work, a novel technique of image watermarking algorithm based on Discrete Orthonormal Stockwell Transform (DOST) and Arithmetic Progression (AP) technique in RGB color space is developed. This technique applied the DOST to make the watermarking scheme more robust against various attacks and more imperceptible. Therefore, the developed algorithm has been applied on three host standard images with size of (512×512) and watermark logo with size (48×48). The performance of the developed algorithm was evaluated using PSNR as performance metrics. Simulation results show that this method is robust against various types of attacks.

REFERENCES

Ahmad, A., Sinha, G., & Kashyap, N. (2014). 3-Level DWT Image Watermarking Against Frequency and Geometrical Attacks. *International Journal of Computer Network and Information Security, 6*(12), 58.

Bansal, R., Romita, & Shikha, S. (2016). Digital Image Watermarking Techniques: Review. *International Journal of Emerging Technology and Advanced Engineering, 6*(3), 717-724.

Chahal, J. S., & Khurana, S. (2013). A Review on Digital Image Watermarking. *International Journal of Emerging Technology and Advanced Engineering, 3*(12).

ITU-T Recommendation J.147 (2002), Objective picture quality measurement method by use of in-service test signals.

Kashyap, N., & Sinha, G. (2012). Image watermarking using 2-level DWT. *Advances in Computational Research, 4*(1), 42-45.

Lai, C.-C., & Tsai, C.-C. (2010). Digital image watermarking using discrete wavelet transform and singular value decomposition. *IEEE Transactions on instrumentation and measurement, 59*(11), 3060-3063.

LI, H.-f., CHANG, N., & CHEN, X.-m. (2010). A study on image digital watermarking based on wavelet transform. *The Journal of China Universities of Posts and Telecommunications, 17*, 122-126.

Malonia, M., & Agarwal, S., Kumar. (2016). Digital Image Watermaking using Discrete Wavelet Transform and Arithmetic

Progression Technique. Paper presented at the *2016 IEEE Students' Conference on Electrical, Electronics and Computer Science*. 5638-4265.

Nin, J., & Ricciardi, S. (2013). Digital watermarking techniques and security issues in the information and communication society. Paper presented at the *Advanced Information Networking and Applications Workshops (WAINA), 2013 27th International Conference on*. 1553-1558.

Rahman, M. A., & Rabbi, M. F. (2015). DWT-SVD based New Watermarking Idea in RGB Color Space. *International Journal of Signal Processing, Image Processing and Pattern Recognition, 8*(6), 193-198.

Santhi, V., & Arulmozhivarman, P. (2013). Hadamard transform based adaptive visible/invisible watermarking scheme for digital images. *Journal of Information Security and Applications, 18*(4), 167-179.

Singh, B., Sharma, K. D., & Jatav, L. S. (2014). New robust watermarking approach for image authentication. Paper presented at the *2014 IEEE 3rd Global Conference on Consumer Electronics (GCCE)*. 285-288.

Sinha, M. K., Rai, R., & Kumar, G. (2014). Literature survey on digital watermarking. *International Journal of Computer Science and Information Technologies, 5*(5), 6538-6542.

Wang, Y., & Orchard, J. (2009). On the use of the Stockwell transform for image compression. Paper presented at the *IS&T/SPIE Electronic Imaging*. 724504-724504-724507

Zheng, D., Liu, Y., Zhao, J., & Saddik, A. E. (2007). 0360-0300. ACM Computing Surveys (CSUR).

ENHANCEMENT OF SELECTIVE MAPPING TECHNIQUE FOR PEAK-TO-AVERAGE POWER RATIO REDUCTION IN OFDM USING NORMALIZED HILBERT MATRIX

[*]H. I. YARIMA, A. M. S. TEKANYI, S. M. SANI AND M. B ABDULRAZAQ
Department of Electrical and Computer Engineering, Ahmadu Bello University, Zaria.
[*]yarimahindu@yahoo.com, amtekanyi@abu.edu.ng,smsani@abu.edu.ng, mbashiray@yahoo.co

ABSTRACT
One of the obstacles of Orthogonal Frequency Division Multiplexing (OFDM) is high Peak-to-Average Power Ratio (PAPR) of the transmitted signal, which results in signal distortion and reduced power amplifier efficiency. There are many techniques to reduce the PAPR values, one of them is Selective Mapping (SLM) technique. However, the performance of this technique in term of PAPR reduction is largely affected by the magnitude of phase rotation vectors. It also requires to transmit the selected phase rotation vectors that produce the signal with the lowest PAPR to the receiver end for the recovery of the original data. In this paper, two normalization procedures in conjunction with the Hilbert matrix are used to obtain phase rotation vectors for the SLM technique to further reduce the PAPR value. The reduction of PAPR is desirable in order to have a better power efficiency of the amplifier. Simulation results indicate that this method achieved much desirable PAPR reduction than any technique. Another benefit of this enhanced technique was that, the Hilbert matrix can be generated at the receiver end to obtain the data signal, thus eliminating the transmission of side information with the original data

Keywords: *Peak-to-Average Power Ratio, Selective Mapping, Normalization, Hilbert Matrix*

1. INTRODUCTION

Orthogonal Frequency Division Multiplexing (OFDM) is an excellent multicarrier technique for high data transmission. It is used for high speed communication systems. OFDM has many benefits such as high spectral efficiency, high transmission rate, and elimination of inter symbol interference. It has already been adopted as the standard transmission technique in the IEEE802.11a wireless LAN systems, Digital Audio Broadcasting (DAB), and Digital Video Broadcasting (DVB) for next generation mobile communication systems. The OFDM signals can be modulated and demodulated using Inverse Fast Fourier Transform (IFFT) and Fast Fourier Transform (FFT) (Sudha*, V*, 2015).

The most prominent demerit of an OFDM system is that it suffers high Peak–to–Average Power Ratio (PAPR). An OFDM signal comprises of a large number of individual modulated subcarriers, which can give rise to a large PAPR when summed up constructively. When N signals aligned in phase they yield a high instantaneous power that is N times the average power. Large PAPR of the transmitted signals results in non–linear distortions of signals, clipping of signals, Bit Error Rate (BER) performance degradation, energy leaking into adjacent channels, inter modulation effects on the subcarriers, as well as increased complexity of the analogue to digital and digital to analogue converters (Girija, *et al.,* 2014). Therefore, it is useful to reduce the PAPR of OFDM systems. To combat the problem of high PAPR, various techniques/schemes have been suggested in literature. The reduction schemes can be categorized into distortion and distortion less schemes. Clipping and filtering fall under distortion schemes. The distortion-based schemes minimized the PAPR of the OFDM symbol but at the expense of increasing clipping to the signal points in the subcarriers (Raja *et al.,* 2015). Distortion schemes are considered to introduce bandwidth re-growth. They do not need any overhead side information to be sent to the receiver and they have low complexity compared to the distortion-less schemes, such as Selective Mapping (SLM) and Partial Transmit Sequence (PTS). Distortion-less schemes do not host bandwidth re-growth but they need transmitted overhead side information.

In SLM technique, modulated data is multiplied with phase rotation vectors then time-domain conversion takes place through IFFT after that PAPR is calculated and finally, signal with minimum PAPR is selected for transmission.

Wang, (2010) proposed the scheme with SLM using randomness in phase sequence selection. This scheme obtained significant PAPR reduction performance with that of ordinary SLM techniques. However, the work did not address the

effect of large magnitude of phase rotation vectors on performance of SLM in terms of PAPR reduction, which results in high power consumption by amplifier in OFDM system. Palanivelan *et al.,* (2011) employed Circulant, Hadamard, and Hilbert matrices to obtain phase rotation vectors for the SLM techniques. Experimental results showed that Hilbert matrix's approach outperformed the other two matrices in terms of PAPR reduction. It is noteworthy that the researchers used the Hilbert matrix without normalization, moreover, the problem of large magnitude of phase rotation vectors which affects the performance of SLM, resulting in deterioration of power in OFMD transceiver was not considered. Florence and Kumari, (2013) reduced the PAPR by using Hadamard SLM technique in a Multiple Input Multiple Output (MIMO) OFDM system. In this research work, the input sequence was convolved by a set of phase sequence and Hadamard transform was applied to each of the sequence. IFFT operation was then used to get the time domain signal. Computer simulations were carried out using 64 subcarriers, 16-Quadrature Amplitude Modulation (QAM), and oversampling factor of L = 4. This method had lower computational complexity. . However, no normalization was done and therefore the effect of large magnitude of phase rotation vectors on performance of SLM in term of PAPR reduction still existed.

In the conventional SLM, the performance of SLM in terms of PAPR reduction is largely affected by the magnitude of Phase Rotation Vectors (PRV) used to generate the candidates signals. Large magnitude phase rotation vectors results in the escalation of amplitudes of signals when summed up coherently, thus leading the signal to exhibit peak power. Signals with peak power affect the power amplifier efficiency used in the OFDM transceiver. In this research work, two different normalization procedures are applied on Hilbert matrix in order to reduce the magnitude of the matrix before using it is rows as PRV. Data blocks were then multiplied with PRV in order to lower the amplitudes of generated signals before their summation at the transmitter and the process leads to further reduction of PAPR.

1.1 OFDM System Model

For OFDM system implementation, IFFT is usually used to modulate its multiple sub-band signals. The source data symbols are sent via serial to parallel converter and modulated with the help of modulation techniques like Quadrature Phase Shift Keying (QPSK), Quadrature Amplitude Modulation (QAM), and Binary Phase Shift Keying (BPSK) to construct a complex vector of size N. The single signal bit is split into N different parallel paths. The N points IFFT and FFT operations are used to modulate and demodulate the data and the resulting complex vector is written (Harne and Zanjade, 2016). as:

$$X=[Xo,X_1,X._{N-1}] \quad (1)$$

where:
X is OFDM data block.
Xo, X_1, $X._{N-1}$ are sequence symbols of the OFDM data block.

In mathematical form, for $0 \le n \ge N-1$, the OFDM symbol is denoted (Harne and Zanjade,(2016) as:

$$x(n) = \frac{1}{\sqrt{N}} \sum_{k=0}^{N-1} X_k \, e^{j2\pi \frac{n}{N}} \quad (2)$$

where:
x(n) is a digital time of OFDM signal vector
$X_{(k)}$ is input data symbol
N is number of subcarriers.
n is an odd integer value.

1.2 Orthogonality in OFDM

OFDM is a superior type of digital multiplexing technique which is mainly desirable for transmitting information over a harsh channel. Diverse carriers are orthogonal against each other by completely standing alone against each other. Two periodic signals are orthogonal if the integral of their multiplication over one complete cycle is equal to zero (Gupta *et al.,* 2013) and for continuous time signals, they are expressed mathematically as:

$$\int_0^T \cos(2\pi nft)\cos(2\pi mft)dt = 0 \quad (3)$$

And, for discrete time signals, the expression of equation (3) becomes:

$$\sum_{k=0}^{N-1} \cos\left(\frac{2\pi kn}{N}\right)\cos\left(\frac{2\pi kn}{N}\right)dt = 0 \quad (4)$$

where:
m is even integer value.
n is odd integer value.
N is number of sub carriers.
t is time for sub carrier to complete one cycle.
f is frequency of sub carrier.

Orthogonality in the context of an OFDM system simply means that two signals are precisely separable in frequency domain by fourier transform as shown in Figure 1.

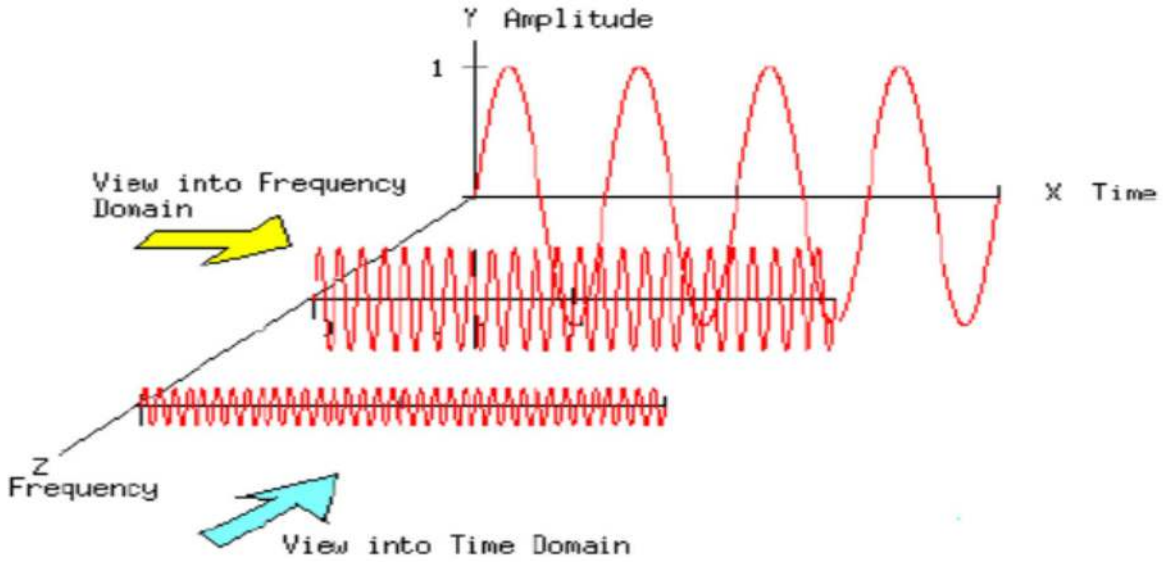


Figure 1: Two Views of OFDM Signal Mukhtar, 2016)

.

1.3 PAPR of OFDM Signal

The PAPR of the transmitted signal $X_{(m)}$ can be express as the ratio of the peak instantaneous power of the signal to average power of the signal. Mathematically, the PAPR of complex pass band signal X_m is written (Kwesi *et al.,* 2015) as:

$$PAPR(X_m) = 10\log_{10}\frac{\max|X_m|^2}{E\left[|X_m|^2\right]} \quad (5)$$

where:

Max $|X_m|^2$ is the peak signal power.

E $[|X_m|^2]$ is the average signal power.

The peak value arises if the number of subcarriers escalates and the peak value is directly related to the amount of subcarriers of the OFDM system (Kwesi *et al.,* 2015). OFDM signal comprises of a number of independently modulated subcarriers, which can give rise to a high PAPR when summed up together. When N signals aligned in phase, they yield a high power that is N times the average power and a large PAPR of the transmitted signals leads to many problems highlighted in the last sentence of the first paragraph in the introduction section.

2. MATERIALS AND METHODS

2.1. Selected Mapping (SLM)

SLM technique was first described by Bauml *et al.,* (1996), the input data sequences are multiplied by each of the phase rotation vectors to generate dissimilar candidates data blocks all representing the same information as the original data block. Each of these candidates' data blocks pass through IFFT operation and then the one with the lowest PAPR is selected for transmission. A block diagram of the SLM technique is shown in Figure 2. Each data block is multiplied by B number of different phase sequences, each of length N of subcarriers, resulting in B number of modified data blocks.

2.2. Block Diagram of SLM

In the midst of the phase generated OFDM data blocks, the one with the minimum PAPR is chosen and transmitted. The scheme can handle any number of subcarriers, it minimizes PAPR without any signal distortion, support all modulation schemes, and PAPR minimization effect is better as the copy of block number U is increased. The setback of this scheme is that, it requires side information to be sent to the receiver (Harne and Zanjade, 2016) to enable the recovery of the original data. Moreover, the performance of this technique is also largely affected by design of phase rotation vectors used in generation of candidates data blocks.

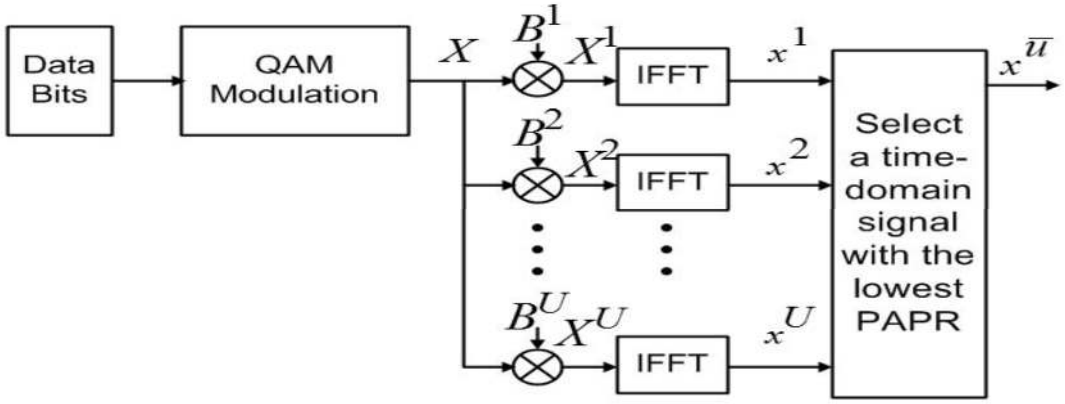


Figure 2: Block Diagram of SLM Technique (Adegbite, *et al*., 2014*)*.

One of the crucial aspects of the SLM technique is the selection of right phase sequence which is random in the presence of phase sequence sets. For instance, in Cheng *et al*., (2007), the shapiro-rudin sequence created recursively.This is also applied to the case of the phase sequence set explained by Bauml, (1996) which is the initial random sequence, and many other researchers. In this enhanced SLM technique, the rows of the normalized Hilbert matrix were used as the phase rotation vectors for PAPR reduction. The Hilbert matrix has a unique definite structure and the receiver can easily generate the matrix for proper decoding of transmitted data. Therefore, this enhanced SLM does not require the transmission of side information to the receiver for decoding the transmitted data.

2.3 Enhanced SLM

In this enhanced SLM, two different normalization procedures were applied on rows of Hilbert matrix to obtain the phase rotation vectors used in enhancing the SLM. The Hilbert matrix was obtained from Cauchy matrix of dimension, m × n with elements, a_{ij} derived from $1 \le i \le m, \text{and} 1 \le \text{j} \le \text{n}$ in the expression of (Palanivelan *et al*., 2011) as:

$$a_{ij} = \frac{1}{x_i - y_j} \qquad (6)$$

where:

$x_i - y_j$ are elements of field F and $x_i - y_j \neq 0$

Hilbert matrix is computed from the Cauchy matrix using the following:

$$x_i - y_j = i + j - 1 \qquad (7)$$

This gives a Hilbert matrix with dimensions m = n = 8 as (Palanivelan *et al.,* 2011):

$$A = \begin{bmatrix} 1 & 1/2 & 1/3 & 1/4 & 1/5 & 1/6 & 1/7 & 1/8 \\ 1/2 & 1/3 & 1/4 & 1/5 & 1/6 & 1/7 & 1/8 & 1/9 \\ 1/3 & 1/4 & 1/5 & 1/6 & 1/7 & 1/8 & 1/9 & 1/10 \\ 1/4 & 1/5 & 1/6 & 1/7 & 1/8 & 1/9 & 1/10 & 1/11 \\ 1/5 & 1/6 & 1/7 & 1/8 & 1/9 & 1/10 & 1/11 & 1/12 \\ 1/6 & 1/7 & 1/8 & 1/9 & 1/10 & 1/11 & 1/12 & 1/13 \\ 1/7 & 1/8 & 1/9 & 1/10 & 1/11 & 1/12 & 1/13 & 1/14 \\ 1/8 & 1/9 & 1/10 & 1/11 & 1/12 & 1/13 & 1/14 & 1/15 \end{bmatrix} \qquad (8)$$

Two normalization schemes were used to normalized the matrix, these are Euclidean normalization (Helm, 2004) and normalization using matrix order (Irukulapati and Chakka, 2009) techniques.

A matrix is normalized when it is norm is equal to one. The matrix is normalized by dividing each of it is elements by it is norm. For example, a matrix x given in equation (8) . (Williams, 2010)

$$x = \begin{bmatrix} 2 \\ 1 \\ 2 \end{bmatrix} \qquad (9)$$

find the norm of the matrix

$||x|| = \sqrt{2^2 + 1^2 + 2^2} = \sqrt{4+1+4} = \sqrt{9} = 3$

Then, the normalized matrix x is now

$$\overline{X} = \frac{X}{\|X\|} = \begin{bmatrix} \frac{2}{3} \\ \frac{1}{3} \\ \frac{2}{3} \end{bmatrix} \quad (10)$$

2.4 Process Procedures of SLM Technique

Step 1: The random data was generated.

Step 2: The generated data was modulated to produce sequence symbols using BPSK.

Step 3: The sequence symbols were converted from series to parallel form and then they were divided into blocks of length N, where N number of subcarriers.

Step 4: Each of the OFDM data block was multiplied with different phase rotation vectors obtained from each row of normalized Hilbert matrix to create new OFDM data blocks.

Step 5: The new OFDM data blocks formed were transformed into time domain using IFFT.

Step 6: Complementary Cumulative Density Function (CCDF) value of the PAPR of each of the block was computed and compared with the respective threshold values.

Step 7: The OFDM data block with the minimum PAPR was finally selected for transmission.

3. Results and Discussion

Extensive computer simulation using communication tool box of MATLAB 2016Ra was carried out to assess the level of PAPR reduction of the proposed enhanced SLM in OFDM communication systems with number of subcarriers to be eight on BPSK modulated data signals. The normalized Hilbert matrix from equation (10) was used for phase rotation vectors. The model simulation parameters were presented in Table 1.

Table 1: Model Simulation Parameters

Modulation	**BPSK**
No of subcarriers (M)	8 symbols
Size of phase sequence	8
Carrier frequency	10MHz
Cyclic prefix	0.1

We use Binary phase shift keying (BPSK) modulation scheme which is considered to be robust among all the modulation schemes due to difference of 180 degree between the constellation point, this is why BPSK was used for the modulation of the generated data to produce sequence symbols. The number of subcarriers are eight, therefore the size of the phase sequence/phase rotation vectors most be eight, because each of the row of the matrix was used to multiply each of the subcarrier.

The simulation results obtained using the model parameters highlighted in Table 3.1 for the respective techniques as shown below with the performance of the enhanced SLM highlighted in green, and black for two different normalization schemes used in this research work. SLM with Hilbert matrix highlighted in blue and the original OFDM signal highlighted in red

Figure 3 shows the CCDF of PAPR results for the SLM with Hilbert matrix, and original OFDM signal, with number of subcarriers set at 8 and phase rotation vector size of 8

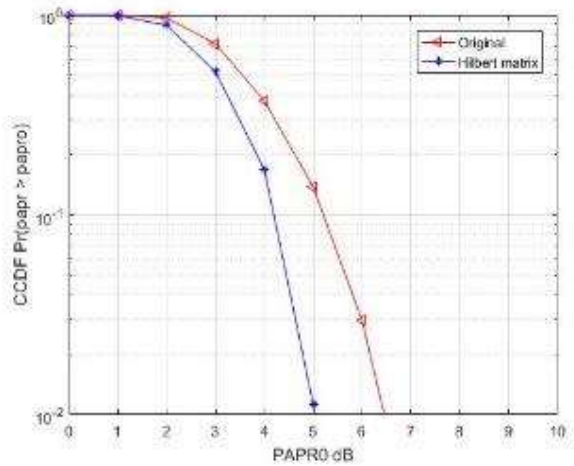


Figure 3: CCDF plot of SLM technique using Hilbert matrix.

From simulations results in Figure 3, at CCDF of 10^{-2} , original signal offers 6.5 dB, while SLM with Hilbert matrix offers 5.0 dB PAPR reduction, which is 1.5dB less than the original This shows the SLM with Hilbert yields an improvement result compared to the original OFDM signal.

Figure 4 shows the CCDF results for the enhanced SLM technique when normalization using Inverse of matrix order was used, SLM with Hilbert matrix, and the original signal, with number of subcarriers set at 8 and phase rotation vector size of 8

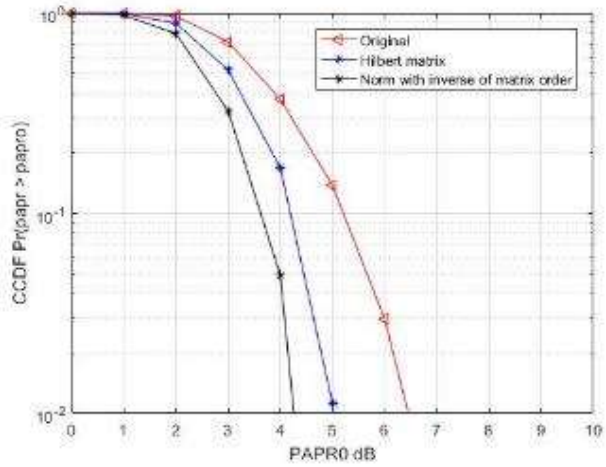


Figure 4: CCDF Plot using Inverse of Matrix order Normalization.

From Figure 4, at CCDF of 10^{-2}, SLM using Hilbert matrix had 5.0dB of a PAPR reduction, while the enhanced SLM using Inverse of matrix order normalization offers reduction of PAPR to 4.29 dB, which is 0.71dB less than SLM using Hilbert matrix. This shows that, the enhanced SLM technique yields a better result compared SLM with Hilbert matrix. The improvement in terms of PAPR reduction offered by the enhanced SLM technique against SLM with SLM technique occurred due to the fact that the normalization reduced the magnitude of the matrix, which led to minimum phase shift when the rows of the matrix are used as phase rotation vectors to generate candidates signals. Due to this minimum phase shift, the amplitudes of sinusoidal subcarriers did not rise to peak level when these subcarriers were summed up together at the input of transmitter. This results in lowering the peak-to-average power ratio.

Figure 5 shows the CCDF of PAPR using Euclidean normalization for the enhanced SLM technique, SLM with Hilbert matrix, and original OFDM signal with number of subcarriers set at 8 and phase rotation vector size of 8.

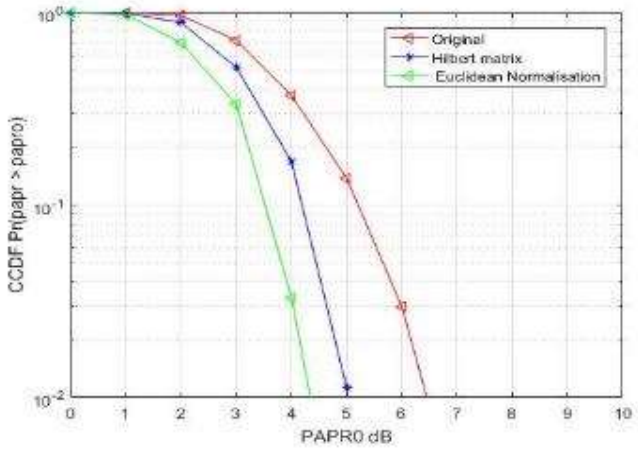


Figure 5: CCDF Plot of PAPR using Euclidean Normalization.

As can be deduced from Figure 5, at CCDF of 10^{-2}, the SLM using Hilbert matrix offers reduction of PAPR to 5.0dB, while the enhanced SLM technique using Euclidean normalization offers reduction of PAPR to 4.3 dB, which is 0.7dB less than SLM using Hilbert matrix .This shows that the enhanced SLM technique with normalized Hilbert matrix yields a better result compared SLM with Hilbert matrix. The improvement in terms of PAPR reduction offered by the enhanced SLM technique against conventional SLM technique occurred due to the fact that the normalization reduced the magnitude of the matrix, which led to minimum phase shift when the rows of the matrix are used as phase rotation vectors to generate candidates signals. Due to this minimum phase shift, the amplitudes of sinusoidal subcarriers did not rise to peak level when these subcarriers were summed up together at the input of transmitter. This results in lowering the peak-to-average power ratio.

From the simulation results, it is noteworthy observed that, PAPR reduction performance of the two normalization procedures are almost the same. This is as result of the fact that, the two normalization procedures did not change internal structure of the Hilbert matrix, but rather reduced it is magnitude

4. Conclusions

In this paper, enhancement of SLM technique for further PAPR reduction in OFDM system using normalized Hilbert matrix has been presented. Phase rotation vectors are obtained by applying two different normalization procedures that is, Euclidean normalization (Helm, 2004) and normalization using inverse matrix order (Irukulapati and Chakka, 2009) techniques on Hilbert matrix.

The following are the conclusions:

(i) From simulation results, it was observed that the proposed method offers better PAPR result of 4.29 and 4.3dB when compared to PAPR value 5.0dB offered by Hilbert without normalization.

(ii) The significant PAPR reduction achieved by the enhanced SLM improved the efficiency of the power amplifier more than conventional SLM schemes. The closer the value of PAPR to zero or the lower the value of PAPR, the less power consumed by RF amplifier during amplification process of the OFDM signals.

(iii) Side information need not be transmitted to the receiver to recover the original signal.

(iv) This scheme can effectively be implemented in 4G and 5G wireless communication systems.

5. **Acknowledgement**

Gratitude and appreciation are to Ahmadu Bello University Management, the lecturers of the Department of Electrical and Computer Engineering, and 9 Mobile Management for their support in my MSc research work.

6. References

Sudha, V., Anilkumar, B., & Sriramkumar, D. (2015). Low-complexity modified SLM method for PAPR reduction in OFDM systems. Paper presented at the Electronics and Communication Systems (ICECS), 2015 2nd International Conference. 1324-1328.

Girija, S., Srinivas, a., Ramudu, K., Sneha, e., Kits, W., & Kakatiyauniversity, k. k. k. (2014). reduction of PAPR using modified SLM technique-application to OFDM systems. International conference on recent advances in communication, VLSI & embedded systems, 75-78.

Raja Et Al. (2015)**. P**apr Reduction Of Ofdm Signal Using Sequential Phase Sequence Slm Based Transceiver Without Side Information. I.J.Wireless And Microwave Technologies,1(8)

Zhong peng Wang," Reduction PAPR of OFDM signals by combining SLM with DCT Transform, school of Information and Electronic Engineering. Zhejiang University of Science and technology, Hangzhou, China, Accepted October6, 2010.

Palanivelan *et al.,* (2011). Matrix based low Complexity PAPR Reduction in OFDM Systems. International Journal of Electronics and Communication Technology, 2(2), 158-162.

Florence, G., & Kumari, U. R. (2013). Reduction of PAPR Using HADAMARD SLM In SFBC MIMO-

OFDM System. International Journal of Engineering Research and Applications, 3(4), 1792-1795.

Harne, S., & Zanjade, A. (2016). PAPR Reduction in OFDM System using Phase Sequence of Riemann Matrix. International Advanced Research Journal in Science, Engineering and Technology, 3(I9), 56-60.

Gupta et al. (2013). PAPR Reduction of OFDM Using a New Phase Sequence in SLM Technique. International Journal of Advanced Electrical and Electronics Engineering (IJAEEE), 2(2), 4.

Abba, M. (2016). Performance Evaluation of OFDM Based Wireless Communication System. (Masters Degree), Jodhpur National University.

Kwesi, M. D., Wang, J., & Sultan, K. (2015). SLM Technique with Hadamard Transform for PAPR Reduction. International Journal of Computer Networks and Communications Security, 3(12), 438–441.

Bauml, R.W., Fischer, R.F.H., and Huber, J.B.: 'Reducing the Peak-to-Average Power ratio of multicarrier modulation by selected mapping', Electron. Letter, 32(22), 2056–2057.

Adegbite, S., McMeekin, S., & Stewart, B. (2014). Low-complexity data decoding using binary phase detection in SLM-OFDM systems. Electronics Letters, 50(7), 560-562.

Cheng et al. (2007). 'Improved SLM for PAPR reduction in OFDM system. Personal, Indoor and Mobile Radio Communications, 10(1109), 1–5.

Helm. (2004). Introduction to Numerical Methods Version One, workbook level 1(3), 1-5.

Irukulapati and Chakka,(2009),ELECTRONICS LETTERS 19th November 2009, 45(24)

Adelaide (2009), How do I normalize a matrix. Retrieved from http://mymathforum.com/linearAlgebra/18218-how-do-i-normalize-matrix.html. 22/04/2017

DESIGN AND SIMULATION OF A PASSIVE BELOW KNEE PROSTHETIC LEG

ABDULLAHI U.M, S. UMARU, AND M.A. ADAMU
Department of Mechanical Engineering, Ahmadu Belo University Zaria.

ABSTRACT
This project presents simulations of a new type of passive ankle prosthesis designed to provide dorsiflexion and plantarflexion of the leg to enable it adjust to rugged terrain. The functional goal is to design a more human like passive prosthesis that will mimic a normal human gait. The static simulation results show a safe design that will withstand an average person of 75 kg. This work supports further research on transtibial prosthetic designs that are lighter and the ankle joint can also be further designed. Also, other material for the foot can also be further work on.

Keywords: *Heel strike, foot flat, and toe off.*

1.0 INTRODUCTION

Prosthesis is an artificial device used to replace a missing body part, such as a limb, tooth, eye, or heart valve. Also prosthesis are intended to restore a degree of normal function to amputees. There is a natural human desire to feel whole and complete, and providing artificial devices has helped to satisfy this need (Al-Khazraji et al, 2012). Amputation is defined as the removal, usually by surgery, of a limb, part, or organ. Its purpose is to remove dead or diseased tissue, to relieve pain, to obtain healing, and/or to rehabilitate the individual. If the amputation level is properly selected and the surgery is performed well, amputation should be considered not as a salvage procedure but as a rescue procedure that is the first step in rehabilitation (Thomas 1993).

In the fitting of any artificial limb, the goal of the prosthetist is simply to restore to the amputee the ability to perform everyday activities in an easy, natural, and comfortable manner. The basic requirements are therefore three in number comfort, function, and appearance, the latter embracing both cosmetic appearance and appearance in use.

Presently one of the major problems in Nigeria with the increase in population is the apparent increase in the number of below-knee amputees in our population due to ageing, accidents, and surgery related to peripheral vascular disease (e.g., arteriosclerosis, diabetes mellitus), cancer, and infection. This increase in the amputee population warrants research that attempts to address issues relevant to prosthetic management. Other causes of amputation in most of the African countries include industrial or environmental accidents, farming accidents, motor vehicle accidents, terrorist attacks, and the lack of basic public health which often leads to diabetes, gangrene, ischemic disease and infection. All of these causes are adding to the number of amputations (Strait, 2006). As stated previously, the objective is to design a more human like below knee prosthetic leg (or simply prosthetic ankle).

2.0 METHODOLOGY

2.1Gait Cycle Terminology

Gait is a periodic phenomenon, and gait cycle can be defined as the time interval between two consecutive occurrences of the same recurring event during walking, where one period is known as a stride. A stride is defined as the duration from when the heel of one leg strikes the ground (0% of stride) to when that same heel strikes the ground again (100% of stride). Key points of that stride are heel strike (0%), foot flat (8%), heel off (43%) and toe off (62%). A stride can be broken into stance phase (or weight bearing) (0-62%) and swing phase (62-100%). Different phases are defined according to the position and kinematic relationships of the limb while walking. Figure 1, identifies the important parts and terms used in describing gait cycle (Herr, 2008).

2.2 Leg Model

The prosthetic leg model is for male left-side unilateral trans-tibial amputee. A typical prosthetic device consists of a custom fitted socket, an internal structure (also called a pylon), ankle, foot and belts that attach it to the body, and in some cases, realistic looking skin. A prosthetic device should of all be lightweight, hence, much of it is made from plastic, depending on the material a designer has in mind. The newest development in prosthesis manufacture has been the use of carbon fiber to form a lightweight pylon.

The figure below shows a light weight prosthesis which comprises a few different components to provide people with a below knee prosthesis. This system includes a pylon, ankle adapter, and keel which is used for alignment purposes and to hold the ankle adapter. The components come in separate pieces, which are easy to assemble and applied. The separate pieces allow height to be addressed while allowing the prosthetic to be aligned properly.

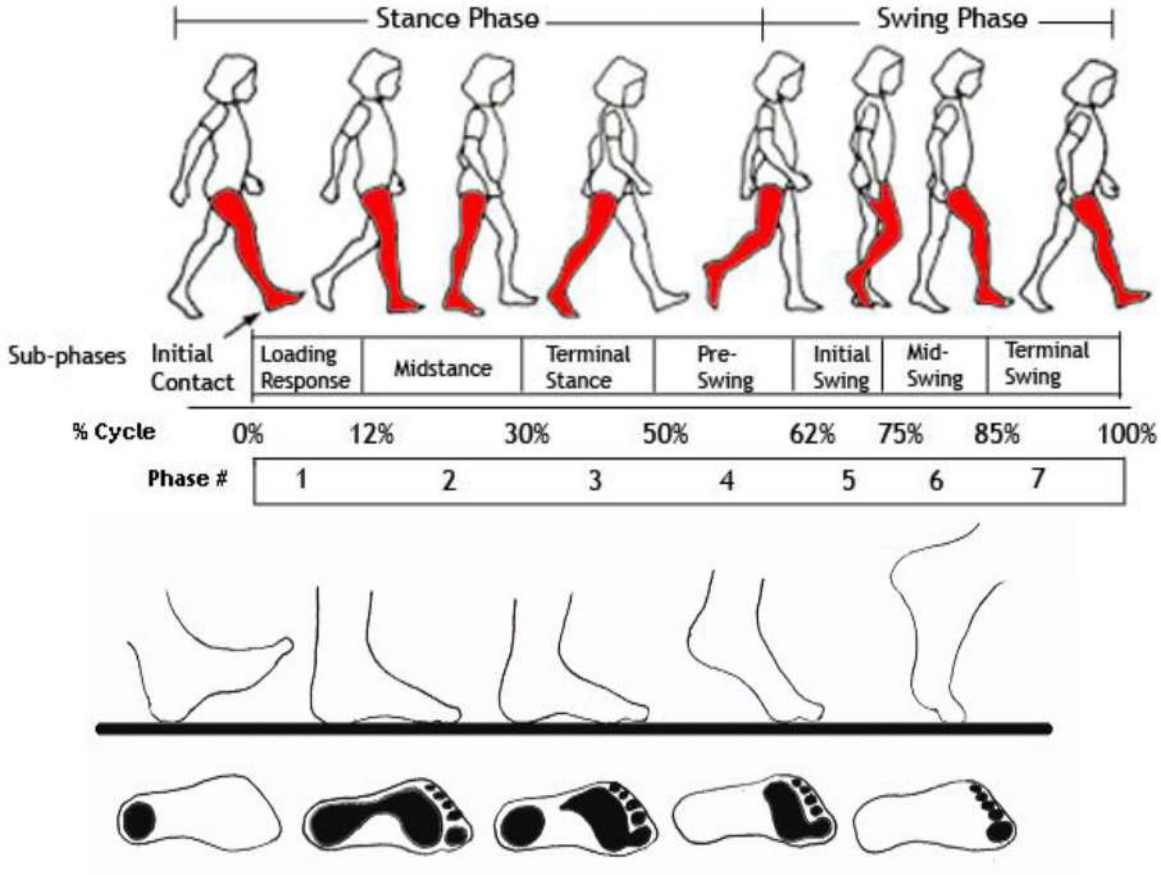


Figure 1: Gait phases and Pressure distribution of foot during gait (Borjian, 2008)

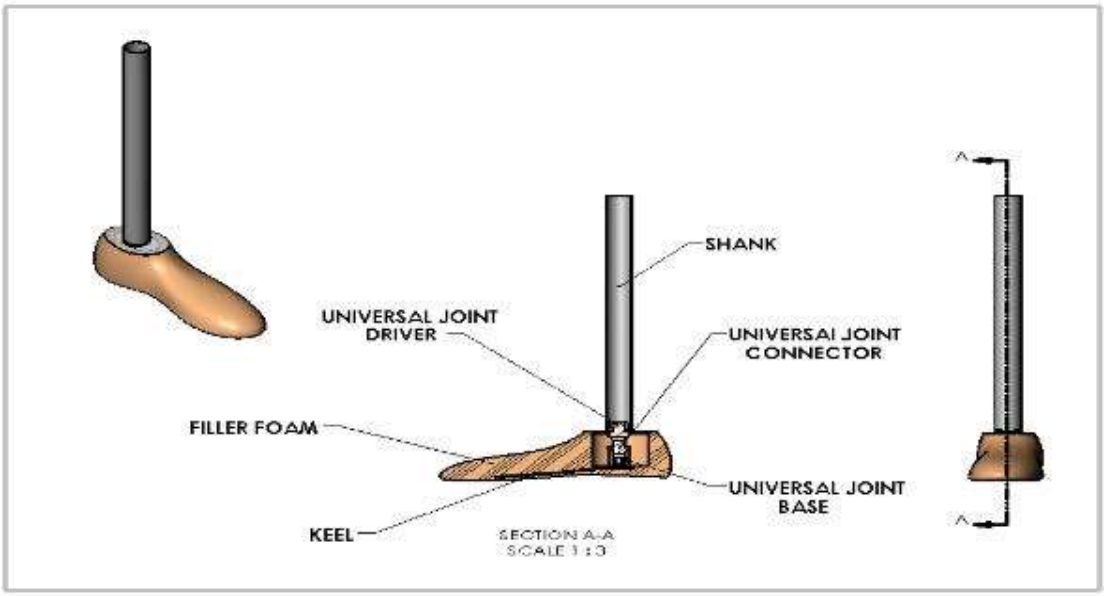


Figure 2: Assembly drawing of design concept.

2.3 Design Considerations

This section explains the design considerations used to guide the prosthesis design. This ankle prosthesis will use purely passive components to convert an adequate amount of energy to propel the body forward and achieve active behavior similar to that of a human ankle. The prosthetic ankle design criteria provided below relate to aspects of physical properties and mechanical performance. The design considerations are:

1. The prosthesis should be compact in size,
2. The prosthesis should be light in weight,

3. The prosthesis should be quiet during its operation,
4. The prosthesis should return to its natural or equilibrium position to prepare for the next gait cycle during swing period (both ankle force and angle should return to zero),
5. The prosthesis should operate in a way similar to that of a human ankle,
6. The prosthesis should be low cost.

2.4 Materials Selection

A prosthetic device should of all be lightweight, hence, much of it is made from plastic, depending on the material a designer has in mind. Lightweight metals such as titanium and aluminum have replaced much of the steel in the pylon. Alloys of these materials are most frequently used. Hence Aluminum is being choose for the pylon because of it low density. Aluminum was chosen as the material for this purpose because it is light weight and cost effective. To further improve the lightness of the system, the pylon was made to be hollow cylindrical rod which supports the foot at the distal end and connects to the socket adapter at the proximal end.

Certain parts of the limb (for example, the feet) have traditionally been made of wood (such as maple, hickory basswood, willow, poplar, and linden) and rubber. Other materials commonly used are plastics such as polyethylene, polypropylene, acrylics, and polyurethane. However, for this project, we are considering silicone rubber for the feet because it is an exceptional rubber in terms of properties.

2.5 Simulation analysis of the passive leg components

Finite element method is a numerical method for solving problem of engineering and physics. It is also referred to as finite element analysis (FEA). FEA is a numerical method that offer a means to find approximation solution. FEA applied in engineering is computational tool for performing engineering solutions.

The Von Mises criterion is the default failure criterion in most software because it gives results closer to the practical value. The von Mises stresses were analyzed through the contour plots which were displayed from the results of the finite element analysis performed in SOLIDWORKS. The two important results are noted and they are:

1. Von Mises elemental stress
2. Displacement.

The Von Mises stresses are displayed through the contour plots to illustrate the stress distributions present throughout the prosthetic leg.

2.6 Applied loads, Boundary conditions and Mesh

Finite element method was used to conduct a stress analysis and show the force distribution along the model. First is to define the locations and directions of loads, the next step is to apply forces and set constraints or supports, these displays the boundary conditions of shank and ankle-foot models. Here the forces are represented by the purple color arrows and the restraints or supports in green color for the loading condition. The finite element model results of the applied load and boundary conditions for shank, ankle-foot are shown in below. A normal load of $735.75\ N$ was applied shank and foot.

3.0 RESULTS AND DISCUSSION

3.1Von Mises Stresses

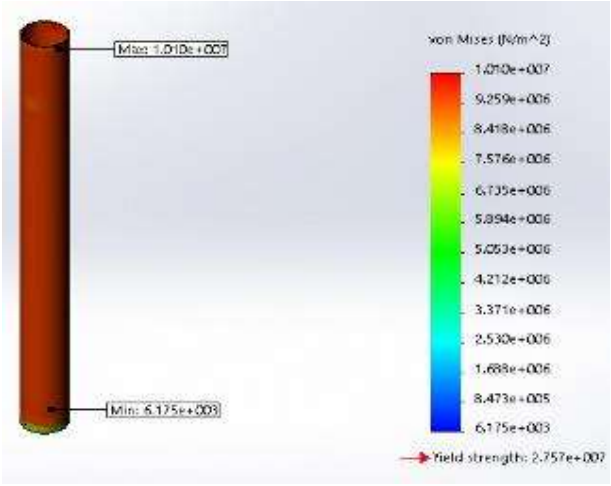


Figure 3.1: The Von Mises stress distribution, in the in the artificial shank model.

From left to right, is the model and finally the color scale for the model. As shown in the stress plots, there are definite areas where maximum Von Mises stresses are occurring on the anterior region of the model. These areas can be visually seen above as red regions on the model; the maximum Von Mises stresses are displayed through the color red in the contour plots. The stresses in the models is uniform and below the Yield Strength.

Table 3.1: Probed Von Mises values for shank

Name	Type	Min	Max
Stress	VON: Von Mises Stress	$6174.64 \times 10^3\ N/m^2$	$1.010 \times 10^7\ N/m^2$

These values detailed above are below the Yield Strength of $2.757\times 10^7\ N/m^2$, which demonstrates that the circular hollow shank model successfully pass the von Mises failure criteria.

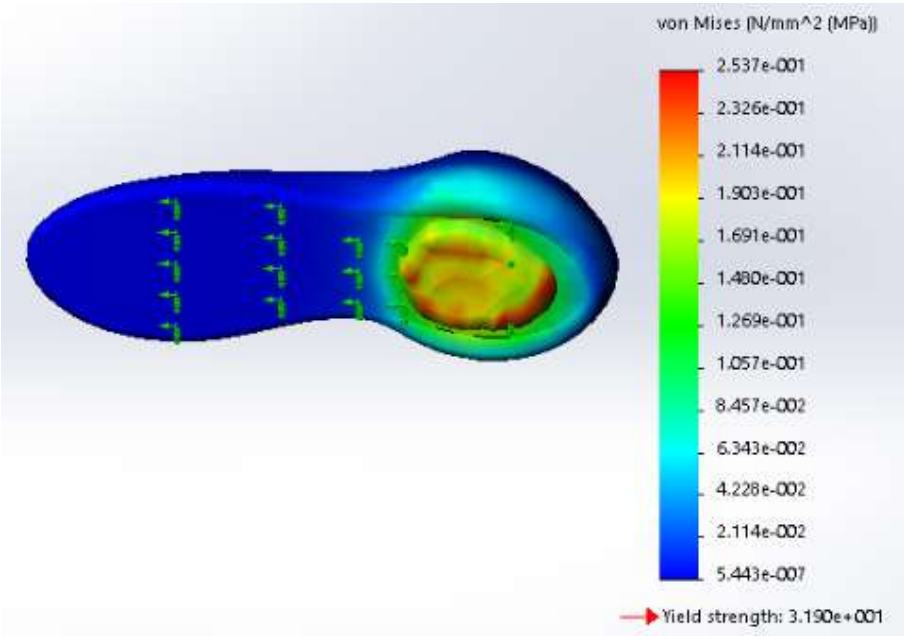


Figure 3.2: The Von Mises stress distribution, in the in the artificial foot model for loading condition I.

Table 3.2: Probed Von Mises values of the foot model for loading condition I.

Name	Type	Min	Max
Stress	VON: Von Mises Stress	$5.44265\times 10^{-7}\ MPa$	$0.253701\ MPa$

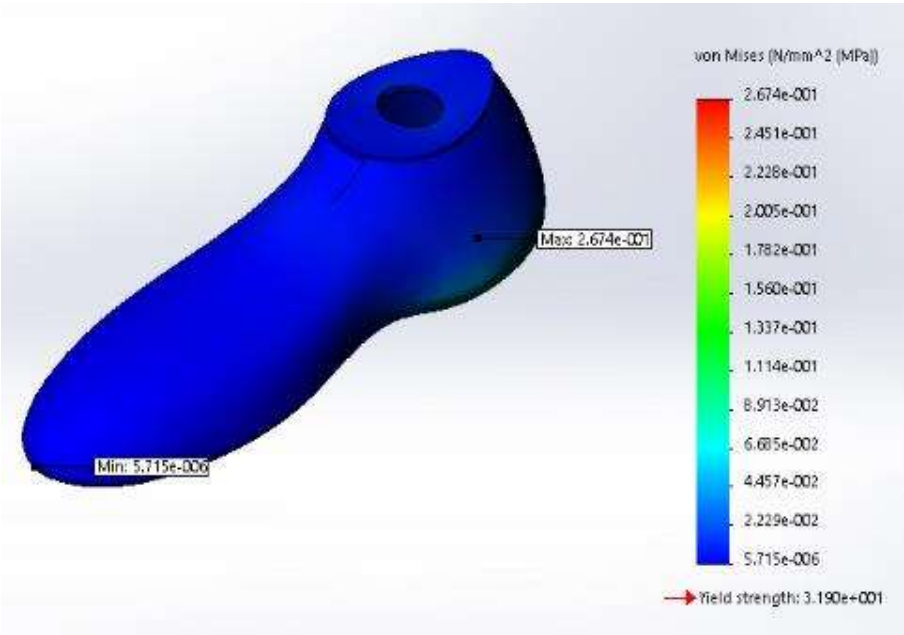


Figure 3.3: The Von Mises stress distribution, in the in the artificial foot model for loading condition II.

Table 3.3: Probed Von Mises values for the foot model for loading condition II.

Name	Type	Min	Max
Stress	VON: Von Mises Stress	$5.71493\times 10^{-6}\ MPa$	$0.267369 MPa$

These values detailed above are below the Yield Strength of 3.190× $10^6\ N/m^2$, which demonstrates that the foot model successfully pass the von Mises failure criteria for loading condition I and II.

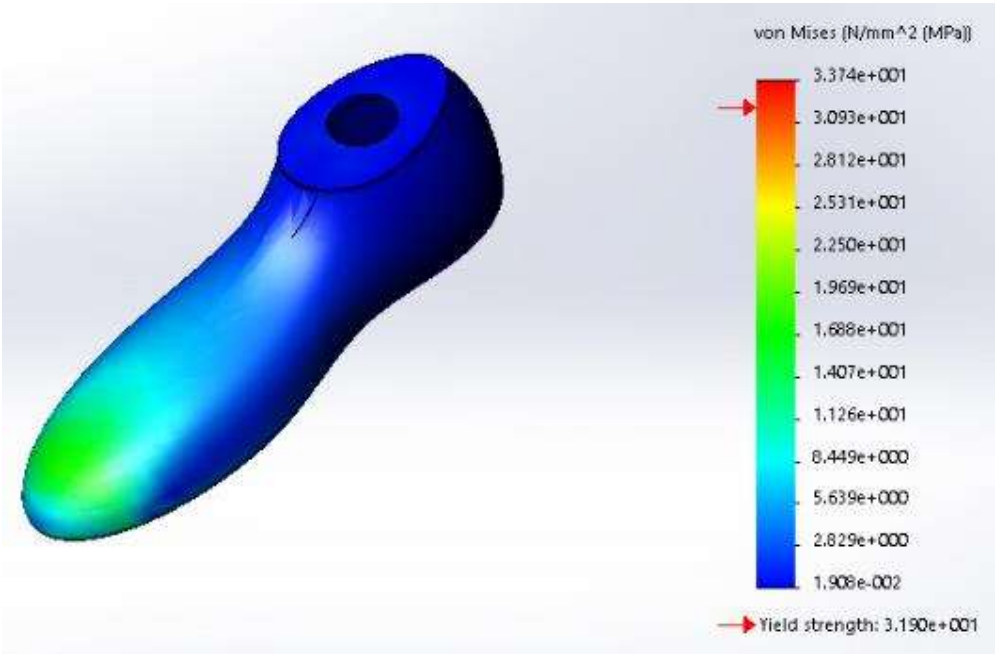


Figure 3.4: The Von Mises stress distribution, in the in the artificial foot model for loading condition III.

Table 3.4: Probed Von Mises values of the foot for loading condition III.

Name	Type	Min	Max
Stress	VON: Von Mises Stress	0.0190791 MPa	33.7389 MPa

These value detailed above for minimum Von Mises criterion is below the Yield Strength of 3.190× $10^6\ N/m^2$, and the maximum value is above the yield strength, which demonstrates that the foot model successfully pass the von Mises failure criteria for the minimum stress.

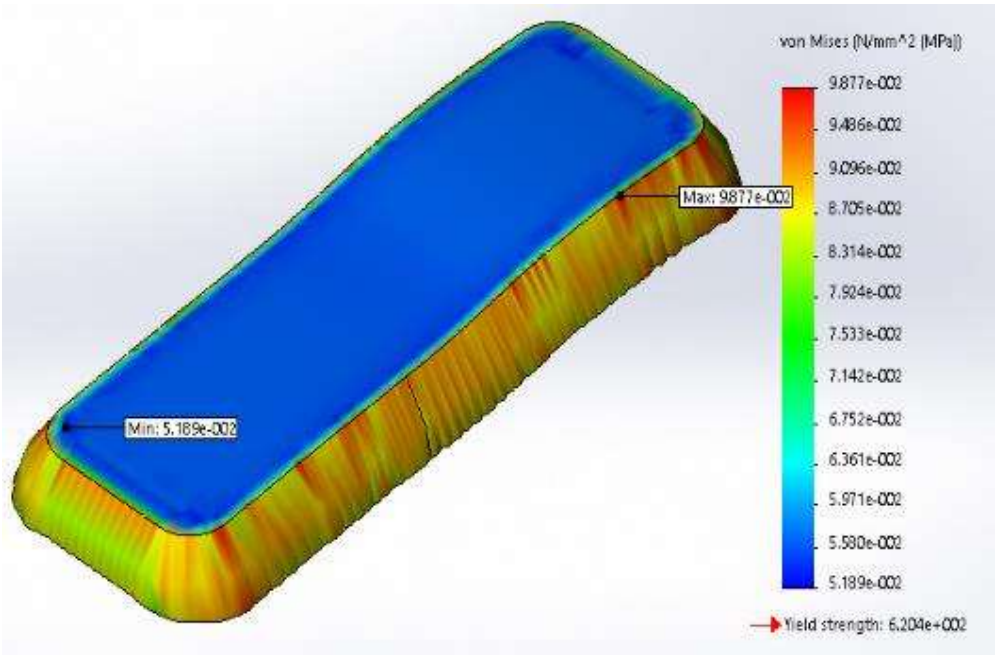


Figure 3.5: The Von Mises stress distribution, in the in the artificial keel model.

Table 3.5: Probed Von Mises values for the keel.

Name	Type	Min	Max
Stress	VON: Von Mises Stress	0.0518938 MPa	0.0987675 MPa

These value detailed above are below the Yield Strength of $620.422\ MPa$, which demonstrates that the keel model successfully pass the von Mises failure criteria.

A decrease in von Mises Stress values is an important aspect of the design to consider; however, there are other effects of a decrease in these values. As the stresses decrease, the displacement values also decrease. Also, an increase in diameter requires more material which contributes to an increase in weight for the limb. An increase in weight would be a negative attribute to the patient as the limb would become heavier and harder to walk with. Although it is important that the Von Mises stresses fall below the Yield Strength line included on the graphs above, the amount that the stresses lie below this value is not as important. Finding a light, flexible limb with Von Mises stresses that are below the Yield Strength is the underlying goal of this project.

4.0 CONCLUSION AND RECOMMENDATION

4.1 Conclusion

The aim of this report is to design a prosthetic foot that uses locally available materials from currently available prosthetic feet. This report has limited the characteristics of a human foot considered. The characteristics are dorsiflexion and plantarflexion using a silicone rubber for the foot and a modified standard universal joint for the ankle joint to provide the flexion of the leg. The segment weight of the leg portion (as defined above) is 0.0465 M, where M is the total weight of the entire body. In this case, a person weighting 75 kg has a corresponding leg mass of 3.4875 kg (Winter, 2005). A body of $75kg$ weight was applied to the foot at stance phase (or weight bearing phase) and simulated to show how the foot deforms, the result shows a safe design. The weight of the leg was found to be $1.1475\ kg$ which is light and is below the weight of the leg of a person of mass $75\ kg$.

4.2 Recommendations

- It is very likely that further improvements and corrections can be made to the prosthesis design. Especially the design of the ankle joint.
- But most importantly, the ideal prosthesis will mimic, as close as possible the characteristics of a normal human foot.

REFERENCES

Al-Khazraji K., Kadhim J. and Ahmed P.S, (2012). "Tensile and Fatigue Characteristics of Lower-Limb Prosthetic Socket Made from Composite Materials". Journal, Materials Engineering Department University of Technology, Baghdad, Iraq.

Borjian R., (2008). "Design, Modeling and of an Active prosthetic knee". Undergraduate project, Mechanical Engineering Department, Waterloo, Ontario, Canada.

David A. W., (2005). Biomechanics and motor control of human movement, 3rd ed., John Wiley & sons Inc.

Geeroms J., (2011). "Study and Design of an Actuated Below Knee Prosthesis". M.Sc. Thesis, Mechanical Engineering Department, Vrije Universiteit Brussel.

Herr H., Samuel K. A. and Peter D., (2006) "An Ankle-Foot Emulation System for the Study of Human Walking Biomechanics" Proceedings of the 2006 IEEE International Conference on Robotics and Automation Orlando, Florida - May 2006.

Mitchell M. D., (2007). "Design and development of an intelligent ankle-foot prosthesis". University of New Brunswick Canada.

Radcliffe, (1955). Digital resource foundation, (http://www.oandplibrary.org/al/), (Accessed online, in July, 2017).

Sanders G. T., May B. J., Hurd R., and Milani J., (1986). Lower Limb Amputations*: A* Guide to Rehabilitation, F. A. Davis, Philadelphia.

The online materials database (matweb.com, accessed on Oct. 2017).

Thomas C. L., (1993), Taber's Cyclopedic Medical Dictionary, 17 ed. F. A. Davis, Philadelphia.

SYNTHESIS AND EVALUATION OF METAL-LOADED ZEOLITE Y FOR CONTROL OF INDOOR CO EMISSIONS

M. PETER[1], D.M KULLA[1], N.O OMINSANYA[1], D.O. OBADA[1*] A.Y. ATTA[2]
[1]*Department of Mechanical Engineering, Ahmadu Bello University, Zaria, Nigeria*
[2]*Department of Chemical Engineering, Ahmadu Bello University, Zaria, Nigeria* [*]
Corresponding author e-mail: obadavid4@gmail.com

ABSTRACT
Cobalt and iron based mixed oxide type catalysts have been prepared using Zeolite Y as supports. The synthesized catalysts were characterized by XRF and XRD. The catalytic activity for CO oxidation was studied in a view of their possible applications in the control of emissions from solid fuel combustion of rural cook-stoves. From the results, Co, Fe, and Co-Fe/ZY catalysts gets activated at about 125, 175 and 200 °C respectively. The Co/ZY catalyst shows approximately 100% CO conversion (T_{100}) at 250 °C for initial CO concentration of 1000 ppm, while this temperature T_{100} was increased to 275 °C and 325 °C for Fe/ZY and Co-Fe/ZY catalyst respectively at space velocity of 20000 h^{-1}. From the characterization studies carried out, these materials could be useful for such reactions where mass transfer is more important than shape and size selectivity.

Keywords: *Mixed oxide catalysts, indoor air pollution, CO oxidation, solid fuel combustion, rural cook-stoves*

1. INTRODUCTION

An estimated 2.5 billion people regularly cook with biomass fuels such as wood or charcoal. Emissions from biomass cook-stoves contribute to global climate change, indoor air quality issues, and related health effects. Exposure to high indoor air pollutant levels from cooking with biomass fuels is responsible for an estimated 1.6 million deaths annually and about 3% of the global burden of disease (Alex *et al*., 2016). Carbon monoxide (CO) has been among the major pollutants released from incomplete combustion of these solid fuels used for the energy requirements (Gordon *et al*., 2004). Carbon monoxide is a product of incomplete combustion and it reduces the blood's ability to carry oxygen. Over exposure (carbon monoxide poisoning) may be fatal. The emission of carbon monoxide from solid fuel combustion due to incomplete combustion cannot be overemphasized

Mixed oxides catalysts based on transitional metals are the potential candidates for many reactions of environmental importance (Li *et al*.,2008; Morales *et al*., 2006; Morales *et al*., 2008; Du *et al*., 2008) and the post combustion control of gaseous emissions in solid fuel cook stoves is no exception. One of the advantages of using these catalysts is their low-cost. In a bid to reduce environmental pollution from these cook stoves, catalytic interventions are required. The catalyst itself is most often a mix of precious metals which include platinum, palladium and rhodium, which are very expensive (Martin *et al*., 2002) and also have hydrothermal and chemical stability issues. From the economic and practical point of view, especially for developing countries, researchers are looking into a series of low-cost metals which can serve approximately the same function without seriously affecting catalytic activities.

Zhang *et al*., (2016) studied copper-ceria catalysts for CO oxidation supported on 4A, 5A, NaX and NaY zeolites prepared by incipient wetness impregnation and excess-solution impregnation. Results revealed that the catalysts were greatly affected by zeolite type and preparation method. The catalytic activity of 4A-ES and NaX-ES was the best among catalysts made by excess-solution (ES) impregnation, demonstrated by the lowest T_{50} at 127 and 129 ^{o}C, respectively.

Hence, the aim of the present investigation is to develop different composition of cobalt- iron mixed oxide based catalysts for CO oxidation with the potential application in biomass based cook stoves.

2. EXPERIMENTAL

Aqueous solutions of the stoichiometric quantity of $Co(NO_3)_2$ and $Fe(NO_3)_3$ were used to prepare metal solutions in deionized water. Catalysts were synthesized by targeted loading of 15wt.% Co and 15wt.% Fe, on zeolite supports. For the mixed metal oxide loading on zeolite support, 7.5 wt.% Co and 7.5 wt.% Fe was targeted. Catalysts were prepared using excess-solution impregnation. Zeolites were pre-treated at 550 ^{o}C for 3 h in air to remove any adsorbed moisture and convert the zeolite to its hydrogen form (H-ZY). For the synthesis procedure in terms of the weight % of metal oxide precursors, 22.0 g $Co(NO_3)_3$.$6H_2O$ and 7.0 g $Fe(NO_3)_3$.$3H_2O$ based on stoichiometric conditions were dissolved into 100.0 mL deionized water to prepare separate

solutions for Co/ZY, Fe/ZY and Co-Fe/ZY catalysts. 5 g zeolites were added into each solution under vigorous stirring (10 min) and further impregnated with the metal oxide solution at room temperature initially and temperature was systematically increased as catalyst precursors were mixed to dryness. Finally, all as-prepared precursors were dried at 100 ºC for 2 h and calcined at 550 ºC in air for 3 h.

Chemical analysis of parent material (zeolites) and synthesized catalysts (modified zeolites) was performed using a X-ray fluorescence spectrometer. Powder X-ray diffraction data was recorded at room temperature and operated at 30 kV and 15 mA with a monochromator and using Cu K-alpha radiation (l = 0.154060 nm). The samples were scanned for 2θ range of 10–90

Catalytic activity of all the synthesized catalysts was investigated for CO oxidation. The steady state gas evaluation assembly equipped with a quartz reactor, precise mass flow controllers and heating system was used to carry out the CO oxidation reaction. 100 mg of catalyst was loaded in a fixed bed quartz reactor. Catalysts were pre-treated in He flow at 200 ºC for 1 h. The reactant gas feed which contained 1000 ppm CO, 10% O_2 and He balance was used for CO oxidation and catalytic activity was subsequently measured at a space velocity of 20,000 h^{-1} (gas hourly space velocity) by oxidizing the exit gas stream for CO using Shimadzu gas chromatograph with molecular sieve 5A column and TCD detector.

3. RESULTS AND DISCUSSION

3.1 Elemental composition of parent material and synthesized catalysts

Table 1 presents the chemical analysis of the samples. Total Si/Al ratios, including both the framework and the extra-framework species, were around 49. For the parent material (zeolite Y), it is noticed that the material is ultra-stable due to its highly siliceous nature based on the Si/Al ratio as observed. The modified catalysts (Co, Fe, Co-Fe/ZY) showed a reduction in Si/Al ratio because of the presence of the metal oxides in the lattice of zeolitic supports. It is worthy of note that the Co/ZY catalyst did not show an appreciable difference in silica to alumina ratio because the instrument could not detect the cobaltite metal. However, Fe/ZY showed an appreciable decrease in Si/Al ratio because the ferrite metal composition (8.276wt %) in the lattice was significant. Interestingly, by observing the Co-Fe/ZY catalyst which had an equal amount of cobalt and iron loadings, and by reason of the instruments 'inability to capture cobalt, it can be noticed that the elemental composition of iron loading was exactly half as compared to Fe/ZY catalysts. This is a strong indication of the accuracy in terms of elemental composition of the parent material and synthesized catalysts.

3.2 XRD patterns of parent material and synthesized catalysts

It is known that thermal treatment could influence the chemical phases present in the impregnated catalysts by virtue of reactions between metal oxides and catalyst supports (Hinot *et al*, 2007; Aneggi *et al*, 2006). In this way, in order to investigate the possible formation of new phases in the supported catalyst after calcination, XRD analysis was performed on the mixed oxide catalysts with reference to the catalyst support itself. Fig. 1 shows zeolite Y and metal loaded zeolite Y (Co, Fe, Co-Fe/ZY) with reflections noticed at 2θ: 6.2, 10.1, 12, 15.8, 20.2, 23.5, and 31 which show a good agreement with the data of zeolite Y in literature (Robson, 2001) and in the library of the instrument. Generally, all the samples tested showed high crystallinity as observed. Major reflections that are ascribed to zeolite Y phases are dominant in all catalyst samples. The results indicate that the calcination at 550 ºC for 3 h did not bring about a change to the crystallinity and points of reflection. In terms of oxide species, only additional diffraction peaks corresponding to CoO_3 were observed in Co/ZY and Co-Fe/ZY at Braggs' angle of about 37º. The XRD result also indicated no chemical interaction was observed between the metal oxide species and the zeolite. It was not possible to identify the presence of the metal oxides due to their low content and high dispersion. This proves that the zeolites' crystalline structure was intact, which was also expected considering the very mild conditions used for metal oxides (Fe and Co) incorporation. This may be responsible for ensuring the preservation of the zeolite -Y framework upon incorporation of the transition metal complexes inside the pores of zeolite-Y.

3.3 CO oxidation activity for metal based zeolite catalyts

Fig. 2 shows CO oxidation activity for all synthesized catalyst. From the results, Co, Fe, and Co-Fe/ZY catalysts gets activated at about 125, 175 and 200 °C respectively. The Co/ZY catalyst shows approximately 100% CO conversion (T_{100}) at 250 °C for initial CO concentration of 1000 ppm, while this temperature T_{100} was increased to 275 °C and 325 °C for Fe/ZY and Co-Fe/ZY catalyst respectively at space velocity of 20000 h^{-1} . This is mainly because of the very high surface area (not reported) as well as ordered, highly porous structure

of zeolite support facilitating mass transfer. The present study therefore infers that zeolites with reasonable pore size can be a very useful catalyst support, especially for the reactions involving relatively smaller molecules like CO as in the present case. As explained by Dyakonov (2003), zeolite pores up to 4 A do not show significant carbon monoxide adsorption and thus mass transfer can be restricted on such zeolitic supports. Adsorptive retention is also reported to increase dramatically at 5 A aperture. This is obviously because the effective diameter of a CO molecule is approximately 4.5 A. In this way, the Y type zeolite used in the present case is quite suitable for the mass transfer of reactants on catalyst sites, thereby showing effective catalytic activity. These results are similar to comparatively higher activity recorded for zeolite based catalysts with the incorporation of precious based metals as reported by (Lokhande, 2015).

4.0 CONCLUSIONS

The results obtained in the present study for CO oxidation clearly suggest that ultra-stable zeolite Y are potential catalyst supports. The synthesis of the catalysts using low cost transition metals is of significance, as most of the metals reported are of high cost. The better activity of Co impregnated zeolite catalyst (Co/ZY) for CO oxidation reactions could be correlated to their redox properties. From the XRD study, it was observed that the present catalyst supports possess the ordered structure, their mesoporous characteristics (not reported) appear to improve the mass transfer of the gaseous reactants, which could also be responsible for their improved activity for CO oxidation.

Table 1: Chemical compositions of the Zeolite Y and modified zeolites

Component	SiO_2	Al_2O_3	Fe_2O_3	TiO_2	MgO	CaO	K_2O	Cl	Si/Al	LOI*
ZY (wt%)	96.404	3.226	0.012	0.023	0.090	0.014	0.015	0.013	50.2	0.06
Co/ZY (wt%)	96.293	3.289	0.031	0.027	0.083	0.005	0.025	0.005	50.1	0.24
Fe/ZY (wt%)	88.235	3.129	8.276	0.035	0.091	0.028	0.016	0.008	47.5	0.18
Co-Fe/ZY (wt%)	91.938	3.156	4.565	0.033	0.075	0.039	0.017	0.006	49.1	0.17

LoI*= Loss on ignition, ZY=zeoliteY; Co/ZY=cobalt/zeoliteY; Fe/ZY=iron/zeoliteY; Co-Fe/ZY=cobalt-iron/zeoliteY; Si/Al; = silica to alumina ratio

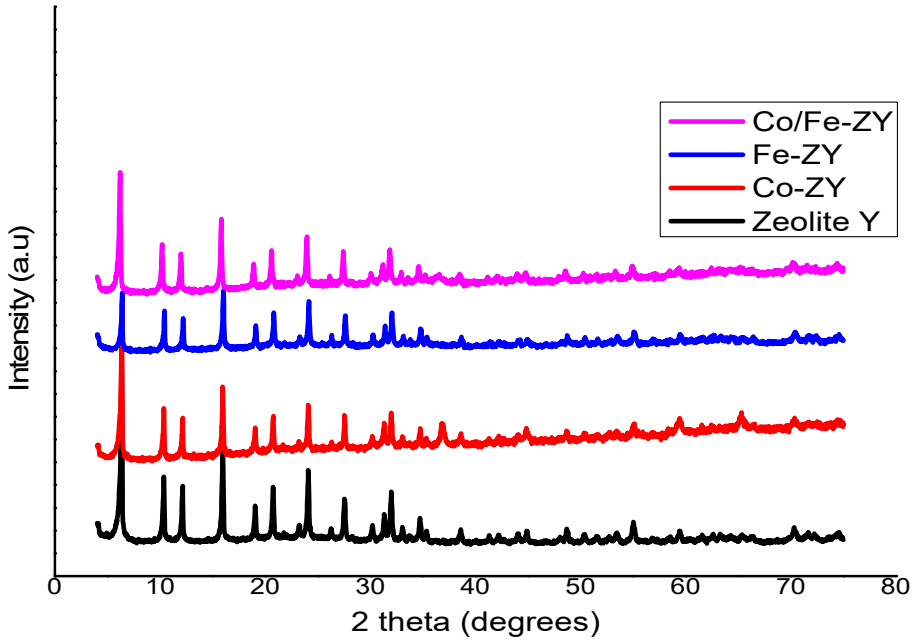


Figure 1: XRD patterns for synthesized catalysts

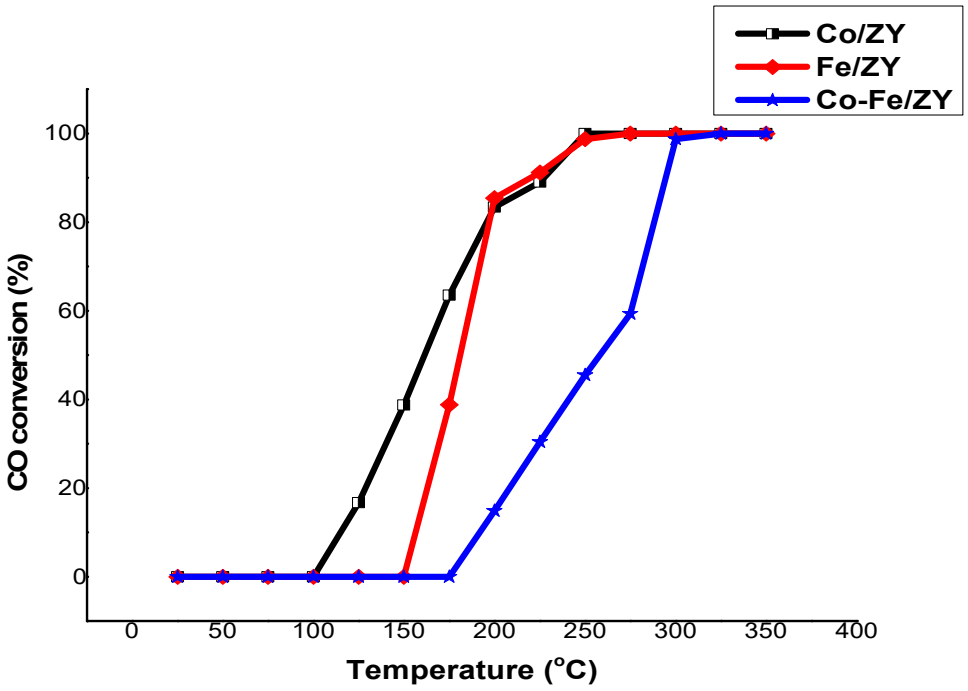


Figure 2: CO oxidation over zeolite based catalysts at 20000 h^{-1} space velocity.

REFERENCES

Alex D. P., Tyler K., Andrew C., Nicholas R. S., Brett A., Ted J.A., and Paul E.Y., (2016). Low-cost, potassium-based, catalytic biomass cookstove for improved indoor air quality. Mainstream Engineering Corporation, Rockledge, FL

Aneggi, E., de Leitenburg, C., Dolcetti, G., & Trovarelli, A. (2006). Promotional effect of rare earths and transition metals in the combustion of diesel soot over CeO_2 and CeO_2–ZrO_2.*Catalysis Today*, 114(1), 40-47.

Du, X., Yuan, Z., Cao, L., Zhang, C., & Wang, S. (2008). Water gas shift reaction over Cu–Mn mixed oxides catalysts: effects of the third metal. *Fuel processing technology*, *89*(2), 131-138.

Dyakonov, A. J. (2003). Abatement of CO from relatively simple and complex mixtures: I. Oxidation on Pd-Ag/zeolite catalysts. *Applied Catalysis B: Environmental*, *45*(4), 241-255.

Gordon, B. A., Mackay, R., & Rehfuess, E. (2004). Inheriting the world: the atlas of children's health and the environment. World Health Organization.

Hinot, K., Burtscher, H., Weber, A.P. and Kasper, G., (2007). The effect of the contact between platinum and soot particles on the catalytic oxidation of soot deposits on a diesel particle filter. *Applied Catalysis B: Environmental*, *71*(3), pp.271-278

Li, W. B., Zhuang, M., & Wang, J. X. (2008). Catalytic combustion of toluene on Cu-Mn/MCM-41 catalysts: Influence of calcination temperature and operating conditions on the catalytic activity. *Catalysis Today*, *137*(2), 340-344.

Martin V, Thomas K, Jurgen G, Gerhard L. (2002). *Automobile Exhaust Control,* in *Ullman's Encyclopedia of Industrial Chemistry,* Wiley-VCH. DOI: 10.1002/14356007

Morales, M. R., Barbero, B. P., & Cadús, L. E. (2006). Total oxidation of ethanol and propane over Mn-Cu mixed oxide catalysts. *Applied Catalysis B: Environmental*, *67*(3), 229-236.

Morales, M. R., Barbero, B. P., & Cadus, L. E. (2008). Evaluation and characterization of Mn–Cu mixed oxide catalysts for ethanol total oxidation: influence of copper content. *Fuel*, *87*(7), 1177-1186.

Robson, H. (2001). Verified synthesis of zeolitic materials" 2nd edition. Published on behalf of the Synthesis Commission of the International Zeolite Association, Amsterdam, Netherlands, Elsevier

Zhang, D., Zhang, H., & Yan, Y. (2016). Catalytic activity of copper-ceria catalysts supported on different zeolites for CO oxidation. *Korean Journal of Chemical Engineering*, *33*(6), 1846-1854.

EVALUATION OF THE DYEING PROPERTIES OF SOME AMINOTHIOPHENE BASED DISPERSED AZO DYES

O.R.A. IYUN [1]*, K.A. BELLO[2], O. J. ABAYEH[3], A. JAURO[4] AND G.Y. KANTIOK[5]*
[1&5*]Department of Chemistry, Ahmadu Bello University, Zaria
[2]Department of Textile Science and Technology, Ahmadu Bello University, Zaria
[3]Department of Pure and Industrial Chemistry, University of Port Harcourt, Port Harcourt
[4]Chemistry Programme, Abubakar Tafawa Balewa University, Bauchi
*kantiokgrace@gmail.com

ABSTRACT
Synthesis of azo disperse dyes derived from 2-aminothiophenes was carried out and their spectroscopic and dyeing properties determined. The electronic absorption spectra cover λ_{max} range of 408-562nm in dimethylformamide with the molar extinction coefficient between l.6-8.7mol^{-1}cm^{-1}x10^4 and gave bright intense hue from pink to green on polyester, due to the variation in polarity. The %exhaustion of the dyes was between 50-98% and the dyed fabrics generally showed good to excellent washing, perspiration, rub fastness on woven polyester fabric.

Key words: *aminothiophene, fastness, disperse dye, exhaustion, polyester.*

INTRODUCTION

Disperse dyes are often substituted azo, anthraquinone or diphenylamine compounds which are non-ionic and contain no water solubilizing groups (Maradiya 2010). The dye particles are thus held in dispersion by the surface-active agent, which consequently are able to retain comparatively better substantivity for hydrophobic fibres, such as polyester, nylon and acetate (Kent, 1992). For the sake of efficient diffusion into textiles, the particles' of disperse dyes are usually as fine as possible comprising low molecular weight molecules in the range of 400-600 (Nkeonye, 1987,).

The most widely used coloured compounds in various fields such as dyeing of textile fibres, colouring of different materials in biological-medical studies and advanced applications in organic synthesis are the azo dyes (Antonio *et al*., 2008). This is due to the simple process of their synthesis by diazotization and azo coupling to the almost endless possibilities presented by variation of the diazo compounds and coupling components to the generally high molar absorptivity (Alimmari *et al*., 2010). This study aimed at the preparation of thienylphenylmaleimide azo disperse dyes and their application on polymeric fibres such as polyester fabric in line with the increasing demand for easily synthesized, high valued, cheap, environmentally friendly dyes that will meet the specifications and aspirations of textile industries.

MATERIALS AND METHODS

Chemicals

All the chemicals used were analytical grade sourced directly from the manufacturing company by the Chemistry Department Kwazulu-Natal University Durban, South Africa. All the solvents were redistilled before they were used for this work.

Synthesis of the Dyes

General Procedure for Diazotization

Sodium nitrite (0.69g, 0.01mol) was added drop wise over a period of 15 minutes with constant stirring to sulphuric acid (5ml) at 10°C and then the mixture was heated to 65°C for 15 minutes. The solution was then cooled to 5°C using an ice bath and a mixture (10ml) of acetic acid-propionic acid (8:1) was slowly added with constant stirring, allowing the temp to rise to 15°C. The reaction mixture was then cooled to 0-5°C. The finely ground aminothiophene (0.01mol) derivatives were slowly added within 30 minutes below 5°C and then the whole mixture was stirred, keeping the temperature low and constant (0-5°C) for 4 hours. Excess nitrous acid was decomposed by using the appropriate volume of urea.

General Procedure for Coupling

N-phenylmaleimide (1.73g, 0.01mol) was slowly dissolved in acetic acid (10ml) and then cooled in an ice bath at 0°C. The diazonium solution previously prepared was added drop wise over a period of 30 minutes with vigorous stirring. The mixture was stirred for an additional 2 hours at 0-5°C, then sodium acetate solution (10%) was added slowly dropwise until the pH became 4-5. The product was then filtered, washed with warm water and then with cold water until acid-free and air dried. It was recrystallized from DMF. The yield was 69% and melting point was 135°C. The purity of the product was checked by thin layer chromatography using ethylacetate and hexane (1:4) as the solvent system.

Application of the dye on polyester
1% solution of phenol was used as a carrier and 1% solution of soap as the dispersing agent on a 1g polyester fabric which was dyed at a 4% shade at a liquor ratio of 50:1. According to the procedure as published by Giles (1974), the polyester was immersed in a dye bath at 40°c and raised gradually to boil in 30mins and the dyeing proceeded for further 90mins. The polyester fibre was scoured in a solution containing 2g/litre $NaCO_3$ and 1g/litre detergent for 30mins at 70°, neutralised in 1ml/litre acetic acid and rinsed thoroughly with water before dyeing commenced. After dyeing the polyester fibre was rinsed well with water and air dried.

Fastness to Washing Test
The prepared dyed sample of polyester was placed in a conical flask with a solution of soap 2.5g/litre and anhydrous sodium carbonate (1g/litre) at a liquor ratio of 50:1 for 30min at 60°C using the ISO3 method for washfastness. The washed samples were rinsed in cold water and then dried at room temperature. The grey scale was used to assess the change in colour between the washed and unwashed samples and the staining of the undyed fabric

Fastness to Light Evaluation
3cm x 2cm dyed polyester fabric was mounted on strips of white card, with half the sample covered by a second strip of card. A set of blue wool standard were similarly mounted, and arranged together with the dyed samples around the xenon lamp. Exposure was terminated when the contrast between the exposed and unexposed portions of the specimen is equal to Grey 3 on the Grey scale for assessing change in colour, unless standard 7 has previously faded to Grade 4 when the test may be terminated. The light fastness of the specimen is the number of the blue standard which show a similar change in colour as the specimen at the point of termination of the test.

Fastness to Rubbing
A white felt was inserted into the groove of the rubbing hand which rubbed 300 times for both the dry and wet test but the white felt was wetted with distilled water before testing for the wet rubbing test. The principle involves rubbing a piece of standard white cloth against the dyed fibre sample under controlled conditions of pressure and speed. The colour transferred to the white felt was compared with a standard grey scale for colour staining assessment.

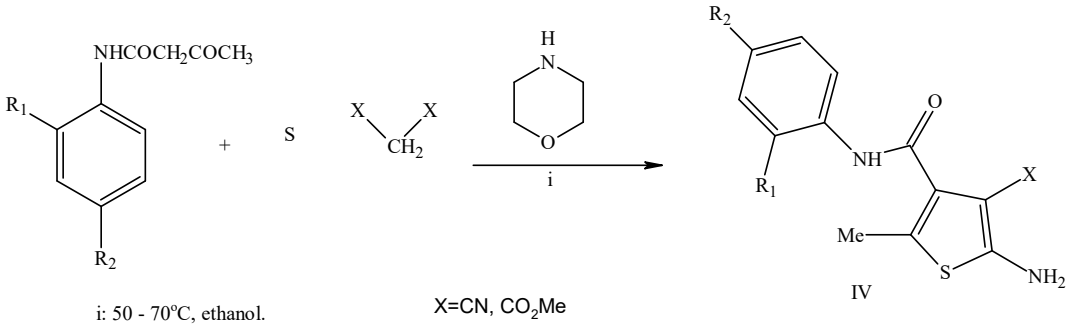
Perspiration Evaluation
Composite samples made of 3cm x 3cm dyed samples sandwiched between two undyed fabrics, were treated in two different solutions (acid and basic solution) containing histidine (immersed in the test solution for 15- 30min and squeezed to 2-2 times its original weight). The samples were then drained and placed between two glass plates of 10cm x 5cm size of 0-15cm thickness under pressure of a weight-piece of mass 5kg. It was kept in an oven for 6h at 38±1^{0}C, the specimen and the adjacent fabrics were dried separately. The grey scales were used to assess the change in colour of each specimen and the staining of the adjacent fibres.

Sublimation Fastness Test
The test for sublimation fastness test was carried out in a temperature regulated oven, the dyed sample was sandwiched between undyed material and the composite specimen was placed between two heated plates for 5minutes at 180°C. The dried fibre was then removed and kept in air for 4hours for conditioning (Maradiya, 2001).

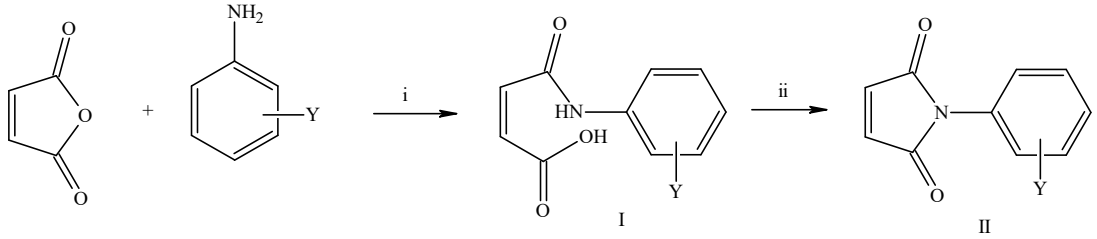
RESULTS AND METHODS

Synthesis of the dyes
Six thienyl N-phenylmaleimide azo disperse dyes were synthesized by diazotising the two diazo components (a) and (b) as shown in scheme1 and coupled them individually with the coupling components 1- 4 in scheme 2. The structures and the physical characteristics of the dyes obtained are shown in Table 1.

Spectra Properties of the Dyes
The absorption spectra of the dyes were recorded in various solvents and the results are summarized in Table 2. The colour of these azo dyes depends on the nature of both the diazo and the coupling components. The electronic spectra of these dyes showed an absorption band in the region 406-435nm in ethanol, 406-427nm in acetone, 405-424nm in toluene and 404-562nm in dimethylformamide (DMF). These bands were due to electronic transitions involving the whole conjugate system both of the phenyl and the five membered sulphur heterocycles and the azo groups as assigned to a transition of $\pi - \pi^*$ type.



Scheme 1: Synthesis of aminothiophene.



Scheme 2: Synthesis of N-phenylmaleimides

Table 1: **STRUCTURE AND PHYSICAL CHARACTERISTICS OF THE SYNTHESIZED DYES**

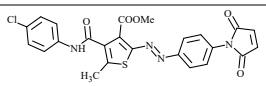
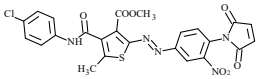
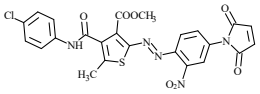
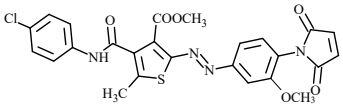
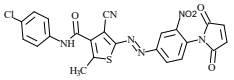
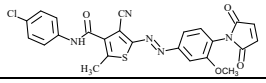
Dye No	Mol formular	Mol wt	Yield%	M.Pt.(°C)	R_f
1a		508.93	76	127	0.88
2a		553.93	69	138-140	0.82
3a		553.93	84	180	0.88
4a		538.95	38	234	0.90
1b		520.90	80	135	0.80
2b		505.93	81	110	0.80538.95

Table 2: VISIBLE ABSORPTION SPECTRA OF THE DYES IN VARIOUS SOLVENTS

Dye No	Mol wt	Maximum Absorption wavelength (λ_{max})nm					Molar Extinction coefficient
		Acetone	Toluene	DMF	Ethanol	Ethanol+HCl	($LMol^{-1}Cm^{-1}$) $X10^4$
1a	508.93	427	424	562	424	431	3.8
2a	553.93	421	411	423	406	403	8.2
3a	553.93	421	420	411	419	417	8.4
4a	538.95	406	405	408	428	404	7.7
1b	520.90	406	419	425	431	427	8.7
2b	505.93	425	420	532	435	435	1.6

Table 3: APPLICATION OF DYE ON FIBRE WITH SHADES OF DYE OBTAINED

Dye No	Polyester fibre	
	%Exhaustion	Colour hue
1a	71	Deep pink
2a	79	Orange
3a	50	Deep orange
4a	98	Brownish purple
1b	58	Green
2b	81	Brown

Table 4: DYEING PROPERTIES OF DYES ON POLYESTER FIBRE

Dye no	Washfastness		Lightfastness	Sublimation		Rubbing		Perspiration			
								Acid		Alkali	
	Cs	Sc		Cs	Sc	Cs	Sc	Cs	Cs	Cs	Cs
1a	5	5	1	5	5	5	3	5	5	5	5
2a	5	5	1	5	4	4	¾	5	5	5	5
3a	5	5	1	5	4			5	5	5	5
4a	5	5	1	5	5	3	3	5	5	5	5
1b	5	5	2	5	5	3	1	5	5	5	5
2b	5	5	3	5	5	3	1	5	5	5	5

Cs-Change of shade of dyed fabric
Sc-staining of cotton
Rating scale: 1-lowest, 5-highest

The introduction of the cyano group as an electron-withdrawing substituent unto the thiophene ring produces a bathochromic shift of the absorption band, while the replacement of the cyano group by a methyl ester exerts a notable hypsochromic shift. This was observed in dyes 1b having λ_{max} of 425nm and 2a with λ_{max} 423nm in DMF. This is attributed to more extensive electron delocalization and the smaller steric requirements of the rod-like cyano group (Hallas, 1999). Bathochromic shifts of the visible absorption band were observed on increasing solvent polarity as seen in the dyes This is expected for a system in which the excited state is more polar than the ground state (Hallas, 1979; Georgiadon, 2002).

The results in Table 2 reveal that the change in λ_{max} value of some of the dyes depend on the position of the substituent on both the diazo and coupling components. The λ_{max} in all these solvents are between 404-562nm. The data reveals that the absorption maximum of the dyes depends on the nature of substitution on the coupling component. No proper generalisation is possible within these series of dyes as far as absorption maxima are concerned.

Solvatochromism of the Dyes

There is a red shift on the visible absorption maxima of the dyes as the solvent polarity increases – this is positive solvatochromism (Antonio *et al*, 2008). The positive solvatochromism is as a result of the increase in the wavelength of absorption with increasing solvent polarity.

Most of the shifts in maximum absorption wavelength observed were bathochromic for many of the dyes where measurements were done in solvent of higher polarity. The maximum absorption wavelength value shifted to longer wavelength when the solvent was changed from ethanol to a more polar solvent such as dimethylformamide (DMF).

Halochromism of the Dyes

Halochromism occurs when the bathochromic shift decreased with the general electron donating capacity of the substituents in the coupling component. The negative halochromism was as a result of the presence of powerful electron donating groups in the coupling component ring of the affected dyes.

The effect of few drops of hydrochloric acid was investigated and the results are summarized in Tables 2. Some of the dyes display positive halochromism, an increase in the λmax of the ethanolic solution on addition of hydrochloric acid. However, majority of the dyes showed negative halochromism a decrease in the λmax in acidic ethanolic solution.

Dyeing Properties of Thienylphenylmaleimide Dyes

The dyeing properties of dyes are given in Table 4 which show that the level of exhaustion and fixation of majority of the dyes ranges from good to excellent. Most of the dyes are pictorially strong brown, orange and deep purple mono azo disperse dyes of low water solubility which are useful for dyeing polymeric materials such as nylon and polyester. The variation in the hues of the dyed fabric resulted from the alteration in both the diazo and coupling components.

The dyes were applied at 4% on polyester fabrics. These dyes gave brown and deep purple hues with excellent brightness, levelness and high tinctorial strength. The addition of dispersing agents (surfactants) helps in promoting levelling by maintaining stability of the dyes and also causing solubilisation of some of the dyes (Datyner,1978; Murray and Mortimer, 1971).The solubilisation of dyes by surfactants is often confused in the technical literature with "increase in solubility", in solubilisation dye interacts with surfactant forming a water soluble species (Arved, 1983) by breaking through dye-water interphase just as in case of oil-water emulsion. In the absence of dispersing agent, there is the risk of deposition of the dye on the surface of the fibre which may result in poor fastness to rubbing.

The dyes were applied on polyester fabric by dyeing with carrier. This was partially successful because of the inability to agitate the dyebath continuously in the domestic pressure pot used for the experiment. Despite this hindrance, it was observed from the result in Table 4 that the colour shades are deeper and the fastness properties are much better (except for lightfastness that is generally poor) and there was no need for alkali clearing because the dyes penetrated well into the fabric without any deposited on the surface.

Shades and Exhaustion Properties of the Dyes

Table 3 shows the shades of dyeing on fibres and exhaustion values of the synthesized dyes which are in the range 50-98%. The dyes produced had different shades and colours ranging from pink to green with good levelness and depth on the fabrics resulting from both the nature and position of the substituent in the coupling components. For instance, dyes 1a-4a were obtained by coupling diazotised 5-Amino-N-(4-chlorophenyl)-4-methoxy-2-methylthiophene-3-carboxide to N-, 2-Nitro, 3-Nitro and 2-Methoxy phenylmaleimides. These series of dyes gave different shades of pink to purple colours. Incorporation of a cyano in place of a methyl ester on the aminothiophene (5-Amino-N-(4-chlorophenyl)-4-cyano-2-methylthiophene-3-carboxide) coupled with 2-Nitro and 2-Methoxy phenylmaleimides gave rise to dyes 1b and 2b, which gave green and brown colours respectively. The trend in the hue of the dyes were generally reflected in those observed for absorption maxima of the dyes in DMF solution (Table 2), which is in agreement with theoretical expectations and previous findings (Choi *et al*, 2000).

Fastness to Washing

The dyes showed fairly good to excellent fastness to washing on polyester fabric. The overall result however, shows that the washfastness of the dyes are very good on polyester as shown on table 4. The synthesized dyes are dispersing dyes that are sparingly soluble in water, hence dyeing takes place from a monomolecular dilute solution of the dye in water, the concentration of which is maintained by the progressive dissolution of solid dye from the finely disperse dye particles in suspension. Therefore, once the dye molecules find their way into the fibre and they are attached to it, they become difficult to remove, more so that it is only sparingly soluble in water. In fact, a remarkable degree of brightness and levelness was observed after washing which shows a clear indication of good penetration and excellent affinity of these dyes to the fibres.

Fastness to Light

The results from Table 4 show that the light fastness of these dyes is generally poor on polyester fibre. In an attempt to trace the relationship between chemical structure and light fastness, it was observed by Maradiya (2010), that there is no absolute value for the light fastness of a dye.

Fastness to Perspiration

The dyeing shows very good (4) to excellent (5) fastness to perspiration properties. The overall results however show that the perspiration fastness values of the dyes are high on the polyester fabric and also better perspiration properties to acid than alkali

CONCLUSION

In conclusion the study showed that a new set of azo disperse dyes (N-Phenylmaleimide Dyes) were synthesized in fairly moderate and good yields and their colour properties examined both in solution and by application on polyester fibre. The diazo component and nature of the substituent in the coupling components also have a great influence on the visible absorption and shade of dyeing. Application of the dye on polyester fibre generally showed good to excellent washing, perspiration and rub but light fastness on the polyester woven fabric

was low. The dyes showed very good to excellent exhaustion and uniform dyeing

ACKNOWLEDGEMENTS

Chemistry Department University of Kwazulu Natal, Durban in South Africa, Chemistry programme, Chemistry Programme, Abubakar Tafawa Balewa University, Bauchi and Ahmadu Bello University Zaria.

REFERENCES

Alimmari, A. S., Marinkovic, A. S., Mijin, D. Z., Valentic, N. V., Todorovic, N. andUscumlic, G. S., (2010). Synthesis, Structure and Solvatochromic Properties of 3-cyano-4,6-diphenyl-5-(3- and 4-substituted phenylazo-2-pyridones) J. Serb. Chem. Soc. 75(8) 1019-103

Antonio, E. H. M., Neuton, M. B., Ligia, M. R., Nkeonye, P. O., and Radim, H. (2008) Study of the Spectropic Properties and First Hyperpolarizabilities of Disperse Azo Dyes Derived from 2-amino-5-nitrothiazole. Journal of photochemistry and Photobiology A: Chemistry 199(2008): 23-33.

Arved, D., (1983) Surfactants in Textile Processing. Mercel Dekker Inc, New York. pp 71-75. `

Choi, J., Sung-Hee, H. and Andrew D. T., (2000): Structure-wetfastness Relationships of some Blue Disperse Dyes for Polyester. Journal of the Society of Dyers and Colourists. 116, pp 276.

Datyner, A., (1978) The Solubilization of Disperse Dyes by Dispersing Agent at 127ºC. Journal of the Society of Dyers and Colourists. 94:256-260.

Georgiadon, K. L. and Tsatsaroni, E. G. Hetarylazo Disperse Dyes Derived from substituted N,N-bis-β-acetoxyethylaniline. Dyes and Pigments. 53, 73-78.

Giles, C.H. (1974). "A laboratory Course in Dyeing", The Society of Dyers and Colourists, Bradford, pp 15-25

Hallas, G. (1979) The Effect of Terminal Group in 4-aminoazobenzene and Disperse Dyes Related Thereto. Journal of Society of Dyers and Colourists. 95, 285-294.

Hallas, G., and Towns A.D (1997) "dyes derived from aminothiophenes Part6: application of some dispersed dyes derived from 2-amino-thiophenes to hydrophobic fibres. Dyes and pigment 33, pp215-28).

Hallas, G. and Jae-Hong, C., (1999). "Synthesis and Properties of Novel Aziridinyl Azo Dyes from 2-aminothiopenes–Part1: Synthesis and Spectral Properties" Dyes and Pigments 40 99-117.

Kent, J. A., (1992), Riegel, s Handbook of Industrial Chemistry, 9th ed., Chapman and Hall, New York. pp 64

Maradiya, H. R., (2001), Synthesis of 2-Azobenzo [b] Theophany Derivatives and their Dyeing Performance on Polyester Fibre. Turk J. Chem 25, 441-450

Maradiya, H. R., (2010), Synthesis and Dyeing Performance of Some Novel Thiazole Azo Disperse Dyes. Journal of Saudi Chemical Society, 14, 77-81.

Murray, A. and Mortimer, K. (1971) Dye Auxiliaries in the Application of Disperse Dyes to Manmade Fibres. Journal of Society of Dyers and Colourists. 87, 173-181.

Nkeonye, P.O (1987), Fundamental Principles of Textiles Dyeing, Printing and finishing. Ahmadu Bello University Press Limited, Zaria, pp 271-275.

KINETIC MODEL FOR GLUCOSE PRODUCTION FROM ELEPHANT GRASS (STEM) USING ASPERGILLUS NIGER

[1*]JIBRIL, A., [1]ADEREMI, B.O., [1]MOMOH, O.R. AND [2]EBENEZER O.

1. Department of Chemical Engineering, Ahmadu Bello University Zaria, Nigeria.
2. Department of Chemical Engineering, University Glasgow, UK.

Keywords: Elephant grass, glucose, Michelis-Menten's constant, reaction rate, *Aspergillus niger*

[*]Corresponding author e-mail: bigdaddynsche@yahoo.co.uk phone: +2348069556596

ABSTRACT

To utilize the economic benefits of elephant grass (pennisetum purpereum) and exploit its potential as biomass for glucose production, the kinetic model for the production of glucose from the grass was investigated at the optimum conditions of hydrolysis (pH 4.5, temperature 45 ^{o}C, time 24 hours). The grass was characterized, pretreated and then hydrolyzed using Aspergillus niger. The effects of particles size (75 - 600 μm), substrate concentration (5 – 100 g/l) and cell loading (0.1 – 1.0 g) were also investigated. Optimum hydrolysis conditions gave the yield of 82.6 % (w/w) glucose. The kinetic model rate expression was tested for the process based on the Michaelis – Menten's kinetics and the kinetic parameters were evaluated from the Lineweaver –Burk plots. The Kinetic parameters – maximum rate of reaction, r_{max}, and Michealis Menten's constant km – obtained are $0.25*10^{-4}$ $g.l^{-1}.s^{-1}$ and 2.85 $g.l^{-1}$ respectively. The model was developed and its reliability was tested with the experimental data. Comparison between the experimental data and those predicted from the rate model indicate good agreement with a correlation coefficient of 0.996.This shows reliability of the model in the design of bioreactor that could be used in the production of glucose from elephant grass.

1.0 INTRODUCTION

The search for eco-friendly and sustainable energy compelled researchers to focus on biomass as the promising fuel source that could relief the world from its energy scarcity and global warming anxiety [1].

In the near future fossil fuel is bound to diminish from the earth surface, hence more work need to be done in the field of biofuels to contend to the future trends. A lot of work has been done and there are so many break-through ranging from the first generation biomass to third generation biomass [3]. Many biofuel plants have been established and production increases all over the years.

However, the second generation biomass (agricultural wastes, grasses, household wastes, other lignocellulosic materials) technology is still not well understood although there are recent improvements.The major setbacks in the development of cellulosic conversion technology are associated primarily with the complex nature of cellulose structure and its resistance to degradation. Other difficulties include the limited number of commercially available enzymes capable of digesting cellulose and the high requirement of enzyme loading coupled with the long period usually needed to attain an appreciable conversion level [10]. These factors make it difficult to run biological systems in a continuous mode. The understanding of biomass reaction kinetics could offer a desirable solution to the aforementioned difficulties.

Chemical kinetics is the study of chemical processes and reactions [9]. This includes analysis of conditions that affect speed of a chemical reaction, understanding reaction mechanisms and transition states, and forming mathematical models to predict and describe a chemical reaction [4]. In enzymatic reactions, the rate of reaction is best described by the Michealis – Menten's reaction kinetics [8]. Where r_{max} (the maximum reaction rate) and k_m (rate constant) are the kinetic parameters, which are needed to be experimentally determined and Cs is substrate concentration.

Many investigators studied the kinetics of biofuel and its intermediate (glucose) production from lignocellulosic biomass so as to provide solutions to the aforementioned problems. [7] reported studies on enzymatic hydrolysis of rice straw using *Trichoderma reseei* cellulase. Also, the effect of cross-linked *Aspergillus niger* cellulase on the hydrolysis of rice hull has been reported by [11]. [12] studied the enzymatic hydrolysis of pretreated rice straw. [1] reported studies on the kinetics of glucose production from rice straw by A*spergillus niger*. [5] developed kinetic model of glucose production from wheat straw by A*spergillus niger*. [2] reported bio-ethanol production from elephant grass using co-cultures of *Aspergillus niger* and *Saccharomyces crevisiae* in simultaneous saccharification and fermentation. Also [3] reported production of bioethanol from elephant grass (stem) by simultaneous saccharification and fermentation.

However, systematic studies on glucose production from elephant grass and evaluation of the relevant kinetic parameters are the principal focus of the present investigation.

2.0 METHODOLOGY

Sample of grass was collected from National Animal Production and Research Institute NAPRI) Zaria provinces. Samples were identified as ***Pennisetum purpureum*** at Biological Sciences Laboratory, Ahmadu Bello University Zaria and were separated into three – the leaves, the inner (soft) stem and the outer (hard) stem. The three samples were dried at 55 °C in an oven for 48 hours, ground to small particles and later sieved using different meshes.

Biomass contents of the three samples were analyzed according to the method of United States National Renewable Energy Laboratory adapted by Animal Science Biochemical Laboratory, Institute of Agricultural Research (IAR) Ahmadu Bello University Zaria. Neutral Detergent Fiber (NDF), Acid Detergent Fiber (ADF), Lignin (L) and other fractions of the grasses were determined. Hemicellulose content of biomass was determined as NDF minus ADF (NDF – ADF), and cellulose content of biomass as 100 minus Lignin minus hemicellulose (100 – Lignin – Hemicellulose). The stem was selected for the conversion.

Pretreatment

100 g of the selected sample was soaked into boiled water and allowed to cool, then filtered and dried at 55 ^{o}C for 48 hours. The filtrate was analyzed for the soluble sugar present. The dried sample was weighed and later separated into two portions. 10 g of one of the portions to be used as treated substrates were added to 100 ml of dilute NH_4OH solution at 25 ^{o}C for 24 hrs. This step was repeated using concentrated NH_4OH solution. The sample was filtered and washed repeatedly with distilled water until pH of 7 was attained. The substrate was then dried in an oven at 55 ^{o}C to a constant dry weight for 48 hours.

Scanning Electron Microscopy (SEM) analyses were carried out for four samples (i.e The untreated, the hot water treated, the dilute ammonium hydroxide solution treated and the concentration ammonium hydroxide solution treated), before the hydrolysis.

Enzymatic hydrolysis

Aspergillus niger was cultured at the Department of Microbiology, Ahmadu Bello University, Zaria and stored in a refrigerator.

In a typical run, 2 g of the substrate was placed in a beaker containing 100 ml of 0.1M solution of sodium acetate at pH 4.5. The temperature of the magnetic stirrer (Sharmond model) was set at constant temperature 45 °C. 0.1g *A. niger* species was added. Sample was being withdrawn after every 30 minutes within 24 hours reaction time for analyses. The concentrations of glucose in the samples were determined by following the method of [9] and [8] which uses a Randox glucose kit and colorimeter (Model WPA 5001, U.S.A.) at 540 nm.

3.0 RESULTS AND DISCUSSION

Development of the kinetic model

The following observations and assumptions are established for convenience:

1. The cells were introduced at their exponential growth phase.
2. The model is targeted to capture only the first segment (initial rate) of the concentration-time curve.
3. Glucose is the main product of interest.
4. A pseudo homogeneous system is being assumed throughout based on solid concentration of 20 g/l
5. The reaction was viewed as enzymes been excreted by the cells into the solution, enabling the overall system to be treated as that of enzyme-substrate kinetics.

Consequently, treatment of kinetic results by graphical differentiation of curves (Figure 1 -7) using the initial rates method [1] afforded the plot of initial rates at different levels of substrate initial concentrations as shown in Figure 8. From this curve, it can be observed that the initial reaction rate is proportional to the substrate concentration (that is, first order reaction) when the substrate concentration is in the low range.

At low concentration of substrate, there is a steep increase in the reaction rate with increasing substrate concentration. The catalytic sites of the enzymes secreted by the cells are probably empty, waiting for substrate to bind, for much of the time, and the rate at which product is formed is limited by the concentration of substrate which is available [6].

Also from the curve, it can be seen that, as the concentration of substrate increases, the reaction rate approaches a constant value indicating that the enzymes become saturated with substrate. As soon as the catalytic sites of the enzymes are empty, more substrate is available to bind and undergo reaction. The rate of formation of product now depends on the activity on the enzymes and not the substrate concentration.

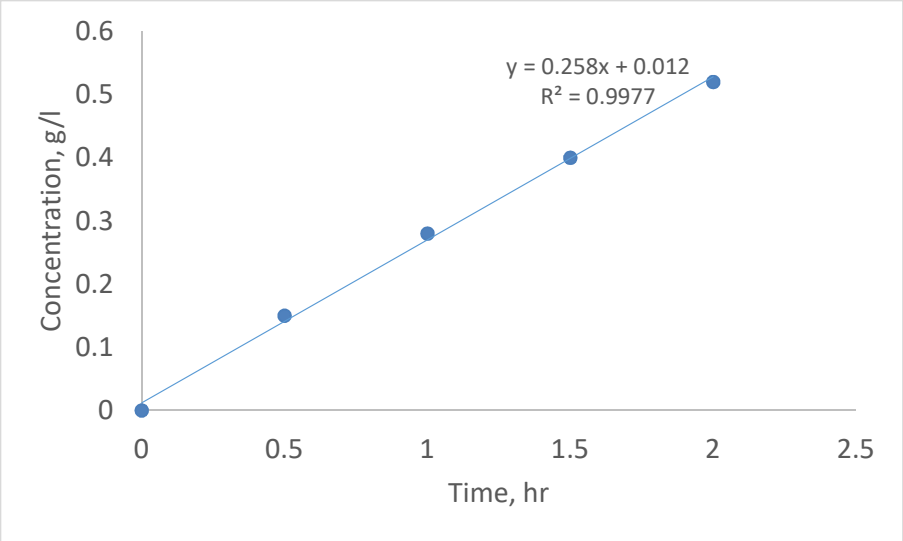


Figure 1: Concentration - Time Plot (Initial substrate, 0.5 g)

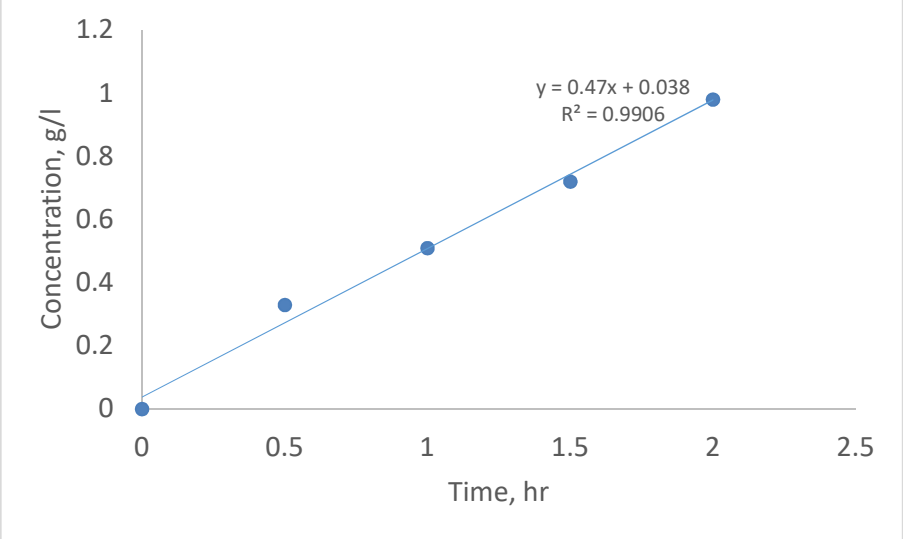


Figure 2: Concentration - Time Plot (Initial substrate, 1.0 g)

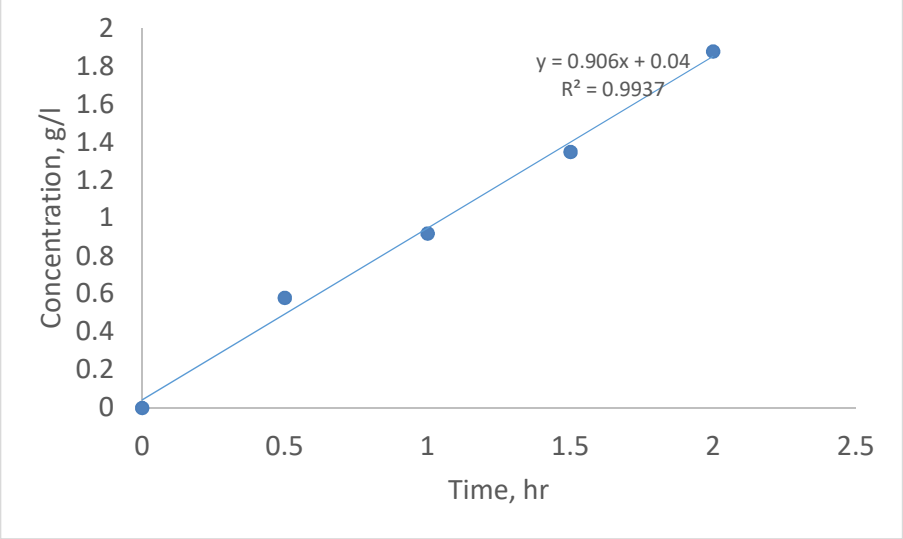


Figure 3: Concentration - Time Plot (Initial substrate, 2.0 g)

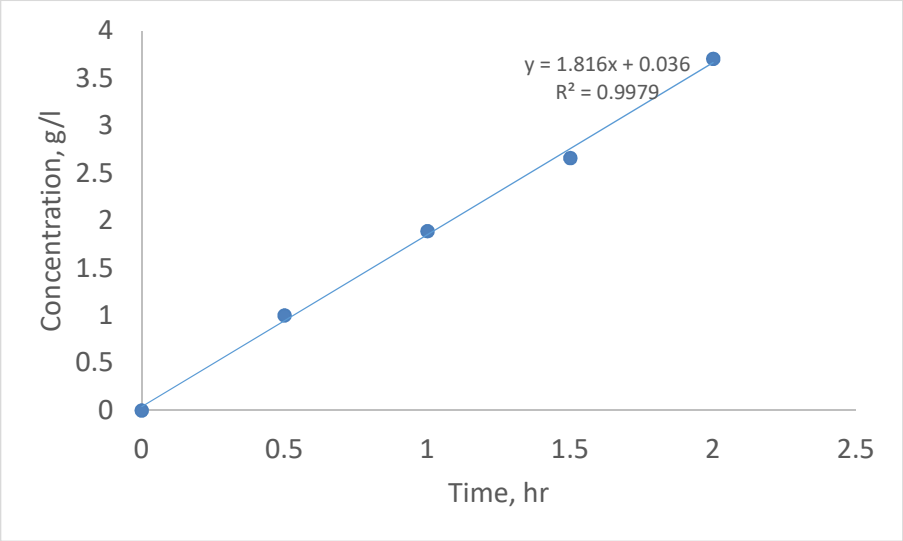


Figure 4: Concentration - Time Plot (Initial substrate, 4.0 g)

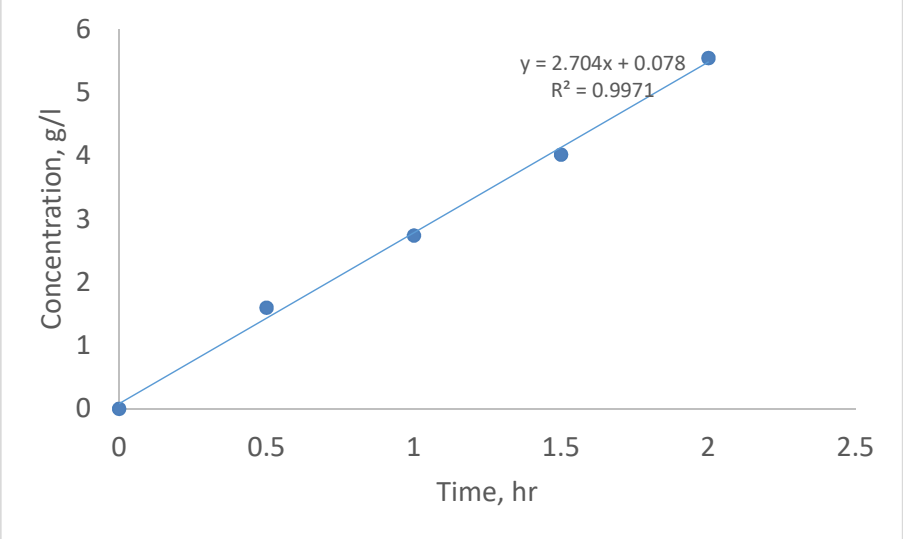


Figure 5: Concentration - Time Plot (Initial substrate, 6.0 g)

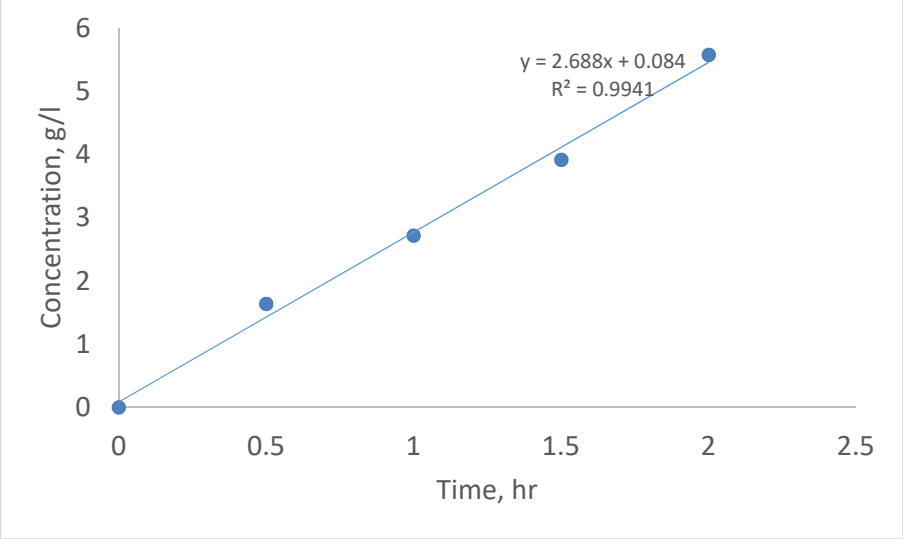


Figure 6: Concentration - Time Plot (Initial substrate, 8.0 g)

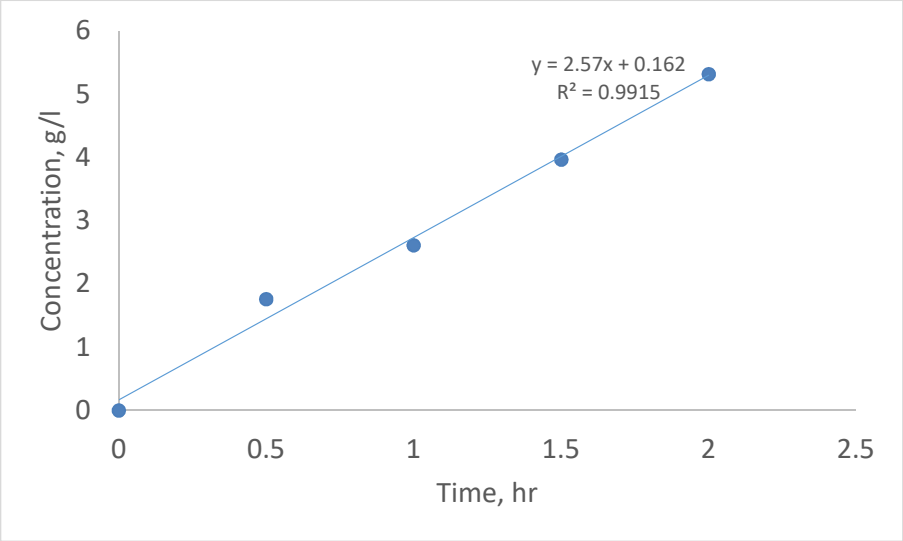


Figure.7: Concentration - Time Plot (Initial substrate, 10.0 g)

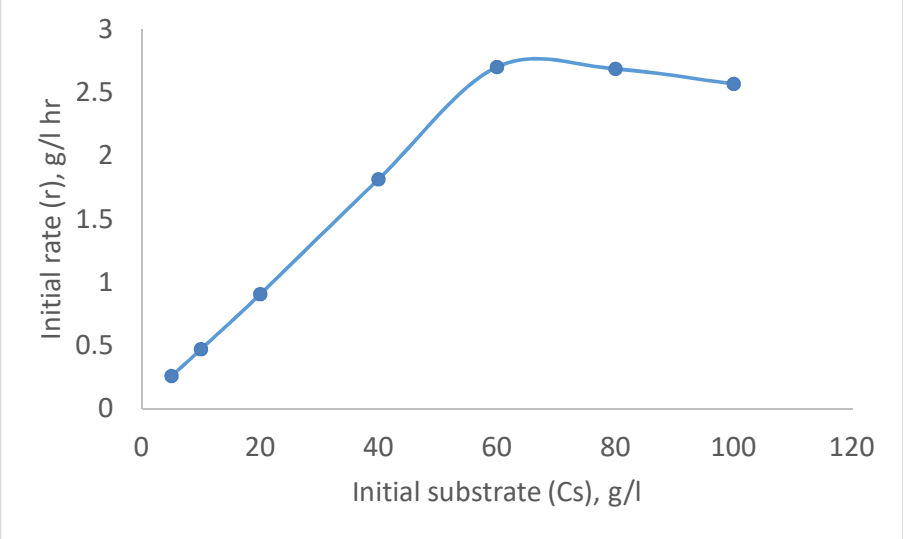


Figure 8: Initial rate versus initial substrate concentration plot

That is, the reaction rate changes gradually from first order to zero order. This form of behavior is commonly described by the Michaelis-Menten kinetic expression:

$$r_p = \frac{r_{max}\, C_s}{K_M + C_s} \quad (1)$$

Where r_{max} (the maximum reaction rate) and k_m (rate constant) are the kinetic parameters, which are needed to be experimentally determined and Cs is the substrate concentration.

Applying the Line weaver – Burk method to linearize the rate expression by inverting equation (1), yields

$$\frac{1}{r_p} = \frac{1}{r_{max}} + \frac{K_M}{r_{max}}\left(\frac{1}{C_s}\right) \quad (2)$$

A plot of the reciprocal of the initial rate r_p versus the reciprocal of the initial substrate concentration Cs is expected to yield a straight line with an intercept $1/r_{max}$ and the slope K_M/r_{max}. A plot of this using the generated experimental data in this work is shown in Figure 4, from which the kinetic parameters (r_{max} and K_M) were estimated as $0.25*10^{-4}$ gl^{-1} s^{-1} and 2.85 gl^{-1}, respectively.

The maximum reaction rate found, conform to the values 0.1910 – 1.7766 * 10^{-4} gl^{-1} s^{-1} reported by [6] when pure enzyme was used on a pure

cellulose in a mixed cellulose system, at a 100% *Aspergillus niger* system (that is no *Trichorderma viride* present).

The reaction rate constant K_M was also found comparable to the value 2.75 gl^{-1} as reported by [6] for hydrolysis of a soluble cellulose (CMC) using the synergetic effects of combined cellulases from *Trichoderma viride* and *A. niger*. K_M represents the strength of binding or affinity of the substrate for the enzyme. Tightly bound substrates have a low K_M and loosely bound substrates have a high K_M. Also the K_M is that concentration of substrate at which half the active sites of the enzyme are filled. This result shows that the K_M is relatively low, hence, the activity of the enzyme will be at constant rate regardless of the variation in substrate concentration.

Also, when K_M is so large compare to Cs, the reaction rate will be first order, and will definitely depend on substrate concentration. On the other hand, when K_M is so small compare to Cs, the reaction rate, r_p will be equal to the maximum reaction rate, r_{max}, hence, the reaction is zero order independent of substrate concentration.

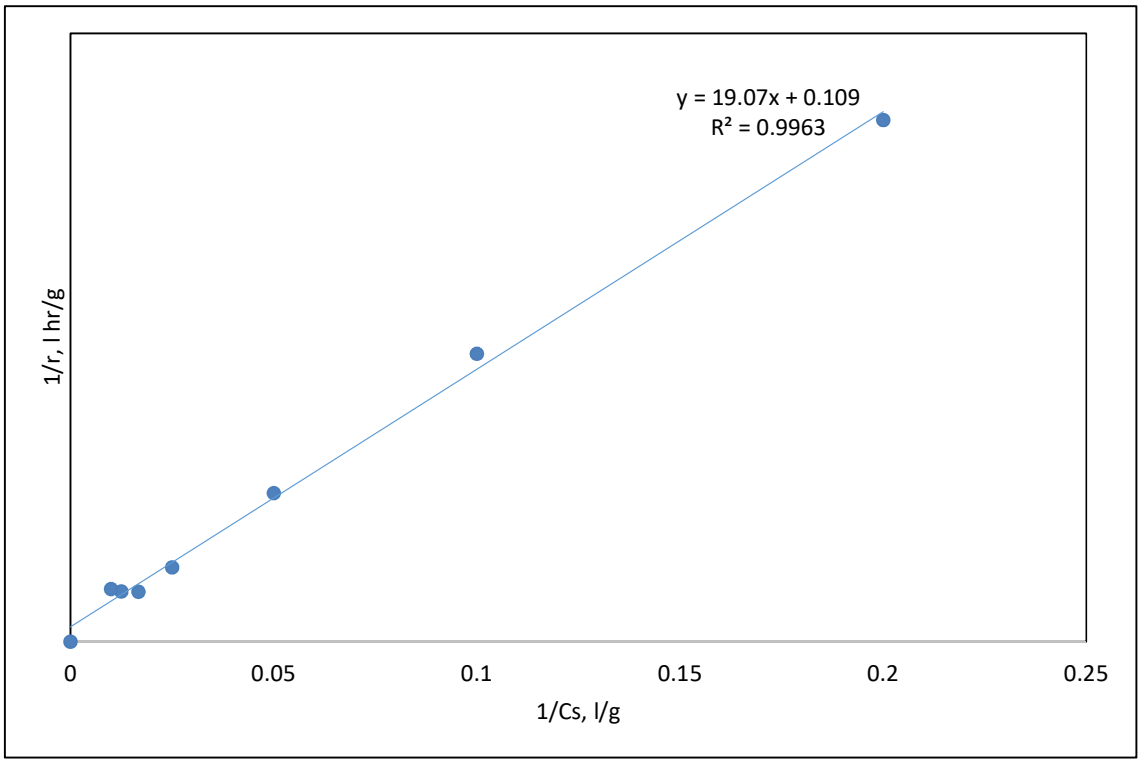


Figure 9. Line-Weaver Burk plot

Based on the evaluated kinetic parameters, the model equation is given as

$$r_p = \frac{0.25 \text{ X } 10^{-4} C_s}{2.85 + C_s} \quad (4.3)$$

The consistency of this model equation was tested with the generated data to evaluate its reliability, statistically. The correlation coefficient (r^2) of the two variables was calculated using this equation:

$$r = \frac{N\sum XY - (\sum X)(\sum Y)}{\sqrt{[(N\sum X^2 - (\sum(X)^2))\,(N\sum Y^2 - (\sum(Y)^2))]}} \quad (4)$$

Where r = correlation coefficient; x = experimental rate values; and y = predicted rate values
After the evaluation, the r^2 was found to be 0.996 indicating fit relationship and good agreement.

CONCLUSIONS

Elephant grass stem contains relatively high amount of cellulose (57 -65 %) and lignin (8 – 11 %) when compared to the leaves which contains 25 % and 7.88 % respectively. Concentrated ammonium hydroxide removes more lignin from a lignocellulosic material than dilute ammonium hydroxide when used for pretreatment. Also enzymes secreted by *Aspergillus niger* in the enzymatic hydrolysis of cellulose are more active at the following optimum conditions: pH 4.5,

temperature 45 °C, particles size range 100 – 150 µm, substrate concentration 20 g/l and cell loading 0.1 g with 82.6 % glucose yield. In the hydrolysis of elephant grass to glucose, the kinetic parameters of the reaction are $r_{max} = 0.25*10^{-4}$ $gl^{-1}s^{-1}$ and $K_M = 2.85gl^{-1}$ as obtained; and the kinetic model established for the process is

$$r_p = \frac{0.25 \text{ X } 10^{-4} \, C_s}{2.85 + C_s}$$

This model equation was found to be consistent with the experimental data with correlation coefficient (r^2) of 0.996.The present study showed that elephant grass is effective for the production of fermentable sugar which can be further processed to bioethanol and other valuable industrial chemicals.

REFERENCES

[1] Aderemi, B.O., Abu, E. and Highina, B.K. (2008). The kinetics of glucose production from rice straw by aspergillus niger. *African Journal of Biotechnology* 7 (11), 1745 – 1752.

[2] Agbodike, T.C. Ado, S.A. and Abdullahi, I.O. (2013). Bio-ethanol production from elephant grass using co-cultures of *Aspergillus niger* and *Saccharomyces crevisiae* in simultaneous saccharification and fermentation. *South Asian Journal of Experimental Biology*, 3 (4), 152-157.

[3] Aiyejagbara, M.O., Aderemi, B.O., and Ameh O.A. (2015). Production of ethanol from elephant grass (Pennisetum purpureum). *International Journal of Innovative mathematics, statistics and energy policies* 4 (1), 1 – 9.

[4] Helmenstine, P. (2015). A review on bioenergy and biofuels: sources and their production. Retrieved from www.researchgate.net/publication.

[5] Highina, B. K., Oladekun, O. A. J. and Abba Aji, M. A. (2011). Kinetic model for glucose production from wheat straw material using Aspergillus niger. J*ournal of applied phytotechnology in environmental sanitation*, 1 (1), 23-28.

[6] Imai M, Ikari K, Suzuki I (2004). High-performance hydrolysis of cellulose using mixed cellulase species and ultrasonification pretreatment. *Journal of Biochem. Eng. 1*7, 79-83

[7] Kaur P.P, Arneja J.S. and Singh J. (1998). Enzymatic hydrolysis of rice straw by crude cellulose from *Trichodernia reseei*. *Bioresource Technology.* 16, 267-269.

[8] Lee, J.M. (1992). Biochemical engineering. Prentice - Hall, inc. London. Pg 259-262.

[9] Lee, Y. and Fan L.T. (1982). Kinetic studies of enzymatic hydrolysis of insoluble cellulose. Analysis of the initial rates. *Biotechnology Bioengineering*, 24 (2), 2383-2406.

[10] Luo J, Xia LM, Lin JP, Cen PL (1997). Kinetics of Simultaneous Saccharification and lactic acid fermentation processes. *Biotechnol. Prog.* 136, 762-767.

[11] Sharma, A., Khane, S.K. and Gupta, M.N. (2001). Hydrolysis of rice hull by cross linked *Aspergillus niger. Bioresource Technology* ,78, 281-284.

[12] Vlasenko, E.Y., Ding, H., Labavitch, J.M. and shoemaker, S.P. (1997). Enzymatic hydrolysis of pretreated rice staw. *Bioresource Technology*, 59 (6), 109-119.

GLUCOSE PRODUCTION FROM ELEPHANT GRASS (PENNISETUM PURPUREUM)

[1*]JIBRIL, A., [1]ADEREMI, B.O., [1]MOMOH, O.R. AND [2]EBENEZER O.

1. Department of Chemical Engineering, Ahmadu Bello University Zaria, Nigeria.
2. Department of Chemical Engineering, University of Glasglow, England.

[*]Corresponding author e-mail: bigdaddynsche@yahoo.co.uk phone: +2348069556596

ABSTRACT

Aforetime, corn, rice, sorghum, wheat and cassava are the main sources of glucose production. But recently, the agricultural waste and grasses have been focused as the alternative method to produce glucose. In this work, elephant grass has been exploited to produce glucose, which is an intermediate product for bioethanol and other industrial chemicals production. The elephant grass was characterized in three parts (the leaves, the inner stem and the outer stem) of which the stem (inner and outer) gave high amount of cellulose available for conversion. The cellulose laden part of the grass was pretreated with hot water, 0.2 M NH_4OH, and 3 M NH_4OH. After the pretreatment, the substrate was hydrolyzed for 24 hours using Aspergillus niger in 0.1 M sodium acetate buffer solution. Effect of various parameters on glucose yield was investigated i.e: time, 8 – 72 hours; pH, 3.5 – 6.5; temperature, 30 – 60 ^oC; particle size range, below 100 – 600 μm; substrate concentration,5 – 100 g/l; and cell loading, 0.1– 1.0 g. The optimum values obtained are 24 hours, 45 ^oC, 4.5, 20 g/l, 100 – 150 μm and 1.0 g, for time, pH, temperature, particles size range, substrate concentration and cell loading, respectively. Glucose production at the obtained optimum conditions gave a glucose yield of 82.6 %. This present study shows that elephant grass is effective for glucose production.

Keywords: *Elephant grass, Cellulose, glucose, Aspergillus niger*

INTRODUCTION

Glucose is an ubiquitous energy source in biological systems [14]. As a simple sugar, glucose is a monosaccharide used in nature as a monomer to create polysaccharides such as starch and cellulose in plants and glycogen in animals. Hence, production of glucose from the natural sources via hydrolysis is more of depolymerization reactions. However, while starch is readily depolymerized to give glucose, cellulosic degradation is more challenging, due to its strong β – 1,4 glycosidic bond when compared to the α – 1,4 glycosidic bond in starch.

According to [10] commercial and cost-effective production of biofuels from biomass remains a daunted task. Although, a lot of breakthrough has been achieved in the field of biomass conversion, the actualization of commercially viable biofuels from second generation biomass is still pending. Researchers are recently, able to produce biofuels from elephant grass in a one-pot simultaneous saccharification and fermentation processes, but the quantification of glucose, an intermediate product formed during fermentation is a critical step to improve biofuel yield [18].

Traditionally, starch from edible crops such as corn, potato, sugar cane, cassava etc. have been the main substrate for glucose production. However, its competition within the food chain compels seeking alternative sources i.e grasses, agricultural wastes, algae etc. among which grasses and lignocellulosic agricultural wastes have been found most promising for abundance and sustainability [14]. Nonetheless, the major setbacks in the development of cellulosic conversion technology are associated primarily with the complex nature of cellulose structure and its resistance to degradation. Other difficulties include the limited number of commercially available enzymes capable of digesting cellulose and the high requirement of enzyme loading coupled with the long period usually needed to attain an appreciable conversion level [11]. These factors make it difficult to run biological systems in a continuous mode.

Attempts at addressing the aforementioned problems have led investigators to use soluble cellulose [4], filter paper [18], sawdust and animal solid wastes [5] with impressive results. [7] reported studies on enzymatic hydrolysis of rice straw using *Trichoderma reseei* cellulase. Also, the effect of cross-linked *Aspergillus niger* cellulase on the hydrolysis of rice hull has been reported by [16]. [17] studied the enzymatic hydrolysis of pretreated rice straw. [1] reported studies on the kinetics of glucose production from rice straw by A*spergillus niger.* Also [2] reported production of bioethanol from elephant grass by simultaneous saccharification and fermentation.

However, systematic studies on glucose production from elephant grass and evaluation of the relevant kinetic parameters are the principal

focus of the present investigation.

METHODOLOGY

Sample of grass was collected from National Animal Production and Research Institute NAPRI) Zaria provinces. Samples were identified as ***Pennisetum purpureum*** at Biological Sciences Laboratory, Ahmadu Bello University Zaria and were separated into three – the leaves, the inner (soft) stem and the outer (hard) stem. The three samples were dried at 55 °C in an oven for 48 hours, ground to small particles and later sieved using different meshes.

Biomass contents of the three samples were analyzed according to the method of United States National Renewable Energy Laboratory adapted by Animal Science Biochemical Laboratory, Institute of Agricultural Research (IAR) Ahmadu Bello University Zaria. Neutral Detergent Fiber (NDF), Acid Detergent Fiber (ADF), Lignin (L) and other fractions of the grasses were determined. Hemicellulose content of biomass was determined as NDF minus ADF (NDF – ADF), and cellulose content of biomass as 100 minus Lignin minus hemicellulose (100 – Lignin – Hemicellulose) [12]. The stem was selected for the conversion.

Pretreatment

100 g of the selected sample was soaked into boiled water and allowed to cool, then filtered and dried at 55 ^{o}C for 48 hours. The filtrate was analyzed for the soluble sugar present. The dried sample was weighed and later separated into two portions. 10 g of one of the portions to be used as treated substrates were added to 100 ml of dilute NH_4OH solution at 25 ^{o}C for 24 hrs. This step was repeated using concentrated NH_4OH solution. The sample was filtered and washed repeatedly with distilled water until pH of 7 was attained. The substrate was then dried in an oven at 55 ^{o}C to a constant dry weight for 48 hours.

Scanning Electron Microscopy (SEM) analyses were carried out for four samples (i.e The untreated, the hot water treated, the dilute ammonium hydroxide solution treated and the concentration ammonium hydroxide solution treated), before the hydrolysis.

Enzymatic hydrolysis

Aspergillus niger was cultured at the Department of Microbiology, Ahmadu Bello University, Zaria and stored in a refrigerator.

In a typical run, 2 g of the substrate was placed in a beaker containing 100 ml of 0.1M solution of sodium acetate at pH 4.5. The temperature of the magnetic stirrer (Sharmond model) was set at constant temperature 45 °C. 0.1g *A. niger* species was added. Sample was being withdrawn after every 30 minutes within 24 hours reaction time for analyses. The concentrations of glucose in the samples were determined by following the method of [9] and [8]which uses a Randox glucose kit and colorimeter (Model WPA 5001, U.S.A.) at 540 nm.

RESULTS AND DISCUSSION

Experimental results obtained are explicitly presented in tables, figures and plates. These results indicate that when elephant grass is adequately exploited, it gives reasonable yield of glucose, which can be further processed to biofuel and other industrial chemical such as hydroxymethylfulfural.

Due to the large number of anticipated experimental runs, some preliminary studies were done to ascertain the practical significance, if any, of delignification on glucose yield. Similarly, the particle size of elephant grass required for optimum reaction rate in favor of the targeted product was also determined.

Elephant grass constituents' analysis

Table 1 shows the fiber fractions and proximate compositions of elephant grass. It could be seen that the stem contains more lignin than the leaves, and this is due to the fact that the stem protecting to the other parts of the plant. The difference in neutral detergent fiber (NDF) and acid detergent fiber (ADF) gives the value of the hemicellulose contents of the plant [12]. The various values of ADF and NDF presented in Table 1 indicates that the leaves contain more hemicellulose than the stem of the plant. In terms of proximate compositions, the leaves contain more crude protein than the stem, while the entire plant has very little oil making it difficult for biodiesel production. The stem also has more carbohydrate contents than the leaves, which shows that the stem will give more sugar than the leaves.

In Table 2, it could be seen that the inner stem has the highest cellulose contents (68.25 %) followed by the inner stem with 57.06 %. Thus, the stem was chosen for the hydrolysis since it contains more cellulose than the leaves. Perhaps, this explains why most researchers often use the stems for biofuel production. For example, [2] in their work used elephant grass stem to produce bioethanol by simultaneous saccharification and fermentation and obtained 78 % yield.

Effect of pretreatment on glucose yield

Table 3 shows the contents of cellulose, hemicellulose and lignin of the stem after pretreatment. The results show that when concentrated ammonium hydroxide is used for pretreatment more lignin was removed than when dilute ammonium hydroxide was used. Also, from the results, it could be observed that pretreatment with hot water removed and dispersed some amount of lignin. This may save some cost of using chemicals for the pretreatment. Hot water was used to remove the soluble sugar content of the elephant grass.

Scanning Electronic Microscopy (SEM) analyses were made for the grass sample both before and after pretreatment and the results are as shown in Plate 1:

Table 1 Fiber fractions of elephant grass

Description	% Lig.	% DM	% ADF	% NDF	% C.P	% C.F	% Oil	% Ash	% NFE
Inner Stem	8.05	75.72	29.66	53.36	2.79	10.24	0.40	3.42	83.15
Outer Stem	10.78	91.64	49.88	82.04	1.36	27.76	0.18	9.76	68.60
Leaves	7.88	58.36	4.62	71.38	6.29	16.84	1.95	2.10	65.16

Table 2 Experimental values for elephant grass composition before pretreatment

Description	% Lignin	% Hemicellulose	% Cellulose
Inner Stem	8.05	23.70	68.25
Outer Stem	10.78	32.16	57.06
Leaves	7.88	66.86	25.26

Table 3 experimental values for elephant grass stem composition after pretreatment

Description	% Lignin	% Hemicellulose	% Cellulose
Inner Stem	1.24	23.70	68.25
Outer Stem	2.78	32.16	57.06
Leaves	0.88	66.86	25.26

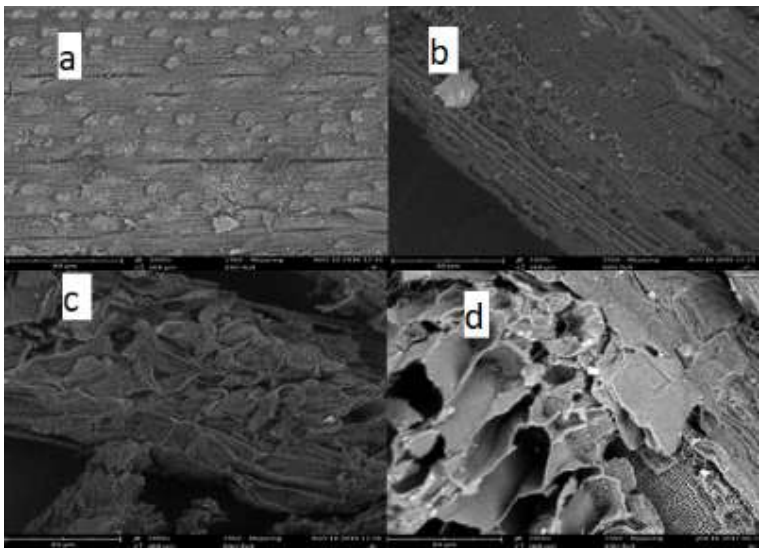


Plate 1: Scanning Electron Microscopy (SEM) view: (a) Untreated (b) Treated with hot water (c) Treated with dilute ammonium hydroxide (d) Treated with concentrated ammonium hydroxide.

Plate 1 (a) shows the untreated sample of elephant grass. It could be seen that lignin accumulated in layers providing shield for the cellulose from enzymes attack. In plate 1 (b), a sample of elephant grass treated with hot water is displayed. Here, lignin was partially dispersed, exposing some parts of the cellulose for enzyme attack. Also plate 1 (c) displayed the sample of elephant grass treated with dilute ammonium hydroxide. In this case, more of lignin was removed but little cellulose was exposed, this may be due to the weakness of the dilute solution. Plate 1 (d) shows clearly that when elephant grass was treated with concentrated ammonium hydroxide, more lignin was removed and dispersed, exposing the cellulose for enzymes attack.

It has been established that when cellulose is exposed to enzymes attack in the appropriate conditions high yield of glucose is expected.

Enzymatic hydrolysis

After the hydrolysis process, glucose concentrations and yields were determined and some parameters were varied and the results obtained with the variation of each parameter are as presented in figures1 – 4

Determination of glucose concentrations

Figure 1 shows the relationship between the absorbance and glucose concentration. It is clear that the relationship is linear, hence, this curve was used as a standard for the determination of the concentrations of the produced glucose.

Effect of reaction time on glucose yield

In figure 2, glucose yield increased with increase in reaction time, but at a certain time no significant changes were observed. It could be seen that at 8 hours only 23.86 %, 25.57 % and 26.10 % yields were obtained for the untreated, dilute ammonium hydroxide treated and concentrated ammonium hydroxide treated substrates, respectively. When the reaction time was extended to 24 hours the yields were 77.19 %, 80.09% and 82.56 %. But at 48 and 72 hours there were no significant changes observed. This indicate that the reaction could be quenched at 24 hours, since no more yield could be obtained after this time. This result also indicates that critical evaluation should be done when deciding for pretreatment since, the difference in yield is not much, considering the amount of money that could be invested for pretreatment.

Effect of pH on glucose yield

The pH of 3.5, 4.0, 4.5, 5.0, 5.5, 6.0 and 6.5 were used to investigate the effect of pH on glucose yield. Other conditions kept constant are as shown at the foot note of Figure 3. From the result, it could be deduced that as the pH increased from 3.5 to 4.5, the glucose yield increased to a maximum of 82.6 %. Increase in pH to 5.0 also gives a reasonable yield of 80.12 %. But further increase in pH to 5.5 resulted in decrease in the yield of glucose. At pH 6.5, there was a drastic decrease in glucose yield indicating that neutral medium does not favour the reaction. The decrease in glucose yield is due to the fact that the cells are more active in mildly acidic medium (pH of 3.5-5.0 for *A. niger* cells), Thus the increase in pH of the medium away from the more acidic medium results in decrease in glucose yield. The reported pH tolerance range for *A. niger* is 3.5-7.0 [14]. Moreso, metabolic processes are generally temperature and pH dependent. Similar result was reported by [1] in hydrolysis of rice straw to produce glucose in which the optimal pH range that gave the highest yield of glucose was 4.5 - 5.0.

Effect of temperature on glucose yield

Figure 4 shows the result of the effect of temperature on glucose yield. This result shows the optimum temperature range of 40 – 50 °C is needed to achieve the best elephant grass conversion to glucose. This is in agreement with the result obtained from the hydrolysis of animal manure lignocellulosic at 50 ^{o}C as reported by [18] and pretreated apple pomace at 40 ^{o}C reported by [3]. It also agrees with the result reported by [1] in their work the kinetic of glucose production from rice straw in which the temperature range was 45 – 50 ^{o}C. [6] also reported optimum glucose yield at 45 ^{O}C, in hydrolysis of wheat straw by *Aspergillus niger.*

In this result, it could be observed that lower temperatures like 30 ^{o}C and 35 ^{o}C favour more formation of glucose than higher temperatures (i.e 55 ^{o}C – 65 ^{o}C). This might be due to the fact that enzyme activity and other chemical reaction in the cells are not favoured at those temperatures.

Effect of particles size on glucose yield

Figure 5 shows how glucose yield varies with changes in particles size ranges. It can be seen from the result that the particle size range of 100 μm – 150 μm gave the highest glucose yield of 82.56 %. But as the particles size ranges increase from 151 μm – 600 μm, glucose yield decreases continuously from 82.56 % to 34.37 %,. This implies that as the particle size increases beyond 150 μm, the surface area available for enzymatic attack decreases. Also agitation during stirring was more effective with smaller particles size than the

larger particle sizes. Further reduction in the particle size below 100 µm has no significant influence on glucose yield (≈ 80 %). This result conforms to the work reported by [18], [1] and [3].

Effect of amount of substrate on glucose concentration

Different initial amounts of substrate were used to investigate how substrate amount varies with product concentration. The amounts of substrate used as indicated in Figure 4.6 were 0.5 g, 1.0 g, 2.0 g, 4.0 g, 6.0 g, 8.0 g and 10.0 g. Other reaction conditions kept constant are as shown in the footnote of figure 4.5. It is clear from the result that glucose concentration increased from 3.6 g/l to 36.34 g/l as the amount of substrate increased from 0.5 g to 10.0 g. This result is expected since more substrate give more product.

Effect of substrate concentration on glucose yield

Figure 7 shows how glucose yield is affected with various substrate concentrations. At the initial stage, the yield increased from 71.3 % to 82 .6 % as substrate concentration increased from 1 mol/l to 6 mol/l. This might be due to inadequate substrate for enzymes attack, thus the cells would rather feed on the product formed, thereby causing the low percentage yield. But the results became stable as the substrate concentration increased from 6 mol/l to 29 mol/l, the product yield drop from 82.6 % to 36.3 %. This decrease in product yield is expected since percentage yield is calculated on weight basis. At high substrate concentration, the enzymes are saturated, since they had enough to feed on, thus, at this point, reaction rate does not depend anymore on substrate concentration indicating zero order reaction. These results conform to the one reported by [3] in the hydrolysis of apple pomace to produce glucose. It also agrees with the results reported by [13] in the hydrolysis of banana stem to produce glucose using stain B.

Effect of cell loading on glucose yield

The effect of *Aspergillus niger* concentration on glucose yield was investigated, while keeping the other parameters constant as indicated in the footnote of Figure 8. The result shows that as *A. niger* concentration increases from 0.1 g to 1.0 g, glucose yield increases from 82.6 % to 90 % after 24 hours of hydrolysis. Similarly, as the cell loading increased, the glucose concentration increased proportionally. This may be due to continuous excretion of enzymes by the cells into the solution. This result agrees with that reported by [1] and [3].

CONCLUSIONS

The cellulose laden part of elephant grass was investigated by characterization and ammonium hydroxide was used for its pretreatment followed by enzymatic hydrolysis with *Aspergillus niger.* Elephant grass stem was found to contain relatively high amount of cellulose (57 -65 %) and lignin (8 – 11 %) when compared to the leaves which contained 25 % and 7.88 % respectively, but when pretreated, the amount of lignin contained in the stem reduced to 1-3 %. Also 82.6 % glucose yield was successfully produced at the following optimum conditions: reaction time 24 hours, pH 4.5, temperature 45 °C, particles size range 100 – 150 µm, substrate concentration 20 g/l and cell loading 0.1 g. The present study showed that elephant grass is effective for the production of fermentable sugar which can be further processed to bioethanol and other valuable industrial chemicals.

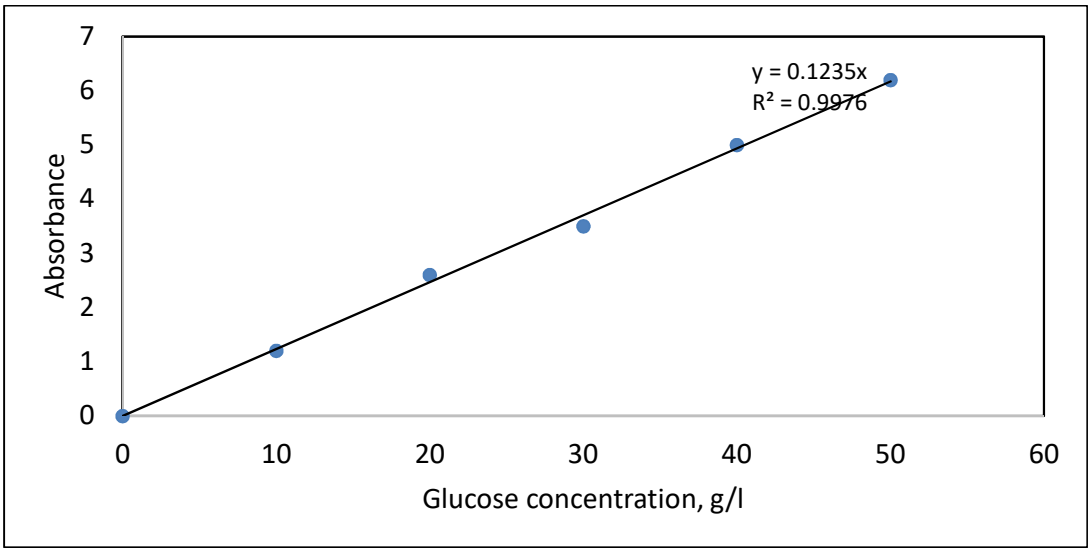


Figure 1 Glucose concentrations standard curve

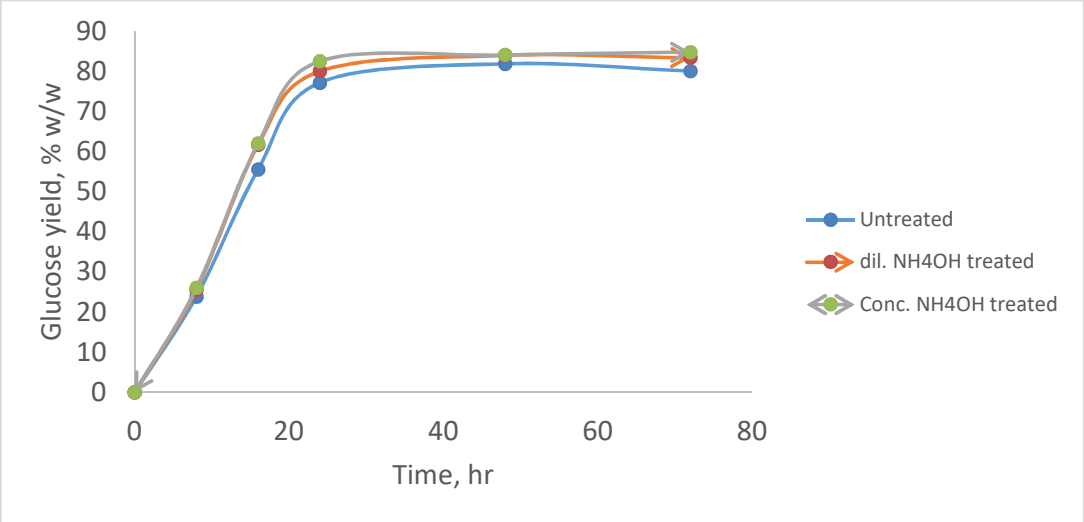


Figure 2: Effect of reaction time on glucose yield (@ 45 °C, pH 4.5, 100 – 150 µm, 20 g/l substrate concentration, 0.1 g cell loading)

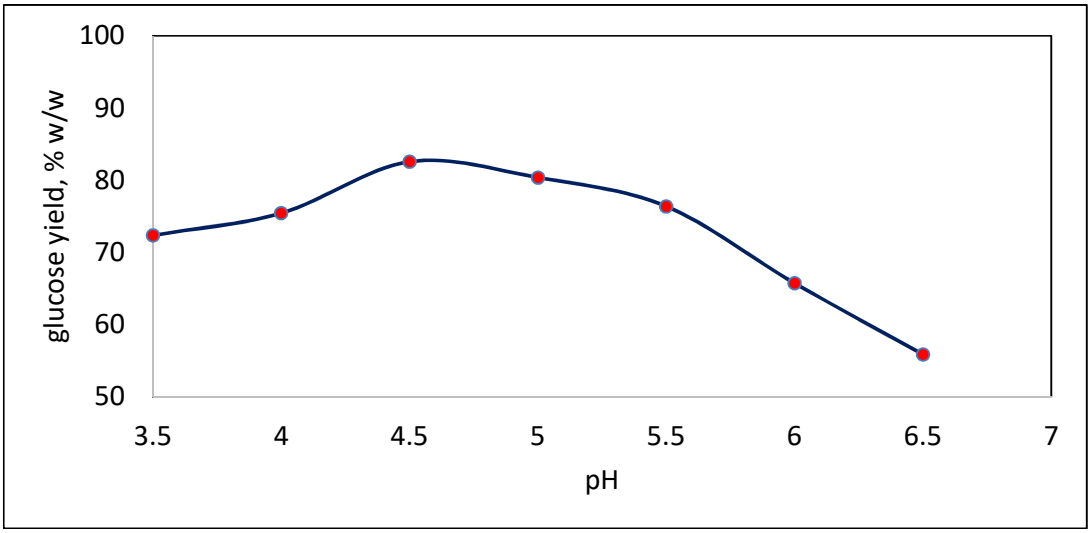


Figure 3: Effect of pH on glucose yield (@ 24 hours, 45 °C, 100 – 150 µm, 20 g/l substrate concentration, 0.1 g cell loading)

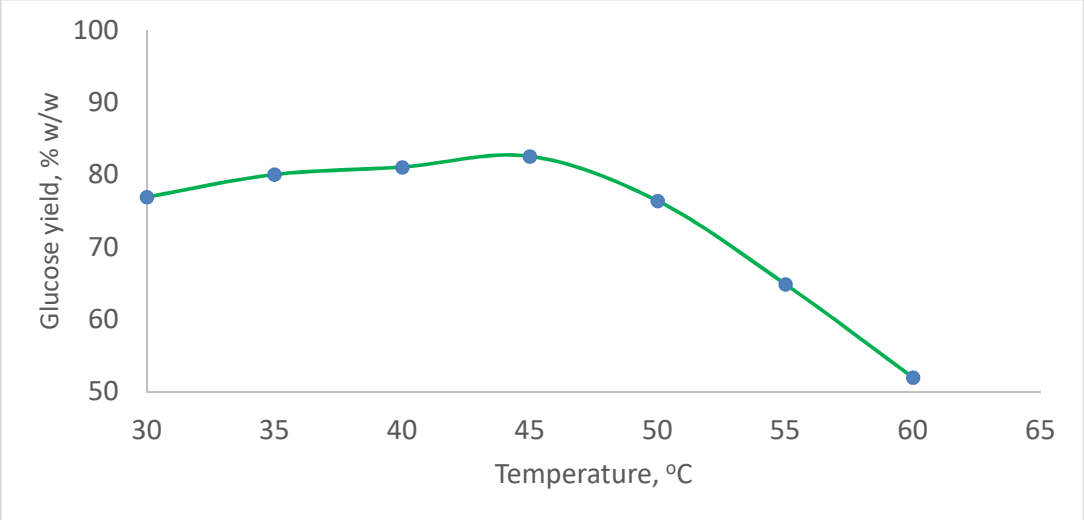


Figure 4: Effect of Temperature on glucose yield (@ 24 hours, pH = 4.5, 100 – 150 µm, 20 g/l substrate concentration, 0.1 g cell loading)

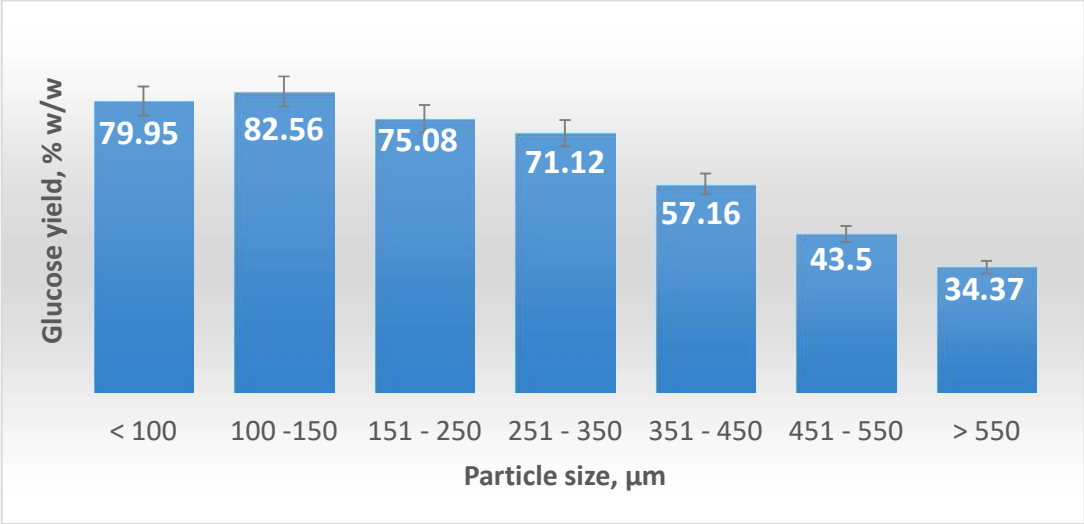


Figure 5: Effect of particle size on glucose yield (@ 24 hours, 45 °C, pH = 4.5, 2 g substrate concentration, 0.1 g cell loading)

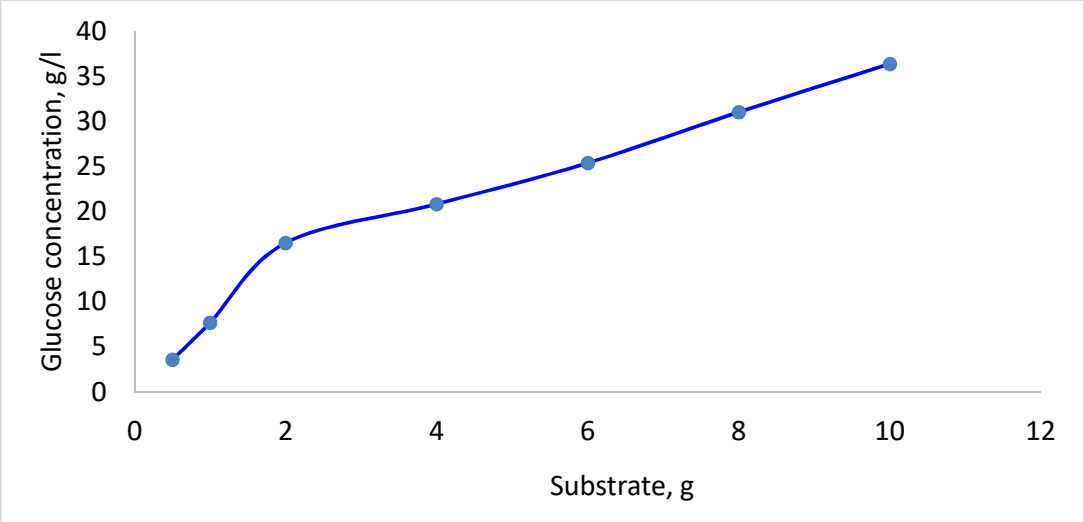


Figure 6: Effect of amount of substrate on glucose concentration (@ 24 hours, 45 °C, 100 – 150 µm, pH = 4.5, 0.1 g cell loading)

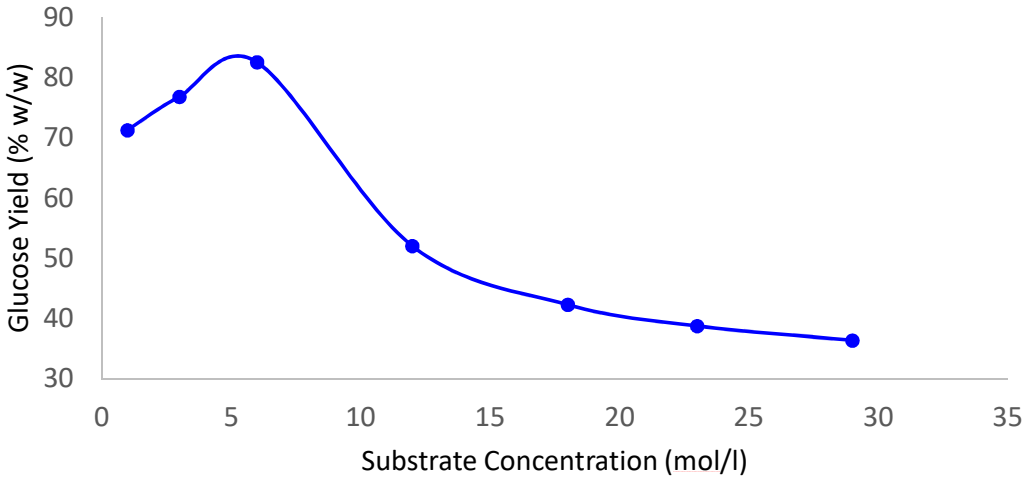


Figure 7: Effect of substrate concentration on glucose yield (@ 24 hours, 45 °C, 100 – 150 µm, pH = 4.5, 0.1 g cell loading)

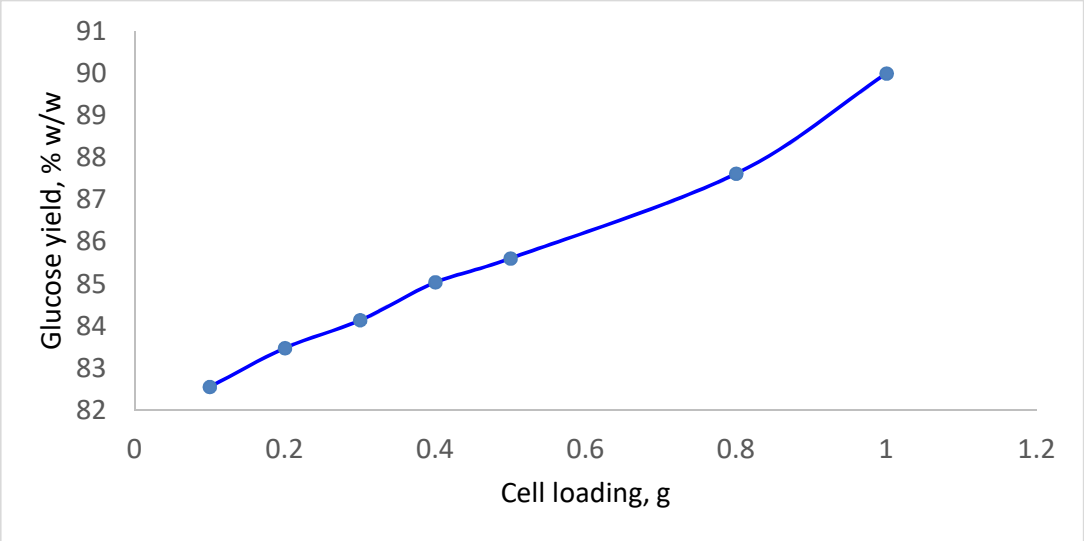


Figure 8: Effect of cell loading on glucose yield (@ 24 hours, 45 °C, 100 – 150 µm, pH = 4.5, 20 g/l substrate concentration)

REFERENCES

Aderemi, B.O., Abu, E. and Highina, B.K. (2008). The kinetics of glucose production from rice straw by aspergillus niger. *African Journal of Biotechnology* vol. 7 (11), pp. 1745 – 1752.

Aiyejagbara, M.O., Aderemi, B.O., and Ameh O.A. (2015). Production of ethanol from elephant grass (Pennisetum purpureum). *International Journal of Innovative mathematics, statistics and energy policies* vol. 4 (1), pp. 1 – 9.

Alexander, D., Richard D., Scott, G. and Ryan P.(2012). Enzymatic Hydrolysis of Cellulosic Biomass for the Production of Second Generation Biofuels. Unpublished MSc. Thesis. Worcester Polytechnic Institute.

Duff, S.J.B. and Murrray, W.D. (1996). Bioconversion of forest products for production of ethanol: a review. *Bioresource Technology,* 55: 1-33.

Gregg, D.I. and Saddler, D.N. (1996). Factors affecting cellulose hydrolysis and the potential of enzyme recycle to enhance the efficiency of an integrated wood to ethanol process. *Biotechnology Bioengineering*, 51:375.

Kaur P.P, Arneja J.S. and Singh J. (1998). Enzymatic hydrolysis of rice straw by crude cellulose from *Trichodernia reseei*. *Bioresource Technology.* 16:267-269.

Lee, J.M. (1992). Biochemical engineering. Prentice - Hall, inc. London. Pg 259-262.

Lee, Y. and Fan L.T. (1982). Kinetic studies of enzymatic hydrolysis of insoluble cellulose. Analysis of the initial rates. *Biotechnology Bioengineering*, 24: 2383-2406.

Liming, X. and Xueling, S. (2004). High yield cellulose production by *Trichoderma ressei* Zu-02 on corn cob residue. *Bioresource Technology* ,91: 259-262.

Luo J, Xia LM, Lin JP, Cen PL (1997). Kinetics of Simultaneous Saccharification and lactic acid fermentation processes. *Biotechnol. Prog.* 136: 762-767.

National Renewable Energy Laboratory, (2013). Proximate analysis manual, USA.

Norhidayu, B. A. (2014). Production of glucose from banana stem waste by using strain B. Retrieved from http: www.malrep.uum.edu.my

Peter, H., Schmauder, H. And Klemm D. (2016). Cellulose: polysaccharides. Wiley online Library. Retrieved from http: www.wiley.com/cellulose

Rezael, P.S., Najafpour,G.O., Shafaghati, H., and Mahjoub, S. (2009). Production of α-Amylase from starch using *Aspergillus niger*. *World applied sciences journal,* 7: 306-311

Sharma, A., Khane, S.K. and Gupta, M.N. (2001). Hydrolysis of rice hull by cross linked *Aspergillus niger*. *Bioresource Technology* ,78: 281-284.

Vlasenko, E.Y., Ding, H., Labavitch, J.M. and shoemaker, S.P. (1997). Enzymatic hydrolysis of pretreated rice staw. *Bioresource Technology*, 59: 109-119.

Wen Z, Liao W, Chen S (2004). Hydrolysis of animal manure lignocellulosic for reducing sugar production. *Bioresource Technology*. 91: 31-39.

DEVELOPMENT OF PEROVSKITE BASED CATALYSTS FOR DIESEL SOOT EMISSION CONTROL

R.T YUSUF[1], A. ANDREWS[2], S. UMARU[1], U.A UMAR[1], D.O. OBADA[1*], AND D. DODOO-ARHIN[3]

[1]Department of Mechanical Engineering, Ahmadu Bello University, Zaria, Nigeria
[2]Department of Materials Engineering, KNUST, Kumasi, Ghana
[3]Department of Materials Science and Engineering, University of Ghana, Legon, Ghana
Corresponding author e-mail: obadavid4@gmail.com

ABSTRACT

Potassium substituted strontium titanate type perovskite catalyst have been developed using the sol-gel and solution combustion methods for diesel particulate oxidation. The synthesized catalysts have been characterized by using XRD, SEM and TG analysis. The catalysts synthesized by the sol-gel method (SrATsg) showed the highest activity in terms of the weight loss of the catalyst which lighted off around 440 °C. The catalytic materials show good thermal stability, while their low cost will also add to their potential for practical applications.

Keywords: *Soot oxidation, Perovskite catalyst, Laboratory scale experiments, Diesel soot*

1. Introduction

During the last decade, diesel engines have increased in popularity compared to gasoline engines all around the world, due to better fuel efficiency, lower operating cost, higher durability, and reliability (Banus *et al*., 2013). However, a major environmental problem associated with diesel is the emission of particulate matter (soot) from the exhaust, which consist mostly of carbonaceous soot and soluble organic fraction (SOF) of hydrocarbon (Abdullah *et al*., 2008).

Significant efforts to seek soot combustion catalysts in the past involved the use of noble metals, (Chien and Huang, 1995, Stein, 1996) zeolites, (Fritz and Pitchon, 1997, Xiao *et al.,* 2001), and mixed oxides (Russo *et al*, 2005, Fino *et al.*, 2006, Bialobok, *et al*., 2007, Peng et *al.*, 2007, Teraoka *et al*., 2001, Teraoka *et al*., 1996, Hong and Lee, 2000). In recent times, huge attention has been paid to the perovskite-group of oxides due to their flexibility, excellent redox properties and high mechanical and thermal stability. Thus they are preferred as ideal materials for catalytic soot oxidation.

Therefore, in this study, substituted perovskite-oxide catalysts ($SrTiO_3$) synthesized using different methods in its unsupported form were evaluated under loose contact situations with model soot and characterized in terms of their catalytic activity for soot oxidation by using thermo-gravimetric analysis.

2. Experimental procedure

$Sr_{1-x}K_xTiO_3$ ($Sr_{0.8}K_{0.2}TiO_3$) based substituted perovskite type materials were prepared by following the sol-gel (SrATsg) and solution combustion (SrATs) routes. The XRD patterns of all the randomly oriented catalyst powder specimens were recorded in the 10.0°- 90° 2θ range with a step size of 0.017° and a counting time of 14 s per step in order to assess their purity and crystalline structure. A scanning and transmission electron microscope was used to analyse the microstructure of the crystal catalyst aggregates. The soot combustion evaluation of the catalysts was analysed by subjecting catalysts to a linear heating ramp between 100°C and 700°C at a rate of 20°C/min in NETZSCH, STA 449 C Jupiter TG/DTA instrument in air atmosphere.

3. Results and Discussion

Fig. 1 show catalysts synthesized at 800 °C for a holding time of 6 h. All reflections of the titanates can be found in the X-ray diffractograms, but there are also very weak reflections of TiO_2 (rutile) and $SrTiO_3$, (strontianite) in the diffractograms of the powders obtained by thermal treatment of the gel precursors at this temperature. The catalysts are obtained in their pure form upon calcination.

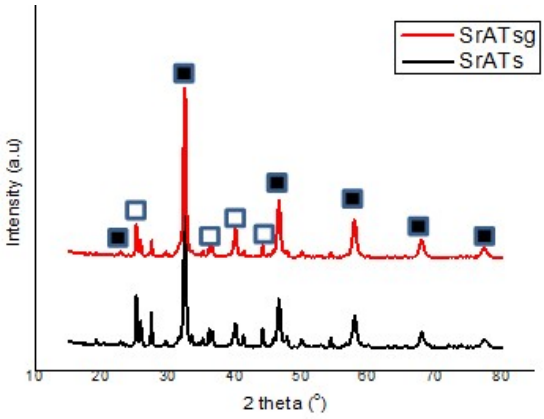


Figure 1: XRD patterns of as-synthesized powders of substituted $SrTiO_3$ prepared with 2 wt % promoter metal (k) using different synthesis methods. All reflections correspond to $SrTiO_3$ or $SrTiO_3$ solid solutions ( ) and TiO_2 ( )

Fig. 2 shows the micrographs of the decomposition products at 800 °C. The perovskite catalysts microstructure appears foamy. During synthesis, the decomposition of reacting precursors generates a large quantity of gaseous product over a very short period, which leads to a spongy catalyst morphology. This feature can be considered a great advantage for soot decomposition. The micrographs of coated catalysts (SSrAT) and bare alumina supports show a uniform coating on the ceramic substrate, which consists of nanoparticles. This coherent interface structure will lead to a strong bond between the coated catalyst and the substrate which is significant for the catalyst life-span since the strong bonding strength between the coated catalyst and the substrate will prevent the scaling off of the catalyst coating from substrate under the pulse-type impact of the engine exhaust gases.

The trend observed for catalytic activity measured by thermo-gravimetry is SrATsg > SrATs > soot as shown in Fig. 4. These results clearly demonstrate the enhanced soot oxidation activity for catalyzed carbon oxidation. The most active substituted perovskite catalyst for soot oxidation i.e. SrATsg showed the highest activity in terms of the weight loss of the catalyst which started around 440 °C.

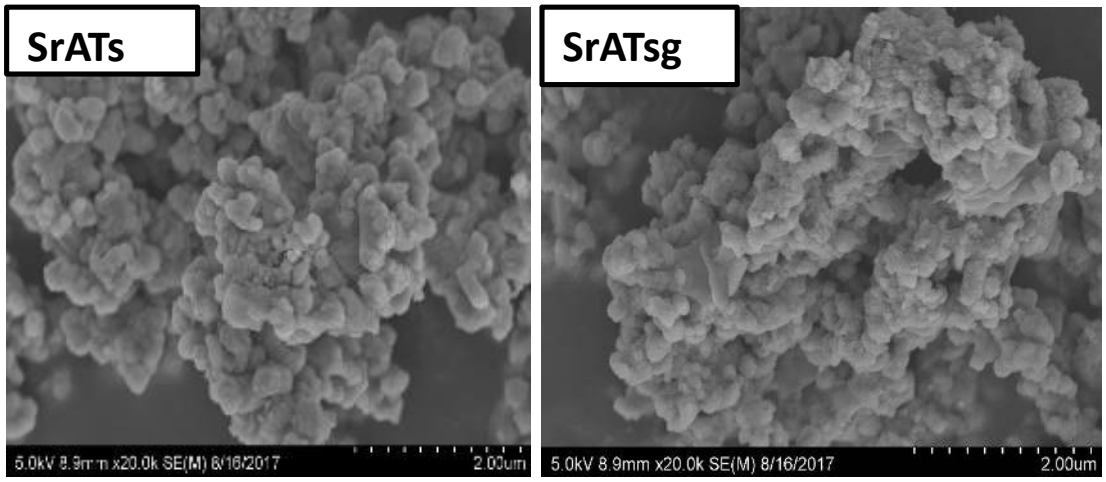


Figure 2: SEM of synthesized catalysts and alumina foam.

The particle sizes for TEM (Fig. 3) images of decomposition products are up to 500 nm for the formed $SrTiO_3$ powder and sharper crystals can be observed for SrATsg.

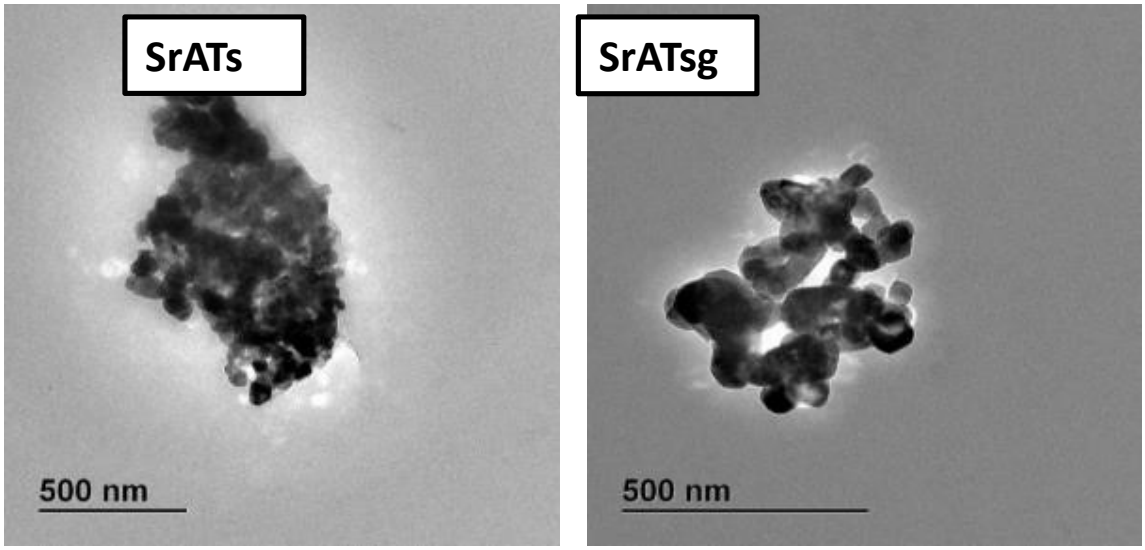


Figure 3: TEM of synthesized catalysts

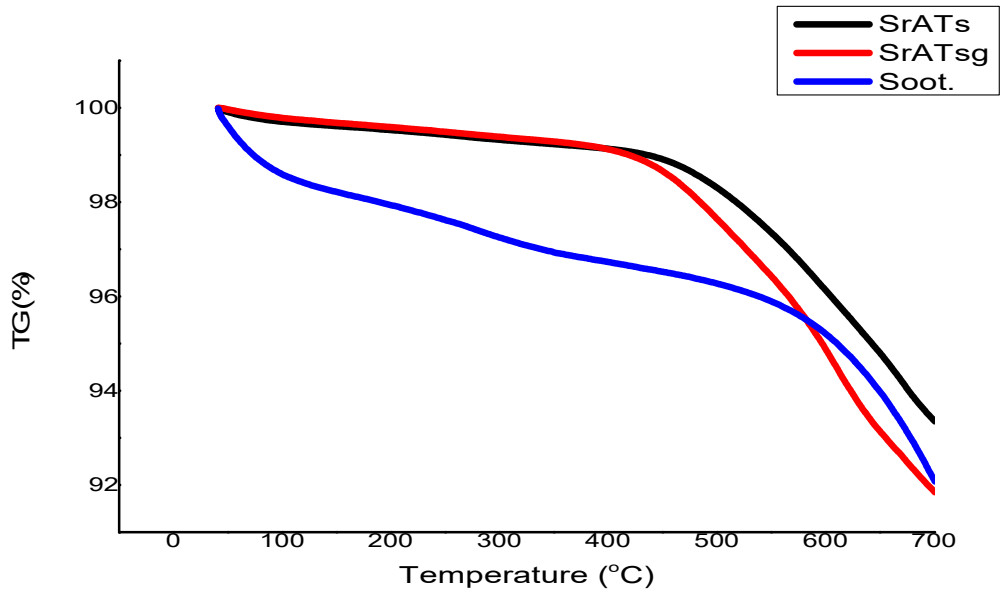


Figure 4: Thermo-gravimetric analysis of synthesized catalysts for soot oxidation

4.0 Conclusion

This work shows that it is possible to synthesize the strontium titanate perovskites by the sol-gel and solution combustion methods and interestingly, these catalysts are quite active for soot combustion.

REFERENCES

Abdullah, A.Z.; Abdullah, H.; Bhatia, S (2008). Improvement of loose contact diesel soot oxidation by synergic effects between metal oxides in K_2O-V_2O_5/ZSM-5 catalysts. *Catal. Commun*., *9*, 1196–1200.

Banús, E.D.; Ulla, M.A.; Miró E.E.; Milt, V.G (2013). Structured catalysts for soot combustion for diesel engines, in diesel engine-combustion. *Emiss. Condit. Monitor*., Ch. 5, 117–142.

Białobok, B., Trawczyński, J., Rzadki, T., Miśta, W., & Zawadzki, M. (2007). Catalytic combustion of soot over alkali doped $SrTiO_3$. *Catalysis Today*, *119*(1), 278-285.

Chien, C. C., & Huang, T. J. (1995). Effect of Copper Content on Pt-Pd-CuO/. gamma.-Alumina Catalysts for Motorcycle Soot Conversion. *Industrial & engineering chemistry research*, *34*(6), 1952-1959.

Fino, D., Russo, N., Cauda, E., Saracco, G., & Specchia, V. (2006). La–Li–Cr perovskite catalysts for diesel particulate combustion. *Catalysis Today*, *114*(1), 31-39.

Fritz, A., & Pitchon, V. (1997). The current state of research on automotive lean NOx catalysis. *Applied Catalysis B: Environmental*, *13*(1), 1-25.

Hong, S. S., & Lee, G. D. (2000). Simultaneous removal of NO and carbon particulates over lanthanoid perovskite-type catalysts. *Catalysis Today*, *63*(2), 397-404.

Peng, X., Lin, H., Shangguan, W., & Huang, Z. (2007). A highly efficient and porous catalyst for simultaneous removal of NOx and diesel soot. *Catalysis Communications*, *8*(2), 157-161.

Russo, N., Fino, D., Saracco, G., & Specchia, V. (2005). Studies on the redox properties of chromite perovskite catalysts for soot combustion. *Journal of Catalysis*, *229*(2), 459-469.

Stein, H. J. (1996). Diesel oxidation catalysts for commercial vehicle engines: strategies on their application for controlling particulate emissions. *Applied Catalysis B: Environmental*, *10*(1-3), 69-82.

Teraoka, Y., Kanada, K., & Kagawa, S. (2001). Synthesis of $La_{1-x}K_xMnO_3$ perovskite-type oxides and their catalytic property for simultaneous removal of NOx and diesel soot particulates. *Applied Catalysis B: Environmental*, *34*(1), 73-78.

Teraoka, Y., Nakano, K., Shangguan, W., & Kagawa, S. (1996). Simultaneous catalytic removal of nitrogen oxides and diesel soot particulate over perovskite-related oxides. *Catalysis Today*, *27*(1-2), 107-113.

Xiao, S., Ma, K., Tang, X., Shaw, H., Pfeffer, R., & Stevens, J. G. (2001). The lean catalytic reduction of nitric oxide by solid carbonaceous materials. *Applied Catalysis B: Environmental*, *32*(1), 107-122.

EFFECTS OF CONCENTRATION AND MOLECULAR WEIGHT ON THE PLASTICIZING EFFICIENCY OF SOME DIALKYL ADIPATES IN PVC SHEETS

[1]*ABBA, H. AND [2]BUKHARI, M. M.
[1]Department of Chemistry, Ahmadu Bello University, P.M.B.1045, Zaria-*810006*, Nigeria.
[2]Department of Polymer and Textile Engineering, Ahmadu Bello University, Zaria.
*Author for Correspondence: habba@abu.edu.ng, hamzaabbah@yahoo.com; +2348028333784

ABSTRACT
In this work, a sheet of pure PVC powder measuring 45 x 9 x 3 mm^3 was prepared by compression moulding method to serve as control. Sheets of the same dimension were also prepared by the same method after addition of 2.5, 5.0, 7.5, 10.0, 12.5, 15.0, 17.5 and 20.0 parts per hundred resin (phr) of three dialkyl adipates (dimethyl, diphenyl and dinonyl). Glass-transition temperature (T_g), elongation at break, tensile strength, leaching and migration of the control and the eight dialkyl adipate-containing PVC sheets were determined to study effects of molecular weight and concentration of the three dialkyl adipates on their plasticizing efficiencies in the PVC sheets. The experimental results showed that although both molecular weight and concentration affected plasticizing efficiency, plasticizer concentration was found to be the most important parameter. Whilst T_g of pure the PVC is 83.98^{o}C, that of 20.0 phr dinonyl adipate-containing sample is 22.21^{o}C, representing a decrease of 61.77^{o}C or 73.55%. Compared to the pure PVC, the T_g of 20.0 phr dipentyl *adipate-containing sample was decreased by 42.00^{o}C or 50.01%. The T_g of 20.0 phr dimethyl adipate-containing sample was decreased by 38.14^{o}C or 45.42% compared to the pure PVC. Although the plasticizer loss values obtained through both leaching are small (indicating strong plasticizer retention) and followed same trend, the amount leached is relatively lower than that migrated. The plasticizing efficiencies (drastic reduction in T_g and increase in elongation at break, slight reduction in tensile strength and strong resistance to weight loss through leaching and migration) of the three adipate s were found to follow the order dinonyl adipate >* dipentyl *adipate > dimethyl adipate. The trends of results in that order are attributed to the difference in size of the three dialkyl adipate molecules represented by their molecular weights. Being larger in size, dinonyl adipate (398.62gmol^{-1}) is retained in the PVC sheets better than the relatively lower molecular weight* dipentyl *adipate (286.41 gmol^{-1}) and dimethyl adipate (174.19 gmol^{-1}) as obtained from their leaching and migration resistance values.*

Keywords*: Adipate, adipic acid, phthalate, plasticizing efficiency, poly(vinyl chloride)*

INTRODUCTION

Although plastics deliver unparalleled design versatility compared to competing materials, constitute an important component of the range of materials used in our modern society as almost all aspects of our daily lives involve plastics in one form or the other, they are rarely used by themselves (Andrady and Neal, 2009; Thompson *et al*., 2009a). Typically, the resins are intimately mixed or "compounded" with additives into formulations that are processed into the shape of the final products to enhance performance (Jia *et al*., 2017). Plasticizers (substances which, when added to a rigid material, makes it flexible, resilient and easier to handle) are the largest group of additives in polymer industry whose molecular weights range from 200 to 700 g mol^{-1} and cover water solubility range of g l^{-1} to sub-µg l^{-1} (Coltro *et al*., 2013).

Second only to polyethylene in terms of production and consumption tonnage, poly(ethene chloride), also known as poly(vinyl chloride), commonly abbreviated PVC, is the world's most versatile plastic that find usage in an enormous range of domestic and industrial products. The versatility is due to its high polarity (chlorine content of 57%) and its ability to accommodate large amounts of additives (e.g., plasticizers) and still maintain its extremely high creep resistance (Björn *et al*., 2007). Being product of addition polymerization of chloroethene (vinyl chloride), unmodified or pure PVC from laboratories or industrial reactors finds application in the construction trades where its rigidity, strength, durability and moldability are useful in pipes, conduits, sidings, window and door frames, bottles for non-food packaging, cards (such as bank or membership): (Klein, 2012).

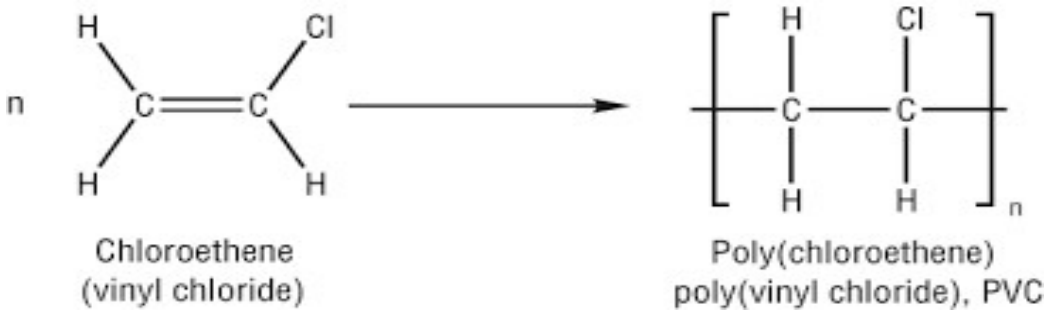


Figure 1: Synthesis of PVC from its chloroethene monomer.

For products to remain flexible especially at low temperatures, PVC is mixed with plasticizes. Plasticized PVC is familiar to consumers as floor tile, garden hose, decorative sheets and imitation leather upholstery, raincoats and shower curtains, inflatable products and many applications where it replaces rubber (Unar *et al*., 2010). PVC is the most versatile and resource efficient thermoplastic with the widest range of applications in virtually all areas of human activity. Today's health care systems are benefiting greatly from medical products made from plasticized PVC that we often take for granted: disposable syringes, surgical equipment, drips, aseptic medical packaging and blister packs for pills, intravenous blood bags, bags and tubing for blood transfusions and infusions, heart valves, artificial corneas and hearing aids, as well as medical devices that keep blood flowing, joints moving and hearts beating (Shaxson, 2009; Talsness *et al*., 2009; Genay *et al*., 2011). Several authors (Tsumura *et al*., 2002; Yano *et al*., 2002; Simmchen *et al*., 2012; Eckert *et al*., 2015) have reported that because of its inertness, durability, and resistance to heat and chemicals, plasticized PVC is also used in such critical applications as children's toys and food packaging to reduce food wastage and preserve meat and vegetables. However, since most of the commercial plasticizers used are not chemically bonded, their tendency to evaporate from surface, leach out of and migrate from the PVC resin and bioaccumulate in living organisms and cause adverse effects on the environment have been the subject of considerable media, legislative and scientific debate (Serodio and Nogueira, 2006; Cao, 2010; Barnes *et al*., 2009). As a result of the heightening health, environment and safety concerns, use of some plasticizers, notably phthalates, was questioned, is strictly controlled or banned (Yano *et al*., 2005; Zhang *et al*., 2008; Chiellini *et al*., 2011). Academia and industry have been collaborating in the search for alternatives to phthalates and other toxic plasticizers to address their increasing toxicological concerns (Crespo *et al*., 2007; Yan *et al*., 2015).

An adipate (OOC-(CH)-COO), a deprotonated anion of adipic acid ($C_6H_{10}O_4$), is the salt and ester of and an alkyd resin derived from, adipic acid. The anionic ($HO_2C(CH_2)_4CO_2^-$) and dianionic ($^-O_2C(CH_2)_4CO_2^-$) forms of adipic acid are also referred to as adipate adipic acid (Reimer *et al*., 2000;

Cano *et al*., 2002; Hao *et al*., 2015). Whilst long chain adipates are used as lubricants due to their light and thermal stability, superior lubricity and corrosion resistance, adipates of short chain lengths (C_5 - C_{10}) are a better choice low-temperature (even arctic) plasticizers because of their high boiling points, compatibility, biodegradability and non-toxicity compared to phthalates of similar alkyl chain length (Lindstrom and Hakkarainen, 2006; Yan *et al*., 2015). Dialkyl adipates are extensively used in household plastic food contact materials, in medical products and packaging due to their higher lipophilicity and a threefold lesser leaching and migration potentials than phthalate-containing PVC products (Tsumura *et al*., 2001; Saito *et al*., 2002; Avelino *et al*., 2015).

The aim of this study was to study the potentials, through glass-transition temperature (T_g), elongation at break, tensile strength, leaching and migration tests, of the three dialkyl adipates (DMA, DPA and DNA) as plasticizers, for use in PVC sheets where flexibility is critical.

2.0 MATERIALS AND METHODS

2.1 Materials

The three dialkyl adipate esters (dimethyl adipaate, dipentyl adipaate and dinonyl adipaate) shown in Table 1 were analytical-grade reagents from Hayashi Pure Chemicals, Osaka, Japan. The analytical-grade PVC powder (M_n 60,000 and M_w 106,000) used was a product of Merck, Darmstadt, Germany.

Table 1: Common and IUPAC names, acronyms, chemical formulae and molecular weights of the three dialkyl adipaate plasticizers used in the study.

Common name	IUPAC name	Molecular formula	Molecular weight ($gmol^{-1}$)
Dimethyl adipate (DMA)	1,6-Dimethyl hexanedioate	$C_8H_{14}O_4$	174.19
Dipentyl adipate (DPA)	1,6-Dipentyl hexanedioate	$C_{16}H_{30}O_4$	286.41
Dinonyl adipate (DNA)	1,6-Dinonyl hexanedioate	$C_{24}H_{46}O_4$	398.62

2.2 Methods

2.2.1 Sample preparation

PVC powder (15 g) was introduced into a beaker containing 100 mL of distilled water and the content spread on a flat tray. After 25 min, a sheet of the pure PVC coupon measuring 45 x 11 x 3 mm^3 was stripped off the tray and air-dried overnight at room temperature (33.6°C) to serve as control. Eight sample coupons of the same dimension were prepared by the same procedure after addition of each dialkyl adipate to PVC in the ratios 2.5:100, 5:100, 7.5:100, 10:100, 12.5:100, 15:100, 17.5:100 and 20:100 representing 2.5, 5, 7.5, 10, 12.5, 15, 17.5 and 20 parts of each of the three dialkyl adipaates listed in Table 1 per hundred parts of the PVC resin (phr).

2.2.2. Determination of glass-transition temperature (T_g)

Glass-transition temperatures of the samples were determined using Perkin Elmer differential scanning
calorimeter (DSC) (Perkin Elmer Instruments Inc. , Norwalk, CT, USA) according to the procedure of Shah and Shertukde (2003).

2.2.3 Leaching test

Each sample was completely immersed in 5 mL of hexane solution containing toluene (2% wt/vol) at room temperature (33.6°C) with continuous agitation for 10 days and the amount of plasticizer leached (expressed as percentage of the total plasticizer content) measured according to the procedure reported by Latini *et al* (2010).

2.2.4 Migration test

Each sample was sandwiched between two un-plasticized PVC sheets of the same shape and maintained in close contact between the glass microscope slides secured by clips and completely immersed in 100 mL deionized water in a flask at room temperature (33.6°C) with continuous mechanical stirring for 10 days. The amount of plasticizer that migrated to the un-plasticized PVC sheets in the 10-day interval was determined according to the procedure of Li *et al* (2012).

2.2.5 Determination of tensile strength and elongation at break

Tensile strength and elongation-at-break of the samples were determined using Universal Tensile Machine (Micro Vision Industries, India, Serial Number 183). The tests were performed with 5000N load cell, cross head speed of 250mm/min and gauge length of 150mm in accordance with the ASTM D-638 procedure (Anon, 2003).

3.0 RESULTS AND DISCUSSION

3.1 Glass-Transition Temperature (T_g)

T_g, the temperature at which a polymer changes phase from an exceedingly strong, glass-like structure (ideal for pipes and window frames) into a flowable or rubber phase, is a fundamental quantity characteristic of rigid plastics related to plasticization because it is only above T_g that plasticiser can penetrate the polymer structure. If the Tg of the polymer is reduced sufficiently, its properties are changed from those of a hard, brittle solid to those associated with a soft, flexible rubber.

Effects of concentration and molecular weight of the three plasticizers (DMA, DPA and DNA) are shown in Figure 2. From the figure, it can be seen that T_g decrease with increase in concentration of plasticizer. While T_g of pure the PVC is 83.98°C, that of 20.0 phr DNA-containing sample is 22.21°C, representing a decrease of 61.77°C or 73.55%. Compared to the pure PVC, the T_g of 20.0 phr DPA-containing sample decreased by 42.00°C or 50.01%. The T_g of 20.0 phr DMA-containing sample decreased by 38.14°C or 45.42% compared to the pure PVC. From Figure 2, the plasticizing efficiencies (reduction in T_g) of the three plasticizers can be seen to follow the order DNA > DPA > DMA. The trend of result in that order is attributed to the difference in size of the three dialkyl adipate molecules represented by their molecular weights (Table 1). Being larger in size, DPA (398.62$gmol^{-1}$) is expected to be more

efficient in reducing the T_g by separating the PVC chains apart to give the chains greater freedom of movement and also reducing the van der Waals forces between the chains, thus increasing the mobility of the chains and increasing the flexibility and extensibility of the PVC sheet. DNA is followed, respectively, by DPA (286.41 $gmol^{-1}$) and DMA (174.19 $gmol^{-1}$), in agreement with literature (Unar *et al*., 2010; Coltro *et al*., 2013).

3.2 Leaching and Migration

Being the most serious challenge facing the plasticizer industry due to its adverse health, safety and environment effects, plasticizer loss from evaporation, hydrolysis, leaching and migration out of and from plasticized material was reported as the most serious challenge facing the plasticizer industry (Latini *et al*., 2010; Li *et al*., 2012).

Results of the effects of concentration and molecular weight of the three plasticizers (DMA, DPA and DNA) on the amount leached and migrated from the plasticized PVC sheets in the 10-day period are presented Figure 3. It can be observed that all the samples showed high resistance to both leaching (removal of a substance from a solid via a liquid extraction media) and migration (any method by which a component leaves a material to a gas, liquid or solid phase), with resistance to migration being comparatively higher than that of leaching. The highest amount leached within the duration of the 10-day test by DMA is 3.25% at plasticizer loading of 20.0phr. With respect to resistance to migration, the maximum amount of the same DMA that migrated during the 10-day period at the same plasticizer loading of 20.0phr is 1.64%. The trends in both plasticizer leaching and migration are basically the same with the amount of plasticizer leached and/or migrated being in the order DMA > DPA > DNA. The trend observed is consistent with the size of the three plasticizers (Table 1). DMA, being comparatively smallest in size (252.22 $gmol^{-1}$), is expected to be lost easily from the plasticized PVC sheets than DPA and DNA. The trend observed (increase in resistance to weight loss with increase in plasticizer size) is in agreement with what was reported earlier (Saito *et al*., 2002; Björn *et al*., 2007).

3.3 Elongation at Break and Tensile Strength

Elongation at break (the extent to which a material can be stretched before it breaks, expressed as a percentage of its original length and tensile strength (a measure of the ability of a material to withstand forces that tend to pull it apart and determines the extent a material stretches before breaking) are the most important mechanical properties of PVC sheets for use in applications where flexibility is crucial.

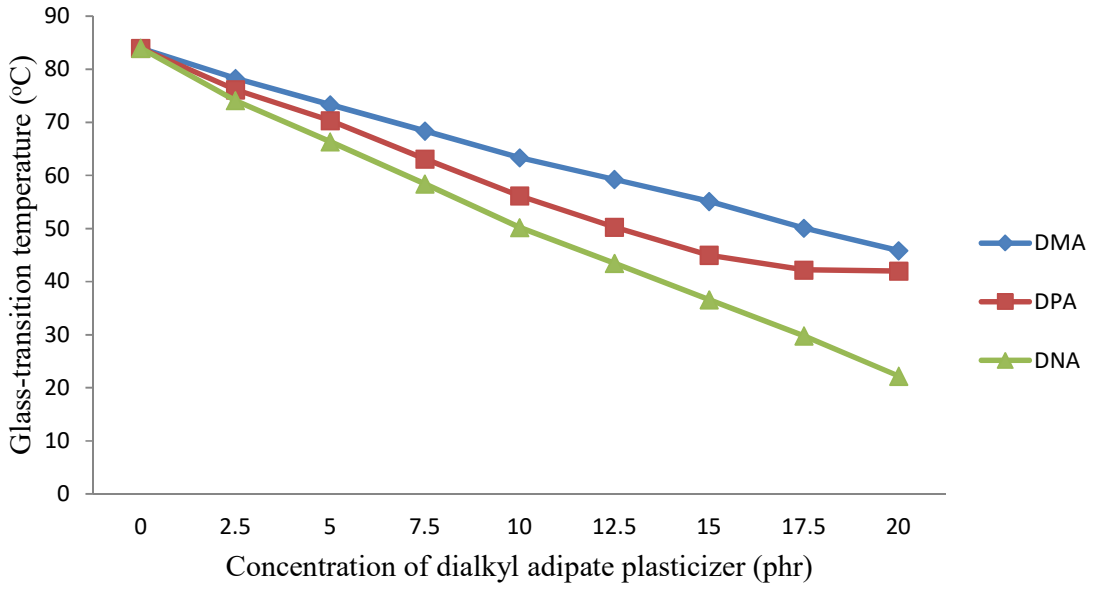


Figure 2: Effect of concentration of the three adipate plasticizers (DMA, DPA and DNA) on glass-transition temperature of PVC sheets.

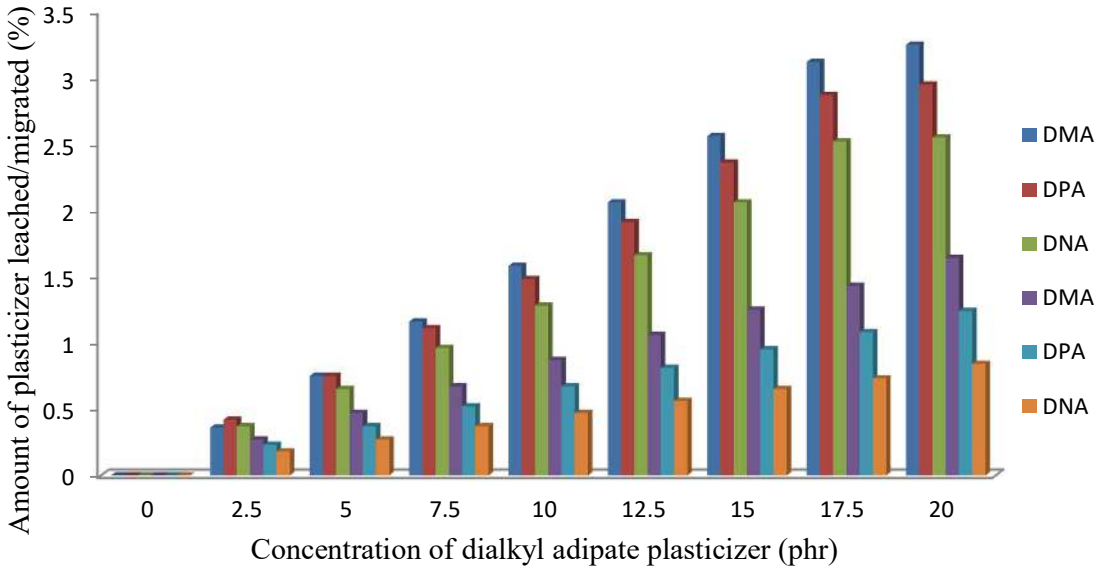


Figure 3: Effect of concentration of the three adipate plasticizers (DMA, DPA and DNA) on their leaching and migration resistance from PVC sheets.

The effect of concentration and molecular weight of the three the three plasticizers (DMA, DPA and DNA) on the mechanical properties of great significance for flexible sheets and films (tensile strength and elongation) in the plasticized PVC sheets are shown in Figure 4. A careful look at the figure shows that elongation at break of the samples increased with increase in plasticizer concentration with DNA having the highest elongation at break value of 151.74% at plasticizer loading of 20.0phr compared to the control of 17.63%. DNA is followed by DPA and DMA with 128.75% and 83.81%, respectively, at the same plasticizer concentration of 20.0phr compared to 17.63% for the control. It can be concluded that the operating order in elongation at break (increase in elongation at break with increase in plasticizer concentration) is DMA > DPA > DNA.

With respect to tensile strength, DNA decreased the tensile strength to 108.43MPa at plasticizer concentration of 20.0phr from 124.94 MPa for the control. DNA is followed, respectively, by DPA (116.04) and DMA (120.75 MPa) at the same 20.0phr plasticizer concentration. In sharp contrast to the operating order in elongation at break, the operating order in tensile strength (decrease in tensile strength with increase in plasticizer concentration) is DNA > DPA > DMA.

Again, the trends observed in both tensile strength and elongation at break can be attributed to the size of the three adipate plasticizers (Table 1) used and were consistent with what were reported in the literature (Lai *et al*., 2012).

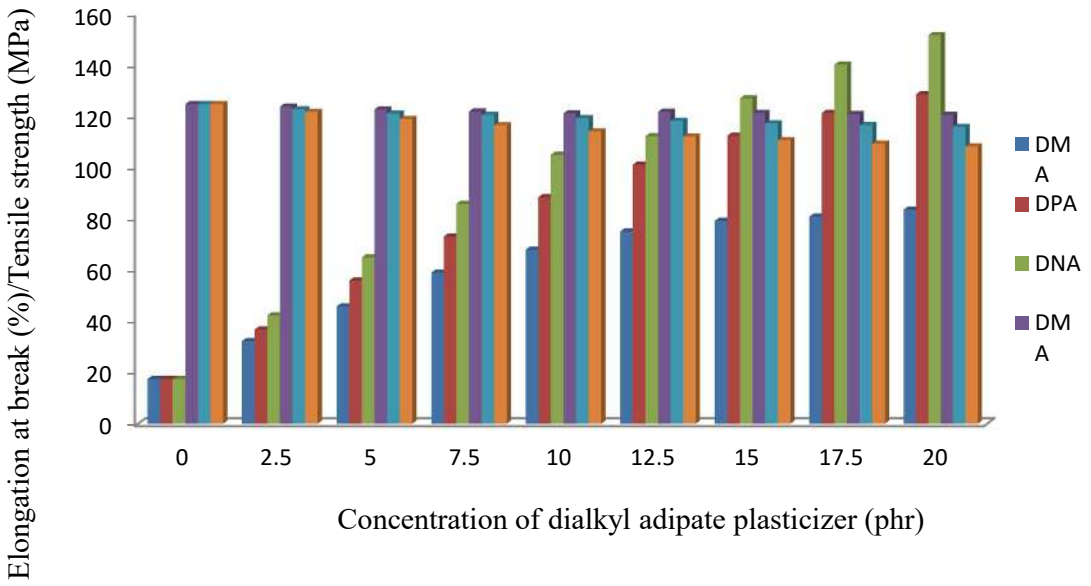


Figure 4: Effect of concentration of the three adipate plasticizers (DMA, DPA and DNA) on elongation at break and tensile strength in PVC sheets.

CONCLUSION

Since the three adipate plasticizers studied are efficient in plasticizing PVC (significantly lowered its T_g, significantly increased its elongation and hence flexibility, greatly resisted leaching and migration from it without significantly compromising its desired tensile strength), biodegradable, nontoxic, highly viscous and non-volatile, they are strongly recommended for use in place of the toxic and environment non-friendly phthalate plasticizers conventionally used in flexible PVC sheets especially where low-temperature performance is required.

REFERENCES

Andrady, A.L. and Neal, M.A. (2009). Applications and societal benefits of plastics. *Philosophical Transactions of the Royal Society of London. Series B: Biological Sciences*, 364: 1977–1984.

Anonymous (2003). Test Method for Tensile Properties of Plastics, ASTM D-638-03. American
Standards for Testing and Materials, Wes t Conshohocken, PA 19428-
2959, pp.674-713.

Avelino, H. M.N.T., Diogo, J.C.F., Caetano, F.J.P. and Fareleira, J.M.N.A. (2015). Viscosity and self-diffusion coefficients of dialkyl adipates: a correlation scheme with predictive capabilities. *Journal of Chemical and Engineering Data, 60*(12): 3696-3702.

Barnes, D.K.A., Galgani, F., Thompson, R.C.,and Barlaz, M. (2009). Accumulation and fragmentation of plastic debris in global environments. *Philosophical Transactions of the Royal Society of London. Series B: Biological Sciences*, 364: 1985–1998.

Björn, A., Hörsing, M., Karlsson, A., Mersiowsky, I. and Ejlertsson, J. (2007). Impacts of temperature on the leaching of organotin compounds from poly(vinyl chloride) plastics — a study conducted under simulated landfill conditions. Journal of *Vinyl* and Additive *Technology,* 13: 176–188.

Cao, X.-L. (2010). Phthalate esters in foods: sources, occurrence, and analytical methods. *Comprehensive Reviews in Food Science and Food Safety*, 9: 21-43.

Cano, J.M., Marin, M.L., Sanchez, A. and Hernandis, V. (2002). Determination of adipate plasticizers in poly(vinyl chloride) by microwave-assisted extraction. *Journal of Chromatography and Analysis*, 963(1-2): 401-409.

Chiellini, F., Ferri, M. and Latini, G. (2011). Physical-chemical assessment of di-(2-ethylhexyl)-phthalate leakage from poly(vinyl chloride) endotracheal tubes after application in high risk newborns.

International Journal of Pharmaceutics, 409(1-2): 57-61.

Coltro, L., Pitta, J.B. and Madaleno, E. (2013). Performance evaluation of new plasticizers for stretch PVC films. *Polymer Testing,* 32(2): 272–278.

Crespo, J., Balart, R., Sanchez, L. and Lopez, J. (2007). Substitution of di(2-ethylhexyl) phthalate by di(isononyl) cyclohexane-1,2-dicarboxylate as a plasticizer for industrial vinyl plastisol formulations. *Journal of Applied Polymer Science*, 104: 1215–1220.

Eckert, E., Muller, J. and Goen, T. (2015). Simultaneous determination of polyvinylchloride plasticizers di(2-ethylhexyl) phthalate and tri(2-ethylhexyl) trimellitate and its degradation products in blood by liquid chromatography-tandem mass spectrometry. *Journal of Chromatography A,* 1410:173-180.

Genay, S., Luciani, C., Decaudin, B., Kambia, N., Dine, T., Azaroual, N., Di Martino, P., Barthelemy, C. and Odou, P. (2011). Experimental study on infusion devices containing polyvinyl chloride: to what extent are they di(2-ethylhexyl)phthalate-free? *International Journal of* Pharmaceutics, 412(1-2): 47-51.

Hao, Y., Yang, H., Zhang, H., Gao, G. and Dong, L. (2015). The simultaneous introduction of low and high molecular weight of biodegradable Poly(diethylene glycol adipate)s to plasticize and toughen polylactide. *Fibers and Polymers*, 16(12): 2519–2528.

Jia, P., Hu, L., Shang, Q., Wang, R., Zhang, M. and Zhou, Y. (2017). Self-plasticization of PVC materials via chemical modification of Mannich base of cardanol butyl ether. *ACS Sustainable Chemistry and Engineering*, *5*(8): 6665-6673.

Klein, D. (2012). Organic Chemistry, John Wiley and Sons, Ltd New Jersey, pp.1139-1169.

Latini, G., Ferri, M. and Chiellini, F. (2010). Materials degradation in PVC medical devices, DEHP leaching and neonatal outcomes. *Current Medicinal Chemistry*, 17(26): 2979-2989.

Li, X., Xiao, Y., Wang, B. and Wang, C. (2012). Effects of poly(1,2-propylene glycol adipate) and nano-$CaCO_3$ on DOP migration and mechanical properties of flexible PVC. *Journal of Applied Polymer Science*, 124(2): 879–1756.

Lindstrom, A. and Hakkarainen, M. (2006). Environmentally friendly plasticizers for poly(vinyl chloride)-improved mechanical properties and compatibility using branched poly(butylenes adipate) as polymeric plasticizer. *Journal of Applied Polymer Science*, 100(3): 2180-2188.

Reimer, R. A., Slaten, C. S., Seapan, M., Koch, T. A. and Triner, V. G. (2000). Adipic Acid Industry — N_2O Abatement. Non-CO_2 Greenhouse Gases: Scientific Understanding, Control and Implementation. Springer, Netherlands, p p.347–358.

Saito, I., Ueno, E., Oshima, H. and Matsumoto, H. (2002). Levels of phthalates and adipates in processed foods migration of di-isononyl adipate from polyvinyl chloride film into foods. *Food Hygiene and Safety Science*, 43(3): 185-189.

Serodio, P. and Nogueira, J.M.F. (2006). Consideration on ultra-trace analysis of phthalates in drinking water. *Water Research,* 40: 2572–2582.

Shah, B.L. and Shertukde, V.V. (2003). Effect of plasticizers on mechanical, electrical, permanence, and thermal properties of poly(vinyl chloride). *Journal of Applied Polymer Science*, 90(12): 3278–3284.

Shaxson, L. (2009). Structuring policy problems for plastics, the environment and human health: reflections from the UK. *Philosophical Transactions of the Royal Society of London. Series B: Biological Sciences*, 364: 2141–2151.

Talsness, C.E., Andrade, A. J. M., Kuriyama, S.N., Taylor, J.A. and vom Saal, F.S. (2009). Components of plastic: experimental studies in animals and relevance for human health. *Philosophical Transactions of the Royal Society of London. Series B: Biological Sciences*, 364: 2079–2096.

Thompson, R.C., Swan, S.H., Moore, C.J. and vom Saal, F. S. (2009a). Our plastic age. *Philosophical Transactions of the Royal Society of Lond on. Series B: Biological Sciences*, 364: 19 73–1976.

Tsumura, Y., Ishimitsu, S., Saito, I., Sakai, H., Kobayashi, Y. and Tonogai, Y. (2001). Eleven Phthalate esters and di(2-ethylhexyl) adipate in one-week duplicate diet samples obtained from hospitals and

their estimated daily intake. *Food Additives and Contaminants*, 18(5): 449-460.

Tsumura, Y., Ishimitsu, S., Kaihara, A. and Tonogai, Y. (2002). Phthalates, adipates, citrate and some of the other plasticizers detected in Japanese retail foods: a survey. *Journal of Health Science*, 48(6): 493-502.

Unar, I.M., Soomro, S.A. and Aziz, S. (2010). Effect of Various Additives on the Physical Properties of Poly(vinyl chloride) Resin. *Pakistani Journal of Analytical and Environmental Chemistry* 11 (2): 44-50.

Yan, Z., Hongyu, L., Dandan, W., Junjia, B., Yanping, H., Guibao, Z., Sanrong, L., Huiliang, Z. and Dong, Lisong, D. (2015). Poly(1,2-propylene glycol adipate) as an environmentally friendly plasticizer for poly(vinyl chloride). *Polymer Korea*, 39(2): 247-255.

Yano, K., Hirosawa, N., Sakamoto, Y., Katayama, H., Moriguchi, T., Joung. K.E., Sheen. Y.Y. and Asaoka, K. (2002). Phthalate levels in beverages in Japan and Korea. *Bulletin of Environmental Contamination and Toxicology*, 68(4): 463–469.

Yano, K., Hirosawa, N., Sakamoto, Y., Katayama, H., Moriguchi, T. and Asaoka, K. (2005). Phthalate levels in baby milk powders sold in several countries. *Bulletin of Environmental Contamination and Toxicology*, 74(2): 373–379.

Zhang, K., Noonan, G.O. and Begley, T.H. (2008). Determination of 2,6-diisopropylnaphthalene (DIPN) and n-dibutylphthalate (DBP) in food and paper packaging materials from US marketplaces. *Food Additives and Contaminants,* 25: 1416–1423.

INVESTIGATION OF CORROSION INHIBITION EFFECT OF MINT LEAVES AND GUAVA LEAVES EXTRACTS IN ACIDIC MEDIA.

B. O. SAMUEL, AND B. DAN-ASABE
Department of Mechanical Engineering, Ahmadu Bello University, Zaria.
basseyokon59@gmail.com

ABSTRACT
This project investigate the corrosion inhibitive effect of plant solution extract of mint leaves (Mentha) and guava leaves (Psidium guajava) on the corrosion of mild steel test specimen immersed in 2M hydrochloric acid(HCL) and 2M sulphuric acid (H_2SO_4). The influence of the active media encountered in service on mild steel over a period of 8 days (192 hours) in the laboratory by the use of weight loss method. Corrosion rate (calculated) in millimeter per year (MPY) was carried out. The results shows that the solution extract of mint leaves could effectively serve as effective inhibitor both in 2M HCL and 2MH_2SO_3. While the extract of guava leaves acts effectively only in H_2SO_4 and deficiently in HCL. Generally, mint leaves has the highest inhibitor efficiency in comparison with guava leaves.

1.0. INTRODUCTION

Several studies over the past 30 years have shown that the annual direct cost of corrosion to an industrial economy is approximately 3.1% of the country's Gross National Product (GNP) (Shaw, 2006). Also, recent years have seen an increasing use of metal prosthetic devices in the body, such as pins, plates, hip joints, pacemakers, and other implants. New alloys and better techniques of implantation have been developed, but corrosion continues to create problems. Examples include failures through broken connections in pacemakers, inflammation caused by corrosion products in the tissue around implants, and fracture of weight-bearing prosthetic devices (Corrosion-doctors.org, 2014). An even more significant problem is corrosion of structures, which can result in severe injuries or even loss of life. Safety is compromised by corrosion contributing to failures of bridges, aircraft, automobiles, gas pipelines etc., the whole complex of metal structures and devices that make up the modern world (Hutsoniap, 2014). Fortunately, uniform corrosion is predictable and is usually controlled by various methods such as painting the surface or applying a layer of a sacrificial metal like zinc to steel (Shaw 2006).

The aim of this work is to investigate the inhibitory effectiveness of some plant leaves extracts in the corrosion of mild steel. This shall be investigated through experimental analysis using plants extract at different concentrations in some acidic media. The plant extract are: guava leaves extract and mint leaves extract. The specific objectives are: to get extracts from guava leaves and mint leaves and to vary the time of exposure of the specimen in the corrosive environment in other to access the effect of concentrations of the inhibitor on the corrosion of steel and compare the results of these extracts with that of a standard inhibitor.

In this work, some literatures have been reviewed in respect to the use of leaves for corrosion inhibitors. Evrim et. al., (Evrim et al., 2016), studied the inhibitory effect of the methanol extract of Gentiana olivieri and its fractions on the corrosion of mild steel in a 0.5 M HCl solution were investigated and EIS results showed maximum inhibition efficiency (93.7%) at an inhibitor concentration of 800 mg/L. Nathiya et. al., (Nathiya et al., 2017) studied the Corrosion inhibition of aluminium in 1 M H_2SO_4 by two different solvent extracts of *Dryopteris cochleata* leaves was studied using weight loss, electrochemical measurements, X-ray diffraction and scanning electron microscopy The result showed that the methanol extract of *D. cochleata* leaves is a better inhibitor than water extract. Muthukrishnan et. al., (Muthukrishnan et. al, 2015) investigated The anticorrosive potential of *Ficus hispida* leaf extract (FHLE) as a corrosion inhibitor in 1 M HCl using weight loss measurement as well as potentiodynamic polarization and electrochemical impedance spectroscopy (EIS) techniques and Temperature studies revealed an increase in inhibition efficiency with decrease in temperature and activation energies increased in the presence of the extract. Alaneme et. al., (Alaneme et al., 2016), investigated the Corrosion inhibition and adsorption characteristics of elephant grass extracts on mild steel in 1 M HCl solution. Their results show that the steel dissolution rate in the acidic solution was sensitive to the extract concentration as mass loss and corrosion rates were observed to decrease with increase in the extract concentration. Loto (Loto, 1998), investigated the effect of vemoia Amolgdalina (Bitter Leaf) solution extract on the corrosion inhibition of mild steel in 0.5M sulphuric acids. In his work, he stated specifically that in some cases the inhibitive effects of some plants solution extract have been attributed to the presence of tannin in their chemical constituents.

The results he obtained showed that the solution extract of the leaves could serve as effective inhibitor only in the 0.5M hydrochloric acid at 28^0C which also has a higher inhibitor efficiency. Eche (Eche, 2001), investigated the corrosion inhibitive effectiveness of solution extracts of locust bean husk, Acacia Nilotica pods, neem leaves, Mahogany leaves on the corrosion of mild steel in 0.5M sulphuric acid. His work showed that locust bean husk have the highest inhibition efficiency followed by Acacia Nilotica pods solution extract. Awulu (Awulu, 2002), research work was set to investigate the effectiveness of plants solution extract as inhibitors of corrosion of mild steel. The solution extracts were gotten from cashew leaves, mango leaves and paw-paw leaves. This research work investigates the effectiveness of plants solution extract as inhibitors of corrosion of mild steel. The solution extracts were gotten from mint leaves and guava leaves. *Mentha* (also known as mint, from Greek *míntha* Linear B *mi-ta*is a genus of plants in the family Lamiaceae (mint family). Due to their tendency to spread unchecked, some mints are considered invasive. Mint grows all year round (Wikipedia, 2014). *Psidium guajava* (common guava, lemon guava) is a small tree in the *Myrtle* family (*Myrtaceae*), native to Mexico, Central America, and northern South America and Africa.

2.0. MATERIALS AND METHODS

Samples used were obtained from the fresh but matured plants at Samaru, Zaria. They were cleaned thoroughly (washed), there after they were air dried and pounded into powder form using pestle and mortar. The powdered sample was then sieved to get fine powder. The powdered samples obtained were taken to the Nigerian Institute of Leather and Chemical Technology (NILEST). They were first extracted using the Soxhlet extraction method and then the following analysis was done: Moisture content, Total soluble, Total solids, Tannins content, Non tannins content, Total acids , Total salts, pH value, Quantitative analysis was used for the determination of chemical components present in the samples used for this experiment. The results of this analysis are as shown in appendix A.

The mild steel coupons were gotten at a standard diameter of 1 inch (25mm), but was machined to 24mm in diameter by turning operation in preparation, using the lathe machine, because of its high degree of surface finish which enhance greater corrosion rate by even distribution on the tested material. Though due to imperfection, the samples varied by considerable tolerances in length.

To ascertain the effectiveness of the samples as inhibitors, test were being carried out. The test were carried out in two stages.

Solution extract was obtained by Soxhlet extraction using ethanol while the concentrate is the dry powder sample in part per million (ppm).

In the first stage, a control experiment was carried out with 2 samples of the mild steel in 2M sulphuric acid and 2M HCL individually without adding any inhibitors and left for 8 days with close observation of 48, 96, 144 and 192 hours respectively.

The second stage was carried out with the corrosive media mixed with the various inhibitors at 10%, 20%, 30% and 40% by volume to determine their effectiveness. The two acids were used with the extracts and concentration and also the standard inhibitor. The standard inhibitor used for this work was Sodium Benzoate (C_5H_2COONa). It is an organic inhibitor and does not promote localized corrosion when used below its critical concentration. Four different concentrations of sodium benzoate were used: 0.1M, 0.2M, 0.3M and 0.5M of sodium benzoate

Corrosion rate was measured using the weight loss method. The corrosion rate can be estimated after another round of cleaning and descaling by measuring weight loss and dividing by measuring weight loss and dividing by the time of exposure. The life of a given component can be predicted by the penetration of corrosion into it. The rate of corrosion of the samples immersed in the various environments was carried out using the relation (Callister, 1997):

$$CPR = \frac{87.6 \times W}{lAt}(mm/yr) \ldots\ldots\ldots\ldots\ldots\ldots (1)$$

Where: CPR = corrosion penetration rate (mm/year), W = weight loss (g), L = density of the mild steel (g/cm^3), A = Area of exposure (cm^2), the density L = 7.85g/cm^3, the area $A = 2\pi RL + 2(\pi R^2) = (2\pi \times 2.4 \times 1.5) + 2(2 \times \pi \times 2.4^2) = 22.6195 + 72.3823 = 95.0018\text{cm}^2$, t = time of observation (hrs). The inhibitor efficiency will then be calculated. Inhibitor efficiency is defined as the percentage of the ratio of the difference between the weight loss in acidic medium and the weight loss in the presence of an inhibitor to the weight loss in acidic medium (Callister 1997).
The efficiency of the inhibitors is given by

$$k = \left(1 - \frac{W}{W_o}\right) \times 100\%$$

where: K = inhibitor efficiency, W = weight loss in the presence of inhibitor, W_0 = weight loss in the absence of inhibitor.

The standard inhibitor used for this work was Sodium Benzoate (C_5H_2COONa). It is an organic inhibitor and does not promote localized corrosion when used below its critical concentration. Four different concentrations of sodium benzoate were used: 0.1M, 0.2M, 0.3M and 0.5M of sodium benzoate.

3.0. RESULTS AND DISCUSSION

Graphs of time against corrosion rates were plotted as indicated in the figures below:

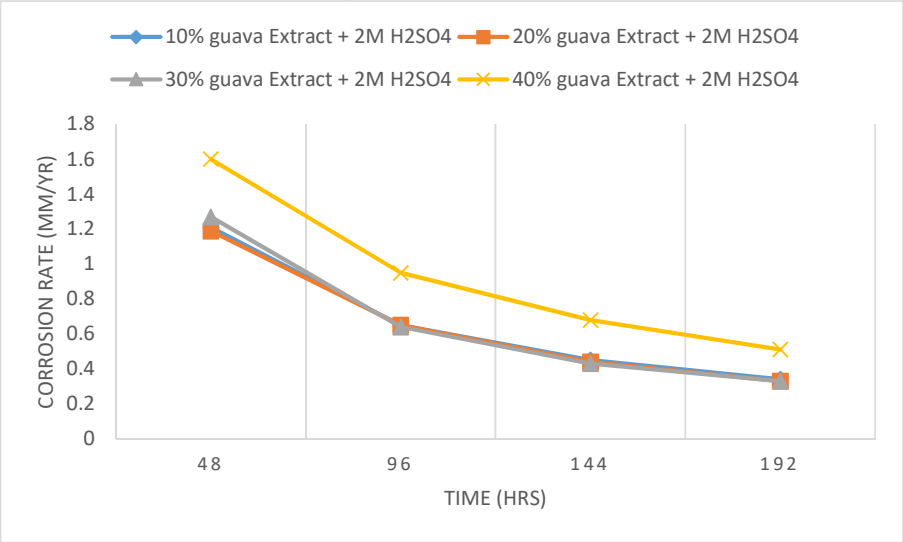


Figure 3.1: Graph of corrosion rate against time for Guava leaf extract in 2M H_2SO_4

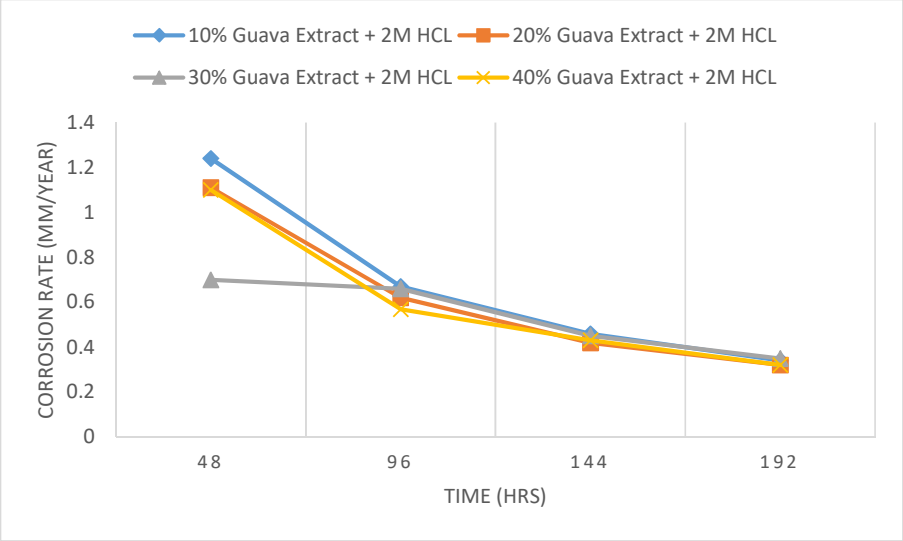


Figure 3.2: Graph of corrosion rate against time for Guava leaf extract in 2M HCL

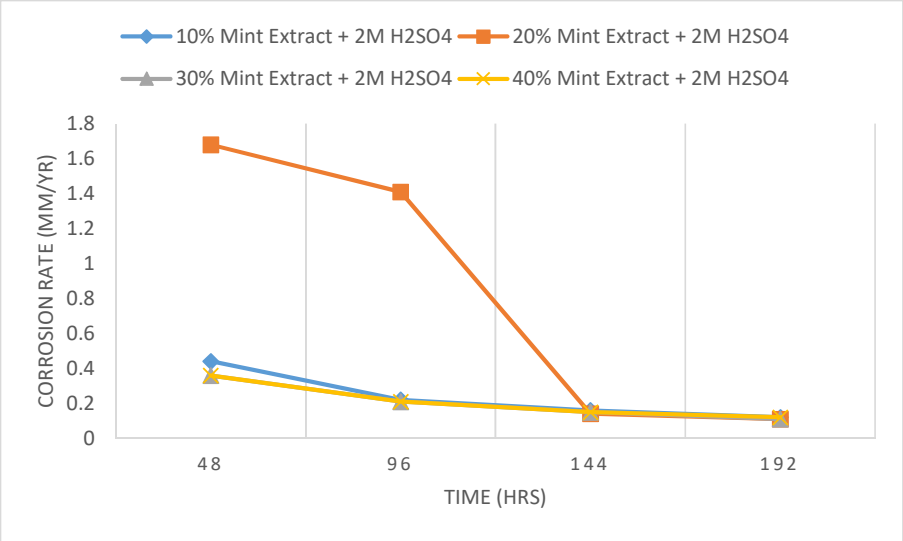


Figure 3.3: Graph of corrosion rate against time for mint leaves extract in 2M H_2SO_4

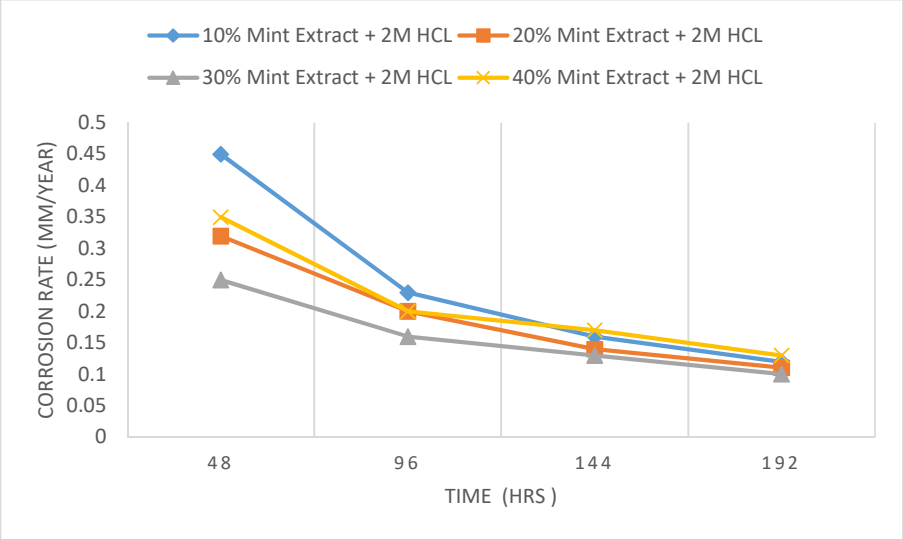


Figure 3.4: Graph of corrosion rate against time for Mint leaves extract in 2M HCL

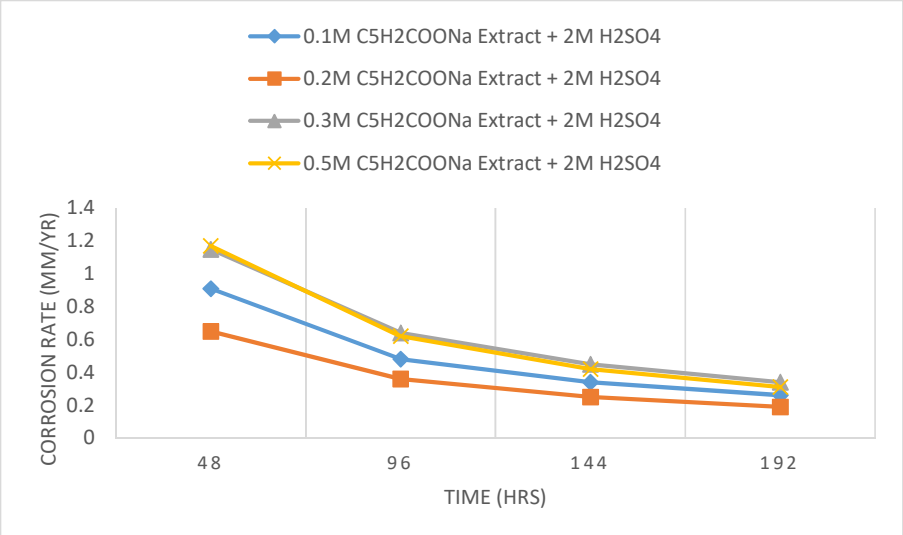


Figure 3.5: Graph of corrosion rate against time for the standard inhibitor C_5H_2COONa in 2M H_2SO_4

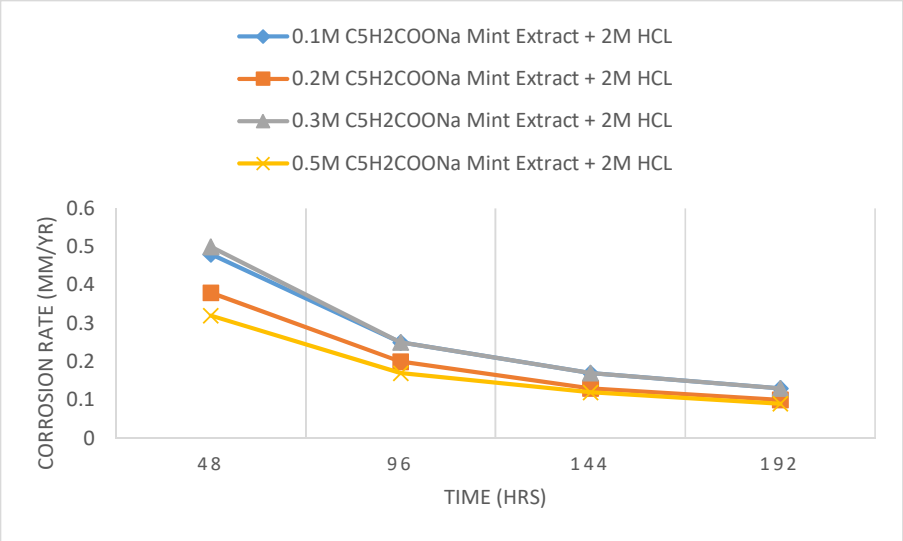


Figure 3.6: Graph of corrosion rate against time for the standard inhibitor C_5H_2COONa in 2M HCL

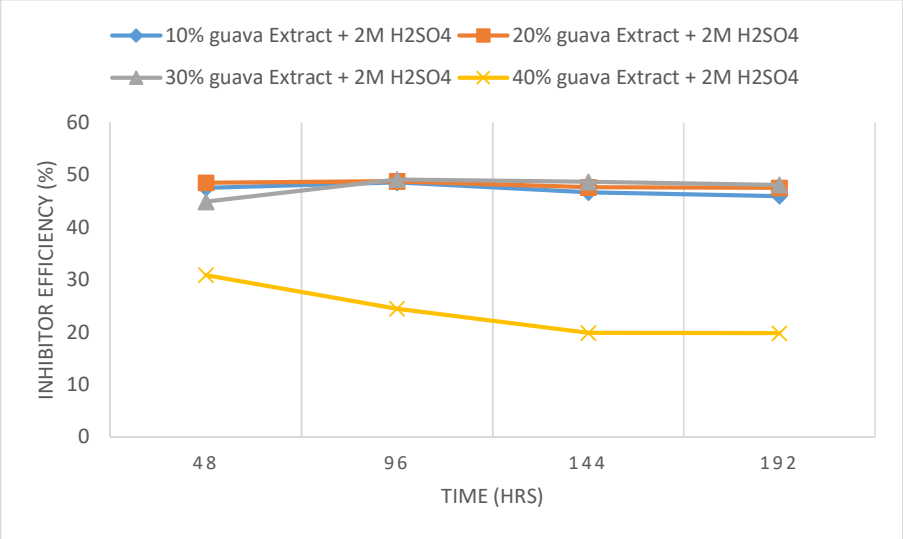


Figure 3.7: Graph of inhibitor efficiency against time for Guava leave extract in 2M H_2SO_4

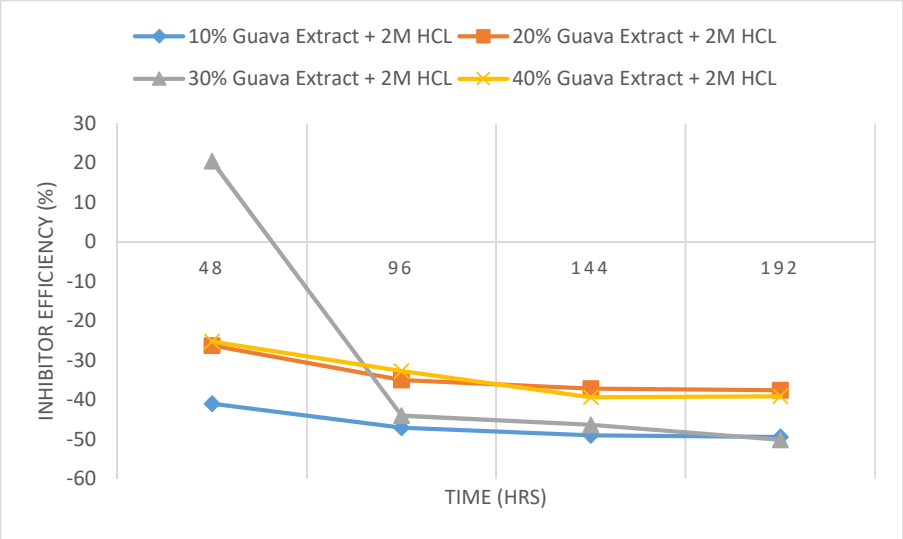


Figure 3.8: Graph of inhibitor efficiency against time for guava leaves extract in 2M HCL

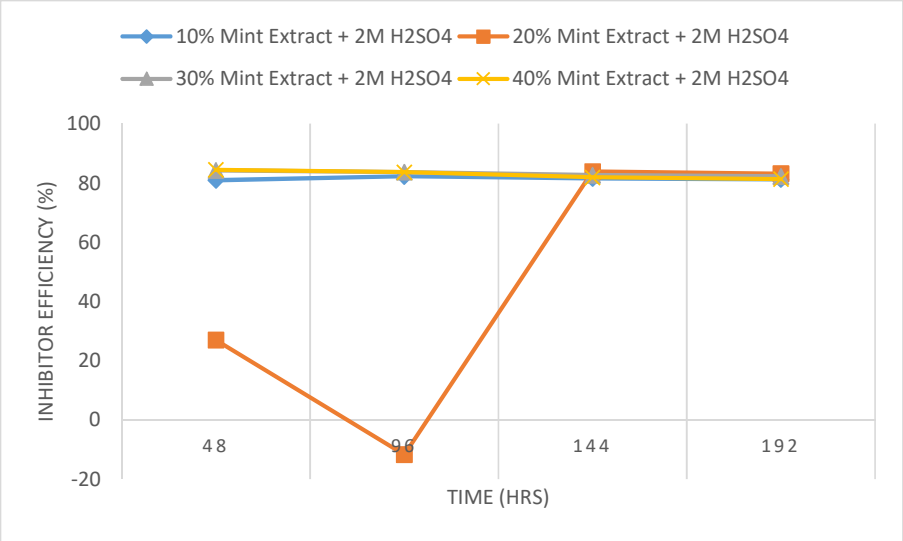


Figure 3.9: Graph of inhibitor efficiency against time for Mint leaves extract in 2M H_2SO_4

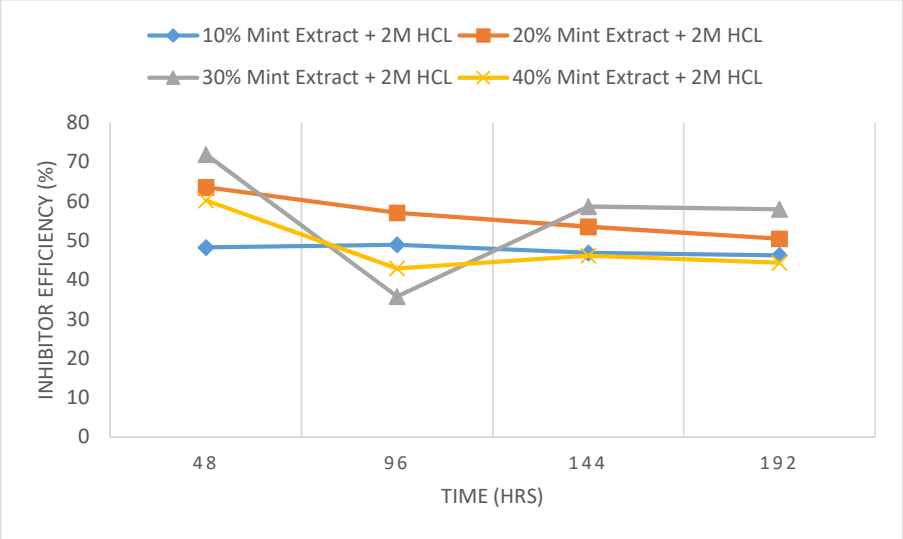


Figure 3.10: Graph of inhibitor efficiency against time for mint leaves extract in 2M HCL

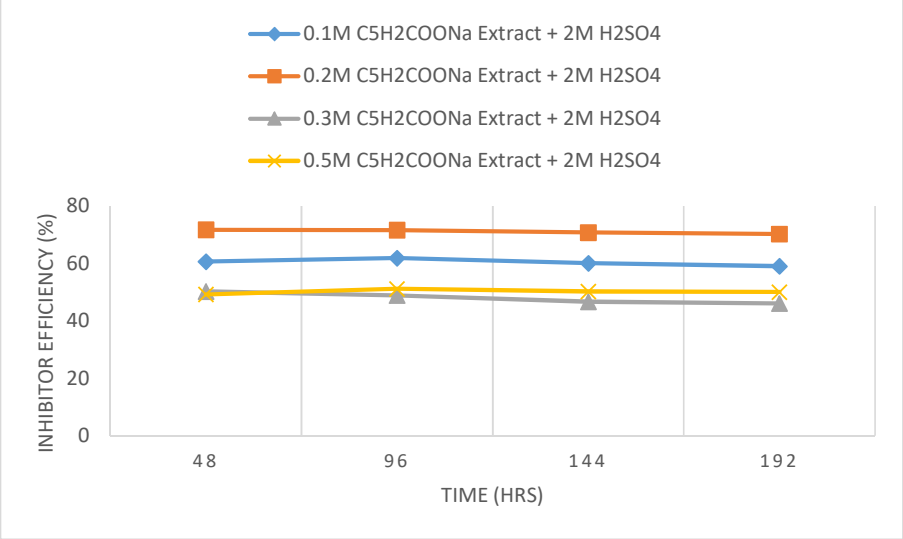


Figure 3.11: Graph of inhibitor efficiency against time for the standard inhibitor C_2H_5COONa in 2M H_2SO_4

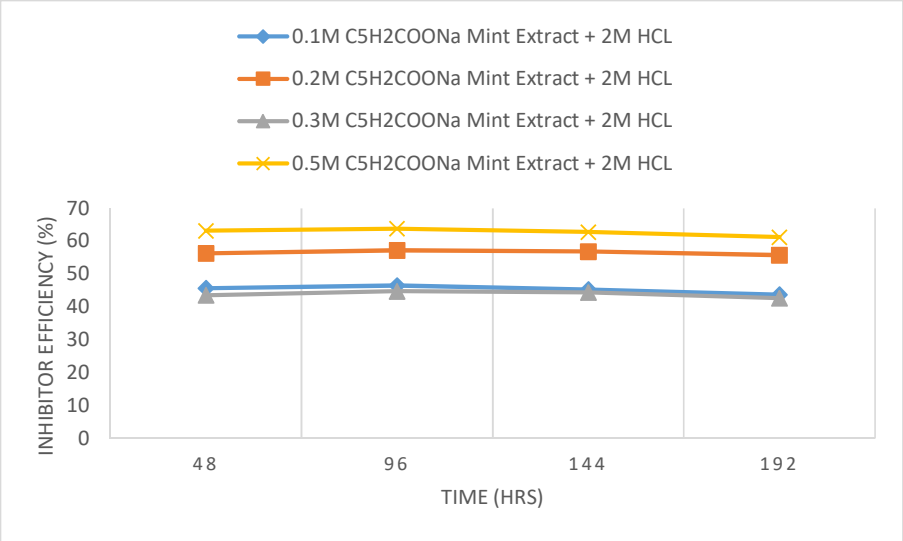


Figure 3.12: Graph of inhibitor efficiency against time for the standard inhibitor C_2H_5COONa in 2M HCL

From the graphical illustration of the results obtained, the extracts of the both leaves were seen to be good inhibitors as they were mostly seen to be having a dropping slope at mostly all percentages of composition with the various acidic media. Having a comparison of each leaf extract with the standard inhibitor performance,

In figure 3.1 which is the Graph of corrosion rate against time for Guava leaf extract in 2M H_2SO_4, we observe that guava leaf extract performed as a good inhibitor with an efficient drop in corrosion rate or weight loss. Just that it had a high initial corrosion rate of above 1.6 mm/yr. before inhibition started taking place as compared to that of the standard inhibitor, i.e. C_2H_5COONa in the same acidic media of sulphuric acid as illustrated in figure 3.5 in which there was corrosion rate of less than 1.2 mm/yr. upon inhibition, and it was highest at the 40% composition. And it was also observed that at composition of 10%, 20%, and 30%, the corrosion rate was almost the same with an initial corrosion rate (that is upon introduction of the metal into the media, after 48hrs. observation) of 1.2mm/yr. Efficiently, in the sulphuric acid media, guava leaf extract inhibited corrosion of the mild steel in the sulphuric acid media from a corrosion rate of 1.4mm/yr. to 0.4mm/yr. after an observation period of 192 hrs. And we could make a prediction of inhibition to a very much lower corrosion rate at a higher exposure time. Guava leaves extract were found out to be good corrosion inhibitors of mild steel at all percentage composition of the leaf extract with sulphuric acid as the corrosive media.

In figure 3.2 which is the Graph of corrosion rate against time for Guava leaf extract in 2M HCL, we could observe that the initial corrosion rate of average 1.2mm/yr. (i.e. observing after 48 hrs.) was much lower than that observed in the sulphuric acid media of 1.6 mm/yr. and also comparing the performance of the guava leaf extract in hydrochloric acid with that of the standard inhibitor shown in figure 3.6, having an average initial corrosion rate of 0.45mm/yr. we could still refer to it as having a good inhibitive capability. Efficiently, we could see that the corrosion rate of the mild steel in the media dropped to 0.4, just as in the case of the sulphuric acid, as we could predict possibly more drop in the corrosion rate at higher time of exposure. In general, it was observed that guava leaves extract performed well as a corrosion inhibitor of mild steel in the presence of HCL as the corrosive media even at different percentages of composition.

In figure 3.3, which shows the graph of corrosion rate against time for mint leaves extract in 2M H_2SO_4 we could see that mint leaves extract performed excellently well as an inhibitor of mild steel corrosion in the presence of sulphuric acid as the corrosive media as it had an efficiently dropping slope with a very good initial corrosion rate of 0.4mm/yr. It could even be observed, upon comparison with the effectiveness of the standard inhibitor in the same corrosive media as in figure 3.5, having an average initial corrosion rate of 1.2mm/yr. that the mint leaf performed very well. On observation of its slope, we could see that at almost all period of observation that the corrosion rate was highly varied as compared to that of the guava leaf extract and the standard inhibitor in still the same corrosive media, having a widely varied corrosion rate at different point of observation though each had a high corrosion rate at the initial. Also, it was observed that at all percentage of composition, the results were almost replicable and the same except at the composition of 20% where

the behavior of the graph in respect to its deviation from others, shows the likelihood of experimental error in the terms of measurement and transfer of the extract and acid during experimentation, or possibly errors arising due to observational procedures. And since we could still observe a slope, we could possibly predict a lower corrosion rate at more time of exposure. In general, from the observation made from this graph, we could see that mint performed well as an inhibitor of mild steel corrosion in the presence of sulphuric acid as a corrosive media.

Also, in figure 3.4 which shows the graph of corrosion rate against time for Mint leaves extract in 2M HCL, it could be observed that just as in the case of sulphuric acid as a corrosive media, mint leaves extract performed very well as an inhibitor of mild steel corrosion in the presence of hydrochloric acid.. With an average initial corrosion rate of 0.35mm/yr. as compared with that of the standard inhibitor of 0.45mm/yr. still in the same corrosive media as shown in figure 3.6, we could say that the leaf extract performed even better than the standard inhibitor as an inhibitor of mils steel corrosion in the presence of hydrochloric acid as the corrosive media. With all percentage composition showing very good corrosion inhibition with the slope highly negative, even having an average corrosion rate of 1.0mm/yr. at an observation period of 192 hrs. We could possibly predict a higher drop in corrosion rate at a higher exposure times. With all compositions showing clearly replicable characteristics, the leaf extract proved to be a very good inhibitor at all percentage of composition.

Figure 3.7 shows the Graph of inhibitor efficiency against time for Guava leave extract in 2M H_2SO_3. All percentages of the composition of the leaves with the corrosive media shows to be satisfactory with an average of 47% efficiency and much lower at the 40% composition as compared to that of the standard inhibitor in still the same corrosive environment having an average compositional efficiency of 60% as seen in figure 3.11.

Also, in figure 3.8, which shows the Graph of inhibitor efficiency against time for guava leaves extract in 2M HCL, we see that the efficiencies were poor. The guava leaves extract in the presence of HCL could be corrosion anti-inhibitive as clearly shown in the graph, as the efficiencies of the inhibitor were even going negative.

Figure 3.9, which shows Graph of inhibitor efficiency against time for Mint leaves extract in 2M H_2SO_4 indicates an excellent inhibition more than that of the standard inhibitor in the same corrosive media as clearly shown in figure 3.11. The efficiency of the mint leaves extract in sulphuric acid was seen to be up to 80% on the average.

Also figure 3.10 shows the Graph of inhibitor efficiency against time for mint leaves extract in 2M HCL. It shows that the inhibitor have an average compositional efficiency of 60% which can be referred to as a good inhibition as compared with that of the standard inhibitor in still the same corrosive media having an average compositional inhibitor efficiency of 50%. Average of all compositional percentages performed very well except with that of 30% performing low at the 2nd observation of 96 hrs. This clearly shows an excellent inhibitor efficiency of the mint leaves as an inhibitor in any of the used corrosive environment as seen in the graphs and discussed above.

4.0. Conclusion

Based on the careful analysis of the results obtained, the following conclusions can be drawn:

1) Mint leaves and guava leaves solution extract have the tannin content of 3.68%/100g sample and 1.25%/100g sample respectively And hydrogen content which are below the maximum of 14%.
2) Mint leaves extract inhibits corrosion more effectively than guava leaves extract in the presence of hydrochloric acid with guava leaves showing a very poor inhibitive capability in the media.
3) Mint leaves extract inhibits corrosion more efficiently than guava leaves extract in the presence of sulphuric acid, though guava leaves proves to be very good inhibitor in this media as compared to its poor performance in the former media.
4) The pH of the media increases and tends towards neutral as the alkaloids in the solution reacts with the acids to form salts.

Conclusively, it can be observed as demonstrated in this project that the corrosion of metal which is one of the major problems faced by engineering, construction industry, and the manufacturing industry can be controlled using guava and mint plant solution extracts which can be easily obtained.

Appendix A

TABLE5.2: SHOWING RESULT OF CHEMICAL ANALYSIS OF PANT SAMPLES

Tests	Mint leaves	Guava leaves
Total acids	50.00%/100g sample	41.67%/100g sample
Total salts	2.0%/g sample	2.33%/g sample
Tannin content	3.68%/100g sample	1.25%/100g sample
Non tannins	1.33%/100g sample	3.75%/100g sample
Total Soluble	80%/g sample	25%/g sample
Total solids	18.62%/g sample	75%/g sample
Moisture content	7%/g sample	7.2%/g sample

Acknowledgement

My Sincere gratitude goes to Dr. Bashir DanAsabe for his intellectual support and contribution as a supervisor throughout the research work.

References

CALLISTER W.D., (1997) Material science and engineering an introduction fourth edition.

CLUBEY B.G: (1988) Chemical inhibitors for corrosion and control. First edition, special publication No 71, Manchester England.

Corrosion-doctors (2011) Corrosion [Online] Available from: http://www.corrosion-doctors.org/ [Accessed: 10th Nov. 2014].

Evrim Baran, Ahmet Cakir, Birgül Yazici, Inhibitory effect of Gentiana olivieri extracts on the corrosion of mild steel in 0.5M HCl: Electrochemical and phytochemical evaluation, Arabian Journal of Chemistry, 2016, , ISSN 1878-5352, https://doi.org/10.1016/j.arabjc.2016.06.008.

JONAH S.A: (1999) Technical Note, Determination of the hydrogen samples from Nigeria using an Am-Be neutron source, CERT, Zaria.

K.K. Alaneme, S.J. Olusegun, A.W. Alo, Corrosion inhibitory properties of elephant grass (Pennisetum purpureum) extract: Effect on mild steel corrosion in 1M HCl solution, In Alexandria Engineering Journal., Volume 55, Issue 2, 2016, Pages 1069-1076, ISSN 1110-0168

LAWUE, F.L: (1978) Corrosion resistance metals and alloys. Second edition, Reinhold publishing company, New York, USA.

LOTO C.A, (1998) the effect of vernomia Amycplaline (Bitter Leaf) solution extract on the corrosion inhibition of mild steel in 0.5M hydrochloric Acid and sulphuric, Nigeria. Corrosion Journal vol. 1 No 1.

P. Muthukrishnan, P. Prakash, B. Jeyaprabha, K. Shankar, Stigmasterol extracted from Ficus hispida leaves as a green inhibitor for the mild steel corrosion in 1M HCl solution, In Arabian Journal of Chemistry, 2015, , ISSN 1878-5352, https://doi.org/10.1016/j.arabjc.2015.09.005.

R.S. Nathiya, Vairamuthu Raj, Evaluation of Dryopteris cochleata leaf extracts as green inhibitor for corrosion of aluminium in 1M H2SO4, In Egyptian Journal of Petroleum, Volume 26, Issue 2, 2017, Pages 313-323, ISSN 1110-0621

Wikipedia, (2014) *Carbon steel* [Online] Available from: http://en.wikipedia.org/wiki/Carbon_steel [Accessed: 10th November 2014].

DEVELOPMENT OF COMPOSITE MATERIAL USING PALM KERNEL SHELL PARTICLES/PHENOLIC RESIN FOR BRAKE PAD APPLICATION

A.A. IBRAHIM, O.P. MICHAEL, A. ALIU, M.B. BALOGUN, S. ABUBAKAR AND N.D. FACI

Department of Mechanical Engineering, Ahmadu Bello University, Zaria-Nigeria

Corresponding author: ahamadii80s@gmail.com

ABSTRACT

This research entails development of asbestos-free composite material for brake pad application due to health hazard recorded from the conventional asbestos based brake pad. Asbestos was replaced with palm kernel shell powder in this research for development of the composite material. Five samples were produced from phenolic resin/palm kernel shell powder at percentage varying compositions ratios from 40% to 60%. Characterizations such as Hardness strength, Abrasion resistance, Impact Strength, Water absorption, Swelling thickness and coefficient of friction were carried out on the composites material samples produced. The results revealed that Hardness strength, Abrasion resistance and Impact strength of the samples decreased with increased filler loading. However, water absorption, swelling thickness and coefficient of friction of the samples increases with increased filler loading from 40% to 60%. Sample A was observed to have most of the properties analyzed within the required standard for automobile vehicles (NIS 323: 1997). Hence, sample A was the most promising among the five composites developed for brake pad application.

Keywords: *asbestos, composite, brake pad, palm kernel shell, phenolic resin*

1.0 Introduction

Environmental pollution is a serious health hazard to humans. Products which wear out and release particles to the atmosphere must be made with materials that are not poisonous to living creatures and human beings. It is universally understood and confirmed that asbestos which is earlier used for the manufacture of brake pad and brake linings of motor vehicle brakes produces asbestos dust that if inhaled by human beings causes cancer of the lungs and brain. (John, 1992). The friction material that was discovered for brake pad ever since was asbestos which during application releases the hazardous gases that is harmful to human health. The use of asbestos as friction material has existed for more than 110years (Sinchair, 2006).

The Palm Oil industry generates large quantity of wastes whose disposal is a challenging task. In the Palm Oil mill, fresh fruit bunches are sterilized after which the oil fruits can be removed from the branches. The empty fruit bunches are left as residues, and the fruits are pressed in oil mills. The Palm Oil fruits are then pressed, and the kernel is separated from the press cake (mesocarp fibers). The palm kernels are then crushed and the kernels then transported and pressed in separate mills. In a typical Palm Oil plantation, almost 70% of the fresh fruit bunches are turned into wastes in the form of empty fruit bunches, fibers and shells, as well as liquid effluent. These by-products can be converted to value-added products or energy to generate additional profit for the Palm Oil Industry (Oyenuga, 1998).

Brake pads are friction material which helps control movement of vehicles that are equipped with disc brakes. Brake pads are steel baking plates with friction material bound to the surface facing the brake disc and it uses friction to transmit force to a moving part of a vehicle (usually the wheels) to slow or stop it completely (Amaren, 2013).

Brake pads convert the kinetic energy of a car to thermal energy by friction when the brake is engaged, the pad or shoe is pressed against a metal disc or drum attached to the wheel, causing it to slow or stop. During this process the pad is heated up by coming into contact with either a drum or rotor, and it starts to transfer small amounts of friction material to the disc or pad. The brake rotor and disk roll the "stick" to each other to provide stopping power. The friction of the pad against the disk is however responsible for the stopping power exhibited (Basha, 2005).

This research aim at developing composite material for automobile brake pads using agro filler (Palm kernel shell) as replacement for the use of asbestos fiber

2.0 Materials and Methods

2.1 Materials

The materials used for the composite production, the manufacturer and grade are as shown in table 2.1.

Table 2.1: Table Showing Materials, Manufacturer, Sources and Grade

S/n	Material	Manufacturer	Sources	Grade
1.	Phenolic Resin	TriveniinterchemPvt Ltd (Group of Triveni Chemicals), Gide, Vapi	Wajson Chemical and Scientific Equipment, Zaria, Kaduna State	INR118
2.	Palm Kernel Shell	-	Samaru-Zaria, Kaduna State	-
3.	Aluminium Oxide	Ashima Petrochemical, Sow Carpet, Chennai	Chemistry Lab., Nilest-Zaria Kaduna State	INR6
4.	Graphite	Intelligent Materials Pvt. Ltd, Village Sundran, DeraBassi	Chemistry Lab., Nilest-Zaria Kaduna State	INR900
5.	Zinc Oxide	G.H Chemicals, Saint Hycinthe, Quebec, Canada	Chemistry Lab., Nilest-Zaria Kaduna State	IRM91 (ASTM)

2.2 Collection and Preparation of Palm Kernel Shell

The palm kernel shell was collected from Sabo Gari market, Kaduna State washed with water to remove dust. The washed palm kernel shell was then sun dried for a week so as to reduce the moisture content in it. The palm kernel shell was crushed to smaller pieces and then grinded to powder using a Laboratory Milling Machine. It was then sieved using sieve Size 72µm in accordance with ASTM D2240.

2.4 Preparation of the palm kernel/Phenolic Resin Composites.

Five (5) samples of different percentage compositions were produced according to the formulation used. Each sample components were mixed using manual mechanical stirrer for 5minutes to achieve homogeneity mixture.

The mixture was filled in a steel mould of 100mm x 80mmx 5mm dimensions and cured on compression moulding machine (carver Hydraulic Press No 4533.4D10B00), at a temperature and pressure of 130ºC and 2.5bar respectively for 10 minutes.

The composite were designated for different samples PKS/PR (A, B, C, D and E) and labeled accordingly as shown in plate 3.3.

2.3 Formulations for Brake Pads

Table 2.2:

S/No	Additives	Samples According to Percentage Compositions Variation(%)				
		A	**B**	**C**	**D**	**E**
1	Phenolic Resin	50	45	40	35	30
2	Palm Kernel Shell	40	45	50	55	60
4	Aluminum Oxide	3.0	3.0	3.0	3.0	3.0
5	Graphite	3.0	3.0	3.0	3.0	3.0
6	Calcium Carbonate	4.0	4.0	4.0	4.0	4.0



Plate 2.1: Showing the various samples developed

3.0 Results and Discussion

3.1 HARDNESS TEST RESULTS

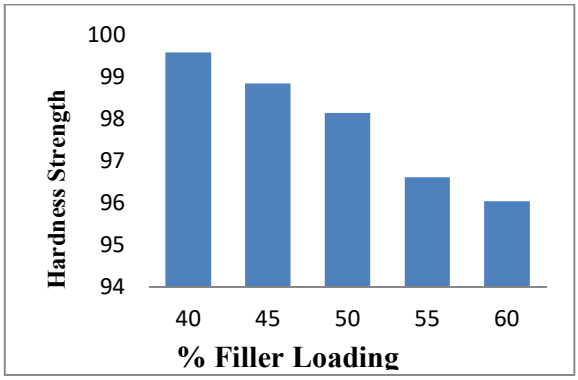


Fig. 3.1: Hardness strength profile for PR/PKS brake pad samples at varying percentage filler content.

Fig. 4.1 above shows the hardness test results for the brake pad produced from Phenolic resin (PR) and Palm kernel shell (PKS) powder. The results show a steady decreased in hardness strength of the brake pad samples produced with increasing filler loading. The decreased hardness strength of the samples produced could be due to the effect of poor binding strength of phenolic resin (binder) since the binder quantity decreases with increasing filler loading.

3.2 ABRASION RESISTANCE TEST RESULTS

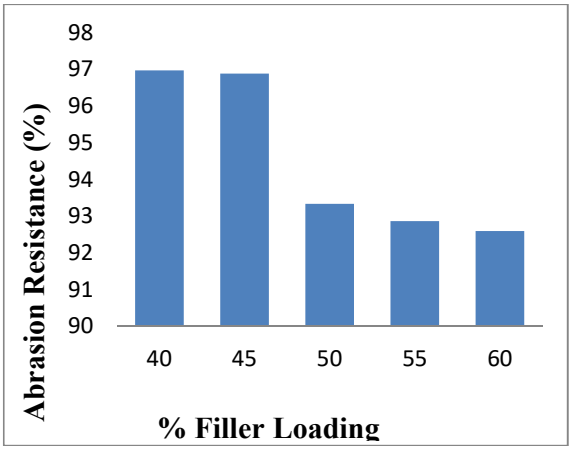


Fig. 4.2: Abrasion resistance profile for PR/PKS brake pad samples at varying percentage filler content.

Fig. 4.2 shows the abrasion resistance test results for the produced brake pads. The chart shows decreased hardness strength of the samples with increasing filler loading. Moreover, a drastic decreased was observed from 50% to 60% as compared to what was observed between 40% and 45% filler loading. This trend could be due to poor interfacial adhesion between the binder (PR) and other components due to poor distribution ratio of the filler quantity in the matrix (binder) as evident by R. O. Ebewele, (2001).

3.3 IMPACT STRENGTH TEST RESULTS

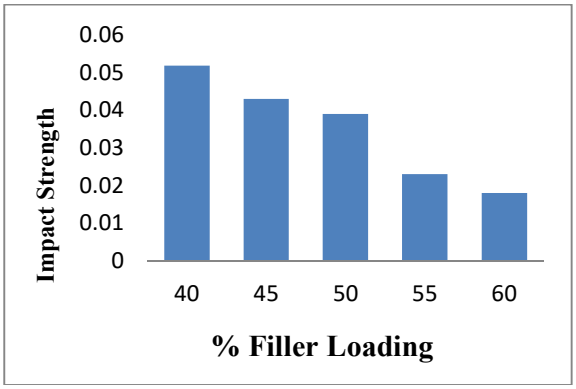


Fig. 4.3: Impact strength profile for PR/PKS brake pad samples at varying percentage filler content.

The impact strength test results are shown in fig 4.3. The results show a decrease trend in the impact strength for the five sample of brake pad produced as the percentage filler loading increased. This could be related to change in the percentage ratio of matrix to filler of the five samples of brake pads produced. Developed composite sample A to D were found to have higher impact strength as compared with required standard impact strength of 0.019J/mm for automobile vehicles (NIS323:1997) except sample E which exhibits lower impact strength of 0.018J/mm.

3.4 WATER ABSORPTION TEST RESULTS

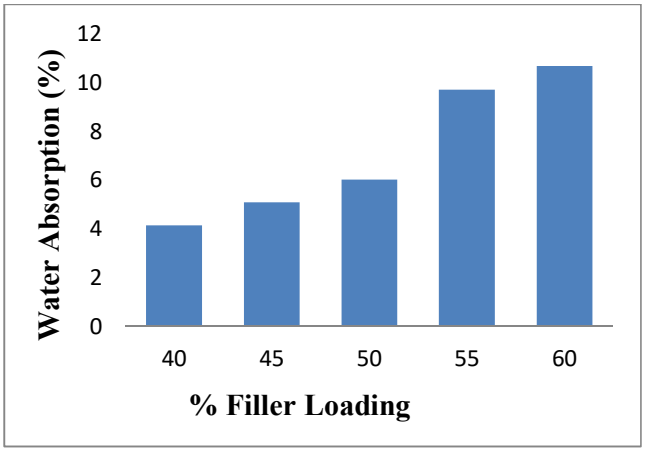


Fig. 4.4: Water absorption profile for PR/PKS samples at varying percentage filler content.

Fig. 4.4 shows the results of water absorption for the brake pad produced. The results show drastic increase in percentage water absorption with increasing filler loading. This trend is expected for the produced brake pads since the binder (hydrophobic component) decreased and the filler load (hydrophilic component) increased in the brake pad system from samples A to E.

4.5 SWELLING THICKNESS TEST RESULTS

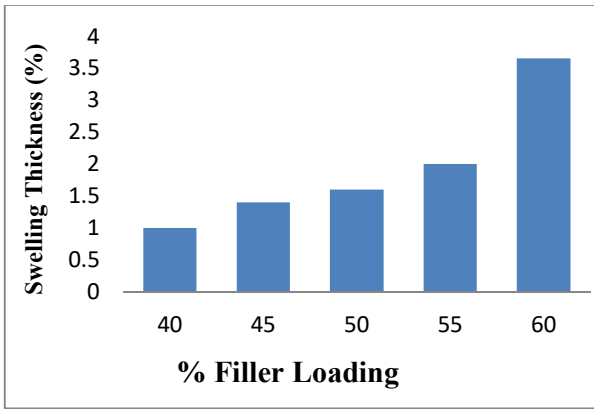


Fig. 4.5: Swelling thickness profile for PR/PKS samples at varying percentage filler content.

Fig. 4.5 shows the results of percentage swelling thickness for the brake pad produced. Percentage swelling thickness of material describes how much it swells when it get in contact with fluid. Swelling thicknessis undesired property in brake pad fabrication as its causes dimensional instability to the brake pad. Hence, may induce brake pad malfunctioning.

The results show drastic increased percentage swelling thickness with increasing filler loading. This trend is expected for the produced brake pads since the binder (hydrophobic component) decreased and the filler load (hydrophilic component) increased in the brake pad system from samples A to E. Furthermore, agro-filler are mostly characterized with increased water absorption whereas polymers usually exhibit low swelling property in water. Meanwhile, in composite formation, all major components will tend to exhibit its individual property bringing about complete unique properties in the final product (composite) as evident by Robert, O. Ebewele (2001). The standard swelling thickness for commercial brake pad is 0.90% (NIS 323: 1997) however values obtained for the developed composites samples A to E tested are 1.00%, 1.50%, 1.60%, 2.00% and 3.65% respectively. Hence, all of the developed samples do not meet the required standard swelling thickness for automobile vehicles except sample Awhich is in the closed range.

4.6 COEFFICIENT OF FRICTION TEST RESULTS

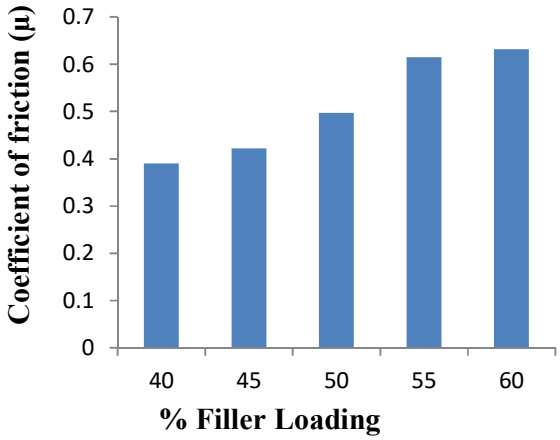


Fig. 4.6: Coefficient of friction profile for PR/PKS brake pad samples at varying percentage filler content.

Fig. 4.6 shows coefficient of friction test results for the developed composites. The results show a steady increase values for the developed composites as the filler loading increased from 40% to 60%. The coefficient of friction for the samples A to E is 0.39, 0.422, 0.497, 0.615 and 0.632 respectively. The standard coefficient of friction for commercial brake pad range from 0.35 – 0.42 (NIS 323: 1997) hence, sample A and B values obtained are within the standard range of coefficient of friction for automobile vehicles.

4.0 Conclusion

Five samples of composite material for brake pad were produced from phenolic resin/palm kernel shell powder at varying percentage compositions ratios. The results revealed that Hardness strength, Abrasion resistance and Impact strength of the samples decreased with increased filler loading. However, water absorption and swelling thickness of the samples increases with increased filler loading.

Moreover, sample A was observed to have most properties closed to the standard properties of automobile vehicle brake pads making it most promising sample for automobile vehicles brake pad among other composites developed in this research.

Recommendation

1. The use of nano partilcle size of filler should be explored for the research purpose.
2. Thermal stability test should be conducted for the samples
3. More combination ratios should be explored and modeled to determine the optimum.

Reference:

John, V. (1992). Introduction to Engineering Materials, 3rd Edition, Macmillan Press Ltd London.

Sinchair W.E. (2006):"Friction Brake"; echanical Design SystemHandbook, ed.Rothbart H.A. McGraw-Hill Book Co. Page 28-38.

Oyenuga, T. K. (1998): Development of Automobile Disk Brake Pad from Local Materials, Ph.D (Manufacturing Engineering) Thesis, University of Benin, Benin City.

Robert O. E. (2001).” Textbook of Polymer Science and Tchnology, 2nd Edition, Department of Polymer Engineering, University of Benin, Benin City.

Basha J.K., Taylor, A.J., and Huband, D.A. (2005): "friction pads for use in Disc Brake,US pat5725077 (United state Patent and Trademark Office).

ENERGY CONSERVATION WITH EFFICIENT LIGHTING: A CASE STUDY OF A PETROLEUM PRODUCTS PRICING REGULATION AGENCY (PPPRA) BUILDING

J. SALEH, P.U. OKORIE AND E. O. OCHUOKPA
Department of Electrical and Computer Engineering, Ahmadu Bello University, Zaria.
* patrickubeokorie@yahoo.com

ABSTRACT
There is a high growing demand of electrical energy in Nigeria. Change in life style, increase in population and technology is the major factor that have increased the demand for energy tremendously. Energy at the national grid is insufficient and also very expensive to purchase hence the need for everyone to save energy. It is important therefore, to use the energy available carefully and judiciously. Lighting forms a major chunk of load on our electrical power system. Energy efficiency in lighting involves building architecture, selection of proper luminaries and light sources. Solid-state lighting (SSL) products made of light-emitting diodes (LEDs) have been considered to offer many potential advantages over conventional lighting technologies. One such advantage is its lower wattage source. However, energy savings is only one measure of effectiveness of an installation. The quantity and quality of illumination and project cost effectiveness are also important. This study evaluates lighting installation to determine the overall suitability of an LED product substitution, including energy savings, illumination quality, cost-effectiveness, human performance, reduction in heat emission and waste disposal. The study also evaluates LED product designed to directly replace traditional lighting system in public buildings.

Keywords: Energy, cost, efficiency, LED, incandescent lamps and fluorescent lamps.

1. INTRODUCTION

Energy is an important measure of prosperity of a nation. Energy is the main stay for continual progress of human civilization. While technological and industrial progress has developed the quality of our lives, it has considerably increased global energy consumption in which Nigeria is not an exemption.

Energy generation in Nigeria is not sufficient with inadequate transmission and distribution facilities. This has affected in no small measure the industrial growth and economic wellbeing of the citizens. The demand for energy is increasing day by day and the cost very high. The available resources of energy are limited. There is need to locate and harness new sources of energy or to use the available ones judiciously so as to make them last longer. Energy conservation is a step in this direction. Broadly speaking, energy conservation is the practice of decreasing the quantity of energy used, and this can only be achieved through efficient energy utilization. In which case energy use is decreased while achieving a similar outcome, or by reduced consumption of energy services.

Energy conservation may result in increase of financial capital, environmental value and human comfort. Individuals and public building that are direct consumers of energy should be able to conserve energy in order to reduce energy costs and promote economic security. Solid-state lighting (SSL) products including light-emitting diodes (LEDs) have been receiving considerable attention because they are thought to offer many potential advantages over conventional lighting technologies. One such advantage is energy savings derived from the lower wattage source.

Today, the variety and number of lighting equipment manufacturers has grown, but the fundamentals of lighting remains the same. These are to supply enough light with proper lighting distribution in space, good spectral qualities and no glare and reasonable costs. The development of light sources and lighting equipment must meet the lighting quality.

Concerning power utilization, 20% to 30% of the world's electricity that is generated is used for lighting **(**http://www.wired.co.uk/news/archive/2011-10/21/eds-solar-energy-consumption**),** mainly in buildings and exterior applications. Over the years, successive administrations in Nigeria have invested a lot of efforts and resources to close the gap between electricity supply and demand in the country. However, such efforts focused largely on capital investments at supply side with little considerations to the demand side management, which is Energy Efficiency and Conservation. Energy efficiency and conservation globally is regarded as the cheapest and fastest form of generation and one of the main drivers of sustainable development in modern energy based economy. The efficient use of energy will enhance the sustainable use of natural resources and in turn contribute to national growth and sustainable

development of a nation. The study by Trifunovic et al (2009), showed a potential energy saving of up to 27% in residential and 30% in the public and commercial sector.

2. LIGHTING FITTING

The various energy lighting source are classified under the following categories:

2.1 LED LAMPS

LED is what is referred to a "solid-state lighting" technology using light emitting diode. Basically, instead of emitting light from a vacuum or a gas, solid-state lighting emits light from a piece of Semiconductor made of a positively charged and a negatively charged component. The light is emitted when electrons move around within the semiconductor structure from the negative to the positive layer. Several studies have been conducted on the benefits of retrofitting conventional lighting systems with the new low Energy ones. Light emitting diode (LED) lamps are more effective than incandescent and compact fluorescent lamp (CFL) bulbs and have a longer lifetime while providing similar luminous. Uddin et al, (2011), found that LED lamps are more expedient than conventional bulbs and also advance in terms of environmental friendliness. Figure 1 shows various components of LED.
(http://continuingeducation.construction.com/crs.php?L=223&C=947)

2.2 INCANDESCENT LIGHT BULBS

Incandescent light bulbs were the most commonly used bulbs. They are also called the "Edison Bulb." They have a simple technology. When connected to a power supply, the electric current heated the wires and tungsten filament to 4,000 degrees Fahrenheit and tungsten begins to evaporate. Without the inert gasses (argon and nitrogen), the tungsten particles would collect on the inside of the glass, causing it to darken. The gasses, however, collect the tungsten particles and send them back to the filament. However, almost 90% of the energy generated by an incandescent bulb is released as heat, not light. Table 1: The range of luminous efficacies for different artificial light sources (US Department of Energy. 2007).

2.3 Fluorescent Lamps

A fluorescent lamp is a low-pressure gas discharge light source. Mainly this light is produced by fluorescent powders activated by ultraviolet radiation generated by discharge in mercury. Generally, this lamp is in form of a long tubular bulb with an electrode at each end, it contains mercury vapor at low pressure with a small amount of inert gas for starting. The electrodes are coated with a material that, when heated upon lamp starting, emits electrons that establish a current across the lamp. Because of the negative voltage-current characteristics of fluorescent lamps it required a device to limit the lamp current, else the ever-increasing current would destroy the lamp.

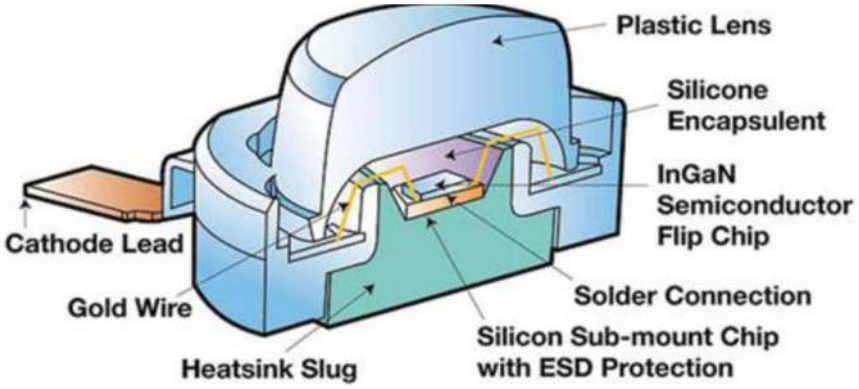


Figure 2.1: Components of a typical light-emitting diode (LED)

Table 1: Luminous Efficacies

Light source	Typical luminous efficacy range in lm/w (varies depending on wattage & lamp type)
Incandescent (no ballast)	10-18
Halogen (no ballast)	15-20
Linear fluorescent (including ballast)	50-100
Compact fluorescent (CFL) (including ballast)	35-60
Metal halide (including ballast)	50-90
Cool white LED->4000K (including driver)	60-92
Warm white LED ->4000K (including driver)	27-54

2.3.1 Compact fluorescent lamps (CFL)

A compact fluorescent lamp (**CFL**), also known as a compact fluorescent lighter energy saving light, is a type of fluorescent lamp. Most CFLs are designed to replace incandescent lamps and fit into most existing light fixtures. Compared to general service incandescent lamps giving the same amount of visible light, CFLs use less power and have a longer rated life. CFLs typically have a rated lifespan of between 6.000 and 10.000 hours, whereas incandescent lamps usually have a lifespan of 750 hours or 1.000 hours. Figure 2 shows compact fluorescent lamps.



Figure 2: Compact Fluorescent Lamp (Philips Lighting Company SAG100 2006)

3 PROPOSED AREA OF RESEARCH

The sample of public building was considered for this study. The Petroleum Products Pricing Regulation Agency (PPPRA) head office building was specifically selected for the evaluation of the lighting system. PPPRA head office building is located at the Central Business District (CBD) of Abuja Federal Capital Territory. Fumo, (2014), Energy security, environmental concerns, thermal comfort, and economic matters are driving factors for the development of research on reducing energy consumption and the associated greenhouse gas emissions in every sector of the economy. Ahmad et al, (2014), the rapid development of human population, buildings and technology application currently has caused electric consumption to grow rapidly. Therefore, efficient energy management and forecasting energy consumption for buildings are important in decision-making for effective energy saving and development in particular places. The building consist of seven floors with wing A and B on each floor illuminated by fluorescent lighting fittings. Access bank is also housed on the ground floor of the building. The working days for both Access bank and PPPRA is five days. Due to the nature of job carried out by the organizations, the working hours is estimated to be 13 hours per day. This information was obtained from the maintenance department and the security unit who are always in the building. Figure 3 described the location and indicating area and Centre of the research work.

3.1 Existing Lighting

The existing lighting lamps in the building are of fluorescent type. It is a two (2) by two (2) ft fitting consisting of four (4) fluorescent tubes with two ballast of thirty six (36W) Watts each meaning, the wattage rating of each fitting is seventy two (72W) Watts. There are a total of Nine Hundred and Eighty four (984) lighting fittings. The number of the lighting fittings were counted manually and the results were double checked with the lighting layout to minimize data gathering error. The lighting layout was obtained from Maintenance Department and it shows the location and type of lamp used in the building in details. It has been identified that the lighting tubes used are Philips and Osram fluorescent lamp. Table 2 present the arrangement of lighting fitting in the building and Figure 4 shows the compacted fluorescent unit lighting fitting.

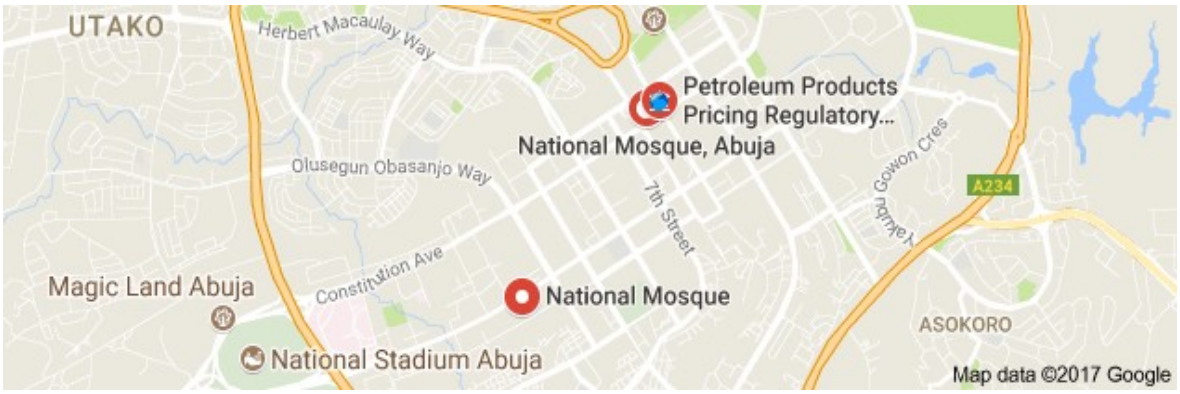


Figure 3. Description location of PPPRA

Table 2: Estimation of Total Number of Lighting Fitting

Floor	Wing A	Wing B	Lobby	Total quantity
G	48	48	14	110
1	51	52	14	117
2	74	64	14	152
3	66	69	14	149
4	79	80	14	173
5	74	81	14	169
6	56	44	14	114
	TOTAL			**984**



Figure 4 Fluorescent tube lighting fitting 72W 2 feet X 2ft

3.2. Potential Energy Saving

LED is a highly energy efficient lighting technology and has the potential to fundamentally change the future of lighting in the world. It uses at least 75% less energy, and last longer life span than fluorescent and incandescent lamp. Widespread use of LED lighting will have great potential impact on energy savings in Nigeria. The computation of daily energy consumption, saving and electricity tariff are given in eqns. 1 to 3:

The total daily energy consumption (EC) is calculated by multiplying the total number of lamps fitting (N), power consumed by the lamp (W), and total hours of operation (OH), which is assumed to be 13 hours. The formula is interpreted in the following equations.

$$EC = \frac{N\ X\ W\ X\ OH}{1000} \qquad (1)$$

Where; EC is energy consumption, N is number of lamps and OH is operating hours per day.

Total energy saving (ES) would be the difference between energy consumption of existing lighting system (ECexisting) and the retrofit lighting system (ECRetrofiting):

$$ES = EC_{existing} - EC_{retrofiting} \qquad (2)$$

Where; ES is energy savings, $EC_{existing}$ is energy consumption of the existing lamps (fluorescent) and $EC_{retrofiting}$ is energy consumption of LED lamp

Bill saving (BS) is calculated by the product of energy saving (ES) with electricity tariff (ET).

$$BS = ES\ X\ ET \qquad (3)$$

Where; BS is bill saving, ES is energy savings and ET is electricity tariff.

4. RESULTS AND DISCUSSION

This section of the report present and discuss extensively the results and analysis performances of the two comparison of energy conservation over one another

4.1. Lighting Audit

A walk-through lighting audit was carried out to ascertain the number of existing fluorescent fittings in the building and the result presented in Table 2 This was necessary to help come up with the required number of LED fittings to be used to retrofit the fluorescent fittings. Furthermore, the rating of the existing fluorescent was also identified to be 72W while a 36W LED fitting was recommended to retrofit the existing fluorescent fitting.

4.2. Energy Consumption

Considering the latest electric tariff rate by Abuja Electricity Distribution Company (AEDC), the electricity provider, the tariff rate for a public building is 47.09 Naira per kWh. In this survey the policy for retrofitting the old lighting system with the new energy Saving LEDs is considered. The variables considered in the analysis are presented in Table 3. The total energy consumption for the lighting application of the selected building for both fluorescent and LED is presented on Table 4.

Equation (1) and the variables in Table 3, were used determine the energy consumption for both LED and fluorescent. Then using equations (1 – 3), we computed energy consumption both, LEDs and Fluorescent fitting, Table 4 is a representation of the summary of the results obtained from the computation.

Table 3: Variable Parameters Analysis

Variables	LED Fittings	Fluorescent Fitting	Unit
Power rating of lamp	36	72	Watts
Single unit provisional Price of lamp	12,000	7,000	Naira
Number of lamps	984	984	Lamps
Running time per day	13	13	Hours
Operational days per month	20	20	Days
Cost of energy/KWh	47.09	47.09	Naira
Life span	50,000	15,000	Hours

Table 4 Energy Consumption Comparison.

Variables	LED Fitting	Fluorescent fitting
Electrical load of lamps in (Watts)	35,424	70,848
Running time per month	260	260
Energy consumption per month (kwh)	9,210.24	18,420.48
Energy to be saved per month (kwh)	**9,210**	0
Total cost of energy per month in Naira	433,710.20	867,420.40
Amount to be saved per month in Naira	**433,710.20**	0
Total Cost of Purchase of lamp	11,808,000	6,888,000
Recovery period of amount spent on purchase of lamp	27 months	0

4.3 Economic Analysis of Led Comparing With Fluorescent

As a result of retrofitting, the overall amount of energy consumption decreases and consequently a decrease in the monthly electricity bill. There is also a significant improvement on the environment because of decrease of the harmful effect of the greenhouse gases. As shown in Table 4.2, the total energy consumption using 72w fluorescent fitting is 18,420.48kwh while the total energy consumption using 36w LED fitting is 9,210.24kwh. The energy to be saved when retrofitting is carried out using the recommended LED is 9,210.24kwh which translates to ₦433,710.20 in savings considering AEDC energy billing rate of 47.09/kwh for public buildings. The lifespan of fluorescent is 15,000 hours translating to three years considering 13 hours of daily operation while the life span of LED is 50,000 hours translating to ten years considering 13 hours of daily operation. Amount of money needed for the purchase of fluorescent fitting is ₦6, 888,000 and the amount needed for the purchase of LED is ₦11, 808,000. In view of the foregoing, it was noted that the initial capital investment for LED is high. However, considering the lifespan of fluorescent and LED, the recovery period for the high initial capital investment on LED is 27 months which is two years 3 months. It is therefore worthy of note that the lifespan of LED provides additional advantage over fluorescent lamp, Figure 5 further present more comparison in chart, which clearly indicates the cost and energy conservation of LED over the fluorescent fitting.

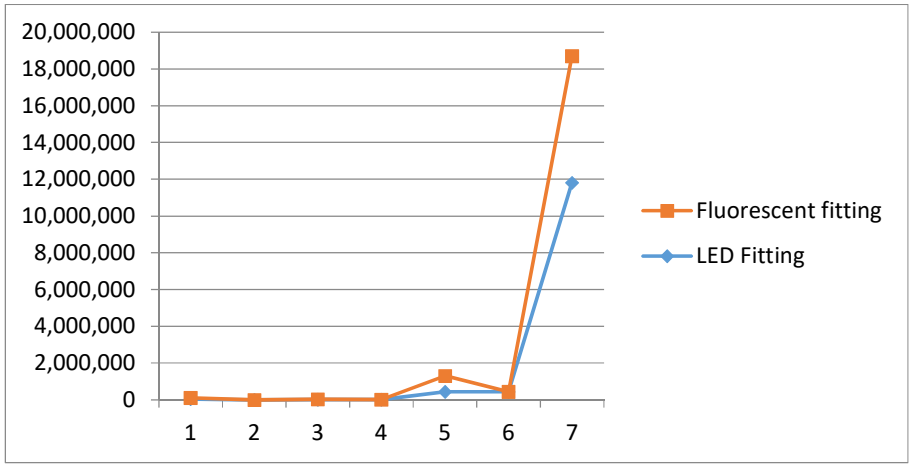


Figure 5 Energy conservation between LED and Fluorescent fitting

The Table 5 offers an easy comparison of the three models of exit sign, while Figure 6 shows the parameters chart.

Table 5: Comparison of three Models

	Incandescent	Fluorescent	LED
Input power (watts)	40	11	2
Yearly energy (kwh)	350	96	18
Lamps Life (years)	0.25-0.5	1-2	20+
Estimated energy cost/year (N47.09)	N16481.5	N4520.64	N847.62

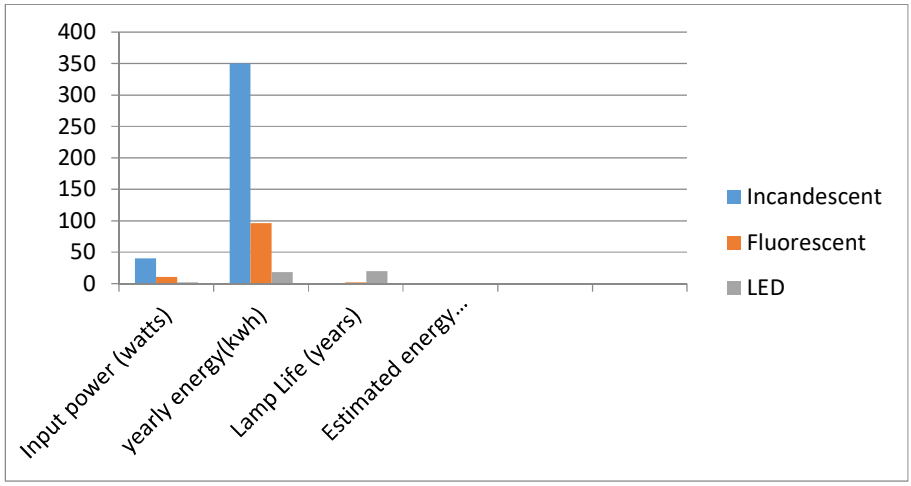


Figure 6 Validation of Three Lighting Fitting

5 CONCLUSSION

In this work energy saving have been analyzed based on the comparison between the conventional lighting system and the proposed LED retrofitting. The policy for retrofitting the old lighting system with the new energy saving LEDs has produced 50% in savings when compared with fluorescent lamps. The result of the life span analysis reveals that after two year three months (27 Months), the selected building will bring profit for the investment. Furthermore, LED is almost maintenance free. This has proven that LED lamp is very productive than the fluorescent lamp because the efficacy is maintained around 90%.

REFERENCES

Ahmad, A. S., Hassan, M. Y., Abdullah, M. P., Rahman, H. A., Hussin, F., Abdullah, H., & Saidur, R. (2014). A review on applications of ANN and SVM for building electrical energy consumption forecasting. *Renewable and Sustainable Energy Reviews*, *33*, 102-109.

Fumo, N. (2014). A review on the basics of building energy estimation. *Renewable and Sustainable Energy Reviews*, *31*, 53-60.

Philips Lighting Company. 2006. Lamp Specification and Application Guide 2006

SAG-100, Philips Lighting Company, Somerset, New Jersey.

Trifunovic, j.; Mikulovic, J.; Djurisic, Z.; Djuric, M,; and Kostic, M. Reductions in electricity consumption and power demand in case of the mass use of compact fluorescent lamps. Science Direct, vol.34, issue 9 (2009) 1355-1363.

Uddin, S. H. Shareef, A. Mohamed, M. A. Hannan, and K. Mohamed, "LEDs as energy efficient lighting systems: a detail review," in *Proceedings of the IEEE* Student Conferenceon Research and Development (SCOReD '11), (2011), pp. 468–472,

US Department of Energy. 2007. ENERGY STAR Program Requirements for Solid State Lighting Luminaires, Eligibility Criteria – Version 1.0. Available at http://www.energystar.gov/ia/partners/prod_development/new_specs/downloads/SSL_FinalCriteria.pdf(January 2009).

CHARACTERISATION OF UNTREATED AND NATURAL LATEX TREATED BORASSUS AETHIOPUM PALM LEAF STALK FIBRE

***[1]ALABI, A.S., [1]SHEHU, U., [1]AUSE, T., [1,2] MBADA, N. I., AND [1]USMAN, I.**
[1]Metallurgical and Materials Engineering Department, Ahmadu Bello University, Zaria
[2]Nigerian Institute of Transport Technology, Zaria.
*ayo.alabi@ymail.com;Phone: 08066150818

ABSTRACT
Demand and use of lignocellulosic fibres as reinforcement in polymer matrices are increasing daily because they address ecological and environmental issues such as recyclability, renewability and non-toxicity. In this work, fibres were extracted from Borassus aethiopum leaf stalk through the combination of water retting and mechanical method, and followed by natural plant latex treatment. The fibre was characterised using fourier transform infrared (FTIR) spectroscopy and single fibre strength test. FTIR showed improved reactivity of fibres due to the introduction of some active functional groups from natural plant latex on the fibre surface. It was concluded that latex treatment will improve fibre – matrix interfacial bonding, through mechanical keying of matrix and fibre matrix reaction at active sites on the fibre surface.

Keywords: *Lignocellulosic fibres, Borassus aethiopum leaf stalk fibre, Natural plant latex, Latex treatment, Mechanical keying*

INTRODUCTION

Borassus aethiopum (Figure 1a), with English names ron palm, borassus palm, African fan palm, fan palm, deleb palm; is known in Nigeria among the Hausa, Igbo and Yoruba as *giginya*; *ubiri* and *agbon-eye,* respectively (Orwa, *et al.*, 2009). It is highly rich in ligno-cellulosic content, and there are many reports on the chemical composition of various parts of this palm from base to crown. The chemical composition of various parts of the tree has shown that the palm is rich in cellulose, hemicellulose and lignin (Ali *et al.*, 2010; Acheampong, 2014; Ngargueudedjim *et al.*, 2015a; Ngargueudedjim *et al.*, 2015b). These components are considered when ligno-cellulosic fibres are used as reinforcement in polymer matrices. Hence, their modifications or interactions with different polymers require the identification of their corresponding absorption bands by the use of fourier transform infrared (FTIR) spectroscopy (Zafeiropoulos, 2011).

Cellulose is the major framework component of natural fibre structure that provides strength, stiffness and stability (Kabir *et al.*, 2012). Its molecular structure (Figure 2a) consists of three hydroxyl groups, two of which form hydrogen bonds within the cellulose (intramolecular), and the other forms hydrogen bond with other cellulose (intermolecular) (Leonard and Martins, 2002; Kabir *et al.*, 2012). Hemicellulose (Figure 2b) is not a form of cellulose at all, the name is just coincidental. It is a polysaccharide that occurs mainly in the primary cell wall, with branched polymers containing five and six carbon sugars (Bledzki and Gassan, 1999; Kabir *et al*., 2012). Aromatic ring structure is the primary chemical constituent in lignin, and these compounds are extremely diverse and present in many forms within the plants and their cell walls. Lignin is a polyphenylpropanoid complex that arises from one or more of the following alcohols (Figure 2c): p-coumaryl (no methoxyl groups ($–O–CH_3$) on the aromatic ring), coniferyl (one methoxyl group at the 3′ position) or sinaple (two methoxyl groups at 3′ and 5′ positions) (Mussig, 2010).

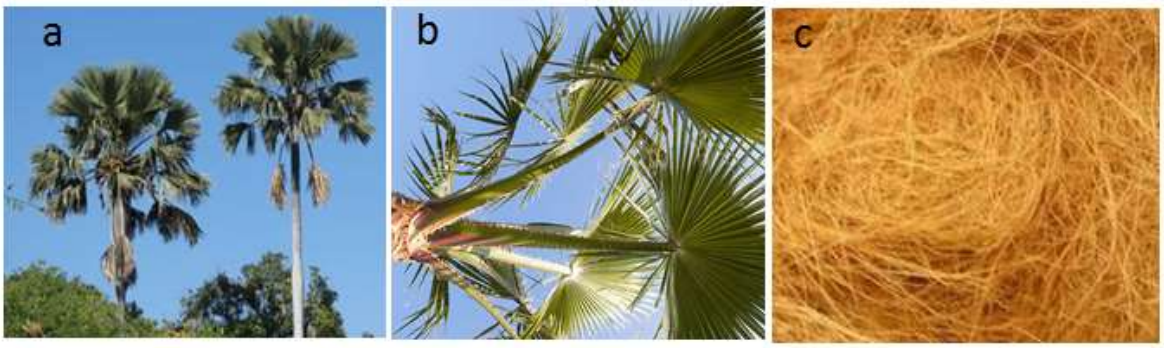


Figure1: (a) *Borassus aethiopum* trees; (b) *Borassus aethiopum* leave stalks; (c) *Borassus aethiopum* extracted fibres

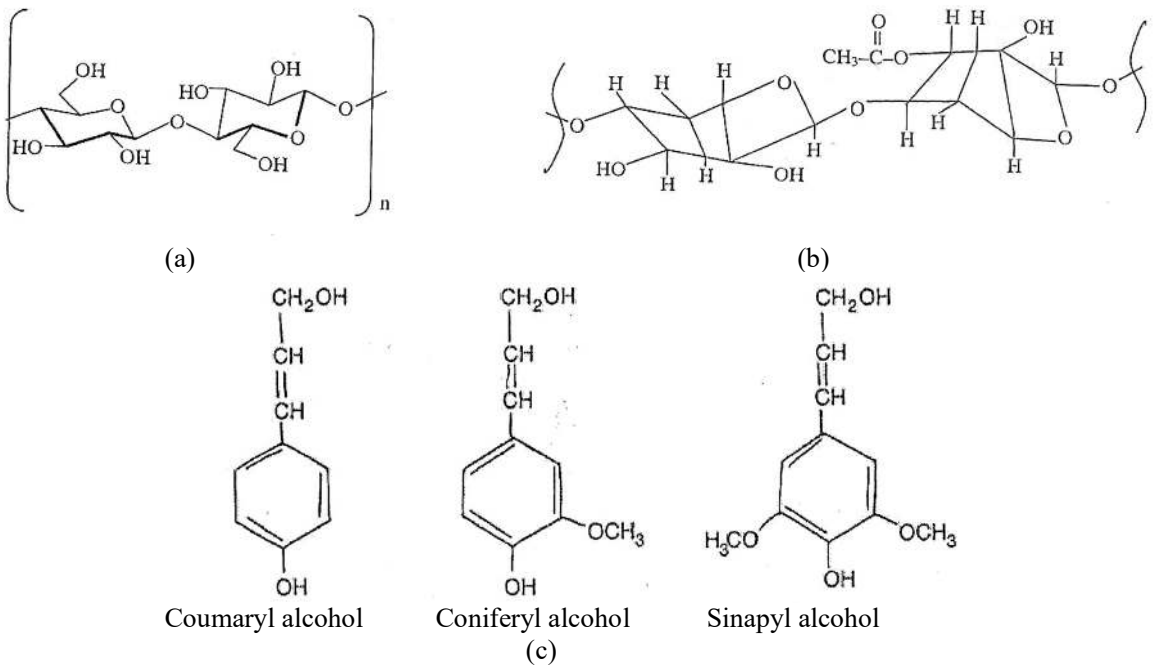


Figure 2: Chemical structure of (a) Cellulose (b) Hemicellulose and (c) Lignin

Insight into the physico-chemical properties and mechanical behaviour of ligno-cellulosic fibres is required to optimise their usage as reinforcements in polymer matrices (Alawar, *et al.*, 2008). The performance of ligno-cellulosic fibres as reinforcement in polymeric materials depends on fibre properties such as strength, stiffness and the interfacial bonding between fibre and polymer matrix. The quality of the fibre–matrix interface is significant for the application of ligno-cellulosic fibres as reinforcement for polymers. Therefore, ligno-cellulosic fibre modifications are considered in modifying the fibre surface properties to improve their adhesion with different matrices (Faruk *et al.,* 2012). Since stress is transferred between matrix and fibres across interface, good interfacial bonding is required to achieve optimum reinforcement and composite properties. The success of the bonding depends on the modification method efficiency, which could be either physical or chemical. The surface of ligno-cellulosic fibre is influenced by fibre composition, fibre modification method (chemical or physical) and processing conditions. Various types of chemical and physical fibre surface modification have been used to enhance natural fibre surface properties. Shukor et *al.* (2013) investigated the effect of NaOH concentration (3%, 6% and 9%) for treating kenaf fibre used as reinforcement in poly lactic acid matrix bio-composite. They found that 6% alkali treatment at ambient temperature is the optimum condition to obtain maximum flexural modulus and impact strength of the composite. Haque *et al.* (2015) investigated effects of acetylation, acrylation, silanisation, alkalisation and permanganate treatment on physical, chemical and mechanical parameters. From their findings, they concluded that treatments such as acetylation, acrylation and silanization can increase interfacial strength, wetting and compatibility between fibre and matrix. Amirou *et al.* (2013) modified date palm fibre by using corona discharge treatment (a physical modification method), which results in surface oxidation. They showed a significant increase in tensile strength and young modulus compared to the composites with untreated fibres, and concluded that the interfacial contact between both components improves because of a higher mechanical anchorage enhanced as a consequence of the etching effect. Han *et al.* (2006) irradiated natural fibres with electron beam to improve adhesion between the fibres and thermoplastics and demonstrated that electron beam irradiation is effective in both impurity removal and functional group development on the surface of natural fibres for better bonding between natural fibre and polymer matrix.

The aim of the present study was to investigate fourier infrared spectroscopy, single fibre tensile strength and morphological characterisation of natural latex treated and untreated *Borassus aethiopum* palm leaf stalk fibre.

MATERIALS AND METHODS

2.1 Materials/ Equipment

The materials and equipment used in this work include: Borassus palm leaf stalk fibre extracted from borassus palm leaf stalk, obtained from a

borassus palm (*Borassus aethiopum*) tree in Daurayi area of Panhauya (11°,7′ N, 7°,37′E) Giwa Local Government, Kaduna State, Nigeria, natural plant latex, tap and distilled water, digital weighing balance (Mettler, AE 160 Model: 8606, Zurich, Switzerland), oven (Model: 60628 Cole and Palmer, London, UK.), sodium hydroxide pellets (Fishers Scientific Company, Fair Lawn, New Jersey, U.S.A.), glacial acetic acid (99% American Chemical Society), attenuated total reflectance infrared spectrometer (Agilent Technologies, Santa Clara, California, U.S.A) optical microscope (NJF – 120A, Zhejiang, China), Zwick/Roell fibre testing machine (BDO – FBO-2005/s, Ulm, Germany).

METHOD

Fibre Extraction

A combination of water retting and mechanical method was used to extract *Borassus aethiopum* palm leaf stalk fibre (Figure 1c) from the leaf stalks (Figure 1b). This was achieved by submerging bundles of leaf stalks in water for 30 days after the thorns at the edges and the bark of the leaf stalk had been shaved. The retted stalk were dried in open air and stored for 7 days to dry. Finally, fibre was seperated by breaking process in which the brittle woody portion of the retted stalks were broken by beating and scraping.

Fibre surface treatment

Surface pretreatment with NaOH was carried out by immersing the fibre in 6 wt.% solution of NaOH for an hour at room temperature (25 - 26°C), after which it was washed with distilled water and the effect of NaOH was neutralised in 2 % glacial acetic acid solution according to Ansell and Aziz (2004); Thomas *et al.* (2004). The fibre was oven-dried for 3 hours at 110°C.The NaOH treated fibre was then given latex coating by dipping into a natural plant latex solution having 10% dry latex content, dissolved in water according to Sreekala *et al.* (2002). Thereafter, the fibre was oven-dried for 3 h at 110°C.

Single fibre tensile test

Single fibres were manually separated from the fibre bundles and cut to the length of 100 mm. The strength of the fibres were determined according to ASTM D – 3379 – 75. Gauge length of 50 mm and cross head speed of 1 mm/min were employed. The machine is equipped with 500 N standard load cell. Specimens were gripped at both end on a Zwick/Roell fabric testing machine and pulled until failure, and load at fracture was then read on a screen. Five readings were taking for each specimen and the average value was recorded.

Single fibre diameter measurement

Optical microscope (model: NJF – 120A) at the Department of Metallurgical and Materials Engineering, Ahmadu Bello University, Zaria, Nigeria in conjunction with a computer software "Digimizer" at the Department of Anatomy, Faculty of Medicine, Ahmadu Bello University, Zaria, Nigeria was used to measure fibre diameter. Prior to the measurement, calibration was done using a laboratory slide. Each sample of fibre consisted of five specimen on which three adjacent readings were taken and averages recorded to the nearest 10 μm.

Fourier transform infrared (FTIR) Spectroscopy

The fourier transform infrared **(**FTIR) spectra of untreated and treated fibres were obtained using the Agilent Technology attenuated total reflection spectrophotometer at the Multi-user Laboratory, Department of Chemistry, Faculty of Physical Sciences, Ahmadu Bello University, Zaria, Nigeria. This was done by clamping the sample tightly on the spectrophotometer and transmitting the IR through the probe. Spectra that corresponded to functional group stretching or vibration were captured on an attached computer and printed out for further analysis.

RESULTS AND DISCUSSION

Single fibre tensile strength and diameter

Figure 3 presents the results of single fibre tensile strengths and average fibre diameters of untreated and latex treated fibres.

A comparison of the untreated and the treated fibres indicated that untreated fibre had the highest average fibre strength (σ_f) of 1250 MPa with average diameter of 350 μm. Latex treated fibre exhibited a lower average strength at fracture of 820 MPa with average diameter of 150 μm.

Reduction in strength of treated fibre as compared to the untreated may be attributed to loss of intracellular hemicellulose and cell-wall lignin between microfibrils during NaOH surface pretreatment, thereby destroying the packing in cellulose chain and causing disorder in crystalline pattern (Zhu *et al.*, 2013). Reduction in average diameter in treated fibre as compared to the untreated was as a result of removal of certain portion of alkali soluble amorphous matters such as impurities, waxes, oil, hemicellulose and lignin (Kabir *et al.*, 2012).

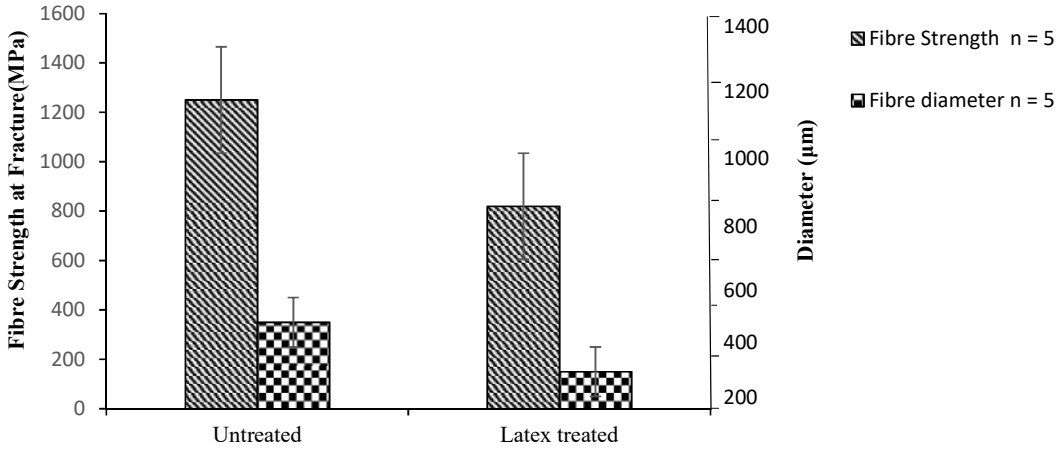


Figure 3: Average fibre strength at fracture and fibre diameter

The finding is in line with (Singha and Rana 2012; Zhu *et al.*, 2013) that reported that aminopropyltriethoxysilane (APS) treatment will destroy packing of the cellulose chain and cause disorder in the crystalline pattern. Thus, the result revealed that effect of surface modifications on ligno-cellulosic fibre strength to be used as reinforcements in composites is an important aspect that requires careful optimization, since the fibre bulk structure may also be altered, especially when the treatment involves extended reaction times or aggressive chemicals. In such cases, increased interfacial strength may be observed when treated fibres are used as reinforcement in polymer matrix composites but decreased fibre strength are exhibited by fibres due to destroyed packing in cellulose chains that may result in crystalline pattern disorder in the fibre structure (Pickering, 2011).

Figures 4 and 5 present the results obtained from attenuated total reflection (ATR) FTIR analysis.

From Figure 4 and 5, it was observed that C – H stretch at 2922.2 cm $^{-1}$ was present in all fibres. The carbonyl peak at 1714.6 cm $^{-1}$ in the untreated fibre was seen to have been reconfigured in the treated fibre. The removal of hemicellulose from the fibre surface caused this peak to disappear. The lignin peak at 1505.8 cm $^{-1}$ in the untreated fibre was altered in the latex treated fibre. Latex treatment introduced amine and asymmetric and symmetric stretch = C – O – C, which could improve the reactivity of the fibre with the matrix. Sgriccia *et al.* (2008) reported that changes in peaks in the FTIR spectrum at 1730, 1625 and 1239 cm $^{-1}$ indicated that the alkali treatment removes hemicellulose and lignin from natural fibre surfaces.

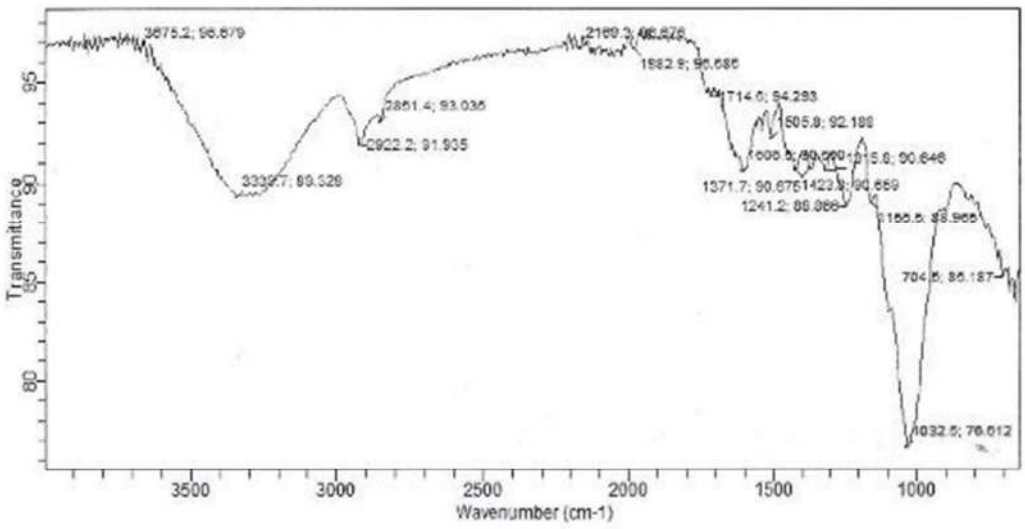


Figure 4: FTIR spectrum for untreated fibre

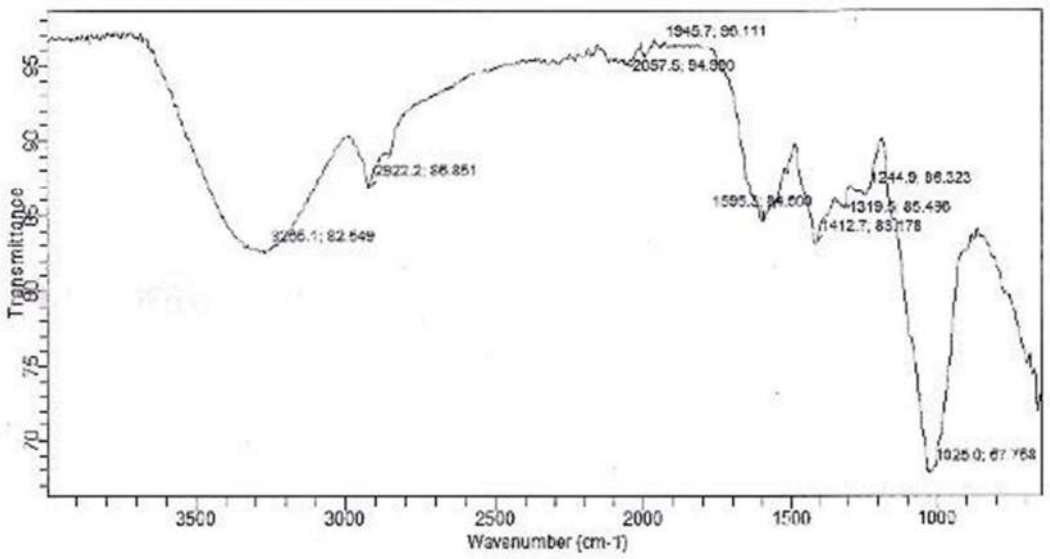


Figure 5: FTIR spectrum for latex treated fibre

CONCLUSION

1. Latex treated fibre at 6 wt.% NaOH pretreatment for 1 hour showed decrease in single fibre tensile strength and corresponding reduction in fibre average diameter.
2. FTIR analysis revealed removal of surface impurities, hemicellulose and lignin and the introduction of amine, which could improve the reactivity of the fibre with the matrix.

RECOMMENDATIONS

1. The fibre could be used as reinforcement to polymeric matrix to improve mechanical properties.
2. Further studies of other physical, chemical or the combination of both surface modifications on the fibre could be investigated.

REFERENCES

Alawar, A., Hamed, A.M., and Al-Kaabi, K. (2009). Characterization of treated date palm tree fibre as composite reinforcement. *Composite, Part B*, 40, 601 – 606.

Ali, A., Fadimatou, B., Tchiegang, C., Saidou, C., and Bouba Adji, M. (2010).Physico-chemical and functional properties of bâtchi or hypocotyle axes of Borassus aethiopum Mart.

Acheampong, J.B. (2014). Physico-chemical properties and natural durability within two varieties of *Borassus aethiopum*. Being a Thesis Submitted to the Department of Wood Science and Technology, Kwame Nkrumah University of Science and Technology, Kumasi, Ghana.

Amirou, S., Zerizer, A., Haddadou, I. and Merlin, A. (2013). Effect of corona discharge treatment on the mechanical properties of biocomposites from polylactic acid and Algerian date palm fibres. *Scientific Research and Essays, 8(21)*, 946 – 952.

Ansell, M.P. and Aziz, S.H. (2004). The effect of alkalization and fibre alignment on the mechanical and thermal properties of kenaf and hemp bast fibre. *Composites: Part 1* – Polyester resin matrix, *Composite Science and Technology 64,* 1219 – 1230.

Bledzki, A.K. and Gassan, J. (1999). Composites reinforced with cellulose based fibre. *Progress in Polymer Science*, *24*, 221-274.

Faruk, O., Bledzki, A.K., Fink, H. and Sain, M. (2012). Biocomposite reinforced with natural fibres: 2000 – 2010. *Progress in Polymer Science, 37*, 1552 – 1596.

Han, S. O., Cho, D., Park, W. H. and Drzal, L. T. (2006). Henequen/poly(butylene succinate) biocomposites: electron beam irradiation effects on henequen fibre and the interfacial properties of biocomposites. *Composite Interfaces, 13(2-3)*, 231-247.

Haque, R., Saxena, M., Shit, S.C., and Asokan, P. (2015). Fibre-matrix adhesion and properties evaluation of sisal polymer composite. *Fibres and Polymer*, 16(1), 146 - 152.

Kabir, M.M., Wang, H., Lau, K.T. and Cardona, F. (2012). Chemical treatment on plant-based natural fibre reinforced polymer

composites: An Overview. *Composites, Part B(43)*, 2883 – 2892.

Leonard, Y.M. and Martin, P.A. (2002). Chemical modification of hemp, sisal, jute and kapok fibres by alkalisation. *Appl Polym Sci,* 84(12):2222–34

Mussig, J. (2010). *Industrial applications of natural fibres: Structure, properties and technical applications*. John Wiley and Sons, Ltd. West Sussene. United Kingdom. 94 – 102.

Ngargueudedjim K., Allarabeye N., K. Charlet, J.F., Destrebecq, R., Moutou Pitti and Robert, J.L (2015a). Mechanical characteristics of fiber palmyra. *Global Journal of Researches in Engineering*, *15*,1 – 9.

Ngargueudedjim K., Bassa B., Nadjitonon N., Allarabeye N., Annouar D. M., Abdel-Rahim M., … Jerome D. (2015b). Mechanical characteristics of tall-palm (*Borassus aethiopum Mart., arecaceae*) of Chad/Central Africa. *International Journal of Engineering and Technical Research*, *3*, 2454-4698.

Orwa, C., Mutua, A., Kindt, R., Jamnadass R. and Anthony,S. (2009). *Agro forestree Database: A Tree Reference and Selection Guide Version 4.0*. retrieved from: (http://www.worldagroforestry.org/sites/treedbs/treedatabases.asp 15th March, 2016.

Sgriccia, N., Hawley, M.C. and Mistra, M. (2008). Characterization of natural fibre surfaces and natural fibre surfaces ad natural composites. *Composites, Part A 39*,1632 – 637.

Shukor, F., Hassan, A., Islam, M.S., Mokhtar, M. and Hassan, M. (2013). Effect of ammonium polyphosphate on flame retardancy, thermal stability and mechanical properties of alkali treated kenaf fiber fill poly lactic acid (PLA) bio-composites. *Materials and Design*, 52: 425-429.

Singha, A.S. and Rana, A.K. (2012). Effect of aminopropyltriethoxysilane (APS) treatment on properties of mercerized lignocellosic *Grewia optiva* fibre. *Journal of Polymer and the Environment*, 1 – 10.

Sreekala, M.S., Kumaran, M.G. and Thomas, S. (2002). Water sorption in oil palm reinforced phenol formaldehyde composites. *Composites, Part A (33),* 763 – 777.

Thomas, S., Jacob, M. and Varughese, K.T. (2004). Mechanical properties of sisal/oil palm hybrid fibre reinforced natural rubber composites. *Composite Science and Technology*, 64, 955 – 965.

Zafeiropoulos, N.E. (2011). *Interface engineering of natural fibre composites for maximum performance*. Woodhead publishing limited. UK, Cambridge.

Zhu, J., Zhu, H., Abhyankar, H. and Njuguna, J. (2013). Effect of fibre treatments on water absorption and tensile properties of flax/tannin composites. A Conference Paper Presentment at the 19th International Conference on Composite Materials, Montreal, Canada.

EVALUATION OF CERAMIC WASTE AS PARTIAL REPLACEMENT OF COARSE AGGREGATE IN HOT MIX ASPHALT

IJIMDIYA, T. S[1]., MANASSEH, J[2]., SANI, J. E[3]., CHUKWUJAMA, I. A[3] AND BAKARE, S. M[4]

[1]Department of Civil Engineering, Ahmadu Bello University, Zaria, Kaduna State.
[2]Department of Civil Engineering, University of Agriculture, Makurdi, Benue State.
[3]Department of Civil Engineering, Nigerian Defence Academy, Kaduna State.
[4]Department of Civil Engineering, Federal Polytechnic, Yaba, Lagos State.

ABSTRACT

This paper present the suitability of ceramic waste aggregate (CWA) as partial replacement for coarse aggregate in asphaltic concrete. In order to achieve this consistency test such as sieve analysis, aggregate crushing and impact value, water absorption, particle shape (flakiness and elongation) and specific gravity was conducted for coarse aggregate and ceramic waste aggregate. Asphalt briquette, using 100% conventional coarse aggregate (control) and variations of ceramic waste aggregate from 10%, 20%, 30%, 40% and 50% were prepared. From the test results, it was observed that the stability value of conventional coarse aggregate (control) gave 4kN and that of CWA of 50% and 20% gave 3.59kN and 4kN respectively as against 3.5kN as minimum value specified in Nigerian General Specification for Roads and Bridges (NGSRB). The corresponding flow, voids in total mix and voids filled with bitumen for sample containing 0% CWA, the values are: 2.88mm, 4.2% and 71.93% respectively, samples containing 20% CWA had flow, voids in total mix and voids filled with bitumen values as 2.77mm, 4.8% and 73.93% respectively and the sample containing 50% CWA had flow, voids in total mix and voids filled with bitumen values as 2.58mm, 10.80% and 85.52% respectively. This shows that the 0% to 20% falls under specification of void in total mix 3% - 5%. The optimum bitumen content of 6.0% and higher stability of 4kN was recorded at a variation of 20% CWA and 80% conventional coarse aggregate. Therefore it can be recommended that ceramics waste aggregate can be used up to 20% as coarse aggregate in asphaltic concrete for a low axle load highway.

Keywords: *Ceramic waste; Coarse aggregate; Hot mix asphalt*

Introduction

The overall relevance of asphaltic concrete in civil engineering practice cannot be overemphasized. The growing concern of resource depletion and global pollution has challenged many researchers and engineers to seek and develop new materials relying on renewable resources. These include the use of by-products and waste materials in highway construction. Although there has been much research conducted on the structural performance of asphalt concrete, these are mostly confined to naturally occurring aggregates, manufactured aggregates and aggregate from industrial by-product. In recent years, initiatives have been instigated on a global and national level to control and regulate waste management. Regulations have become increasingly rigorous and consequently, options which are still rarely used at present, such as minimizing or recycling waste, are becoming economically attractive. All recycling and reuse of waste products involves research aimed at acquiring a full understanding of such products in order to determine suitable and specific applications (Sanchez, Marin, Frais, & Rivera, 2007).

Flexible pavements are designed to have a long life span say 20 years therefore the load distributions that would occur on these structures must also be calculated and included in the design process (Serin, Morova, Saltan, & Terzi, 2012).

The current research focuses on economically increasing the performance and life span of roads through the use of ceramic waste as partial replacement for coarse aggregate. This will also reduce the cost of deposition of ceramic waste on landfill which will reduce the overdependence on natural resources thus saving energy and protection the environment (Mehta, 2001). (Wang, Hung, Lo, & Yapijakis, 2006) reported that the inclusion of higher percentage of ceramics waste as filler in asphalt concrete led to improvements in stability value and the Marshall stability. (Evangelista, de Brito, & Dhir, 2007) analyzed the feasibility of reusing CWA as aggregate in concretes, in proportion of 30% in concrete without noting any relevant reduction in compressive strength.

(Gonzalez & Martinez, 2005) established maximum proportions of ceramic waste as aggregate as 50% in concrete in order to achieve strength characteristic greater than 30 N/mm^2 with the need to increase the water/cement ratio by approximately 6%.

(Dennis, 2009) reported that the results of tests on the performance of asphalt binder mixed with fine fiber reinforcing plastic (FRP) powder and thermoplastic shows that the thermoplastic melted during mixing and separated from the asphalt after being cooled. Therefore, there is a need to use materials that do not melt to avoid changes in the performance of binder. That is why the research aimed at evaluating the use of ceramics waste which does not melt as partial replacement of coarse aggregate in the production of asphalt concrete for highway pavement.

MATERIALS AND METHODS

MATERIALS

Bitumen: The bitumen was sourced from Nigerian National Petroleum Corporation (NNPC) refinery, Kaduna and the laboratory test conducted on the bitumen includes; specific gravity, softening point, flash and fire point, solubility, penetration, viscosity and ductility test according to the (ASTM, 2005) clauses D70, D36, D92, D4, D5, D4402 and D113 respectively

Coarse Aggregate: The coarse aggregate were obtained from quarry site in Zaria, Kaduna State and the laboratory test conducted on the coarse aggregate includes; sieve analysis (BS, 1377), water absorption (BS812, Part 2: 1975), particle shape (flakiness and elongation) test (ASTMC33) and (BS812, 1982), aggregate crushing value test (BS812, 1982), aggregate impact value test (BS812, 1982), and specific gravity test (ASTM, C136)

Fine Aggregate: The fine aggregate was obtained from a block production industry in Samaru, Zaria, Kaduna State. The fine aggregates sizes ranges from 4.75mm (sieve No. 4 to 75µm (sieve No. 200). The laboratory test conducted on it includes the sieve analysis and the specific gravity test.

Mineral Filler: Dangote brand of Ordinary Portland Cement was used in the experiment. Some preliminary tests like setting time and soundness tests were carried out on the cement in accordance with the provision of (BS, EN 196 Part 3 1995)

METHODS

Marshall Mix Design: The aggregate (conventional aggregate and ceramic waste aggregate) were first dry sieved, into the desired size fractions. The amount of each size fraction required to produce a batch that will give a high compacted specimen is the weighed in a separate pan for each test specimen; this is about 1.2kg of the dry aggregate. Three specimens were prepared for each combination of aggregates and bitumen. The pans were then placed in an oven until the dry aggregate achieved the required mix temperature. When the batch aggregate have reached the mixing temperature, a mixing bowl was charged with the heated aggregates, the required quantity of bitumen was added, and mixing was carried out until all the aggregate particles are fully coated. For light design traffic category which was designed for, 35 blows were applied, with the compacted hammer to each end of the specimen. After compaction, the specimens were allowed to cool in air at room temperature until no deformation results when removing each from the mould. Each compacted test specimen is subjected to the stability and flow test, density and voids analysis. For the stability and flow testing, the specimens were immersed in water bath at 60^0C for 30 to 40 minutes. The Marshall testing machine, a compression teating device, was designed to apply loads to test specimens through cylindrical segment testing heads at a constant rate of vertical strain of 51 mm per minute. Loading was applied until specimen failure occurs. The Marshall testing machine is equipped with a calibrated proving ring for determining the applied testing load. The force in Newton required to produce failure of the test specimen was recorded as its Marshall Stability value and the magnitude of deformation of the specimen at the point of failure was recorded as the flow value. The point of failure was defined by the maximum load reading obtained.

DISCUSSION OF RESULTS

Properties of Constituent Materials

The properties of the preliminary test conducted on the bitumen is shown in Table 1 and the properties of the aggregates (fine and coarse) used together with the ceramic waste aggregate are presented in Table 2. The initial and final setting time of mineral filler (Dangote brand of Ordinary Portland Cement) is shown in Table 3.

Table 1: Result of preliminary tests on bitumen

Test	Test Method (ASTM)	Specification by codes for penetration Grade			Result Obtained
		40/50	60/70	80/100	
Penetration at 25^0C	D5	40 – 50	60 – 70	80 – 100	70
Softening point (^{0}C)	D36	49 – 59	46 – 56	42 – 51	46.5
Flash point and Fire point (^{0}C) Min.	D92	232	232	219	205
Solubility in trichloroethylene (^{0}C) Min.	D2042	99	99	99	99
Specific gravity at 25^0C Min.	D70	0.97 – 1.02	0.97 – 1.02	0.97 – 1.02	0.99
Ductility at 25^0C Min.	D113	-	50	75	80
Viscosity at 60^0C (mm^2/s)	D4402	220 - 400	120 - 250	75 – 150	173

Table 2: Result of preliminary tests on aggregate

Test	Code Used	Results Obtained	Value according to codes
Aggregate Crushing Value (CWA) %	BS 812 Part 112	23.3	<30
Aggregate Impact Value (%)	BS 812 Part 112	17.8	<30
Aggregate Crushing Value (Coarse Aggregate) (%)	BS 812	22.95	<30
Specific Gravity (Coarse Aggregate	ASTM C136	2.67	2.6 – 2.9
Specific Gravity CWA g/cc	ASTM C136	2.63	2.6 – 2.9
Specific Gravity (Fine Aggregate) g/cc	ASTM C136	2.65	2.6 – 2.9
Specific Gravity (Cement) g/cc	ASTM C188	3.15	3.15
Water Absorption (Coarse Aggregate)	BS 812 Part 2	0.3	0.2 – 0.6
Water Absorption (CWA)	BS 812 Part 2	0.6	0.2 – 0.6
Flakiness Index (Coarse Aggregate)	ASTM C33, BS 812	22	11 – 35
Flakiness Index (CWA)	ASTM C33, BS 812	29	11 – 35
Elongation Index (Coarse Aggregate)	ASTM C33, BS 812	21	10 – 37
Elongation Index (CWA)	ASTM C33, BS 812	32	10 – 37

Table 3: Summary of physical properties of Cement

Test	Code Used	Average result	Code recommendation
Initial Setting Time	BS EN 196 Part 3 (1995)	121 minutes	>45 minutes
Final Setting Time	BS EN 196 Part 3 (1995)	3 Hrs 26 minutes	< 10 Hours

Particle Size Distribution

The particle size distribution curve of coarse aggregate, ceramic waste aggregate, fine aggregate are shown in Figure 1 – 3 while the particle size distribution curve for combination of filer, coarse and fine aggregate is shown in Figure 4. The design gradation adopted (see Figure 4) shows that it's a well graded and proportioned for the mix design since it fell between the upper and lower boundary of the specification.

Effect of Ceramic Waste Aggregate on Stability

The variation of stability with bitumen content at varying ceramic waste aggregate is shown in Figure 5. Generally as the bitumen content increases the stability increases to optimum bitumen content of 6% and thereafter decreases for all percentage of ceramic waste aggregate used. This is attributed to the strength property (aggregate crushing and impact value) of the ceramics waste which is lesser compare to the coarse aggregate. As the bitumen content increases with increase in ceramic waste, the stability of the sample decreases i.e. higher CWA content had the lowest stability. The optimum stability of 4.0kN was obtained at 20% CWA and 6% bitumen which fall within the permissible limit 2 – 4 kN. The finding is in agreement with that of (Çağdaş & Murat, 2015) and (Dhieyatul, Ratnasamy, & Eltaher, 2016)

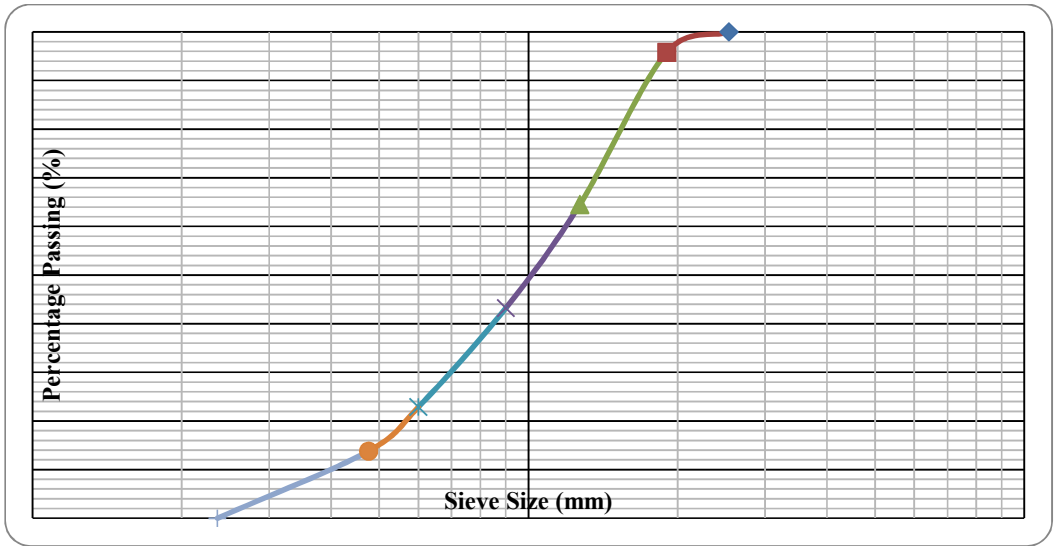


Figure 1: Particle Size Distribution Curve for Coarse Aggregate

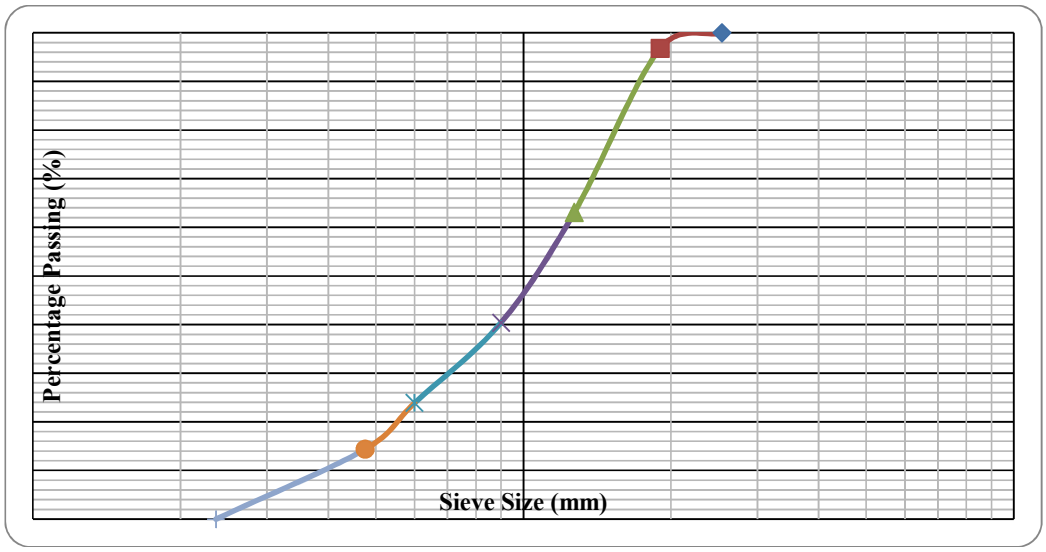


Figure 2: Particle Size Distribution Curve for Ceramic Waste Aggregate

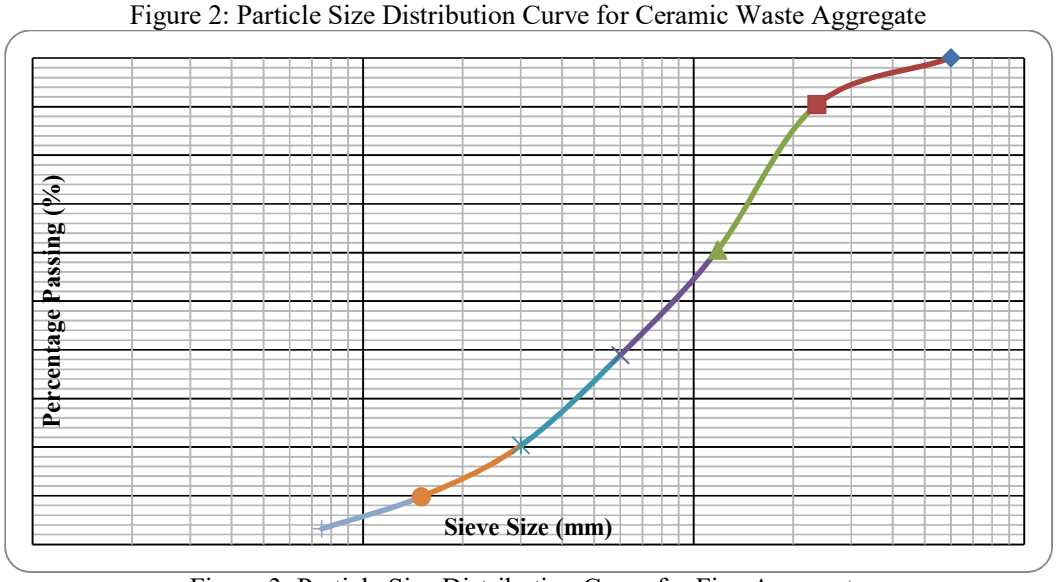


Figure 3: Particle Size Distribution Curve for Fine Aggregate

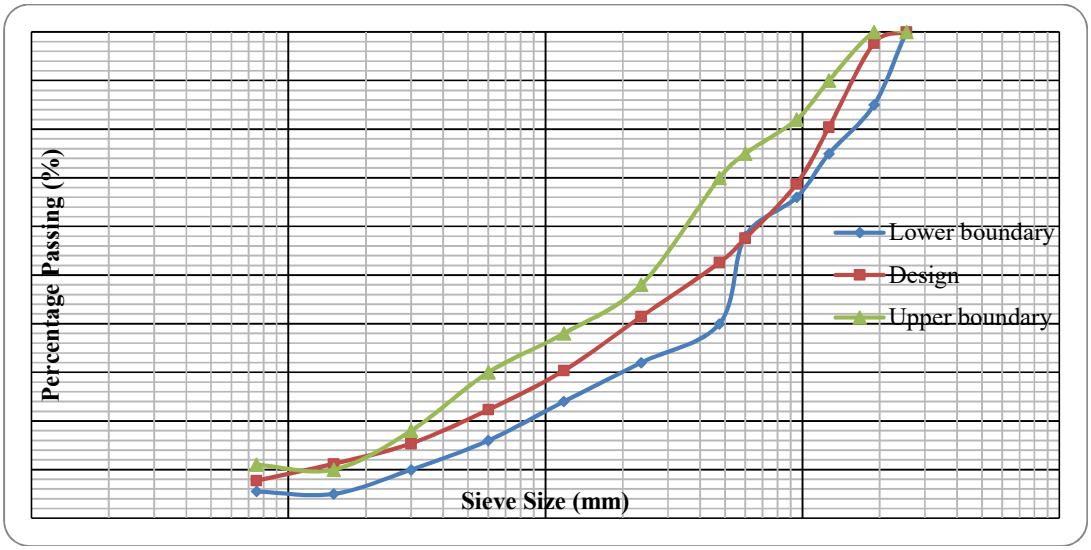


Figure 4: Particle Size Distribution of Combination of Filler, Coarse and Fine Aggregate showing Lower and Upper boundary of the specification and the design mix

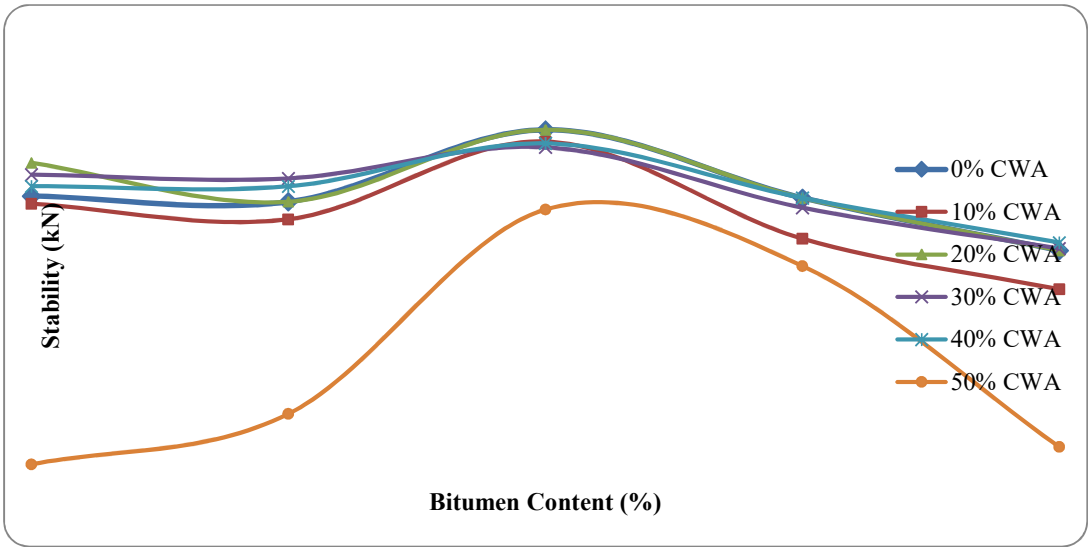


Figure 5: Variation of Stability with Bitumen Content at Varying Ceramic Waste Aggregate

Effect of Ceramic Waste Aggregate on Flow

The variation of flow with bitumen content at varying ceramic waste aggregate is shown in Figure 6. Generally the result shows that flow increases with increase in bitumen content for all percentage of ceramic waste aggregate except at 50% CWA where the flow increases and later decreases with increase bitumen content which may be as a result of the stiffness of the bitumen in the mix, when the mixes becomes less flexible and the resistance to deformation increases then the flow value decreases. The finding is in agreement with that of (Çağdaş & Murat, 2015).

Effect of Ceramic Waste Aggregate on Compacted Density of Mix (CDM)

The variation of Compacted Density of Mix with bitumen content at varying ceramic waste aggregate is shown in Figure 7. Generally compacted density of mix increased slightly as the bitumen content increased at 5.5% then decreased subsequently with increasing the bitumen content. The initial increase at 5.5% bitumen content may be attributed to the absorption rate and strong bonding between the aggregate but as the bitumen content increased and the CWA content increased the bond elapse which leads to less density. Thereby, for the decrease implies that as the bitumen content increased there was no one on one contact of the aggregate particles and as load was transmitted by hydrostatics pressure through the bitumen, the strength of the mix reduced. The finding is in agreement with that of (Çağdaş & Murat, 2015).

Effect of Ceramic Waste Aggregate on Voids in Total Mix (VIM)

The variation of Voids in Total Mix with bitumen content at varying ceramic waste aggregate is shown in Figure 8. Generally the void in total mix decreases as the bitumen content increased for all percentage of CWA. At 5% bitumen content as the ceramic waste aggregate content exceeds 20% CWA the voids in air increases to the extent of exceeding the maximum property of voids in total mix specified by Nigerian Specification for Roads and Bridges. These may be due to the low specific gravity of the CWA. The finding is in agreement with that of (Çağdaş & Murat, 2015).

Effect of Ceramic Waste Aggregate on the Voids in Mineral Aggregate (VMA)

The variation of Voids in Mineral Aggregate with bitumen content at varying ceramic waste aggregate is shown in Figure 9. Generally voids in mineral aggregate increases as the bitumen content increased for all percentage of CWA. The finding is in agreement with that of (Çağdaş & Murat, 2015).

Effect of Ceramic Waste Aggregate on Voids Filled with Bitumen (VFB)

The variation of Voids Filled with Bitumen with bitumen content at varying ceramic waste aggregate is shown in Figure 10. Generally Voids Filled with Bitumen increases to an optimum value at 6% bitumen and thereafter decreases for all percentage of CWA. The finding is in agreement with that of (Çağdaş & Murat, 2015).

Optimum Bitumen Content

The bitumen or binder content is a very important parameter in Marshal Mix design. The basic parameters in mix design are selected and the corresponding binder content was determined. Such parameters include stability, CDM and VIM. The above listed parameters and their corresponding averages of bitumen content for various CWA contents are shown in Table 4. According to the Nigerian general specification for rads and bridges, it shows that as the ceramic waste aggregate increases the void in total mix increases which decreases the stability and also the average optimum bitumen content cannot be obtained because the VIM is beyond the optimum parameter value stipulated as 4%.

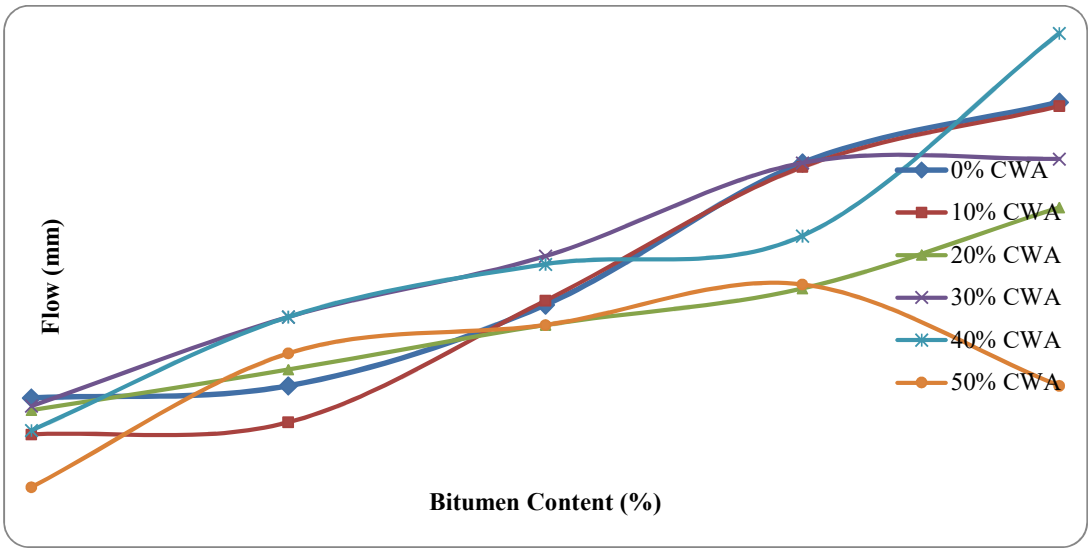


Figure 6: Variation of Flow with Bitumen content at Varying Ceramic Waste Aggregate

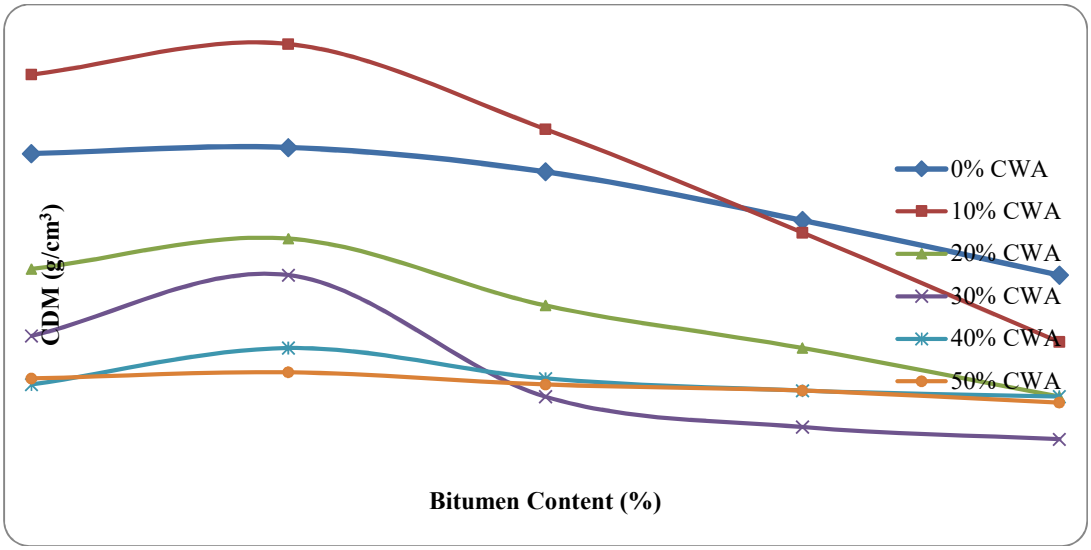


Figure 7: Variation of Compacted Density of Mix with Bitumen content at Varying Ceramic Waste Aggregate

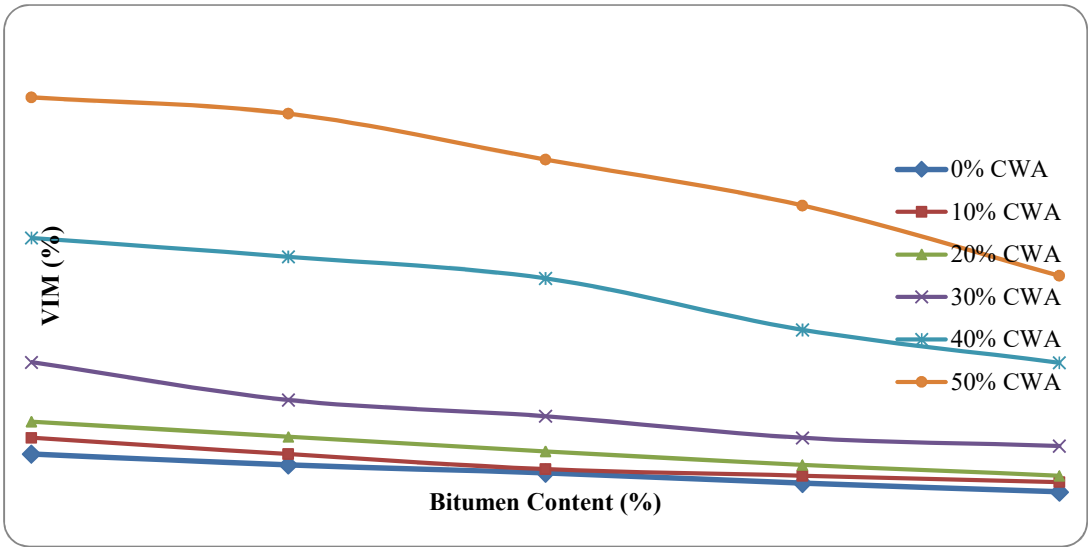


Figure 8: Variation of Voids in Total Mix with Bitumen content at Varying Ceramic Waste Aggregate

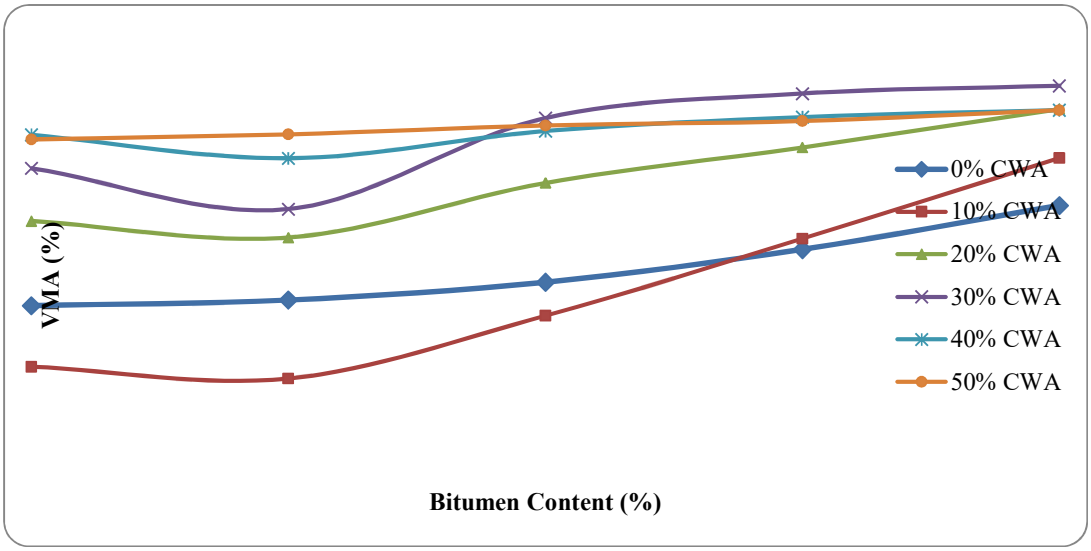


Figure 9: Variation of Voids in Mineral Aggregate with Bitumen content at Varying Ceramic Waste Aggregate

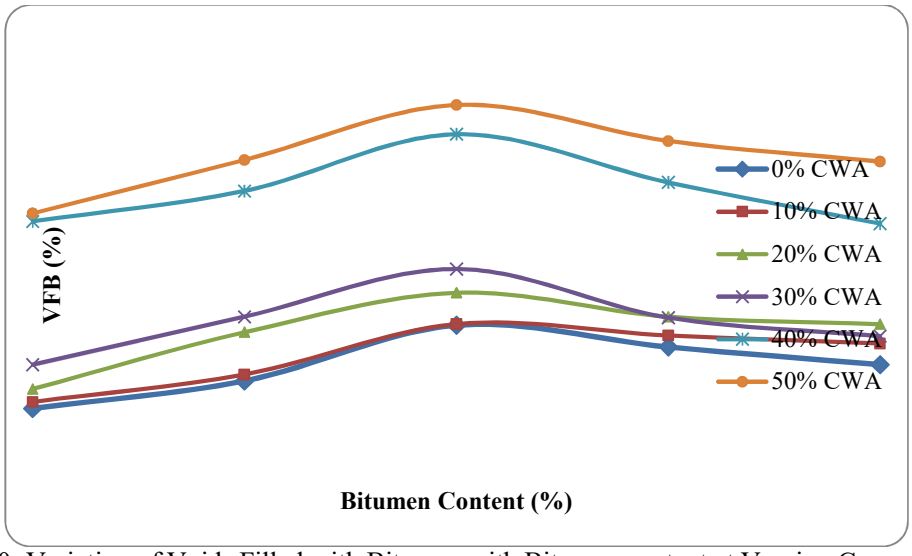


Figure 10: Variation of Voids Filled with Bitumen with Bitumen content at Varying Ceramic Waste Aggregate

Table 4: Optimum parameters for various percentage of CWA

Parameters		Stability	CDM	VIM	Average binder content
0% CWA	Optimum parameter value	4.0	2.21	4.0	-
	Optimum binder content (%)	6.0	5.5	5.5	5.7
10% CWA	Optimum parameter value	3.94	2.18	4.0	-
	Optimum binder content (%)	6.0	5.5	5.9	5.8
20% CWA	Optimum parameter value	4.0	2.06	4.0	-
	Optimum binder content (%)	6.0	5.5	6.5	6.0
30% CWA	Optimum parameter value	3.91	2.0	4.0	-
	Optimum binder content (%)	6.0	5.5	-	5.8
40% CWA	Optimum parameter value	3.93	1.88	4.0	-
	Optimum binder content (%)	6.0	5.5	-	5.8
50% CWA	Optimum parameter value	3.59	1.84	4.0	-
	Optimum binder content (%)	6.0	5.5	-	5.8

CONCLUSIONS

From the results of the findings, the following conclusions can be made:

1. The bitumen is of 60/70 grade which fall within the code specification and can be used for bituminous mix design
2. The aggregate crushing value of the coarse aggregate is 23.3% which satisfies the recommendation of (BS812, 1982) part 112 and the aggregate impact value for coarse aggregate is 17.8% which meets the requirement of (BS812, 1982) part 111.
3. The specific gravity for both coarse aggregate and fine aggregate are 2.67 and 2.65 g/cm^3 respectively.
4. The water absorption value of ceramic waste aggregate falls within specification but shows it absorption is more than that of conventional coarse aggregate.
5. The optimum bitumen content for the stability mix design is 6.0% and the least value of stability is 3.59kN corresponding to a CWA content of 50% while the highest is that of control and 20% whose value is 4.0kN

6. The higher the bitumen content, the higher the flow. However, the flow of 2mm is constant between 5.0 – 5.5 bitumen content and the optimum content of 5.5% gave rise to an optimum CDM value of 2.0g/cm^3.
7. The VFB increases with increase in bitumen content. At ceramic waste aggregate of 0% to 20%, the value of VFB falls within specification by the (Federal Ministry of Works and Highway, 2013).
8. It is recommended that a maximum of 20% partial replacement of CWA with coarse aggregate for use in the production of asphalt for a lightly trafficked highway which will reduce the construction cost

References

ASTM. (2005). American Standard of Testing Materials.

ASTM. (C136). *Standard Test Method for Specific gravity Test of coarse aggregate* .

ASTMC33. (n.d.). American Society of Testing and Materials Standards and Specification for concrete aggregates.

BS. (1377). British Standard Specification for aggregate .

BS. (EN 196 Part 3 1995). *Standard Test Methods for setting time and soundness test* .

BS812. (1982). *British Standard Specification for aggregates from natural source for concrete* .

BS812. (Part 2: 1975). British Standard Specification for aggregate from natural sources for concrete.

Çağdaş, K., & Murat, K. (2015). Use of Ceramic Wastes in Road Pavement Design. *Proceedings of the World Congress on New Technologies (NewTech 2015) Barcelona, Spain – July 15 - 17, 2015Paper No. 226* , 1 - 6.

Dennis, B. C. (2009). The Impact of Small-Scale Ceramics Industries on National Developement . *Ashaku Journal of Ceramics 24(2)* , 13 - 15 .

Dhieyatul, H. I., Ratnasamy, M., & Eltaher, A. (2016). Utilization of Ceramic Waste Materials as Alternative Aggregate in Hot Mix Asphalt (HMA) Mixtures. *Australian Journal of Basic and Applied Sciences 10(13)* , 147 - 154 .

Evangelista, R. V., de Brito, J., & Dhir, R. K. (2007). Properties and composition of recycled aggregates from construction and demolition waste suitable for concrete production. *Constr. Build. Mater. Vol. 65* , 201 - 217.

Federal Ministry of Works and Highway. (2013). *Highway manual Part 2: Maintenance work Abuja Nigeria* .

Gonzalez, B., & Martinez, F. (2005). Recycled aggregate concrete: aggregate and mix properties. . *Materiales de Construccion Vol. 55* .

Mehta, P. K. (2001). Reducing the environment impact of concrete. Concrete can be durable and environmentally friendly. *Concr Int http://www.ce.berkeley.edu/*paulmont/CE60New/Concrete%20and20the%20 Environment.pdf Vol. 10* , 61 - 66 .

Sanchez, M., Marin, F., Frais, M., & Rivera, J. (2007). Reciclado de cascote ceramic en construction. Seminario S12. *Recycled de materials en el sector de la construction* , 95 - 105.

Serin, S., Morova, N., Saltan, M., & Terzi, S. (2012). Investigation of usability of steel fibers in asphalt concrete mixture. . *Construction Build Mater Vol. 36* , 234 - 244.

Wang, L. K., Hung, Y. T., Lo, H. H., & Yapijakis, C. (2006). *Handbook of Industrial and Hazardous Waste Treatment. Second Edition.* Marcel Dekker: ISBN 0-203-02651-9 New York.

A REVIEW OF MATERIALS, METHODS AND MODERN TECHNOLOGY OF SIZING AND DESIZING OF COTTON IN TEXTILE INDUSTRIES.

SALISU, ABDUL.
Samaru College of Agriculture, Division of Agricultural Colleges, Ahmadu Bello University, Zaria.
Correspondence: sirabdu2080@gmail.com, +2327035586840.

ABSTRACT
Researches on the sizing Material is on the increase yearly. The global need for sizing agents all over the world is estimated to be more than 10 million tons per year. Therefore, a serious research focus on the development of improved, cost-effective, and environment-friendly process of size formulation for cotton yarn weaving is still a challenge and priority to researchers. Another significant operation in the process chain of manufacturing a woven cotton fabric, before actual finishing, is fabric desizing, which is an additional challenge. This research work is review of several researches of the past, present and up to date development of Size materials, formulation application and Desizing of cotton materials.

Keywords: Sizing agents, Desizing

1.0 Introduction

Scholars of weaving have considered sizing to be the heart of weaving. Weaving process depends upon a complexity of factors which include the material characteristics, the sizing ingredients, the sizing operation, and the yarn parameters. In the weaving process, the warp yarns on a loom undergo extremely harsh mechanical actions of repeated stresses and strains as well as substantial abrasion due to friction (Wallace, Hyunyoung and Heungsup, 2007). This result to unsatisfactory fabric formation during weaving with a lot of problem such as generation of lint, formation of balls in dense warps, inter fiber clinging and inter yarn entanglements, and, consequently, excessive yarn breakages, loom stoppages, and, hence, production and quality interruptions (Pleva and Rieger, 1992). To avoid these problems in weaving, the warp yarns, for centuries, have always been coated with a thin strong film of a suitable adhesive, generally any ordinary or modified starch (Mangesh and Tesfaye, 2016).

Sizing and desizing remain important wet-processes in textile industries. Sizing is the addition of starchy material to warp yarns (Cavaco-Paulo and Gübitz, 2003). The size mixture not only covers the yarn surface with a thin film, but it is also absorbed into the yarn core, thus gluing and cementing the projecting fibers to the yarn surface, increasing the yarn smoothness and strength, and, thereby, facilitating the weaving process (Patel and Thakkar, 2013). This process of coating the warp yarns on a slasher is called sizing or slashing. The sizing agent does not only contain starchy material (Kiro, 2014). It contains other formulation chemical additives (Emel and Cigdem 2016). The processing of raw cotton in order to improve its performance in further finishing stages consists of three consecutive steps: desizing, scouring and bleaching (Mangesh and Tesfaye, 2016). Desizing removes the size applied to warp yarns prior to weaving; scouring breaks down pectins and waxes and helps remove other impurities present in cotton fibres to improve water absorptivity (Charles, 1992; Karmakar, 1999). In another word desizing is a typical process in pretreatment of cotton woven fabrics and cotton blends but also necessary for all grey synthetic materials containing (Kiro, 2014). The sizing agents on the warp yarns, have to be removed before further processing in textile finishing (Cavaco and Gübitz 2003; Hashem, 2007).

2.0 Conventional and Modern Sizing Technology

The need for the development of different sizing agents other than starch and its derivatives was prompted by the introduction of new spinning and weaving technologies (Karmakar, 1999). Although the textile chemists and technologists worldwide are continuously trying to develop new and improved size formulations and methods of size application, the classical or traditional size and sizing method, which were introduced in the industry more than 140 years ago, are still very much used without any substantial changes at more than 85 % of textile mills in the world today (Dumitras, Sawhney and Bologa 2004).

New and modified techniques for improving the sizing process and sizing materials are continuing to be developed. For example, it has been found that wetting before sizing with hot water, modifying the fiber surface, and modifying the size formulation improve the effectiveness of the sizing process (Pleva and Rieger 1992; Wallace, Hyunyoung and Heungsup, 2007). However, the conventional sizing process continues to be very

inefficient and uneconomical for short runs. As cited in Dumitras, Sawhney and Bologa (2004), the yarn immersion in the sizing mixture with the subsequent squeezing of the yarn still remains the main sizing procedure with all its technological weaknesses, drawbacks and difficulties. In several countries, however, progressive methods, such as warp yarn sizing with deposit rollers; sizing with porous sintering rolls; hot melt sizing; foam sizing; pre-wet yarn sizing; and mechanical methods of starch splitting during size preparation, have been developed and applied. But these relatively new developments are still applied with caution and are not widely used by the industry (Goswami, Anandjuwale and Hall 2004).

Modern sizing technology increases the efficiency of looms, brings savings of sizing agents and energy, and improves the quality of the sized warp. In spite of huge progress in sizing technology, there is a series of theoretical and practical problems concerning the optimisation of size coat. Since no standardised test methods yet exist, which could show to what extent end breakage rate would decrease on a loom after sizing, difficulties exist in planning the efficiency of looms and the quality of the end product. It is believed that size coat will enable minimization of end breakage rate on a loom (Pleva and Rieger 1992). Single-end sizing is an approach to eliminate the problems associated with the traditional method by applying size to individual yarns and drying each yarn separately (Mangesh and Tesfaye 2016). Currently single-end sizing machines are commercially available; however, these machines are primarily used for sizing filament yarns. The method of applying size is similar to conventional sizing in that size is applied by pulling individual yarns through a size bath and squeezing them to remove excess moisture; however the yarns are dried in a hot-air dryer (Pleva and Rieger 1992).

3.0 Requirement of Sizing Materials

Review literatures showed that in the past size formulation requirement was a problem. There was no standard of evaluation of sizing materials (Cavaco and Gübitz, 2003; Hashem, 2007). Researchers of sizing material where able to overcome the challenges of standardization size requirement of specific type of yarn. The performance of the yarn during weaving can also be ascertained (Karmakar, 1999). This achievement has solve the problem of weavers to certain level during weaving. The ingredient of sizing material are basically three. Thus, we have Adhesive substances, lubricant and antiseptic agent. The composition of this ingredient varies from one size to another. Generally, a size material is required to cheap and readily available. It should not be detrimental to the substrate in which it is been applied to. It should have short curing time. It should not react or change colour of the substrate. Ease of removal after sizing is also considered. The size should increase the tensile strength of the substrate (Pleva and Rieger 1992; Wallace, Hyunyoung and Heungsup, 2007).

3.1 Effect of Sizing on Weavability

It is well known that the objective of sizing is to solve problem arising from weaving. Indeed sizing reduces rate of warp yarn breakage during weaving. According to (Patel and Thakkar, 2013) purpose of sizing is to achieve yarn weavability features, such as improve yarn quality, increased weaving efficiency, smooth fabric surface, in desizing ease of removal size from surface of fabric and reducing high cost of manufacturing fabric. weaving machine efficiency is directly proportional the appropriate sizing process (Kiro, 2014). It has been cited that many attempts have been made to evaluate the variable that effect size performance without attempt for weaving trial. A bulk of literature showed that tensile test on sized yarn cannot stand as a means of predicting and judging beaking rate in weaving. Selecting an appropriate size mix is an aspect of sizing. It is again a well established fact that size mix selection is govern fibre substrate consideration. Size add-on is one of the factors that affect physical properties of yarn. Increasing the size add-on will tend to increase the performance of certain size substrate. The effectiveness of sizing defend not only on adhesion between size and yarn but also on the film forming properties of the size material, the properties of the yarn themselves and the machine parameters.

Increasing the size add-on beyond the optimum, in fact, has a detrimental effect on weaving performance since the warp breaks increase (Behera and Joshi 2006). Excessive size add-on leads to an increased penetration of the size, which makes the yarn inflexible. Also, higher size add-on may tend to coat the yarn with a very thick film of size which is not sufficiently anchored to the fibers. Such a thick coating of size film may have a lower extensibility compared to the extensibility of the warp yarn itself (Behera and Joshi 2006). Inflexibility of the yarn and a size film not bound securely have a net effect of size film shedding due to its easy rupturing, thus making the yarn vulnerable to intensive abrasion action and leading to a higher warp breakage rate (Hashem, 2007). The best weaving efficiency region consistent with optimal size add-on is usually achieved in practice by trial and error.

4.0 Technique of desizing textile materials

After satisfactory weaving of yarn to fabric, the size become the major threat to finishing processing. The knowledge of size application helps in removing the size when the need arise during desizing (Behera and Joshi, 2006). In desizing factors that defend on size removal has to be considered (Dumitras, Sawhney and Bologa, 2004). Viscosity of the size in solution, Ease of dissolution of the size film on the yarn. Amount of size applied, Nature and the amount of the plasticizers, and Fabric construction, have to be considered in desizing of textile material (Charles 1992.). There are different methods of desizing. Methods such as enzymatic desizing, oxidative desizing, acid steeping, rot steeping (use of bacteria), desizing with hot caustic soda treatment, and hot washing with detergents were still usefull in the removal of size from textile material (Emel and Cigdem, 2016). Table 1 shows various size materials and their substrates.

Table 1: Material Size and substrate

SIZE MATERIAL	SUBSTRATE	DESIZEABILITY	SIZE RECOVERY
CMC	Cellulose Acetate, Viscose Rayon	Emzyme desizing	20-30%
Acrylics	Nylon Filament Yarn	Hydrolisis	60-90%
Polyester resin	Polyester filament	Hydrolisis	90-100%
Venyl acetate	Glass fibres, Acetate and polyester filament	Hydrolisis	70-80%
Styrene/maleic anhydride	Acetate rayon	Hydrolisis and oxidation desizing	50-60%
PVA	Cotton	Hydrolisis	80-90%
Starch	Cotton, Rayon, polyester and PC blend	Hydrolisis	20-30%

5.0 Conclusion

Summarizing all the facts mentioned above, we can state that the sizing and desizing processes deployed in the weaving industry today demand too much amount of heat and electric energy, human resources, water consumption, and sewage water treatment. In addition, the use of various chemical reagents (perhaps, toxins of complex compositions) that may be harmful to the environment is alarming. Therefore, a serious research focus on the development of improved, cost-effective, and environment-friendly process of warp sizing for cotton yarn and other substrates will continue to be a high priority.

References

Behera B. K. and Joshi V.K. (2006) Effect of sizing on weaveability of dref yarn. AUTEX Research Journal Vol.6 No 3 http://www.autexj.org/no1-2006/018.pdf

Cavaco-Paulo A. & Gübitz G. M. (2003). Cambridge: Woodhead Publishing, *Textile processing with enzyme*. 17–169, ISBN 18557366101.

Charles Tomasino, (1992.) *Chemistry & Technology of Fabric Preparation & Finishing,* Raleigh, North Carolina,

Dumitras P.G., Sawhney P.S., Bologa M.K., (2004), Some New Perspectives On Improving Weaving Process Of Cotton Yarns № 1, С. 82–87.

Emel C. S., and Cigdem S. (2016) Optimization of sizing parameters with a taguchi method India Journal of Fibre and Textile Research Vol. 41 P73-77.

Goswami B. S., Anandjuwale R.R., and Hall D. M. (2004) Textile Sizing. Marcel Dakkar, Inc. New York Basel http://www.deekker.com

Hashem, M.M. (2007). An approach to a single pretreatment recipe for different types of cotton. *Fibers Text. East. Eur.,* 15(2), 85.

Karmakar S.R., (1999) *Chemical Technology in the Pre-treatment Processes of Textile,* Elsevier, Amsterdam,

Kiro Mojsov (2014) Enzymatic Desizing of Cotton: A Review International Journal of Management, IT and Engineering http://www.ijmra.us

Mangesh D. T. and Tesfaye Tolessa Adere (2016) Short and Efficient Desizing and Scouring Process of Cotton Textile Materials *In ternational Journal of Engineering Trends and Technology (IJETT) – Vol. 35 No.6.*

Patel P. R. and Thakkar (2013) Analysing Performance of Esterified Starch against thin Boiling Starch for warp sizing Application. International Journal for Scientific Research and Development Vol. 1 Issue 2

Pleva R., Rieger W., (1992) Measurement and Optimization of Size Pick-up, Textil Praxis International, 47 3, 230-232.

Wallace W. C., Hyunyoung OK, and Heungsup P. (2007) Single-end Sizing of Yarn Using a Slot Applicator. Textile Research Journal ttps://www.researchgate.net/publication/258195794.

COMPARATIVE STUDY OF HYDROXYAPATITE NANOCRYSTALS SYNTHESIZED AT PHYSIOLOGICAL CONDITIONS USING THE CHEMICAL PRECIPITATION AND HYDOTHERMAL TECHNIQUES

V. OCHIGBO[1], V.O. AJIBOLA[2], E.B. AGBAJI[2], A. GIWA[3], J.T. BARMINAS[1], P. MANNIVASAKAN[4], V. RAJENDRAN[4]

[1]National Research Institute for Chemical Technology (NARICT), Zaria-Nigeria
[2]Department of Chemistry, Ahmadu Bello University Zaria-Nigeria
[3]Department of Textile Science and Technology, Ahmadu Bello University Zaria-Nigeria
[4]Centre for Nanoscience and Technology, K.S.Rangasamy College of Technology, Tiruchengode-637 215, Tamil Nadu India..
Corresponding Email:*ochigbovic@gmail.com*

ABSTRACT
Nano crystalline hydroxyapatite were prepared at physiological conditions of pH (7.4) and temperature (37^oC) by precipitation and hydrothermal methods using $Ca(NO_3).4H_2O$ and $NH_4H_2PO_4$ as precursors. The prepared samples were characterized via Particle size Analyser (PSA), Fourier transform infrared spectroscope (FT-IR), energy dispersive X-ray fluorescence (XRF/EDX), X-ray diffraction (XRD), Brunauer–EmmettTeller (BET), Scanning electron microscopy(SEM), Transmission electron microscopy (TEM) and Thermogravimetric /Differential thermal analyser (TG/DTA). Nanocrystals were successfully synthesized via both techniques used. The wet precipitated and hydrothermally synthesized powders revealed Ca/P of 1.65 and 1.66, average particle size distribution of 26nm and 29nm, specific surface area/ pore size/pore volume before and after calcination of (106 and 96m^2g^{-1}/18and 21.35nm/0.65 and 0.48ccg^{-1}) and (102 and 95m^2g^{-1}/19.40and 22.6nm/0.62 and 0.43ccg^{-1}), crystalline size (D)/ degree of crystallinity (Xc) of (5.03nm/0.53) and (5.08nm/1.82), a highly agglomerated uneven rod-like structures respectively. The crystallinity/size and morphology as revealed by XRD and SEM were confirmed from the TEM images having sizes less than 100nm and the crystalline nature of both powders. TG/DTA revealed the thermal stabilities of both powders beyond 800^oC.

Keywords: *Comparative, hydroxyapatite, nanocrystals, physiological, precipitation Hydrothermal*

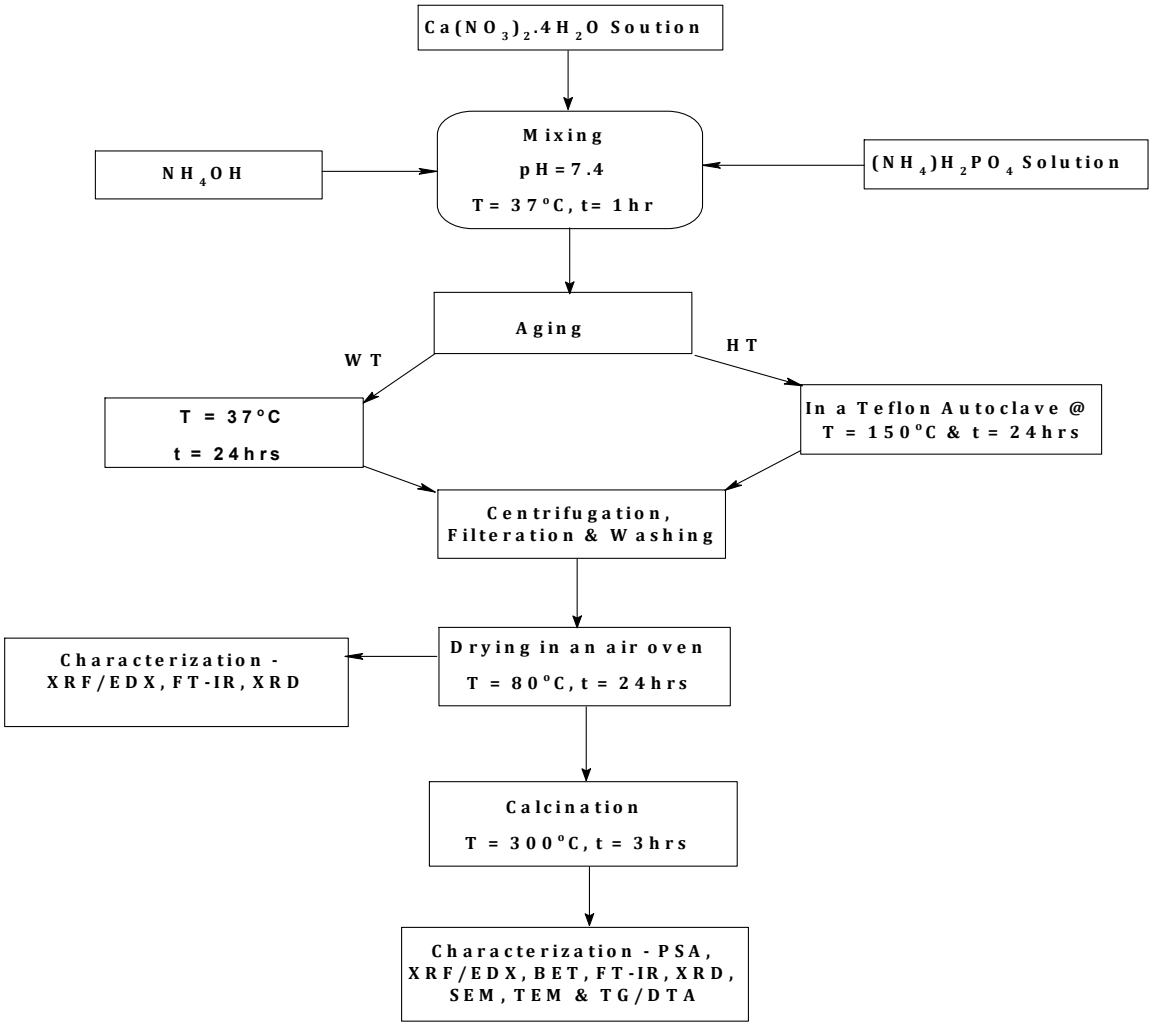
INTRODUCTION

The resorption property of Calcium phosphates depends on Ca/P ratio, degree of crystallinity and crystal structure. A remarkable property of the synthetic HA is its bioactivity, in particular the ability to form chemical bonding with surrounding hard tissues after implantation (Fathi *et al*., 2008). However, most synthetic apatites are formed via high temperature processes, resulting in a well-crystallized structure, which has little or no activity toward bioresoption. To produce synthetic HA powders with the desired properties, wet-chemical methods (precipitation, hydrothermal technique, and hydrolysis of other calcium phosphate) and dry processes (solid-state reaction) can be used (Young and Holcomb, 1982).

Also, there were various techniques reported in literature for the production of nano-sized HA particles but none reports on its production at physiological conditions which is an integral part to its used as biomaterials; particularly, in these hydrothermal and precipitation techniques, moreover, there has being little attempt to investigate the effects of processing conditions on HA particle size, as the only processing variable reported is the effect of calcinations temperature on particle size (Feng *et al*., 2005, Fathi and Hanifi, 2007, 2008). So the effect of processing parameters like pH and temperature on particle size is a serious challenge that needs attention.

MATERIALS AND METHODS

$Ca(NO_3)2{\cdot}4H_2O$ (98% MERCK), NH_4H_2PO4 (99% MERCK), NH_4OH (25% MERCK) and ultrapure water (Arium 611UF; Sartorius AG) as the starting materials were used as received without any further purification. The experimental procedures are as shown in the flow chart.



Scheme 3.1: Flow chart for the synthesis of HA via hydrothermal and wet precipitation method.

RESULTS AND DISCUSSION

The chemical composition of the apatite (Table 4.4) from XRF/EDX studies confirmed the presence of calcium and phosphate in the apatite. Based on these XRF/EDX signatures, the Ca/P ratio of the hydroxyapatite obtained by the hydrothermal and wet precipitation methods were calculated as 1.66 and 1.65 respectively. The Ca/P ratios of HA powder obtained from the hydrothermal method appeared slightly higher compared to that obtained from the wet precipitation method, and this difference could be attributed to the elevated aging temperature which favours particle agglomeration, due to faster reaction that resulted to larger crystal formation and a more complex reaction with different phases of calcium phosphate formation under our experimental conditions, with respect to the wet precipitation method (Anita *et al.,* 2015).

The FT-IR spectra of the synthesized HA (Figure 4.12 and Table 4.1) showed bands at 3572cm^{-1} and 631cm^{-1} corresponding to the hydroxyl group stretching and vibration modes respectively. The intense band at 962cm^{-1} corresponded to P – O stretching vibration modes whereas the doublet at 603 – 567cm^{-1} corresponds to O – P – O bending (Nejati *et al.,* 2009). Furthermore, the broad band at 3425 and 1640 cm^{-1} were attributed to absorbed water, while the sharp bands at 3572cm^{-1}was attributed to the stretching vibration of the lattice OH. PO_4^{3-} characteristics peaks appear at 568, 602, 962, 1040 and 1092cm^{-1}. The observation of the asymmetric P–O stretching vibration of the PO_4^{3-} band at 962cm^{-1} is a distinguishable band alongside the sharp bands at 633, 602, 568cm^{-1}, corresponding to the triply degenerate bending vibrations of PO_4^{3-} in hydroxyapatite. Some CO_3^{2-} derived bands were observed at 870cm^{-1} and around 1420-1480 cm^{-1}indicating that a minute amount of carbonate substitution occurred (Elliot, 1994), which might be due to the adsorption of atmospheric carbon dioxide during the sample preparation, but, because carbonates are

constituents of bone structures (Rajabi-Zamani *et al*., 2008) the presence of CO_3^{2-} may play a vital role in the bioactivity of HA rather than being a cause of concern. The bands of absorbed water (H-O-H) around 1630 and 3450 cm^{-1} appear narrower and sharper in the hydrothermal than the wet precipitation method. The band around 870cm^{-1} which corresponds to carbonate ion (CO_3^{2-}) group was more pronounced in the HA obtained by the wet precipitation than in the hydrothermal method. The band around 3572cm^{-1} which corresponds to the hydroxyl ion (OH^-) group appear sharper, with higher intensity for HA powder from the hydrothermal than the wet precipitation method. These variations in band intensities andappearance could be attributed to the elevated aging temperature of the hydrothermal method, otherwise all characteristic bands of the HA appeared similar in position. These results are in conformity with those reported by Maryam and Ramakrishna, (2004) and Negati*et al.,*(2009) using the same synthetic routes but different reaction temperatures.

Table 4.4: Elemental Compositions and Ca/P ratio of Hydroxyapatite (HA) obtained at Wet Precipitation and Hydrothermal Methods.

S/N	Elements	Hydrothermal	Wet precipitation
1	Ca	57.305	58.863
2	P	34.521	34.716
3	Si	7.788	6.384
4	Fe	0.7005	0.013
5	Cu	0.1995	0.010
6	Sr	0.1845	0.006
7	**Ca/P**	**1.66**	**1.65**

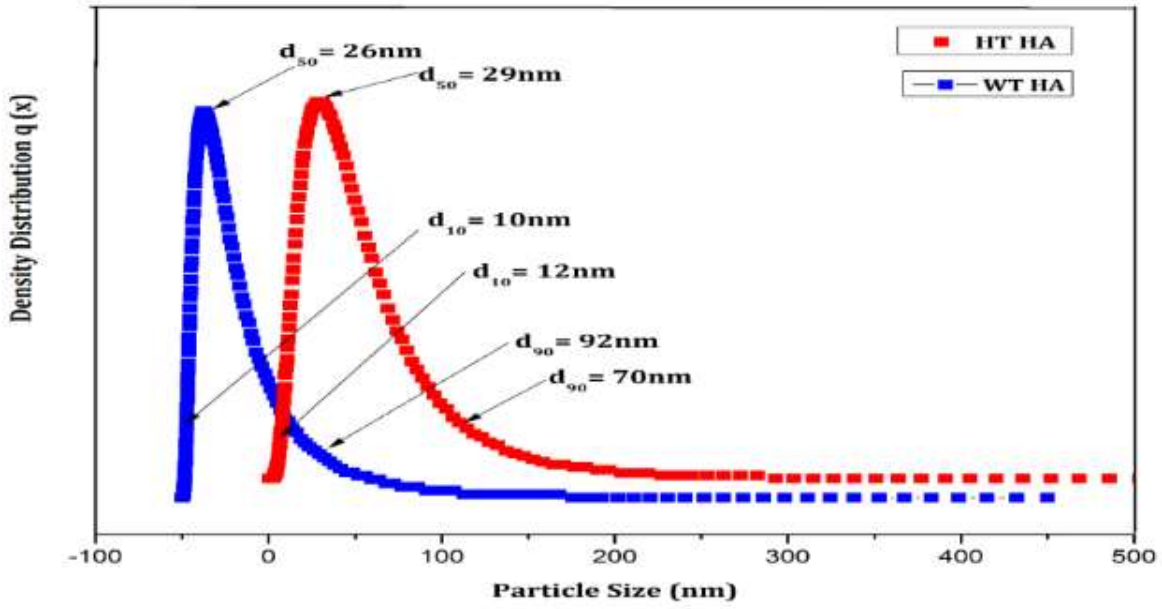


Fig. 4.12: Particle Size Distribution of Hydroxyapatite (HA) Synthesized via Hydrothermal (HT) and Wet Precipitation (WT)

Table 4.5: Specific Surface Area (SSA), Pore Size (PS), Pore Volume (PV) and Average Particle size (D_A) of Hydroxyapatite (HA) before and after Calcinations from BET analysis

S/N	Apatite (HA)	SSA(m^2/g)	PV(nm)	PS(cc/g)	D_A(nm)
1	HA WT (A)	106	0.65	18.67	17.91
2	HA WT (B)	96	0.48	21.32	19.77
3	HA HT (A)	102	0.62	19.40	18.61
4	HA HT (B)	95	0.43	22.60	19.98

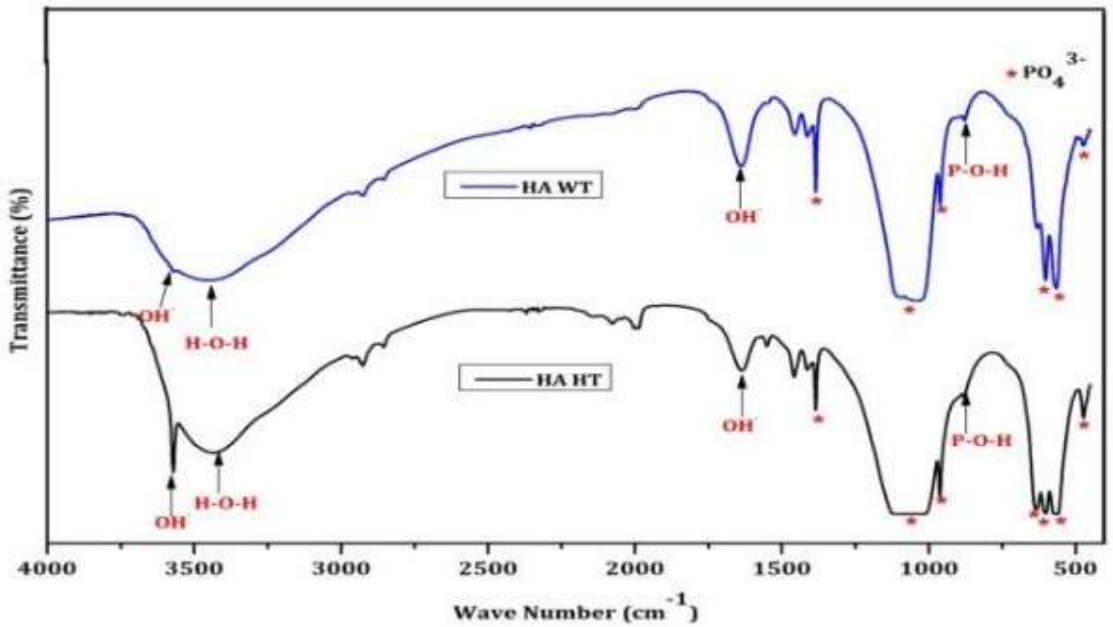


Fig. 4.11: FTIR spectra of HA synthesized via Hydrothermal (HT) & Wet precipitation (WT)

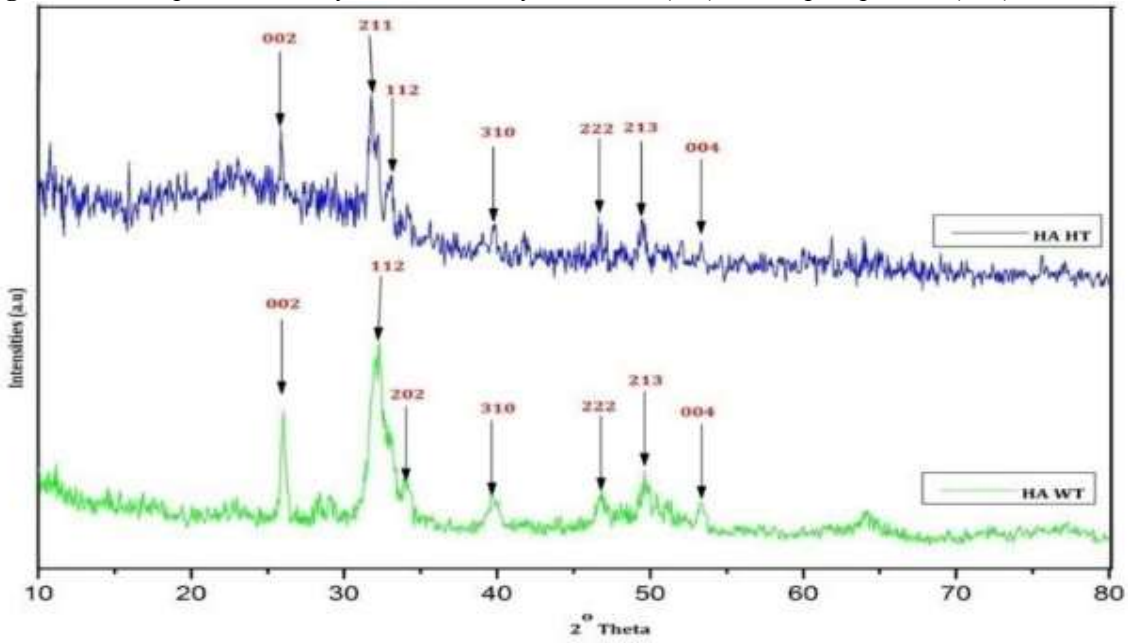


Fig. 4.27: XRD pattern of HA synthesized via Hydrothermal (HT) & Wet precipitation (WT)

Table 4.9: The Crystallite Size (D), Degree of Crystallinity (Xc) and the Lattice Parameters of Hydroxyapatite(HA) synthesized via Hydrothermal and Wet Precipitation Methods

Parameters / Methods	**Crystal Size parameters**		**Crystal Lattice parameters**			
	Crystallite size D (nm)	Degree of crystallinity (Xc)	HA (Theoretical)		HA (Experimental)	
			a(nm)	c(nm)	a(nm)	c(nm)
WET PRECIPITATION	5.0316	0.5374	0.942	0.688	0.942	0.686
HYDROTHERMAL	5.0812	1.8136	0.942	0.688	0.943	0.689

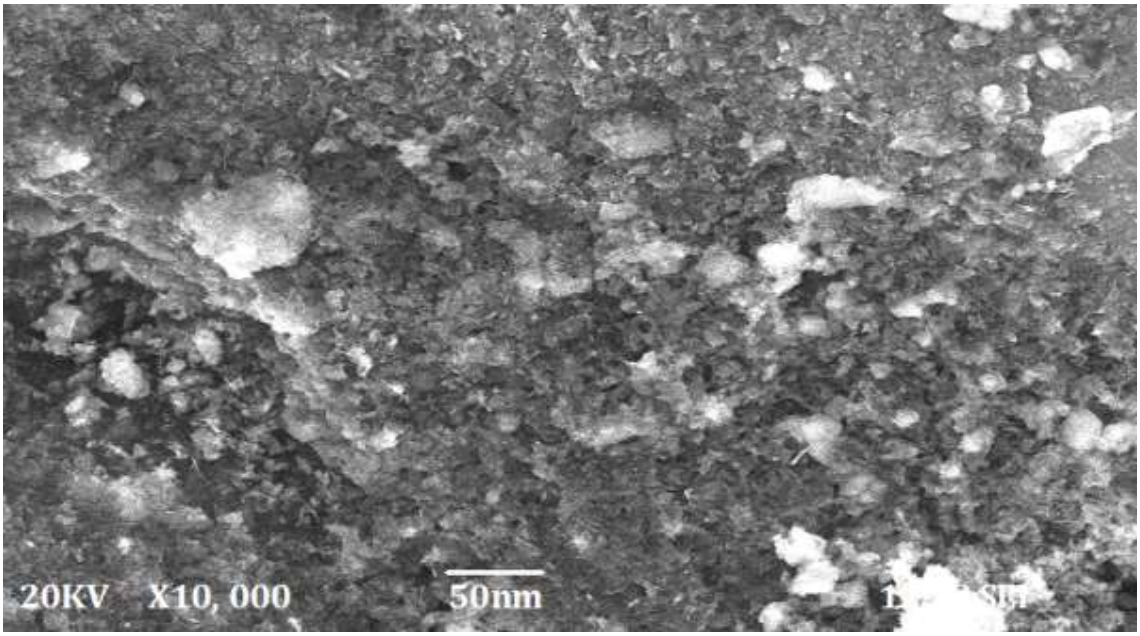


Fig. 4.31: SEM Image of HA synthesized via Hydrothermal (HT) Method

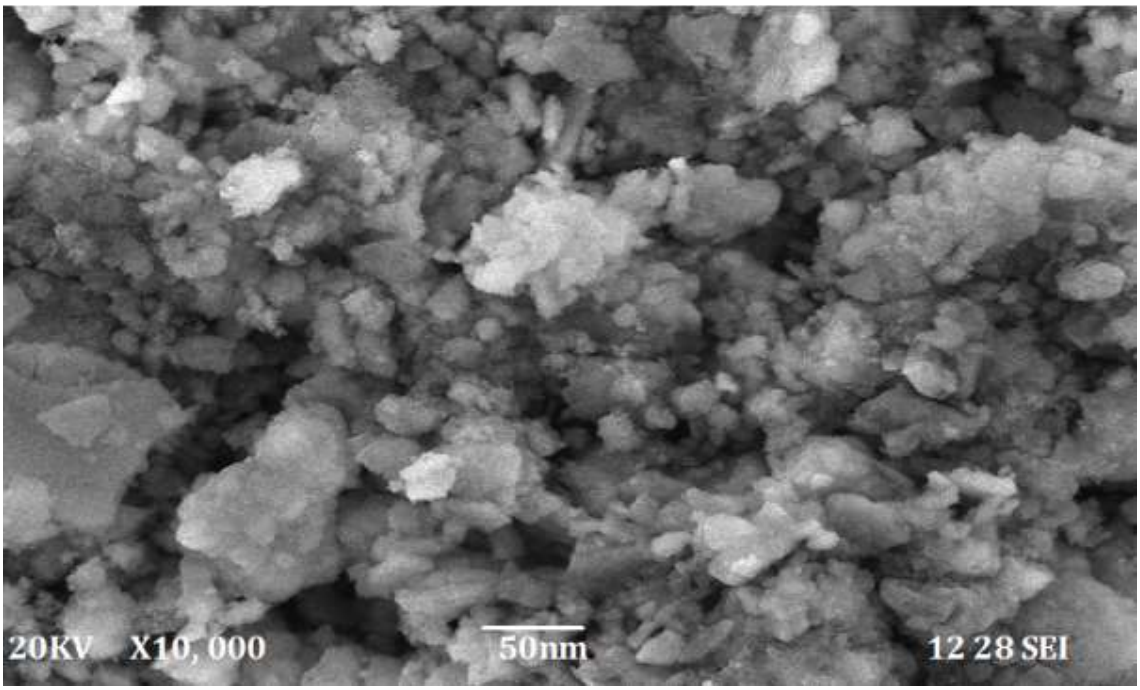
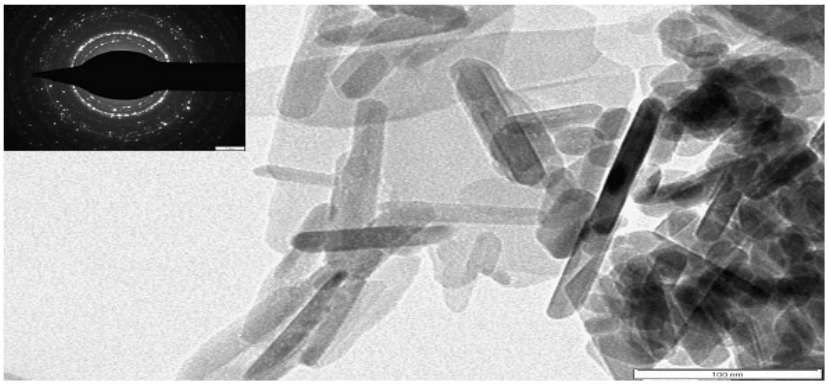


Fig. 4.32: SEM Image of HA synthesized via Wet precipitation (WT) Method



4.17: TEM image for hydrothermally synthesized Hydroxyapatite (HA)

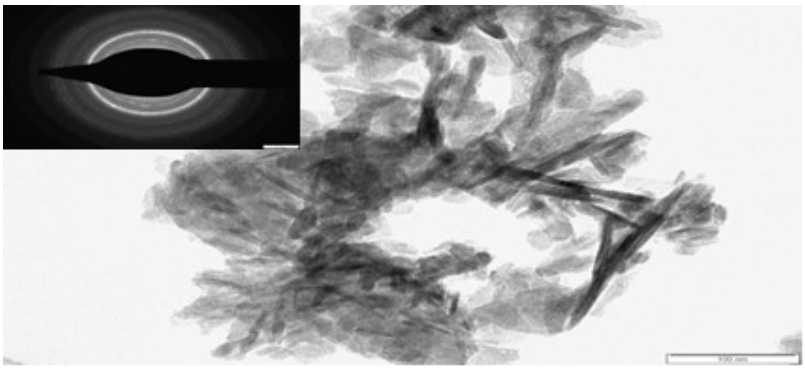


Figure 4.17: TEM image for wet precipitated Hydroxyapatite (HA)

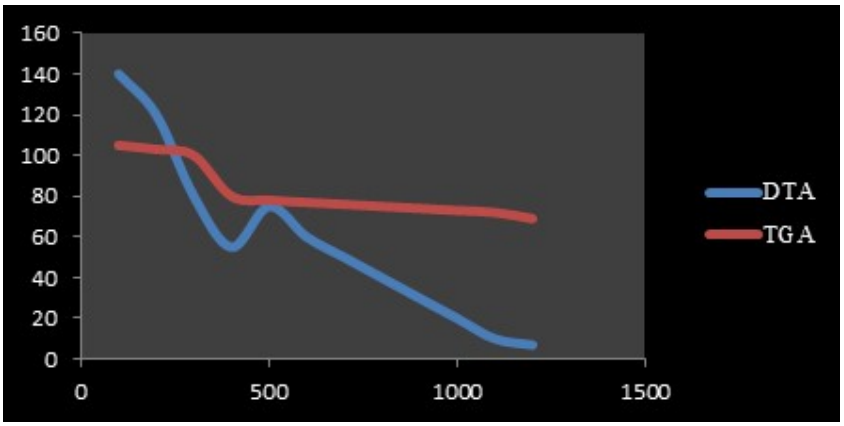


Fig. 4.48: TG/DTA curve of HA synthesized via Hydrothermal (HT) Method

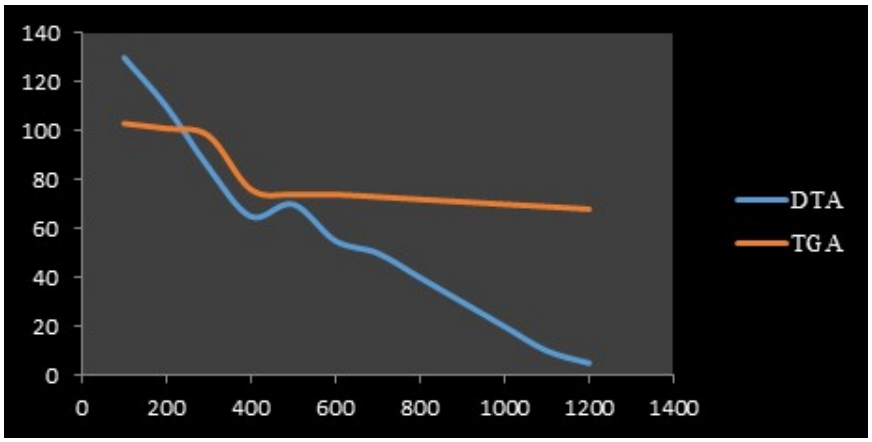


Fig. 4.49: TG/DTA curve of HA synthesized via Wet precipitation (WT) Method

From Figure 4.12, the average particle size distribution (PSD) of the hydroxyapatite nanoparticles for the hydrothermal and wet precipitation methods were 29nm ± 5% and 26nm ± 5% respectively, suggesting that greater percentage of these particle were within these sizes. Expectedly, the HA obtained by wet precipitation method had smaller particle size considering the particle size distribution, than the hydrothermal method, which by virtue of its higher temperature of aging should produce larger crystals, as hydrothermal treatment temperature can assist apatite crystal growth through provision of a highly active surface for the small apatite precipitate particles to bind to each other and grow into larger crystals compared to the wet precipitation where aging was done at ambient temperature (Zhang and Vecchio, 2007; Watanabe *et al*., 2009). Calcination of the HA powders resulted to a crystal with a decreased specific surface area (SSA) and pore volume (PV) with a increased pore size (PS), irrespective of the synthetic method (Table 4.5). This is attributable to the fact that Calcination increases the temperature of the crystal particle, which in turn leads to increase in particle size and the degree of agglomeration (Toledo-Antonio *et al*., 2003). Furthermore, there was a sharp decrease in SSA of the samples after calcinations. This sharp decrease in SSA of the samples after calcinations might be attributed to the presence of ammonia which might have enter the system during pH adjustment that was not completely washed during filtration\washing processes, and might also be due to the presence of chemically bonded water during the synthesis. HA crystals obtained by hydrothermal method had a smaller SSA and PV and an increased PS before and after calcination, compared to the HA obtained by wet precipitation method. The crystallite size (D) increases with calcination, as the hydrothermal method produced larger crystal sizes than the wet precipitation method, this difference observed could be attributed to the different aging temperatures. Comparing the average particle size (D_A) estimated by BET to the average crystallite size (D) estimated by XRD (Table 4.3), the average particle size calculated by BET was larger than the crystallite size calculated by XRD. This suggests that the particles contain several crystallites (Sergent *et al*., 2002).

Structural information on the apatite via XRD (Figure 4.13) shows that, the hydrothermally prepared hydroxyapatite has major diffraction peaks located at 2θ = 25.7º(002), 2θ = 39.8º (310), 32.9º (300), 2θ = 46.7º (222), 2θ = 49.5º (213), 2θ = 53.4º (004), while HA obtained from wet precipitation had its major diffraction peaks at 2θ = 25.9º (002), 2θ = 32.2º(112), 2θ = 34.0º (202), 2θ = 39.7º(310), 2θ = 46.8º(222), 2θ = 49.5º(212), 2θ = 53.1º (004) as seen in Table 4.6. These diffraction peaks when compared to standard peaks from the International Centre for Crystal Diffraction (ICCD), and literature values were found to be consistent and the predominant phase were confirmed as hydroxyapatite (HA) when matched with the Joint Committee for Powder Diffraction Standards (JCPDS), for calcium phosphates file number 00 – 009 – 0432. Furthermore, the crystallite size (D) and degree of crystallinity (Xc) were higher in the HA nanocrystals, obtained from the hydrothermal method than the wet precipitation method (Table 4.13). The lattice parameters (a and c) for the HA were 0.943 and 0.689 nm and 0.942 and 0.686 nm respectively for the hydrothermal and wet precipitation methods. The crystallites size (D) and the degree of crystallinity (X_c) of the HA estimated using the Debye scherrer equation were found to be 5.08 and 1.81 nm for the hydrothermally prepared HA and 5.03 and 0.54 nm for HA prepared by wet precipitation(Table 4.12). This observation was supported by result of particle size distribution (PSD), where the HA obtained from the wet precipitation method has smaller average particle size distribution of 26nm ± 5% to 29nm ± 5% for the hydrothermal method. Comparing these average crystallite sizes (D) estimated by XRD to the average particle sizes (D_A) estimated by BET (Table 4.3), the average particle size calculated by BET was larger than the crystallite size calculated by XRD. This suggests that the particles contain several crystallites (Sergent *et al*., 2002).

From the surface morphology of the HA, samples were examined using SEM analysis (Figure 4.14 and 4.15), the hydrothermally synthesized HA showed a non-uniformly distributed rod like crystals, with high agglomeration (Fig 4.14) while the hydroxyapatite prepared by wet precipitation exhibited less agglomerated uneven structure crystals (Fig 4.15), with numerous spherical and plate like crystals that were agglomerated together to form rod like shape. The morphology for the wet precipitation method has a non-uniformed size of particle with various size distributions whereas the morphology of the hydrothermal method showed an obvious change with increasing average particle size and more agglomeration among the particles due to the elevated aging temperature. On the other hand, all the particles exhibited a rod-like shape with varying degrees of agglomeration among fine particles, making the particles size

difficult to measure. The image of HA from the hydrothermal method (Fig 4.16) showed a closely agglomerated, non-uniform spherical nano particles, whereas the HA from the wet precipitation method (Fig 4.17) showed less agglomerated particles, with non-uniform shapes. The hydrothermally prepared hydroxyapatite powder showed particles with high degree of agglomeration caused by elevated aging temperature, which resulted to mutual interaction between particles arising from some forces like the Van-der-Waals forces, capillary forces and electrostatic forces (Pug and Bergstrom, 1994; Cukrov *et al*., 2001). This observation is consistent with those observed from the SEM micrographs and the result of Muthusamy *et al*., (2012). Furthermore, from the selected area electron diffraction (SAED) pattern, hydroxyapatite (HA) obtained by both the wet precipitation and the hydrothermal methods were characterized by diffraction rings, this suggests a fully crystallized nature of the apatite. However, in addition to the diffraction rings, the hydrothermally prepared hydroxyapatite has some discrete spots that indicate that it was fully crystallized with polycrystalline nature.

Thermal study of the apatite done via Thermogravimetric/Differential Thermal (TG/DTA) Analysis (Figure 4.18 and 4.19) shows that there was a weight loss of about 6% for temperature up to 380°C and 12% for temperature between 380°C to 400°C, for HA prepared by hydrothermal method and about 9% for temperature up to 220°C and approximately 24% for a range between 220°C to 380°C, for HA prepared by wet precipitation method. Similarly, about 9% weight loss was also observed for temperature up to about 800°C for HA prepared by hydrothermal method and about 6% weight loss was observed for temperature up to 800°C for HA prepared by wet precipitation method. In the first stage, an obvious weight loss was observed indicating that there was an evaporation of the absorbed water from the surface and pores (Furedi-Milhofer *et al.,* 1979, Larmas *et al*., 1993). Beyond 800°C to 1200°C, no significant weight loss was observed since an almost stable curve was noticed within this temperature range, suggesting thermal stability of the HA. Since there was no significant weight loss beyond 800 to 1200°C, it thus supports thermal stability beyond the temperature 1050°C as proposed for HA by dean-Mo *et al*., 2002.

The DTA curve shows an endothermic sharp peak and broad peak around 400°C for HA prepared by hydrothermal and wet precipitation methods respectively. This is because removal of water molecules from Calcium nitrate tetrahydrates ($Ca(NO_3)_2.4H_2O$)had occurred, corresponding to physical loss of absorbed water molecules and the removal of crystallized water. Similarly, the endothermic peak at around 600°C in the curve of HA prepared by wet precipitation method is related to the removal of groups like decarboxylation or addition of other groups during the preparation of HA powder. However, the sharp exothermic peaks observed at around 500°C and 450°C for HA prepared by hydrothermal and wet precipitation methods respectively, indicated the crystallization of HA, thus confirming its formation.

CONCLUSION

A pure HA nano-crystals were successful synthesized from the wet precipitation and hydrothermal methods respectively, with the resulting powder from the wet precipitation producing particle in smaller nano regime than the hydrothermal at the physiological conditions employed for these syntheses. As indicated by the results of characterization, XRF/EDX confirms the presence of calcium and phosphorus with Ca/P ratio estimated as 1.66 and 1.65, for hydrothermal and wet precipitation, which shows good similarity to those of natural bone apatite (Ca/P=1.67). FTIR confirms the characteristics bands of the hydroxyapatite (HA), XRD patterns indicated major predominant peaks as HA using JCPDS 2001 with file no: 09-0432, as well as confirming its degree of crystallinity (X_C) and crystallite size (D), all within the nano regime. Evidences from BET analysis, SEM, TEM all confirmed the morphological and structural properties as being in nano regime while TG/DTA confirms its thermal stability up to 1200ºC which is typical of hydroxyapatite (HA).

REFERENCES

Anita, L.J., Ravichandran, K. And Sundareswari, M (2015). The study on the synthetic methodologies for manoeuvring the morphology crystalinity and particle size of hydroxyapatite. *Journal of chemical and Pharmaceutical Research*, 7(2): 231-239.

Carrodeguas, R. G. and Aza, S. D. (2011). α-tricalcum phosphate: synthesis properties and biomedical applications.*Acta Biomaterialia*, 7, 3536-3546.

Cukrov, L. M., McCormick, P. G., Galatis, K. and Wlodarski, W. (2001). Gas sensing properties of nanosized tin oxide synthesized by mechano-chemical processing. *Sensors and actuators B. chemical*, 77(1) 491-495

Dean-Mo Liu, T. Troczynski, Wenjea J. Tseng. (2001). Water-based sol-gel synthesis ofhydroxyapatite: process development. *Biomaterials,* 22, 1721-1730.

Elliott, J. C. (1994). Structure and Chemistry of the Apatites and Other Calcium Orthophosphates, *Elsevier*, Amsterdam, p. 111.

Fatehi, K., Moztarzadeh, F., Soalti-Hashjin, M., Tahriri, M., Rezvannia, M. and Ravarian, R. (2008). *In vitro* biomimetic deposition of apatite on alkaline and heat treated Ti6A14V alloy surface. *Bulletin Material Science*, 31, 101-108.

Fathi, M., Hanifi, A. and Mortazavi, V. (2008). Preparation and bioactivity evaluation of bone – like hydroxyapatite nanopowder. *Journal of Materials Processing Technology*, 202, 536 – 542.

Feng, W., Mu-sen, L., Yu-peng, L. and Sheng-song, G. (2005). Synthesis and microstructure of hydroxyapatite powders in stimulated body fluid. *Journal of Materials Science*, 40, 2073 – 6.

Feng, W., Mu-sen, L., Yu-peng, L. and Sheng-song, G. (2005). Synthesis and microstructure of hydroxyapatite powders in stimulated body fluid. *Journal of Materials Science*, 40, 2073 – 6.

Furedi-milhofer, H., Hlady, V., Baker, F. S., Beebe, R. A., Wolejko-wikholm, N. and kittelberger, J. S. (1979). Temperature programmed dehydration of Hydroxyapatite. *Journal of colloid interface science*, 70: 1 – 9.

Kumta, P. N., Sfeir, C., Lee, D. H., Olton, D. and Choi, D. (2005). Nano Structured calcium – phosphate for biomedical applications: novel synthesis and characterization. *Acta Biomaterialia*, 1, 65–83,

Larmas, M. A., Hayrynen, H and Lajunen, L. H. J. (1993). Thermo gravimetric studies on sound and carious human enamel and dentin as well as hydroxyapatite. *Scandinavian journal of dental research*, 101 185 – 191

Murugan, R. and Ramakrishna, S. (2004). Bioresorbable composite bone paste using polysaccharide based Nano hydroxyapatite. *Biomaterials*, 25: 3829–3835.

Muthusamy, P., Kandiah, K., Palanisamy, M., Venkatachalam, R. and Palanisami, K. (2012). Synthesis, Characterization and Biological response of magnesium substituted Namobioactive glass particles for biomedical applications. *Ceramic International.* (39): 1683-1694.

Nejatic, E., Firouzdor, V., Eslaminejad, M.B. and Bagheri. (2009). Needle-like Nano hydroxyapatite/poly (L-Lactic acid) Composite Scaffold for Bone tissue engineering application. *Materials Science and Engineering* C, 29, 942-949.

Pugh R. J and Bergstrom, L (1994). Surface and colloid chemistry in advanced ceramic processing Marcel Dekker, New York. 273.

Rajabi-zamani, A. H., Behnamghader, A., kazemzadeh, A. (2008). Synthesis of nano crystalline carbonated hydroxyapatite power via nonalkoxide sol-gel method. *Materials science and engineering*, 28: 1326 – 1329.

Renu, S., Ravi, R. P., Anubha, A. G., Satabhisa, K and Marshal, D. (2012). In situ amino functionalization and microstructure formation of hydroxyapatite Nanoparticles synthesized at different pH by precipitation route. *Materials Chemistry and Physics*. 133 (2-3): 718-725

Saeri, M. R. (2003). The Wet Precipitation Process of Hydroxyapatite. *Materials Letters*, 57, 4064 – 4069.

Sergent, N., Gelin, P., Perier-Camby, H., Praliaud, H. and Thomas, G. (2002). Interaction of water, hydrogen and their mixtures with SnO_2 based materials: the role of hydroxyl group in detection mechanism. *Sensors and actuators B. chemical*, 84: 176.

Song, K. C. and Kang, Y. (2000). Preparation of high surface area tin oxide powders by a homogeneous preparation method. *Materials letters,* 42(5): 283-289

Toledo-Antonio. J. A., Baez, R. G., Sebastian, P. J. and Vazquez, A. (2003). Thermal stability and structural deformation of rutile SnO_2 nanoparticles. *Journal of solid state chemistry,* 174: 241

Watanabe, T., Kawachig, G., Kamitakahara, M., Kikuta, K and Ohtsuki, C (2009). Formation of needle-like hydroxyapatite by hydrothermal treatment of $CaHPO_4.2H_2O$ combined with β-$Ca_3(PO_4)_2$. *Journal of the Ceramic Society of Japan,* 117 (1366): 759-764

Young, R. A. and Holcomb, D. W. (1982). Variability of Hydroxyapatite Preparations, *Calcified Tissue International*, 34, 17–32.

Zhang, X. and Vecchio, K. S. (2007). Hydrothermal synthesis of hydroxyapatite rods. *Journal of Crystal Growth*, 308, 133 – 140.

PRELIMINARY INVESTIGATION OF THE EFFECT OF PRECURSOR CONCENTRATION AND CALCINATION TEMPERATURES ON HYDROXYAPATITE NANOCRYSTALS SYNTHESIZED AT PHYSIOLOGICAL CONDITION USING WET PRECIPITATION METHOD

V. OCHIGBO[1], V.O. AJIBOLA[2], E.B. AGBAJI[2], A. GIWA[3], J.T. BARMINAS[2], B.S. ZURU[1], P. MANNIVASAKAN[4], V. RAJENDRAN[4]

[1]*National Research Institute for Chemical Technology (NARICT), Zaria-Nigeria*
[2]*Department of Chemistry, Ahmadu Bello University Zaria-Nigeria*
[3]*Department of Textile Science and Technology, Ahmadu Bello University Zaria-Nigeria*
[4]*Centre for Nanoscience and Technology, K.S.Rangasamy College of Technology, Tiruchengode-637 215, Tamil Nadu India.*
Corresponding Email:*ochigbovic@gmail.com*

ABSTRACT
In this study, Hydroxyapatite (HA) was synthesized at physiological conditions of pH (7.4) and temperature (37ºC) using the wet precipitation method. Different concentrations of precursors, viz. 0.5, 1.0, 1.5 and 2.0 M were studied and calcination was done at 300, 500, 800 and 1100 ºC. The results indicated that nano-size HA particles were obtained at all the precursor concentrations. The synthesized hydroxyapatites were characterized by energy dispersive X-ray fluorescence (XRF/EDX), X-ray diffraction (XRD) and Fourier transforms infrared spectroscopic (FT-IR) studies. XRD studies revealed characteristic peaks of hydroxyapatite (HA) as confirmed by JCPDS 2001. XRD also revealed the crystalline nature of the powder and the crystallite size (D) and degree of crystallinity (Xc) estimated from pattern using the Derby Scherrer equation indicated that both quantities increases with increase in precursor concentrations and calcination temperatures. FT-IR revealed HA characteristic bands of OH^- and PO_4^{3-}. XRF/EDX revealed the elemental composition of the samples, where the Ca/P ratio was estimated as 1.65; similar to those of natural bone or theoretical value of 1.67 at the precursor concentration of 0.5M and calcination temperature of 300ºC.

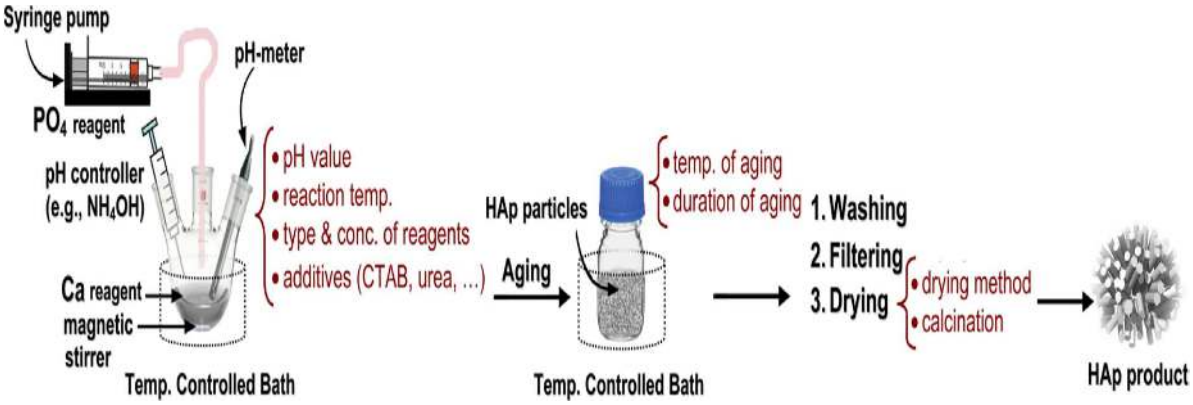
Keywords: Hydroxyapatite, Nanocrystals, physiological, wet precipitation, calcination.

INTRODUCTION
The rapidly growing development of nanotechnology is due to the unique properties of nanocrystalline materials in comparison with their large-grained analogs. Hydroxyapatite (HA)-$[Ca_{10}(PO_4)_6(OH)_2]$ is a calcium phosphate ceramic mineral present in the human body. It has for many decades been used as a key material in biomedical engineering as bone implants and prosthesis for dental and bone repair (Cuneyt *et al*., 1997). Biomaterials with nanostructures have unique physicochemical properties and many nano-rooms for the functionalization of biomolecules, and to act as carriers for therapeutics (Subbiah *et al*., 2010). Morphologically controlled hydroxyapatite nanostructures fulfil multifunctional roles, such as in the form of biosensors (Wang *et al*., 2010), photo catalysts (Vukomanovic *et al.,* 2012), carriers for drug delivery (Cheng *et al.,* 2006), appliances in tissue engineering and regenerative medicine (Ebaretonbofa and Evans, 2002), as well as membranes for the removal of heavy metals from polluted water (Takagi et al., 2004). These functional properties of HA strongly depend on their morphology, stoichiometric ratio, crystallinity and crystal size distribution. However, acquiring the desired morphology by controlling the synthesis parameters is difficult and thus it is a challenge to attain the desired morphology with required properties. Hence, researchers have focused on producing HA nanostructures with well distributed and high crystalline nanostructures. Many attempts have being made to improve the powder properties by controlling microstructural morphology. The specific characteristics, crystallization process and bioactivity of diverse nano HA crystals have led to different clinical application (Hench, 1991). If the crystal can be presented not only as rods and needles but also in spherical and flaky shapes, the nano size HA can be exploited in many other new fields (Wang *et al.,* 2006). Nano sized size HA can provide large interfaces, giving high bioactivity and great adsorption capability in the catalysis and separation fields. The important methods for the preparation of HA powders are solid state reaction, precipitation and hydrolysis of calcium phosphates (Thangamani *et al*., 2002). A processing method was designed to improve and control the powder properties such as crystallinity, particle size, particle size distribution and powder morphology. The processing method was divided into two parts:

calcination (to improve the crystallinity), and concentration (to reduce the particle size, narrow the distribution and alter the powder morphology) (kotHApalli *et al*., 2004).In the present work, nano-sized HA powder was synthesized via wet chemical precipitation at physiological conditions of pH and Temperature considering the reactant concentrations and calcination temperatures.

MATERIALS AND METHODS

$Ca(NO_3)2{\cdot}4H_2O$ (98% MERCK), NH_4H_2PO4 (99% MERCK), NH_4OH(25% MERCK)and ultrapure water (Arium 611UF; Sartorius AG) as the starting materials were used as received without any further purification. Firstly, an analytical weighing scale was used to accurately weigh $Ca(NO_3)2{\cdot}4H_2O$ and $NH_4H_2PO_4$ and were respectively dissolved in 500 ml of ultrapure water in a 1000 ml beaker, and the pH of each solution was brought up to 7.4 by adding few drops of ammonia solution and the beakers were covered to avoid possible contamination via contact with atmospheric conditions. The temperature of the reaction (37° C) was maintained by a thermostat-controlled water bath. The phosphate solution was added into each of the calcium solution in a drop-wise manner in a beaker to make slurry. The slurry was agitated at 2000 rpm using a digital display thermostat water bath cauldron for 1hr at 37 ºC. They were then centrifuged, washed with distilled water until the traces of ammonia were removed, filtered under mild suction and dried at 80 ºC for 24 hours and calcinated in air oven at 300, 500, 800 and 1100 ºC respectively for 3hrs to produce HA powder, and ground to powders using a mortar and pestle and then characterized via XRF/EDX, FT-IR and XRD.



Scheme 3.2: Preparation of HA nanoparticles via conventional chemical precipitation

RESULTS AND DISCUSSION

The FT–IR spectra of the HA powder (Figures 4.1 – 4.8) possesses bands for (OH^-) group in the region of 3400 – 3500cm^{-1} and 1640cm^{-1}(Liu, *et al*., 2003, Wang *et al*., 2006) for all precursor concentrations and calcination temperatures, except for calcination temperature of 1100ºC. The bands for (PO_4^{3-}) groups were observed in the region of 1000 – 1500cm^{-1}. The presence of these characteristics functional groups (OH^- and PO_4^{3-}) in the powder confirmed the formation of hydroxyapatite (HA). These bands became more distinct, narrower with the intensities increased, irrespective of the calcination temperature as the precursor concentration was changed from 0.5M to 2.0M. Decrease in the calcination temperature irrespective of the precursor concentration resulted to an increase in the band intensities, particularly for bands around the 3450 cm^{-1}, 1630 cm^{-1} region corresponding to the OH^- functional groups. This may be attributed to loss of absorbed water as the temperature of calcinations increases. While the bands around 570 cm^{-1}, 1140 cm^{-1}, and 870 cm^{-1}that corresponds to the PO_4^{3-} functional groups increased with increase in the calcination temperatures, bands around 1420 cm^{-1} corresponding to CO_3^{2-} functional group also decreased with calcinations temperatures from 300 °C to 800°C where it appeared lowest and disappeared at 1100°C calcination temperature, this suggests the decomposition of the carbonate group. However, the increase in band intensities with increase in calcination temperature is attributed to the loss of adsorbed water from the powder, faster particle agglomeration and resultant larger particle size, at high calcination temperatures. Furthermore, the bands in the region of 470-1400 cm^{-1} generally appeared clumsy with non-distinctive bands due to the presence of several phases, particularly for samples calcinated at 800°C and 1100°C for all the precursor concentrations.

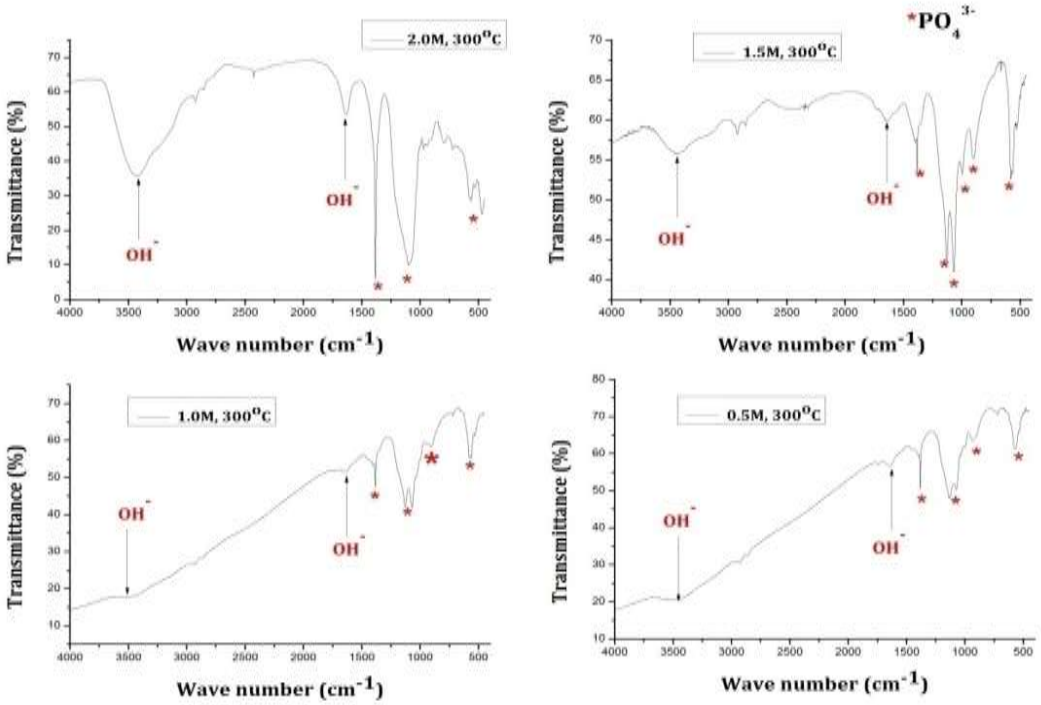


Fig. 4.3: FTIR spectra of HA synthesized via WT method using different initial precursor concentrations, calcinated at 300°C.

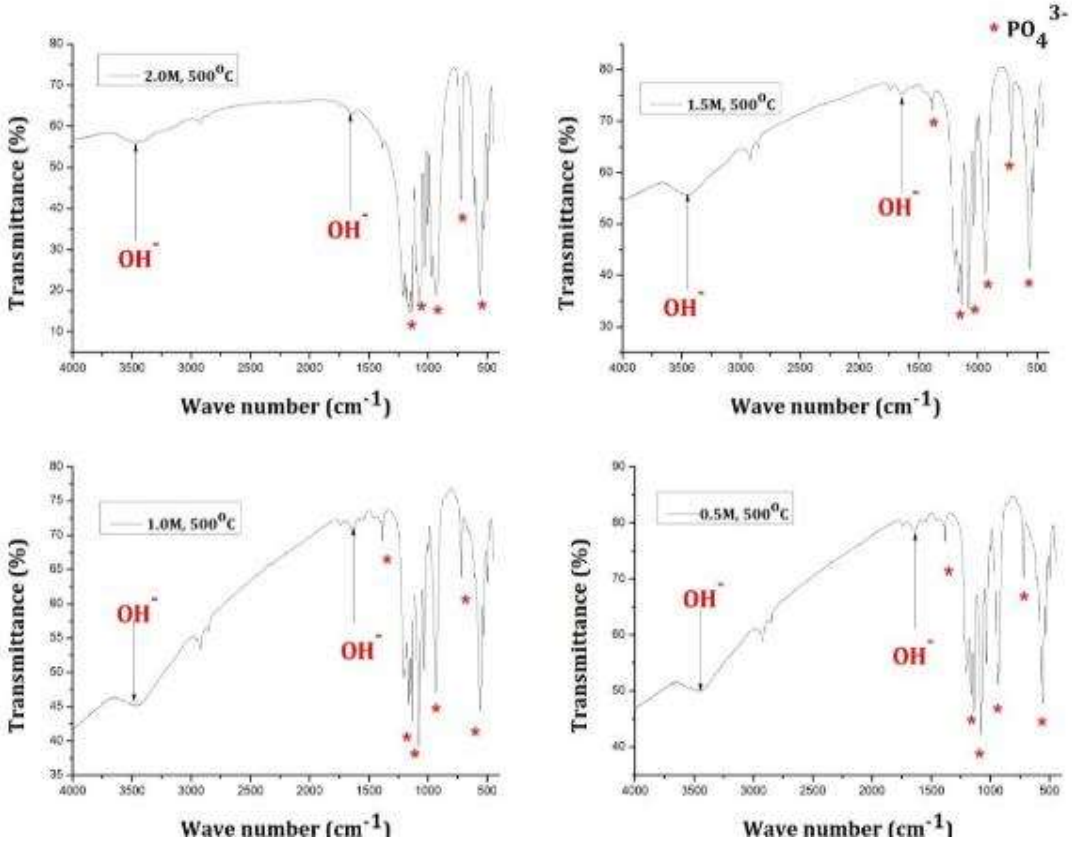


Fig. 4.4: FTIR spectra of HA synthesized via WT method using different initial precursor concentrations, calcinated at 500°C.

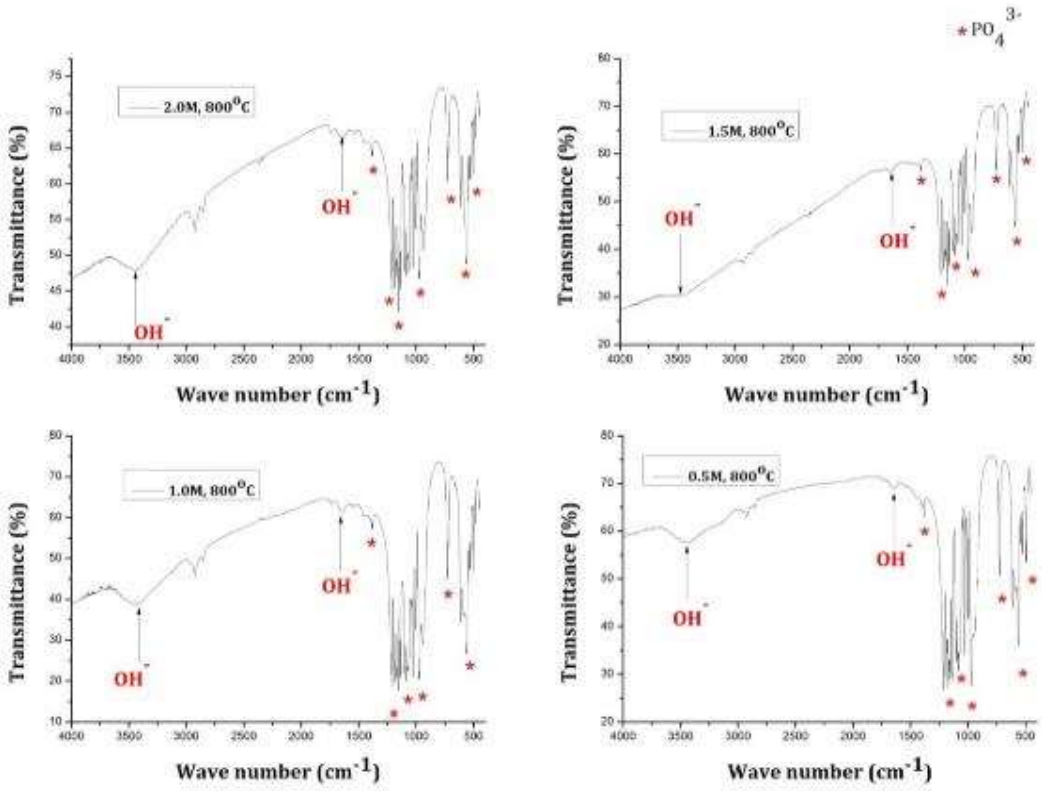


Fig. 4.5: FTIR spectra of HA synthesized via WT method using different initial precursor concentrations, calcinated at 800ºC.

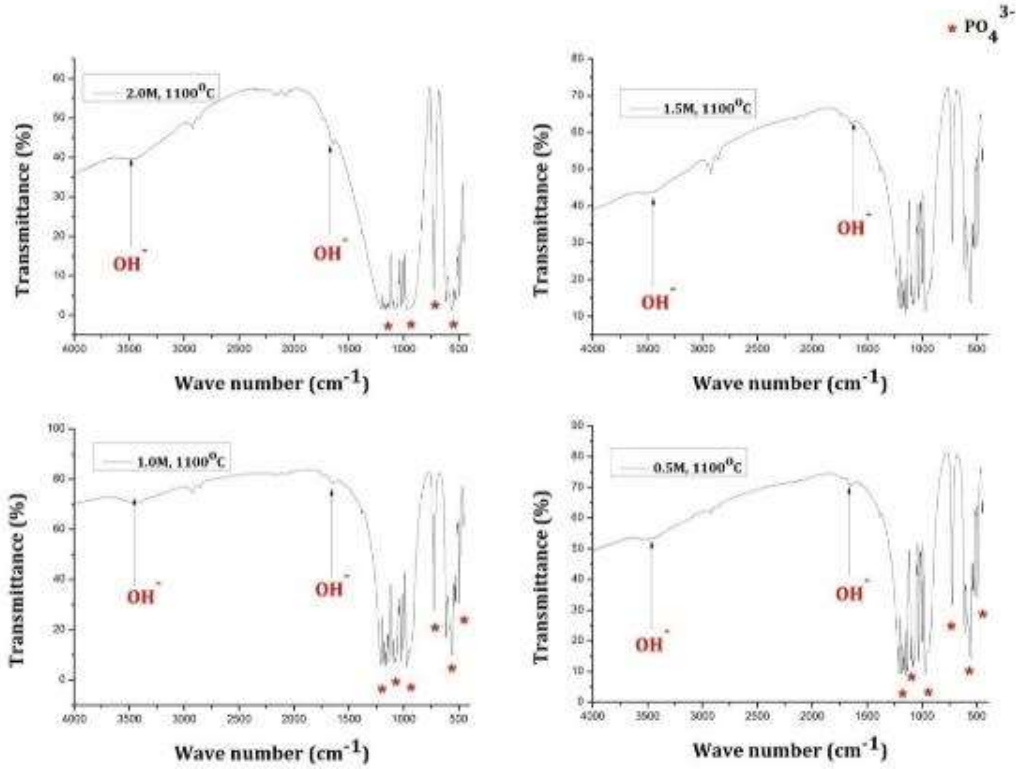


Fig.4.6: FTIR spectra of HA synthesized via WT method using different initial precursor concentrations, calcinated at 1100ºC.

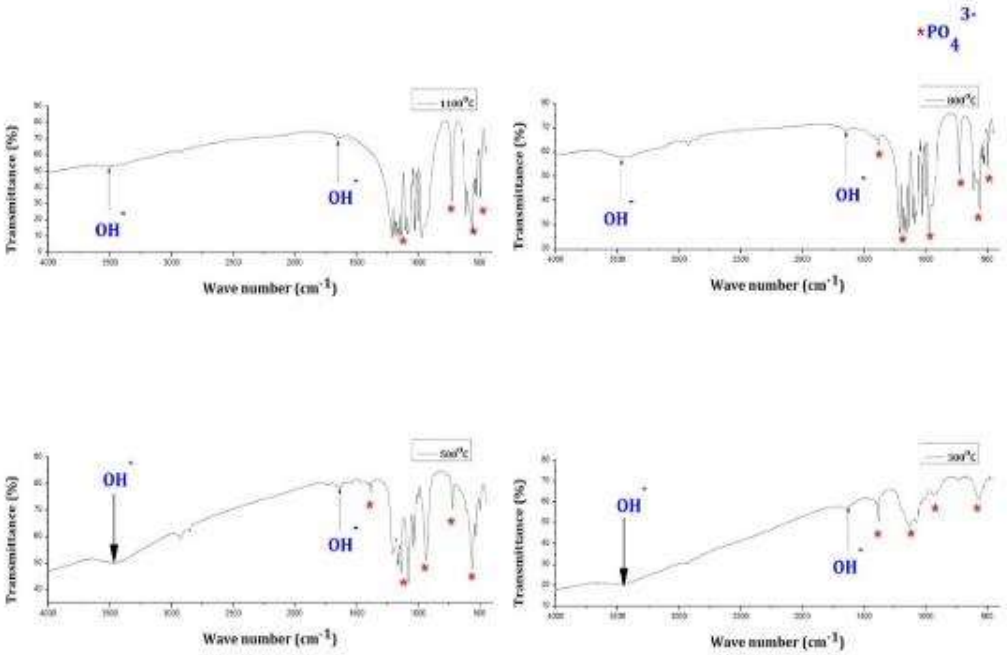


Fig. 4.7: FTIR spectra of HA synthesized using initial precursor concentration of 0.5M, calcinated at different temperatures.

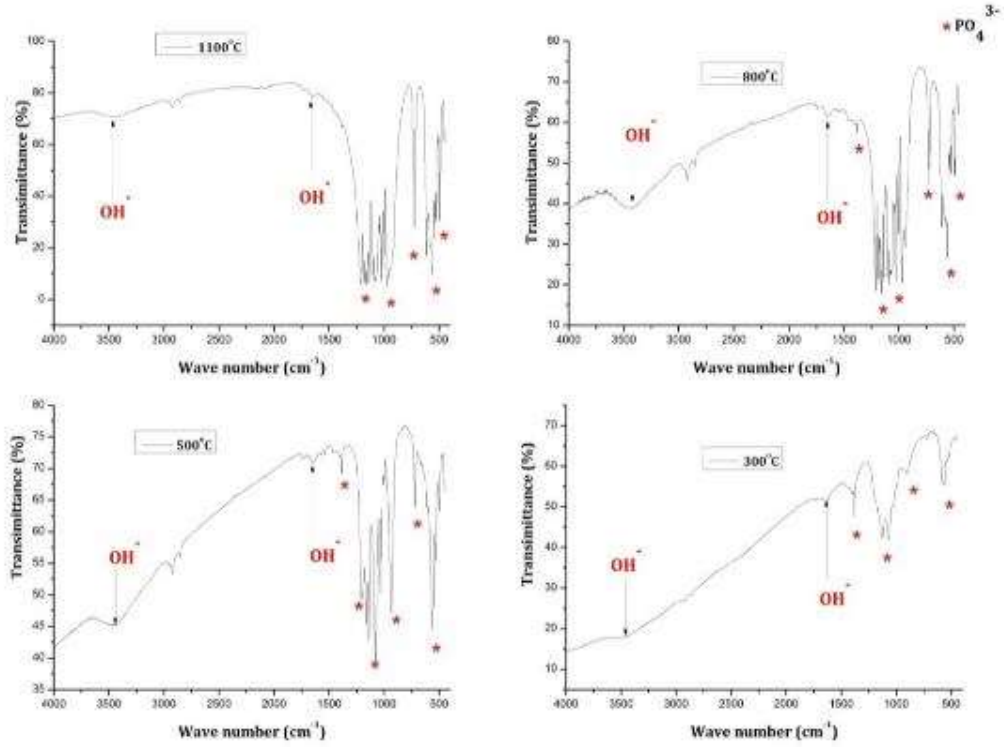


Fig. 4.8: FTIR spectra of HA synthesized using initial precursor concentration of 1.0M, calcinated at different temperatures.

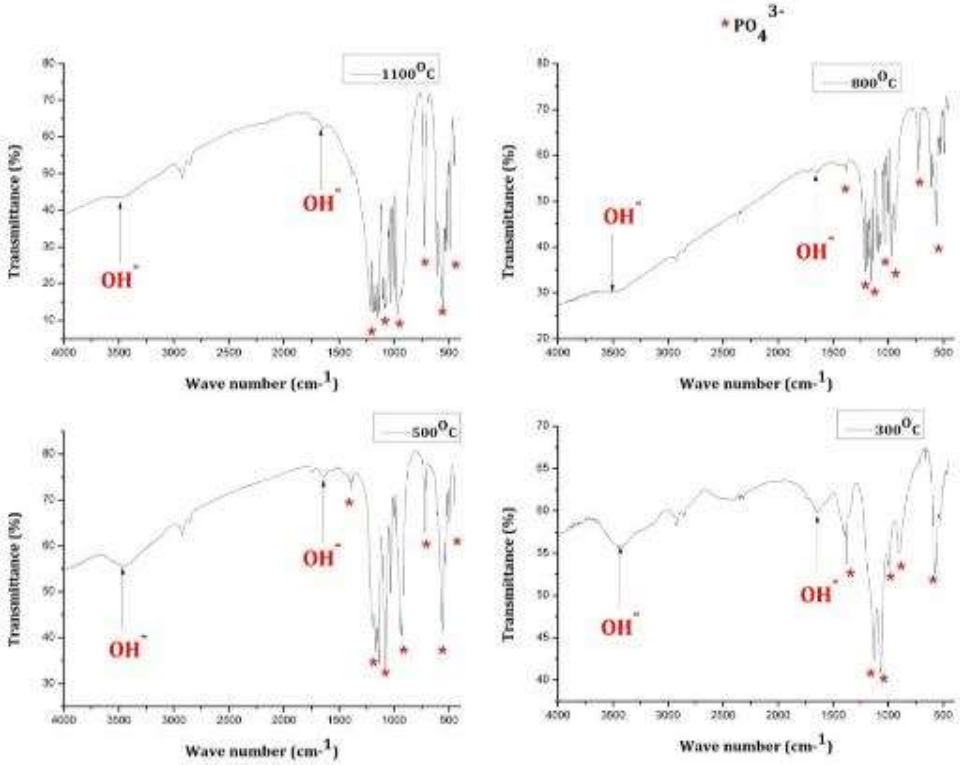


Fig. 4.9: FTIR spectra of HA synthesized using initial precursor concentration of 1.5M, calcinated at different temperatures.

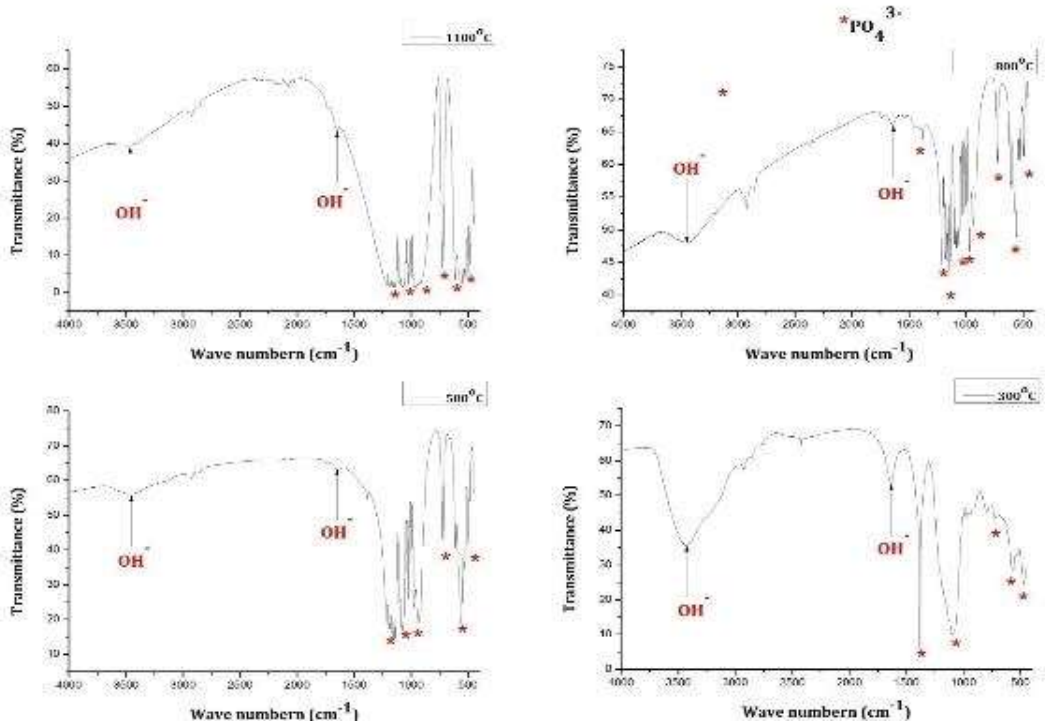


Fig. 4.10: FTIR spectra of HA synthesized using initial precursor concentration of 2.0M, calcinated at different temperatures.

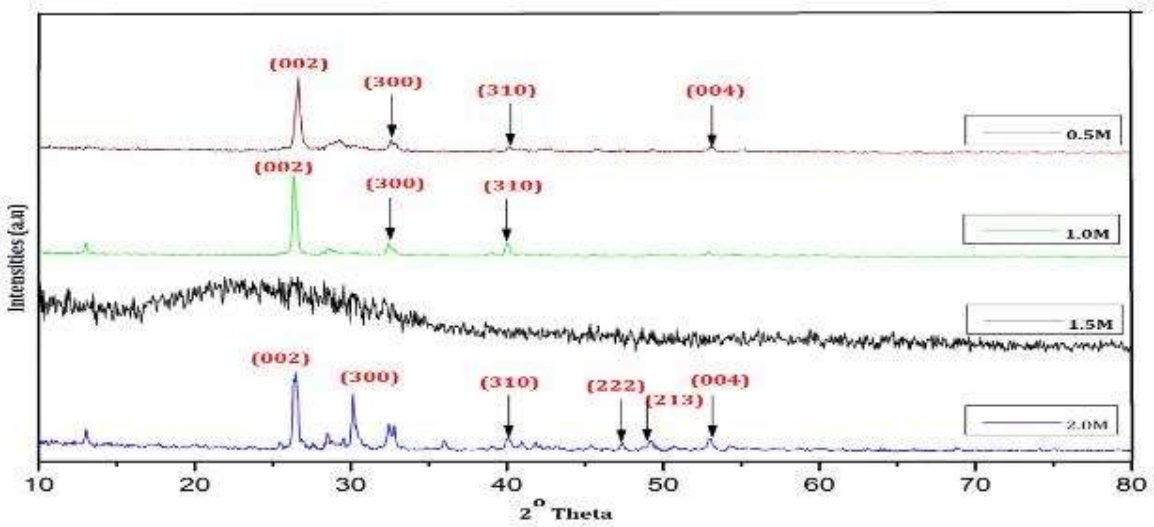


Fig. 4.11: XRD pattern of HA synthesized via WT method using different initial precursor Concentrations and calcinated at 300°C.

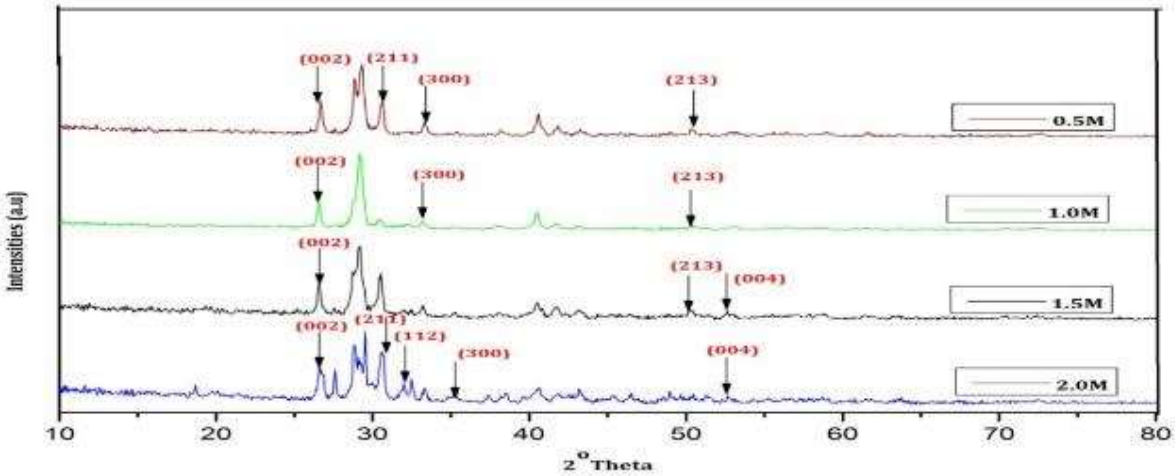


Fig. 4.12: XRD pattern of HA synthesized via WT method using different initial precursor concentrations and calcinated at 500°C.

Table 4.1: Major elemental composition and Ca/P ratio of hydroxyapatite (HA) synthesized via wet precipitation at various reactant concentrations and calcination temperatures respectively

Reactant concentration (M)	**300°C**			**500°C**		
	Ca%	P%	Ca/P	Ca%	P%	Ca/P
0.5	58.863	35.716	1.65	62.239	34.299	1.81
1.0	58.794	36.655	1.60	60.733	34.386	1.77
1.5	60.903	35.393	1.72	66.784	32.577	2.05
2.0	60.303	33.628	1.79	61.708	33.072	1.89

Table 4.2: The crystallite size (D) and degree of crystallinity (Xc) of hydroxyapatite (HA) synthesized via wet precipitation at various reactant concentrations and calcination temperatures respectively.

Reactant concentration (M)	**300°C**		**500°C**	
	Crystallite size D (nm)	Degree of crystallinity (Xc)	Crystallite size D (nm)	Degree of crystallinity (Xc)
0.5	3.7796	0.2268	7.5593	1.8136
1.0	6.0443	0.9286	7.5593	1.8136
1.5	-	-	7.4889	1.8136
2.0	15.1106	14.5089	10.0808	4.2989

The elemental compositions of the synthesized hydroxyapatite (HA) particles were ascertained using XRF/EDX (Table 4.2). The Ca/P ratio increased as calcination temperature increased. This could be attributed to the fact that at higher temperature of calcination, there was an increase in crystal size as a result of the agglomeration of smaller crystals and its constituent elements (Evis and Webster, 2011). Meanwhile, at a particular calcination temperature, increase in the precursor concentration shows an irregular increase in the Ca/P ratio, an indication of a weak effect of precursor concentration on Ca/P ratio (Raynaud *et al*., 2000). While comparing the experimental Ca/P ratio to the theoretical (Ca/P=1.67), the hydroxyapatite synthesized using precursor concentrations of 0.5 and 1.5M and calcinated at 300°C gave Ca/P ratio that are in conformity with the theoretical value, suggesting their similarity to the natural apatite than HA prepared at other precursor concentrations and calcination temperatures. This may be attributed to the fact that, at higher temperature of calcination irrespective of the precursor concentrations, hydroxyl group of the hydroxyapatite tend to be lost and thus forms other calcium phosphate minerals like alpha and beta tricalcium phosphate (α and β -TCP) with higher Ca/P ratios. Furthermore, the Ca/P ratio close to 1.67 as seen from 0.5M at 300°C suggests that no CaO content was present and the HA with Ca/P close to 1.75 and above suggests formation of small amounts of CaO (Sanosh *et al*., 2009).

The XRD pattern of the synthesized hydroxyapatite (HA) (Figure 4.9 – 4.10), indicated that the diffraction patterns gave sharp and clear reflections with varying intensities which confirms the phase purity and crystallinity associated with each samples. The major diffraction peaks located at 2θ = 25.9° (002), 2θ = 53.1° (004), and 2θ = 25.9° (002), 2θ = 53.1° (004) for HA from the hydrothermal and wet precipitation methods were found to match with the International Centre for Powder Diffraction Studies- Joint committee for Powder Diffraction Studies (JCPDS, 2001) files for calcium phosphate. The predominant HA phase were confirmed as they matched with JCPDS files numbers 00 – 009 – 0432. These data confirm the major phase as hydroxyapatite particles. The crystallite size (D) and degree of crystallinity (X_C) (Table 4.3) varies with precursor concentration and the calcination temperatures. The degree of crystallinity (X_c) increased with temperature of calcination, which was attributed to the increased crystallite sizes implying more crystal planes at high temperature due to particle agglomeration, while at a particular calcination temperature(300 or 500 ^oC), crystallite size (D) and degree of crystallinity (X_c) increased with increase in precursor concentration. These variations observed are in agreement with the work reported by Syed and Murtaza, (2013), Sanosh *et al.,*(2009) and Bouyer *et al.,*(2000). Furthermore, it was observed that HA calcined at higher temperature (500°C) exhibited high crystallinity. This high crystallinity could be attributed to the fact that high calcination temperature would lead to an increase in crystal size translating to more crystal planes, as nanocrystals tend to agglomerate forming large crystals, hence, the high crystallinity observed than calcination at lower temperature (Mobasherpour *et al.,* 2007). However, this high crystallinity has little or lacks bioresorptive potentials, which is the major property of HA as an implant material (Gergely *et al*., 2010).

In this optimization, the hydroxyapatite prepared using precursor concentration of 0.5M and calcination temperature of 300°C with (Ca/P = 1.65) gave better similarity to those of the natural bone apatite (Ca/P = 1.67), the desired crystallinity and smaller particle size. So, on the basis of Ca\P ratio being closely similar to those of natural bone (Ca\P ═ 1.67) (Fathi *et al.,* 2008), the smaller particle size with reduced crystallinity depicting bioresorptive potentials (Wang *et al*., 2010, Dorozhkin, 2010) and the absence of impurities like CaO, α–TCP and β–TCP as observed from the different characterization techniques (FTIR, XRF\EDX and XRD) using the wet chemical methods at physiological conditions for synthesis of HA indicated high purity of the method compared to the use of other synthetic methods like the dry methods and the high temperature processes (Sanosa *et al*., 2009), 0.5M precursor concentration and calcinations temperature of 300°C were adopted as the optimum conditions for synthesis of biomimetic HA at physiological conditions for the subsequent synthesis.

Conclusively, Hydroxyapatite (HA) was successfully synthesized at all the precursor concentrations of 0.5, 1.0, 1.5 and 2.0M, by wet precipitation at physiological conditions. As calcinations temperature increase, crystallinity increases and crystal size tends to micron from nano as a result of loss of hydroxyl group.

REFERENCES

Bouyer E, Gitzhofer F and Boulos M I 2000 J. Mater. Sci.Mater. Med. 11 523

Cheng W.P, Gray A.I, Tetley L, Hang T.L.B, Schätzlein A.G and Uchegbu I.F (2006).

Polyelectrolyte nanoparticles with high drug loading enhance the oral uptake of hydrophobic compounds. *Bio-macromolecules* 7: 1509-1520.

Cuneyt Tas A, Korkusuz F, Timucin M and Akkas N (1997). An investigation of the chemical synthesis and high-temperature sintering behaviour of calcium hydroxyapatite (HAp) and tricalciumphosphate (TCP) bioceramics. *J. Mater. Sci: Mater. Med*. 8: 91-96.

Ebaretonbofa E and Evans J.R.G (2002). High porosity hydroxyapatite foam scaffolds for bone substitute. J. Porous Mater. 9: 257-263.

Hench,L.L. (1991). Bioceramics: from concept to clinic, *J Am Ceram Soc*.;74:1487– 510.

KotHApalli, C. Wei,M. Vasiliev, A.M.Shaw, T. (2004). Influence of temperature and concentration on the sintering behavior and mechanical properties of hydroxyapatite, *Acta Materialia*, 52, 5655-5663.

Liu, J. B., Ye, X. Y. and Wang, H. (2003). The Influence of pH and temperatures on the morphology of hydroxyapatite synthesized by hydrothermal method. *Ceramics International*, 29: 629 – 633.

Mobasherpour, I., Heshajin, M. S, Kazemzadeh, A. and Zakeri, M. (2007). Synthesis of naocrystaline hydroxyapatite by using precipitation method. *Journal of Alloys Compounds,* 430-330

Sanosh, K. P., Chu, M. C., Balakrishnan, A., Kim, T. N. and Cho, S. J. (2009). Utilization of biowaste eggshells to synthesize nanocrystalline hydroxyapatite powders. *Materials letters*: 63: 2100-2102

Subbiah R, Veerapandian M and Yun K.S (2010). Nanoparticles:Functionalization and multifunc- tional applications in biomedical sciences. *Curr. Med. Chem*. 17: 4559-4577.

Takagi O, Kuramoto N, Ozawa M and Suzuki S (2004). Adsorption/desorption of acidic and basic proteins on needle-like hydroxyapatite filter prepared by slip casting. *Ceram. Int*. 30: 139-143.

Thangamani,N. Chinnakali,K. Gnanam, F. D. (2002). The effect of powder processing on densification, microstructure and mechanical properties of hydroxyapatite, *Ceramics International,* 28, 355-362.

Vukomanovic M, Zunic V, Otonicar M, Repnik U, Turk B, Skapin S and Suvorov D (2012). Hydroxya- patite/platinum bio-photocatalyst: a biomaterial approach to self-cleaning. *J. Mater. Chem.* 22: 10571-10580.

Wang S, Lei Y, Zhang Y, Tang J, Shen G and Yu R (2010). Hydroxyapatite nanoarray-based cyanide biosensor. *Anal. Biochem*. 398: 191-197.

Wang, L., Li, Y. and Na, Y. (2006). Single-crystal nanorods as multicolor luminescent materials. *Nano Letters*, 6: 1645–1649.

Wang, Y. J. Chen,J.D. Wei, K. Zhang, S.H. Wang,X.D. (2006). Surfactant-assisted synthesis of hydroxyapatite particles, *Materials Letters* 60, 3227–3231

INFLUENCE OF PROCESS VARIABLES ON ADSORPTION OF COLOUR FROM TEXTILE WASTE WATER USING ACTIVATED CARBONS FROM SOME AGRICULTURAL WASTES

R.O. OKPUWHARA, B.M. DAUDA AND K.O. FASHOLA
Department of Textile Science and Technology, Ahmadu Bello University, Zaria, Nigeria
oghenetega7@gmail.com

ABSTRACT
The adsorption of colour from textile wastewater using activated carbon derived from cassava peel, maize, and groundnut and rice husks has been investigated. Textile wastewater containing a mixture of Basic Yellow and Basic Green dyes collected from the effluent reservoir of a textile mill in Kaduna-Nigeria was used for the study. Batch adsorption experiments were carried out as a function of parameters such as pH, time, adsorbent dose, particle size and adsorbate concentration. Adsorption parameters for Langmuir and Freudlich isotherm models were examined for dye adsorption and for the validity of the models. Analyses of the equilibrium data, show that Langmuir model fits better for the removal of the Basic Yellow dye and Freundlich model fits better for the removal of the Basic Green dye contained in the effluent. According to linear regression criterion, the Freundlich isotherm model fits better than Langmuir model for dye adsorption, though both models have high fitness for this biosorption.

Keywords: *adsorption, agricultural wastes, carbon, isotherms.*

INTRODUTION

The effluents emanating from textile industries often contain high concentrations of colouring matter as a result of unused dyes (Easton, 1995). About 15% of the dye that is manufactured and used by the industry is discharged into the water. Of this, approximately 2-3% is discharged by the dye manufacturing industry and about 14-15% by the textile dyeing industry. That amounts to about 18000 tonnes of dye being discharged in wastewater, leading to considerable environmental pollution (Zollinger, 1987 and Aksu, 2005).

The presence of dyes in watercourses can also cause many water-borne diseases like nausea, haemorrhage, ulceration of skin and mucous membrane and so forth. Dark colour dyes block sunlight from entering the water, thus inhibiting photosynthesis and killing aquatic flora and fauna (Strickland and Perkins, 1995). Negative impact of dyes on human health and aquatic animals has led to regulatory actions in several countries.Apart from the toxicologicalproperties of dyes, their colour is one of the first signs of contamination recognized in a wastewater. Since a very small quantity of dyes in water is highly visible, it often affects theaesthetic merit and water transparency (Banat *et al*., 1996).

Adsorption techniques have gained favour recently due to their efficiency in the removal of pollutants which are too stable for conventional methods. Decolourization is influenced by many physico-chemical factors such as, dye/sorbent interaction, sorbent surface area, particle size, temperature, pH, and contact time. Performance is dependent on the type of carbon used and the characteristics of the wastewater (Thakur, 2006). Adsorption is in general seen as more acceptable than chemical oxidation processes using chlorine or ozone which tends to leave oxidation by-products in solution which in turn may themselves have possible health risks (Tebutt, 1998).

MATERIALS AND METHODS

MATERIALS

Chemicals and Reagents

All chemicals and reagents used are of analytical grade and include the following:
Phosphoric acid (H_3PO_4), Zinc chloride ($ZnCl_2$), Sulphuric acid (H_2SO_4), Sodium hydroxide(NaOH), Sodium hydrogen carbonate ($NaHCO_3$),), Commercial Activated Carbon (CAC).

Glass Wares/Apparatus

Beakers, measuring cylinders, funnels, pipettes, , burettes, wash bottles, shaking vessels stoppers ,volumetric flasks pyrex dishes, filter paper (whatman 110mmø)desiccator crucibles air tight plastic container.

Equipment

The equipment used in this research work includes the following:
Water still (Aquatron; Model: A4000), Grinding mill (Thomas Wiley; Model 4), Digital weighing balance (Sartorius; Model: ED2245, Ohaus - Adventurer TM; AR2130) , Muffle furnace (SearchTech; Model: SXL – 1030), Oven (Gallenkamp, Model: IC 0990), Laboratory

blender (Christon; Model: 38BL40), Electronic test sieve shaker (Endecott; Model: E.F.L.1; MK II 7416), Digital pH meter (Labtech), Test tube shaker (IKA® KS -WERKE; Model: 130 Basic D -79219), Scanning spectrophotometer, SpectroUV – VIS dual beam (split beam) (Labo Med; Model: UVS – 2700/UVS 2800).

Adsorbents /Adsorbates

The materials used for the production of adsorbents include the following agricultural wastes: Maize husk (MHAC), groundnut husk (GHAC), rice husk (RHAC) and cassava peel (CHAC). Materials removed as adsorbates are: Dye effluent from textile mill (mixture of basic green dye (BGD)and basic lemon yellow dye(BYD)).

Collection and Preparation of Biomass Waste Samples

The agricultural waste samples were collected locally from Zaria environs. The collected samples were washed with water to remove dirt, other particulate matter and air dried. The dried samples were crushed using grinding mill fitted with sieves of 0.5mm mesh (Rice Husk), 1mm mesh (cassava peel), 2mm mesh (Maize and Groundnut husks). Samples were then labelled and stored in tight plastic containers.

Collection and Preparation of Adsorbate

The Adsorbate (industrial dye wastewater) was collected from the untreated effluent reservoir at Chellco Textiles Nigeria Limited, Kaduna, Nigeria. The dyeing waste effluent was collected by dipping a 2-litres bottle under the wastewater until it was full.

The dye-containing wastewater was used without further purification and diluted to the required concentration. A 1000ppm (1000mg/l) concentration was first prepared and from which series of working concentrations of 2ppm, 4ppm, 5ppm, 6ppm, 8ppm and 10ppm were prepared as described by Kardirvelu *et al*. (2003). The maximum wavelength (λ_{max}) of the effluent was determined with a UV spectrophotometer. Graphs were plotted using different concentrations and concentration factor (slope from graph, that is, concentration divided by absorbance, to get concentration factor) was calculated. The absorbance readings were taken at the Beer Lambert λ_{max} and multiplied by concentration factor to give the amount of dye in a particular effluent sample (Mudoga *et al*., 2002).

METHODS

The methods for production of activated carbon using chemical activation of the agricultural wastes and adsorption experiment have been discussed in the paper titled Colour Removal from Textile Waste Water Using Activated Carbons From Some Agricultural Wastses (Okpuwhara *et al*, 2013).

ADSORPTION ISOTHERM

The equilibrium data on the adsorption experiments of the adsorbate and adsorbent interaction were fitted to isotherm models, namely, the Langmuir and the Freundlich to determine the adsorption characteristics. The adsorptive capacity of the Langmuir and Freundlich isotherm is given by the Equation 1.

$$qe = V\left[\frac{C_o - C_e}{m}\right] \ldots\ldots\ldots (1)$$

Where:

V = Volume of adsorbate used (mg/dm^3)

qe =Amount adsorbed per unit mass of adsorbent (mg/g)

C_o = Initial concentration

C_e= Equilibrium concentration

m = Weight of adsorbent used (g)

A linear plot of 1/qe against 1/Cewas employed to provide values of Q^o and b from the intercept and slope of the Langmuir isotherm plots as displayed in Figures 1 to100. For the Freundlich isotherm, a linear plot of log q_e against log $C_e$was employed to determine values of the empirical constants K_f and n by the intercept and slope of the linear regression, which are also displayed in Figures 1 to 100. The isotherms for the adsorbent samples for the effluent adsorbate were all plotted as displayed in Figures 1 to 100. The isotherm constant values and correlation regression or coefficients were then extrapolated from the isotherms. The summary of the effluent adsorption isotherm data and correlation analysis for the experimental parameters are shown in Tables 1 and 2. The adsorption isotherm data were calculated as explained below.

3.6.1 Langmuir Adsorption Isotherm

The mathematical expression of the Langmuir isotherm model equation is presented in Equation 2. This equation was compared with the isotherm equations and the constants were then extrapolated.

$$\frac{1}{q_e} = \left(\frac{1}{Q^o b}\right)\left(\frac{1}{C_e}\right) + \frac{1}{Q^o} \ldots\ldots\ldots (2)$$

where:

Q^o = Langmuir constant which is a measure of the monolayer adsorption capacity (mg/g)

b = Langmuir constant which is a measure of the surfaceenergy (mg/dm^3).
The intercept Q^o from the isotherms was first calculated by the expression $1/Q^o$ and the answers were then used to calculate the slope $1/Q^o b$ (Nkeonye, 1989).

3.6.2 Freundlich Adsorption Isotherm

For linearization of the data, the mathematical expression of the Freundlich isotherm model was written in logarithmic form. This is represented by Equation 3.

$$\text{Log } q_e = \text{Log } K_f + \frac{1}{n}\text{Log}C_e \ldots\ldots\ldots (3)$$

where
K_f = Freundlich constant which is the measure of adsorption or binding capacity(mg/g)
$\frac{1}{n}$ = Freundlich constant which is the intensity of adsorption, which characterizes the affinity between the sorbent and sorbate.

The intercept Log K_f and the slope n (calculated by the expression 1/n)were both extrapolated from the Freundlich isotherms.

RESULTS AND DISCUSSION

The results of the Langmuir and Freundlich isotherm constant data are displayed in Tables 1 and 2, the isotherms of the effluent are given in Figures 1 to 100.

4.1 ADSORPTION ISOTHERM STUDIES

Analysis of the isotherm data is important in order to develop an equation that accurately represents the results and which could be used for design purposes (Mahvi *et al*., 2004). The Langmuir and Freundlich parameters along with the correlation coefficients were computed from the intercept and the slope of the fitted Langmuir and Freundlich equation as stated in Equations 2 and 3 (Chingombe *et al*., 2006). The results of correlation analysis along with the isotherm parameters are given Tables 1and 2 for the effluent.Considering the many factors that research have indicated play significant role in adsorption process, mixtures of dyes can present particular problems for efficient separation and adsorption processes (Allen and Koumanova, 2005).

Three different adsorption isotherm surface plots have been carried out using the Langmuir and Freundlich models which are two-parameter models to test their applicability (Figures 1 to 100). They were used to analyze the adsorption equilibrium to describe the relationship between the amount of dye adsorbed (qe) and its equilibrium concentration (Ce) for all the ACs based on the work of Kratochvil and Volesky (1998) who suggested that the qe uptake calculated, should be used as three different adsorption isotherm surface plots which is given as:

1. For the uptake of BYD: yielding the effect of BGD on BYD.
2. For the uptake ofBGD: yielding the effect of BYD on BGD.
3. For the total uptake in the effluent that is, BYD + BGD uptake.

Regression Coefficient (R^2) Value

The goodness of the fit is discussed using the regression or correlation coefficient (R^2) values which are a measure of goodness-of-fit as displayed in Tables 1 and 2, which show that both the Langmuir and Freundlich isotherm models can adequately describe the adsorption data with high correlation coefficient (R^2 in some instance equals 1).

Table 1: Adsorption Equilibrium Isotherm Constants and Regression Coefficient for Effluent.

Type of Adsorbent	Parameter	Effluent Yellow Dye						Effluent Green Dye					
		Langmuir			Freundlich			Langmuir			Freundlich		
		Q^o	b	R^2	K_f	n	R^2	Q^o	b	R^2	K_f	n	R^2
CAC													
	pH	1.74	7.37	1.00	2.01	-5.06	1.00	2.31	-131.21	1.00	2.25	24.69	1.00
	Time	2.43	-2060.00	0.44	2.35	-64.94	0.84	2.47	-13500.00	0.49	2.42	-151.52	0.87
	Dosage	4.78	3.64	0.61	4.25	1.93	0.78	3.34	17.72	0.62	5.79	2.18	0.83
	Particle Size	0.99	-12616.25	0.80	1.02	-212.77	0.95	0.99	-5066.00	0.98	1.03	-156.25	0.99
	Concentration	0.99	-12647.50	0.56	1.03	-169.49	0.86	0.84	174.21	0.31	1.91	3.54	0.32
MHAC													
	pH	1.88	-11.39	1.00	2.04	-6.54	1.00	2.33	-165.15	1.00	2.27	-27.70	1.00
	Time	2.48	-10095.00	0.82	2.44	-208.33	0.95	2.33	-2149.50	0.47	2.33	-2149.50	0.94
	Dosage	0.55	-20.43	0.55	0.03	-0.63	0.37	0.33	-12.63	0.51	0.01	-0.25	0.31
	Particle Size	2.46	-4060.00	0.86	2.42	-131.58	0.97	2.45	1.00	0.75	2.39	-100.00	0.93
	Concentration	0.92	-375.48	0.01	0.50	9.09	0.01	4.91	33.95	0.44	0.02	1.26	0.55

Table 2: Adsorption Equilibrium Isotherm Constants and Regression Coefficient for Effluent

Type of Adsorbent	Parameter	Effluent Yellow Dye						Effluent Green Dye					
		Langmuir			Freundlich			Langmuir			Freundlich		
		Q^0	b	R^2	K_f	n	R^2	Q^0	b	R^2	K_f	n	R^2
GHAC													
	pH	1.85	-10.30	0.99	2.02	-6.15	1.00	2.33	-215.00	0.99	2.26	-27.03	1.00
	Time	2.42	-1032.50	0.80	2.36	-61.73	0.95	2.48	-40270.00	0.77	2.45	-312.50	0.93
	Dosage	1.71	33.38	0.06	3.37	2.45	0.30	1.76	126.27	0.11	5.98	2.38	0.37
	Particle Size	1.63	-2040.33	0.98	1.60	-100.00	1.00	1.66	-20136.67	0.83	1.64	-294.12	0.96
	Concentration	1.59	76.55	0.39	8.91	1.79	0.70	-62.50	-1.54	0.67	16.52	1.59	0.68
RHAC													
	pH	1.86	-11.52	1.00	2.03	-6.54	1.00	2.31	-127.53	0.99	2.24	-24.27	1.00
	Time	2.40	-1041.50	0.50	2.30	-44.25	0.89	2.46	-10167.50	0.30	2.39	-105.26	0.79
	Dosage	1.90	14.51	0.05	4.11	1.68	0.37	0.01	1.53	653.04	7.83	2.02	0.31
	Particle Size	1.62	-1031.83	0.83	1.57	-61.73	0.96	1.66	-20136.67	0.93	1.64	-294.12	0.98
	Concentration	3.66	15.61	0.62	7.89	1.74	0.72	10.70	9.44	0.78	28.51	1.33	0.82
CPAC													
	pH	0.84	-1.56	0.91	2.10	-1.56	0.98	1.36	-5.05	0.93	1.84	-3.38	0.98
	Time	0.91	-4.58	0.68	1.55	-2.41	0.90	0.70	-3.75	0.34	1.47	-1.68	0.75
	Dosage	17.86	0.25	0.94	2.94	1.41	0.92	2.69	4.39	1.00	2.03	2.97	0.91
	Particle Size	0.75	-84.72	0.95	1.37	-18.48	0.99	0.76	-137.85	0.91	1.34	-23.26	0.98
	Concentration	0.91	-4.58	0.68	1.55	-2.41	0.90	0.70	-3.75	0.34	1.47	1.68	0.75

The Langmuir plots of the effluent are shown in Figures 1 to 100 and the values of the constants are shown in Tables 1 and 2. Results in this analysis gave a comparatively good linearity with reasonably high linear correlation coefficients. For the effluent in Table 1, R^2 values for BYD was averagely 0.679– 0.998 and for BGD, it was averagely 0.667 – 0.997 suggesting that the adsorption process obeys the Langmuir model. Therefore, the adsorption of BYD and BGD on the ACs can be said to be monolayer-type and this agrees with the observation that the adsorption from an aqueous solution usually forms a layer on the adsorbent surface.

The Freundlich plots of the effluent are shown in Figures 1 to 100 and the values of the constants are shown in Tables 1 and 2. The graphs are linear and the linear correlation coefficient values are high suggesting that this model is suitable for the description of the adsorption process. The R^2 value for BYD in effluent was averagely 0.780 – 0.999 and for BGD was 0.830 – 1.000. The Green dyes had higher R^2 except for CPAC, which had better results with yellow dye removal and also the highest R^2 with the Langmuir isotherm model.

The observed linear relationships are significant as evident from the correlation coefficients (R^2values) close to unity, which indicate the applicability of these two adsorption isotherms and the monolayer and heterogenous coverage of BYD and BGD on the carbon surface. In general, according to R^2 criterion, Freundlich model fits better for dye adsorption for the present adsorption study. The values of Langmuir constants indicate favourable conditions for adsorption but low values of correlation coefficients show that Langmuir model is less fitted to present adsorption compared to Freundlich model. Therefore the individual dye had the same dye uptake from the effluent, that is, the yielding effect was not so significant.

Langmuir Constants (Q^o and b values)

The Langmuir isotherm model is a monolayer adsorption on active sites of the adsorbent and is presented in Equation 2. The use of this isotherm implies the existence of a monolayer of adsorbate at the outer surface of the adsorbent.

Q^0 is the amount of adsorbate adsorbed per unit mass of adsorbent corresponding to complete monolayer coverage, the monolayer adsorption capacity or the maximum adsorbable value of qe. Q^ovalue (Tables 1 and 2) indicates that the ACs is better adsorbent for BYD compared to BGD. This could be linked to the formation of mesopores created by the chemical modification of the biosorbent. The magnitude of Q^0 indicates that the amount of BYD per unit weight of adsorbent to form a complete monolayer on the surface appears to be significantly higher in comparison to BGD.

b is Langmuir adsorption constant and increases with an increase in the binding energy of adsorption and with a decrease in temperature. Also, b is a constant independent of qe. The b value for dyes and effluent was relatively very low as shown in Tables 1 and 2. A low value of b indicates that the adsorbents have high affinity for the adsorbate (Qaiser *et al*., 2007).

LANGMUIR AND FREUNDLICH ISOTHERMS FOR EFFLUENT

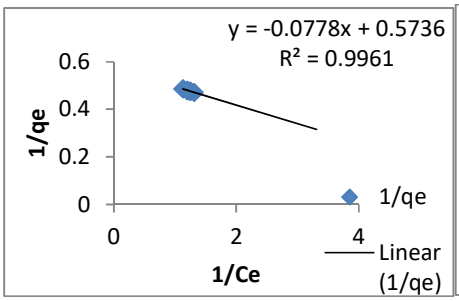


Fig.1 Langmuir pH for EBYD by CAC

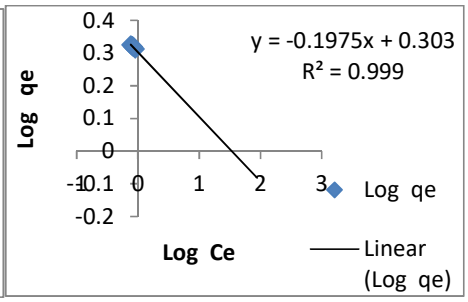


Fig.2 Freundlich pH for EBYD by CAC

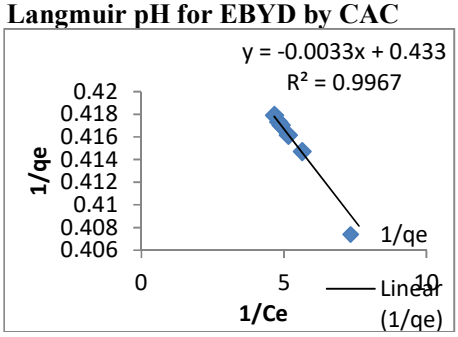


Fig.3 Langmuir pH for EBGD by CAC

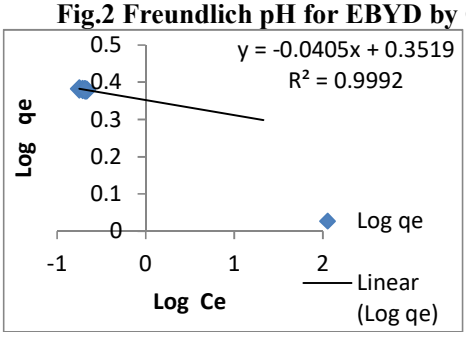


Fig.4 Freundlich pH for EBGD by CAC

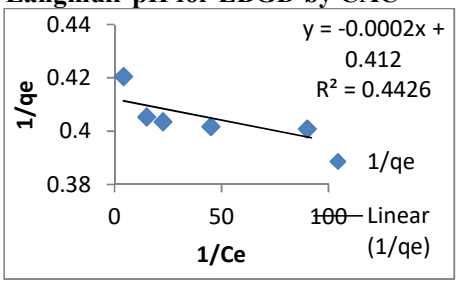


Fig.5 Langmuir Time for EBYD by CAC

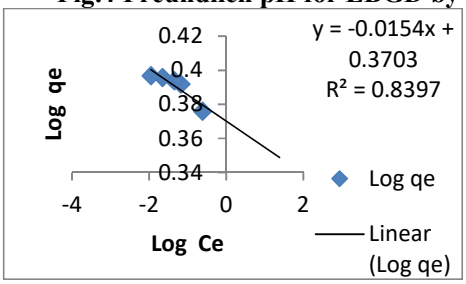


Fig.6 FreundlichTime for EBYD by CAC

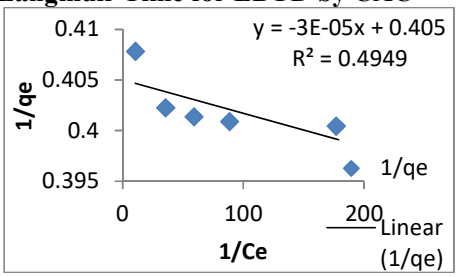


Fig.7 Langmuir Time for EBGD by CAC

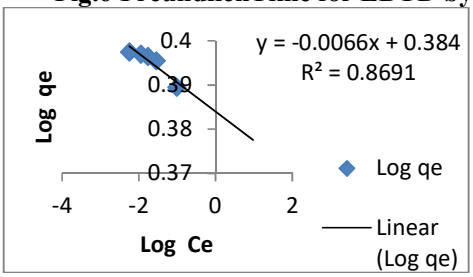


Fig.8 FreundlichTime for EBGD by CAC

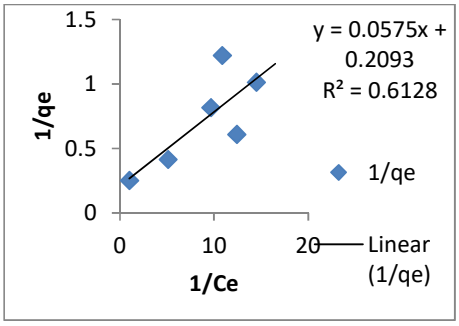


Fig.9 Langmuir Dosage for EBYD by CAC

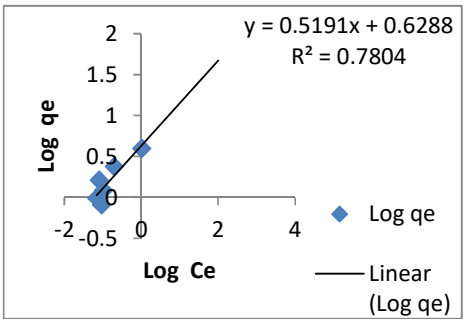
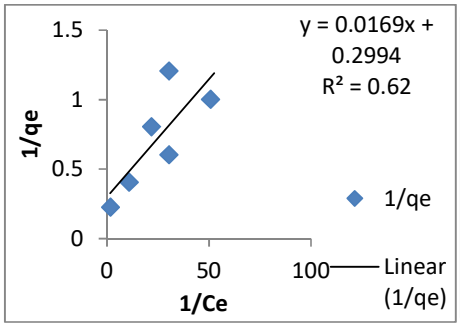


Fig.10 Freundlich Dosage for EBYD by CAC



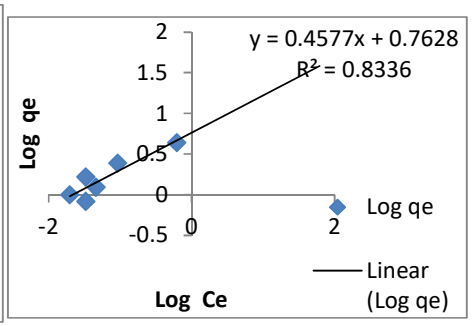
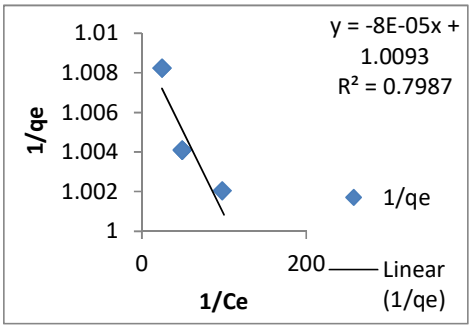


Fig.11 Langmuir Dosage for EBGD by CAC Fig.12 Freundlich Dosage for EBGD by CAC



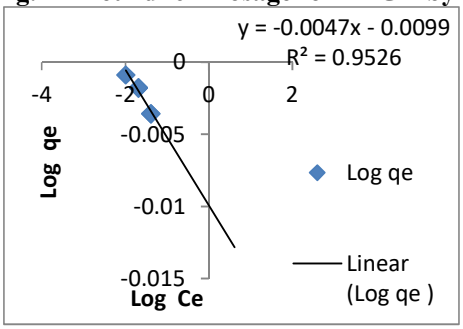
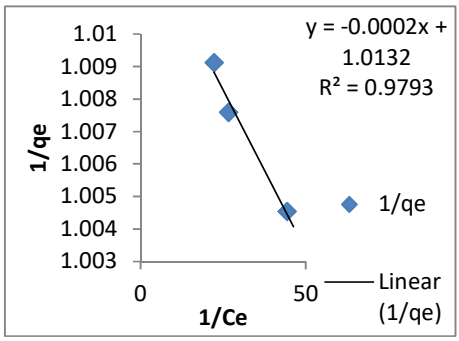


Fig.13 Langmuir Part. Size for EBYD by CAC Fig.14 Freundlich Part. Size for EBYD by CAC



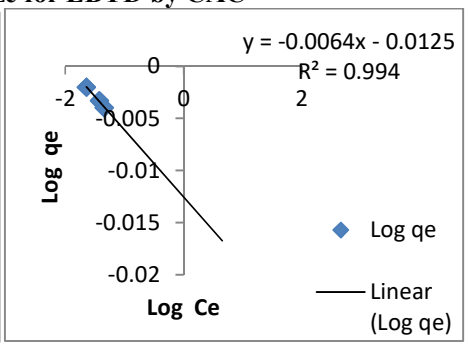
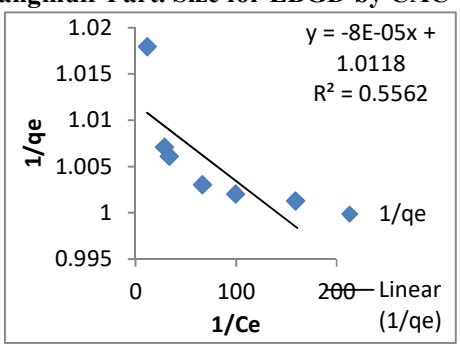


Fig.15 Langmuir Part. Size for EBGD by CAC Fig.16 FreundlichPart.Size for EBGD by CAC



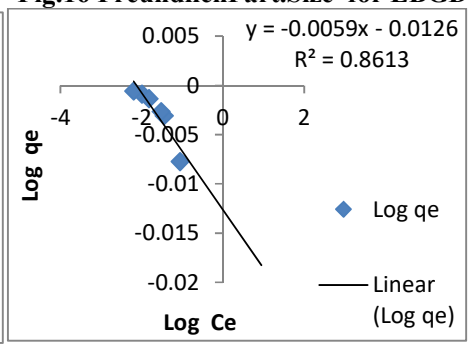
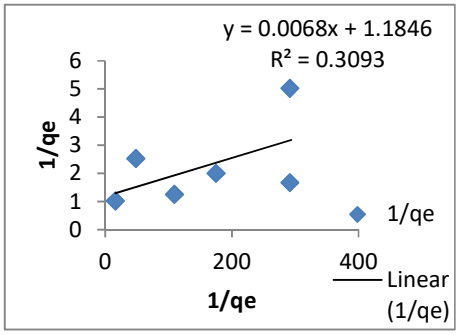


Fig.17 Langmuir Conc. for EBYD by CAC Fig.18 Frendulich Conc. for EBYD by CAC



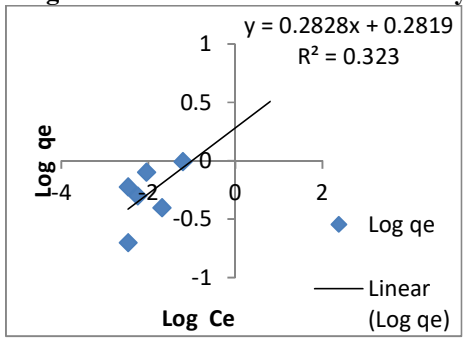


Fig.19 Langmuir Conc. for EBGD by CACFig.20 Freundlich Conc. for EBGD by CAC

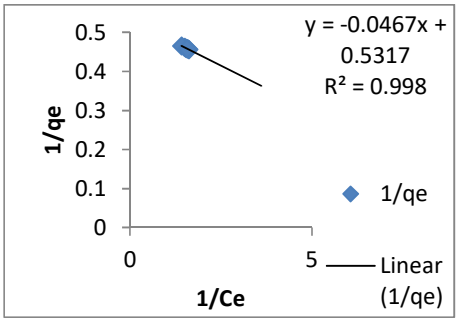


Fig.21 Langmuir pH for EBYD by MHAC

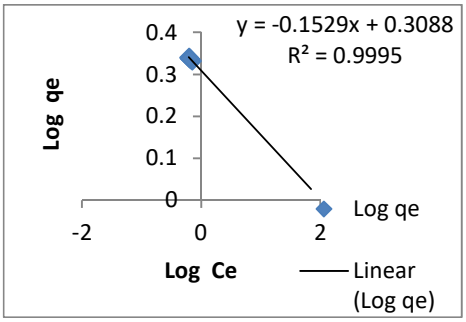


Fig.22 Freundlich pH for EBYD by MHAC

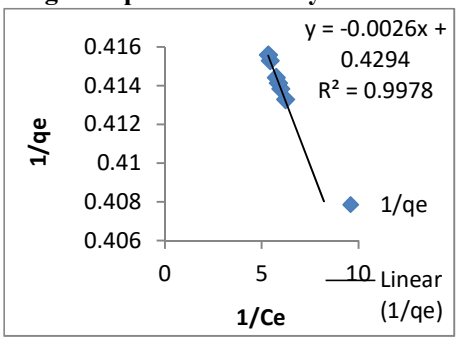


Fig.23 Langmuir pH for EBGD by MHAC

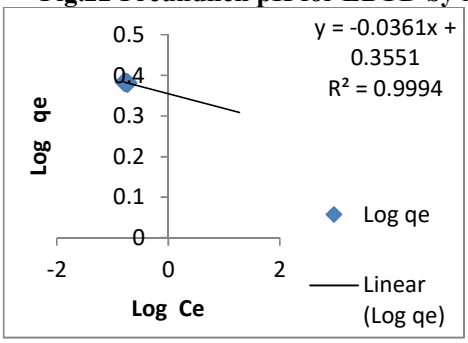


Fig.24 Freundlich pH for EBGD by MHAC

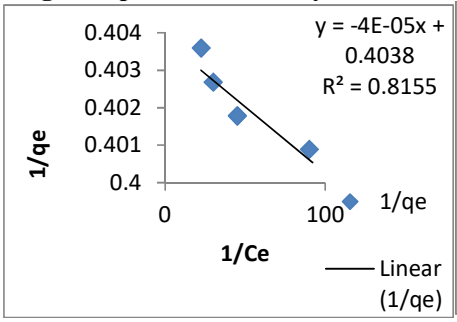


Fig.25 Langmuir Time for EBYD by MHAC

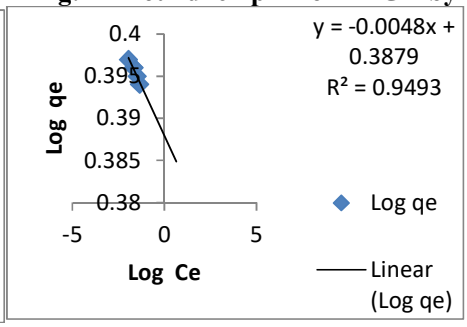


Fig.26 FreundlichTime for EBYD by MHAC

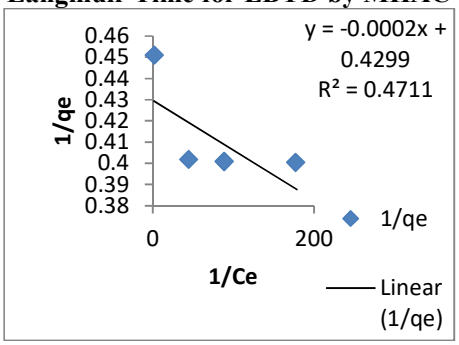


Fig.27 Langmuir Time for EBGD by MHAC

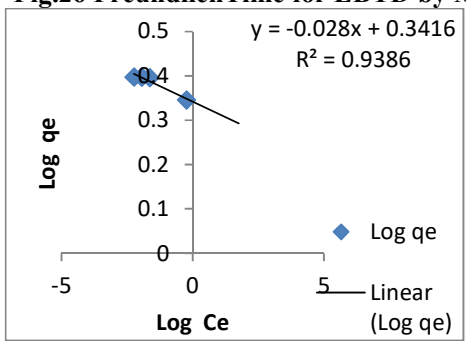


Fig.28 Freundlich Time for EBGD by MHAC

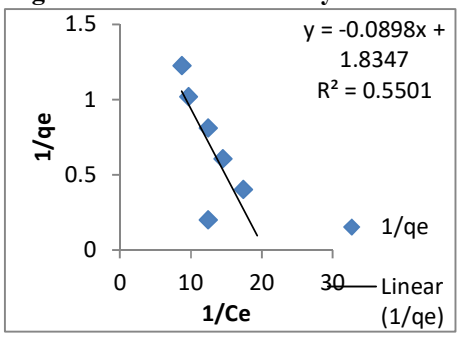


Fig.29 Langmuir Dosage for EBYD MHAC

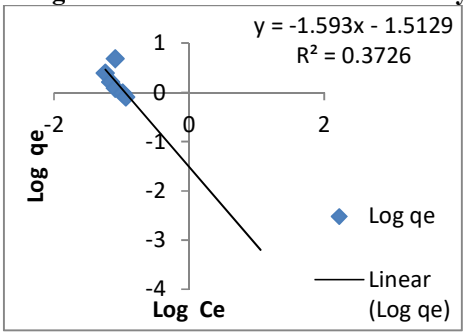


Fig.30 Freundlich Dosage for EBYD by MHAC

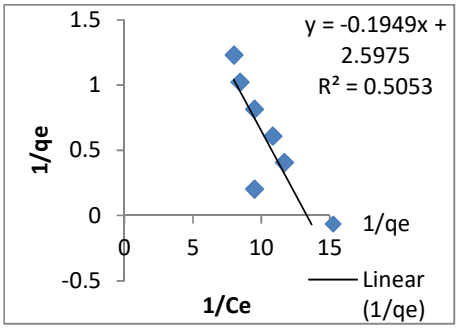


Fig.31 Langmuir Dosage for EBGD by MHAC

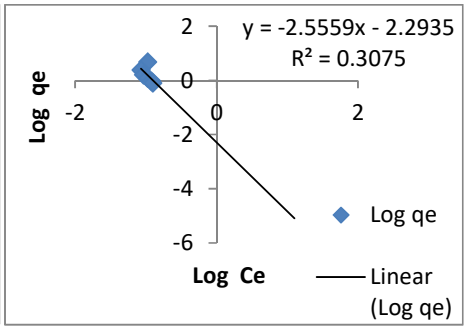


Fig.32 Freundlich Dosage for EBGD by MHAC

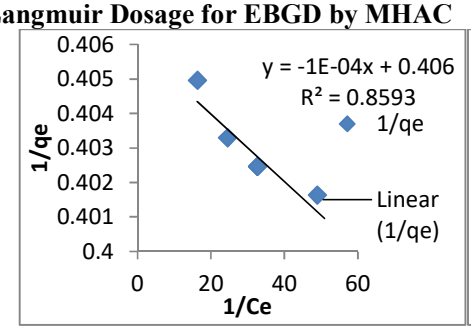


Fig.33 Langmuir Part. Size for EBYD by MHAC

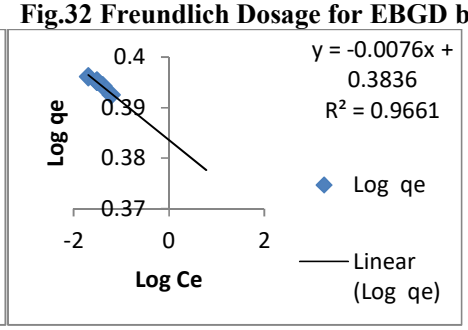


Fig.34 Freundlich Par. Size for EBYD by MHAC

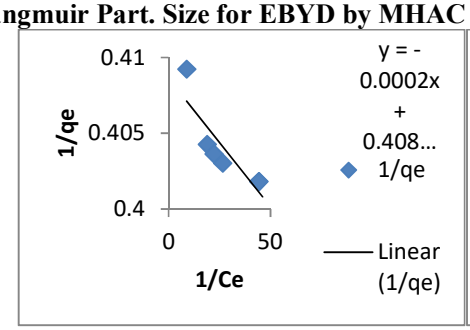


Fig.35 Langmuir Part. Size for EBGD by MHAC

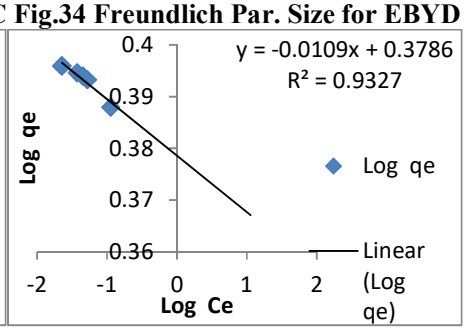


Fig.36 FreundlichPart.Size EBGD by MHAC

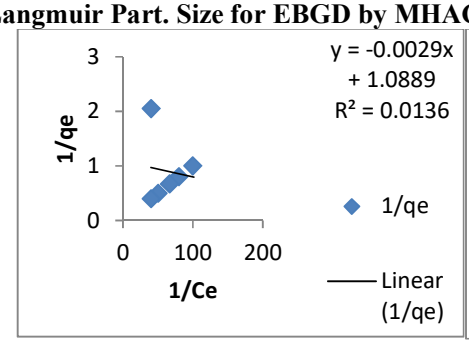


Fig.37 Langmuir Conc.for EBYD by MHAC

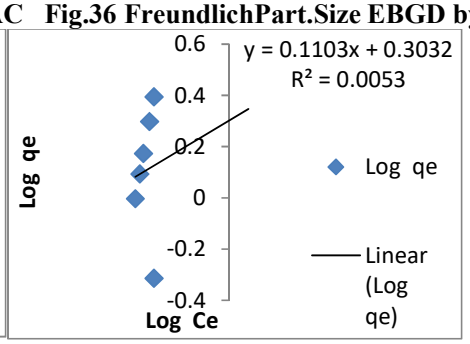


Fig.38 Freundlich Conc. forEBYD by MHAC

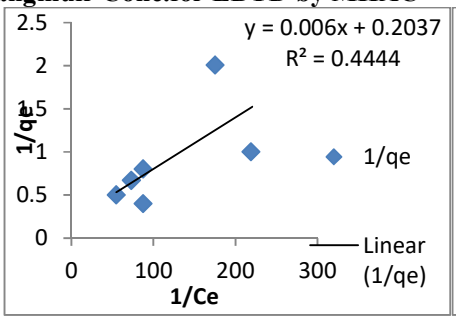


Fig.39 Langmuir Conc.for EBGD by MHAC

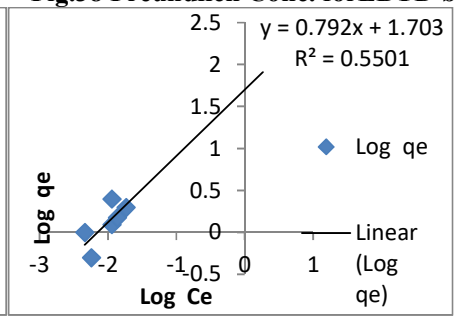


Fig.40 FrendulichConc.forEBGD by MHAC

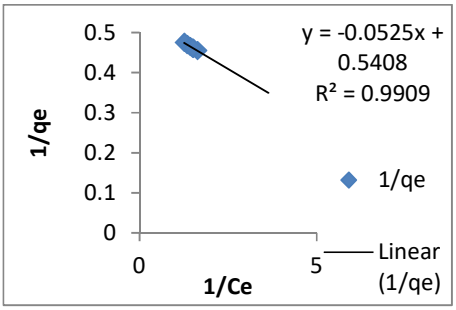


Fig.41 Langmuir pH for EBYD by GHAC

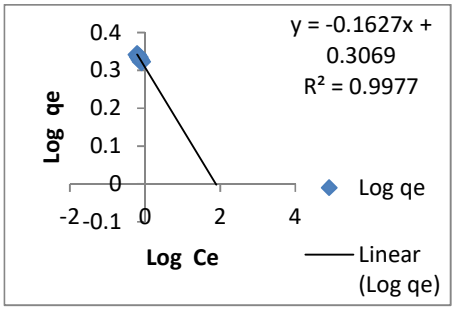


Fig.42 Freundlich pH for EBYD by GHAC

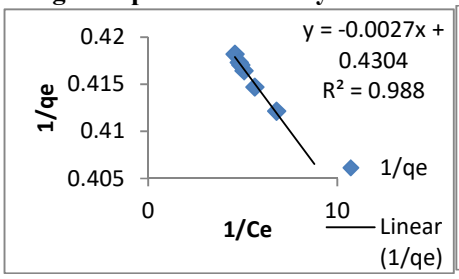


Fig.43 Langmuir pH for EBGD by GHAC

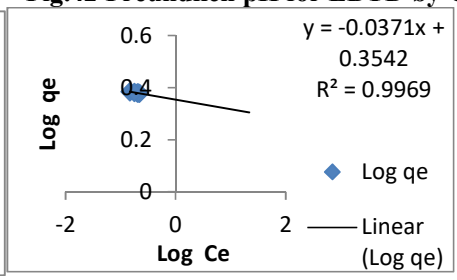


Fig.44 Freundlich pH for EBGD by GHAC

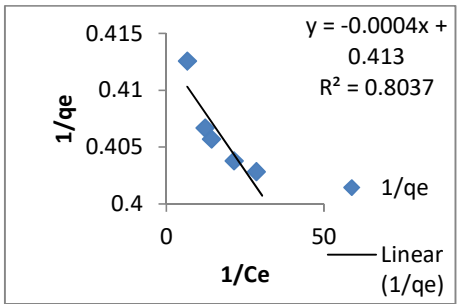


Fig.45 Langmuir Time for EBYD by GHAC

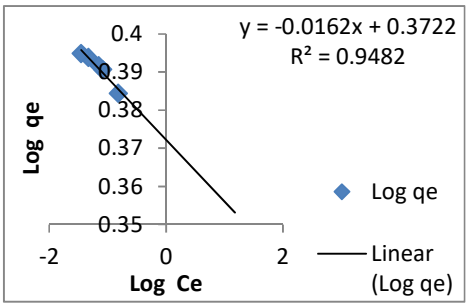


Fig.46 Freundlich Time for EBYD by GHAC

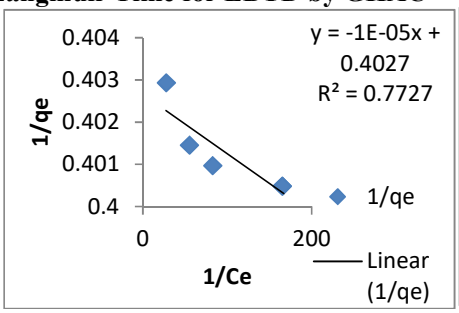


Fig.47 Langmuir Time for EBGD by GHAC

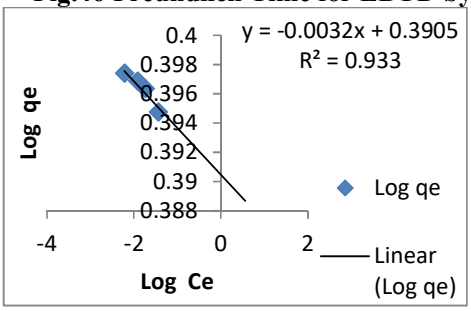


Fig.48 Freundlich Time for EBGD by GHA

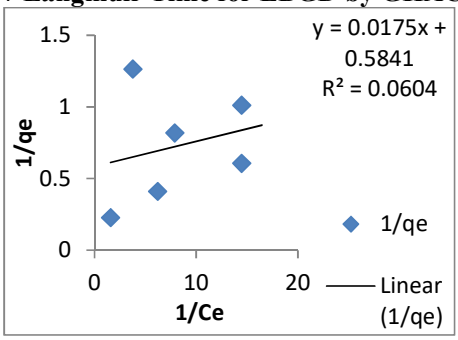


Fig.49 Langmuir Dosage for EBYD by GHAC

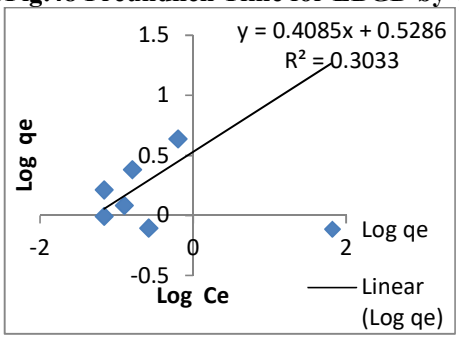


Fig.50 Freundlich Dosage for EBYD by GHAC

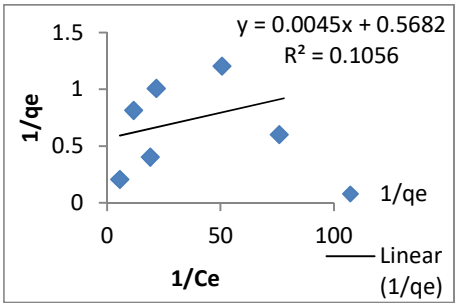


Fig.51 Langmuir Dosage for EBGD by GHAC

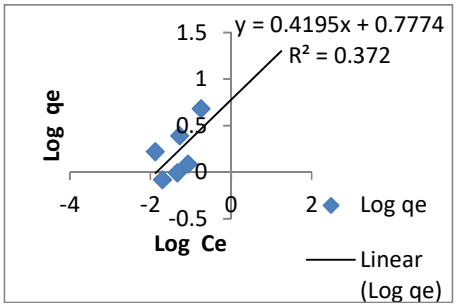


Fig.52 Freundlich Dosage for EBGD by GHAC

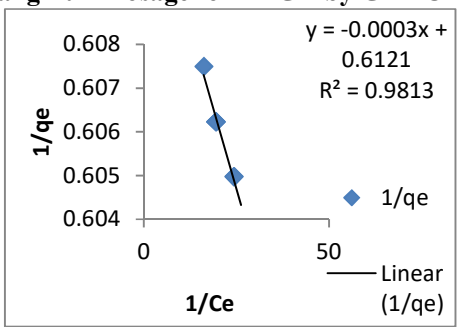


Fig.53 Langmuir Part. Size for EBYD by GHAC

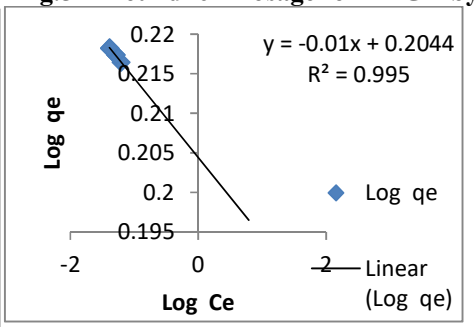


Fig.54 Freundlich Part. Size for EBYD by GHAC

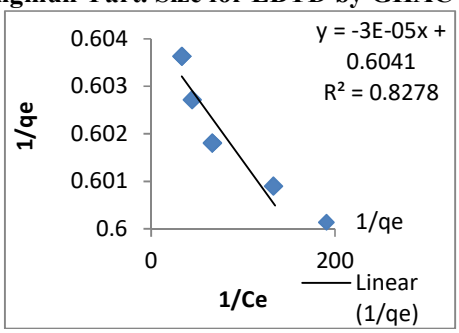


Fig.55 Langmuir Part. Size for EBGD by GHAC

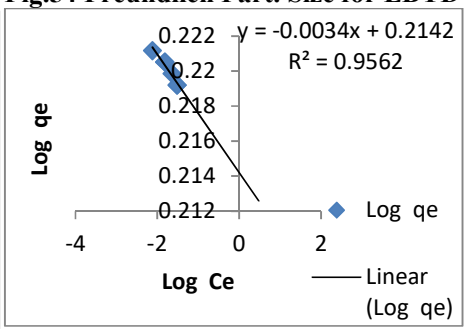


Fig.56 Freundlich Part. Size for EBGD by GHAC

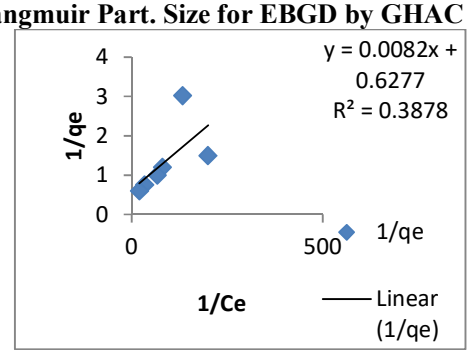


Fig.57 Langmuir Conc. for EBYD by GHAC

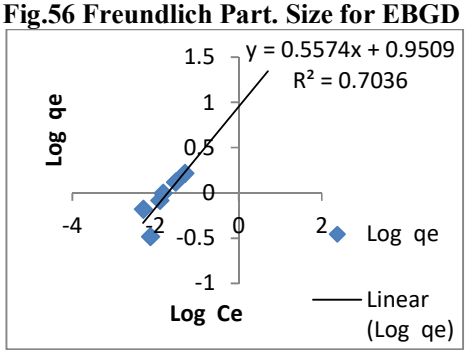


Fig.58 Freundlich Conc. for EBYD by GHAC

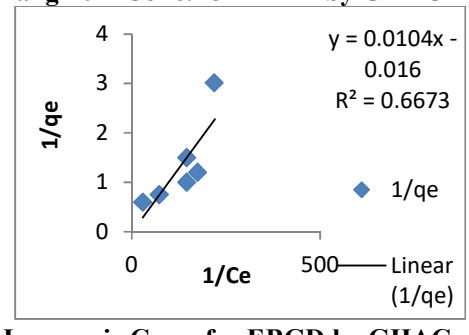


Fig.59 Langmuir Conc. for EBGD by GHAC

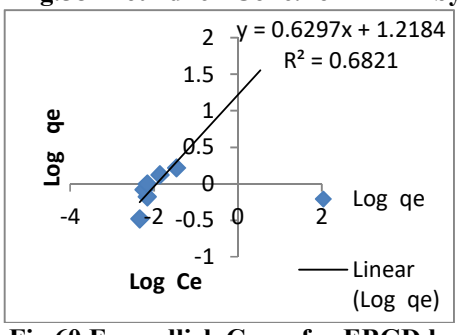


Fig.60 Freundlich Conc. for EBGD by GHAC

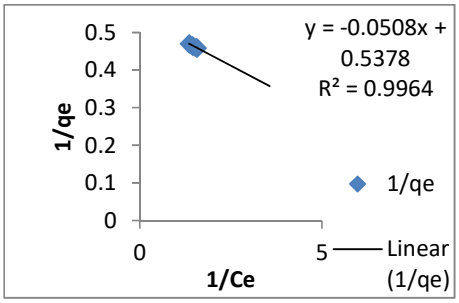


Fig.61 Langmuir pH for EBYD by RHAC

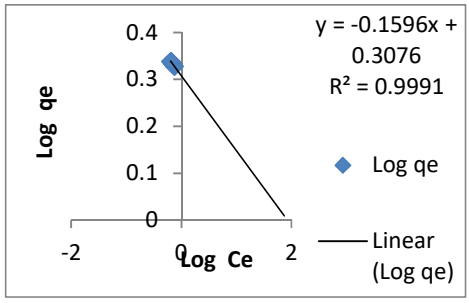


Fig.62 FreundlichpH for EBYD by RHAC

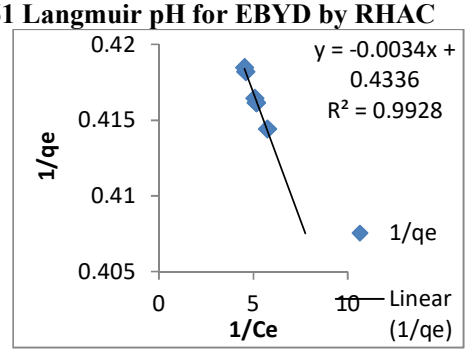


Fig.63 Langmuir pH for EBGD by RHAC

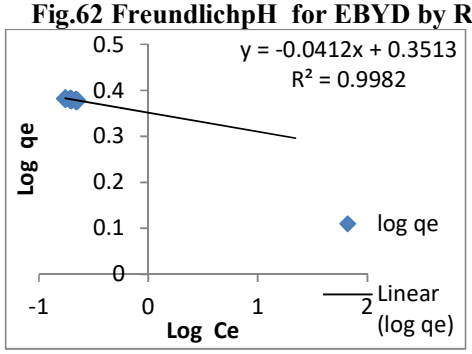


Fig.64 Freundlich pH for EBGD by RHAC

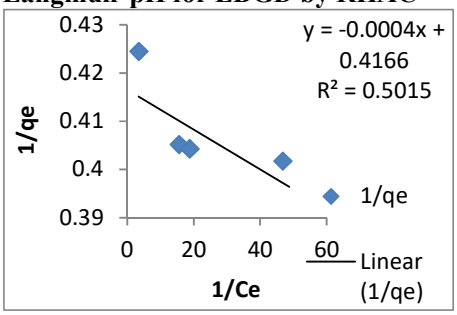


Fig.65 Langmuir Time for EBYD by RHAC

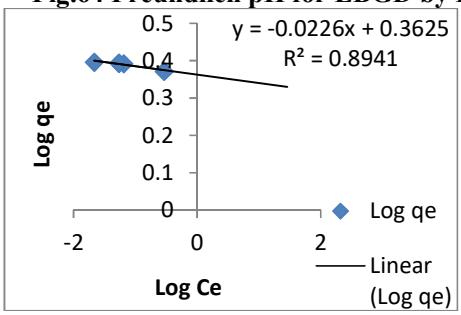


Fig.66 Freundlich Time for EBYD by RHAC

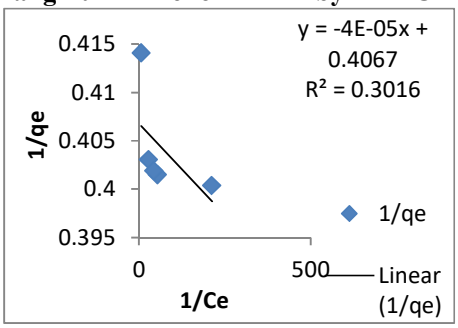


Fig.67 Langmuir Time for EBGD by RHAC

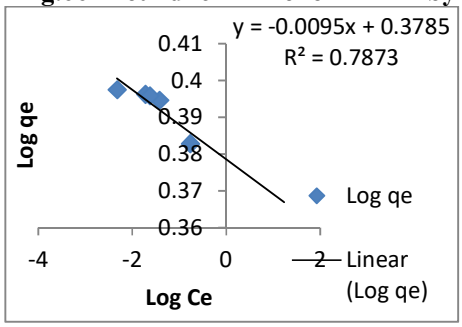


Fig.68 Freundlich Time for EBGD by RHAC

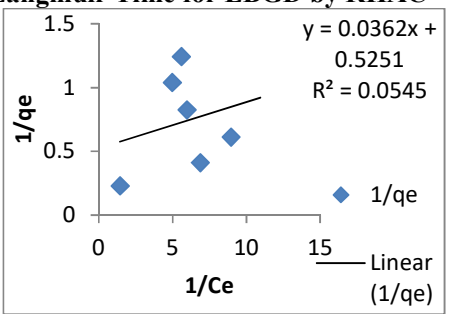


Fig.69 Langmuir Dosage for EBYD by RHAC

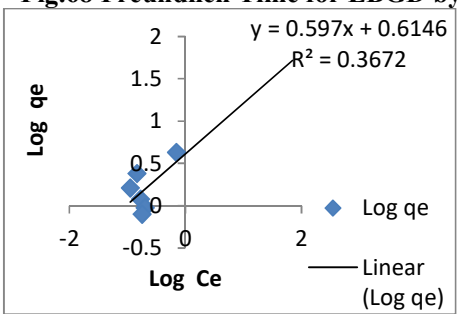


Fig.70 Freundlich Dosage for EBYD by RHAC

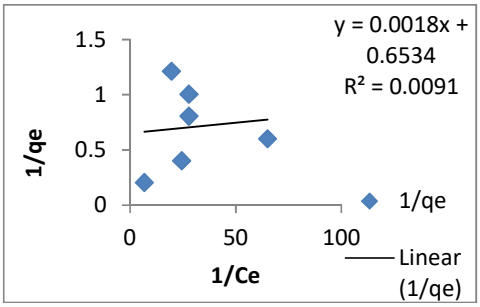


Fig.71 Langmuir Dosage for EBGD by RHAC

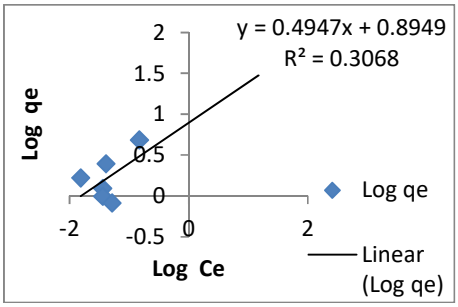


Fig.72 Freundlich Dosage for EBGD by RHAC

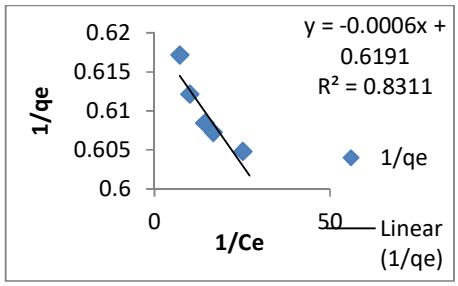


Fig.73 Langmuir Part. Size for EBYD by RHAC

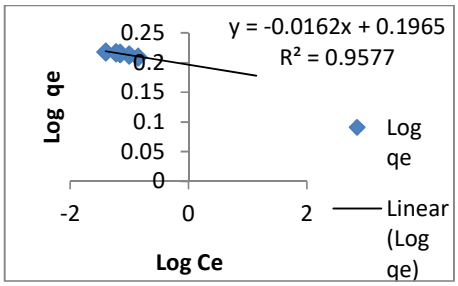


Fig.74Freundlich Part. Size for EBYD by RHAC

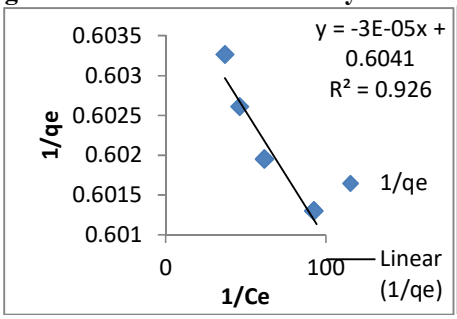


Fig.75 Langmuir Pat. Size for EBGD by RHAC

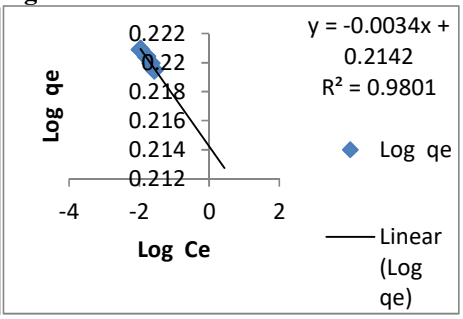


Fig.76Freundlich Part. Size for EBGD by RHAC

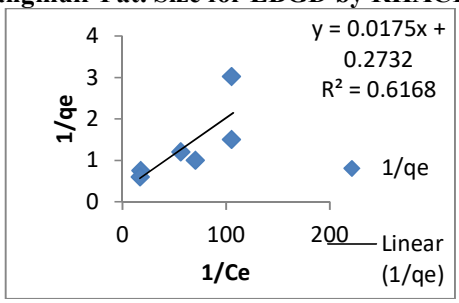


Fig.77 Langmuir Conc. for EBYD by RHAC

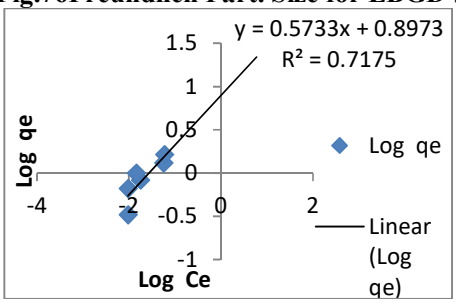


Fig.78 Freundlich Conc. for EBYD by RHAC

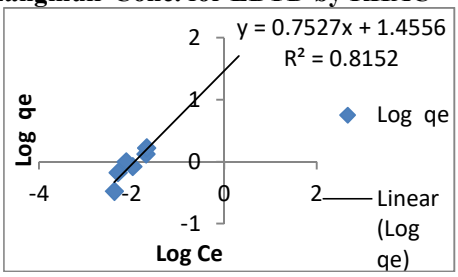


Fig.79 Freundlich Conc. for EBGD by RHAC

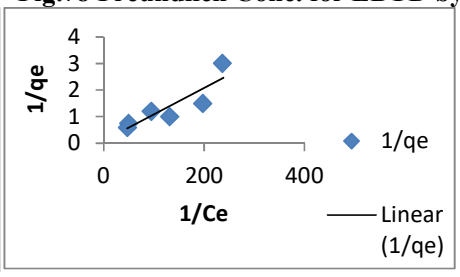


Fig.80 Langmuir Conc. for EBGD by RHAC

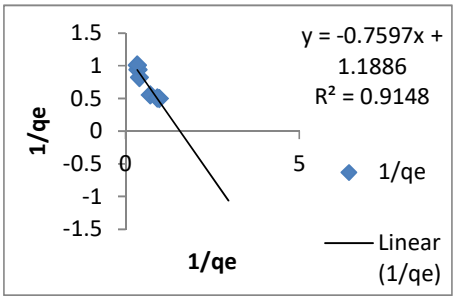


Fig.81 Langmuir pH for EBYD by CPAC

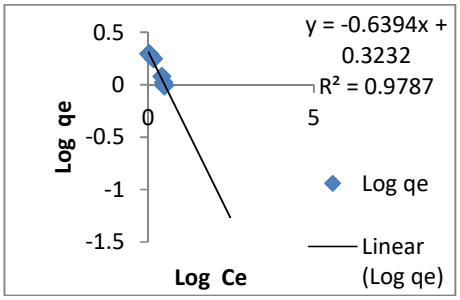


Fig.82 Freundlich pH for EBYD by CPAC

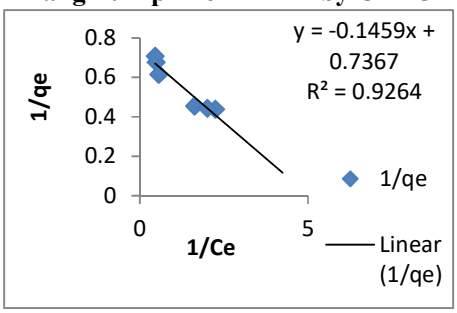


Fig.83 Langmuir pH for EBGD by CPAC

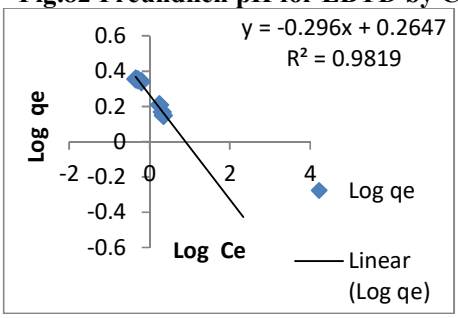


Fig.84 Freundlich pH for EBGD by CPAC

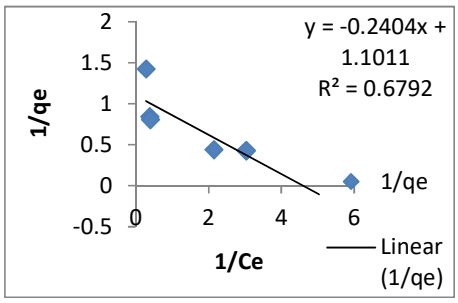


Fig.85 Langmuir Time for EBYD by CPAC

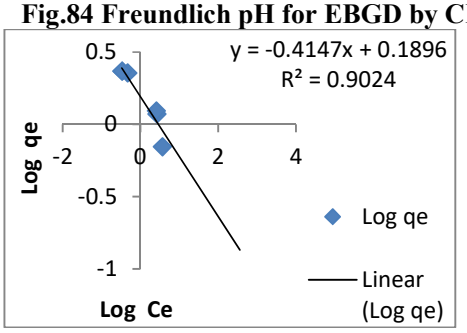


Fig.86 FreundlichTime for EBYD by CPAC

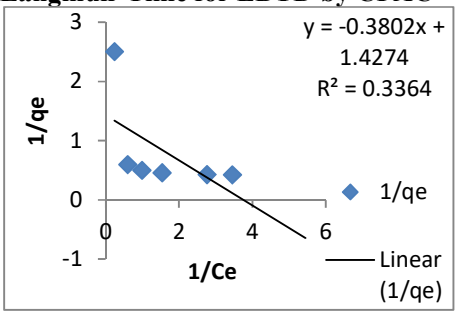


Fig.87 Langmuir Time for EBGD by CPAC

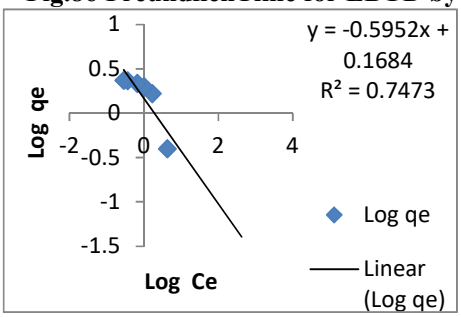


Fig.88 Freundlich Time for EBGD by CPAC

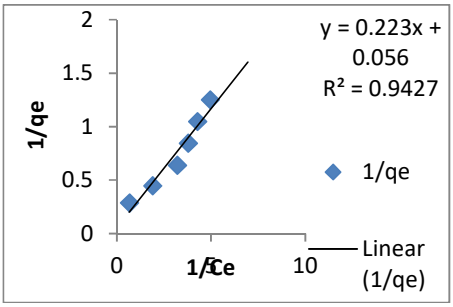


Fig.89 Langmuir Dosage for EBYD by CPAC

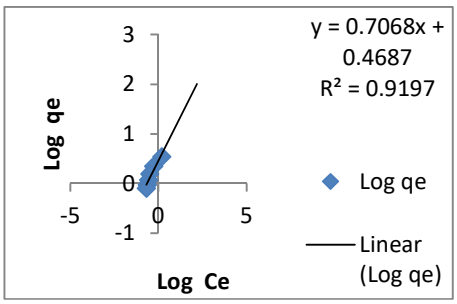


Fig.90Freundlich Dosage for EBYD by CPAC

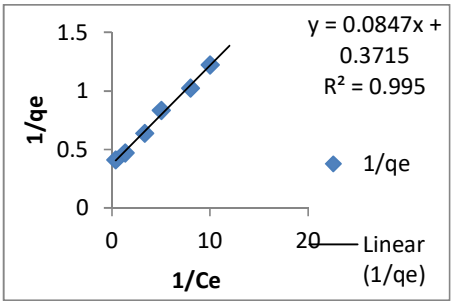


Fig.91 Langmuir Dosage for EBGD by CPAC

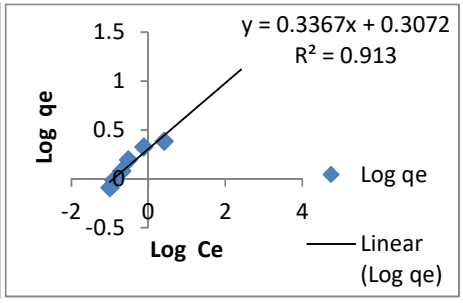


Fig.92 Freundlich Dosage for EBGD by CPAC

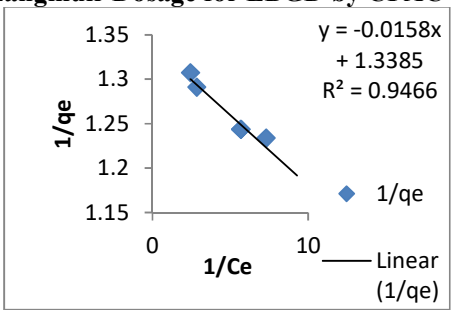


Fig.93 Langmuir Part. Size for EBYD by CPAC

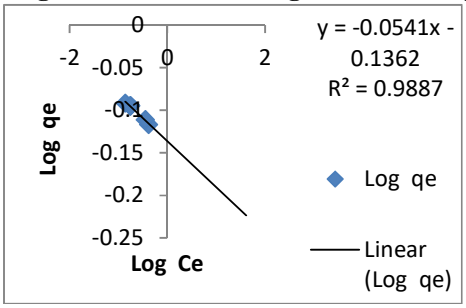


Fig.94FreundlichPart. Size for EBYD by CPAC

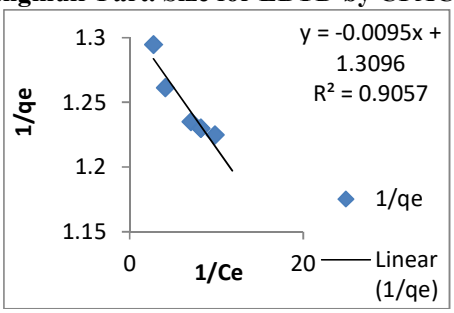


Fig.95 Langmuir Part. Size for EBGD by CPAC

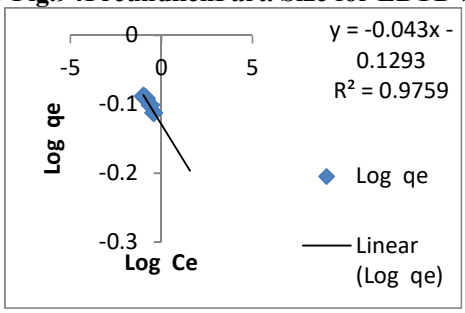


Fig.96 Freundlich Part. Size for EBGD by CPAC

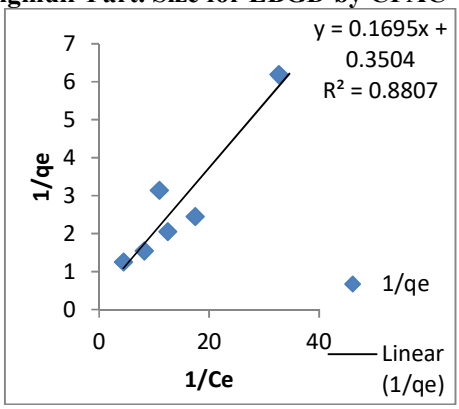


Fig.97 Langmuir Conc. for EBYD by CPAC

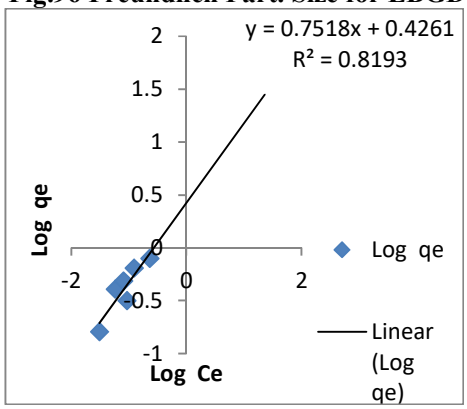


Fig.98 Freundlich Conc. for EBYD by CPAC

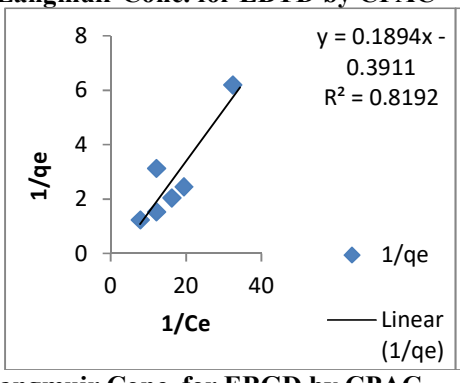


Fig.99 Langmuir Conc. for EBGD by CPAC

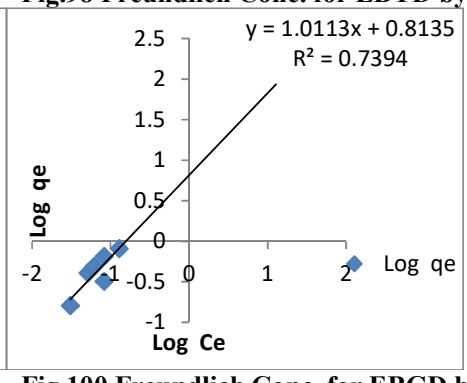


Fig.100 Freundlich Conc. for EBGD by CPAC

Freundlich Constants (K_f and n values)

The Freundlich isotherm equation as presented in Equation 3 considers heterogeneous surfaces and is based on the idea that the adsorption depends on the energy of the adsorption sites. Where K_f is the constant for function of energy of adsorption and temperature which measures adsorption capacity and n is constant representing the intensity of adsorption (Eckenfelder, 2000).The higher the value of K_f, the easier the uptake of dye from the effluent (Rengaraj *et al*., 2002). From the isotherm data, RHAC had the highest favoured values of K_f then GHAC, MHAC, CAC and CPAC respectively.

The n value, which reflects the intensity of adsorption, presents the opposite trend to that of R^2, but as seen from Tables 1 and 2 for all the adsorbents and adsorbate, 1/n values were found high enough for separation which signifies that the surface of the ACs are heterogeneous in nature (Khalid *et al*., 2000). For a good adsorbent, the slope 1/n, ranging between 0 and 1, precisely, $0.2<1/n<0.8$ which is a measure for the adsorption intensity or surface heterogeneity and indicates favourable adsorption (Kumar *et al.,*2010). A smaller value of 1/n indicates better adsorption mechanism and formation of rather strong bond between the adsorbate and adsorbent (Patil *et al*., 2006).

Isotherm data reveals that the adsorption process follows both Freundlich and Langmuir isotherm for effluent and that the adsorption is favourable. The BYD was better described by Langmuir model in comparison to Freundlich model. Therefore, the ACs is observed to have higher adsorption capacity with the BYD than the BGD. In addition, although both Langmuir and Freundlich models are also well suited to fit the data on the BGD, the adsorption data represented acceptable fit to the Freundlich isotherm equation and not as perfect as to the Langmuir isotherm.

Therefore,it is apparent that the adsorption data for the ACs fits the Freundlich isotherms better than the Langmuir isotherm because the R^2 values for the former were comparatively higher than the latter suggesting the existence of multilayer adsorption of dyes on a relatively heterogenous ACs surface. The adsorption data also showed a constrasting result in that there were negative values of the constants which imply that k_f and n was not favourable for removal of the dyes from the effluent at certain dosage.

CONCLUSION

In this study, Freundlich model gave higher coefficient of correlation (R^2) as compared to the Langmuir model. The BGD also gave higher R^2 except for CPAC, which had better dye removal results with BYD and also the highest R^2 with the Langmuir isotherm model.

The Freundlich constant K_f which indicates a high rate of adsorbate removal as its rate increases shows that RHAC had the highest favourable values of K_f thenGHAC, MHAC,CAC and CPAC respectively. The Freundlich constant 1/n; when small indicates stronger bond between the adsorbate and adsorbent. From the isotherm data,1/n had small values overall which shows that adsorption is favoured.

The isotherm data revealed that the adsorption process fitted both the Freundlich and Langmuir isotherm models for both dyes and effluent and that their adsorption is favourable. The BYD was better described by Langmuir model in comparison to Freundlich model. Therefore, the ACs are observed to have higher adsorption capacity with the BYD than the BGD. The adsorption data for the BGD, represented acceptable fit to the Freundlich isotherm equation and was not as perfect as to the Langmuir isotherm.

The adsorption capacities investigated showed that the Freundlich adsorption isotherm is superior to Langmuir adsorption isotherm with higher coefficient of regression values, although, both isotherm models had comparably high fit for adsorption.

The magnitude of the Langmuir constant, Q^0 results indicates that the amount of BYD in the effluent per unit weight of adsorbent to form a complete monolayer on the surface is significantly higher in comparison to BGD. Therefore, The Langmuir model possesses greater agreement with the experimental data. Langmuir constant b was relatively low overall, confirming high affinity between the adsorbents and adsorbates.

REFERENCES

Aksu, Z., (2005). Application of Biosorption for the Removal of Organic Pollutants: A Review. Process Biochemistry, 40: 997–1026.

Allen, S.J. and Koumanova, B. (2005). Decolourisation of Water/Wastewater Using Adsorption (Review). *Journal of the University of Chemical Technology and Metallurgy*, 40(3): 175-192.

Banat I.M, Nigam P and Marchant R. (1996). Microbial Decolorization of Textile-Dye Containing Effluents: A Review.*Bioresource Technology*, 58:217–227.

Chingombe, P., Saha, B. and Wakeman R.J. (2006). Effect of Surface Modification of An Engineered Activated Carbon on the Sorption of 2,4-Dichlorophenoxy Acetic Acid and Benazolin from Water. *Journal of Colloid and Interface Science*, 297: 434 - 442.

Easton, J.R. (1995). The dye makers's view. In: Cooper, P. (Ed). *Colour in Dyehouse Effluent*.Society of Dyers and Colourists, Bradford, United Kingdom, pp.11.

Eckenfelder, W.W., Jr. (Ed.). (2000). *Industrial Water Pollution Control*. Series in Environmental Engineering Mcgraw – Hill Book Company. Singapore.

Kadirvelu, K., Kavipriya, M., Karthika, C., Radhika, M., Vennilamani, N. and Pattabhi, S. (2003). Utilisation of Various Agricultural Wastes for Activated Carbon Preparation and Application for the Removal of Dyes and Metal Ions from Aqueous Solution *Bioresource Technology,* 87: 129-132.

Khalid, N., Ahmad,S., Toheed, A. and Ahmad J. (2000) Potential of Rice Husks for Antimony Removal.*Applied Radiation and Isotopes*, 52: 30-38.

Kratochvil, D. and Volesky, B. (1998). Evaluation of Two-Metal Equilibrium Biosorption Advances in Biosorption of Heavy Metals.

Kumar, A.G, Perinbama, K., Kamatchia, P., Nageshb, N. and Sekaranc, G. (2010). In Situ Immobilization of Acid Protease on Mesoporous Activated Carbon Packed Column for the Production of Protein Hydrolysates. *Bioresource Technology*, 101 (4): 1377–1379.

Mahvi, A.H.; Maleki, A. and Eslami, A. (2004).Potential of Rice Husk and Rice Husk Ash for Phenol Removalin Aqueous Systems. *American Journal of Applied Sciences,* 1(4): 321-326.

Nkeonye, P.O. (1989). *Fundamental PrinciplesOf Textile Dyeing, Printing and Finishing.* Ahmadu Bello University Press Ltd. Zaria – Nigeria.

Okpuwhara, R.O. (2013). Adsorption of Colour From Textile Wastewater Using Activated Carbon Derived From Cassava Peel, Maize, Groundnut and Rice Husks. M.Sc.Thesis, Department of Textile Science and Technology, Ahmadu Bello University, Zaria - Nigeria.

Patil, S., Bhole, A. and Natrajah, G. (2006). Seavenging of Ni (II) Metal Ion by Adsorption on PAC and Babhul, *Journal of Environmental Science and Engineering*, 48 (3): 203- 208.

Qaiser,S., Saleemi, A.R. and Ahmad, M.M. (2007). Heavy Metal Uptake by Agro Based Waste Materials. Electronic Journal of Biotechnology, 10(3): 409 – 416.

Strickland, A.F. and Perkins, W.C. (1995).*Textile Chemist and Colourist*, 27(5): 11-15.

Tebbutt, T.H.Y. (Ed.) (1998). *Principles of Water Quality Control*. Butterworth Heinemann, Oxford.

Thakur, I.S. (2006). *Environmental Biotechnology: Basic Concept and Application*. I. K. International Pvt. Limited., New Delhi, Numbai, Bangalore.

Zollinger, H. (1987). *Azo Dyes and Pigments, Colour Chemistry-Synthesis, Properties and Applications of Organic Dyes and Pigments*.New York:VCH,Wiley Science Publishing. Available from NetLibrary database, pp. 92.Retrieved July 25 from http://onlinelibrary.wiley.com/doi/10.1002/9783527615438.fmatter/pdf.

EVALUATION OF VARIATIONS IN INDOOR AIR QUALITY IN SELECTED HOUSEHOLDS WITHIN KADUNA METROPOLIS

F.B. IBRAHIM AND D. E. ASUKU
Department of Water Resources & Environmental Engineering, Ahmadu Bello University Zaria

ABSTRACT
Indoor air quality has been cited by the EPA as one of the top five most urgent environmental risks to public health.it is in line with this that the assessment of variations in indoor air quality of selected households was carried out in Ungwan Rimi (low density) and Sabon Tasha(high density) areas of Kaduna State. Monitoring and analysis of relevant indoor air pollutants such as relative humidity, temperature, carbon monoxide (CO), carbon dioxide (CO_2) and particulate matter PM_{10} (>10ug/m^3) using portable air quality monitoring device. A total of thirty (30) randomly selected households were assessed twice a day, in the morning and evening at peak periods to determine the variations in the IAQ at the two periods; in the living rooms and kitchen; and in the two selected areas. The results obtained revealed that there was high variation in CO between the two study areas with coefficient of variation (CV) of 57.5%; moderate variation in PM_{10} with CV of 26.9%; and low variations in relative humidity, temperature and CO_2 with CV of 4.0%, 2.2% and 4.0% respectively. Variations between the IAQ in the mornings and evenings was low in the two study areas with CV ranging from 3.7% to 13.2% and 2.9% to 14.2 % in Ungwan Rimi and Sabon Tasha respectively for all the parameters measured. The variations between livingroom and kitchen air quality was low for all the parameters in the two study areas except for CO and CO_2 in the two study areas. The study recommends the use of proper air control measures where necessary for cleaner air and healthier environment.

Keywords: *indoor air quality, variation, CO, CO_2, particulate matter, relative humidity*

1.0 INTRODUCTION

Indoor air quality (IAQ) is a term which refers to the air quality within and around buildings and structures, especially as it relates to the health and comfort of building occupants. Indoor air quality is a major concern to businesses, homes, schools, offices and industrial environments. It has been cited by the EPA as one of the top five most urgent environmental risks to public health. Most people spend up to 90% of their time indoors, not to mention workers who spend very long hours in office environments. This goes to show that for the better part of most the day, people are exposed to indoor pollution. (Occupational Safety and Health Administration, www.osha.gov)

Every building has its own set of peculiarities, Air quality may be determined by the site of the building, its original design, and renovations, whether air handling systems have been installed, occupant densities, activities conducted within the building, and the occupants' satisfaction with their environment. (Occupational Safety and Health Administration, www.osha.gov)

The basis for which the population density is categorized as densely, moderately and sparsely distributed is as a result of the obvious extents of congestion. Living condition has a direct impact on public health, and any impact on public health includes largely the effects of air composition. This then affects indoor air quality as the number of persons affects number of activities and hence affects the air and its quality.

Symptoms related to poor IAQ are varied depending on the type of contaminant. They can easily be mistaken for symptoms of other illnesses such as allergies, stress, colds, and influenza. The usual clue is that people feel ill while inside the building, and the symptoms go away shortly after leaving the building, or when away from the building for a period of time (such as on weekends or a vacation). Failure of building owners and operators to respond quickly and effectively to IAQ problems can lead to numerous adverse health consequences. Health effects from indoor air pollutants may be experienced soon after exposure or, possibly, years. Symptoms may include irritation of the eyes, nose, and throat; headaches; dizziness; rashes; and muscle pain and fatigue. Diseases linked to poor IAQ include asthma and hypersensitivity pneumonitis. The specific pollutant, the concentration of exposure, and the frequency and duration of exposure are all important factors in the type and severity of health effects resulting from poor IAQ. Age and preexisting medical conditions such as asthma and allergies may also influence the severity of the effects. Long term effects due to indoor air pollutants may include respiratory diseases, heart

disease, and cancer, all of which can be severely debilitating or fatal (OSHA 2011)

At this time, it cannot be certain the extent to which indoor air pollution if left unchecked can grow and what future effects increase in the level of common IAPs can have. However, an awareness of the possible effects is necessary to educate people on the likely events, especially adverse effects to human health. In this light, it is necessary that data on indoor air quality is obtained through carefully selected methods of air sampling. IAQ measurements can provide knowledge on the presence and severity of air pollutants, hence; proffer solutions for a comfortable and healthy environment for human dwelling purposes. The justification for this study lies in the fact that people spend most of their time indoors so the quality of indoor air has major implications on health, also indoor air pollution is largely the result of human activity such as tobacco smoking, burning fuel for heat or cooking, the use of cleaning materials and solvents and even breathing.

2.0 METHODOLOGY

2.1 Sample Size and Sampling Technique

The sampling frame for this research consists of the residents of Sabon Tasha (high density) and Ungwan Rimi (low density) communities in Kaduna metropolis. A number of models have been developed to estimate sample size. The sample size of this research is calculated by using Taro Yamane (1973) formula for 95% confidence level (according 20,693,000 persons from the data of Beijing China district official report 2012). The calculation formula of Yamane is presented as follows:

$$n = \frac{N}{1 + N(e)^2}$$

where,
n= sample size
N= population size
e=level of significance (set at 0.05 for this study)

The above formula was used for Ungwan Rimi with 4,606 households and Sabon Tasha with 6,023 households (NPC, 2006). Sample sizes of 368 and 375 were obtained respectively. However, 20% of the sample size was carefully distributed around both areas, bringing the total number of distributed questionnaires to one hundred and fifty.

A total of one hundred and fifty questionnaires were administered to inhabitants of the study areas, seventy-five in each area. This was achieved by sectionalizing the areas and ensuring the whole area covered. The researcher distributed questionnaire prior to carrying out air sampling in randomly selected households amongst the one hundred and fifty households in each area.

2.2 Air Sampling and Analysis

Two areas, Sabon Tasha for densely and Ungwan Rimi for sparsely populated were the areas of study. Households were selected randomly based on the population size estimated and a total number of 30 households were chosen, fifteen per area of study.

In each of the randomly selected households, air quality was monitored in the living room and kitchen area with the assistance of research personnel from KEPA, Kaduna Environmental Protection Agency. In each household, five (5) air quality monitoring parameters were measured; suspended particulate matter (PM_{10}), Carbon Monoxide (CO), temperature (^0C), relative humidity (%) and Carbon dioxide (CO_2).

Concentration of gaseous pollutant in the ambient air was measured using the gas analyzers and sensors handheld air quality measurements equipment. The equipment was switched on at each time of sampling and allowed to suck in air for a minimum of 2 minutes after which the ambient concentration of the pollutants having been measured was displayed on the screen for recording. Readings were taken and recorded on a prepared sheet in the morning between 7:00am–10: 00am and 4:00pm-6:30pm in the evening. The prevailing climatic condition which happened to be rainy season as the study was conducted in the month of June, was also put into consideration.

2.3 Data Analysis Technique

All statistical analyses were carried out using IBM SPSS version 20 statistical program and Microsoft Excel 2010.

3.0 RESULTS AND DISCUSSIONS

The results obtained from the air quality assessment of the two study areas are as given in Tables 1 - 4. The analysis of the data in terms of its variations in the morning and evenings; living room and kitchen; and in the low density (Ungwan Rimi) and high density (Sabon Tasha) areas are given in Tables 5 – 8 discussed as follows.

Table 1: Air Quality in the Morning in Households in Ungwan Rimi

No of house holds	Relative Humidity (%)		Temp (^{0}C)		CO (ppm)		CO_2 (ppm)		PM_{10} (ug/m^3)	
	living Room	Kitchen	Living Room	Kitchen	Living Room	Kitchen	Living Room	Kitchen	Living Room	Kitchen
1	66.10	69.70	27.9	27.6	1.00	5.00	492	452	7.00	18.00
2	68.20	69.00	27.6	27.4	4.00	5.00	1241	817	6.00	10.00
3	75.90	77.90	25.7	25.9	6.00	11.50	474	176	10.00	13.30
4	66.10	69.70	27.9	27.6	1.00	5.00	492	452	7.00	18.00
5	75.90	77.90	25.7	25.9	6.00	11.50	474	176	10.00	13.30
6	75.90	74.20	26.6	26.8	8.25	13.50	1037	899	9.30	12.25
7	78.10	78.60	25.6	25.7	8.70	8.50	663	497	10.10	7.20
8	76.70	75.20	26.2	26.5	7.82	10.00	701	698	9.25	7.28
9	75.00	72.6	26.3	26.6	7.25	15.70	612	681	9.30	7.80
10	76.40	73.00	26.3	26.7	7.5	17.6	630	980	9.70	11.80
11	76.10	74.80	26.8	26.8	8.70	16.90	1065	1144	7.80	8.70
12	76.10	74.80	26.8	26.8	8.70	16.90	1065	1144	7.80	8.70
13	75.70	74.60	26.5	26.6	17.70	8.97	771	772	8.67	7.80
14	78.20	77.90	25.2	27.3	7.50	13.20	1125	936	7.90	8.40
15	72.60	71.60	26.5	26.8	7.79	11.20	712	689	9.43	7.31

Table 2 Air Quality in the evening in Households in Ungwan Rimi

No of house holds	Relative Humidity (%)		Temp (^{0}C)		CO (ppm)		CO_2 (ppm)		PM_{10} (ug/m^3)	
	living Room	Kitchen	Living Room	Kitchen	Living Room	Kitchen	Living Room	Kitchen	Living Room	Kitchen
1	52.70	59.80	32.7	32.1	7.20	21.10	725	994	6.80	6.28
2	57.50	54.20	31.6	31.4	4.20	8.90	1165	1135	6.50	7.20
3	54.20	56.80	33.1	32.7	9.60	22.60	554	665	8.60	9.80
4	51.70	50.20	32.0	35.6	4.50	6.90	673	715	7.75	9.30
5	59.20	57.60	29.2	28.9	7.10	21.10	613	669	8.10	11.40
6	59.20	57.60	29.2	28.9	7.10	21.10	613	669	8.10	11.40
7	63.80	62.90	28.3	29.6	10.90	11.30	628	713	7.30	8.90
8	67.80	66.40	30.1	31.3	8.50	14.90	625	991	7.80	9.20
9	74.10	73.80	28.7	29.2	7.40	20.50	749	1148	8.10	14.50
10	75.20	74.20	27.8	28.2	6.50	18.90	321	628	8.75	9.31
11	75.20	74.20	27.8	28.2	6.50	18.90	321	628	8.75	9.31
12	70.10	69.90	26.5	26.9	9.80	12.60	426	986	14.40	9.80
13	63.80	62.90	30.1	31.3	4.50	8.20	374	583	162	189
14	66.20	64.80	28.9	29.2	7.50	10.30	421	596	14.90	11.16
15	66.20	64.80	28..9	29.2	7.50	10.30	421	596	14.90	11.16

Table 3 Air Quality in the morning for Households in Sabon Tasha

No of households	Relative Humidity (%)		Temp (^{0}C)		CO (ppm)		CO_2 (ppm)		PM_{10} (ug/m^3)	
	living Room	Kitchen	Living Room	Kitchen	Living Room	Kitchen	Living Room	Kitchen	Living Room	Kitchen
1	81.40	78.10	24.9	26.0	6.80	18.25	803	810	7.60	11.25
2	73.40	77.60	26.5	26.0	9.68	18.25	1245	1440	6.78	10.28
3	74.50	74.30	26.6	26.8	8.90	14.25	567	754	9.78	10.50
4	72.30	73.40	26.6	26.6	34.20	12.37	818	623	10.80	19.00
5	70.40	67.10	27.8	26.9	9.28	19.10	787	734	7.66	10.28
6	67.10	69.80	28.0	27.5	34.60	19.80	513	500	15.60	10.00
7	66.80	63.90	28.5	28.9	11.98	36.70	863	829	9.96	18.10
8	67.50	69.30	28.4	28.2	25.68	8.00	626	744	17.60	8.98
9	66.60	68.20	28.9	29.1	26.01	39.60	509	441	11.80	17.80
10	62.50	59.20	30.3	31.4	16.80	60.87	445	176	14.80	25.60
11	62.50	59.20	30.3	31.3	16.80	60.87	445	176	14.80	25.60
12	62.50	59.20	30.3	31.3	16.80	60.87	445	176	14.80	25.60
13	61.40	65.70	30.2	29.2	20.80	35.80	1412	428	14.80	18.80
14	61.40	65.70	30.2	29.2	20.80	35.80	1412	428	14.80	18.80
15	58.80	58.80	30.8	30.8	50.80	50.80	548	1067	26.80	26.86

Table 4 Air Quality in the Evening in Households in Sabon Tasha

No of households	Relative Humidity (%)		Temp (^{0}C)		CO (ppm)		CO_2 (ppm)		PM_{10} (ug/m^3)	
	living Room	Kitchen	Living Room	Kitchen	Living Room	Kitchen	Living Room	Kitchen	Living Room	Kitchen
1	63.80	62.90	31.1	31.0	8.20	17.80	583	681	9.70	12.30
2	63.20	61.70	30.5	30.2	9.15	10.20	670	878	7.80	9.20
3	61.10	63.50	30.1	29.9	9.25	16.20	361	1518	8.20	10.30
4	61.90	65.20	30.1	30.2	11.78	26.70	507	323	9.71	17.80
5	59.20	57.70	29.7	29.4	6.90	22.10	626	715	7.85	10.30
6	63.80	62.90	28.8	28.9	9.85	15.83	411	1523	11.28	10.50
7	62.80	66.90	28.6	28.4	10.01	19.80	583	374	10.68	24.30
8	67.70	66.60	27.8	27.7	13.30	26.76	416	353	10.80	14.30
9	63.80	60.9	28.3	29.1	8.78	17.82	566	1211	8.80	9.80
10	61.80	61.20	29.7	31.8	62.81	18.8	449	628	26.80	12.40
11	61.80	61.20	29.7	31.8	62.81	18.8	449	628	26.80	12.40
12	61.80	61.20	29.7	31.8	62.81	18.8	449	628	26.80	12.40
13	62.80	66.70	28.6	28.9	20.01	10.01	373	593	14.30	11.26
14	64.70	61.30	29.7	31.2	38.5	21.6	436	986	19.80	13.80
15	64.70	61.30	29.7	31.2	38.5	21.6	436	986	19.80	13.80

Table 5 Coefficient of Variation of Parameters Measured in the Two Study Areas

	Relative humidity (%)	Temperature (^{0}C)	Carbon Monoxide (ppm)	Carbon Dioxide (ppm)	Particulate Matter (ug/m^3)
Ugwan Rimi	68.86	28.28	10.25	706.87	9.89
Sabon Tasha	65.08	29.19	24.28	668.4	14.49
Mean	66.97	28.735	17.265	687.635	12.19
STD	2.672864	0.643467	9.920708	27.2024	3.25
CV	0.039911	0.022393	0.574614	0.039559	0.2668
CV*100 (%)	3.991136	2.239315	57.46139	3.955936	26.68
Decisiom					

Table 6 Coefficient of Variation between Morning and Evening

		Relative Humidity	Temperature	Carbon Monoxide	Carbon Dioxide	Particulate Matter
UNGWAN RIMI	**Morning**	74.15	26.62	9.28	735.57	9.63
	Evening	63.57	29.93	11.21	678.17	10.15
	Mean	68.86	28.275	10.245	706.87	9.89
	STD	7.48119	2.340523	1.364716	40.58793	0.367696
	CV	0.108643	0.082777	0.133208	0.057419	0.037179
	CV*100	10.86435	8.277713	13.3208	5.741923	3.717852
SABON TASHA	**Morning**	67.28	28.58	26.71	692.13	15.19
	Evening	62.87	29.79	21.85	644.67	13.79
	Mean	65.075	29.185	24.28	668.4	14.49
	STD	3.118341	0.855599	3.436539	33.55929	0.989949
	CV	0.047919	0.029316	0.141538	0.050208	0.068319
	CV*100	4.791918	2.93164	14.15378	5.020839	6.83195

Table 7: Variations between living room and kitchen in Ungwan Rimi

UNGWAN RIMI		Relative Humidity	Temperature	Carbon Monoxide	Carbon Dioxide	Particulate Matter
MORNING	**Living Room**	74.2	26.51	7.19	770.27	8.62
	Kitchen	74.1	26.73	11.36	700.87	10.66
	Mean	74.15	26.62	9.275	735.57	9.64
	STD	0.07071068	0.155563	2.948635	49.07321	1.442498
	CV	0.00095362	0.005844	0.317912	0.066715	0.149637
	CV*100	0.09536167	0.584386	31.79122	6.671454	14.96367
EVENING	**Living Room**	63.79	29.71	7.25	575.27	9.79
	Kitchen	63.34	30.18	15.17	781.07	10.51
	Mean	63.565	29.945	11.21	678.17	10.15
	STD	0.31819805	0.33234	5.600286	145.5226	0.509117
	CV	0.00500587	0.011098	0.499579	0.214581	0.050159
	CV*100	0.50058688	1.109835	49.95795	21.45813	5.01593

Table 8: Variations between living room and kitchen in Sabon Tasha

SABON TASHA		Relative Humidity	Temperature	Carbon Monoxide	Carbon Dioxide	Particulate Matter
Morning	**Living Room**	67.27	28.55	20.66	762.53	13.23
	Kitchen	67.3	28.61	32.76	621.73	17.16
	Mean	67.285	28.58	26.71	692.13	15.195
	STD	0.0212132	0.042426	8.555992	99.56063	2.77893
	CV	0.00031527	0.001484	0.320329	0.143847	0.182884
	CV*100	0.03152739	0.148448	32.03292	14.38467	18.28845
Evening	**Living Room**	67.3	29.47	24.84	487.67	14.61
	Kitchen	62.99	30.1	18.85	801.67	12.99
	Mean	65.145	29.785	21.845	644.67	13.8
	STD	3.04763023	0.445477	4.23557	222.0315	1.145513
	CV	0.04678226	0.014956	0.193892	0.344411	0.083008
	CV*100	4.67822585	1.495643	19.38919	34.44111	8.300819

3.1 Relative Humidity

The values of the relative humidity in the study areas are as given in Table 3. The result shows that relative humidity in Ungwan Rimi range from 50.2 to 75.2 % and 66.1 to 78.6% in the mornings and evenings respectively while Sabon Tasha had range of 58.8 to 81.4% and 57.7 respectively. This indicates that relative humidity was higher in the evening in Ungwan Rimi while it is higher in the mornings in Sabon Tasha.

The coefficient of variation in relative humidity between the two study areas was 4.0% which shows that there is low variation between them. The coefficient of variation between relative humidity values in the morning and evening was 10.86% in Ungwan Rimi and 4.79 % in Sabon Tasha which suggests that the indoor air quality is more stable Sabon Tasha.

Also, the coefficient of variation for relative humidity between the living room and kitchen in Ungwan Rimi in the morning was found to be 0.095% and 0.501% in the evening, while in Sabon Tasha it was found to be 0.032% in the morning and 4.68% in the evening. This suggests that the relative humidity between the living rooms and kitchens of households have negligible variation.

3.2 Temperature

The values of the temperatures in the study areas are given in Table 4. It was found from the result that the temperature in the morning in Ungwan Rimi ranged between 25.2^0C - 27.9^0C and between 24.9^0C - 31.80^0C in Sabon Tasha while the evening temperatures ranged between 26.5^0C-33.1^0C in Ungwan Rimi and 27.7^0C - 31.90^0C Sabon Tasha. This indicates a higher temperature in Sabon Tasha especially in the evening which is an inverse of the relative humidity which is lower in Sabon Tasha in the evenings. This is because warm air can hold more water vapor than cool air, therefore relative humidity falls when the temperature rises if no moisture is added to the air.

Considering the two study areas, the coefficient of variation between them for temperature was found to be 2.24% and this indicated negligible variation between the study areas. Also, between the morning and evenings in Ungwan Rimi and Sabon Tasha the CV was found to be low in both areas, with 8.28% and 2.93% respectively.

The CV between the living rooms and kitchens in both areas were found to be very low in the evenings and even lower in the mornings, with the CV in the morning being 0.58% and 0.148% for the study areas respectively and in the evenings Ungwan Rimi was found to have a CV between living room and kitchen of 1.11% and Sabon Tasha had a CV of 1.49%. This indicates minimal variation in temperature between the living rooms and kitchens in both areas and can be attributed to kitchen to living room proximity which does not allow for significant temperature difference within the households.

3.3 Carbon monoxide

The values of CO in the study areas are as given in Tables 1-4. The results shows that CO levels ranged from 1ppm to 20.50ppm in Ungwan Rimi and 6.80ppm to 62.81ppm in Sabon Tasha. The result shows very significant coefficient of variation (57.46%) between the study areas. This could be as a result of the difference in fuels used for heating and cooking and the availability of ventilation in the two study areas (Asuku, 2017).

In Ungwan Rimi the coefficient of variation between the morning and evening CO levels was low at 13.32%, while it was 14.15% in Sabon

Tasha. However, in Ungwan Rimi the morning average was found to be 9.28ppm and evening was 11.21ppm, while Sabon Tasha had higher CO of 26.71ppm and 21.85ppm as the morning and evening averages.

The CO levels were observed to be higher in the kitchens than the living rooms in all cases. The results showed moderately high coefficient of variation of CO between the living rooms and kitchens, in the mornings and evening in both study areas. For Ungwan Rimi in the morning and evening, CVs of 31.79% and 49.96% were obtained while Sabon Tasha had CV of 32.03% and 19.39% for morning and evening respectively.

3.4 Carbon dioxide

The values of carbon dioxide in the study areas are as given in Tables 1-4. The level of carbon dioxide ranged between 421ppm-1241ppm in Ungwan Rimi and 176ppm - 1440ppm in Sabon Tasha. The coefficient of variation between the areas was found to be very low at 3.96%

In Ungwan Rimi the CV between morning and evening readings was found to be 5.74% and in Sabon Tasha it was 5.02%. This low coefficient of variations indicates that the data in both areas for the morning and evening readings vary only slightly.

The coefficient of variations in the living rooms and kitchens were also determined in the mornings and evenings. In the morning in Ungwn Rimi it was found to be significantly low at 6.67% and moderately low in Sabon Tasha at 14.38%. The evening values had moderately high CV with 21.46% in Ungwan Rimi and 34.44% in Sabon Tasha. This suggests that the living rooms and kitchens had higher variations in the evenings than in the mornings.

3.5 Particulates (PM_{10})

The values of particulate matter in the study areas had a range of 6ppm to 18ppm in Ungwan Rimi and 6.78ppm to 26.80ppm in Sabon Tasha. The result shows that the variation of PM_{10} between the two areas was significant. This could be as a result of the difference in fuels used for cooking and dust accumulation in the households. While, some households within a study area use gas some were noted to use coal and firewood.

In Ungwan Rimi the coefficient of variation between morning and evening was found to be 3.72% and in Sabon Tasha it was obtained to be 6.83%, both being low indicating that the PM10 in the morning and evening was stable.

The coefficient of variation between the living room and the kitchen in Ungwan was found to be moderately high in the mornings and low in the evening at 14.56% and 5.02% respectively. Sabon Tasha on the other hand had moderately high coefficient of variation in the morning at 18.29% and low coefficient of variation of 8.301% in the evening. These variations could be as a result of more activities taking place in the kitchen than the living rooms in the mornings.

These activities include domestic cleaning and cooking activities, cooking activities being influenced by the type of fuel used.

4.0 CONCLUSION

The study showed that for all the parameters measured, the concentrations of were generally higher in the mornings than the evenings although the coefficient of variation between mornings and evenings were low (2.9-13.32%). Variations in the air quality between the two study areas were stable except for CO which high variation with CV of 57.5% and moderate variation in PM_{10} with CV of 26.68%. The highest variations were observed between the living rooms and the kitchen where the variations in CO, CO_2 and PM_{10} concentrations were quite high.

The study recommends increase in ventilation especially in the mornings when the concentrations of most of the measured parameters are high.

5.0 REFERENCES

Asuku D.E. (2017) Assessment of Indoor Air Quality of Selected Households Within Kaduna Metropolis: Case Studies of Ungwan Rimi And Sabon Tasha Areas, Kaduna. An undergraduate project submitted to the Deaprtment of Water Resources & Environmental Engineering, Ahmadu Bello University Zaria.

NPC (2006), National Population Commission

OSHA (2011), *'Indoor air quality in commercial and institution buildings (2011)*', US department of labour, occupational safety and health administration. http:/www.osha.gov

USEPA (2006) US Environmental Protection Agency, Office of Air Quality Planning and Standards, Washington, DC.http://www.epa.gov/air/criteria.html

Yamane T. (1976). Statistics: An Introductory Analysis. Published by New York Harper and Row, USA.

COMPOSITES FABRICATION AND CHARACTERIZATION

J. BABA ALI AND A. GIWA
Department of Polymer and Textile Engineering, Ahmadu Bello University, Zaria
*Corresponding author email; jamilahbabaali@gmail.com; Phone; +234(80) 8664-2026.

ABSTRACT
Composite materials play a vital role in many industrial applications. Researchers are working on fabrication of new composite materials worldwide to enhance the applicability of these materials. In view of this, the objective of the present work is to study the methods of fabrication/preparation and characterization of composites. The fabrication/preparation of composites material generally depends on the constituent materials i.e the matrix and reinforcement, the matrix material could be either polymer, carbon, ceramic or metal matrix and the reinforcement material could be in the form of particulate, fibrous or whisker. The reinforcement/filler type plays an important role in the determination of mechanical properties of composite. The most crucial factor affecting the mechanical properties of composites is the reinforcement /matrix interfacial bonding. Thus, the general properties of composites depend on the nature of the matrix, the reinforcement and rule of mixture, the method of composites fabrication depends on the type of the matrix, the reinforcement and the end use application(s).

1.0 INTRODUCTION

1.1 COMPOSITE

Composite material is a material composed of two or more distinct phases (matrix phase and reinforcing phase) and having bulk properties significantly different from those of any of the constituents (Fig. 1). Also, Composites are engineering materials made from two or more constituent material that remain separate and distinct on microscope level while forming a single component (Fig. 2).

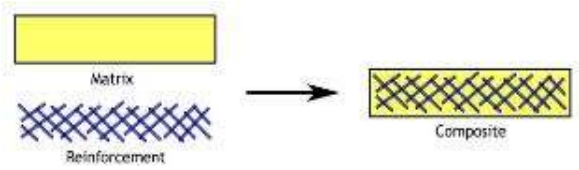


Fig. 1: Matrix and reinforcement in a composite material

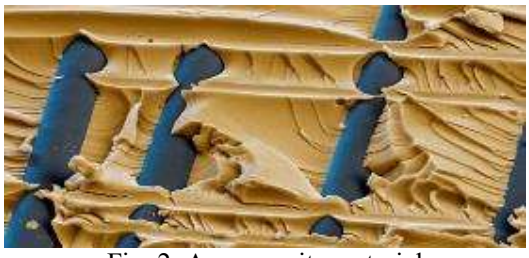


Fig. 2: A composite material

There are two categories of constituent materials: matrix and reinforcement. At least one portion of each type is required. The matrix material surrounds and supports the reinforcement material by maintaining their relative position. The reinforcement impacts their special mechanical properties to enhance the matrix properties. A synergism produces materials properties unavailable from the individual constituent materials, while the wide variety of matrix strengthening materials allows the designer of the product or structure to choose an optimum combination. Engineered composite materials must be forced to shape. The matrix material can be introduced to the reinforcement before or after the reinforcement material is placed into the mold cavity or onto mold surface. The matrix material experiences a melding event, after which the part shape is essentially set. Depending on the nature of the matrix material, this melding event can occur in various ways such as chemical polymerization or solidification from the melted state (Ananda and Sudupt, 2008).

High performance composites consist of high modulus, high strength filaments bonded together by a much softer matrix to form structure material marked by high modulus and high strength. Properties are variable depending primarily on fibres and matrix properties, volume content of these constituents, and the orientation and geometry of fibres. All are controllable and selected by a fabricator to fulfill structural requirement for a given application. Composites are anisotropic, having properties dependent on the axis of testing (Ananda and Sudupt, 2008).

1.2CONSTITUENTS OF COMPOSITE

There are two categories of constituent materials: matrix and reinforcement.

1.2.1 MATRIX

This is the continuous phase of material, and its role is primarily that of a glue or binder. A resin is a type of matrix, which must have the proper viscosity for easy process ability-namely; it must have the proper viscosity and evolve minimum

amount of volatile product during cure. Most useful matrix materials are cross-linked polymers of the thermosetting type. The main matrix materials for advance composites are usually thermosets, e.g. epoxy, polyester, phenolic, vinyl ester, and polyamide. Some thermoplastics are also in use; these thermoplastic polyester, polyethylene, polysulphanone and polyetherketone (peek).

1.2.2 REINFORCEMENT

These are discrete inclusions used to improve the structural characteristics of materials. They can be continuous in form (fibre, filament or tape) or discontinuous in form (whiskers, flake or particulate). Reinforcements reduce cost, improve formality and electrical properties, increase the ratios of strength of density and stiffness to density; increase resistance to corrosion, fatigue creep, stress rupture, and reduced the coefficient of thermal expansion. Reinforcements allow the material to be tailored to the material. Fillers are considered to be cheap extenders and diluents used to reduce the cost of a compound (Joel, 2007).

1.3 CLASSIFICATION OF COMPOSITES

Composite materials are classified based on the basis of matrix material or the basis of filler material (Sudipt and Ananda, 2008) (Fig. 3).

1.3.1 ON THE BASIS OF MATRIX

The Fig.4 shows the classification of composites on the basis of matrices.

1. Metal Matrix Composites (MMC)

Metal Matrix Composites are composed of a metallic matrix (aluminium, magnesium, iron, cobalt, copper) and a dispersed ceramic (oxides, carbides) or metallic (lead, tungsten, molybdenum) phase. Metallic Reinforcement may be tungsten, beryllium etc. MMCs are used for Space Shuttle, commercial airliners, electronic substrates, bicycles, automobiles, golf clubs and a variety of other applications. From a material point of view, when compared to polymer matrix composites, the advantages of MMCs lie in their retention of strength and stiffness at elevated temperature, good abrasion and creep resistance properties. Most MMCs are still in the development stage or the early stages of production and are not so widely established as polymer matrix composites (Hashim *et al*, 1999)

2. Ceramic Matrix Composites (CMC)

Ceramic Matrix Composites are composed of a ceramic matrix and imbedded fibres of other ceramic material (dispersed phase).

3. Polymer Matrix Composites (PMC)

This type of matrix often determines the maximum service temperature, since it normally softens, melts or degrades at a much lower temperature than the fibre reinforcement. The most widely utilized polymer resins are the polyester and vinyl esters namely; thermoplastics resins [polypropylene, polyphenylene, siphone, polymide etc] and thermo set resins [polyesters, phenolic, melamine, silicones, polyurethanes, etc]. The role of polymer matrix in a fibre reinforced composites is to transfer stress between the fibres, to provide a barrier against an adverse environment and to protect the surface of the fibre from mechanical abrasion. The matrix plays a major role in the tensile load carrying capacity of a composites structure. The binding agent or matrix in the composites is of critical importance. Polymer resins have been broadly divided into two categories: Thermosetting and Thermoplastic resin. (Sudipt and Ananda, 2008)

1.3.2 ON THE BASIS OF FILLER MATERIAL

1. Particulate Composites

Particulate Composites consist of a matrix reinforced by a dispersed phase in form of particles.

a. Composites with random orientation of particles.
b. Composites with preferred orientation of particles. Dispersed phase of these materials consists of two-dimensional flat platelets (flakes), laid parallel to each other.

2. Fibrous Composites

a. Short-fibre reinforced composites. Short-fibre reinforced composites consist of a matrix reinforced by a dispersed phase in form of discontinuous fibres (length < 100 diameter).
b. Composites with random orientation of fibres.
c. Composites with preferred orientation of fibres.

3. Long-fibre reinforced composites.

Long-fibre reinforced composites consist of a matrix reinforced by a dispersed phase in form of continuous fibres.

1.4 RULE OF MIXTURES

Rule of Mixtures is a method of approach to approximate estimation of composites material properties, based on an assumption that a composite property is the volume weighted

average of the phases (matrix and dispersed phase) properties. According to Rule of Mixtures properties of composite materials are estimated as follows:

In developing the rule of mixture, the following assumptions are made:

- Fibres are uniform, parallel and continuous.
- Perfect bonding between fibre and matrix.
- Longitudinal load produces equal strain in fibre and matrix

1.5 METHODS OF COMPOSITES FABRICATION

A variety of molding methods (Fig. 6) can be used according to the design requirements. The principal factors are the nature of the chosen matrix and reinforcement materials. Another important factor is the gross quantity of the material to be produced. Large quantities can be used to justify high capital expenditure for rapid and automated manufacturing technology. Small production quantities are accommodated with lower capital expenditure but higher labour and tooling costs at a correspondingly slow rate (Danladi and Shuaib, 2014)

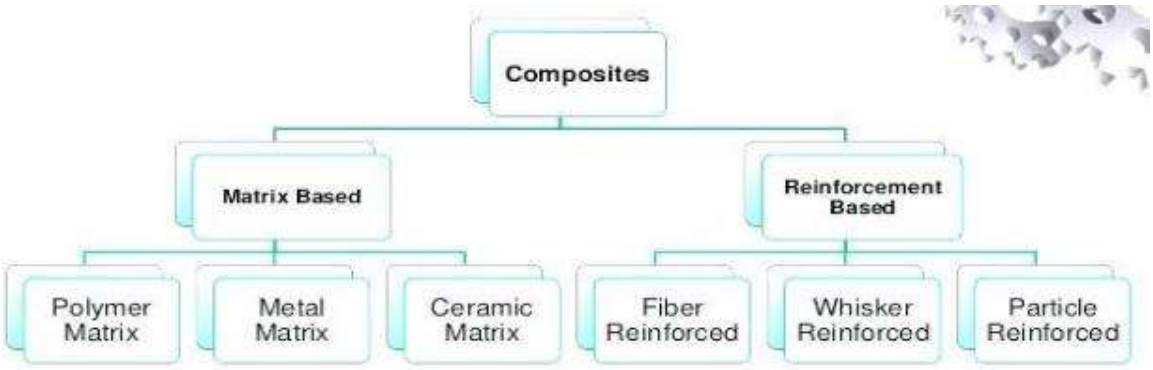


Fig.3: Showing general classification of composite.

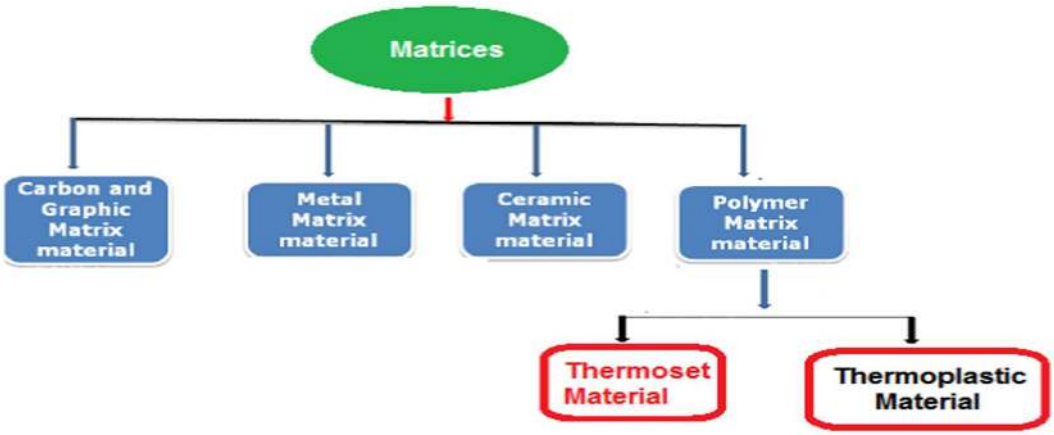


Fig.4: Classification of composites on the basis of matrices.

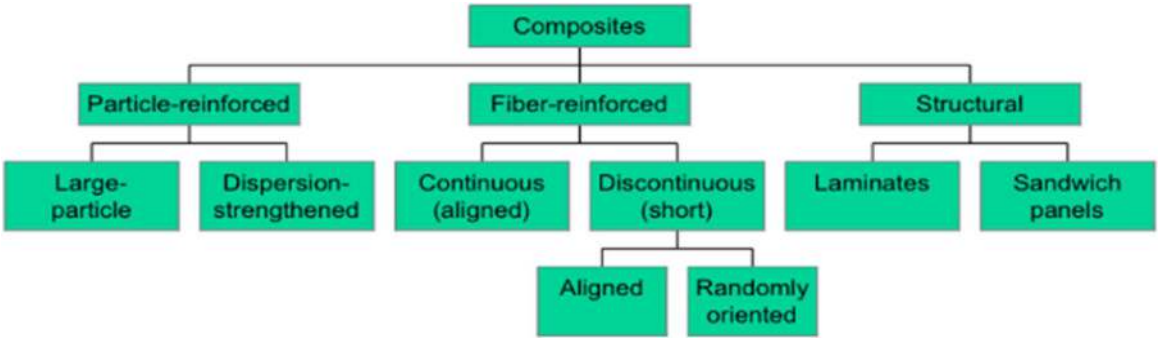


Fig. 5: Showing the classification of composites on the basis of filler material.

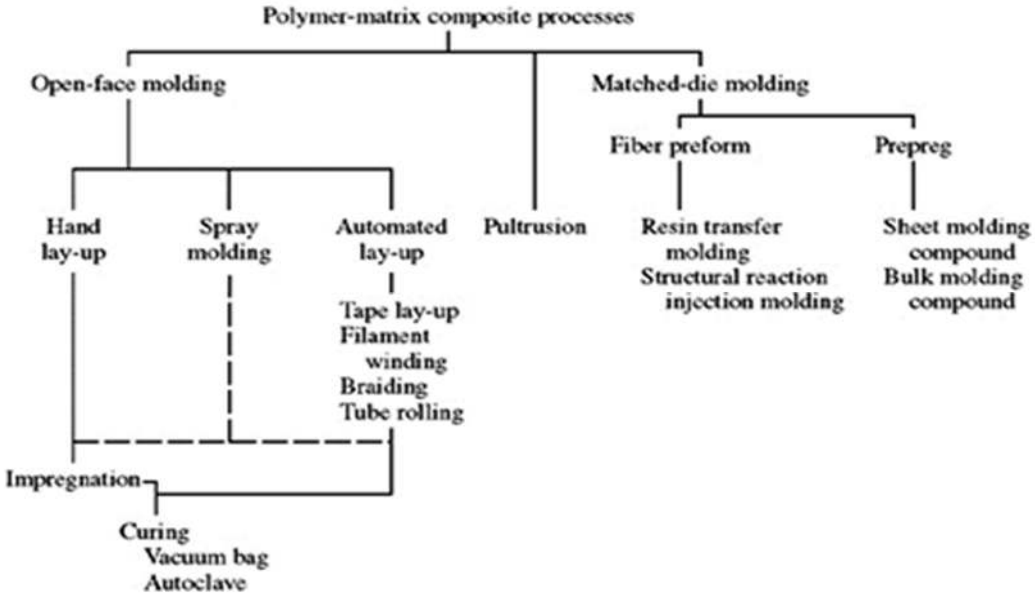


Fig.6: Showing Polymer Matrix composite processing methods.

In general, the reinforcing and matrix materials are combined, compacted and processed to undergo a melting event. After which the part shape is essentially set, although it can undergo a melting event. After which the part shape is essentially set although it can deform under certain process conditions. For a thermo sets polymeric matrix material, the melting event is a curing reaction that is initiated by the application or addition of heat or chemical reactivity such as organic peroxide. For a thermoplastic polymeric matrix, the melting event is solidification from the melted state. For a metal matrix material such as titanium foil, the melting event is fusing at high pressure and temperature near the melt point. For many molding methods, it is convenient to refer to one mold piece as a ‘’lower’’ mold and another mold piece as ‘’upper‘’ mold. Lower and upper refers to the different faces of the molded panel, not the mold ‘’ mold. Lower and upper refers to the different faces of the molded panel, not the mold configuration in space. In this convention, there is always a lower mold and sometimes an upper mold. Past construction begins by applying materials to the lower mold. The molded product is often referred to as a panel. For certain geometric and materials contributions, it can be referred to as a casting. For certain continuous processes, it can be referred to as a profile (Joel, 2007).

1.5.1 OPEN MOLDING

A process using one sided mold which shapes only one surface of the panel the opposite surface is determined by the amount of material placed upon the lower mold. Reinforcement material can be placed manually or robotically. They include continuous fibre forms fashioned into textile constructions and chopped fibre. The matrix is generally a resin, and can be applied with a pressure roller, a spray device or manually. This process is generally done at ambient temperature and atmospheric pressure.

1.5.2.1 Hand Lay-Up Method

Hand lay-up techniques is the simplest and oldest open molding method of the composites fabrication processes. It is a low volume, labor intensive method suited especially for large composites, such as boat hull, Glass or other reinforcing mat or woven fabric or roving is positioned manually in the open mold and resin is poured, brushed or sprayed over and into the glass piles. Entrapped air is removed manually with squeegees or rollers. Room temperature curing thermosets resins e.g, polyester and epoxy resins are the most commonly used matrix resin. Curing is initiated by a catalyst in the resin system which hardens the fibre reinforced resin composites. A pigmented gel is first applied to the mold surface for easy removal (Joel R, 2007)



Fig.7: Showing Hand lay-up method

- Advantages:
  - low cost tools
  - versatile: wide range of products
- Disadvantages:
  - time consuming
  - easy to form air bubbles and disorientation of fibers
  - inconsistency

1.5.2.2 Spray-Up Method

Similar to hand lay-up in simplicity, spray-up offers greater shape complexity and faster production. Spray-up utilizes a low-cost open mold, room temperature curing resin, and is ideal for producing large parts such as tub/shower units and vent hoods in low to moderate quantities. Chopped fiber reinforcement and catalyzed resin are deposited in the mold from a chopper/spray gun.



Fig.8: Showing Spray-Up Method

As with lay-up, manual rolling removes entrapped air and wets the fibre reinforcement. Woven roving is often added in specific areas for thickness or greater strength. Pigmented gel coats can be used to produce a smooth, colourful surface.

1.5.3 VACUUM BAG MOLDING

A process using a two-sided mold set that shapes both surface of the panel. On the lower side is a rigid mold and on the upper side is a flexible membrane. The flexible membrane can be a reusable silicon material or an extruded polymer film such as nylon. Reinforcement materials can be placed on the lower mold manually or robotically, generally as continuous fire forms fashioned into textile constructions. The matrix is generally a resin. The fibre form may be pre-impregnated with the resin in the form of prepared fabrics or unidirectional tapes. (Joel, 2007).

1.5.4 AUTOCLAVE MOLDING

A process using a two-sided mold set that forms both surface of the panel. On the lower side is a rigid mold and on the upper side is a flexible membrane made from silicone or an extruded polymer film such as nylon. Reinforcement materials can be placed manually or robotically. They included continuous fibre forms fashioned into textile constructions. Most often, they are pre-impregnated with resin in the form of prepared fabrics or unidirectional tapes. In some instance, a resin film is placed upon the lower mold and dry reinforcement is placed above. The upper mold is installed and vacuum is applied to the mold cavity. Then the assembly is placed into an autoclave pressure vessel. and low void content for maximum structural efficiency (Danladi, and Shuaib, 2014).

1.5.5 RESIN TRANSFORMER MOLDING

A process using a two-sided mold set that forms both surfaces of the panel. The lower side is a rigid mold. The upper side can be a rigid or flexible mold. Flexible mold can be made from composite materials, silicone or extruded polymer films such as nylon. The two side fit together to produce a mold cavity. The distinguishing feature of resin transfer molding is that the reinforcement materials are placed into this cavity and the mold set is closed prior to the introduction of matrix material. Resin transfer molding includes numerous variety which differ in the mechanics of how the resin is introduced to the reinforcement in the mold cavity. These variations include everything from vacuum infusion to vacuum assisted resin transfer molding.

1.5.6 THE PLASTIC INJECTION MOLDING PROCESS

Because of its high viscosity, in order for plastic injection molding to be successful melted polymer must be injected into a hollow mold with a large force.

Feeding the polymer resin (pellets) down to the auger (screw) is a large open-bottomed container. An electric (or hydraulic) motor is responsible for turning the auger inside a heated cylinder which feeds the pellets up through the grooves of the auger. A gate before the mold cavity restricts the flow of the melt into the mold and limits backflow. The pressure created by pushing the forward through the grooves up to the gate also produces heat on the inside of the cylinder which helps to melt the polymer and prepare it for injection into the mold. As the auger moves forward it injects polymer melt into the mold at high pressure (typically 10,000 - 30,000 psi), holds it, and adds more melt to ensure the contraction due to cooling and solidification does not leave gaps in the final product. Eventually the gate solidifies and isolates the mold from the injection cylinder (Joel, 2007)

1.6 TESTING OF COMPOSITES

Evaluation of physical, mechanical and other characteristics of object made from plastic is a function, which the plastic engines is frequently required to perform. The purpose may be control of quality in production, acceptance testing against specifications, establishment of data for engineering and design or other end of substantial economic importance.

1.7 MECHANICAL TESTS

The test of physical properties using mechanical testing of plastics is among the most important. These tests determine the strength, stability, hardness and bending properties of materials.The five most important mechanical tests are tensile (ASTM D638), Izod impact (ASTM D256), Rockwell Hardness (ASTM D785), Durometer Hardness (ASTM D2240) and flexural strength (ASTMD790) (Siti Rabiatull *et al*, 2012).

1.7.1 TENSILE PROPERTIES

Tensile test measure the maximum stress that a material can withstand while being stretched or pulled. The properties derived from the tensile test are the most important indications of strength of a material. The force necessary to pull a specimen apart, as well as how the material stretches before breaking indicates how tough or brittle the material may be. Plastic materials produce stress-strain diagrams that offer clear indications of the various points of yielding as the load is increased.

1.7.2 IMPACT STRENGTH

This is the measure of the work done to break a test piece. It is the ability of a material to withstand shock loading or the work done in fracturing under shock loading. In practical terms, where the fabricated objects are to encounter dynamic force such as shock, impact strength may be more important than tensile strength. There are several types of impact testing machines. Impact strength is measured in joules per meter (j/m) (SitiRabiatull *et al,* 2012)

1.7.3 HARDNESS

This is described as the process of surface deformation of a material due to indentation. This test is employed using 2 types of durometer hardness machine i.e. type A and type D, usually for measuring the indentation that is hardness, a material that is ranging from soft rubber to hard rubber and plastic (SitiRabiatull *et al*, 2012)

1.7.4 FLEXURAL STRENGTH

The flexural strength represents the highest stress experienced within the material at its moment of rupture. It is measured in terms of stress. The transverse blending test is mostly employed, in which a sample having either a circular or rectangular cross-section is bent until fracture or yielding, using a three-point or four-point flexural test techniques. Flexural strength is calculated in (Mpa) (Hodgkinson, 2000).

1.7.5 COMPRESSION STRENGTH

Compression strength is the capacity of a material or structure to withstand load tending to reduce size, in other words compressive strength resists compression (being pushed together).The application of compressive load on the cross-section can be done in three ways.

1. Directly applying the compressive load on the end of a specimen.
2. Loading the edges in shear and mixed shear.
3. Directly loading on the specimen. (Urbane and Johnson, 2014)

CONCLUSION

In conclusion, the properties of composites depend on the nature of the matrix, the reinforcement and the rule of mixture. Similarly, the method of composites fabrication depends on the type of the matrix, the reinforcement and the end use application(s).

REFERENCES

Ananda T.J and Sudipt K,(2008). Metal matrix composites Production and characterization of aluminum-fly ash composite using stir casting method.Pp.15-25.

Bharath K.S,Madhusudhana R.H and Ravi B .C (2014). Experimental investigation of mechanical properties of sisal fiber and rice husk reinforced polymer composite. Journal of Mechanical and Civil Engineering (IOSR-JMCE) e-ISSN: 2278-1684,p-ISSN: 2320-334X, Volume 11, Issue 4 Ver., PP 05-11.

Danladi.A, and Shuaib.J, (2014)"Fabrication and properties of Pineapple fibre/High density polyethylene composites"American Journal of Material Science,4(3):139-143DOI:10.5923/j.materials.20140403.04.

Hashim, J. Looney. L. and Hashim, M.S.J. (1999)"Metal matrix composites production by the stir casting method,' 'Journal of Materials processing technology, 92-93: 1-7.

Hodgkinson.J.M, (2000).Mechanical testing of Advance fibre composites, Cambridge: woodhead publishing Ltd, P132-133.

Ishiaku U.S, Sahoo .S, Nakai. A, Kolaki, Mohanty.A.K, Misra.M, and Hamada.H,(2007). Mechanical properties

and durability of jute reinforced thermosetting composites.Journal of Biobased Materials and Bioenergy.1(3):427-436. DOI:10.1166/Jbmb.2007.019.0.65.

Joel R.Fried,"Polymer Science and Technology"(2007)Second Edition New Delhi, Pp.76, 77.

Sitirabiatull Aisha and Hardinnawirda.K, (2012). Effect of rice husk as fillers in polymer matrix composites, Journal of Mechanical Engineering and Sciences, e-ISSN: 2231-8380: Vol.2, pp181-186

Sudipt K and Ananda T.J(2008). Metal matrix composites Production and characterization of aluminum-fly ash composite using stir casting method.Pp.15-25.

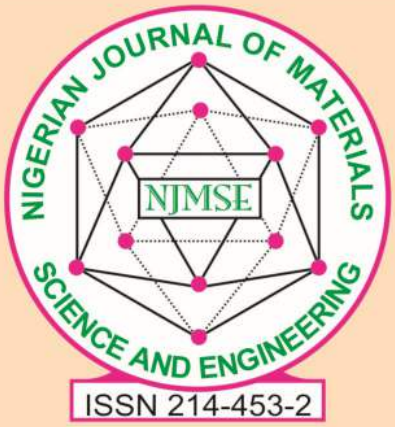
Urbane K.T,Lee and Johnson(2006)"Column Compression strength of tabular packaging forms. Page 34,6. Journal of testing and evaluation.

Composites Molding Images .Retrieved via www.Substech.com at 4:31pm on 23/01/2016.

Nigerian Journal Of Materials Science and Engineering (NJMSE)

Vol. 9 Number 1 ISSN 214-453-2 June, 2018

Materials Science and Technology Society of Nigeria (MSN)



An International Journal of the Materials Science and Technology Society of Nigeria

You can Publish with us bi-annually